THE BEHAVIOUR OF ROADBASE MATERIALS UNDER REPEATED LOADING

b y

JOHN MURRAY HANSON, M.Phil.

Thesis submitted to the University of Nottingham
for the degree of Doctor of Philosophy
October 1971

ABSTRACT

A standard testing machine has been modified to perform constant frequency strain-controlled repeated loading tests on laboratory prepared samples of flexible roadbase materials. Tests over a temperature range of 0°C to +40°C have been performed on specimens of hard and soft dense bitumen macadam, dense tar macadam and hot rolled asphalt, together with a limited number of stress- and strain-controlled tests on dry lean concrete.

The effect on stiffness of strain, strain rate and temperature has been established for all materials studied, both from tests designed specifically for this purpose and from the initial stiffness values of specimens tested in repeated loading. From these results the compound shapes of the stiffness/strain relationships of the materials investigated have been evolved.

The stress level of dry lean concrete tested in repeated loading has been related to both the number of load applications to fracture and the strain at which fracture occurs. Strain-controlled tests on bituminous materials have shown a progressive fall in stiffness under the repeated applications of load. Mathematical expressions have been developed for the strain level and number of applications of load required to cause various reductions in initial stiffness, leading to theoretical relationships between the number of load applications sustained and the resulting fall in stiffness.

Parallel plate and coaxial cylinder viscometers have been developed to measure binder viscosity in both static and steady shear conditions and results of these tests have been used to support a proposed theory for structural breakdown of binder under repeated applications of load.

Test results have been utilized in a theoretical analysis of layered systems employing an established elastic theory computer programme and resulting pavement service lives established.

Recommendations are made for ways in which flexible road pavement materials might be improved in view of the experimental results obtained.

ACKNOWLEDGEMENTS

The experimental work reported in this Thesis was carried out in the Department of Civil Engineering, the University of Nottingham. The Author would like to express his gratitude to the Science Research Council for its sponsorship and to Professor R.C. Coates for facilities made available.

The Author also wishes to thank the Secretarial and Laboratory Staff for their assistance, and Messrs. Ellis and Everard Ltd., Shell International Petroleum Company Ltd., and Midland Tar Distillers Ltd. for the supply of materials.

Finally, sincere thanks are extended to Professor P.S. Pell for his supervision and guidance throughout the experimental period.

CONTENTS

		Page
CHAPTER 1 -	INTRODUCTION	I
	Introduction	
	Road Pavement Components	
	Road Pavement Materials	
	Pavement Thickness Design	
	Equivalence of Road Pavement Materials	
	Assessment of Road Pavement Performance	
	Road Pavement Failures	
	Laboratory Studies	
	Background to work in Thesis	
CHAPTER 2 -	WORK IN THESIS	I7
	Introduction	
	Scope of Investigation	
	Form of Thesis	
CHAPTER 3 -	PHYSICAL CHEMISTRY OF BITUMINOUS AND CEMENTITIOUS BINDERS	I9
	Introduction	
	Tar	
	Bitumen	
	Cement Paste	
CHAPTER 4 -	RHEOLOGICAL BEHAVIOUR OF BITUMINOUS BINDERS AND MIXTURES	23
	Introduction	
	Bituminous Binders at Constant Temperature	
	Bituminous Binders at Various Temperatures	
	Bituminous Mixtures	
	Non-linear Behaviour of Bituminous Materials	
CHAPTER 5 -	REVIEW OF PREVIOUS WORK	35
	Introduction	
	Stiffness Properties of Bituminous Materials	
	Behaviour of Bituminous Materials under Repeated Loading	
	Static properties of Concrete	
	Behaviour of Concrete under Repeated Loading	

Page

CHAPTER 6 - PRELIMINARY EXPERIMENTAL AND DEVELOPMENT WORK 85

Method of Testing
Specimen Size
Specimen Compaction
Specimen Extrusion
Specimen Void Measurement
Bonding of Specimens to End Caps
Specimen Mounting for Testing
Specimen Temperature Control

CHAPTER 7 - DEVELOPMENT OF TESTING APPARATUS 92

Specimen Deformation Measurement
Specimen Testing Equipment
Binder Viscosity Tests
Binder tests in steady shear

CHAPTER 8 - EXPERIMENTAL PROCEDURES AND TECHNIQUES 101

Experimental Procedures - Bituminous Materials
Experimental Techniques - Bituminous Materials
Experimental Procedures - Cement Bound Materials
Experimental Techniques - Cement Bound Materials
Binder Viscosity Tests
Binder Tests in Steady Shear
Standard Tests on Binders

CHAPTER 9 - EXPERIMENTAL RESULTS PRIOR TO MAIN TEST PROGRAMME 123

Calibration of Test Equipment
Tests on Materials, Mixtures and Specimens prior to Dynamic testing
Dynamic tests on Bituminous Specimens
Dynamic tests on Concrete Specimens

CHAPTER 10 - EXPERIMENTAL RESULTS OF MAIN TEST PROGRAMME 137

Voids in Specimens
Stiffness Measurements
Stiffness/Strain Relationships
Repeated Loading Tests on Bituminous Materials
Repeated Loading Tests on Dry Lean Concrete
Binder Viscosity Tests
Static Tests on Binders

Page

CHAPTER 11 - DISCUSSION OF EXPERIMENTAL RESULTS I64

Voids in Specimens

Stiffness Measurements

Stiffness/Strain Relationships

Repeated Loading Tests on Bituminous Materials

Repeated Loading Tests on Dry Lean Concrete

CHAPTER 12 - EFFECT OF ROADBASE STIFFNESS ON THEORETICAL PAVEMENT STRENGTH I9I

CHAPTER 13 - CONCLUSIONS I96

CHAPTER 14 - APPLICATION OF EXPERIMENTAL RESULTS TO PRACTICE 20I

CHAPTER 15 - RECOMMENDATIONS FOR FURTHER WORK 204

BIBLIOGRAPHY 206

PLATES 222

FIGURES 245

TABLES 399

APPENDICES 437

CHAPTER ONE

INTRODUCTION

INTRODUCTION

The ever increasing magnitude and intensity of commercial vehicle wheel loads make heavy demands on modern road pavements. With the expanding network of motorways and improved trunk roads, road transport is becoming an increasingly attractive proposition. The by-passing of built-up areas together with the elimination of sharp bends and steep gradients encourage the passage of loads both larger and heavier than ever before. The highway engineer is therefore faced with the problem of designing and improving roads to be capable of withstanding these increasingly heavy demands.

The function of a road pavement is to provide a safe, comfortable, convenient and economic running surface for the passage of fast moving traffic. Its structure must be capable of spreading the wheel loads to a level acceptable to the native soil on which it is constructed. The repeated application of wheel loads on a road pavement may lead to a deterioration of one or more of the component layers resulting in surface irregularities and possibly cracking. Once the road pavement surface condition falls below a specified standard remedial measures become necessary. These are both costly and inconvenient and should be kept to an absolute minimum, if not eliminated completely.

ROAD PAVEMENT COMPONENTS

Road pavements are constructed in a series of horizontal layers of different materials. Each layer has a specific function to perform and the appropriate materials and layer thicknesses are selected with due regard to efficiency and economy.

Road constructions may be of either "flexible" or "rigid" design depending upon the application, ground and traffic conditions, economics and to some degree personal choice. Flexible construction consists of both unbound and bituminous-bound materials whereas rigid construction consists of unbound and cement-bound materials. Specifications include dry lean concrete as a roadbase material for flexible pavement construction but, as will be shown later, the structure remains essentially flexible. Rigid pavements for heavily trafficked roads are always of reinforced concrete but may include a thin overlay of bituminous

surfacing material. This thesis is concerned only with roadbase materials used in flexible road pavement construction and remarks will, therefore, be confined to this form of structure.

Figure 1 shows a typical cross section of flexible pavement construction used in new motorways and major trunk road improvements in Great Britain, which are expected to carry in excess of 4,500 commercial vehicles per day 20 years after construction. Although the materials in layer thicknesses will be discussed in more detail in the following sections, those shown are intended to provide a broad indication of the materials and corresponding thicknesses involved.

Wearing course - The function of the wearing course is to provide an even, impermeable, skid resistant running surface for the passage of traffic. The material should be stiff enough to resist excessive deformation under the action of moving and stationary traffic and flexible enough to accommodate slight irregularities arising from any permanent movements of the underlying layers. The wearing course should be sufficiently impermeable to resist the ingress of water into itself and the underlying layers. In this country, where pavements are surface dressed to increase resistance to skidding, the wearing course should be capable of accepting surface dressing or precoated chippings.

A wearing course material which will satisfactorily perform the functions set out above will also possess considerable load spreading properties. Although the wearing course is not specifically designed to be a structural member of the road pavement, it does contribute significantly to the load spreading characteristics of the structure.

Base-course - A smooth, level, running surface is best achieved by laying a thin wearing course layer on a smooth level base. One of the functions of the base-course is therefore to provide such a surface on which to lay the wearing course. Base-course material generally contains less binder and filler than the wearing course, since impermeability is much less important, but it nevertheless possesses good load spreading properties and is designed as a structural member. The base-course material is also required to resist excessive deformations yet accommodate local deformations without cracking.

Roadbase - The roadbase is generally considered to be the main structural member of the road pavement. Since it is protected from extremes of temperature and from the ingress of moisture by the wearing course and

base-course, a cheaper, more open textured material is most commonly used. Due to its thickness, bituminous roadbase materials are placed in a number of layers each of up to $3\frac{1}{2}$-inches in thickness (1).* With layers of this depth, and also due to the fact that, when laid, the underlying layers are still generally warm, it is most difficult to achieve a good smooth surface of specified level. It would, therefore, be impossible to lay an even surfaced wearing course straight on to the surface of the roadbase.

Like the wearing course and the base-course materials, roadbase materials should be able to resist excessive deformations at the same time possessing a certain degree of flexibility. The intensities of stresses at various points in the roadbase will be considerably less than those in the wearing course and base-course, the actual values under a given wheel load depending upon the modular ratios of the layers and those of the underlying materials. Although a more inferior material may well suffice for the roadbase, it will be shown subsequently that considerable short-term and long-term economies are to be gained by the appropriate selection of carefully designed and manufactured roadbase materials.

Sub-base - Many subgrade materials are susceptible to frost and the subsequent frost heave may well have an adverse effect upon the road pavement structure. In order to protect the subgrade from frost damage, a minimum thickness of construction above it may be estimated. In this country for a strong, but frost susceptible, subgrade this thickness for heavily trafficked roads is taken as between 17 and 20-inches, depending upon the type of roadbase material used (2). To make up this thickness by increasing the depth of the roadbase would be most uneconomical. A cheaper sub-base material is therefore employed to replace the additional thickness of the more expensive roadbase material.

The sub-base should be a well graded and well compacted granular material. Such a material has excellent load-spreading properties and makes a significant contribution to the structural rigidity of the road pavement. The thickness of the sub-base is further increased to assist in reducing the load transmitted to lower quality subgrades.

A carefully selected and well compacted sub-base material is a most stable and economical load-spreading member. However, since significant tensile forces are present at considerable depths in a road pavement, an unbound sub-base material can only be used below depths,

---

* Figures in parenthesis refer to references at the end of the Thesis.

under bound layers, at which tensile forces are minimal.

Sub-grade - The subgrade is usually the native soil which has been compacted and levelled to the formation level. The strength of the subgrade determines the depth of construction above it which is generally effected by changing the sub-base thickness. Subgrade soils which fall below a specified strength are replaced by other well compacted soils or fine granular materials.

ROAD PAVEMENT MATERIALS

Bituminous road pavement materials may be classified into two broad groups, namely continuously-graded and gap-graded mixtures. The former is used extensively in the United States of America and many other countries and is known as "asphaltic concrete." When used in Great Britain a dense continuously-graded bituminous mixture is referred to as "dense bitumen macadam" or "dense tar macadam." The gap-graded type of bituminous mixture is peculiar to Great Britain and is known as "hot rolled asphalt." Both asphaltic concrete and hot rolled asphalt employ bitumen as the binder, although tar has been used in the United States of America on some occasions.

Continuously-graded bituminous materials - The load-bearing capacity of a continuously-graded bituminous mixture is derived mainly from the frictional interaction of the aggregate particles and partly from the visco-elastic properties of the binder. The viscosity of the binder may be increased by the addition of some fine inorganic powder, such as cement or crushed limestone, which will also act as an extender to the binder helping to fill the aggregate voids. The function of the binder is twofold. First it provides lubrication for the dry aggregate during compaction and secondly, in the constructed pavement, it inhibits the ingress of water and contributes greatly to the tensile properties and general stability of the mixture.

In the United States of America and certain other countries following American highway engineering practice, continuously graded mixtures are generally designed by means of empirical test methods (3-6). For a particular aggregate type and grading the "optimum" binder content is evaluated from test results of a series of specimens covering a range of binder contents. The optimum binder content is that which satisfies certain specified compaction, strength and deformation characteristics. The required characteristics are specified in accordance with the

requirements of the road pavement and with the position of the material in the structure.

In Great Britain and many Continental countries continuously-graded mixtures are designed in accordance with specifications based on practical experience rather than the results of mechanical tests. The specification used in this country (1) caters for both dense and open textured macadams for road pavement construction.

Gap-graded bituminous materials - a gap-graded mixture consists essentially of a sand asphalt with a proportion of relatively coarse stone. The load bearing capacity of the mixture is gained essentially from the strength of the sand/(filler)/binder matrix the stone acting mainly as an extender to the matrix.

The aggregate grading of a gap-graded bituminous material is such that it will accommodate a higher content of binder than will a continuously-graded material. This additional binder provides greater durability against the inclement weather conditions experienced in this country and also enables the wearing course to accept a surface dressing. Moreover, the nature of the aggregate grading results in a far more workable mix than a continuously-graded material. It is therefore possible to employ binders of higher viscosity resulting in most stable mixtures possessing considerable load spreading characteristics.

Hot rolled asphalts in Great Britain are designed in accordance with B.S.S. 594 (7). This document takes into account traffic and weather conditions, and provides tabulated data for mix design based on practical experience accumulated over a number of years.

Dry lean concrete - The aggregate grading of dry lean concrete used in flexible road pavement construction is also of a continuous nature. It is common practice in this country to use river gravel as the concrete aggregate which, unlike crushed rock, contains very little material finer than a No. 100 mesh sieve size. The strength of dry lean concrete is derived mainly from the cement matrix and is strongly dependent upon the adhesion between the matrix and the aggregate. This aspect is dealt with in more detail in Chapter 5.

In Great Britain dry lean concrete for flexible roadbases is designed in accordance with the Specification for Road and Bridge Works (1). As the name implies, dry lean concrete has a low water and cement content to achieve a relatively flexible material and to ensure high density microcracking rather than low density macrocracking.

Unbound granular materials - A continuously-graded, well compacted, dry, granular material possesses excellent compression and shear transmission characteristics. Load spreading properties are increased by the use of more angular, rough-textured aggregates and under the action of external compressive forces. Tensile properties of dry granular materials are low but are increased somewhat under the action of lateral compression. The application of this type of material is therefore limited to circumstances where tensile forces are small.

In Great Britain granular roadbases and sub-bases are designed in accordance with the current Specification for Road and Bridge Works (1). Granular roadbase materials may either be premixed with a small amount of water, or the coarse aggregate first placed dry and the finer material rolled in. Granular materials used in sub-base construction are bound with either an organic (clay) or an inorganic (crushed limestone dust) material and occasionally with cement and water.

PAVEMENT THICKNESS DESIGN

The structural function of a road pavement is to spread wheel loads to an intensity such that the repeated applications of load will not cause excessive deformation or shear failure of the subgrade. The thickness of an efficient structure will depend upon its [illegible], the seasonal levels of the water table, the strength of the subgrade, the load spreading properties of the component layers and their behaviour under repeated applications of load, the magnitude and intensity of wheel loads and the climatic conditions prevailing.

The thickness of a road pavement may be determined using theoretical design methods, empirical design methods based on correlated field and laboratory performance data, or purely on the properties of the subgrade.

In several districts, including many parts of West Germany (8), pavement design thickness is based solely upon the frost-susceptibility of the subgrade. The determined pavement thickness is made up of layers the depths of which depend upon the intensity of traffic and the type of materials used.

An early pavement thickness design method, upon which several design procedures are based today, is the Soil Classification Method (9). The maximum bearing capacity of the native soil is evaluated by some form of penetration or triaxial loading test. The stress distribution theory of Boussinesq is then used to evaluate the depth at which the stress imposed by the design wheel load is equal to the bearing

capacity of the subgrade. This depth of soil is then replaced by the same depth of pavement structure. An example of a current design method based on this principle is that employed by the North Carolina State Highway Commission (10). Here the strength of the subgrade is evaluated from its California Bearing Ratio (C.B.R.) value. The design wheel load is dependent upon the traffic density, and the component layer thicknesses are dependent upon the type of materials to be used.

Many current pavement thickness design procedures are based upon C.B.R. design methods (11), the C.B.R. value of the subgrade being taken as a relative measure of its strength. Design curves, based on the results of previous practical experience or on the results of full scale trials, relate the C.B.R. value of the subgrade to the required pavement thickness appropriate to the traffic conditions and (possibly) the environmental conditions prevailing. The thickness of the component layers is sometimes specified but often left to the experience and intuition of the engineer. Many such methods are outlined in Sessions 1, 6, 7 and 8 of the First International Conference on the Structural Design of Asphalt Pavements and also in Highway Research Records 13, 46, 71 and 291.

A further empirical thickness design method is the Group Index Method (12) employed, among others, by the U.S. Highway Engineers Group (13). In this method a group index is ascribed to the subgrade soil evaluated from its clay content and Atterburg Limits, leading to the selection of the appropriate pavement thickness.

In Great Britain pavement thickness design is carried out in accordance with the recommendations laid down in Road Note 29 (2)*. This document provides design charts based upon practical experience of road pavement performances and is periodically updated in the light of recently appraised full scale road trials. The appropriate road pavement thickness is selected from a knowledge, or estimation, of the C.B.R. value of the subgrade and depends upon the daily number of commercial vehicles anticipated 20 years after construction. The design chart for Class 1 type flexible road pavement construction is shown in Figure 1. Here the thickness of the surfacing and roadbase layers are stipulated and the sub-base thickness varies from 6 to 19½-inches depending on the C.B.R. value of the subgrade.

---

*Since the preparation of this Thesis Road Note 29 has been superceded by a third edition. Comments and diagrams referring to this Note should be studied in conjunction with the third edition.

In all the above design methods the total pavement thickness is specified for the local soil, traffic and environmental conditions. This total thickness is achieved by the use of several layers of materials, their individual thicknesses being selected with due regard to their characteristics and economy. Lee and Croney (14) have concluded, from full scale road trials performed in this country, that the type of surfacing and base materials have a far greater influence in the determination of pavement performance than does the overall pavement thickness. Lee and Croney are of the opinion that pavement thickness cannot be related to subgrade strengths and state that a considerable saving in pavement thickness may be achieved when using strong surfacing and base materials.

Based on the results of the A.A.S.H.O. road test (15) a thickness design method has been evolved (16, 17) whereby a "structural number" is ascribed to structure. This structural number is evaluated from the C.B.R. value of the subgrade and functions of traffic and climatic conditions. The component layers are selected such that the summation of the products of the relative strength and thickness of each layer is equal to the structural number of the system.

Dynamic tests may also be performed on the subgrade and overlying layers to determine pavement thickness. The California Division of Highways have developed a design method whereby the resilient properties of the various component layers are evaluated by means of repeated loading tests in compression (431). Using the stress distribution theory of Boussinesq, the estimated stress level of each layer is used to determine its appropriate resilience. The sum of the predicted resilient deformations of each layer and the subgrade enable the amount of surface deflection to be estimated. These surface deflections are used to determine the efficacy of the assumed design thicknesses.

With the advent of the electronic digital computer many theoretical mathematical analyses of the stresses and strains in multi-layered road pavement systems have been proposed. A theoretical analysis, together with a thorough knowledge of the properties of road pavement materials, will lead to a more rational and economical approach to pavement thickness design.

It is generally assumed that the road pavement consists of a number of homogeneous, isotropic, linear, elastic stratified horizontal layers, of either finite or infinite boundaries, resting on a semi-infinite elastic mass. Most analyses are based on the work of Burminster (19)

although new approaches using finite element techniques are being introduced. More complex analyses have recently been developed to take account of the visco-elastic nature of bituminous-bound materials (20, 21); however, Thrower (22) has noted that the characteristic elastic wave velocities of road structures are considerably greater than the vehicle speeds. Good agreement has been observed between calculated and measured stresses and strains in road pavement structures by several investigators (23-26) indicating that an elastic analysis is sufficiently precise pending a better understanding of basic material properties.

The basic elastic theory has been employed by the Shell Petroleum Company (27-29) in the presentation of design curves (30) for the structural design of road pavements. Compound layer thicknesses evaluated from these design curves are such that, under the design load, critical stresses and strains do not exceed those of the materials employed. The critical conditions in this case are taken as the maximum tensile strain in the bituminous-bound layers, occurring on the underside of the roadbase, and the vertical stress on the subgrade.

A review of theoretical approaches to pavement analysis and design is presented by Brown and Pell (31) together with a proposed procedure for flexible pavement design.

EQUIVALENCE OF ROAD PAVEMENT MATERIALS

It will be appreciated from the preceding section that, with the trend towards a more rational approach to pavement thickness design, considerable economic advantages are to be achieved with the use of high quality road pavement materials. In reducing layer thickness, the superior load spreading properties of a road material offer a twofold economic saving. First a thinner layer thickness results in a saving in material, or at least enables the reduced thickness to be replaced by a less costly unbound material. Secondly, a reduction in layer thickness may enable the number of passes of the road laying equipment to be reduced thus affecting substantial economics.

Attempts have been made to ascribe equivalence factors to various types of road pavement materials based on the performances of full scale road tests. At the Alconbury Hill road trial (32) it was found that, for sections of similar performance, the 'thickness factors' (T) given by the relationship:-

$$T = 2 \times \text{thickness of bituminous bound layers} + 1 \times \text{thickness of unbound base} + \tfrac{3}{4} \times \text{thickness of sub-base}$$

were in close agreement one with another. This suggests that 1-inch of bituminous material is equivalent to 2-inches of unbound base material and $2\frac{2}{3}$-inches of sub-base material.

Results from the A.A.S.H.O. road test (15,33) suggest that 1-inch of asphaltic concrete surfacing is equivalent to:-

1.3-inches of asphaltic concrete base

1.9-inches of cement-bound base

3.1-inches of unbound granular base

4.6-inches of sandy gravel sub-base

6.3-inches of sandy gravel base

The actual equivalence factors will depend upon the temperature and loading conditions of the bituminous bound layers and their positions within the structure. The above figures represent typical average values.

The advantages of the higher load-spreading properties of bituminous-bound materials have also been exemplified by the theoretical work of Coffman et al (34) and laboratory studies of Monismith et al (35). Both groups of investigators point out that, owing to the complexities of stress distributions and loading conditions, no unique values could be ascribed to various road-making materials. In practical applications, however, the equivalences assessed by full scale road trials may prove a valuable guide to pavement thickness design.

ASSESSMENT OF ROAD PAVEMENT PERFORMANCE

It has been stated earlier that the function of a road pavement is to provide a safe, comfortable, convenient and economic running surface for the passage of fast moving traffic. A road surface is considered structurally unserviceable when its general riding qualities are impaired due to one or a combination of permanent deformation, cracking or surface disintegration.

The traditional method of assessment of road pavement performance is by a panel of trained observers making a visual appraisal of the surface condition and possibly an evaluation of riding quality after driving over the section. Stringent rules for the personal assessment of road pavement performance are laid down by the Canadian Good Roads Association (36) and the Road Research Laboratory (37).

Based upon the assessment of pavement performances of sections of the A.A.S.H.O. road test by a panel of observers, a mathematical expression for "serviceability index" (p) has been established (15) in the form:-

$$p = 5.03 - 1.91 \log (1+SV) - 0.01 \; C+P - 1.38 \; RD^2$$

where SV = slope variance (longtitudinal variation)

RD = rut depth (average depth under 4 ft straight edge)

C = cracking (cracked area/1000 ft^2 of surface)

p = patching (patch area/1000 ft^2 of surface)

Surface irregularities may be measured by means of precise levelling (38) or by continuous records of the deviation of pavement surface evenness from a reference point maintained by a multi-wheel device (39 Other methods are discussed by Hveem (40) and Peattie (41).

Hutchinson (42) considers that not only pavement roughness but also vehicle dynamics and human response should be considered when assessing pavement performance. Results are presented of pavement performance tests based on the ability of a vehicle passenger to trace a triangular waveform on a moving chart.

Serviceability evaluations by a panel of observers have shown (36) that the road surface deflection under a moving wheel load is a significant parameter in predicting the performance of flexible pavements. Deflection measurements are now widely used as an assessment of pavement performance, although several authorities (36, 43, 44) are of the opinion that radius of curvature, rather than vertical deformation, is a better indication of serviceability.

Vertical deformation under a moving wheel load is generally performed by means of the Benkleman Beam, developed during the W.A.S.H.O. road test in 1953 (45). The Benkleman Beam consists essentially of a 12 ft long beam pivoted 8 ft from one end carrying a sensing point in contact with the pavement surface. The other end of the beam carries a vertically mounted dial gauge also in contact with the pavement surface. The dial gauge, or electronic displacement transducer, therefore indicates $\frac{2}{3}$ of the deformation of the pavement surface under the contact point. The vertical deformation of the pavement surface is measured while loaded by the dual wheels of a standard axle load straddling the beam. This standard axle load may be driven off, or onto, the beam under controlled conditions.

A semi-continuous method of vertical deformation measurement has been developed in France and is known as the Lacroix Deflectograph (37). Here two Benkleman Beam-type devices are mounted between the rear and front wheels of a standard rear axle-weight lorry. As the vehicle progresses forward at creep speed, the dual rear wheels astride the beams, the maximum vertical surface deformations are recorded. The beams are then drawn forward and the vehicle again passes over the beams. This

procedure is repeated continuously.

Tests on road structures of similar road pavement materials but different thicknesses have shown a positive relationship between dynamic vertical surface deformation and long term surface deformation such as rutting. This enables a prediction of pavement life to be assessed, although Peattie (46) has shown that this is not applicable to road structures of dissimilar roadbase materials. A knowledge of the structural members of the road pavement is therefore necessary before an assessment of remaining service life can be made. In many cases tolerable deflection criteria is specified as an assessment of potential pavement performance (see references 2 - 8 of reference 18).

ROAD PAVEMENT FAILURES

The methods of assessment of road pavement performance have been outlined in the preceding section. Road pavement failure is generally a progressive state and is usually deemed to have occurred when certain limits of road pavement performance have been exceeded.

The most common form of road failure in this country is that of excessive deformation, generally in the form of longitudinal rutting.

Excessive deformation of a newly constructed road pavement surface may be attributed to excessive settlement of one or more of its component layers, as a result of densification and/or lateral displacement. These effects are the direct consequence of the action of traffic resulting in a greater compactive effort than that achieved during construction. In-situ tests on sub-base materials, using wage propagation techniques, have indicated a threefold increase in the modulus of sand and a twofold increase in the modulus of slag (47) under traffic. Similar, although less marked, trends have been observed in the overlying bituminous-bound layers. Excessive surface deformation in the early life of a flexible road pavement should not, therefore, be regarded as an indication of premature failure.

Excessive surface deformation in a mature road pavement is generally attributed to either the lateral displacement of its layers or a deterioration in the load bearing characteristics of its component materials. Local rutting may result in the development of tensile stresses in excess of the breaking strength of the surfacing material. The ensuing cracking may well constitute a road surface failure in its own right but is nevertheless a direct result of the primary cause of excessive surface deformation. Further, in-situ wave propagation tests have shown that structural deterioration of existing road pavement

materials in this country is confined almost exclusively to the sub-base and subgrade layers (47).

The gap-graded type of bituminous road pavement material prevalent in this country is sufficiently ductile to accommodate surface irregularities in the underlying layers. It is therefore most unlikely that tensile stresses will develop in its lower surface sufficient to cause cracking and subsequent road pavement failure. The densely graded, high stiffness, asphaltic concretes used in the United States of America and elsewhere, however, tend to act as a slab bridging surfacing irregularities in the underlying layers. The constant repetition of loading may therefore result in the initiation of tensile cracking propagating to the surface and leading to distress and loss of serviceability. Further cracking may initiate on or near the surface due to its constant flexure under the action of rolling wheel loads.

Cracking of a road pavement surface may constitute a failure although not necessarily resulting in a deterioration in the structural performance of the system. Such cracking, not associated with excessive surface deformation, is loosely referred to as a "fatigue" phenomena. The term "fatigue" is used in this context to describe that change in condition resulting from the repeated applications of load which would not occur from a single application of load of equal magnitude. This definition covers a very wide range of eventualities and is used in this section purely in deference to practising highway engineers.

Many cases of "alligator" or "chicken wire" cracking in bituminous road pavement surfaces have been cited, especially in the United States of America, and have mainly been attributed by their observers to "fatigue", The possibility of "fatigue" failure in flexible road pavements was postulated by Hveem and Carmany (48) in 1948 and proposed by Hveem (49) as an explanation of surface cracking in the W.A.S.H.O. road test in 1955 (50). Many subsequent cases of "fatigue" failure have been reported both in test tracks and in service road pavements (e.g. 51, 52) and model test tracks (e.g. 53).

It is inappropriate at this juncture to discuss whether or not surface cracking not associated with excessive deformation is entirely a fatigue phenomenon. It should be noted, however, that references have been made to alligator cracking in bituminous road surfaces which have not been ascribed to fatigue (e.g. 43). The application of the term "fatigue" to surface cracking is a matter of conjecture. This is probably the result of a basic misunderstanding of the definition of terms rather than of the performance of the material. This subject will be dealt with in more detail later in this thesis.

The increasing magnitude and intensity of wheel loads in this country is the potential cause of a considerable number of road pavement failures due to rutting. To overcome this problem the tendency is to adopt a more continuously-graded type of bituminous material for road surfacings. For the reasons discussed above, the adoption of a high stiffness, continuously-graded, asphalt surfacing in this country, while reducing rutting, is likely to create a further problem of surface cracking. The superior load-spreading properties of dense, bound, road-base materials is now universally accepted and their adoption in this country will also provide a less deformable base for the road surfacing. Such roadbases are essential if asphaltic concrete-type surfacing materials are to be used without cracking.

Surface cracking and the degredation of the structural properties of flexible road pavements is at present a problem in the United States of America. It is likely to become a real problem in Great Britain and consequently the behaviour of flexible road surfacing and base materials is the subject of much speculation and investigation.

LABORATORY STUDIES

The structural performance of a road pavement is a function not only of the properties and thicknesses of the component layers but also upon such factors as pavement width and shoulder support, subgrade drainage, environmental conditions such as ambient temperature, rainfall and level of water table, traffic volume and composition, pavement age, previous and potential traffic history, and other effects such as surface treatments and traffic behaviour. The analysis of existing road pavement behaviour is therefore extremely complex and a basic understanding and prediction of structural performance is generally based upon the results of laboratory tests performed under idealised conditions. Practical difficulties preclude the construction of a full scale road pavement under idealised loading and climatic conditions. Laboratory studies are therefore confined to scale model structures or fundamental tests on the component materials.

The rational design of road pavement structures demands a thorough understanding of the behaviour of its component materials and the stress conditions to which they are subjected. Due to the complexity of the stress distribution within a road structure fundamental tests are generally performed on specimens of road pavement materials subjected to simple uniaxial, biaxial or triaxial loading under carefully controlled conditions. These properties are then employed in the theoretical analysis and the results compared with known pavement behaviour.

One of the main difficulties in the planning of laboratory tests on road pavement materials is the selection of appropriate specimen dimensions and loading conditions. A laboratory specimen is considered to represent an element in the structure and ideally should be stressed accordingly. Since the stresses and strains in one layer of the structure vary continuously with depth and position relative to load, the element should be sufficiently small such that changes in conditions throughout its volume are negligible. Alternatively the specimen should be loaded in a manner identical to that in practice. Since the load pattern depends upon the material under investigation it cannot be predicted. Further, if the load pattern were estimated, the practical difficulties of applying it to a laboratory specimen will be readily appreciated.

The maximum size of aggregate used in road pavement construction ranges from $\frac{3}{4}$ to $1\frac{1}{2}$-inches depending upon the material and its position in the structure. A laboratory specimen should ideally possess minimum dimensions in excess of four times the maximum particle size in order that the behaviour of the material as a whole might be assessed. Clearly this is many orders of magnitude greater than the element previously considered over which changes in loading conditions may be considered negligible. (No advantage is to be gained from the use of scaled down mixtures since the ideal element is a fixed proportion of the maximum particle size.) Laboratory specimens are therefore, of necessity, far larger than would be desired and it is assumed that their behaviour is in some way indicative of the behaviour of the finer matrix in the ideal element.

The results of laboratory tests on road pavement materials have been used in theoretical analyses of pavement structures with a reasonable degree of correlation. Reference to session V and VI of the Second International Conference on the Structural Design of Asphalt Pavements will show that measured and calculated strains within a factor of two have been obtained and are generally considered satisfactory. These results have been achieved, however, mainly on the assumption that the materials are elastic and no account is generally taken of the stress dependency of the materials considered. With new theoretical methods, such as finite element techniques, a greater knowledge of the behaviour of road pavement materials will enable better correlation between theory and practice to be obtained. The validity of new theoretical analyses can only be established with data pertaining to the characteristics of road pavement materials under load. A better understanding of pavement material behaviour is therefore essential if advances in the rational approach to the structural design of road pavements are to be achieved.

BACKGROUND TO WORK IN THESIS

Over the past two decades an ever increasing interest has been shown in the behaviour of flexible road pavements under repeated applications of load. Early work by Nijboer and Van der Poel, published in 1952 (54-56), confirmed suggestions that bitumen-bound road pavement materials show signs of distress after a number of repeated applications of load. Since then a multiplicity of test methods and results have been reported ranging from studies on simple uniaxially loaded cylinder to model road structures.

Much investigation over the past 15 years has been carried out under the auspices of Monismith and Pell, the former at the University of California and the latter at the University of Nottingham. Both investigators are performing studies into both material behaviour and pavement design each with an emphasis on the materials, constructions and problems of his particular country.

Early work by Pell was concentrated on road surfacing materials being formed into necked, circular cross-section specimens, tested in stress-controlled rotating bending. A unique relationship was found between initial strain and fracture life and consequently, a strain-controlled torsion test was developed with identically shaped specimens. Further stress-controlled testing, by later investigators, was performed on wearing course and base-course materials necessitating a scaled up version of the original necked specimen to accommodate the larger maximum aggregate size. An extensive test programme has yielded much information about the effect of testing and mixture variables on fracture life.

The testing of roadbase materials, with which this thesis is concerned, necessitated a new form of test method. It was felt that the greater maximum aggregate size and the more open textured nature of roadbase materials would result in high voids on the surface of the conventional necked specimens. Since surface stresses are high, it was considered likely that the inherent local weaknesses would lead to premature failure. Further, the testing of a larger necked specimen would present considerable practical difficulties. It was, therefore, decided to attempt uniaxial reversed stress testing of cylinders.

A small temperature controlled laboratory was made available for this research project. Also, a 10,000 lb. capacity, reversed stress, Instron testing machine was ordered for testing purposes, prior to the date on which the author took up his duties. This machine has been modified and used throughout the test period to study the behaviour of roadbase materials under repeated loading.

CHAPTER TWO

WORK IN THESIS

INTRODUCTION

The work reported in this thesis is concerned with the behaviour of typical British roadbase materials under repeated applications of load. A split console, 10,000 lb. reversed stress Instron testing machine was provided for this purpose, the testing frame being situated in a small temperature controlled laboratory with a working temperature range of $-10^{o}C$ to $+40^{o}C$.

SCOPE OF INVESTIGATION

A method of special preparation, void analysis and mounting into specially designed end caps has been developed and the Instron testing machine has been modified to perform stress or strain-controlled testing at a pre-selected frequency. Rigid and adjustable mountings have been designed to secure specimens into the testing machine. Mounting devices for specimen deformation tranducers have also been developed, together with associated electronic equipment.

Tests have been performed on two types of dense bitumen macadam, dense tar macadam, hot rolled asphalt and dry lean concrete roadbase materials. Stiffness and service life relationships have been established for the bituminous materials covering a wide range of temperatures and loading levels. Stiffness and service life relationships have also been established for dry lean concrete at a single temperature.

Standard tests have been performed on the bituminous binders both as received and after heating prior to mixing. These tests have also been performed on the bitumen binders recovered, by an outside organisation, from compacted specimens.

A viscometer has been developed to measure the viscosities of the bituminous binders at the temperatures at which material properties were assessed. These values have been used to evaluate theoretical mixture stiffness values to compare with practical results and also to study the influence of the binder in mixture properties. A standard shear vane apparatus has been modified for a preliminary and brief investigation into the behaviour of bituminous binders under constant shear.

The results of material stiffnesses have been used in the Shell Bistro computer programme, for the stress distributions in layered systems,

in order to assess the (theoretical) effect of roadbase material on road pavement performance under extremes of temperature and frequency of loading,

Experimental results from the bituminous materials, together with limited work on binder behaviour, have led to the presentation of a possible explanation of material behaviour under repeated applications of load. The behaviour of dry lean concrete has also been considered. Stiffness results for all materials have been discussed in the light of accepted rheological phenomena and results of previous investigators. Finally, failure mechanisms have been discussed, both for the materials and testing conditions considered and for in-service flexible road pavement structures.

FORM OF THESIS

In the presentation of conclusions drawn from the experimental results submitted in this thesis, references have been made to the chemical structure and rheological properties of the bituminous binders and mixtures considered. Reference is also made to the test methods and results of previous investigators.

Rheology is now a well established science and numerous textbooks are available on the subject. Whereas a detailed study of rheology is well outside the scope of this thesis, it is felt that a brief background might be found useful when considering the implications of the experimental results discussed. A succinct chapter on basic rheology is therefore included which is deemed pertinent to the contents of this thesis. This chapter is prefaced by notes on the chemical properties of tars and bitumens.

A review of previous work is presented to illustrate the present state of knowledge on the behaviour of bound road pavement materials under dynamic loading, and the test methods from which this knowledge has been derived.

Details are also presented of the development of apparatus used in this investigation, the experimental procedures adopted and the experimental techniques evolved.

CHAPTER THREE

PHYSICAL CHEMISTRY OF BITUMINOUS AND CEMENTITIOUS BINDERS.

INTRODUCTION

Reference will be made in subsequent chapters to certain aspects of bituminous and cementitious binders including standard tests and their physio-chemical composition and structure. The tests referred to are included in all standard text books on the subject and are not described in this thesis. Whereas the structure of bituminous and cementitious binders is also adequately described elsewhere, it is felt desirable to remind the reader of those aspects considered relevant to this thesis.

TAR

Tar is a dark brown to black, aromatic, amorphous, thermoplastic substance derived from carbonized organic materials or organic materials which are destructively distilled in the absence of air. It consists essentially of hydrocarbons with small quantities of hydroxy compounds, paraffinic hydrocarbons and heterocyclic compounds. It has a high molecular weight range and the proportion of certain molecular weight ranges, as determined by solvent fractionisation, is used to define the chemical composition of tar. Dickinson (57) utilizes n-hexane, benzene and pyridine as solvents to describe the tar by five fractions.

Dickinson (57) has supported the postulate of Nellensteyn (58,59) that tar may be considered as a colloidal structure. Wood and Philips (60) have expressed doubts regarding the validity of the colloidal hypothesis and suggest that tar should be considered as a supercooled multicomponent liquid.

The majority of road tars are predominantly viscous in nature and are classified by means of one or two standard tests, the standard tar viscometer and the equiviscous temperature viscometer. These tests are adequately described, among others, in references 69 and 70.

BITUMEN

Bitumen is a black to dark brown, amorphous, aliphatic, thermoplastic substance derived from petroleum oil residue. It may be manufactured by distillation, precipitation by solvents or oxidation, or found in natural occurrences. It is completely soluble in carbon

disulphide and consists of hydrocarbons and hydrocarbon compounds with a wide range of molecular weights. By means of solvent fractionisation using petroleum ether or n-heptane, bitumen is divided into two distinct components the properties of which are used in its classification.

Nellensteyn (62) has put forward the hypothesis that, like tar, bitumen may be considered to be a colloidal structure and he has been supported by Pfeiffer and Van Doormaal (63) although disputed by Mack (64). It has subsequently been claimed proven by Pfeiffer and Saal (65) and utilized by Pfeiffer (66) and Labout (67) in their analysis of bitumen types.

On the basis of a colloidal hypothesis the precipitate of high molecular weight disperse phase (micelles) is defined as asphaltenes and the continuous phase as maltenes. Saal and Labout (61) have suggested that the miceller disperse phase consists not only of asphaltenes but also a proportion of maltenes depending upon the temperature, the remaining maltenes forming the viscous Newtonian-type continuous phase. The distinction between asphaltenes and maltenes is dependent upon the nature of the solvent used and can therefore be subdivided into various molecular weight groups by the use of a variety of solvents. Labout (67) states that if the micelles are well peptized (they behave as independent entities with virtually no mutual attraction, therefore with only hydro dynamic interaction) then the bitumen will behave as a sol. If the micelles are partly flocculated (two or more linked together) the bitumen will behave as a gel. Saal and Labout (68) have shown that free micelles or isolated small agglomerates of micelles, considered as free micelles, may be present in gel-type bitumens as well as sol-type bitumens. For bitumens with extremely low asphaltene content, the colloidal structure is almost exclusively that of the continuous (maltene) phase and behaves as a Newtonian-type viscous liquid. The elastic properties of a bitumen are attributed to the disperse phase and therefore become more dominant as asphaltene content increases.

Bitumens are generally classified in one of three groups: pitch-type (low asphaltene content, predominently viscous) sol-type (medium asphaltene content, visco-elastic) and gel-type (high asphaltene content, predominently elastic).

It will be noticed that a far greater emphasis is placed upon the categorization of bitumen types than of tar. Apart from its wider application throughout the world, after processing, bitumen, unlike tar, exhibits certain properties peculiar to its source and method of process.

The two standard tests for bitumens are the penetration test and the ring and ball softening point test. These are carried out in accordance with B.S.3235 (71) and described in many other sources including reference 70.

Bitumens of different type (i.e. source and/or process) can be detected when differences between the ring and ball softening point temperatures and that at a standard penetration are at variance. For bitumens of similar type the relative hardnesses are indicated by the temperature differences between the ring and ball softening points. The type of bitumen is defined by its penetration index, evolved by Pfeiffer and Van Doormaal (63), which describes the difference between the ring and ball softening point temperature and the standard penetration temperature by a single parameter. The nomograph for the determination of penetration index is reproduced in Figure 7. Penetration indices range in practice from -2.5 to -2 for low asphaltene content, pitch-type bitumens, with small difference between ring and ball softening point temperature and standard penetration temperature; from -2 to +2 for sol-type bitumens of medium asphaltene content and temperature difference, and from +2 to +6 for high asphaltene content gel-type bitumens exhibiting large temperature differences.

CEMENT PASTE

Cement paste consists of dry cement powder which is activated by the addition of water during mixing immediately prior to use. Cement used in flexible road pavement construction is produced by the intimate association of materials containing calcium carbonate (limestone or chalk) with materials containing silica, alumina, and ferric oxide (clay or shale). These constituents are mixed together in water to form a slurry which is heated in a kiln at high temperature. The resulting cement clinker is ground in the presence of a small quantity of gypsum (to retard setting) to form cement powder. Variations in cement type are effected by altering the proportions of raw materials, the kiln temperature and/or the fineness of the grinding. Portland cement consists of tri calcium silicate, responsible for most of the early strength; di calcium silicate, responsible for mature strength; tri calcium aluminate, responsible for some of the very early strength; and tetra calcium alumino ferrite which is relatively inactive. This is the Bogue composition thought to be the conversion of anhydrous calcium silicates into an hydrated form.

When water is added to dry cement powder the process of hydration is initiated. Freyssinet (163) has stated that, as the cement powder is dissolved by the water, saline ions are liberated. These saline ions combine with water to form hydrated crystals which build up into a close nodular crystalline structure with an interstice of capillary and gel voids partially filled with water. The structure offers increasing resistance to the movement of free water until further crystal growth is inhibited.

It is often found that, whereas there is ample free water available, a crystalline crust may form around certain larger cement particles inhibiting the ingress of water and resulting in an unhydrated nucleus. Reneus (160) has described cement paste as a mixture of unhydrated cement particles and a cement gel, the latter comprising crystals of colloidal size and water. The view that the gel crystals are of colloidal dimensions has also been expressed by Powers and Brownyard (161) and Lea (162).

CHAPTER FOUR

RHEOLOGICAL BEHAVIOUR OF BITUMINOUS MATERIALS

INTRODUCTION

Rheology is the study of deformation and flow of matter. Much theory of rheology deals with idealised cases based on first order differential equations, on the assumption that constants of these equations do not vary with recognised variables. Rheology is generally concerned with reversible phenomena but in practice non-reversibility is often found where properties exhibit changes with time or deformation.

In this thesis it is intended to deal only with the qualitative aspect of rheology as a means of explaining experimental phenomena, a quantitative approach would demand a large amount of work both theoretical and experimental, beyond the terms of reference of this thesis. Where relevant, recommendations are made as to how qualitative behaviour may be quantified.

The behaviour of idealized bodies may be described by three basic components, elasticity, viscosity and plasticity. The elastic component is that which stores energy and determines deformation. The viscous component is that which dissipates energy and determines rate of deformation. The plastic component is essentially an elastic component with a yield value above which no energy is stored and the body exhibits permanent deformation or flow. These three basic elements may be described in a number of ways, the two most common being the mechanical and the electrical analagies. In mechanical terms the elastic element, storing energy, is represented by a spring, the viscous element, dissipating energy, by a dashpot and the plastic element, limiting stored energy, by a friction model. In electrical terms resistors, capacitors and inductores are used to represent energy storing and dissipating elements, their configuration depending on whether voltage or current is used to represent overall rheological behaviour, The mechanical elements subsequently used are shown in Figure 2a.

By definition, the elastic (solid) element is considered linear in that it obeys Hooke's law, viz. shear stress is proportional to shear strain, or, $G = \frac{\tau}{\gamma}$ where "G" is the constant of elastic shear modulus, and "τ" the shear stress at a shear strain "γ". The viscous (liquid) element obeys Newton's law, viz. shear stress is proportional to rate of shear

strain, or $\tau = \eta \dot{\gamma}$ where "η" is the constant of coefficient of viscosity, and "τ" the shear stress resulting from a rate of shear strain "$\dot{\gamma}$". As described previously the plastic element is defined as elastic up to a limiting (yield) stress above which the stress deformation is infinite.

These three basic elements may be arranged in various combinations to form models representing the behaviour of complex bodies. Those bodies exhibiting both elastic (time-independent) and viscous (time-dependent) properties are termed visco-elastic bodies.

Figure 2b shows the three simplest forms of visco-elastic behaviour. The Kelvin (or Voigt) model represents a visco-elastic solid exhibiting retarded elasticity and recoverable deformation, defined as firmo-viscous behaviour. The Maxwell model represents a visco-elastic liquid exhibiting rate-and time-dependent elasticity and non-recoverable deformation and is defined as elastico-viscous. The Bingham model, representing a plastic liquid is defined as plastico-viscous.

A large number of these models may further be arranged in various combinations to describe the behaviour of highly complex visco-elastic bodies. Whereas complex models lose their illustrative value, they are useful in assisting in the building up of first order differential equations to describe the behaviour of a visco-elastic body.

It cannot be over emphasised at this stage that the function of these mechanical analagies is purely illustrative and that the various elements are in no way intended to represent any chemical or physical component of the body whose behaviour they describe.

BITUMINOUS BINDERS AT CONSTANT TEMPERATURE

The complex modulus, or stiffness, of a bituminous binder may be determined under three quite distinct conditions of loading. First, under the application of a constant stress the resulting deformation pattern enables stiffness to be determined after various intervals of time. Here, stiffness is defined as the ratio of applied stress to strain resulting after the time of loading considered. Secondly, under the application of a constant rate of deformation the resulting load pattern enables stiffness to be determined after any time of loading as before. Thirdly, for continuous dynamic sinusoidal loading stiffness may be determined from the ratio of stress range to strain range for various frequencies.

In his work on the stiffness properties of bitumens, Van der Poel (72) has shown that at any particular time of loading the ratio of maximum

to minimum stiffness, as determined by each of the conditions of loading described above, is less than two. Van der Poel suggests that, for practical purposes, a graphical representation of bitumen stiffness may be built up from the results of tests carried out using any of the three loading methods described. Heukelom (73) has endorsed Van der Poel's assumption of continuity considering a factor of 2 in bitumen stiffness to be small over a range of bitumen stiffness of 1.10^{10}. Monismith et al (74), reviewing results of stiffness measurement tests using various loading methods, consider the static creep test to be the most simple and reliable loading method available.

Saal (75) has suggested that the rheological behaviour of all bitumens may be illustrated (although not defined) by the simple Burger model shown in Figure 3b. The log. stiffness/log. time relationship of a Burger model, representing the behaviour of an elastico-viscous binder, is bounded by elastic and viscous asymptotes similar to a Maxwell model (see Appendix 1), the shape of the visco-elastic "transition" between the "elastic" and " viscous" portions of the stiffness/time relationship being dependent upon the model parameters, As elastic recovery of a binder becomes complete so the dominance of the series dashpot is reduced until a Burger model with no series dashpot, representing the behaviour of a binder exhibiting complete elastic recovery at the cessation of loading, is bounded by two elastic asymptotes.

Saal and Labout (61) have shown that at a constant temperature the pitch-, sol-and gel-type bitumens referred to in Chapter 3 have quite different rheological properties. Reference to Figure 4 will show that the rheological behaviour of bitumen "a", like the majority of tars, approximates closely to that of an ideal Maxwell liquid. This bitumen "a" is typical of those of the pitch-type with low asphaltene content and a penetration index of less than -2. Properties of bitumens within this group range from almost purely elastic to almost purely viscous within a relatively short range of loading time, with little evidence of any retarded elasticity. There is no partial recovery after removal of load and therefore the "transition" between "elastic" and "viscous" behaviour is acute.

Bitumen "b" is typical of the sol-type group of bitumens with penetration indices ranging from -2 to +2. Bitumens within this group exhibit a high degree of retarded elasticity after removal of load and their rheological behaviour may be illustrated by the Burger model.

As the penetration index increases the viscous element of the Maxwell portion becomes less dominant and stiffness becomes less sensitive to changes in time of loading.

Gel-type bitumens are typified by bitumen "c". Bitumens in this group have high asphaltene contents and penetration indices in excess of +2. Changes in time of loading have relatively small effect in changes in stiffness and the high degree of elastic recovery indicates the relative insignificance of the series dashpot in the Burger model analogy of rheological behaviour.

Saal and Labout have attributed these rheological behaviours directly to the asphaltene content of the bitumens and the colloidal structure (if any) it forms. Clearly there are not any distinct divisions between these three groups of bitumens and it is possible that certain external factors may change the structure of a particular bitumen and hence its classification group.

As the asphaltene content of a bitumen is increased the rheological behaviour is less like that of a Maxwell liquid and several investigators have attempted to represent the behaviour of both binders by means of more complex rheological models. Monismith and Secor (74,76,77) have found that whereas a 3- and 4- model system may represent the rheological behaviour of the material during loading, poor agreement is found during relaxation. Papizan (78) has found more favourable agreement with overall behaviour using a 5-model system but at this stage the mathematics becomes rather complex.

BITUMINOUS BINDERS AT VARIOUS TEMPERATURES

In common with all linear polymers (79,80) all the relaxation times of a bituminous binder depend identically upon temperature and the effect of temperature on stiffness may be represented by a shift in the time scale of the log. stiffness/log. time relationship (73,71,82). The temperature sensitivity is defined by the bulk modulus of the binder which is in turn dependent upon its colloidal nature. Temperature sensitivity is reduced as bitumen penetration index is increased and therefore, the sharper the transition of the log stiffness/log time curve, the greater is the temperature shift factor.

Van der Poel (83) has produced a nomograph for the determination of the stiffness of bitumen based on the results of many tests. From this nomograph, reproduced in Figure 8, the stiffness of a bitumen may be estimated from a knowledge of its type (defined by its penetration index),

its hardness (defined by the difference between the ring and ball softening point temperature and the temperature considered) and the time of loading. Van der Poel has claimed an accuracy in nomograph stiffness of within a factor of two and has found that all bitumens, irrespective of type and hardness, approach an elastic asymptote stiffness of 3.10^9 N/M^2 ($4.35.10^5$ lb/in^2). An equivalent value for tar has been found elsewhere to approximate to 4.10^9 N/M^2 ($5.8.10^5$ lb/in^2). These elastic asymptote values are independent of temperature in accordance with those of rigid elastic bodies which alter by only a few hundredths of a per cent per degree centigrade change in temperature (84 p.11). The dissimilarity in the behaviour of bitumen to that of rubberlike solids is exemplified by the latter's greater temperature sensitivity at short loading times (86).

Heukelom (73) has expressed doubts regarding the accuracy of Van der Poel's nomograph for low penetration index bitumens and Heukelom and Klomp (86) have developed a modified nomograph reproduced in Figure 9.

BITUMINOUS COMPOSITIONS

The rheological properties of a bituminous composition are to a great extent dependent upon the rheological properties of the binder. Thrower (87) has shown that for a tar-bound road surfacing material under constant load its change in rate of deformation with change in temperature is identical to that of the binder alone. The same effect has been found to apply to bitumen binders on which a greater amount of work has been performed.

In 1906 Einstein (88) found that for very dilute suspensions of non-interacting small rigid spheres the viscosity of the solution is given by:-

$\eta_s = \eta (1 + 2.5 \phi)$ where η_s = viscosity of solution

η = viscosity of continuous phase

ϕ = volume concentration of disperse phase.

Arnstein and Reiner (89) have since found that cement mortars of volume concentrations of up to 60% obey this law, although this high concentration may be offset by the high viscosity of the material ($10^{17} - 10^{18}$ poise).

Roscoe (90) has suggested that for high volume concentrations of uniformly sized particles:-

$\eta_s = \eta (1 - 1.35 \phi)^{-2.5}$ and for particles of diverse size:-

$\eta_s = \eta (1 - \phi)^{-2.5}$.

Due to the large number of variables in bituminous materials it is generally found preferable to estimate stiffness from simple relationships subject to a certain degree of error rather than to analyse each variable and compute the resulting stiffness from the contribution of each to the whole.

Van der Poel has complemented his nomograph for the determination of bitumen stiffness with a further nomograph to determine the stiffness of a bitumen-aggregate composition (91), reproduced in Figure 10. The mix factor is dependent upon the aggregate concentration and is applicable to densely graded aggregates resulting in material voids of less than 3%.

Heukelom and Klomp (86) have proposed:-

$$S_{mix} = S_{bit}\left(1+\frac{2.5}{n}\cdot\frac{Cv}{1-Cv}\right)^{n}$$

where S_{mix} = stiffness of mixture

S_{bit} = stiffness of bitumen

C_v = volume in concentration of aggregate.

$$n = 0.83 \log_{10}\left(\frac{4.10^5}{S_{bit}}\right)$$

(where S_{bit} is in Kg/cm^2)

The results of this relationship shown in Figure 11 have been supported by Monismith et al (74) although they report lower than predicted stiffnesses which they attributed to high void contents. Van Draat and Sommer (209) have suggested that for materials with high void contents in excess of 3% the C_v term should be replaced by the modified form:-

$$C_v{}^1 = \frac{C_v}{1+(V_v-0.03)}$$

where V_v = proportion by volume of voids in mixture.

It should be emphasised that in the determination of material stiffness the properties of the recovered binder should be used in the determination of binder stiffness. This practice assumes that the rheological properties of a heated binder are similar to those of an unheated binder of equivalent type and hardness.

NON-LINEAR BEHAVIOUR OF BITUMINOUS MATERIALS

The basic rheology described at the beginning of this chapter and subsequent comments on the behaviour of bituminous binders and mixtures have been based on the assumption that the visco-elastic behaviour of the materials is linear. A linear material is defined as one in which the ratio of stress range to strain range is constant. The material may therefore be defined by a constant dynamic modulus, stiffness in the case of bituminous materials, at the conditions prevailing. Non-linearity of a visco-elastic model may be ascribed to non-linearity of one or more of

its components. The causes of non-linearity may therefore be considered in terms of each element.

The relationship between stress and strain for apparently rigid materials is generally linear up to the yield stress which occurs at a relatively low strain. Visco-elastic solids or liquids exhibit greater flow before rupture and the relationship is generally non-linear at higher strains. Van Wazer et al (84) have stated that, regardless of how complicated the function relating the viscous and elastic deformation to the applied stress, the relationship between stress and strain is approximately linear at small strains. Macdonald et al (100) have shown that for large strains in polymers, viscosity and shear modulus both decrease with increasing shear strain. The change in shear modulus, and hence elastic modulus, is reported to decrease proportionally more than the viscosity. Little information is available on the determination of yield stresses in bituminous binders but the constant elastic asymptote value of Van der Poel (83) and Henkelom and Klomp (86) suggest that elastic yield stresses are not significant under practical loading conditions, any effect being obscured by non-linear viscous behaviour.

Non-linearity of the viscous component of a visco-elastic material may result from either, or both, of two quite independent effects, non-Newtonian behaviour due to stress-dependence on rate of shear strain, or time-dependence at constant strain rate.

Stress-dependence - A Newtonian liquid is linear insomuch as shear stress is proportional to rate of shear strain. When log. shear stress is plotted against log shear rate a linear relationship with slope "n" denotes a power low liquid, i.e. $\tau = \tau_1 \left(\frac{\dot{\gamma}}{\dot{\gamma}_1}\right)^n$ or $\eta_s = \eta_1 \dot{\gamma}^{n-1}$ where suffix 1 represents a reference condition $\dot{\gamma} = 1$, and η_s is the structural viscosity at shear rate $\dot{\gamma}$. (The structural viscosity is the instantaneous viscosity at a particular stress at shear strain rate whilst the apparent viscosity " η_a " is the secant modulus viscosity. It can be shown that $\eta_s = \eta_a \cdot n$). Non-Newtonian liquids which exhibit a less than linear increase in shear stress with unit increase in shear rate ($n<1$) are termed pseudoplastics and those exhibiting a greater than linear increase ($n>1$) are termed dilatent. These non-linear effects are illustrated in Figure 6b.

Many authors indicate that pseudoplastic materials are far more common than dilatent materials. Pseudoplasticity has been shown by Coombes and Traxler (93) when illustrating the non-Newtonian characteristics of bitumens. Pell and McCarthy (94) have shown stress-dependent non-linearity in bitumen tested in torsional strain and stress-dependence is common

in bituminous mixtures. Lee et al (95) have related the plastic flow index ($\equiv \frac{1}{n} > 1$) to temperature for a range of bitumens as shown in Figure 5. No literature has been found on the stress-dependent properties of tar but bitumen may certainly be taken as a pseudoplastic material.

Explaining pseudoplasticity, Eisenschitz (96) has suggested that at low strains (hence low stresses) stress relaxation cannot occur at a rate comparable with the rate of deformation, whereas at higher strains (hence higher stresses) the stress relaxes faster resulting in a reduced viscosity. Scott Blair (97, p93) observes that if shearing causes a strain either in the compressible dispersed particles of a suspension or disperse phase of a colloidal system such that rise in entropy is involved, the viscosity will fall with increasing stress. Wilkinson (98) suggests that with increasing rate of shear strain asymetric particles or molecules will become progressively aligned and the resulting viscosity will drop. This trend will continue until all the particles or molecules are aligned when Newtonian flow will occur. The logical progression from Wilkinson's theory is that the larger the molecular (polymer) chain, the greater the degree of non-Newtonian behaviour. This is supported by work done by Edelmann (99) who has related the degree of non-Newtonian behaviour to the molecular weight of the macro molecules defining the dimensions of the molecular chains. Van Wazer (84, p22) has stated that there is a minimum shear stress below which even the largest known polymer chain liquids behave as Newtonian liquids. This minimum stress of some 1.10^3 dynes/cm^2 ($1.45.10^{-2}$ lb/in^2) is that required to disentangle the polymer chains sufficiently to give a configuration appreciably different to that of the unsheared state.

Bitumens may well exhibit a yield stress, hence being defined as a Bingham plastic. This yield stress is attributed (84) to the interference between particles of the disperse phase and consequently single phase liquids do not possess a yield value. This yield value may well coincide with the onset of non-Newtonian behaviour since Thrower (87) has suggested that bitumens may possess a yield stress less than 5.10^3 dynes/cm^2 ($7.25.10^{-2}$ lb/in^2).

Dilatency has been attributed by Oscar Reynolds to the dense packing characteristics of the disperse phase in high disperse phase content liquids. Under the action of increasing shear rate greater resistance to movement is offered by the disperse phase particles which must "dilate" before flow can occur. As "dilation" of these particles continues the "void content"

increases and the volume of free lubricant offered by the continuous phase is reduced, hence the greater resistance to flow. The term dilatent therefore refers to the action of the particles rather than to the behaviour of the liquid as a whole. This explanation is the subject of much controversy but few more feasible suggestions have yet been made.

Time-dependence - Stress-dependent type non-Newtonian viscous liquids exhibit a viscosity dependent upon the shear stress, or rate of shear strain, prevailing. Whatever this value of viscosity it will remain constant as long as the shear stress, or rate of shear strain, remains constant.

Some liquids, however, exhibit a change in viscosity under the sustained application of constant rate of shear, or constant stress, and are termed time-dependent liquids. It will be appreciated that in this case constant rate of shear strain and constant shear stress will result in differing changes in viscosity over equal periods of time.

Liquids which exhibit an increase in viscosity with time are classified as rheopectic liquids and those which exhibit a decrease in viscosity with time are classified as thixotropic liquids as shown in Figure 6c.

Thrower (87) has reported that thixotropy is evident in sol-type and gel-type bitumens, the effect becoming more conspicuous as asphaltene content is increased. Saal and Labout (68) and Pfeiffer and Saal (65) have shown thixotropy in gel-type bitumens at various shear stresses. Thixotropy has also been shown by Coombes and Traxler (93) in air-blown Venezuelan bitumen (gel-type). Saal and Labout (61) have attributed a slope of greater than unity in the logarithmic plot of stiffness against time for pure bitumen, to thixotropy and hence stated that this gradual collapse of structure is peculiar to gel-type bitumens.

Wilkinson (98) has stated that if a thixotropic material is continuously sheared at a constant rate of shear after a period of rest, the structure will be progressively broken down and the apparent viscosity decrease with time. This theory is also put forward for bitumens by Saal and Labout (61,68). The rate of breakdown of structure will be dependent upon the number of linkages available for breaking and must therefore decrease with time. The simultaneous reformation of structure will increase as the number of new structural linkages is increased. Eventually a state of dynamic equilibrim is reached where the rate of building of linkages is equal to the rate of breakdown. This equilibrium position depends on the rate of shear strain and moves towards greater breakdown

as the rate increases.

Scott Blair (97,p.90) has stated that thixotropy is "clearly" due to the disorientation of suspended particles during shear and their subsequent reorientation on resting.

A thixotropic material has been defined by Weltman (101) as being one which undergoes a gel-sol-gel transformation upon agitation and subsequent rest. Traxler (102) has suggested, however, that in the case of bitumen it is not necessary for the gel structure to be completely destroyed. A partial breakdown of structure followed by recovery is evidence of thixotropy.

Thixotropy is the process of a breakdown in structure but Scott Blair (97) has qualified this by stating that the process must be completely reversible. Further, Scott-Blair states that thixotropy is a truly reversible gel-sol transformation, in which the "set" (gel) form should possess infinite viscosity and finite modulus (i.e. elastic) and the sol form finite (not necessarily constant) viscosity and no appreciable yield value. Materials which do not satisfy Scott-Blair's definition are defined by Pryce-Jones (103) as "false-bodies." Here the material undergoes a partial dispersion of its gel-type structure under the influence of shear and the reformation of its gel structure on the removal of the shear. The yield value of a false body is reduced under the action of shear and is recoverable.

If a time dependent material is sheared at a constant rate in a concentric cylinder type apparatus and the shear stopped, a drop off in torque will result, the gel structure of Scott-Blair's thixotropic material (by definition) having been transformed to a sol. Since this material is a true viscous liquid when the shear action is stopped, the drop off in torque will be complete since the viscous liquid is incapable of storing energy. Thus on reformation of the original gel structure, no torque remains. Conversely, a false body will store a certain amount of energy thus exhibiting a finite torque on the reformation of the original structure. This simple test may be applied to a bitumen to assess whether it is thixotropic or a false body. However, the shear thinning effect of time dependent materials is, for the purpose of this thesis, described as thixotropy. A complete gel-sol-gel transformation is not an essential part of the definition used hereafter.

A simple theoretical analysis of non-linear effects on the stiffness properties of bituminous binders and mixtures has been evolved for the purposes of explaining experimental results reported later in this Thesis. Due to the complexity of material models and the lack of access to suitable apparatus this theoretical approach cannot be quantified and is not, therefore, presented. However, recommendations are made for ways in which certain premises may be quantified later in this Thesis.

STIFFNESS VARIATION IN TENSION AND COMPRESSION

In comments on the linear and non-linear behaviour of binders made hitherto it has been assumed that the particular aspect of behaviour discussed has been independent of direction of deformation.

Lodge (104) has stated that the behaviour of a rubber-like liquid in steady elongation differs from its behaviour in steady shear. Lodge (p. 114) shows that in steady elongation, if $\dot{\varepsilon} < \frac{1}{2\tau}$,

$$\lambda = 3\eta\,(1-2\dot{\varepsilon}\tau)^{-1}(1+\dot{\varepsilon}\tau)^{-1}$$

where λ = elongational viscosity
η = viscosity
$\dot{\varepsilon}$ = rate of elongation
τ = relaxation time.

If $\dot{\varepsilon} \ll \frac{1}{2\tau}$ then $\lambda \to 3\eta$ (Trouten's coefficient of viscous traction). However, as $\dot{\varepsilon} \to \frac{1}{2\tau}$, $\lambda \to \infty$. Thus the elongational viscosity (λ) increases rapidly with increasing rate of elongation ($\dot{\varepsilon}$), whereas for a Newtonian liquid the viscosity is independent of rate of shear. Lodge attributes this difference in behaviour between elongation and shear to the fact that in constant elongation the three principle axes are constant whereas in steady shear only one principle axis remains constant.

Applying the relationship of Lodge, as well as that of others, Wanket (105) has replaced the positive rate of elongation for tension by a negative term for compression. Hence we have

$$\lambda_T = 3\eta\,(1-2\dot{\varepsilon}\tau)^{-1}(1+\dot{\varepsilon}\tau)^{-1}$$
$$\lambda_c = 3\eta\,(1+2\dot{\varepsilon}\tau)^{-1}(1-\dot{\varepsilon}\tau)^{-1}$$

where suffix "T" represents tensile deformation and "c" represent compressive deformation. Therefore if $\dot{\varepsilon} \ll \frac{1}{2\tau}$ then $\lambda_T \to 3\eta$ & $\lambda_c \to 3\eta$. However, as $\dot{\varepsilon} \to \frac{1}{2\tau}$, $\lambda_T \to \infty$ but $\lambda_c \to 3\eta$. Wanket claims that the behaviour in compression is not, therefore, the same as the behaviour in tension, the tensile viscosity being greater than the compressive viscosity. The difference has been attributed to the fact that in steady elongational flow the long-chain molecules are progressively aligned along the axis of flow whereas in steady compressional flow the molecules are aligned in planes

perpendicular to the flow axis.

No evidence of unequal tensile and compressive stiffnesses for binders has been found, although unequal stiffnesses have been reported in bituminous mixtures. This aspect is covered in Chapter 5.

CHAPTER FIVE

REVIEW OF PREVIOUS WORK

INTRODUCTION

The experimental work reported in this thesis may, for the purposes of discussion be divided into two distinct parts. The first part covers stiffness measurements which have been performed on both specimens tested specifically for this purpose and on those specimens tested under repeated loading. The second part covers the majority of specimens which have been tested under the action of repeated applications of load.

The review of previous work on these two aspects of bituminous material behaviour is considered separately. First, methods of describing the stiffness of bituminous materials are reviewed together with certain specific aspects of material stiffness. Secondly, test methods and trends in results of the behaviour of bituminous materials under the action of repeated loading are reviewed. The behaviour of cement bound materials is discussed separately.

STIFFNESS PROPERTIES OF BITUMINOUS MATERIALS

METHODS OF DESCRIBING STIFFNESS

It was stated in the Introduction to this Thesis that a knowledge of the stiffness characteristics of bituminous materials is essential to several aspects of pavement design. An understanding of the effect on stiffness of such factors as frequency of application of load, intensity of load and ambient temperature is necessary in the rational design of road pavements. Only when a thorough understanding of the effect of these factors on stiffness is established may the appropriate bituminous mixture be selected and utilized to full advantage. A relatively stiff material may be considered unsuitable for road pavement constructions due to its brittle properties or temperatures susceptibility. Brittle fracture resulting from excessive dynamic or static stresses, or from thermal stresses, has been related to mixture stiffness and this aspect will be considered briefly in due course.

It will be shown later that the stiffness of a bituminous material used in road pavement construction has a considerable influence on its behaviour under the action of repeated applications of load. Therefore, from this aspect also, an appreciation of the factors affecting stiffness

is necessary in the design of mixtures for road pavement materials.

Expressions based on component characteristics - Stiffness may be described by means of a mathematical expression built up from the contributions of component characteristics to the stiffness of the whole. The material stiffness will be determined, in varying degrees, by all mixture component characteristics. Aggregate interaction alone has been shown (106) to be a function of the grading, mean particle size, shape and surface texture of each size range of aggregate used. Binder stiffness has been shown previously to be dependent upon its type, hardness and viscosity. The stiffness of the material is then defined by the aggregate interaction, the binder stiffness and some function of the degree of compacting affecting material voids and aggregate distribution and orientation. External conditions such as frequency, magnitude and direction of load and temperature will further determine the value of stiffness. Whereas it is theoretically possible to define numerically these functions and build up a mathematical expression for stiffness the practical limitations are self evident.

Attempts have been made to present mathematical relationships describing material stiffness based upon what the investigators consider the more relevant factors. The application of these expressions is extremely limited since the assessed degree of relevance of component characteristics is applicable only to small changes in material composition.

Finn et al (107) have suggested that the dynamic modulus of cores extracted from road pavements may be defined by:-

$$\log_e M = -1.86 - 0.016P + 0.047\rho + 2.58S$$

where M = dynamic modulus x 10^{-3}

P = penetration of bitumen

ρ = density of material

S = percentage of sand in aggregate.

Shook and Kallas (108) have proposed two mathematical expressions for the determination of material stiffness at a frequency of 4 cycles/second:

$$\log_{10} M = 1.54536 + 0.020108\,(x1) - 0.0318606\,(x2) + 0.068142\,(x3) - 0.00127003\,(x4)^{0.4}\,(x5)^{1.4}$$

$$\text{Log}_{10} M = 3.12197 + 0.0248722\,(x1) - 0.0345875\,(x2) - 9.02594\,\frac{(x4)^{0.19}}{(x6)^{0.9}}$$

where M = dynamic modulus in 10^5 lb/in^2

x1 = percentage of aggregate passing 200 sieve

x2 = percentage of air voids in material

x3 = bitumen viscosity at 70°F in 10^6 poise

x4 = percentage of bitumen in mixture by weight

x5 = test temperature in °F

x6 = $\log_{10}$ viscosity of binder at test temps. in poise.

Here the dynamic modulus has been determined on continuously graded specimens 4 inches in diameter and 8 inches long, subjected to axial sinusoidal loading. Both field and laboratory prepared specimens have been studied.

It will be noticed that no provision has been made for changes in test frequency in the equations of either Finn et al Shook and Kallas.

Expressions based on emperical tests - It is also possible to describe the stiffness of a bituminous material by an expression built up from the results of emperical tests. Shook and Kallas (108) have reported several attempts to relate the results of the Marshall test to stiffness and report no evidence of any other emperical test being used. The Marshall test is used to evaluate the load bearing capacity of a specimen (stability) and the deformation undergone by the specimen before its load bearing capacity is achieved (flow). This test is widely described elsewhere (e.g. 70). The Marshall test is performed on specimens 4 inches in diameter and $2\frac{1}{2}$ inches high tested on their side in a state of semi-unconfined compression. The dynamic modulus has been described as:-

$$\frac{\text{Stability (lb)}}{2.5 \times 4} \Big/ \frac{\text{Flow (0.01 in)}}{100 \times 4} = 40 \frac{\text{Stability}}{\text{Flow}}$$

This relationship has been used frequently by McLeod (109,110), and Heukelom and Klomp (86) suggest that it is equivalent to a loading time of 4 seconds. Since the criterion of Marshall failure is generally considered to be that of shear this derived modulus should be viewed with caution.

Shook and Kallas (108) have proposed the "promising " relationships:

$$\log_{10} |E^*| = -0.124262 + 1.25469\ K - 0.061215V$$

where $|E^*|$ = dynamic modulus in 10^5 lb/in^2

$K = \log_{10} \frac{\text{stability (lb)}}{100 \text{ flow (0.01 in)}}$

V = percentage voids in material - those of Marshall specimen.

The modulus is that at a frequency of 4 cycles per second and is applicable over the temperature range 40°F to 100°F.

At a Marshall stability of 2000 lb. and flow of 20 units (0.2 in) the previous expression for dynamic modulus renders a value of 4.10^3 lb/in^2 and that of Shook and Kallas, assuming 3% voids, $4.9.10^4$ lb/in^2. From the nomograph of Van der Poel (83) at a test temperature equal to that of the ring and ball softening point of the binder, bitumen stiffness at 4 cycles per second is 100 times that at a loading time of 4 seconds. Applying Heukelom and Klomp's mix factor correction (86) for $C_v = 0.8$, the mixture stiffness ratio is 50. That of the above is 12.

Shook and Kallas (108) have also attempted to relate stiffness to other emperical tests such as Hveem stability, Hveem cohesion and direct and indirect tension. Only Marshall results produced stiffness to an acceptable degree of accuracy, within 40% of estimated modulus.

Expressions based on theoretical binder behaviour - Stiffness may also be described by the use of a mathematical expression relating stiffness to binder behaviour and aggregate characteristics. This method generally employs the use of rheological models to build up a generalized expression for the behaviour of the binder. The material stiffness is then determined from the binder stiffness and a suitable mix factor. This method of defining stiffness has been discussed in principle in Chapter 4.

Secor and Monismith (111) have attempted to describe the behaviour of asphaltic concrete by a simple three element model consisting of a Maxwell model in parallel with a spring. While describing the dynamic behaviour of the material adequately, poor correlation was obtained with the creep recovery stage. The addition of a dashpot in series with this three element model (76,77) has produced better correlation with creep. A Burger's model with four additional Kelvin models has been employed by Papizan (78) to obtain a reasonable degree of correlation with mixture behaviour. Further details on the comparison of these methods are presented by Monismith et al (74) who summarize their review by stating that these model representations are of limited applicability in predicting material behaviour.

Expressions based on measured stiffnesses - The final method employed to describe stiffnessis by building up expressions based on the results of measured stiffness values at various conditions. Expressions may be either in the form of mathematical or graphical representations.

The method of fitting a mathematical expression to experimental results would be performed by regression analysis. Due to the complexity of the mathematics this system is seldom used and results are generally expressed graphically.

Graphical representations may be either in the form of stiffness/time curves with appropriate temperature shift factors or in the form of nomographs. Relationships are usually presented for binder behaviour alone and corresponding mixture stiffness determined by the use of an appropriate mix factor.

As described in Chapter 4, the most well established binder stiffness nomographs are those of Van der Poel (83) and Heukelom and Klomp (86).

Mix factors are determined either from the nomograph of Van der Poel (91) or from the mathematical expression of Heukelom and Klomp (86) applying the correction of Van Draat and Sommer (92). The expression of Heukelom and Klomp is presented in nomographic form together with the other binder stiffness and mix factor nomographs in Figures 8-11.

INFLUENCE OF MIXTURE AND TESTING VARIABLES

Binder stiffness - The stiffness of a bituminous material is largely governed by the stiffness of the binder. It has been shown in Chapter 4 how binder hardness and type, temperature, time and method of loading determine the stiffness of the binder. It was shown that method of loading has a relatively small effect on the magnitude of stiffness and for practical purposes is generally ignored. Binder hardness and type determine the stiffness of the binder and consequently largely determine the stiffness of the material. The nomographs of Van der Poel (83) and Heukelom and Klomp (86), shown in Figures 10 and 11 respectively, show that as the bitumen stiffness is increased so is the additional stiffening effect of the aggregate decreased.

Binder content - Moderate changes in binder content of up to 1½% either side of the optimum value have been shown by Goetz (112) and Shook and Kallas (108) to have little effect on material stiffness. Shook and Kallas have shown, however, that if compactive effort is adjusted to provide constant void content at varying binder content, then at a void content of 4%, an increase in binder content from 4% to 6% will reduce the stiffness by a factor of two.

It is well known that in the Marshall test additional binder to a dry mixture will increase the stability. After an optimum binder content is reached, additional binder serves to reduce the stability and increase the flow. The relationship: dynamic modulus = 40 stability/flow, may be utilized to study the effect of binder content on dynamic modulus or stiffness.

The mix factors of Heukelom and Klomp (86) also indicate the effect of binder content on the stiffness of dense bituminous materials. Here a continual increase in stiffness is suggested when binder content is reduced, assuming a constant, low void content. In this case a binder content of 1½% less than an assumed optimum of 6% results in an increase in stiffness of a factor of 2.2. A mixture richer in binder by 1½% would result in a reduction in material stiffness of a factor of 1.6.

Void content - The effect of air voids on the stiffness of dense bituminous materials has been illustrated by Jiminez and Galloway (113). Tests on bituminous diaphragms clamped on their peripheries and loaded centrally have indicated a linear relationship between the logarithm of dynamic modulus (or stiffness) and density. The stiffness was found to increase by 50% when voids were reduced by an estimated 10%.

For sinusoidal bending of a square section cantilever, Bazin and Saunier (114) have produced aggregate mix factors based solely on material voids. This system, for use with continuously graded aggregates, indicates a 100% increase in stiffness when voids are decreased by 10%.

By applying the void correction of Van Draat and Sommer (92) to the mix factors of Heukelom and Klomp (86), a reduction in voids from 15% to 5% suggests an increase in stiffness of a factor of two. This factor at a binder stiffness of 1.10^4 Kg/cm^2 ($1.42.10^5$ lb/in^2) is increased to five when binder stiffness is reduced to 1.10^2 Kg/cm^2 ($1.42.10^3$ lb/in^2).

In sinusoidal axial testing, Shook and Kallas (108) have reported that, for a densely graded aggregate, a decrease in material voids from 12% to 4% resulted in an increase in stiffness of a factor of two at 5°C and three at 35°C. This is in close agreement with the mix factor trends detailed above.

Shook and Kallas (108) have related stiffness to Marshall test results and material voids. If the ratio of Marshall stability to flow stays sensibly constant then a 10% decrease in void content would result in only a minimal increase in stiffness. This suggests that at the optimum binder content only the ratio stability to flow defines stiffness. Previous work by the Author (106) has shown that flow is increased with increasing voids with relatively little increase in stability. Voids would therefore have a greater influence on stiffness than the expression of Shook and Kallas might at first suggest.

Aggregate type and grading - Finn (115) has found that aggregate grading has a greater influence on material stiffness, at constant binder content, than does aggregate type. This finding may be expected since a wide range of aggregate gradings have a range of optimum binder contents far greater than various aggregate types at a common grading. Previous work by the Author (106), testing the Marshall properties of materials made with a wide range of aggregate types and gradings, has supported the findings of Finn. At optimum binder content the voids and stiffness (estimated from the relationship 40 x stability/flow) vary very little for different aggregate types. However, stiffness is increased and voids are decreased, when the

maximum size and stone content is increased. These trends are confirmed by Paeger and Ku (116).

For continuously graded aggregates Fin et al (107) have related material stiffness to bitumen penetration, material density (voids) and sand content. A greater weighting is given to the sand content than to the void content, although the former may well determine the latter.

Shook and Kallas (108) have considered the voids, aggregate concentration and proportion of aggregate finer than a 200 mesh sieve the most dominant factors. It is difficult to assess the more influential factor in this case. Although aggregate content is the greatest term, large alterations in this factor are unlikely.

NON-LINEARITY IN STRESS/STRAIN RELATIONSHIPS

Non-linearity in a bituminous material may be due to either non-linearity in the binder and/or the non-linear behaviour of the binder/aggregate composition.

It was shown in Chapter 4 that non-linear behaviour of a binder is probably attributable to its non-Newtonian characteristics. These non-Newtonian characteristics have been described as stress-dependence and time-dependence and both effects are manifest in road bitumens under certain conditions. Bitumens of high asphaltene content and high penetration index were shown to be more prone to non-Newtonian behaviour than those of low asphaltene content and low penetration index.

Pell and McCarthy (94) have shown that the stiffness of a 40/50 penetration bitumen is reduced as torsional strains are increased. However, since the absolute values of stiffness are subject to error, only the trends may be considered. The numerous other indications of non-linearity in bitumen, reported in Chapter 4, are the results of shear tests, either in sliding plate or concentric cylinder viscometers. Limits of pseudoplasticity and thixotropy are inapplicable to the results of the road pavement materials, since the performance of these is generally assessed in either flexure or axial loading testing conditions.

Non-linearity in bitumen-aggregate compositions has been widely reported but it is difficult to assess whether this is a result of non-linearity of the binder, effects of the aggregate or a combined effect of the two. No evidence of any reports of stiffness (or repeated loading) work on tar-bound bituminous materials has been found.

Stiffness measurements on bituminous materials fall into two categories, static (creep) tests in tension or compression and dynamic tests cycling either in tension or compression or tension and cpmpression, relative to the initial state. Static and dynamic tests fall into two further groups, stress-and strain-controlled tests where one parameter is kept constant and the behaviour of the other observed.

In comparing various test methods for stiffness measurements, Monismith (74) has reported linear behaviour in dense asphaltic concrete tested in tensile or compressive creep, tensile stress relaxation and tensile or compressive constant rate of deformation. In all test methods the linear range was found to apply to strains of up to 1.10^{-3} in/in over a temperature range 5°C to 45°C. The only exception was in the tensile creep test where a limiting strain of 1.10^{-4} in/in was found. The stress in static tests was varied from 11 lb/in^2 to 88 lb/in^2 and the constant rate of deformation from 0.07 in/in/minute to 0.53 in/in/minute.

Pagan and Ku (116), in assessing the effect of binder viscosity on the mechanical properties of dense asphaltic concrete, have reported linear behaviour in compressive creep tests up to strains of $1,10^{-4}$ in/in. This applied for stresses ranging from 3 lb/in^2 to 80 lb/in^2 at temperatures between 5°C and 40°C. Pagan and Ku have also found that after 3 or 4 "conditioning" cycles of load this linear range was increased.

Compressive testing under repeated applications of sinusoidal loading has been reported by Gardner and Skok (117), Papizan (78) and Kallas and Riley (118). For dense asphalt compositions all investigators have found reasonably linear behaviour up to strains of 5.10^{-5} in/in over a temperature range 5°C to 40°C. Gardner and Skok have covered a stress range of 19 lb/in^2 to 40 lb/in^2 at 1 cycle/second, Papizan, 4 lb/in^2 to 35 lb/in^2 at 1.7 cycles/second to 137 cycles/second and Kallas and Riley 17.5 lb/in^2 to 70 lb/in^2. Gardner and Skok have assumed a linear material when applying stiffness results to a mathematical 4-element model. Papizan has described the material as "reasonably linear" and Kallas and Riley consider the effect of vertical stress load as of "no practical importance." Similar studies by Coffman et al (119) support these conclusions.

Sayegh (120) has performed tests on dense asphaltic concrete using longitudinal harmonic vibrations at frequencies of 4, 10 and 40 cycles/second. Here linearity has been found up to a strain of 2.10^{-5} in/in at temperatures of between 25°C and 40°C. Sayegh has expressed concern at reports of linearity in excess of 1.10^{-3} which he considers "quite excessive for heterogeneous material such as bituminous concrete." Sayegh has shown that non-linearity increases in magnitude with increasing temperature or

decreasing frequency, and suggests that the secant modulus of stiffness be described as $\frac{\text{Young's modulus}}{1 + \text{dev. from linearity \%}}$.

In four point repeated tensile flexure tests on asphaltic concrete beams at 25°C., Deacon and Monismith (121) and Kallas and Riley (118) have recorded non-linear behaviour as stress level is increased. Over a stress range of 50 lb/in^2 to 150 lb/in^2, the results of Deacon and Monismith show a stiffness drop of 7½% while those of Kallas and Riley indicate a drop of 25%. It should be remembered that in these tests the wave form is not continuous. Deacon and Monismith have a square wave of 0.1 second duration while Kallas and Riley apply a sine wave over 0.2 seconds. Monismith et al (35) have shown that the degree of non-linearity is more acute for dense surfacing materials than for less dense base materials tested under similar conditions. Good agreement in flexural stiffness behaviour of "asphalt-cement-treated base" materials has been found between beams prepared in the laboratory and those taken from the field. For this material tested at 20°C., linear behaviour is indicated for flexural strains of up to 5.10^{-4} in/in.

Torsion tests reported by Pell and McCarthy (94) on bitumen and sand asphalt specimens have revealed non-linearity over the temperature range -20°C to +40°C for all torsional strains in excess of 1.10^{-4} in/in. The degree of non-linearity increased with temperature but was not affected greatly by aggregate content at constant temperature. Torsional stiffness results indicate a greater drop in stiffness at higher temperatures over a similar range of strain. These stiffness results, similar to those of gap-graded asphalts tested in rotating bending (123), suggest that stiffness reduces to a constant value at high stress levels. Pell and Taylor (124, 125) have shown with more sophisticated measuring equipment that this trend is, in fact, reversed. As would be expected, constant stiffnesses indicating linear behaviour were associated with lower stress levels. The erroneous results of Pell and McCarthy (94) and Pell (123) have been attributed by Taylor (124) to the inaccuracy of the load and deformation measuring equipment. The main conclusion of Pell and McCarthy, that fall in stiffness with increase in strain is more acute with less stiff materials, is nevertheless of considerable importance.

Pell and Taylor (123-125) have reported non-linearity in both continuously graded and gap-graded asphalts in bending. Sinusoidal tension-compression tests at +10°C have indicated a stiffness drop of some 25% for gap-graded asphalts and over 30% for continuously graded asphalts, resulting

from an increase in strain from 4.10^{-5} in/in to $1.6.10^{-4}$ in/in. In contrast to torsion tests, Pell reports a greater reduction in stiffness at lower temperatures over the same stress range but in this case the material was of a gap-graded nature. An analysis of the results of Taylor, covering a wide range of gap-graded materials at various test temperatures and frequencies, indicates that non-linear behaviour occurs at a strain of approximately 1.10^{-4} in/in. Continuously graded materials indicate a lower strain level of approximately 5.10^{-5} in/in.

Non-linear behaviour is also reported by Eisenmann (126) in cylindrical dense asphalt compositions subjected to shear. Here the reduction in stiffness with similar stress increase is greatly increased as the stiffness is decreased.

In view of the foregoing results it may be assumed that, in dense bituminous materials, the strains level at the onset of non-linear behaviour is higher for static tests than for dynamic tests. Static tests in both tension and compression reveal linearity up to strains of approximately 1.10^{-3} in/in, except at high temperatures in excess of $+40^{\circ}C$ where this strain is reduced. Dynamic tests on materials in axial compression and tensile flexure have been found to exhibit linear behaviour up to strains of approximately 1.10^{-4} in/in for frequencies between 1 and 140 cycles/sec. and temperatures from $5^{\circ}C$ to $40^{\circ}C$. Onset of non-linear behaviour has been reported in one case as occurring at strains of 2.10^{-5} in/in although the test method precludes a direct comparison with other results. Gap-graded asphalts tested in bending also display linear characteristics up to strains of approximately 1.10^{-4} in/in, but this will be reduced for continuously graded aggregates.

In general it would appear that the degree of non-linearity is increased with stiffer materials, although conflicting reports are found on this aspect.

TENSILE AND COMPRESSIVE PROPERTIES

The onset of non-linear behaviour in bituminous materials in tension, compresion or reversed stress systems has been reviewed. The stiffness of a material, however, is independent of its degree of linearity and may differ in tension and compression.

In comparing calculated and measured deflections in layered systems Monismith and Secor (77) have observed that, while good agreement was found at low temperatures, at temperatures approaching $+40^{\circ}C$ significant deviation

was evident. Monismith and Secor suggest that this may be due to a change in the ratio tensile to compressive stiffness, being more acute at higher temperatures. Direct tension, compression and bending creep tests were performed on beams of dense asphaltic concrete at +25°C. Results showed that the instantaneous strain occurring on the application of stress is equal for both direct tension and direct compression. After 100 minutes at an applied stress of 1.35 lb/in^2 the tensile strain equalled $3\frac{1}{2}$ times the compressive strain and four times after 200 minutes. In bending, instantaneous strains were again equal but after 100 minutes tensile strains were reported equal to $1\frac{1}{2}$ times the compressive strains. In this case equal linear stiffnesses were recorded up to a strain of 2.10^{-4} in/in.

On further creep tests Monismith et al (74), reporting the results of Alexander (127) for similar sized beams, have shown that at +5°C stiffnesses are equal up to five minutes. After this tensile strains exceed compressive strains. A moment of 0.55 lb.in at +25°C has resulted in tensile strains double those of compressive strains after 10 minutes of flexured creep.

Kallas (128), in a paper specifically concerned with the relative behaviour of dense asphaltic concrete in sinusoidal tension, compression and tension-compression loading, has studied a wide variety of materials. Two binder types have been reported in mixtures of varying binder content and compactive effort. Results show that for both binders and all binder and void contents, material stiffness was greater in compression than in tension at high temperatures and low frequencies but equal at low temperatures. The softer (88 pen.) binder at optimum binder content produced a ratio of tensile to compressive material stiffness of 1 at 5°C, $\frac{3}{4}$ at 25°C and $\frac{1}{2}$ at 40°C. The harder (59 pen.) bitumen produced ratios of 1 at 5°C and $\frac{2}{3}$ at 100°C, both at a frequency of 1 cycle/second. Kallas considers these differences of little significance relative to the magnitude of stiffness. Changes in phase angle are considered of greater importance. At +40°C the phase angle in tension is double that in compression indicating that the viscous portion contributes more to the inelastic behaviour of the material in tension than in compression.

A certain amount of work has been performed on a study of the ultimate strength of bitumen and bituminous materials in compression and (mainly) in tension. An analysis of the criterion of failure may be useful in assessing the causes of non equality in tensile and compressive stiffnesses.

Heukelom (73) has performed compression tests on cylindrical specimens of pure bitumen at constant rates of deformation and at a variety of temperatures. Heukelom has observed that, at the point of maximum load, cracks appeared running in the direction of applied stress. Upon further deformation the familar cone shaped failure planes occurred, indicating a final breakdown in the region of maximum shear stress. Heukelom suggests that it is unlikely that shear failure is the criterion of maximum stress but rather the excessive tangential strain. Since tangential strain is related to axial strain by Poissan's ratio, Heukelom proposes that, for incompressible binders, the ultimate compressive strength is double the ultimate tensile strength, ($\varepsilon_T = \mu \varepsilon_C \therefore \sigma_C = 2\sigma_T$).

On tests with dense asphaltic concrete Heukelom has shown that in compression the ultimate strength is proportional to the ultimate compressive strength of the bitumen. In tension the ultimate strength is proportional to the ultimate tensile strength of the bitumen for bitumen stiffnesses up to 500 Kg/cm^2 ($7.25.10^3$ lb/in^2). Failure beyond this stress is attributed to excessive hydrostatic tension. The constants of proportionality have been termed mix factors, hence:

$$\sigma_{T mix} = M_T \sigma_{T bit}$$
$$\sigma_{C mix} = M_C \sigma_{C bit}$$

where: σ_{mix} = strength of composition
σ_{bit} = strength of bitumen
M = mix factor of ultimate strength.

Suffix 'T' refers to tension and 'C' to compression.
Heukelom has found that these mix factors are functions solely of the aggregate type, grading and content and independent of binder stiffness, (cf. Figure 10), and that $M_C \cong 1.5 M_T$.
Heukelom combines his equations to give:

$$\sigma_{C mix} = 2 \frac{M_C}{M_T} \cdot \sigma_{T mix} \cong 3 \sigma_{T mix} \quad \text{and} \quad \sigma_{T bit} = \frac{1}{2 M_C} \cdot \sigma_{C mix} .$$

Hargett (129) has stated that the stability of a bituminous road surface is determined by the shearing resistance of the surfacing material. This shearing resistance consists of the cohesive strength of the binder and the internal friction of the aggregate. Hargett suggests that the tensile strength of a bituminous material is that of the cohesive strength of the binder whilst the compressive strength is due to the shearing resistance. Results have shown that the compressive strength of asphaltic concrete at room temperature and constant rate of deformation is five times that of the tensile strength. At failure, compressive strains averaged $5.2.10^{-2}$ in/in and tensile strains $1.8.10^{-2}$ in/in. This strength ratio compares favourably with that of Heukelom (73).

It is reasonable to assume that the factors governing failure in a bituminous composition will also contribute to the behaviour of the material

prior to failure. The conclusion drawn from the tests of Heukelom and Hargett is that the cohesive strength of the binder and the internal friction of the aggregate both contribute to the stiffness both in tension and compression. At very small strains the net contribution of binder and aggregate is equal in tension and compression. As strain is increased the internal friction contributes more to the compressive stiffness and less to the tensile stiffness. Since the strength derived from internal friction is greater than that from binder cohesion, the compression stiffness will exceed the tensile stiffness to an increasing degree as strain is increased. Non-linearity may be attributed to increasing hydrostatic pressures in the binder as well as to any non-linearity in the binder itself. The ratio of compressive to tensile stiffness will increase to a maximum of $\frac{M_c}{M_T}$ when failure occurs due to tensile stresses in the binder exceeding its tensile strength.

Regarding the ultimate tensile strength properties of bituminous binders and compositions, Heukelom (73) and Pfeiffer and Saal (130) have found that the elongation of pure bitumen at fracture is a function of the stiffness of the bitumen. The elongation is dependent upon type and hardness of the bitumen only insomuch as these factors determine the bitumen stiffness. Heukelom has produced a nomograph relating the elongation at fracture to the time of loading, the difference between the test temperature and that of the ring and ball softening point of the bitumen and the penetration index of the bitumen. This nomograph is reproduced in Figure 12. By applying the appropriate value of the mix factor M_T, the elongation to failure and ultimate tensile strength of bituminous materials may be ascertained. Heukelom has not produced values of mix factor M_T for various aggregate combinations.

Epps, (131) on fracture strengths of bitumen bound materials, has found values of M_T of 0.85 for continuously graded granite aggregate mixtures with 6% of bitumen. Values of M_T of 0.5 were found for a similar aggregate type and grading but with a binder content of 5.2%, B.S. 594 gap-graded mixtures produced M_T values approaching 0.9 as might be expected from a richer mixture. An increase in filler content from 4% to 12% in a granite aggregate mixture increased the value of M_T from 0.64 to 1.03.

BEHAVIOUR OF BITUMINOUS MATERIALS UNDER REPEATED LOADING

INTRODUCTION

A comprehensive review of the various test methods used in assessing the behaviour of both metals and bituminous materials under repeated

applications of load has been presented by Deacon (110) for work carried out prior to 1965. Taylor (124) has extended this review with a detailed analysis of bituminous materials testing up to September 1968. Particular reference is paid by Taylor to results of the rotating bending type testing carried out at Nottingham University. A review of testing methods applicable to bituminous materials is presented by Pell and Taylor (132) who include details of work in rotating bending detailed more fully in reference 125.

A brief review of the methods employed in assessing the behaviour of bituminous road materials under repeated loading is included below. It is hoped that this will enable subsequent comments on factors affecting behaviour under repeated loading and experimental results discussed in Chapters 10 and 11 to be more fully appreciated in the light of the method of testing used.

Stress-controlled testing - The first investigation performed specifically to study the behaviour of bituminous materials under repeated applications of load is stated by Taylor (124) to be that of Nijboer and Van der Poel (54-56), first published in 1952. Reversed stress testing on sandsheet mixtures was performed on cylindrical specimens $1\frac{1}{2}$ inches in diameter and 4 inches long. Specimens were mounted as a horizontal cantilever and tested in rotating bending at a frequency of 25 cycles/second. Nijboer and Van der Poel found that when plotted on logarithmic scales a linear relationship existed between the maximum tensile stress and the number of cycles required to induce fracture.

In 1958, Monismith (133) published a paper concerned with the behaviour of dense asphaltic concrete mixtures under the action of repeated loading. Monismith tested laboratory prepared specimens 3 inches wide, 2 inches deep and 12 inches long. Specimens were tested on a flexible diaphragm supported by a multi-spring base very similar to that used by Thomas (134) in 1948. A square wave load was applied centrally onto the specimen and the deformation and subsequent elastic recovery recorded by means of a displacement transducer at a point of loading. After a predetermined number of load applications, the specimen was simply supported on a 10 inch span and loaded centrally to failure at a rate of 0.25 in/min. The maximum load sustained by the specimen and the corresponding deflection were used to calculate the modulus of rupture of the specimen. By dividing this modulus of rupture by that of a similar unflexed specimen the degree of damage sustained by the repeated application of load was assessed. Service life was defined as the number of load applications required to cause a 10% drop in the modulus of rupture. When plotted on logarithmic scales a linear relationship was

found between maximum tensile stress and service life.

Papizan and Baker (135) in 1959 reported the results of repeated flexure tests on beams $1\frac{1}{2}$ inches wide and of varying depths simply supported on a 9 inch span. A transverse steel spring of variable stiffness provided additional support at centre span. A sinusoidal load was applied mid span over a period of 0.2 seconds and at 105 applications per minute. Papizan and Baker defined the service life in relation to the increased deformation resulting from the repeated applications of load. Linear logarithmic relationships were found both between maximum tensile stress and service life and between the initial deformation and service life. The former linear relationship was found to apply for all beam depths tested.

Tests on pure bitumen and sandsheet specimens in pure bending have been performed by Pell (136) and first reported by Saal and Pell in 1960 (137). Here specimens were rotated in a vertical position and subjected to a couple applied to the free end, imposing pure reversed stress bending on the specimen. Specimens 2 inches in diameter and $10\frac{1}{2}$ inches long were necked down to $1\frac{1}{2}$ inches in diameter at the centre in order to eliminate complications due to geometric stress concentrations. During rotating bending tests Pell measured no increase in deformation during the test until just before the fracture occurred. Pell has found that over a wide range of testing speeds and temperatures and for various mixture compositions, in each condition a linear relationship existed between the logarithms of stress amplitude and the number of cycles to specimen fracture. Using the nomographs of Van der Poel (83) and Heukelom and Klomp (86) the strain amplitudes at the beginning of the tests were also calculated. For a particular mixture composition, when plotted on logarithmic scales, a common linear relationship was found for all the test temperatures and frequencies studied. Different lines were obtained for materials of different mixtures.

The constant stress testing of bituminous materials in rotating bending initiated by Pell has been extended by other investigators (94, 138, 139). In 1962 attention was shifted to BS594 gap-graded materials and larger specimens with a $2\frac{1}{2}$ inch diameter neck were employed. A modified single point loading system was utilized in order to impose greater loads and the resulting shear force imposed on the specimen was not considered to have any influence upon results (140). Again, when plotted on logarithmic scales linear relationships were obtained between stress amplitude and fracture life and for initial strain a common line for all testing conditions of a particular mixture composition.

Also in 1962 results were published of work by Jimenez and Gallaway

(113) who subjected to repeated applications of load a diaphragm 17½ inches in diameter and 1 inch thick. The diaphragm, produced from dense asphaltic concrete, was rigidly clamped around its periphery and supported, on a membrane, by oil pressure. A sinusoidal load was applied over 5 square inches at 11 cycles/second. The resulting deflection was recorded and plotted on a double logarithmic scale, against the number of elapsed cycles. The service life was defined as the number of cycles at which the relationship deviated from the linear.

Deacon (141) has used a 4-point loading system to study the effect of cumulative damage on dense asphaltic concrete. Specimens 1½ x 1½ x 15 ins. sawn from laboratory prepared slabs, were simply supported on a 12 inch span and loaded at the third points. This loading system provides a constant bending moment over the middle third length of the span. In this sytem, reported in 1965 (141) and first published in 1967 (121, 142), equal loading was applied through the loading points and held for a predetermined time then reversed such that the specimen was returned to its original unflexed position. This procedure was repeated until fracture. Deacon has found that, on logarithmic scales, there was a linear relationship between maximum tensile stress and fracture life, but a curved relationship between fracture life and maximum initial strain.

Reversed stress testing has been reported in 1962 by Lucas et al (143) and Bazin and Saunier (114). Here sawn, rectangular section, trapezoidal specimens of sandsheet were fixed at their thicker ends and tested as vertical cantilevers. This shape ensured a point of maximum stress well away from both the fixed end and the loaded free end. Specimens were oscillated at a frequency of 50 cycles/second and again a common linear logarithmic relationship was found between initial strain and fracture life. Results have been correlated with those obtained from a small road machine, 10 feet in diameter which is trafficked by a 1 ton wheel travelling at 10 m.p.h.

A simple 3-point bending system has been reported in 1969 by Majidzadeh et al (144) to study the rate of crack propagation in sand asphalt specimens under repeated flexure. Laboratory prepared specimens, 1 x 1 x 12 inches in size, were subjected to sinusoidal load cycling at a frequency of 30 cycles/minute and at temperatures of between 0°C and 15°C. Only one material has been studied which produced linear parallel relationships between the logarithms of load amplitude and fracture life for different temperatures. Strain values have not been presented.

Strain-controlled testing - The earliest work on the behaviour of bituminous road pavement materials under repeated load applications has been quoted by Deacon (141) as being that of Hennes and Chen (145), first reported in 1950. Although essentially measuring the dynamic modulus of rupture of asphaltic concrete materials, certain repeated loading tests were carried out. Laboratory prepared specimens 2 x 2 x 12 inches in size were tested, on a simply supported leaf spring, under conditions of controlled deformation at a frequency of 37 cycles/minute. It was found that when plotted on logarithmic scales a linear relationship occurred between the initial, calculated, stress and the number of cycles to fracture, a fracture life of one cycle corresponding to the modulus of rupture of the material.

This form of testing with continuous flexible support intended to represent the supporting action of underlying layers in a road structure has also been reported in 1955 by Hveem (49). This work was initiated by Hveem in order to assess the degree of damage sustained by road pavement materials under the action of traffic. Hveem has sawn specimens 2 x 2 x 12 inches from beams taken from the road. These were mounted on rigid supports at the ends and on a sponge rubber support along their length. A load was applied centrally by a cam profiled to represent the loading wave of a multi-wheel vehicle. Service life in this strain controlled test was defined by cracking. Hveem has found a linear relationship betweem the logarithms of deflection and service life. Hveem has also found shorter service lines from those specimens taken from road surfacings more prone to distress under the action of traffic.

The fact that fracture life was found by Pell (136, 137) to be a function of initial strain in rotating bending type reversed stress testing led McCarthy (136)in 1960 to develop a constant strain torsion machine. Specimens identical to those used by Pell in pure bending were mounted vertically, locked at the lower end and subjected to torsional oscillations at the upper free end at a frequency of 24 cycles/second. Fracture life was detected by crack propagation at the neck of the specimen. In this case, although linear, the relationships between the logarithms of strain and fracture life did not coincide for specimens at various testing temperatures.

In 1961, Monismith et al (147) reported results obtained from strain-controlled testing of asphalt concrete beams 3 inches wide, 2 inches deep and 12 inches long. The beams were rigidly clamped at their ends and loaded at the centre point. Monismith et al have shown that specimens whose lower face is flexed in tension, compression, or reversal strain exhibit similar behaviour under the action of repeated applications of load when flexed at

equal deformation ranges.

Monismith (148-150) has also reported strain-controlled testing of asphaltic concrete using the stress-controlled spring base test system previously described. As before the specimen was loaded at its central point but deflection was monitored by strain gauges mounted on the underside of the beam. The deflection was maintained for a predetermined time after which the load was released and the spring bed reverted the beam to its original unflexed position. Service life was defined, as before, as the number of cycles required to reduce the modulus of rupture by 10%. When plotted on logarithmic scales Monismith has found a linear relationship between strain and service life. In agreement with Pell and McCarthy (94) Monismith has also found non-coincidence in strain/service life relationships for specimens tested at various testing conditions.

In 1967 Kirk (151) published details of strain-controlled testing of dense bituminous mixtures in the form of beams, 5 x 7 x 53 cm. (2 x $2\frac{3}{4}$ x 20 inches), sawn from laboratory prepared slabs. Four-point loading was employed in a manner similar to that of Deacon (141) and specimens subjected to reversal strain controlled loading at a frequency of 50 cycles/second. Kirk has defined service life as the number of cycles required to reduce the initial load by 50%. Again a linear logarithmic plot was obtained between strain and service life with non-coincidence at various testing conditions.

It will be apparent that over the wide range of testing methods employed, for both stress-and strain-controlled testing of dense bituminous materials, one factor predominates; when plotted on logarithmic scales a linear relationship was generally found between initial strain and service or fracture life. In controlled stress testing, lines were common for a mixture tested at a variety of temperatures and frequencies, in controlled strain testing they were not.

INFLUENCE OF MIXTURE AND TESTING VARIABLES ON SERVICE LIFE

Of the thirteen methods of testing the behaviour of dense bituminous road pavement materials outlined above, nine are in some form of flexure, three in rotating bending and one in torsion. In all cases service life or fracture life has been related to the maximum extreme fibre stresses or strains, and in no case is the stress or strain constant over the cross section of the specimen. Trends in lives appear to be similar for mixture variables, irrespective of testing method used, where stress reversal occurs across the cross section. Mixture variables and testing variables will

therefore be considered individually, comments applying to all testing methods unless otherwise stated.

Binder grade and type - Pell (123, 140) has shown the effect of binder grade on gap-graded materials in the single load rotating bending machine. Tests on materials consisting of 7.2%, by weight, of 40/50 and of 90/110 penetration bitumen have been performed at 0°C. Taking the logarithm of stress axis as the abscissa, slopes of logarithm of fracture lives were formed to be 7.1 and 5.5 for mixtures made with 40/50 and 90/110 penetration bitumens respectively. Corresponding fracture lives at a bending stress of 200 lb/in^2 were $1.5.10^7$ cycles and $1.1.10^6$ cycles. When reduced to derived strain by means of nomographs, fracture lives were found to coincide, within the limits of experimental error. Here the slope was 5.3 and the fracture life at a strain of 2.10^{-4} im/in was $1.2.10^5$ cycles.

The four point bending stress-controlled apparatus of Deacon (141) has been used by Epps (131) to study the effect of binder grade on the service life of continuously graded granite materials at 25°C. Epps has used three grades of bitumen ranging from 40/50 to 85/100 penetration at a constant binder content of 6%. In agreement with Pell, Epps has also found longer lives associated with the harder binders. At a bending stress amplitude of 200 lb/in^2 service lives were found to be $9.5.10^3$ cycles and $1.1.10^2$ cycles for the 40/50 and 85/100 penetration bitumens respectively, with slope factors of 5.0 and 4.0. When the logarithm of service life was plotted against the logarithm of the initial bending strain, Epps has found that lines of different bitumen grades were not coincident. The harder bitumens exhibited greater sensitivity in lives to given changes in strain. The slopes for the 40/50 and 85/100 penetration bitumen materials were 4.0 and 2.8 with service lives at an initial bending strain of 2.10^{-4} in/in of $8.0.10^4$ cycles and $8.7.10^4$ cycles respectively.

Bazin and Saunier (114) have confirmed the findings of Epps, studying 40/50 and 85/100 penetration grade bitumens in both sandsheet and dense asphalt specimens. The binder content of the sandsheet was 9.5% and the dense asphalt 6%. The trapezoidal cantilever was subjected to stress-controlled cycling with 50 cycles/second at a temperature of +10°C. For the sandsheet, logarithmic plots of initial strain against fracture life were 5.4 and 4.0 respectively. For the dense asphalt, 4.3 and 3.3. Fracture lives at an initial strain of 2.10^{-4} in/in were $1.0.10^6$ cycles and $2.0.10^5$ cycles for the sandsheet and $3.1.10^4$ cycles and $1.6.10^4$ cycles for the dense asphalt.

Monismith (150) has reported the results of Jiminez (152) on the effect of bitumen penetration and viscosity on the service lives of asphaltic concretes. A reduction in bitumen penetration from 120 to 90 was found to increase mixture life by a factor of 7 and a further reduction from 90 to 60 by a further factor of 6.

Under conditions of controlled strain, Monismith (150) has studied the effect of three binder grades on the service lives of continuously graded granite mixtures assessed by the spring bed flexure test. Bitumens studied were 40/50, 85/100 and 120/150 penetrations all from the same source, mixture binder content being constant at 5.9%. Tests at $+5^{\circ}C$ showed that for the 40/50 and 85/100 penetration bitumen mixtures slopes of the logarithmic strain/service life relationships were 5.9 and 6.6. Lives at a bending strain of 2.10^{-4} in/in were $6.2.10^{5}$ cycles and $3.8.10^{6}$ cycles respectively, For two 85/100 pen. bitumens from different sources Monismith has detected a slight increase in service life for the higher viscosity material.

Kirk (151) has reported results of tests on specimens of dense crushed granite aggregate mixtures, tested in strain controlled 4-point bending, at 50 cycles/second. The service lives of specimens consisting of $5\frac{1}{2}\%$ of 180/200 penetration bitumen were found to be common for a given strain level over a temperature range $-5^{\circ}C$ to $+15^{\circ}C$. Kirk has also reported that the strain level resulting in a service life of 1.10^{6} cycles is sensibly constant for mixtures of 10/20, 40/50, 80/100 and 180/210 penetration bitumens, at $1.4.10^{-4}$ in/in. A further 10/20 penetration bitumen which was a blown type, resulted in somewhat longer lives.

Although it is impossible to relate the results of different test methods with different materials and different criterion of service life certain trends are evident. In controlled stress testing under identical testing conditions, mixtures with lower penetration bitumens produce longer lives at equal stress levels. The service lives of these materials are also more sensitive to changes in bending stress. When reduced to initial bending strain, the service lives of the harder bitumen compositions show a greater sensitivity to changes in strain. Longer lives at given strain levels are suggested where the maximum bending strain occurs at one position but not where bending strain is uniform over a large portion of the specimen. These trends are common for both gap-graded and continuously graded mixtures over a wide range of maximum particle size and binder content.

Under conditions of controlled-strain testing, for maximum bending stress occurring at one position on the test specimen, contrary to the

findings of stress-controlled testing, service lives of the harder bitumen mixtures are less sensitive to changes in strain level and have shorter service lives at a given strain. The results of tests where a uniform bending strain occurs over a large area, no difference in sensitivity or service life is reported for various binder grades.

In both forms of strain-controlled testing greater service lives are evident with lower penetration index bitumens of similar penetration.

Binder content - It is generally accepted that the service lives of bituminous materials are increased with increasing binder content, all other mixture components and testing conditions remaining constant.

Monismith (133), using the stress-controlled spring bed apparatus, has observed an increase in service life of a factor of approximately 50 for an open textured asphalt when binder content is increased from $3\frac{1}{2}\%$ to 5% and a factor of some 200 for a dense asphalt over the range 4% to 7%. All tests were performed on compositions with an 85/100 penetration bitumen and $\frac{3}{8}$ inch maximum size aggregate under a load amplitude of 60 lb. at $+25^{\circ}C$.

The stress-controlled diaphragm of Jiminez and Gallaway (113) has indicated an optimum binder content for fracture life. Tests on dense asphaltic concrete, with a crushed granite aggregate, revealed a twofold increase in fracture life for each additional 0.5% of binder from 6.6 to 7.5%. After the optimum binder content of 7.5% fracture life was reduced by a factor of $1\frac{1}{2}$ for a further 0.5% increase in binder content.

Pell and Taylor (123,125) have studied the effect of binder content on fracture life of gap-graded materials in rotating bending. Testing was carried out at a stress level of 165 lb/in^2, in a frequency of 1000 cycles/minute, and atemperature of $+100^{\circ}C$. It was found that in the binder content range 4% to 6%, a 0.5% increase in binder content resulted in an increase in fracture life of a factor of 2.5. At binder contents in excess of 6% fracture life increased less rapidly until maximum life was achieved at a binder content of 7.5%. Upon further increase in binder content to 12.5%, a gradual reduction in life was observed. The optimum binder content for maximum fracture life is the same binder content as that for maximum stiffness. This has also been found by Epps (153) in stress controlled four point bending.

Tests in reversed stress bending by Pell (137) have confirmed longer fracture lives for high binder contents. Tests on sandsheet mixtures with $9\frac{1}{2}\%$ and 14% of 40/50 penetration bitumen at $0^{\circ}C$ have shown that when plotted on logarithmic scales, the higher binder content mixture showed a tenfold

increase in fracture life with a slope factor slightly less than the leaner mixture. These sandsheet specimens have also been tested in strain controlled torsion as reported by Pell (139). A richer (mastic) mixture of 28% binder content, and a pure bitumen specimen have also been tested. Further results are presented for mastic type mixtures made with single sized glass spheres of average sand particle size. All results show that as the volume concentrations of the binder in the mixture increase, so does the service life of the material at a given strain. All lives on a logarithmic plot of strain against service life are roughly parallel, being slightly less steep for higher bitumen contents.

In all cases of stress-or strain-controlled testing, an increase in binder content up to and above the normal working binder content results in an increase in service life. In the case of practical mixtures an optimum binder content is evident for maximum service life, generally slightly above the normal binder content, corresponding to maximum stiffness. In mixtures where there is little or no particle interaction, maximum service life appears to occur with the richest, pure bitumen samples.

Test temperature - The effect of temperature on the service lives of bituminous materials under the action of repeated loading is identical to the effect of bitumen grade. A decrease in testing temperature has the same effect as a decrease in bitumen penetration. It was observed that a lower penetration bitumen produced not only longer service lives under conditions of controlled stress testing, but also a greater sensitivity of life to changes in stress.

A similar trend for changes in test temperatures has been found by Pell and Taylor (123-125), for a gap-graded material with 6% of 40/50 penetration bitumen, tested at 1000 cycles/minute. Here linear relationships were found between the logarithms of bending stress and fracture life. At a bending stress of 200 lb/in^2 fracture lives were $8.2.10^2$ cycles (extrapolated), $2.0.10^4$ cycles and $1.2.10^5$ cycles for temperatures of +20°C, + 10°C and 0°C respectively. Corresponding slopes were 4.2, 5.8, and 5.9. Derived strain values resolved to a common relationship between initial strain and fracture life. Deriving initial strains from measured stiffness values results in a non-linear logarithmic relationship as found by Epps (131).

Work of other investigators support the findings of Pell and Taylor that a common relationship exhibits between initial strain and service life, where stress is applied to a local area. Results of tests on dense asphaltic

concrete, in stress-controlled four point bending reported by Monismith (150), show that on a basis of derived initial strain, results at +5°C and +20°C do not resolve to a common line. Longer service lives, associated with greater sensitivity in life with change in initial strain, resulted from higher testing temperatures. Tests on denser surfacing material did, however, indicate a common derived strain/service life relationship.

Pell (139) has reported the results of tests on plain bitumen in pure bending tested over a range of temperatures and frequencies. On a strain basis fracture lives were found not to reduce to a common line. Although parallel, longer lives were associated with higher temperatures (and lower frequencies of loading). Tests in strain-controlled torsion have confirmed this trend. Pell (139) has shown that over a range of temperatures from -11°C to +10°C the service life of pure bitumen is increased with increase in temperature. At a tensile strain of 1.10^{-3} service lives were found to be $1.8.10^{5}$ cycles, $9.0.10^{5}$ cycles and $1.0.10^{7}$ cycles (extrapolated) for temperatures of -11°C, 0°C and +10°C respectively. The slopes of the logarithmic plots of tensile strain and service life are sensibly constant at approximately 4.7.

Further tests in strain controlled torsion by Pell (139) on sandsheet specimens have shown that at low temperatures, between -20°C and 0°C, service life is sensibly independent of test temperature. As test temperatures were increased to +40°C, longer lives resulted, with less sensitivity in life to changes in strain. At temperatures below 0°C a slope of 7.4 was found, similar to that at +15°C. At +30°C the slope was 5.8 and at +40°C, 4.1. Lives at a constant strain of 4.10^{-4} in/in at temperatures below 0°C were $3.0.10^{4}$ cycles, at 15°C $1.3.10^{5}$ cycles at +30°C $8.0.10^{6}$ cycles and at +40°C $2.5.10^{7}$ cycles (extrapolated).

Strain-controlled tests on practical stone filled materials also reflect longer lives at higher temperatures. Monismith (148-150) has shown that when dense asphaltic concrete is tested on the spring bed apparatus at constant strain, logarithmic plots of bending strain against service life produce parallel lines for different temperatures. A granite asphalt with 5.9% of 40/50 penetration bitumen has shown an increase in service life of a factor of 9 when the temperature is increased from +5°C to +20°C. A gravel asphalt with identical binder type and content has shown an increase in service life of a factor of 15.5 over a similar temperature rise. The slopes of these two aggregate type mixtures were similar at approximately 6.5 and the service lives of both mixtures at +5°C at a strain of 2.10^{-4} in/in was found to be $1.0.10^{6}$ cycles.

In both stress-and strain-controlled testing, on the basis of derived or imposed initial strain, longer service lives are associated with higher testing temperatures. It would appear that at very low testing temperatures service lives are similar. As the temperature is increased so is the service life increased at a progressively greater rate.

Frequency of loading - It is generally accepted that the effect of frequency of loading on the behaviour of bituminous materials under repeated loading is similar to that of test temperature and binder grade. An increase in frequency of loading, as a decrease in test temperature results in a stiffer binder and hence increase in service life for a particular bending stress.

Pell and Taylor (125) have shown that in single load rotating bending at $+10^{\circ}C$, fracture life is increased with increasing frequency of loading. Tests on a gap-graded basecourse mixture show that the increase in fracture life decreases with high frequencies where the material becomes more linear. With a stress amplitude of 165 lb/in^2 an increase in testing frequency from 60 to 130 cycles/minute resulted in a tenfold increase in fracture life, whereas for a further tenfold increase in fracture life frequency was increased from 130 to 1500 cycles/minute.

Kirk (151), testing dense asphaltic concrete in strain controlled 4-point bending, has reported "only negligible" effect on service life when frequency was decreased from 50 cycles/second to 10 cycles/second. According to Pell and Taylor (135) such an increase in frequency would, for gap-graded materials, result in an increase in fracture life of a factor of 2.5.

Void content - The effect of voids on the fracture life of sandsheet specimens of constant mixture components has been illustrated by Saal and Pell (137). In pure rotating bending at $0^{\circ}C$ at 3000 cycles/minute and a stress amplitude of 400 lb/in^2, a linear relationship was found between voids and the logarithm of fracture life. A decrease in void content from 10% to 1% resulted in an increase of fracture life of a factor of 16. Pell (139) has stated that this reduction in life with increase in voids is far greater than would be expected from the corresponding reduction in cross-sectional area. Further, the surface finish had no effect on fracture life where the internal voids remained constant.

Pell and Taylor (125) have extended this trend to the results of gap-graded base course asphalts tested at 1000 cycles/minute and at $+10^{\circ}C$. Results over a wide range of stresses, when expressed in terms of initial

strain, indicated that a reduction in voids from 10% to 1% would increase the fracture life by a factor of 35. It should be noted that, unlike the sandsheet materials of Saal and Pell, these mixtures contained no added filler.

In correlating the fracture life of sandsheet specimens in stress-controlled flexure and in a small road machine, Bazin and Saunier (114) have found that a decrease in voids resulted in an increase in fracture life. At a test temperature of $+10^{\circ}C$ and a frequency of 50 cycles/second, a reduction in mixture voids from 9% to 4.5% resulted in an increasein fracture life of 3.2 at an initial strain of 2.10^{-4} in/in and 2.2 at a strain of 5.10^{-4} in/in. According to Saal and Pell (137) a comparable reduction in voids would result in an increase in fracture life of a factor of 4.3.

Epps (131) has studied the effect of voids on the service life of gap- and continuously-graded materials in the stress-controlled 4-point bending apparatus of Deacon (141). At a common temperature of $+20^{\circ}C$ and stress level of 150 lb/in^2 a linear relationship was found between voids and the logarithm of service life. For a gap-graded mixture a reduction in voids from 10% to 1% resulted in an increase in life of a factor of 8.0 (extrapolated below 4% voids). For a fine graded asphaltic concrete the increase was 200 (extrapolated beyond 3% and 9% voids) and for a coarse graded asphaltic concrete the increase was 35 (extrapolated beyond 3% and 7% voids).

Kirk (151) has shown that, for both gap-and continuously-graded aggregates tested in strain-controlled four-point bending, voids will reduce service life only if the ratio of binder content, by volume, to void content is less than five. Below five the reduction in service life with increase in voids becomes more acute as the ratio is reduced. Hence, for a gap graded material with 6% binder, by weight, void contents less than 3% would not be expected to affect service life. For a sandsheet with a binder content of $9\frac{1}{2}$% the critical void content would be 4%. For an open textured macadam type material with 4% binder the critical void content would be 2%. These results have been produced on a basis of strain-controlled testing. The results of Saal and Pell, and Pell and Taylor, outlined above, pertain to stress-controlled testing where the definition of service life is that of complete fracture.

In stress-controlled testing all investigators report a reduction in service life with increase in mixture voids. The influence of voids on service life is more acute with denser aggregate gradings. In strain controlled testing the influence of voids on service life appears to be less severe than in stress-controlled cycling.

Aggregate type and grading - It is extremely difficult to assess the influence of aggregate type and grading on the service lives of bituminous materials. A fine, angular, rough textured, hydrophilic aggregate requires more binder for equivalent material voids than does a coarse, rounded, smooth hydrophobic aggregate. Conversely, the former aggregate mixture will produce more material voids at equivalent binder content than the latter. When preparing bituminous materials of various aggregate properties it is most difficult to produce specimens of equal binder and void contents. If this were done by means of varying the compactive effort subjected by the material during sample preparation, results of service lives under repeated loading would be meaningless since some mixture would be considered rich while other would be considered dry. If mixtures were prepared with practical binder contents then the results of repeated loading tests would be masked by the effect of binder and void content.

Controlled-stress testing by Jiminez and Gallaway (113), using the diaphragm apparatus, have shown that for continuously graded mixtures of both rough textured granite and smooth textured sand, an optimum binder content exists for maximum material fracture life. At an optimum binder content of 7½% the granite mixture produced a fracture life five times that of the gravel mixture at its optimum of 6%. At a common binder content of 6% the gravel aggregate mixture showed an increase in fracture life of 1.3 over the granite aggregate mixture at 7% the effect was reversed with a granite fracture life ten times that of the gravel. Material voids were not presented. The difficulty of assessing mixture performance is adequately illustrated in this example.

In stress-controlled rotating bending tests on gap-graded wearing course asphalts, Pell and Boyd (123,140) have studied the effect of aggregate grading on fracture life. With constant aggregate type, derived strain/fracture life lines were found to be parallel but the lower stone content mixtures exhibited longer lines. These lower stone content mixtures did, however, contain greater quantities of binder. Pell and Taylor (123,125) have continued this investigation on gap-graded base course asphalts and for common measured strains report no increase in fracture life for different aggregate types. With an increase in fineness of the sand fraction at constant binder type and content Pell and Taylor have reported an increase in fracture life. At 6% sand passing a number 200 mesh sieve a fracture life ten times that with no passing 200 mesh sand was found, and was doubled with 14% sand passing a 200 mesh sieve. On a basis of measured strains, materials with greater than 6% of sand passing

a 200 mesh sieve produce a typical logarithmic relationship, allowing for slight variations in material voids. Mixture with less than 6% of sand passing a 200 mesh sieve exhibit higher material voids and corresponding reduction in fracture lives. A similar trend is reported for various quantities of limestone filler, changes in lives being attributed to material voids and stiffnesses. Bazin and Saunier (114) have studied the relative behaviour of sandsheet, rolled lean and crushed dense materials in stress-controlled flexure tests using the trapezoidal shaped specimens described previously. Longest fracture lives at a common initial strain were associated with the sandsheet and shortest fracture lives with the lean mix. However, the sandsheet binder content was 9.5% while that of the lean mix was 4%. Voids were higher for the sandsheet at 22.2%, being 14.4% for the lean mix. In this case it is not possible to assess the relative contributions of binder content and aggregate grading (if any) to fracture life.

Four-point stress-controlled bending tests by Epps (131), have shown no statistical evidence of any effect on service life of either aggregate type or grading for common binder and test conditions. In this investigation Epps took care to maintain constant void contents throughout the range of materials examined by adjusting the comparative effort to suit the aggregate covering a range of fineness in continuous grading. The tests to assess the effect of aggregate type were conducted on materials whose binder contents were such that equal California stabilities were obtained. The variation in binder content was, however, within $\frac{1}{2}\%$.

Monismith (150) has reported greater service lives for materials composed of crushed granite than for those of uncrushed gravel. The granite mixtures, however, contained more bitumen than the gravel mixtures. These tests were carried out in the strain controlled 4-point bending spring bed apparatus.

Kirk (151), testing in strain-controlled 4-point bending, has shown that the relationship between the strain at a service life of 1.10^6 cycles and ratio of volume of binder to volume of voids, is independent of aggregate type and grading. Kirk states that it must be concluded that the effect of aggregate type and grading has only negligible effect on service life.

CAUSE OF INFLUENCE OF MIXTURE AND TESTING VARIABLES ON SERVICE LIFE

Since the stiffness of aggregate particles in a bituminous material is extremely large compared with the stiffness of the binder, it is reasonable

to assume that the strain in the material is accounted for by the strain in the bitumen. The postulate of Pell (136,139), that the service life of a bituminous material subject to repeated applications of loading is dependent upon the strain in the binder, is now widely accepted.

Considering an idealized case of stress-controlled testing, where no change in stiffness and hence strain occurs during the test. If service life is defined as the number of loading cycles to crack initiation, then for a particular material a common relationship would exist between service life and strain. This relationship would be common for all testing conditions and would be peculiar to the method of testing employed.

The results of stress-controlled testing by many investigators have indicated that a common relationship does not exist between initial strain and service life. At a particular initial strain longer service lives are generally found for materials produced with less stiff bitumens. The less stiff bitumen may be a result of the bitumen grade or of the testing conditions. This trend is confirmed in strain-controlled testing where longer service lives are associated with softer bitumens, higher testing temperatures or lower testing frequencies. Pell (136,139) has pointed out that service life, however defined, will include a certain amount of crack propagation. At a common initial strain lower stiffness materials will be subjected to lower stresses. Since the rate of crack propagation is dependent upon the stress level prevailing, being greater with higher stresses, it follows that the rate of crack propagation will be greater for stiffer materials. Pell attributes increases in service life for less stiff material to the reduced rate of crack propagation.

This crack propagation theory of Pell may be used to explain certain other phenomena found in stress and strain/service life relationships. It was reported earlier in this Chapter that logarithmic plots of initial strain against service life, for both stress-and strain-controlled testing, showed that the service lives of stiffer materials were less sensitive to changes in strain. At higher material stiffnesses crack propagation time is very short and so service lives are very little longer than the number of cycles required to cause crack initiation. As mixture stiffness is reduced a greater proportion of the service life is due to crack propagation resulting in a greater sensitivity of service life to changes in strain. The significance of crack propagation is illustrated by Pell (139) with strain-controlled torsional tests on sandsheet specimens of constant mixture composition. At temperatures of between $-20^{\circ}C$ and $0^{\circ}C$ very little difference in service life was observed at a common strain implying almost instantaneous crack propagation. At a strain of 4.10^{-4} in/in the service

life at +40°C was 1000 times that of the low temperatures. A close study of the fracture planes and surfaces of the sandsheet and pure bitumen specimens, tested in bending, has been shown by Pell to reveal an increased crack growth at higher temperatures. It would appear, therefore, that the stress level prevailing affects not only the rate of crack propagation, but also the amount of crack growth before failure.

In stress-controlled testing it has been widely reported that the longer service lives of stiffer materials are more sensitive to changes in stress than the shorter lives of less stiff materials. Heukelom (73) has shown that under conditions where the binder behaves more elastically and hence less viscously, the number of cycles required to induce fracture is increased. An increase in slope of the logarithmic plot of stress against service life (with stress as the abscissa) would therefore indicate a greater degree of elasticity at lower stresses as bitumen stiffness is increased. This in turn would indicate non-linearity, or stress dependency of the material. Taylor (124) has continued this argument by observing that a greater dependence of service life on stress level is evident with non-linear materials than with linear materials.

The effect of binder content on service life is self explanatory in the light of the strain in bitumen concept of Pell.

Pell and Taylor (125) have shown the effect of void content on the fracture life of gap-graded base course asphalts. This relationship may be employed to predict (at a datum void content) the fracture lives of similar gap-graded type materials with various void contents. If this operation is performed on the fracture life results of specimens of mixtures of varying binder contents, a predicted relationship between binder content and service life at zero voids may be obtained. On plotting stiffness against the logarithm of the corresponding equivalent service life for zero mixture voids at each binder content, a linear relationship is obtained. The strain in bitumen concept of Pell, then, applies to mixtures of varying binder content. Under testing conditions of controlled stress, the reduction in service life resulting from a reduced material stiffness at higher binder contents, is far less than the increase in service life resulting from the binder strain. An increase in mixture voids will reduce stiffness which will in turn reduce the potential service life of a void-less material. The void content will further reduce the potential service life. The effect of voids in service life is therefore very significant.

The presence of voids in a bituminous material has two distinct effects on material performance. First they reduce the cross-sectional

area of load bearing material thus increasing the stress. Secondly, they act as stress raisers. Pell (139) has reported some correlation between the size of surface voids in pure bitumen under strain controlled torsion and the fracture life at low temperatures. Epps (131) has shown, by means of the Ingles (154) equation for stress at crack or void edge, that both the size and shape of voids influence the magnitude of stress concentration. Epps has stated that the more elongated the air void, perpendicular to the applied stress, the greater the stress concentration at the tip. Gap-graded materials with rounded aggregate fines are suggested by Epps to contain smaller more rounded voids than continuously graded materials with angular aggregates. The former materials produce longer service lives for equal void contents.

As stated earlier, results of repeated loading trials on bituminous compositions suggest that the shape, texture and grading of the aggregate affect service life only insomuch as they define void content, void shape and binder content.

CAUSE OF INITIATION OF FAILURE PROCESSES

Pell (139) has used the theories of crack initiation and crack propagation to explain the various phenomena associated with the behaviour of bituminous materials under the action of repeated loading. These theories have also been employed above to explain the evident effects. The cause of crack initiation has not, however, been discussed.

Bituminous road materials are inherently inhomogenous and crack initiation will occur at the weakest point(s) where strain-raising flaws give rise to local stresses in excess of the breaking strength of the binder. Andrews (155) has stated that these flaws may occur as either physical discontinuities such as crack (or air voids), discontinuities of elastic modulii such as particles of material embedded in the matrix of a second, or irregularities in the ordering of atoms such as discolations in a crystal lattice. Clearly, there are many potential stress-raising flaws in bituminous materials.

Cracking in a bituminous material, subjected to repeated application of load, may be initiated by changes in the stress-raising flaw conditions such that critical local stresses occur. Unless the shapes of voids are altered, for example by compaction or other particle reorientating effects, crack initiation must be induced by changes in the rheological nature of the

binder. Alternatively, cracking may be initiated from the very first application of load and service life is then a measure of the rate of crack propagation before "failure."

It is accepted that in metals and crystalline bodies the initiation of cracking due to stress fluctuations is due to localized slip and plastic deformation. Majidzadeh et al (144) have stated that, while the induction period of crack initiation in metals may account for a major portion of the fracture life, in alloys crack initiation occurs at the first cycle of loading. In this case of polymers Majidzadeh et al feel that it is reasonable to assume that crack initiation also occurs at the first cycle of loading. This is due to the abundance of stress-raising flaws in polymers - and more especially in bituminous materials - which also occur in alloys.

Pell (139) has shown that at low temperatures where the binder stiffness is relatively high, the fracture lives of sandsheet materials tested in strain controlled torsion are similar for equal strain amplitudes, It is likely, therefore, that at these low temperatures the pattern of rate of crack propagation is approximately constant and crack initiation at the first cycle. The effect of temperature on service life is then a measure of the average rate of crack propagation under the various stress and temperature conditions prevailing.

Many investigators have found that in stress-controlled testing, the relationship between service life and initial strain is independent of frequency of loading. This indicates that the crack initiation (if any) and crack propagation are time-independent functions.

The rate of crack propagation is dependent upon the energy balance at the tip of the crack. Heukelom (73) has shown that the energy dissipated by the delayed elastic strain determines the rate of crack propagation. Heukelom has shown that for pure bitumen:-

$$\left(\frac{\varepsilon_d}{\varepsilon_b}\right)^2 = \frac{S}{E-S} \cdot \frac{K}{\sqrt{N}}$$

where ε_d = delayed elastic strain in repeated loading

ε_b = delayed elastic strain in static test to failure

S = bitumen stiffness

E = elastic stiffness of bitumens

N = number of load repetitions.

The constant "K" has been found to be dependent upon the method of testing employed. A value of 40 is quoted for stress-controlled cycling and about 50 for strain-controlled cycling depending upon the criterion of failure. In the (hypothetical) case of an elastic bitumen, fracture will

not occur. For a viscoelastic bitumens failure will always occur after a finite number of cycles and there is therefore no suggestion of a "fatigue limit".

Andrews (155) and Majidzadeh et al (144), have stated that where plastic deformation occurs, the radius of curvature of the crack tip is increased, resulting in a slower rate of crack propagation and, hence a longer fracture life. This supports the evidence of several investigators that longer fracture lives are associated with more viscous binder conditions at equal strain.

A deterioration in the rheological properties of the binder may also cause the initiation of cracking in a bituminous material subjected to repeated applications of load. If the local stiffness of the binder is reduced to its breaking strength then cracking will initiate and propagate at a rate dependent upon the testing conditions prevailing. If the rheological changes in the binder were similar at low temperatures and crack propagation time was instantaneous, then the finding of Pell (137) described earlier could equally well be described by this behaviour. No evidence has been found of any literature pertaining to any aspect of this possible phenomena.

EFFECT OF COMPLEX LOADING ON SERVICE LIFE

The review of previous work so far has been concerned with the behaviour of bituminous road pavement materials under the continual repeated applications of load. These tests have been controlled either by stress or strain limits and the control function has been kept constant throughout the period of test. A limited number of studies have been carried out by certain research workers to investigate the effects of cumulative damage, rest periods and long term effects on bituminous materials.

Cumulative damage - A brief study of the effect of cumulative damage on the behaviour of dense asphaltic concrete has been performed by Shelly (153) using the spring base, single point, strain controlled bending test equipment developed by Monismith (148) described earlier. Reporting the work of Shelly, Deacon (141) states that only three levels of strain were studied, each block being imposed for 7500 applications. Shelly has tentatively concluded that the linear summation of cycle ratios hypothesis of Bradbury (156) (also known as Miner's hypothesis) may well be valid for bituminous mixtures. This hypothesis states that at failure

$\sum \frac{n_i}{N_i} = 1$ where n_i is the number of applications of strain ε_i and N_i is the number of applications of strain ε_i resulting in failure under conditions of simple continuous loading.

This work has been extended by Deacon (121,141) using four-point bending. Load has been applied over a period of 0.05 seconds, held for a further 0.05 seconds and the beam specimen then returned to its original unflexed position. This controlled stress testing was performed on dense asphaltic concrete specimens at +25°C and at frequency of 100 applications per minute. Deacon has shown that a Miner hypothesis was applicable and is expressed in the form:

$$N_s = \frac{N_s(K)}{\sum p_i \left(\frac{\sigma(K)}{\sigma_i}\right)^b}$$

where N_s = service life in compound loading

$N_s(K)$ = service life at stress $\sigma(K)$ in simple loading

p_i = proportion of load duration at stress σ_i

b = slope of relationship log. N_s x log. σ for simple loading.

Deacon has shown that the service life of a decreasing stress sequence of loading exceeds that of an increasing stress sequence where the longer of the two stress levels is applied for less than 20% of the fracture life. Otherwise the above relationships describe the behaviour adequately. Further tests by Deacon on both random and block loading showed no significant differences in service life for these two conditions of loading. The material, therefore, shows no stress history effects. Work is currently being undertaken at Nottingham University to study the effect of cumulative damage in stress-controlled rotating bending.

Rest periods - The effect of the rest periods on the service life on a sandsheet material tested in pure rotating bending has been reported by Pell (139). Specimens have been tested at 0°C and run to one half of their predicted life. Specimens were rested for up to 24 hours at room temperature and others for one or two hours at +40°C. In no case was any beneficial effect found to service life. Testing gap-graded materials in rotating bending at +10°C, Taylor (124) has run specimens for periods of $\frac{1}{2}$, $\frac{1}{3}$ and 1/10 of their predicted fracture lives resting them overnight at a temperature of +30°C. In agreement with Pell no increase in predicted service life was found.

Stress-controlled testing by Monismith et al (147), using the

spring-base three point bending apparatus of Monismith, has shown no beneficial effect on rest periods between individual applications of load. It should be remembered that in this testing method duration of loading was 1 second and testing frequencies did not exceed 30 applications per minute. Therefore, in no case was the period between loading cycles less than 1 second. Monismith et al have found this non-beneficial effect for a variety of materials tested at $+25^{\circ}C$.

Bazin and Saunier (114), testing trapezoidal dense asphaltic concrete and sandsheet specimens in stress controlled flexure at $+10^{\circ}C$, have shown significant increases in service life after periods of rest. In this form of test dynamic strain was found to increase slowly throughout the test until a few cycles before fracture when a rapid increase in strain was observed. Tests were carried out and stopped when this increase in strain just prior to failure was achieved. Specimens were then left to rest, at room temperature, either in a vertical or horizontal position. After a predetermined rest period, ranging from a few hours to 100 days, specimens were retested to failure. Bazin and Saunier have found that for the dense asphaltic concrete specimens, stored vertically, the second test run produced lives 20% of the first run after 6 hours, 60% after 1 day, 100% (complete recovery) after 15 days and 110% after 100 days. For the asphaltic concrete specimens stored horizontally a second test produced lives of between 10% and 20% of the first run. Increases in rest periods above 1 day did not increase the fracture lives of the second test runs. All the sandsheet specimens were stored vertically and here a 25% life was found after a 1 day rest, 50% after 10 days, and 110% after 100 days. The greater healing effect of those specimens stored vertically is attributed by Bazin and Saunier to the stress imposed by the dead weight of the specimen on the potential fracture surface. It was concluded that the rate and degree of healing is dependent upon the temperature, time and applied stress during rest and upon the mixture composition.

Pell (139) has reported further results of tests on sandsheet materials in strain controlled torsion. As was the case in pure bending, no increase in fracture life was found in sandsheet specimens rested overnight at room temperature. In the case of pure bitumen specimens in torsion at $-4^{\circ}C$ an increase in life was found when run for half the predicted life and rested for 17 hours at $-4^{\circ}C$. Mean lives were increased from a predicted life of $1.24.10^{6}$ cycles to 1.9410^{6} cycles. Bitumen specimens rested for the same period but at room temperature showed a mean life of $7.5.10^{6}$ cycles.

Strain-controlled testing in four point bending reported by Kirk (151) has shown that for tensile strains applied over a period of 0.02 seconds and a rest between each cycle of about 0.5 seconds, increased lives are associated with higher test temperatures. The logarithmic relationships between strain and service life are linear and parallel for all test temperatures. At a common strain level the service life at $0^{o}C$ was found to be ten times the life under simple loading and at $+25^{o}C$, 300 times that of simple loading.

It would appear from the foregoing that rest periods have a beneficial effect on the service lives of dense bituminous materials. The healing process is accelerated at higher storage temperatures and higher compressive stresses. The fact that Pell and Taylor have apparently found less evidence of healing is undoubtedly due to the definition of service life employed. The test methods of both Bazin and Saunier and Kirk enabled the potential service lives of specimens to be accurately assessed. In the test methods of Pell and Taylor, only an average predicted service life based on previous test specimens was available on which to assess any increase in service life with rest periods. The assessment of increased life is therefore open to significant inaccuracy.

EFFECT OF LONG TERM BINDER HARDENING

Bituminous binders are known to harden with age due to oxidation and loss of volatile oils resulting in more viscous, brittle properties. Heating or working of a binder will reduce the viscosity and arrest the hardening process. Vallerga et al (157) have suggested that embrittlement of lightly trafficked cul-de-sacs is due to hardening. This effect is not found in more heavily trafficked pavements since stresses imposed during loading tend to break down any hardening structure that might tend to form.

Monismith and Secor (158) have shown that although the viscosity of a bitumen may increase by a factor of 4 after 3 days and 7 after 18 days, the original viscosity is regained upon heating. Further, repeated loading tests on materials made with this type of binder showed no increase in service life at various ages up to 10 days.

The effect of bitumen ageing has also been studied by Vallerga et al (157). Specimens of dense asphaltic concrete have been tested in the four point stress-controlled system of Deacon (141). Materials have been produced with bitumens of 85, 64, 42 and 13 penetration and also with

batches of a 120/150 penetration bitumen aged in a rolling thin film over at 165°C, also to penetration of 85, 64, 42 and 13. Results of repeated loading tests indicated one common line for all aged bitumen materials when initial strain was plotted against service life. On logarithmic scales these relationships were found to be linear. At an initial strain of 1.10^{-3} in/in no difference in life was found between the service lives and the aged and unaged bitumen materials. At an initial strain of 2.10^{-4} in/in the service lives of the aged bitumen mixture lives were almost double those of the unaged bitumen materials.

Since harder bitumens of similar grade have also been reported by Epps (131), Monismith (150) and Kirk (151) to produce longer service lives, it is concluded that bitumen hardening does increase the service lives of bituminous road pavement materials under the action of repeated applications of load.

STATIC PROPERTIES OF CONCRETE

FACTORS CAUSING INTERNAL STRESSES

Upon cooling after hot mixing and compaction, bituminous materials may be subjected to internal stresses due to the differential thermal contractions of the constituent components. However, due to the viscous nature of bituminous binders, being more fluid when differential movements are greatest, it is most unlikely that any internal stresses will be evident in the material prior to external loading.

Unlike bituminous materials, however, it is well known that prior to loading, internal stresses are set up in concrete due to both curing and shrinkage.

Curing - After a concrete has been mixed and compacted the continual process of hydration of cement results first in setting and secondly in hardening of the concrete. Since hydration cannot occur in the absence of water, fresh concrete is kept moist for at least 24 hours after placing and left for a further period, generally a minimum period of 7 days before loading. During this initial curing period, internal stresses are set up within the structure, although it will be appreciated that the secondary curing, or ageing, period extends over many years during which time internal stresses will continue to be set up although diminishing in magnitude.

Hansen (166) has stated that an expansion of the cement paste is due to hydration of the cement oxides whilst Serafim and Guerreiro (167) simply attribute it to the volume of absorbed water. The expansion of the cement paste results in internal compressive stresses in the concrete. These compressive forces acting on the aggregate particles may well induce tensile stresses elsewhere in the cement matrix resulting, possibly, in microcracking.

Shrinkage - Once a saturated concrete is exposed to the atmosphere a drying-out process commences. The migration of water from the gel pores results in negative pore water pressures causing tensile forces to be set up in the cement matrix. Meyers et al (168) have stated that this process will continue not until the specimen is completely dry but rather until a state of hydraulic equilibrium is achieved. This explains the presence of free water in a nominally dry concrete, the significance of which will be illustrated in section headed 'Rest period and healing' later in this chapter. These tensile shrinkage stresses may result in bond cracks between the coarse aggregate and the sand cement matrix or between the sand and the cement paste or in microcracks within the cement paste itself. Once formed, these cracks act as potential stress raisers and may be the cause of cracking in roadbase construction where relatively high tensile forces are present.

CREEP

From the instant a load is applied, concrete will deform, at a decreasing rate, almost indefinitely. The total deformation at any period of time is equal to the sum of the instantaneous recoverable elastic deformation, the time dependent recoverable delayed elastic deformation and the time dependent non-recoverable creep deformation. Creep is not analogous to viscous flow in bituminous materials since the rate of deformation under constant stress decreases with time. Further, as will be shown below, unlike viscous deformation, creep is a semi irreversible process.

The term creep is often used loosely to include the delayed elastic deformation of concrete. Illston (169) has attributed the delayed elastic effect to the interaction between the solid and fluid phases of the concrete mortar. Although referring to the delayed elastic deformation as primary creep, Glucklitch (170), like Illston, stresses that this and creep are the result of two entirely independent mechanisms.

In their review of literature on creep, Fluck and Washa (171) have found creep attributed to four effects. First, the closure of internal voids, presumably equally applicable in tension as in compression, secondly, viscous flow of cement paste, thirdly, crystalline flow of the aggregate, and fourthly, migration of water from the concrete. Illston (169) also includes microcracking as a cause of creep.

Ward and Cook (172) describe the mechanism of creep as being related to the movement of physically bound water in the gel structure and attribute creep deformation to progressive microcracking. Rehbinder, Schreiner and Zhigach are quoted as finding that the absorption of liquids will cause microcracks to propagate and that tensile creep is higher than creep in compression due to accelerated cracking. The microcracking component of creep has been stated by Meyer et al (168) as propagating from bond cracks or matrix cracks initiated by curing and shrinkage. Cracks do not initiate under creep conditions, but will propagate from cracks initiated on the application of the creep loads.

Both Neville (173) and Glucklich (170) suggest that the viscous component of creep is due to the viscous nature of the cement paste resulting in a gradual transfer of load from the matrix to the aggregate.

Mobility of free water has been offered as a reason for creep and Glucklich (174) has outlined three reasons why this creep component is non-reversible. First, under the action of external forces, free water may be diverted to undersaturated zones. This water is then firmly bound by high adhesion forces augmented by the gel structure. Secondly, water expelled to the atmosphere by external forces is not recovered upon removal of the load. This restricts the reformation of the original shape since the meniscuses formed at the free end of the capillaries. Thirdly, water displaced by an external force may be used for further hydration. The mobility of free water theory has also been proffered by Slate and Meyer (159) and the finding of Neville (173), that creep is greater in a drying concrete than either a wet or dry concrete, supports this. Further, McHenry (175) has found that creep deformation is reduced with concrete age when moisture movement is inhibited.

Illston (176) has found that the rate of creep in tension is considerably more than that in compression under similar conditions. Up to 50% of the ultimate loads, creep deformations in both tension and compression have been found to be proportional to the applied stress.

Fluck and Washa (171) in their review of literature on creep of concrete have found that creep is increased with lower heat cements and

that, whereas it is increased with increasing cement particle size for low heat cements, it is reduced with increasing cement particle size for normal portland cement. Creep is increased with decreasing maximum aggregate size and increasing mixture voids. Creep is also increased with increasing aggregate adsorption, water cement ratio and cement volume. Although the curing conditions were found to have no significant effect on creep, creep was increased in testing conditions which accelerated drying. Creep was found to be reduced with increasing hydration of the cement paste. Finally, although creep has been found to increase with increasing applied stress level, creep has been found evident at stress levels as low as 1% of the maximum bearing stress.

All the foregoing factors have been found to apply to concrete tested in tension, torsion, bending and compression. Creep is greater under the action of uniaxial tension than under uniaxial compression during the initial stages of a creep test, although ultimate values of creep deformation in tension and compression are similar.

In view of the proposed mechanisms of creep outlined previously, the factors increasing creep deformation are all as would be expected.

In applications of structural concrete creep is generally a problem. However, in roadbase construction, where settlement of the underlying layers would result in high tensile stresses in the underside of the unsupported concrete, creep may well be a desirable concrete characteristic. The foregoing factors suggest ways in which creep in dry lean concrete roadbase materials may be encouraged.

MODULUS AND STRESS/STRAIN RELATIONSHIPS

Attempts have been made to define the instantaneous elastic modulus of concrete by mathematical expressions.

Hansen (177) has reported Chetdeville and Dantu as proposing, for uniform mixture strain:-

$$E_{conc} = V_{mortar} E_{mortar} + V_{agg} E_{agg}$$

where V = volume concentration

E = elastic modulus

Hansen suggests that for uniform mixture stress:-

$$E_{conc} = \frac{1}{\frac{V_{mortar}}{E_{mortar}} + \frac{V_{agg}}{E_{agg}}} \qquad \text{where } E_{agg} > E_{mortar}$$

Hansen reports Ishai as suggesting that:-

$$E_{mortar} = (1 + KV_{agg})\, E_{cem.paste}$$

and Powers

$$E_{cem.paste} = V_{gel}^{3} \cdot E_{gel}$$

The four foregoing relationships assume no bond between the aggregate and the mortar.

From the relationships of Einstein, $\eta_s = \eta\,(1+2.5v)$ Hansen has shown that $E_{conc} = E_{mortar}\,(1+2.5V_{agg})$ is a fair approximation for aggregate concentration up to 60% Thereafter, Hansen suggests:-

$$E_{conc} = \frac{E_{mortar}}{1 - V_{agg}}$$

The stress-strain relationship of concrete is generally accepted as being non-linear, stiffness, as defined previously, decreasing with increasing stress or strain. In fact Grimer (182) has suggested that there is no reason why the stress-strain relationship should be linear since external deformations are not necessarily indicative of internal deformations.

Johnson (178), reviewing the results of uniaxial and flexural tests on concrete, has found that when plotting the ratio of stress to ultimate stress, against the ratio of strain to strain at ultimate stress, a non-linear relationship is obtained. For uniaxial tension this curve is defined by a strain ratio of $40 \pm 3\%$ at a stress ratio of 50% and is independent of mixture parameters. Johnson has also found near-linear relationships to exist between the ultimate strengths of uniaxial tension, indirect tension and flexure tests. The relationships between these and uniaxial compression was found to be non-linear.

Glucklich (170) and Illston (176) have suggested that the stress-strain relationship for concrete is linear for instantaneous loading conditions and that the practical non-linearity is due to delayed elastic deformation. Non-linearity has been attributed by Plowman (179) to creep and the stress-strain slope is therefore a function of rate of application of load near the ultimate failure stress. On 4 inch diameter cylinders 12 inches long subjected to axial compression, Plowman has found the stress-strain relationship to be linear for up to stress ratios of $\frac{1}{3}$.

Barnard (180) and Popovics (181) both attribute non-linearity of the stress-strain relationship to progressive microcracking due to excessive local tensile strains. Popovics has found that non-linearity

is greater for concrete than for mortar and greater for mortar than cement paste. This suggests, possibly that the majority of microcracking is due to a breakdown in bond between the coarse aggregate and the mortar.

Grimer (182) has suggested that when reduced to ratios "stress to maximum stress" and "strain to strain at maximum stress", the stress-strain relationship may be considered a power law curve. Grimer considers concrete as a diphase system with a discontinuous aggregate phase in a continuous matrix phase. Due to the different modulii of the phase- a system of internal stresses is induced under the action of external loading. These internal stresses result in progressive tensile microcracking leading to non-linearity and plasticity of the material. Lower modulii aggregates have been shown to produce more linear stress-strain relationships and Neville (183) has also found greater linearity with increasing matrix strength.

Plastic-type materials withstand considerable loads at strains well in excess of that at maximum stress. Grimer (182) has found that for concrete made with a variety of aggregate types, at double the strain at maximum load, 75% of this maximum load is still withstood by a gravel aggregate concrete and 40% with an artificial "Lytag" aggregate concrete.

STATIC FAILURE MECHANISM AND STRENGTH

The failure mechanism of concrete has been shown by Oladapo (184) to be the result of a gradual build up of microcracks, attributed to bond failures between the coarse aggregate and the mortar. The critical stage is that at which the microcracks propagate to such an extent that they link up to form a continuous network. Since this cracking is random Oladapo states that overall strain at failure is not a constant. Oladapo attributes bond cracking to the difference in modulus between the mortar and the aggregate. Further cracking linking up to form the ultimate crack network may result from cracks in the mortar and rupture of the aggregate (sic.).

Baker (185) and Anson (186) consider that the aggregate forms a lattice in the weaker mortar. Failure is then a result of the breakdown of the lattice leading to excessive tensile stresses in the mortar, or by a failure of the aggregate-matrix bond.

Ackroyd (187) has also supported the foregoing theories in stating that since results of undrained tests in triaxial compression do not obey Coulomb's law, cohesion and angle of friction cannot be considered as basic parameters.

Confirmation of the bond failure mechanism has also been claimed by Scholer (166). Here, mortar has been cast on to a plain rock face and it

was found that when tested wet, the factors influencing bond also influenced the strength of concrete made with the same rock as aggregate. These tests were performed on wet specimens since it was considered that drying, causing shrinkage cracks, would affect the results. Scholer has not, in fact, studied the effect of shrinkage on his results.

Jones and Kaplan (188), studying the effect of aggregate type on the strength of concrete cubes and beams, have also attributed failure to a breakdown in adhesion between the coarse aggregate and cement. It was found that cracks first appeared in cubes produced with gravel aggregate at 49% of the ultimate stress whereas with crushed limestone aggregate cracks did not appear until 69% of the compressive strength. After cracking, Jones and Kaplan have found that the mechanical interlock of the aggregate particles contributes to the strength of the concrete cubes. The crushing strength of lean mix concrete cubes is well in excess of that of plain mortar cubes. In flexure the only property of the coarse aggregate relevant is that which determines the aggregate/cement matrix bond. Further, Jones and Kaplan report that the flexural strength of concrete is less than that of the mortar.

Failure of concrete on a crystalline scale has been studied by Reinius (160) who states that (in 1956) very little is known of the internal mechanism of concrete. Reinius postulates that load is transmitted from one aggregate particle to another by the crystal lattice. Mortar failure is initiated in a concrete specimen subjected to compressive loading when the tensile strength of the lattice crystals perpendicular to the direction of load is exceeded. Cracks will form parallel to the direction of application of load. Under the application of hydrostatic compression failure is due to the exceedence of the compressive strength of lattice crystals. Further, if a specimen of concrete is compressed in direction x then some crystals in the perpendicular directions y and z will fail in tension. The modulus of elasticity in the z- direction is then reduced due to the fractured crystals in the y-direction. This theory has been substantiated by experimental results.

It has been pointed out by Bresler and Pister (189) that the strength of concrete is a function of the state of stress and cannot be predicted by limitations of tensile, compressive or shearing stresses independently of one another. The ultimate stress at failure is therefore dependent upon drying conditions, restraint of movement, settlement, duration of loading and stress history.

Krishnaswamy (190) has subjected 4-inch cubes to both uniaxial and triaxial compressive loading. A microscopic examination of sections was made at various proportions of the predicted ultimate strength. Cracking was found due to a separation of the individual components of the concrete and also in the mortar and aggregate. An increase in compressive strength of a factor of 6 was found when a bilateral stress equal to one quarter of the ultimate uniaxial compressive strength was applied. The strength gain was progressively less as the confining pressure was increased.

A review of multiaxial stressing of concrete has been presented by Kupfer et al (191) who have found reports of strength increases in concrete subjected to hydrostatic compression of between 80% and 350%. Testing 8 x 8 x 2 inch concrete slabs in biaxial stress Kupfer et al have found an increase of 27% over the multiaxial strength. The ultimate strength was found to be less in compression with a normal tensile stress. Further, the biaxial tensile strength was found to be identical to the uniaxial tensile strength.

The effect of test method on the strength of concrete has been discussed by Wright and Garwood (192). A review of work on the relationships between various test methods, has been shown by Popovics (193) to suggest that the ratio uniaxial tensile strength to flexural strength is 0.56. This relationship is independent of magnitude of strength. Further, the ratio flexural strength to compressive strength is in the order of 0.20 which increases slightly with decrease in strength. Other investigators suggest the ratio is equal to $\frac{10}{f_c}$. However, the two ratios indicate that one may expect a tensile strength in the order of one tenth of the cube strength.

The ultimate tensile and compressive strengths of concrete have been found by Johnson (194) to be increased with decreasing water/cement ratio, increasing aggregate surface area and aggregate strength. The aggregate/cement ratio was found to have little effect on strength for paste volumes of 30% and 40% although workability is affected.

It might be expected that these trends apply equally well to dry lean concrete roadbase material. Williams and Patankar (195) have found marked increases in the compressive and flexural strengths of dry lean concrete with a granite aggregate. Workability, however, was reduced. A decrease in water content from 8% to 5% was found to increase the

equivalent cube strength from 1160 to 2270 lb/in^2 using a gravel aggregate concrete.

BEHAVIOUR OF CONCRETE UNDER REPEATED LOADING

INTRODUCTION

It is now well established that concrete is liable to show signs of distress under the repeated applications of load. Due to the brittle nature of concrete, variations of stress due to the continual fluctuations of temperature and moisture content may well combine with dynamic loading to cause failure.

In previous sections of this Chapter no reference has been made to the term "fatigue". This term has not been used,due partly to the diverse interpretations of the word, and partly to the complex mechanism of failure of bituminous materials under repeated loading. In concrete the word "fatigue" is understood to describe the failure resulting from the repeated applications of loads each smaller than a single static load which would cause failure. Although the definition of fatigue in concrete is the same as that used in metal fatigue, the mechanism of failure is quite different. The ensuing review of interpretations of the mechanism of failure of concrete under the action of repeated loading will suggest that the term "fatigue" in concrete is applied rather loosely. However, in order to comply with current practice, the term "fatigue" will be used to describe the failure of concrete under the action of repeated loading. Other fatigue terminology used has the same meaning as that in mental fatigue work.

Fatigue curves for concrete are generally presented in the form stress to the logarithm of the corresponding fatigue life. "Stress ratio" is the ratio of stress range to the ultimate stress and is usually expressed as a percentage. The "fatigue strength" at a certain fatigue life is defined as the maximum stress range the concrete will withstand for this particular critical number of cycles of loading and mean stress level. The "fatigue limit" or "endurance limit" is the stress range below which an infinite fatigue life is achieved. Not all materials exhibit a fatigue limit, if stress range is plotted against $(\frac{10^4}{N})^{\frac{1}{4}}$ on linear scales a linear relationship indicates that the material has a fatigue limit. The intercept of this straight line with the stress axis indicates the value of the fatigue limit (see reference 196). Non-linear relationships pass through the origin and therefore indicate no fatigue limit.

Fatigue results of concrete are often represented by means of a modified Goodman diagram as shown in Figure 13. Here the stress ratio is plotted against an acute, dimensionless axis o–a representing the minimum stress level. For a particular fatigue life the maximum stress level is plotted vertically above the corresponding minimum stress level as described by line o–a. From a number of fatigue tests at a variety of stress ranges and mean stress levels, the envelope b–a thus produced may be used to predict the stress range at a given mean stress or at a given maximum or minimum stress level.

Repeated loading tests – The earliest investigator to study the behaviour of cement-bound materials under the repeated applications of load is reported by Nordby (197) as being de Joly (198) in 1898. De Joly has performed both compressive tests on cubes and tensile tests on dumbell shaped specimens of cement mortar. Nordby also cites the works of Van Ornum, reporting results of repeated loading tests on cubes in 1903 and Feret, who reported the results of tests on cubes, beams and cylinders in 1906.

Comprehensive reviews of investigations into the behaviour of plain concrete under the action of repeated applications of load have been presented by Nordby (197), Murdock (199) and Raithby and Wiffin (200). The majority of the work on concrete reported by these reviewers and elsewhere has been concerned with structural plain concrete. Although very little work has been reported on the behaviour of dry lean concrete under repeated loading, it may well be possible to apply or extend the results of tests on structural plain concrete to dry lean concrete used for roadbases.

The majority of repeated loading tests are performed either in compression or flexure. Although plastic deformation undoubtedly occurs during both forms of test, only the "fatigue" life is generally reported. Certain investigators have, however, presented hysteresis loops or stress/strain lines for the loading half of the cycle, at various stages during the test. It has been found that the stress/strain relationship of cycle 1, as described earlier, indicates a progressive reduction in modulus of elasticity with increasing load. After a number of repetitions of stress controlled load, the relationship becomes linear and later concave, indicating an increase in modulus with stress level. Although the modulus increases during the loading half of the load cycle, its magnitude is generally less than the instantaneous modulus of the first cycle. Hysteresis loop areas are found to reduce from cycle 1, reach a minimum value when the stress/strain relationship is roughly linear and then increase to failure. These effects have been illustrated, among others, by Van Ornum (201), Bennett (202), Raju (203) and Popovics (181).

Trott and Fox (204) have reported that after a small number of

applications of load the stress/strain relationship for concrete is more linear than when loaded under static conditions. Under static loading the onset of non-linearity occurred at a strain of $7.7.10^{-5}$in/in, whereas under dynamic loading this was doubled to $1.55.10^{-4}$in/in. In either case the magnitudes of modulus of elasticity over the linear range were almost equal at $6.2.10^{6}$ lb/in^{2}.

Linger and Gillespie (205) have been reported by Raithby and Wiffin (200) as finding that the fatigue lives for given stress ratios are equal in compression and tension. Tests on cylindrical specimens were performed in direct axial compression and indirect tension by loading the specimens on their sides. Raithby and Wiffin state that this phenomenon suggests a similar mechanism of failure both in tension and compression.

In their reviews neither Nordby (197) nor Raithby and Wiffin (200) have found any evidence of a fatigue limit in plain concrete. Kesler (206), Bennett (202) and Antrim and McLaughlin (194) have run tests for 10 million cycles and have found no fatigue limit.

Factors affecting fatigue life - Little information is available on the fatigue life of plain concrete. Of the results published it would appear that when expressed in terms of stress ratio, mixture variables have very little effect on fatigue life. Nordby(197) and Raithby and Wiffin(200) have found literature providing evidence of a slight reduction in fatigue strength for leaner mixes although the reduction is not considered significant. Antrim and McLaughlin(207) have tested 3 inch in diameter and 6 inch long cylinders in axial compression. They have found a common relationship between stress ratio and fatigue life for normal concrete with air voids within the range 0.5% to 2% and air entrained concrete with 7.5% to 10.5% air voids. Testing frequencies were between 500 and 1000 cycles/minute. Bennett (202) has also found a common stress ratio/fatigue life relationship for concrete mixes covering a range of aggregate sizes, water cement ratios and water contents.

The frequency of loading has also been found to have little effect on the fatigue life of concrete. Here, ample evidence is available to support this statement. Raithby and Wiffin (200) have found that most investigators consider that frequency affects fatigue life only insomuch as the speed of loading influences the ultimate strength of concrete. Assimacopoulos et al (208) have found that when the frequency of loading is increased from 500 to 9000 cycles/minute the internal temperature of the concrete increased from 25°C to 80°C. Fatigue life, however, was unaffected. Other investigators have found no influence from test

frequency for frequencies down to 2 cycles/minute (200).

The effect of eccentricity of loading on the fatigue strength of concrete has been studied by Ople and Hulshos (209). It was found that the fatigue strength of 6 inch diameter by 12 inch long cylinders tested in vertical compression was increased from 65% to 75%, at a fatigue life of 2.10^6 cycles, when the axial loading was changed to eccentric loading. The eccentric loading was such that the stress ranged from zero to maximum compressive stress across the circular section.

Mechanism of failure under repeated loading - Tests by Antrim (210) on cylinders of cement paste and concrete loaded axially have provided evidence to suggest that the fatigue characteristics of concrete are governed by the fatigue characteristics of the cement paste. In a review of theories of failure, Antrim has found a general agreement that cracks propagate under repeated applications of load, resulting in "fatigue" failure.

Doyle et al (193) suggest that fatigue cracks in concrete propagate from the aggregate-mortar interface in the same way as they do in static tests. Shrinkage, causing residual stress concentraions around the coarse aggregate, was not found to influence the static or fatigue strengths. Nordby (197), however, attributes crack initiation to shrinkage stresses. The longer lives resulting from wetter mixes is attributed to the less brittle cement paste and its ability to readjust its structure. This delays the built-up of stress concentrations and thus reduces the rate of crack propagation. Nordby has reported shorter lives for concrete than for equivalent cement paste specimens and suggests that this is due to bond failures in the concrete.

Murdock has found literature to suggest that fatigue failure is probably due entirely to the progressive breakdown in bond between the aggregate and the mortar.

Trott and Fox (204) have put forward the theory that there is a "limiting tensile strain" at which cracking initiates. Trott and Fox suggest that the "limiting tensile strain" under repeated applications of load is less than that under static loading conditions, although there was found to be little reliable information on this matter. Raithby and Wiffin (200) quote Hilsdorf and Kesler (211) as stating that failure of beams in flexure occurs as soon as the maximum surface strain reaches a strain of $2.5.10^{-4}$ in/in. Raithby and Wiffin point out that this conclusion was based on rather inconclusive evidence.

It was reported earlier that Bresler and Pister (189) have stated that static strength of concrete cannot be predicted by limiting tensile, compressive or shearing stresses independently of one another. On the assumption that this statement is equally applicable to fatigue failure, then the "limiting tensile strain" of Trott and Fox (204) and Hilsdorf and Kesler (211), if applicable, will be peculiar to the method of testing employed.

Although information on the matter is sparce, it would appear that the mechanism of failure in static tests is similar to that in dynamic tests. Little evidence is available to indicate whether the critical crack patterns are similar. Raju (203) has proposed that under static testing conditions the load and cracks increase simultaneously leading to failure. Under dynamic testing conditions, however, only a small amount of energy is absorbed by crack propagation in each cycle. Raju suggests that this encourages the formation of many bond microcracks leading ultimately to a critical crack network.

Cumulative damage and "strain hardening" - Hilsdorf and Kesler (211) have performed cumulative damage tests on 6 inch square cross section plain concrete beams subjected to three point bending on a 60 inch span. Tests were carried out at a frequency of 450 cycles/minute at two alternating block stress levels. On tests where the stress level was altered once Hilsdorf and Kesler found that when the higher stress level was applied before the lower stress level then the resulting life was greater than that predicted by Miner's theory. Conversely, when the lower stress level was applied first, the resulting life was less than the Miner prediction. It was suggested that on drying, shrinkage in the cement paste sets up tensile stresses in the concrete. When loaded in flexure or compression a permanent set is observed which sets up compressive stresses tending to neutralize the existing tensile stresses. This new (partially) stress-relieved system will result in a higher ultimate strength thus effectively reducing the magnitude of the stress ratio. The rate of crack propagation will be decelerated resulting in a longer life. This change of state is similar to the strain hardening process in metals.

This strain hardening effect has been observed by many investigators manifesting itself in the form of increasing modulus. Bennett (202) has found this effect in concrete specimens subjected to repeated applications of load. After 1.10^6 cycles the compressive strengths of concrete specimens were found to be over 10% higher than those in an unloaded condition.

Raithby and Wiffin (200) have cited the results of repeated loading tests reported by Linder and Gillispie (205). It was found that under alternating compressive loading both the tangent and secant modulii fell rapidly over the first 15% of the fracture life. Between 15% and 80% of the fracture life the falls in modulii were less acute until a further fall to failure. The effect was more acute with the secant modulus values. It is probable that the reduction in rate of decrease of modulii in the early stages of the test was due to strain hardening thus inhibiting crack propagation.

Rest period and healing - Each reviewer mentioned previously (197,199,200) has found reports of beneficial effects after rest periods. De Joly (198) is reported by Nordby (197) as finding a beneficial effect of rest periods on mortar cubes in 1898.

Hilsdorf and Kesler (211) testing plain concrete beams in three-point bending have studied the effects of rest periods. With no rest periods a linear relationship was found between the stress ratio and the logarithm of fracture life. At a stress ratio of 85% the fracture life was found to be 1.10^2 cycles and at 62%, 1.10^7 cycles. Further specimens were tested for 4500 cycles (10 minutes cyclic loading) then rested for a predetermined period. This was repeated until failure. The predetermined periods were 1, 5, 10 20 and 27 minutes. It was found that the fatigue strength at 1.10^7 cycles was increased from 62% to 68% when the rest periods were increased from 0 to 5 minutes. For rest periods in excess of 5 minutes, no further recovery was found. In all rest period durations no change in the stress ratio/fracture life relationship was found for fracture lives less than 1.10^4 cycles.

Hatt and Crepps (212) have subjected 4 x 4 x 30 inch concrete cantilever specimens to cyclic loading at 10 cycles/minute. It was found that in general rest periods had a beneficial effect on the concrete. In one case, after 5 weeks rest a specimen exhibited almost complete recovery after being on the verge of failure.

Whitman (213) has found a considerable improvement in the compressive strength of 5 inch diameter cylinders 10 inches long subjected to a number of loading cycles in compression. Since the rest periods involved ranged from 3 days to one year it is difficult to differentiate between the effects of rest periods, strain hardening and ageing.

Menon (214) has reported complete recovery of mortar briquettes after fracture and complete separation in tension. After breaking, the fracture surfaces were tightly held together under water for a period of time.

The probable cause of strength recovery is that of autogenus healing. Autogenous healing is the process of hydration of newly exposed unhydrated surfaces of cement. These unhydrated surfaces may be exposed either by cracking or by internal reorientation of the lattice structure. Serafim and Guerreiro (215) have shown that the hydration of unhydrated free lime sets up internal stresses. These new stresses may well counteract those set up in the concrete due to repeated applications of load.

It was shown earlier in this Chapter that larger cement particles may well possess nucleii of unhydrated cement. Freyssinet (163) has suggested that upon stressing the lattice structure will be distorted permitting a further movement of free water. Newly exposed unhydrated cement will then be dissolved in the water resulting in the formation of more crystals, thus increasing the strength of the lattice structure and hence the concrete. Reinius (160) has further stated that under the action of repeated loading the lattice crystals are progressively broken down. Therefore, if the loading is temporarily suspended and restarted the second modulus should be resumed. Since this is not the case, but the elastic modulus exceeds the second modulus then fractured crystals are being replaced (in part) by a new crystal structure.

It will be appreciated from the foregoing that concrete has a very complex structure. Although its mechanism is not yet fully understood, the theories of crack initiation, propagation, failure and healing are now generally accepted. For satisfactory dry lean concrete roadbase materials, it should be possible from the results of tests on higher strength plain concrete to encourage such factors as healing and creep by suitable mix design.

CHAPTER SIX

PRELIMINARY EXPERIMENTAL AND DEVELOPMENT WORK

METHOD OF TESTING

The stresses imposed by a loaded area on a layered system are extremely complex. Under the repeated applications of a given constant load the dynamic modulus of a member of the structure may change in value, resulting in a redistribution of stresses throughout the system. Theoretical analyses and practical results have shown that neither the stress nor the strain amplitude remain constant on any element during this process. In simple testing the decision had therefore to be made whether to adopt a stress-controlled or a strain controlled method of test.

The review of previous work has shown that the selection of the control mode is not related to any material application or position in the structure but is generally selected to suit the testing equipment employed. Stress-controlled testing is found easier to develop and has the advantage of a very well defined catastrophic failure, although it should be remembered that in practice "failure" may occur well before laboratory fracture.

Monismith (216) has suggested that for bituminous-bound layers in a road structure, the appropriate test method might be determined by the layer thickness. Monismith has presented theoretical relationships between the (maximum) horizontal stress and strain occurring at the underside of the bound layer and the modulus of the bound layer for different layer thicknesses, shown in Figure 14. It will be seen that when the modulus of the bituminous-bound layer is reduced from 1.10^6 lb/in^2 to 3.10^5 lb/in^2 the stress for a 1 inch layer thickness falls by a factor of 3.0 whilst the strain increases by a factor of 1.2. For a 4 inch layer the stress decreases by 1.8 and the strain increases by 2.2. For a 9 inch layer the stress decreases by 1.6 and the strain increases by 2.5. On the basis of these results Monismith has suggested that for layer thicknesses less than $2\frac{1}{2}$ inches strain-controlled testing is more appropriate since changes in strain are less than those of stress. Conversely, for layer thicknesses greater than 4 inches, stress controlled testing is more appropriate.

If the theoretical results of Monismith are valid, assuming a linear elastic material, then the testing limits, be they stress or strain, should ideally be altered by the amount determined by the layer thickness and transient modulus. It is felt that if the testing limits are kept constant then the specimen experiences loading patterns which deviate from practice

to such an extent that the recommendations of Monismith may cease to be well founded.

The choice of testing method may also be selected upon consideration of the behaviour of supported and unsupported slabs. If a slab is unsupported and is repeatedly loaded, as the stiffness falls the recoverable and non-recoverable deflections of the slab progressively increase until failure. In a supported slab, however, the increase in recoverable deformation of the slab will be considerably less due to the support and the slab will be forced back to its original position with subsequently no non-recoverable component of deflection. Although the roadbase layer does not conform to either of the above analogies, it might be argued that it approximates closer to the supported case, thus suggesting that a controlled strain form of test might be more appropriate.

The case for a controlled strain form of test for roadbase materials is further strengthened by the fact that the materials are far from homogeneous A reduction of stiffness is likely to be confined to local areas and the unloaded surrounding material will tend to force the local area back to its original position. Only when the reduction of stiffness in these local areas is sufficient to significantly affect the surrounding material are these conditions likely to be changed.

In view of the foregoing comments it was decided to adopt a controlled strain form of testing. Preliminary tests have been performed under conditions of controlled stress in order to detect any relationship between the lives of uniaxial and rotating bending tests using similar materials. Subsequent tests were of the controlled strain type.

SPECIMEN SIZE

In selecting the specimen size three factors were borne in mind. First, the specimen diameter should be the same as a standard core cutter in order that cored specimens might be tested, if deemed necessary, at some later date. Secondly, the specimen diameter should ideally be at least four times the maximum size of the aggregate used. Thirdly, the specimen diameter should be such that the testing machine would be capable of imposing sufficiently high stresses on the specimen. It was decided to limit the maximum aggregate size to 1 inch and adopt a 4 inch diameter specimen. This would enable a standard laboratory compactor and extruder to be used during specimen manufacture, and permit a maximum axial stress of almost 800 lb/in^2 to be imposed by the Instron testing machine.

A specimen length of approximately 8 inches was selected in order to minimize shear plane interference.

SPECIMEN COMPACTION

The necked specimens used in rotating bending, referred to earlier, have always been compacted by means of hand rodding followed by axial compression in an hydraulic jack. These specimens were predominantly of a gap-graded rich nature of relatively workable consistency. British road-base materials are generally leaner continuously-graded mixtures and it was felt that the high degree of particle interaction of the densely graded granite aggregate would result in poor compaction and possibly aggregate fracture under direct compression. The possibility of employing an automatic Proctor compactor was studied, this providing a compactive effort of 10 lb weight falling through 18 inches. The machine is designed such that the base supporting the 4 inch internal diameter mould rotates eccentrically, beneath the 2 inch diameter compacting foot, through approximately 30° after each blow. It was hoped that roadbase materials compacted by this method would have their larger aggregate particles worked into their most stable positions, as is the case with insitu rolling.

Compaction moulds, base plates and extrusion collars were designed and manufactured in steel. These are shown in Plate 1 and in cross-section in Figure 19. The automatic Proctor compactor is shown in Plate 2.

Initial compaction trials were performed by introducing the hot bituminous material into the preheated mould in three roughly equal layers. Each layer was rodded and compacted by twenty-five blows of the automatic compactor. In the preparation of dense bitumen macadam specimens designed to Ministry of Transport specifications (1), (see Table 1 and Figure 15) average internal voids were found to be 5.8% with a standard deviation of 0.5%. Average surface voids, as opposed to end voids (see below), were 6.3% with a standard deviation of 1.4%. After testing to failure it was observed that specimens fractured apparently at the interfaces of the three compacted layers.

Further specimens were prepared in both three and single layers. The latter was performed by introducing the material into the mould in approximately five layers tamping each layer with a $\frac{1}{2}$ inch diameter steel rod and then subjecting each end of the specimen in turn to twenty-five blows from the automatic compactor. Internal voids in dense bitumen macadam specimens prepared in this manner were found to be some 1% higher than the previous method at 6.7% but with a lower standard deviation of 0.3%.

(Voids of up to 10% are acceptable for this type of mix (217)). Surface voids were slighly less than before at 6.0% and with a reduced standard deviation of 0.6%.

Six additional samples were prepared, three by each of the above two methods but with the larger stone sizes picked out after mixing in order to assess any improvement in surface voids. In each method of compaction internal voids remained virtually unchanged. Surface voids in the three layer method of compaction were reduced by some 2% but reducing the maximum stone size had little effect on the surface voids of specimens produced by single layer compaction from both ends.

Density variation throughout the lengths of the specimens made by each of the four techniques mentioned above were measured by means of a radioactive scanning device developed and built by the Road Research Laboratory (218). Typical traces in Figure 16 clearly show two distinct planes of low density material in specimens compacted in three layers,, verifying the presence of planes of acute inhomogenuity. Subsequent specimen failures occurred virtually horizontally at one of these planes of weakness. Traces of specimens compacted in a single layer show the expected reduction in density towards the centre, in the order of 5% to 10%. Test fractures for these specimens were irregular and occurred in this middle third region of lower density material.

The method of compacting specimens in a single layer from both ends has consequently been adopted for all specimen preparations subsequent to this initial study.

SPECIMEN EXTRUSION

A hydraulic jack was available for the extrusion of compacted specimens from their moulds. This has two main drawbacks. First, the pumping rate is very slow and secondly the travel of the ram is less than the height of the specimen. The process of suspending jacking to insert the required packing pieces is both difficult and time consuming for a single operator. A standard soil mechanics extruder was therefore used to extrude all the bituminous specimens produced. This is shown in Plate 3.

It was required to extrude the dry lean concrete specimens one day after production and it was not felt desirable to employ the horizontal extruder used for the bituminous materials. In view of the difficulties of using the hydraulic jack referred to above, a vertically mounted pneumatic hydraulic jack was developed and is shown on the left of the hydraulic jack in Plate 4. This pneumatic jack is run from the laboratory compressed air

supply and employs the piston and cylinder of a double acting pneumatic ram with a 24 inch stroke. The ram has been converted to operate from oil, pressurised by the compressed air, in order to eliminate compressibility problems associated with pneumatic equipment.

It was not found possible to extrude bituminous specimens with this jack due to the low working pressure of the system.

SPECIMEN VOID MEASUREMENT

One of the main disadvantages of laboratory prepared specimens in relatively small moulds is the occurrence of large surface and end voids. These voids, included in an overall void content, do not represent the true internal voids, making a direct comparison with insitu values impossible.

Figure 17 shows the form in which voids are present in the specimen. It will be appreciated that, whilst the surface voids are relevant in the performance of the specimen under test, only internal voids provide a true comparison of specimen density with practical mixes. Since the end voids are filled with adhesive under test they are not relevant either to test behaviour or in a practical comparison.

It was therefore felt necessary to measure both internal voids and internal plus surface voids. The latter is achieved while the specimen is still in its mould by carefully filling each end in turn with 0.2 mm Ballotini (nominally spherical glass particles). From a knowledge of the bulk density of the Ballotini and the weight required to fill the end volumes of the mould, the volume of specimen is easily ascertained. After extrusion, weighings in air and water enable total, internal and surface voids to be determined.

Ballotini was selected because of its potentially greater reproducability of packing than sand particles. The size was chosen to provide the greatest accuracy of measurement while not possessing any cohesive properties due to ionisation of smaller particles. Further, it was estimated to have a similar viscosity to the adhesive used to bond the specimens to their end caps, thus penetrating end voids to roughly the same degree.

BONDING OF SPECIMENS TO END CAPS

It was anticipated that difficulty might be experienced in bonding specimens directly into end caps for tensile loading. It was expected that special end treatment of the specimens and possibly casting the specimens

into end caps during manufacture would be necessary.

The possibility of bonding with an epoxy resin was investigated using Araldite GY250 resin and X83/144 hardener. This epoxy resin has been specially developed for use in the repair of concrete, it is relatively viscous when mixed and will cure within a few hours at room temperature. It has the added feature that it may be applied and will subsequently set and cure under water.

An initial trial was performed bonding a pure bitumen cylinder 4 inches long and 2 inches in diameter into 2 inch diameter steel end caps used for tests on microconcrete. The end caps were gripped in a tensile testing machine and pulled apart at room temperature. In no case did the bitumen pull out of the end caps.

Prototype end caps and specimen mounting jigs were designed and manufactured in steel. These are shown in Plates 5 and 6 and details of the end caps in Figure 20. The jigs ensure that the end cap plates remain parallel to one another and perpendicular to the axis of the specimen during setting and curing. This system proved quite satisfactory and subsequent end caps were case hardened after manufacture to avoid damage during cleaning operations. The six prototype pairs of end caps were later turned down to 20 thou undersize and grooved, as shown in Plate 5, to accommodate the rubber "O" rings securing the membranes used in the testing of concrete specimens.

SPECIMEN MOUNTING FOR TESTING

End cap and load cell adaptors designed to secure the mounted specimen in the testing machine were manufactured in steel. These are shown in cross section in Figure 20 and in position in Figure 18 and Plate 7.

When mounting specimens in the testing machine, up to 15 thou inch eccentricity was sometimes detected between the perimeter of the upper end cap and that of the load cell adaptor. This is due to the limitations of the specimen mounting jig. Whereas the bituminous specimens could accommodate this amount of eccentricity with no apparent signs of distress when the upper end cap bolts were tightened, the concrete specimens tended to crack at one or other of the end caps. Ball jointed adaptors were therefore developed using 2 inch diameter hardened steel balls in mild steel cages. These ball jointed adaptors, shown in Figure 21 and Plate 8, were designed to accept end cap eccentricities far in excess of any

likely to be encountered in practice. In use the axis of the specimen will not be truly vertical but the resulting inaccuracy is considered of minor importance. These ball jointed adaptors were only employed when testing concrete due both to their relatively low load bearing capacity and to difficulties experienced with the extensometer mountings discussed later.

SPECIMEN TEMPERATURE CONTROL

The loading frame of the Instron testing machine is situated well away from air currents in a temperature controlled room. Although the scale factor of the electronic displacement transducers employed is virtually unaffected by temperature change, it was found that the null point, or electrical zero, drifts slightly with changes in ambient temperature. This is attributed to the thermal expansion of the slug spindle. It was felt necessary to protect the extensometers and specimen from draughts bringing slight variations in temperature and also from temperature rises during defrosting periods when testing at sub-ambient temperatures. This was effectively performed by placing two sheets of 1/16-inch Perspex one to the front and one to the rear of the area between the moving crosshead and the upper fixed crosshead, providing a temperature stable chamber.

A Negretti and Zambra four-channel galvanometric recorder was installed to record temperature changes in the temperature controlled room. One of the hereus resistive elements is attached to the rear Perspex guard, close to the specimen and extensometers as shown in Plate 8, to monitor temperature variations in this area.

CHAPTER SEVEN

DEVELOPMENT OF TESTING APPARATUS

SPECIMEN DEFORMATION MEASUREMENT

Extensometer mounting - Deformations of specimens under test are monitored both by 1/10 thou inch dial gauges for setting up and for visual observations and by electronic transducers for an electrical output to a permanent record. These transducers are mounted such that the slug spindles lie on a specimen diameter equally spaced from the vertical axis of the specimen. This ensures that only the average specimen deformation is recorded, any eccentricities being readily detected by means of the dial gauges.

Each extensometer and dial gauge assembly is mounted on a brass block in turn secured to a $\frac{3}{8}$ inch diameter silver steel carrier rod, as shown in Plate 7. The lower end of the carrier rod passes through a linear bearing mounted permanently on the lower end cap adaptor. The upper half of the carrier rod is tapped $\frac{3}{8}$ inch B.S.B. thread and passes through the upper end cap mounting bracket. Coarse vertical adjustment is affected by means of the two brass nuts clamping the rod to the bracket as shown in Plate 7, fine adjustment being performed electronically.

When a bituminous sample is being set up, the upper end cap remains virtually horizontal due to the stiffness of the load cell and hence the carrier rods ride freely in the bearings. It was stated earlier that the concrete specimens required a modified adaptor which would accommodate high degrees of eccentricity in the end caps. In this case the axes of the carrier rods would not be concentric with the linear bearings and so shortened carrier rods were made. The resulting free hanging extensometer assemblies are shown in Plate 8. This system has the potential drawback that slight non-vertical movements of the upper end cap, due to inhomogenuities of the specimen, might result in a wandering of the extensometer spindle with consequent loss of zero. This phenomenon was not, however, observed in practice.

Extensometer electronics - Electronic measurements of specimen deformations are measured by two Linear Variable Differential Transformer (LVDT) displacement transducers. The LVDT operates from a 24 volt direct current supply and contains an exciter which alternates the supply voltage at 2000 cycles/second. This alternating voltage passes through a primary coil and a

movable slug induces an alternating current in a secondary coil on the transformer principle. The output from the secondary coil is demodulated and is fed out as a direct current voltage, the magnitude of which is proportional to the displacement of the slug from its central null position. The output of all Schaevitz (Electro Mechanisms) LVDT's is 12 volts full scale deflection. The recommended electrical loading of LVDT's varies with range and is stated by the manufacturer. The impedence of the LVDT is in the order of 7K ohms.

Deformations of preliminary test specimens were measured by means of a single LVDT with a range of $\pm$0.400 inches and consequently an output of 15 volts/inch. Once the magnitude of specimen deformations likely to be encountered during testing had been assessed, a nominally matched pair of LVDT's was acquired each with a range of $\pm$0.050 inches (output 120 volts/inch). These LVDT's were mounted diametrically opposite one another and connected electronically in series. The electrical power from the LVDT's was sufficient to drive one channel of a Rikadenki 3-pen potentiometric strip chart recorder whose input impedence is 35K ohms. A series of π-type impedence balancing pads was designed to balance the impedences of supply and load, while alternating the signal to produce a full scale (10 mV) deflection of the recorder corresponding to 1,2,5,10,20 and 50 thou-inch overall deformation of the specimen. Recorder range was selected by means of a double pole rotary switch and zero suppression by means of 1 10-turn rotary potentiometer acting as a potential divider across the 24 volts supply. The circuit diagram is shown in Figure 23.

Early experimental work indicated the need for an accurately controlled strain cycling system. It was therefore decided to feed the extensometer output of the two LVDT's into the potentiometric recorder of the Instron testing machine. This recorder feedback potentiometer slide wire spindle is connected directly to three adjustable cams each with a microswitch. Each cam is adjusted to actuate its microswitch when the recorder pen is at a desired proportion of full scale deflection. Two microswitches control the reversing mechanism of the loading moving crosshead whilst the third microswitch activates a cycle counter. By utilising the Instron recorder limit cams to operate at given deformations this system permits cycling of specimen deformations down to some 0.1 thou inch corresponding to a specimen strain of approximately $1.5.10^{-5}$ in/in. If required this value may be reduced by adjusting the extensometer attenuation.

The load cell amplifier output, normally driving the recorder, is diverted to channel 1 of the 3-pen recorder and also to a centre off,

double pole, two-way switch. The attenuated extensometer output is also led to the two-way switch and to channel 2 of the 3-pen recorder. This switch, shown in the centre of the upper auxiliary instrument control panel of the Instron in Plate 10, enables the Instron recorder to be driven from either load cell or extensometer output, thus enabling load or extension controlled testing to be performed.

Due to the low input impedence of the Instron pen recorder, in the order of 1 to 2 K ohms, it was found that insufficient power was available from the twin LVDT's to drive both the Instron and Rikadenki recorders using the previously developed impedence balancing pads. A new system was therefore developed using a single channel operational amplifier module serving the joint functions of an attenuator and emmiter follower. Zero suppression is effected by means of a 10-turn helical potentiometer used as a trim resistor and the recorder sensitivity altered by means of suitable feedback resistors, selected by a double pole rotary switch. The circuit diagram of this system, used throughout the main test programme, is shown in Figure 24 and 25 and the control equipment in the lower auxiliary instrument panel of the Instron shown in Plate 10.

SPECIMEN TESTING EQUIPMENT

Introduction - The Instron testing machine used in this research project is a versatile testing machine capable in its standard form of performing either load or extension controlled cycling of specimens, or a simple combination of the two. Limits of load are determined by the positioning of cams connected directly to the load recorder slide wire. Limits of extension are determined by the setting of adjustable limit switches on the lead screws of the moving crosshead.

The layout of the Instron crosshead control system is shown in Figure 27. A synchronous motor drives two main drive shafts whose speed ratio is 10:1. By the selection of appropriate gears between one of these drive shafts and the driven shaft a reference transformer is rotated at a predetermined speed. A series of magnetic clutches between the driven shaft and the reference transformer enable the latter to be rotated in either direction or kept stationery. The output of the reference transformer is fed through an amplifier to the main drive motor which is geared to the lead screws of the lower moving crosshead of the testing frame. The output of a feedback generator is fed to the reference transformer acting as a pacer to ensure that the positions (rather than the velocities)

of the two units are identical. The speed and direction of the reference transformer, therefore, determine the speed and direction of the moving crosshead. The speed of the reference transformer is determined by the gears selected and its direction by push buttons on the front panel activating the appropriate clutch magnet. When the machine is set to automatic cycling the limit microswitches perform the same function as the manual push buttons in activating the clutch magnets.

A 10,000 lb load cell is mounted in the upper fixed crosshead and the specimen is connected between this and the lower crosshead. The distance travelled by the lower crosshead therefore, is equal to the sum of the deformation of the specimen and the deformation of the load cell and associated fittings. The deformation of the load cell and associated fittings in both tension and compression was found to be in the order of 1.5 thou inch/1000 lb.

If a specimen is subjected to load controlled cycling, as the stiffness falls, the specimen deformation increases, the crosshead (moving at a constant speed) has further to travel and so the frequency falls. For example, consider a specimen of 6 inch gauge length whose stiffness falls by 40% during the course of a test, with a crosshead speed of 0.2 in/min and triangular wave form:-

specimen stiffness	1.10^6 lb/in^2	6.10^5 lb/in^2
stress	100 lb/in^2	100 lb/in^2
load	1260 lb	1260 lb
load cell deformation	1.89 thou	1.89 thou
strain	$1.00.10^{-4}$in/in	$1.67.10^{-4}$in/in
specimen deformation	0.60 thou	1.00 thou
total deformation	2.49 thou	2.89 thou
frequency	40.2 cy/min	34.6 cy/min

Figure 28 illustrates the change in frequency of specimens under load controlled testing.

If a specimen is subjected to deformation controlled testing, utilising the recorder limit switches, as the stiffness falls, the load decreases, the crosshead has less far to travel and so the frequency rises. In the above example:-

specimen stiffness	1.10^6lb/in^2	6.10^5lb/in^2
strain	1.10^{-4}in/in	1.10^{-4}in/in
specimen deformation	0.60 thou	0.60 thou
stress	100 lb/in^2	60 lb/in^2
load	1260 lb	756 lb
load cell deformation	1.89 thou	1.13 thou
total deformation	2.49 thou	1.73 thou
frequency	40.2 cy/min	57.8 cy/min

This effect is also illustrated in Figure 28. Here it will be noticed that the frequency of cycling tends to level out at some 52 cycles/minute. This is due to the inertia of the testing machine. The rise in strain is due to overshoot of the system and to a change in the viscoelastic properties of the material. These aspects will be dealt with more fully in Chapter 10.

In the case of extension cycling of the specimen, by cycling between preset limits of crosshead movement, as the specimen stiffness falls, the load decreases, the load cell deformation decreases and the specimen deformation increases. In the case of the above example:-

specimen stiffness	1.10^6 lb/in^2	6.10^5 lb/in^2
total deformation	2.49 thou	2.49 thou
stress	100 lb/in^2	60 lb/in^2
load	1260 lb	756 lb
load cell deformation	1.89 thou	1.13 thou
specimen deformation	0.60 thou	1.36 thou
strain	$1.00.10^{-4}$ in/in	$2.27.10^{-4}$ in/in

The first two examples above illustrate the changes in testing frequency likely to be encountered in load- or deformation-controlled testing. The third example illustrates the limitations of the basic "extension" cycling facility of the Instron testing machine, this method of control was not pursued.

It was shown in Chapter 4 how the stiffness of a bituminous material is affected by the frequency, or rate of application of load. This factor has to be eradicated in laboratory testing in order that the behaviour of the material under stress-or strain-controlled cyclic conditions may be assessed. It was therefore endeavoured to devise a system whereby the frequency of loading could be kept constant throughout the course of the test. This would enable an accurate assessment to be made of the variation of specimen stiffness with time, or number of cycles, under conditions of controlled stress or controlled strain cycling.

Frequency modulator - The only method of controlling frequency of loading and hence rate of application of load in the present system lies in the control of crosshead speed. It has been shown in Figure 27 that under normal conditions the desired crosshead speed of the Instron testing machine may be attained by the use of appropriate gears between the synchronous drive output shaft and the reference transformer input shaft.

Utilising the synchronous output drive of the standard Instron a simple system of cone drive was devised as shown in Figure 31a. This enabled the crosshead speed to be varied from the standard speed, as determined by the Instron gears, by the ratio of the cone diameters in

contact with the jockey wheel. It was felt that a speed reduction of 2:1 would be adequate for this purpose.

An electronic monitoring system was developed and built in conjunction with the Faculty's Electronics Department, the principle of which is set out in Figures 29 and 30. The unused contacts of the Instron cycle counter microswitch are utilised in circuit to trigger an isolating relay. This output is fed to a binary (bistable) unit which serves the purpose of providing one output pulse for every two input pulses, thus eliminating any errors arising from the counter microswitch not actuating exactly midway between the cycle limits. This output is fed via a second relay to a pulse shaper and period timer unit and also directly to a computer. The output of the period timer is also fed into the comparitor. When the second relay operates, the period timer runs for a preset duration which is equal to the required time for one cycle. If the actual time for one cycle is different from the preset time then the comparitor detects the difference and an error signal is sent via power relays to the actuator motor. The actuator motor runs in the appropriate direction for the duration of the error signal thus altering the ratio of the driver to driven cone shaft speeds and hence the crosshead speed. A small correction is carried out each cycle until the error is eliminated.

Cones were originally made of brass with knurled surfaces and the jockey wheel fitted with a rubber "O" ring. This produced a certain amount of slip, quite unacceptable in the system, especially at low speeds. Since the Instron gears were generally fitted as a reduction gear the cone arrangement was altered to the position shown in Figure 31b with the variable speed device before the gear reduction and hence operating at a higher speed. Although slipping was reduced it was still at an unacceptable level. The cones were then turned down and coated with silicone rubber, being machined down to a thickness of 0.025-inches. The original jockey wheel was replaced by a knurled aluminium wheel and this system reduced variations in output speed (as measured by a d.c. generator tachometer) to as little as $\pm 1\%$. The result of a test on a bituminous specimen using this form of frequency control is shown in Figure 47. It will be seen that 1000 cycles elapsed before the test frequency rose to the preset frequency at which stage the modulator held the frequency to the preset level. In use, however, the silicone rubber quickly wore and acute slipping occurred. This was remedied temporarily by the inclusion of 20% emery flour into the silicone rubber but wear could not be avoided.

It was clear that the use of a friction drive was impracticable in the small scale required and that the only alternative would be a system of constant mesh gears transmitting a positive continuous drive at all times.

The range of speeds required was, in the light of experience gained with the cone system, of the order of 150% to 20% of the standard Instron speed when cycling with strain control. Stress-controlled testing could be equally well performed by starting the test at the lower speed end of the device since frequency tends to decrease in this case.

Reducing the speed of a d.c. motor to 15% of its maximum is quite impracticable due to the fall-off in torque. Consequently, it was decided to try an epicyclic differential system shown in Figure 32 whereby the Instron synchronous motor would be used to provide the standard speed and a separate d.c. shunt wound motor, with a variable resistor in series with the field winding, used to provide the necessary speed change. It will be appreciated that by the selection of the appropriate gear ratios a small change in speed of the d.c. motor would result in a large change in output speed, thus the required $7\frac{1}{2}$ times reduction in overall speed could be effected by a 28% reduction in d.c. motor speed. This change in d.c. motor speed was easily achieved by altering the field resistance without undue fall-off in torque. On trial this drive system proved quite unsatisfactory since the difference in power of the two geared motor outputs caused the Instron synchronous motor to race and hence cause a varying output to the reference transformer. Although this problem could well have been overcome by fitting a worm gear to the synchronous motor and altering the gearing of the epicyclic gear box other difficulties which became apparent led to this epicyclic system being abandoned.

The discovery and acquisition of a Kopp Variator, an infinitely variable speed gearbox, led to the development of the present system shown diagramatically in Figure 33 and in Plate 11. Plate 12 shows the unit together with the associated electronic equipment and Plate 10 the chain drive to the Instron reference transformer.

This frequency modulator derives its power from a synchronous motor which drives, via the Kopp Variator and fixed gears, the Instron reference transformer. The Variator provides a speed range of 283% to 35% of the input speed and gears were selected such that the output shaft of the unit will run at speeds in the range 151% to 21% of the Instron synchronous motor output shaft. By the selection of the appropriate Instron gears at the beginning of each test adequate crosshead speed variation is available to compensate for any change in frequency encountered.

A d.c. tachometer generator is fitted to the output shaft of the

unit (coupled directly by chain drive to the reference transformer) its output being directly proportional to the crosshead speed. The generator tachometer has an output of 20 volts/1000 r.p.m. corresponding to 0.74 volts output for a crosshead speed of 1 inch/minute. This signal, suitably attenuated, is fed to the third channel of the 3-pen recorder enabling a permanent record of crosshead speed to be made throughout the course of the test.

BINDER VISCOSITY TESTS

During the course of testing the bituminous specimens, three types of which differed only in the type of binder, it became apparent that a knowledge of the viscosity of the binder, at the temperature of test, might be useful in explaining certain experimental phenomena. The majority of viscometers measure directly, or indirectly, the viscosity of the material under test either at a particular temperature, high enough for the material to flow, or measure the temperature at which a certain phenomenon occurs. Only two types of viscometer enable viscosity determinations to be made at any desired temperature, the rotating cylinder type viscometer and the cone and plate type viscometer. The rotating cylinder type viscometer is of limited use for bituminous binders in that it covers only a small range of viscosities. The cone and plate type viscometer is ideal for the present application but these models are expensive to purchase and one was not available for the present study.

It was therefore decided to construct a simple parallel plate viscometer along the lines of one developed by Diennes and Klemm (219) for the viscosity determination of high polymers, particularly polyethylene resins. The theory is based on the work of Stefan.

The viscometer, shown in Plate 14 and in cross section in Figure 34, consists essentially of two parallel plates 2 inches in diameter. The lower plate is integral with the lower jig plate whose overall diameter is $3\frac{1}{4}$ inches. The upper plate moves on the axis of, and parallel to, the lower plate by means of a silver steel plunger in a brass bush mounted in the upper jig platen. The jig platens are located by three detachable posts. Suitable spacers on the plunger between the upper plate and upper jig platen permit the initial separation of the plates to be varied in units of $1/16$ inch down from $\frac{1}{4}$ inch.

A bituminous binder is placed between the parallel plates at the required thickness and the upper plate located in position by means of a locking ring and release lever. During test the sample is loaded through

a 1 inch ball bearing on the upper plate plunger. Loading is effected by a standard oedometer loading frame, as shown in Plate 16, enabling loads from 1.5 kg to 500 kg using hanger weights from $\frac{1}{4}$ lb to 100 lb. Loads less than 1 kg are applied directly as shown in Plate 15.
Recommended loadings are presented in Table 1.

Upon freeing the release lever, plate separations at certain time intervals are evaluated from the dial gauge readings.
From the basic relationship:-

$$t = \frac{3\pi\eta a^4}{4F}\left(\frac{1}{d_2^2} - \frac{1}{d_1^2}\right)$$

where t = time taken for plates to separate from d_1 to d_2

η = viscosity

a = loaded area of specimen

F = force acting on specimen

The viscosity is given by:-

$$\eta = \frac{L}{15.5} \cdot s \text{ poise}$$

where L = load on specimen in kg

s = slope of linear portion of graph of time against $1/d^2$

d = separation of plates

BINDER TESTS IN STEADY SHEAR

A standard shear vane apparatus has been modified to assess the effect of the continual application of shear on the viscosities of bituminous binders. The shear vane apparatus has been modified, as shown in Plate 17, to accept an equiviscous temperature apparatus (e.v.t.) cylinder. A steel base accepts the e.v.t. cup which is located by a removable collar. The drive has also been modified by replacing the standard "O" ring and pulleys with a toothed rubber belt and toothed pulleys. The torque in the binder under test is shown by an indicator on a circular scale in the standard manner. This apparatus is also used in the temperature controlled room at the road-base specimen test temperature.

CHAPTER EIGHT

EXPERIMENTAL PROCEDURES AND TECHNIQUES

EXPERIMENTAL PROCEDURES - BITUMINOUS MATERIALS

Material preparation - Prior to the main testing programme sufficient aggregate for the project was sieved and stored in bins. Ten sieve sizes were employed, being 1", $\frac{3}{4}$", $\frac{1}{2}$", $\frac{3}{8}$" followed by a half sieve size progression to a number 100 mesh sieve. Stone larger than $^3/16$" was washed before storing.

Specimens were prepared in batches of six and 3500 gm of dry aggregate, sufficient for one specimen, was weighed into each of six trays according to the appropriate aggregate grading set out in Table 2 and Figure 15. During weighing out of the larger granite stone sizes any elongated or flaky aggregate was discarded. Trays of aggregates were placed in an oven, at a temperature 25°C higher than the appropriate binder temperature specified in Table 2, and left overnight.

The following morning the specified binder was transferred from its drum into the appropriate air jacketed heating pot. It was stirred occasionally whilst being brought to temperature over a period of approximately one hour. During heating and over the $\frac{3}{4}$ hour mixing period the binder was kept covered at all times when not in use. Binders were never reheatedand discarded if overheated by more than 5°C.

An hour before commencing the mixing of bituminous materials six specimen moulds and two end plates were placed in the oven with the aggregate. At the same time low gas flames were directed on to the automatic compactor foot and a $\frac{1}{2}$ inch diameter tamping rod in order to eliminate adhesion to the mixed material. The heating element in the oil jacket sun and planet mixer was also switched on some one hour prior to mixing and its thermostat set to operate at an oil temperature equal to that of the binder.

Specimen preparation - A trayful of heated aggregate was emptied into the mixer, the tray returned to the oven, and the aggregate mechanically stirred for 10 to 15 seconds. A central depression was made in the mixed aggregate and the correct amount of binder weighed in by difference. Dry aggregate was then folded in over the binder and the material mixed mechanically for a period of one minute. Collections of rich material were scraped off the mixer blades and bowl side by means of a spatula and the material mixed for a further minute. Rich material was again removed from the mixer blades, the mixture discharged into the heated tray and returned to the oven where it was covered with a suitable aluminium plate to reduce oxidation. This procedure

was repeated for the five remaining mixtures.

Approximately one hour after the beginning of mixing operations specimen compaction was commenced. A mould and base plate were removed from the oven and assembled near the compactor. The first trayful of mixed material was thoroughly mixed and introduced into the mould in four roughly equal layers by means of a flat spoon. Each layer was distributed by 15 well placed blows of the preheated tamping rod. After the final layer was tamped its surface was domed in order to reduce the number of larger stones being displaced by the compactor foot. The tamping rod was replaced on the low gas, the compacting foot gas removed and the base plate and filled mould assembly located on the compactor. The material was then subjected to 25 blows of the automatic compactor using a 10 lb weight falling through 18 inches. The assembly was then removed from the compactor, the second preheated base plate located on the compacted end and the mould inverted. The original base plate was then removed and replaced in the oven and the assembly returned to the compactor where it was subjected to a further 25 blows of the automatic compactor. After compaction the assembly was removed and the 4 inch diameter cooling base located in the uppermost end. The mould was again inverted, the base plate removed and returned to the oven. The mould was finally numbered with a wax crayon and set on one side to cool. The compactor foot was scraped clean if necessary and its gas flame replaced. This procedure was repeated for the five remaining mixtures using the materials in the order in which they were prepared.

Void measurements - Some 24 hours after the preparation of thebituminous specimens end void measurements were taken prior to extrusion. Initially, loose material was removed from the specimen ends by means of a sieve cleaning wire brush. The first specimen mould was then stood upright in a 12 x 18 inch tray and 0.2 mm Ballotini poured into the mould end in a rotary manner from a 200 cc polythene beaker. When the Ballotini was proud of the mould end it was struck off level by means of a steel rule. This was achieved by placing the rule vertically across a diameter of the mould and resting on the mould perimeter. The rule was then drawn outwards keeping it in contact with the mould end. This was repeated striking the remainder of the proud Ballotini from the mould end in the opposite direction. This procedure was repeated using a diameter roughly perpendicular to the original position. The Ballotini filling the mould end was then emptied into a second tray and transferred via a funnel into a 100 cc glass beaker. This beaker was then placed on an electric balance having previously been zeroed with the

empty beaker, and the weight of Ballotini recorded. This Ballotini, together with the overspill from the first tray, was then transferred, via the funnel, into the polythene beaker and the above procedure repeated twice. The specimen mould was then inverted and the above procedure repeated in the "lower" end. This system was repeated for the five remaining specimens.

After extrusion specimens were weighed in air and water enabling internal, surface and total air voids to be evaluated.

Specimen extrusion - After end void measurements specimens were extruded by means of a soil mechanics screw jack extruder. Each specimen was pushed from its lower end and was numbered after extrusion. After weighing in air and water, specimens were stood vertically, on their lower ends, on a grill, and left to dry. When dry they were stored in a similar position on a flat surface.

Specimen mounting in end caps - The ends and end inches of the sides of each bituminous specimen were degreased with trichloroethylene. Three parts of Araldite X83/144 hardener was weighed into ten parts of GY 250 resin and the adhesive thoroughly mixed. The adhesive was then placed sparingly into the end caps and on to the specimen ends. The end caps were located onto the specimen ends, worked in to expel any trapped air, and the assembly clamped into the specimen mounting jig. The jig was then placed in the temperature controlled room, operating at the desired test temperature, and left for the adhesive to set and cure. The remaining five specimens were mounted in a similar manner.

Specimen mounting in testing machine - When required for testing the specimen, mounted in end caps, was removed from its mounting jig and stood in the Instron testing machine with its lower end cap located in the lower crosshead adaptor. The moving crosshead was set in motion in an upward direction and stopped when the upper end cap was within $\frac{1}{8}$-inch of the load cell adaptor. The eight end cap retaining screws were then inserted rotating the specimen, if necessary, in order to line up the upper end cap screw holes. Upward movement of the moving crosshead was resumed until the load cell output registered a few pounds compression. The eight retaining screws were then tightened in diametrically opposed pairs, care being taken to ensure that the specimen was not subjected to more than a few pounds tensile or compressive load. If an eccentricity of more than some 10 thou inches was evident between the perimeters of the upper end cap and

the load cell adaptor this gap was shimmed before the retaining screws were tightened. When all eight retaining screws were fully tightened the position of the lower moving crosshead was adjusted to eliminate any load on the specimen.

Extensometers were next installed by first locating the lower extensometer clamp loosely around the lower end cap. The extensometer carrier rods were next positioned in the linear bearings and the lower clamp tightened in position. The upper extensometer clamp was then located and tightened in such a position that both carrier rods rode freely in their bearings. Carrier rod spacers and nuts were then located to finger tightness, each pair of carrier rod nuts being adjusted such that the dial gauges indicated a predetermined zero. The extensometer plugs were next connected, the LVDT slugs positioned in their appropriate extensometer and the power supply switched on. Carrier rod nuts were then finally tightened with a spanner such that the output from the LVDT was approximately zero.

A magnetic base dial gauge was finally located on the upper crosshead to monitor total crosshead deformation and the draught excluder baffles positioned to front and rear of the testing frame.

During this setting up process care was taken to ensure that no load, resulting from viscous flow of the material, was permitted to develop. Testing was commenced only when the specimen had been in a stress free state for at least 15 minutes.

Specimen testing - stiffness measurement tests - Each series oftests to determine the service life characteristics of a specific bituminous material at a specific temperature, was preceded by a series of stiffness measurement tests. These stiffness tests, on between three and six specimens, were performed primarily to assess the effect of rate of application of strain (strain rate) on specimen stiffness. They also served, however, as a guide to the approximate limit switch settings and crosshead speeds required to produce specific strain level and frequency requirements in subsequent tests at that temperature.

All testing of bituminous specimens was conducted under conditions of controlled strain with the exception of a few preliminary stress-controlled and single shot tests described later.

With the specimen in a stress free state the extensometer output range was selected and the signal switched to both the Instron and Rikadeski 3-pen recorders. The extensometer amplifier trim potentiometer was then adjusted

to suppress the zero to 50% full scale deflection on the Instron recorder. The appropriate load range from the Instron load cell amplifier was next selected and the load signal suppressed also to provide a 50% full scale deflection on channel 1 of the 3-pen recorder. The deformation channel (2) of the 3-pen recorder was adjusted, if necessary, also to 50% full scale deflection. The Instron limit microswitch positions were next adjusted symmetrically about the 50% full scale deformation position with due regard to extensometer output range and pen overshoot. In these stiffness measurement tests the Instron crosshead speed control was used in its standard form. The appropriate crosshead speed gears were therefore chosen and located and the 3-pen recorder chart speed selected. Finally the Instron cycling made switch was set to 'load' (cam) cycling.

The testing apparatus was then ready for specimen testing.

In both stiffness measurement and service life tests, cycling was always commenced in a downward direction resulting in tensile loading for the first quarter cycle.

For each stiffness measurement the specimen was cycled for 10 cycles only to reduce changes in condition to a minimum. During this 10 cycles the time taken for 5 cycles was recorded in order to calculate the cycle frequency.

Cycling was stopped by pressing the Instron stop button when the specimen was being subjected to a compressive load and the deformation was approaching zero. The crosshead position was then adjusted by means of the manual positioning knob such that both load and deformation were zero.

A new combination of extensometer output range, load cell output range, limit switch position and crosshead speed was selected and the procedure repeated. Some 5 minutes were left between each test where the strain level just studied was less than 2.10^{-4} in/in and 10 minutes for strain levels greater than this.

This whole procedure was repeated on large number of times over a wide range of strain levels and testing frequencies until the specimen was permanently damaged.

Testing frequencies were changed in a random manner but strain levels were progressively increased in order to acquire the maximum amount of information from a specimen before it sustained permanent damage. Periodically an early strain setting was repeated in order to ensure that no permanent damage had been sustained by the specimen. When this occurred the test was terminated and the specimen removed.

At each strain level and frequency combination the stiffness of the

specimen on the first cycle was determined from the total load range and the total extension range. The assumption was made that the cross sectional area of the specimen remained constant throughout the test. Specimen strain was also calculated, together with the strain rate computed from the strain level and the frequency. Calculated stiffness was finally plotted against strain on double logarithmic graph paper noting strain rate at each position.

From the resulting graph the effect of strain rate on stiffness at a given strain level was determined for the specimen tested.

Specimen testing - service life tests - In the determination of service life under strain- (or stress-) controlled conditions, using the frequency modulator, an effort was made to select a starting crosshead speed which would result in a test frequency as close as possible to that selected. Modulator correction would therefore be kept to a minimum in this early vulnerable part of the specimen life. To this end, specimens of low strain level, whose service lives were predicted to be in excess of 1000 cycles, were subjected to a setting up trial of less than 10 cycles of loading at the appropriate cam settings and estimated crosshead speed as indicated by the stiffness measurement tests. These trial cycles were timed and if necessary the crosshead speed control adjusted to correct for error in frequency. Generally these initial frequency trials were performed when a new specimen had been set up in the evening after previous testing. This provided a period of at least 12 hours for the specimen to recover and experience indicates that little irrecoverable damage is done at low strain levels in these first few cycles.

This procedure was not adopted for specimens whose service lives were predicted to be less than 1000 cycles since any permanent damage sustained would influence the test results . Further it was felt that the more rapid change in specimen behaviour at these higher stresses and strains would reduce the significance of changes in frequency.

Specimens tested at a strain level resulting in a predicted service life of less than 50 cycles were tested without frequency control (at constant crosshead speed). This policy was adopted since it was found difficult to predict the required crosshead speed at these high strains. Modulator corrections would invariably be greater than changes in frequency, due to the reduction in stiffness.

Tests were never started until the specimen had been in a stress free state for at least 1 hour.

Prior to the start of testing, with the frequency modulator drive motor switched off, the tachometer generator output range was selected and the third channel of the 3-pen recorder zeroed. The appropriate gears on the frequency modulator were fitted and the modulator drive motor then switched on leaving the actuator motor isolated. The cycle counter was zeroed and the undred-cycles indicator electronics reset.

Further procedures prior to test were identical to those detailed for stiffness measurement tests. These were selecting the output ranges of the extensometers and the load cell amplifier and zeroing these outputs to 50% full scale deflection. The Instron recorder mode switch was set to extension and the microswitch cams positioned. The Instron cycle mode selector switch was finally set to 'load' (cam) cycling.

Testing was started and stopped in an identical manner to that described above for stiffness measurement tests. The frequency modulator actuator motor was only switched on after the first complete cycle in order to avoid any erroneous correction resulting from spurious signals at the start of testing. Frequency correction was then performed automatically throughout the course of the test.

The 3-pen recorder was run for the first 1000 cycles then at 100 cycles either side of cycles 1500, 2000, 3000, 5000, 7000, 10,000 and 20,000. This enabled specimen stiffness to be measured at cycles 1, 2, 5, 10, 25, 50, 100, 200, 300, 500, 700, 1000, 1500, 2000, 3000, 5000. 7000, 10,000 and 20,000 or less if service life was exceeded. In early tests hysteresis loops were taken with a Houston X-Y Plotter at these cycles but the practice was discontinued in later testing programmes due to the difficulty of measurement, limitations of the recorder and lack of useful information from the results. Testing frequency was also measured at the above cycles by recording the time taken to perform 5 cycles.

Testing was terminated when the specimen stiffness had fallen to less than 60% of the stiffness at cycle 1.

At the above cycles up to the specimen service life, stiffnesses, strains and strain rates were calculated and the stiffness plotted against elapsed cycles on a double logarithmic plot. This graph enabled a tentative estimate to be made of the number of cycles required to reduce the stiffness to 90%, 75% and 60% of the initial stiffness. These values were subsequently corrected if the change in strain or strain rate over the test period exceeded 10%. This aspect is dealt with more fully in Chapter 9.

Certain specimens were retested after a period of time in order to study the effect of rest periods on service life.

Either three or six specimens were tested at each strain level enabling relationships to be established between strain and cycles to 90%, 75% and 60% of initial stiffness for each material, temperature and rate studied.

Removal of specimen from testing machine - At the end of each test, or series of tests, the 3-pen recorder, extensometer power supply and frequency modulator actuator motor were switched off. The draught baffles, magnetic based dial gauge and extensometer fittings were removed. The Instron recorder mode was set to load and the load cell output signal attenuated to the upper limit microswitch position. The Instron cycle mode selector switch was set to 'load' (cam) cycling and the specimen load cycled from zero to tension. The load cell output range was increased after every 20 to 50 cycles until the specimen was pulled into two separate parts. It was hoped that under these conditions the specimen would fail at its weakest plane which might be the source of locally high strains during strain-controlled testing.

The specimen end caps were unbolted from the testing frame and the fractured portions removed from the machine. The nature of the fracture surface was observed and the profile of the fracture recorded by measuring the distance of the fracture surface from the lower end cap at eight roughly equally spaced positions around the specimen perimeter.

A hammer and cold chisel were employed to fracture the specimen across the end caps and the two portions of the fractured specimens were reunited, marked and stored for future reference.

Cleaning of end caps - When a number of filled end caps had accumulated they were placed in a furnace oven at a temperature of approximately 400°C. After some 15 minutes an end cap was removed and the hot bituminous material and resin scraped out with a spatula. This operation was performed under a fume extractor and was repeated for the remaining end caps.

Upon cooling the end caps were generally sufficiently clean for re-use. Occasionally, when carbon deposits were evident, the end caps were clamped in a lathe and the insides polished with a fine emery cloth.

EXPERIMENTAL TECHNIQUES - BITUMINOUS MATERIALS

Material preparation - The granite aggregate used throughout in the preparation of dense macadams, and as the stone fraction in the hot rolled asphalt, was received from the quarry in the following nominal sizes:-

1", ¾", ½", ⅜", ¼ and ⅛" to dust. The 1", ¾" and ½" aggregate sizes were washed and sieved manually on ¾", ½" and ⅜" sieves respectively and stored when dry. The ⅜" and ¼" aggregate sizes were blended in equal proportions and washed and sieved on a 3/16" sieve, then stored when dry. Material passing this 3/16" sieve was added to the ⅛" to dust aggregate and sieved mechanically on number 7, 14, 25, 52 and 100 mesh sieves. These sand sizes were not washed but stored directly from the discharge chutes of the sieving machine.

The flint gravel aggregate used as the sand fraction in the hot rolled asphalt was also sieved mechanically on number 7, 14, 25, 52 and 100 mesh sieves and the material passing these sizes stored without washing.

In weighing out, the various aggregate sizes were blended to the maximum accuracy permitted by the particle weight. This was found to be in the order of $\pm$ 2 gm for the larger stone sizes and within balance accuracy for sand sizes. Final total aggregate weights were seldom more than 10 gm out side the 3500 gm target weight.

Harder 40/50 and 90/110 pen. bitumens were removed from their drums by means of a hammer and chisel but the soft 190/210 pen. bitumen and the 54 e.v.t. tar were scooped out of their drums with a heated knife blade. It was fully appreciated that as the supply of binder was gradually used up its nature would differ due to sedimentation in the supply drum. It was felt, however, that this difference in consistency would be obscured by the predicted random and experimental errors in specimen preparation and testing. No action was therefore taken to remedy this effect.

During the heating of bituminous binders great care was exercised in order to avoid any overheating of the binder and the materials kept covered in order to reduce hardening due to oxidation with loss of volatile oils. All binders were heated to a temperature resulting in a predicted binder viscosity of 2 poise, although the temperature of the 190/210 pen. bitumen was modified slightly in order to give material internal voids compatible with the other macadams.

Surplus binder was discarded after the conclusion of mixing.

Specimen preparation - Binder was weighed into the dry aggregate by weight difference. This operation was generally performed with either two or three attempts and was executed to $\pm$ 1 gm in a minimum binder weight of 146 gm. This represents a binder content of 4 $\pm$ 0.03%.

When the mixed material was taken from the oven for specimen compaction, it was thoroughly mixed with a flat spoon in order to distribute

the coarse aggregate evenly throughout the material. Every care was taken to ensure that each spoonful of material placed into the compaction mould was a truly representative sample.

Rodding each of the four layers was performed partly to compact the material but mainly to distribute the finer material evenly around the surface of the mould. Particular attention was paid to avoid any concentrations of coarse material at the surface which would result in high surface voids and its associated undesirable features.

No difficulty was encountered in removing the base plates during specimen preparation provided the plates were rotated before being lifted off.

With experience it was found that the mixing of six trays of material took some 40 minutes and the compacting of six specimens a further 40 minutes. The period from the first mix to the last compaction was therefore some 1 hour 40 minutes.

Voids measurements - In the preparation of bituminous materials it was generally found that, whereas the lower end of the specimen was relatively smooth, the upper end contained a moderate proportion of end voids. When the Ballotini was placed in the upper end some material ran down the inside of the mould filling surface voids which were continuous with the end voids. The mould was therefore rotated whilst being inclined in order to discharge any Ballotini trapped in these voids. In some cases, where a surface void was linked to the end by only a small continuous void, a steady trickle of Ballotini from a surface void indicated that it would be some considerable time before the flow of Ballotini would cease. In such cases discretion was exercised in terminating the discharge and it was felt that the resulting errors would be relatively small.

The weight of Ballotini required to fill the mould end volume was in the order of 350 gm. Weights were recorded to the nearest 0.1 gm and the three determinations seldom differed by more than 1.5 gm.

After measuring the end voids of each batch of six specimens the Ballotini was inevitably contaminated with small particles of bituminous material. These were removed by sieving the Ballotini on a number 72 mesh sieve. The Ballotini was replaced periodically and a check made of its bulk density under conditions of filling similar to its practical application.

End void measurements on six specimens took approximately 30 minutes.

Internal and total voids were determined after extrusion by weighing each specimen in air and water. In the latter operation the specimen was rotated through at least one complete revolution under water before placing in the weighing stirrup, in order to avoid erroneous readings resulting from trapped air pockets. Weights in air were in the order of 3500 gm and in water, 2000 gm. Weighings were performed to the nearest $\frac{1}{2}$ gm and air and water weighings for six specimens took approximately 15 minutes.

Specimen extrusion - Extrusion of each batch of six specimens was straightforward but exhausting and was found to take between 20 and 30 minutes.

After extrusion of the specimens moulds were checked for damage sustained during compaction and deburred with a half round file if necessary.

Only after the preparation of rich gap graded materials did the moulds require cleaning in paraffin.

Specimen mounting in end caps - The epoxy resin used to stick the specimens into the end caps has a workable life of only 10 to 15 minutes and this time is reduced with quantities greater than 50 gm in weight. Consequently, sufficient resin for three end caps only was prepared at one time. After the six lower ends had been worked into their end caps the upper ends were treated in a similar manner. For smooth ended specimens 10 gm of resin was mixed with 3 gm of hardener and the most irregular of ends seldom required more than 20 gm of resin.

Upon location and tightening in the mounting jigs small quantities of resin were inevitably exuded from between the specimen and the end caps. This surplus resin was removed with a spatula and the specimen/end cap corners cleared out to remove any fillet of resin. During setting, small quantities of resin flowed up between the specimen and the end cap forming a slight fillet which was not removed.

Preliminary bonded specimens were left to set and cure at room temperature before being placed in the temperature controlled room for climatization before testing. After about an hour at a temperature of $0^{\circ}C$ it was found that cracks appeared in the resin around the specimen/end cap interface. This was attributed to the differential thermal contractions of the two materials. As a direct result of this phenomenon, specimens tested at below ambient temperatures ($+10^{\circ}C$ and $0^{\circ}C$) were stored at the appropriate temperature prior to bonding into the end caps. Specimens were removed from the temperature controlled room, cleaned and mounted and

immediately returned to the temperature controlled room. This procedure eliminated resin cracking and would result in a tightening of the end caps onto the specimens. Specimens tested at above ambient temperatures were stored in the laboratory, mounted, then placed in the temperature controlled room to climatize. The resin in freshly mounted specimens, therefore, was always left to set and cure at the specimen testing temperature.

Cleansing and bonding of six specimens into their end caps was found to take some 45 minutes.

Specimen mounting in testing machine - During the mounting of test specimens in the Instron testing machine great care was exercised in order to keep loading of the specimen to an absolute minimum. When the specimen was located in the lower crosshead adaptor, the recorder mode was set to load, the load cell output switched to its most sensitive range (200 lb full scale deflection) and the limit switches set some two divisions (4 lb) either side of the no load zero position. By setting the lower limit switch to "cycle" and the upper limit switch to "stop", when set in motion, the moving crosshead would proceed in an upward direction until a 4 lb compressive load was reached whereupon the crosshead would stop. When tightening the end cap screws, any tensile loading developed would automatically be relieved. When the specimen was set up the cycle switches were reversed, with a low crosshead speed selected, such that any compressive load set up during mounting was dissipated.

When locating the extensometer carrier rods in their linear bearings prior to tightening up the lower extensometer clamp, each rod was stood on a $\frac{1}{2}$" thick block and the dial gauge spindles held in their uppermost position by means of crocodile clips. This enabled the lower extensometer clamp to be finally located and tightened with no mechanical interference from the dial gauge spindles. As soon as the lower extensometer clamp was fully tightened the blocks and clips were removed.

When the carrier rod nuts were finally tightened care was taken to ensure that the extensometer spindles lay on a specimen diameter as indicated by scribed lines on the lower extensometer bearing plates. Each specimen took approximately 20 minutes to set up in the testing machine.

Specimen testing - During stiffness measurement tests the appropriate crosshead speed for a required frequency was selected from a knowledge of the deformation range, the predicted overshoot, and load cell deformation and on the assumption that the deformation wave form is triangular. This

system was only adopted when testing under new conditions such as material or temperature. In practice, however, once one test had been performed on a particular material at a particular temperature, different crosshead speeds were selected on the assumption that to double the crosshead speed would double the frequency. This guide would predict a frequency somewhat higher than that resulting due to the fact that a higher crosshead speed increases stiffness, hence load, hence load cell deformation, hence crosshead distance thus reducing the theoretical frequency. In this way, frequencies were restricted to 40 cycles/minute (or up to 50 cycles/minute for very short periods) avoiding damage to the testing machine.

In order to build up a relationship for stiffness variation with strain and strain rate the range of crosshead speeds was generally kept constant. This was done in preference to keeping the frequency constant since the strain rate increases only slightly as the strain range is increased at constant crosshead speed. By retaining a range of testing frequencies, the strain rate would increase as the strain range is increased, thus rendering an analysis of results more difficult.

From trends in specimen stiffness with strain at various frequencies, a reasonably accurate estimate could be made of the appropriate initial crosshead speed required for specific conditions. Therefore, when setting up a specimen for a service life determination, the appropriate crosshead speed could be selected with some confidence. The required crosshead gears were fitted and the frequency modulator gearbox ratio adjusted for the requisite crosshead speed. The modulator is fitted with a manual override button which causes the actuator motor to run in the direction which increases crosshead speed. This button may, therefore, be employed. Alternatively, the Instron cycle counter microswitch activated once only. The modulator electronics detects a low frequency and the actuator motor compensates automatically. Conversely, by activating the microswitch fairly rapidly, the modulator electronics detects a high frequency causing the actuator to reduce the crosshead speed accordingly. By these means, the appropriate crosshead speed is easily obtained.

During long term tests the change in specimen stiffness per cycle was found to be extremely small. The sensitivity of the frequency modulator is such, however, that even at very small frequency errors the actuator motor is activated momentarily. In order to avoid unnecessary wear on the modulator it was therefore switched off and only used periodically to eliminate any significant frequency error which might accrue. Errors were deemed significant when they were in excess of 1% of the required frequency. This is equal to the accuracy of the frequency measuring system,

the limiting factor here being the 0.1 second response of both the timer and the operator.

The time taken for stiffness measurements to be made on one specimen was up to 4 hours, depending on how many tests the specimen would withstand before irrevocable damage was manifest. Service life tests ran from a few minutes to 12 hours, depending on strain level and testing conditions.

Removal of specimen from testing machine - This operation was found to take some 15 minutes, the exact time being determined by the number of cycles required to fracture the specimen. Generally, removal of the specimen assembly itself took about 10 minutes.

Cleaning of end caps - Cleaning of the end caps was usually performed by an assistant and the time of operation was not determined. It is estimated that the cleaning of one pair of end caps would take approximately 5 minutes.

EXPERIMENTAL PROCEDURES - CEMENT BOUND MATERIALS

Material preparation - As was the case with the aggregates for the bituminous specimens, sufficient aggregate was prepared for all the concrete testing. Sieve sizes were $\frac{3}{4}$", $\frac{1}{2}$", $\frac{3}{8}$" and subsequent half sieve sizes to a number 100 mesh sieve. Stone larger than $^3/_{16}$" was washed before storing.

Concrete specimens were prepared in batches of six with three cubes each on the first and last batching days. The concrete aggregate was graded as shown in Table 2 and Figure 15 and 3500 gm of dry aggregate, sufficient for one specimen, was weighed out into each of six trays. Aggregate for cubes was also weighed out separately and 2500 gm was prepared for each 4-inch cube. These aggregate weights include the Ordinary Portland Cement which was weighed out with the dry aggregate. Prior to testing the compaction moulds and base plates were lightly oiled to prevent adhesion of the set concrete to the steel.

Specimen preparation - A trayful of dry aggregate was emptied into the cold sun and planet mixer and mechanically mixed for 1.10 to 1.15 seconds. A central depression was formed in the aggregate and the appropriate quantity of preweighed water added. The dry aggregate was then folded in over the water and the material mixed mechanically for one minute. Any cement paste was next removed from the mixer side and blades by means of a spatula and the material mixed for a further one minute. Any rich cement paste was again removed from the mixer side and blades and the mixed material scooped out into its tray.

Compaction was performed, immediately after mixing, in a manner identical to that of the bituminous materials but with cold equipment. Upon compaction of the second face and the positioning of the 4 inch diameter "cooling" base, the specimen mould was inverted, numbered, and placed in a curing tank with a water level some $\frac{1}{4}$ inch below the upper end of the compaction mould. The upper end of the mould was covered with a flat plate to reduce evaporation to a minimum. This procedure was repeated for the five remaining mixtures.

Control cubes were also produced, three each at the beginning and end of the concrete series of specimens, cube mixtures being prepared in an identical manner to that of the specimen mixtures. The mixed material was introduced into the 4-inch cube moulds in three roughly equal layers with each layer rodded some 20 times. The final layer was also compacted by means of a 2 inch square bar applied three times at nine evenly spaced positions over the cube surface. Surplus material was then floated off and the cubes covered with damp sacking.

Void measurements - No end void measurements were taken on the dry lean concrete series of specimens. Typical internal void measurements were made on six fractured specimens after dynamic testing. These specimens were weighed saturated in water, saturated surface dry and bone dry after 24 hours in an oven at a temperature of 110°C.

Specimen extrusion - Dry lean concrete specimens were extruded 24 hours after compaction by means of the pneumatic/hydraulic jack mentioned earlier. Specimens were extruded from their lower end, numbered, and returned to the curing tank where they remained until required for testing.

Control cubes were also stripped after 24 hours and stored in the curing tank until required for testing. Preliminary mix design and control cubes were tested at 7 and 28 days.

Specimen mounting in end caps - Dry lean concrete specimens were mounted and tested at least three months after compaction. A specimen was removed from the curing tank and its ends and end inches of the side degreased with a scrubbing brush and Teepol. These areas were then rinsed in cold water and the surface water removed by means of a dry cloth. The insides of the special end caps were degreased with trichlorothylene and the appropriate amount of adhesive prepared. The same epoxy resin was used for the concrete specimens as for the bituminous materials, namely Araldite GY250

resin and X83/144 hardener. Sticking and mounting in the jig was performed in an identical manner to that of the bituminous materials. After mounting the assembly was immediately placed in the curing tank where the adhesive set and cured.

Six specimens were prepared in this manner at one time and the mounted specimens left under water at room temperature until required for testing.

Specimen mounting in testing machine - Prior to the testing of concrete specimens the special flexible adaptors were fitted to the Instron testing machine. Larger draught baffles were used to accommodate the increased distance between the upper and the lower crossheads.

When required for testing a mounting jig assembly was taken from the water bath and the mounted specimen removed. A 4 inch diameter rubber membrane, some 10 inches long was placed around the specimen and the specimen sealed by means of rubber "O" rings securing the membrane to the end caps. These "O" rings were located in the groove provided in the specially turned-down end caps.

The lower crosshead adaptor was lightly clamped in a near horizontal position and the specimen located on this adaptor. The lower end cap was then bolted relatively tightly in place and the moving crosshead raised until the upper end cap was within some $\frac{1}{8}$" of the load cell adaptor. The four upper end cap screws were next located in the load cell adaptor and the crosshead adaptor screws released. The specimen assembly was therefore free to be rotated about into vertical axis. Finally, the crosshead was raised until the load cell indicated a few pounds compression and all sixteen screws fully tightened. Care was taken to ensure that no tensile force was exerted on the specimen during this operation. The lower crosshead position was then adjusted to relieve any loading imposed on the specimen.

Two pieces of 15 thou inch brass shim were employed to protect the rubber membrane from damage from the extensometer clamps. The shims were 1 inch wide and 14.1 inches long. A shim was placed around the lower end caps with the butt joint to the rear of the specimen and the lower extensometer clamp located in position and fully tightened. The upper extensometer clamp was located on the second shim around the upper end cap in a similar manner. For concrete specimens the extensometer assemblies were fitted to short carrier rods and these were hung from the upper extensometer clamp. Adjustment of the extensometers was performed by

means of the carrier rod nuts as before and the extensometers zeroed mechanically and electronically as described previously.

A larger rod was fitted to the magnetic base dial gauge and this was located on the upper crosshead, bearing onto the lower crosshead. Draught baffles were finally fitted.

Specimen testing - All testing of concrete specimens was performed at a temperature of +20°C since the review of previous work has shown that temperature variations over the range considered has little effect on dynamic behaviour.

Stiffness tests were performed on three dry lean concrete specimens to assess the effect of rate of application of strain on stiffness. These tests were performed in a manner identical to that described for the bituminous materials.

For reasons discussed in Chapter 9, after a few preliminary service life tests under strain-controlled conditions, the majority of dry lean concrete specimens were tested under conditions of controlled stress cycling. Due to the fact that frequency of loading within the range considered showed no effect on specimen stiffness, all dry lean concrete specimens were tested with no frequency control, using fixed crosshead speed gears. In all other respects the method of test was identical to that procedure followed for the bituminous materials, stress-controlled cycling differing only insomuch as the Instron recorder mode was set to "load" rather than "extension." Stress-controlled cyclic testing continued until complete fracture of the specimen occurred.

Removal of specimen from testing machine - After complete fracture of the tested specimen, the extensometer power supply was switched off and the draught baffles, magnetic based dial gauge and extensometer fittings removed. The specimen end caps were unbolted from the flexible adaptors and the specimen taken out. After removal of the "O" rings and rubber membrane the specimen was separated from the end caps using a hammer and cold chisel. The specimen was finally marked for future identification and stored.

Cleaning of end caps - The cleaning of end caps was carried out in exactly the same way as that of the bituminous specimen end caps. Upon removal from the oven the concrete was easily removed by levering it out of the end cap with a spatula.

EXPERIMENTAL TECHNIQUES - CEMENT BOUND MATERIALS

Material prepratain - Gravel aggregate for the preparation of dry lean concrete specimens was received from the pit in the standard concrete aggregate sizes of $\frac{3}{4}$", $\frac{3}{8}$" and $^3/16$" sand. As with the granite aggregates stone sizes of $\frac{3}{4}$", $\frac{1}{2}$" and $\frac{3}{8}$" were washed and hand sieved whilst the $^3/16$" stone and the 7, 14, 25, 52 and 100 mesh sieve sizes were screened mechanically and stored without washing. Cement was weighed out with the aggregate and the accuracy of individual and cumulative weighings was the same as for the bituminous material aggregates.

Specimen preparation - No special techniques were employed in the preparation of dry lean concrete specimens. The precautions and compactions exercised in the preparation of bituminous specimens were closely followed in the case of dry lean concrete specimens.

Specimen extrusion - The specially developed pneumatic/hydraulic jack was employed to extrude the dry lean concrete specimens in a vertical position. Certain specimens exhibited a high initial resistance to extrusion which could not be overcome by the jack. These were started off in the hydraulic jack shown to the right in Plate 4 and then transferred to the pneumatic/hydraulic jack for final extrusion.

Specimen mounting in end caps - Although wet, no special techniques were developed for the mounting of dry lean concrete specimens into their end caps.

Specimen mounting in testing machine - The technique of setting the Instron cycle cams to a low load level to keep stresses on the specimen to a minimum was also used in the setting up of the dry lean concrete specimens. Since the material behaves quasi-elastically in a short term static state, when set up, any compressive load was removed by a single movement of the crosshead by the manual positioning knob.

Due to the shortened extensometer carrier rods the lower extensometer clamp was located and tightened in position in a single operation. The upper clamp was next located, the extensometer carrier rods positioned and the retaining nuts adjusted to finger tightness. The upper clamp was then rotated on the end cap until the extensometers were in the correct position relative to the lower extensometer bearing plates. When this position was achieved both the upper clamp and the carrier rods nuts were fully tightened.

The LVDT spindles were finally inserted and the upper extensometer clamp released, repositioned and retightened if necessary.

Specimen testing - No form of frequency control was employed in the testing of dry lean concrete specimens. Consequently, no setting-up trials were performed but all tests carried out at fixed crosshead speeds. The procedures and techniques employed in starting both stiffness measurement tests and service life tests were identical to those used for stiffness measurements of the bituminous specimens. In certain service life tests conditions of controlled stress were employed. This only required the Instron recorder mode to be set at "load" rather than "extension."

During load cycling both the dynamic extension range and the permanent deformation increased as damage was incurred. It was therefore necessary to either suppress or attenuate the extensometer output in order to keep the signal within the range of the recorder. Insufficient suppression was available to cater for the total permanent deformation of dry lean concrete specimens and the output signal was therefore attenuated when it exceeded the range of the recorder. Since the dynamic deformation also increased the accuracy of measurement was not impaired with attenuation.

Removal of specimen from testing machine and cleaning of end caps - These operations were carried out in an identical manner to those of the bituminous materials and no special techniques were developed.

BINDER VISCOSITY TESTS

Binder preparation - Approximately 500 gm of each of the four bituminous binders used in the preparation of the dense bituminous roadbase materials investigated, were removed from their delivery drums, by the methods previously described, and placed in clean tins, some 4 inches in diameter and 6 inches long. Four further tins were filled with the binders which had been heated ready for specimen material preparation. Small samples of recovered bitumens were also set aside for viscosity tests. All containers were covered to reduce any loss of volatile oils and also to prevent the ingress of dust.

When required for testing the appropriate tin of binder was heated, covered, in an oven to a temperature some 50°C less than that used in mixing operations. The material was then sufficiently fluid to permit it to flow relatively easily. About 25 gm of binder was then poured onto a flat metal plate some 6 inches square resulting in a spread approximately

$^3/_{16}$" thick. If in time the thickness flowed out to less than $\frac{1}{8}$" fresh binder was added to make up the thickness. Binders were not kept on plates for more than a few days due to contamination from the atmosphere.

Viscometer preparation - The required spacer was located on the upper plate shaft, the shaft positioned in the bearing and the collar fitted hard down on the release lever. The faces of both the upper and lower plates were heated slightly with a bunsen flame in order to aid adhesion of the binder to the steel. These faces were then wiped dry with a tissue and degreased with trichloroethylene. An area of binder sufficiently large to cover the 2" diameter viscometer plates was removed from the plate, with a warm palette knife, and placed on the lower plate of the viscometer. The upper viscometer frame was then located in place on the support posts and the socket head retaining screws fully tightened in turn by degrees. A piece of hacksaw blade, the teeth of which had previously been ground off and the broken end dressed up like a chisel blade, was warmed and used to clean off the excess binder. This excess binder was discarded.

A second viscometer was loaded in a similar manner and the pair transferred to the temperature controlled room for climatization.

Each viscometer took 10 minutes to prepare.

Binder testing - Each pair of viscometers was left overnight in the temperature controlled room before testing to ensure that the binder and viscometer had reached the required testing temperature.

For predicted binder viscosities above 1.10^4 poise tests were performed in a standard oedometer. An empty viscometer with a shim representing the initial binder thickness in position was located in the oedometer. The loading ball was positioned on the viscometer shaft and the loading arm lowered into position. Finally, the adjustable platform was set and clamped in such a position that the lever arm was horizontal. This platform position was only altered when a different initial binder thickness was studied. In this case the above oedometer preparation procedure was repeated.

The loaded viscometer was positioned in the oedometer frame, the loading ball located and the unweighted loading arm lowered gently onto the ball. The loading arm support spindle was next raised until it held the arm just clear of the loading ball. From a knowledge of the predicted binder viscosity the appropriate hanger weights were selected and placed on the hanger of the loading arm. The loading arm support spindle was

next lowered until the arm just nipped the loading ball and the dial gauge assembly fitted and zeroed. The apparatus was then ready for the commencement of testing.

The viscosity test was started by first freeing the viscometer release lever then lowering the loading arm support spindle. On the instant that the dial gauge indicated movement of the upper plate a stop clock was started. The dial gauge reading, from which the plate separation could be calculated, was recorded at the following time intervals:- $\frac{1}{4}$, $\frac{1}{2}$, $\frac{3}{4}$, 1, $1\frac{1}{2}$, 2, 3, 5, 7, 10, 15, 20, 25, 30, 40, 50 and 60 minutes. In the case of the binders with predicted viscosities less than 1.10^4 poise the samples were loaded directly. In this case the stop clock was started and the release lever freed simultaneously. Dial gauge readings were taken at the same time intervals. In either case a graph of the reciprocal of the square of the plate separation against time was plotted on linear graph paper and a straight line drawn through the linear portion. From the slope of this line the viscosity of the binder was calculated.

This test was repeated at least twice for each condition and covered the entire range of binders and temperatures studied.

Cleaning of viscometer - When binder viscosity tests were carried out at $0^{\circ}C$ the binders were extremely brittle. The viscometers were taken from the temperature controlled room, the retaining screws removed and a thin wedge tapped into the face of the binder. The binder readily shattered and was easily removed from the viscometer plates.

At higher temperatures the retaining screws were removed and the plates separated by means of the heated palette knife. The bulk of the binder was then removed with the reheated knife and the remainder cleaned off with solvent.

After thorough cleansing of the whole viscometer, which took in the order of 5 minutes, the shaft was lightly oiled to prevent rusting and to reduce friction in the bearing.

BINDER TESTS IN STEADY SHEAR

Viscometer preparation - The inner cylinder of a standard equi-viscous temperature (e.v.t.) apparatus was cleaned with trichlorethylene and located in the adaptor which was in turn fitted into the shear vane apparatus.

A few grammes of binder was heated in an oven to a temperature some $50^{\circ}C$ below that used in the preparation of bituminous materials and poured into the e.v.t. cup. The correct depth was obtained using the depth gauge

provided with the e.v.t. apparatus. As soon as the required depth had been obtained and while the binder was still relatively fluid, the cup was located in the special base plate of the shear vane apparatus and the locking ring tightened in position. The shear vane assembly with the inner cylinder in position was next lowered into the cup full of binder until the top of the inner cylinder was level with the top of the cup.

The apparatus was finally transferred to the temperature controlled room where it was left overnight before testing commenced.

Binder testing - When ready for test the shear vane torque indicator was zeroed, the motor switched on and the stop clock started simultaneously. The torque was recorded and plotted against time on linear graph paper at the following intervals:- 10, 20, 30, 45 seconds, 1, 1½, 2, 3, 5, 7, 10, 15, 20, 25, 30, 40, 50, 60 minutes and every 30 minutes thereafter. The duration of the test varied from between 1 and 12 hours.

Cleaning of viscometer - At the conclusion of each test the inner cylinder was disconnected from its adaptor and the locking ring removed. The cup with binder and inner cylinder were then transferred to an oven at roughly 100°C. When the binder was sufficiently fluid to flow relatively easily the inner cylinder was removed and the binder poured out of the cup. The cup and cylinder were then cleaned in paraffin and finally cleansed with trichlorethylene.

Once the binder was fluid, setting up and cleaning of the apparatus took approximately 5 minutes.

STANDARD TESTS ON BINDERS

Experimental procedures - Standard tests were also performed on the four binders used in the investigation, as received, after heating and after mixing. Tests were the penetration test, the ring and ball softening point test and the equi-viscous temperature test and all were performed in the manner set out in the appropriate specification.

CHAPTER NINE

EXPERIMENTAL RESULTS PRIOR TO MAIN TEST PROGRAMME

CALIBRATION OF TEST EQUIPMENT

Load cell calibration - The results of the static and dynamic tests for load cell calibration are shown in Tables 4a, 4b and 4c.

The results of Table 4a taken from the actual trace in Figure 36 show the high degree of linearity of the Instron load cell, amplifier and recorder for tensile loads of up to 100 lb. The $1\frac{1}{2}$ lb discrepancy in descending loads is attributed to the dead band of the recorder. The dead bands of both the Instron (Leeds and Northrup) and Rikadenki recorders are specified as $1\frac{1}{2}\%$ f.s.d. corresponding, in this load cell calibration setting, to 2 lb. It was found that these dead band specifications were liberal and $\frac{1}{2}\%$ f.s.d. could be achieved with careful adjustment of amplifier gain and damping.

Table 4b tabulates the results of a static calibration of the load cell in compression up to 375 lb after calibrating at 100 lb in tension. Results indicate good correlation between the load cell amplifier and recorder and the proving ring.

Dynamic compressive test results shown in Table 4c indicate the good response of the load cell amplifier over a crosshead speed range of 0.01 to 2 inches/minute; at this maximum speed of 2 inches/minute the rate of increase of load of this proving ring is 72.5 lb/second. The response of the Instron and Rikadenki recorders are specified at $\frac{1}{4}$ second and $\frac{1}{2}$ second full scale deflection respectively and should, therefore, follow load increases of 2000 and 1000 lb/second respectively at this load cell calibration range. During specimen testing, frequencies of loading rarely exceeded 40 cycles/minute. This represents a loading time of $\frac{3}{4}$ second which is well in excess of the limitations of the recorders. Both pen recorders will therefore follow the load cell amplifier output during testing and this load cell amplifier appears to follow the change of load on the load cell satisfactorily over the range examined.

Deformation of load cell and fittings - The results of compressive and tensile tests to calibrate the deformation of the load cell and fittings are set out in Table 5 and in Figures 35a and 35b. Deformations over a load range of 1000 lb compression to 1000 lb tension are taken from Table 5 and are shown plotted in Figure 35b. Here it will be seen that the deformation of load cell and fittings is in the order of 1.5 thou. inch/1000 lb.

The fact that deformations in tension are greater than those in compression is attributed mainly to the fact that the load cell adaptor is screwed hard onto the load cell spindle thread. Thus, in compression load is transmitted to the load cell through the core of the threaded spindle whilst in tension the load is transmitted through the spindle thread. The gradual change in deformations from compression to tension indicates a progressive change in loading from spindle core to spindle thread. Another contributory factor to the differences in deformation characteristics in tension and compression is the characteristics of the load cell and end cap retaining screws.

The load cell and fittings have been calibrated and results are included in this thesis in order to show the magnitude of load cell deformation. The calibration is not, however, used in any other than illustrative calculations.

Backlash of testing equipment - The trace of load on a dummy specimen of 2 inch diameter steel tube with $\frac{1}{8}$ inch wall thickness (illustrated in Figure 22) loaded between 500 lb tension and 500 lb compression is shown in Figure 37. It will be seen that backlash of the testing equipment, which also includes the threads on the steel tube, is minimal and has been assumed insignificant for calculation purposes.

Instron turn-round time - The turn-round time of the Instron testing machine is specified as being inversely proportional to the crosshead speed and between 2 and 3 seconds at the lowest setting. Thus the turn-round time would be within the range 2 to 3 seconds at a crosshead speed of 0.002 inches/minute and 2 to 3 milliseconds at 2 inches/minute. At a crosshead speed of 0.002 inches/minute and a compressive load of 510 lb a turn-round time of 2.81 seconds was measured from the load output on the Rikadenki strip chart recorder. This apparent turn-round time includes the dead band of the recorder which, if assumed to be $\frac{3}{4}\%$ f.s.d. reduces the turn-round time to 2.06 seconds.

Ignoring the acceleration and deceleration times of the moving crosshead, which could not be detected on the load cell output, the wave form of the crosshead is sensibly trapezoidal as shown in Figure 38. At a frequency of 40 cycles/minute and a crosshead speed of 0.5 inches/minute the turn-round time represents only 1.1% of the cycle time or some 1% of the loading time. In this case the wave form may be considered triangular.

It will be shown later that the load and deformation waves of the bound roadbase specimens studied are not triangular due to the viscous

characteristics of the materials. Since these characteristics dominate the wave patterns, especially at low speeds of loading where turn-round time is significant, the crosshead deformation wave form is assumed triangular.

Crosshead response time - During cam limit microswitch control of cycling a delay occurs between the instant the microswitch is actuated and when the crosshead stops. This delay time is due to the response of the limit microswitch, the electronic circuitry, the crosshead speed clutches and the main crosshead drive motor brake coil. These are estimated by Messrs. Instron to total some 200 milliseconds representing an overshoot of 1.7 thou. inches at a crosshead speed of 0.5 inches/minute. This overshoot is further increased by the inertia of the system. As crosshead speed is reduced so is the crosshead response time reduced thus resulting in reduced overshoot and specimen strains.

Frequency modulator crosshead speeds - With crosshead speed gears AX:AX representing a fixed crosshead speed of 1 inch/minute and the frequency modulator speed at 100% the moving crosshead travels a distance of 15.037 inches in 10 minutes $\pm$ 0.1 seconds. This represents a crosshead speed of 1.504 inches/minute. At an indicated speed of 50% the distance travelled in 10 minutes is 7.491 inches.

The infinitely variable speed gearbox used in the frequency modulator is therefore taken as linear (as specified) and the crosshead speed taken as 1.5 times the fixed speed given by the crosshead speed gears. These crosshead speeds are shown in Figure 39.

Temperature sensitivity of extensometers - An aluminium tube 4 inches in diameter with an $\frac{1}{8}$ inch wall thickness, 8 inches long was load cycled in compression. Figure 40 shows the variation in extensometer output due to changes in ambient temperature of some 1°C. When the extensometers were protected by baffles to front and rear of the specimen the resulting output of the extensometers will be seen from Figure 41 to be much improved.

With the baffles in position the LVDT extensometers were calibrated at each test temperature but were not found to vary.

It is concluded that the variation in the LVDT's extensometer output is due to the thermal movement of the spindles and that the calibration of the LVDT's is not temperature sensitive over the range 0°C to +40°C. In theory the spindle deformation and hence zero drift of the extensometers is approximately 0.02 thou. inch/°C.

Hysteresis losses in the system - Figure 42 shows an actual trace of the hysteresis loops for the system with the steel dumbell in the testing machine as shown in Plate 9. The small hysteresis losses are due to both the epoxy resin used to secure the dumbell into the end caps and to the characteristics of the electronics of the testing and recording system. The difficulty of measuring loop areas recorded by this plotter due to its poor response time will be readily appreciated.

Further loops formed during low frequency testing of the steel dumbell in the flexible end cap adaptors are shown in Figure 43. These loops havebeen drawn from load and extensions taken from the three-pen recorder. If hysteresis losses of specimens were to be measured, the hysteresis loop areas of the calibration system would have to be measured at various loads and rates of loading, and the hysteresis loss of the system subtracted from the recorded hysteresis loss of the specimen. This aspect was not pursued.

Behaviour of resin bond - Again using the steel dumbell system as shown in Plate 9, the resulting stiffnesses of steel at various strains and rates of strain are shown in Figure 44. It will be seen that for a similar range of strains and rates of strains examined with the roadbase material specimens, the stiffness of the steel is recorded as decreasing by 10% over a strain range of 23. This slight drop in stiffness is attributed to the deformation of the resin bonding material. Since the loads on the resin with the steel dumbell are well in excess of those likely to be encountered in routine testing, the deformation of the resin is not considered in the calculation of roadbase specimen stiffness.

The steel dumbell has been cycled under conditions of controlled strain for 10,000 cycles at a resulting load of some 1400 lb. Reference to Figure 45 will show that there is no decay in the resin bond during this number of load cycles.

Changes in measured stiffnesses of roadbase specimens, tested under various conditions of load and number of load applications, are considered to be indicative of changes in the material itself and not in any way changes in the stiffness of the resin bond or testing and recording equipment.

TESTS ON MATERIALS, MIXTURES AND SPECIMENS PRIOR TO DYNAMIC TESTING

Specific gravity tests - The results of specific gravity tests on graded aggregates, by water displacement, and bituminous binders, by weights in air and water, are shown in Table 5. Results will be seen to be quite reproducable and are used with confidence in the calculations of specimen voids.

Temperatures of hot materials - The temperatures of a batch of six dense bitumen macadam mixtures were recorded at various stages in the preparation of specimens. The oven in which the aggregate was heated overnight was set at 175°C and the aggregate temperature of the mixture for specimen 171 was 172°C. After mixing the materials were all at 165°C irrespective of their position in the oven and the temperature of specimen 171 prior to compaction was 158°C.

These temperatures are considered satisfactory.

Void measurements of bituminous specimens - The results of density tests on Ballotini, introduced into a volume similar to that of a mould with a specimen inside by different methods, is shown in Table 8. It will be seen that the method adopted (method 1) has an extremely low scatter of results and is more reproducable than the other methods studied.

The lengths of the six moulds used in the preparation of specimens are shown in Table 9. The average length is taken to calculate an average mould volume of 1855.3 cc.

Climatization of bituminous specimens - A small number of sand asphalt specimens with thermocouples was produced. The internal temperature of one such specimen was monitored whilst it was climatizing from room temperature to a test temperature of +10°C. The cooling curve is shown in Figure 46 where it will be seen that the specimen takes a period of three hours to reach the test temperature. In cases where the test temperature is about 20°C different from room temperature it is anticipated that some 5 to 6 hours should be allowed for full climatization. In practice, specimens were left for at least 12 hours in the temperature controlled laboratory prior to testing.

Mix design for dry lean concrete - The specification for dry lean concrete for roadbase construction calls for a cube strength 1000 lb/in^2 at 7 days and 1500 lb/in^2 at 28 days.

Cube tests on three dry lean concrete cubes with an aggregate cement ratio of 17.5:1 resulted in an average 7 day strength of 825 lb/in^2. Tests on six cubes with an aggregate cement ratio of 15:1 resulted in an average 7 day strength of 1238 lb/in^2 and six further cubes of a similar composition in an average 28 day strength of 1490 lb/in^2. Since the average 28 day strength was brought down by a particularly low value the mixture was considered satisfactory. Results are set out in Table 6 for the above mixtures produced with the aggregate grading shown in Table 2 and Figure 15.

Trial concrete specimen - During the preparation of test cubes in dry lean concrete mix design, a trial specimen of dry lean concrete was cast in the manner described in Chapter 8. This specimen had an aggregate cement ratio of 17.5:1 and was produced in order to discover any shortcomings in the proposed methods of production, mounting and testing.

The surfaces of the specimen were good and free from large surface voids. After one week of curing under water the specimen was bonded into the steel end caps, under water, using the epoxy resin employed for the bonding of bituminous specimens. The specimen was left overnight under water for the resin to cure and then removed from the water bath, surface dried with a cloth and coated with molten wax to eliminate moisture losses. The specimen was then mounted in the testing machine and subjected to dynamic loading. The results of these dynamic tests are reported later in this Chapter.

All aspects of this study proved satisfactory but it became apparent that coating the specimen with wax was both time consuming and would not permit an inspection of the specimen during test. It was therefore decided to reduce moisture losses by means of a rubber membrane.

Moisture loss from concrete specimen - Certain dry lean concrete specimens were to be tested in a saturated state. The effectiveness of a 4 inch diameter rubber membrane was investigated by comparing the drying out of two initially saturated surface dry specimens. Each was stuck into end caps and one covered with a rubber membrane which was retained by "O" rings in the standard manner. The drying out results are shown in Table 7.

All concrete specimens were tested within 24 hours of removal from the waterbath and covering with the rubber membrane. Results from Table 7 show that the specimen remains fully saturated during this period.

DYNAMIC TESTS ON BITUMINOUS SPECIMENS

Details of all specimens, their test temperatures and method of test, are set out in Table 3. Exploratory tests were performed on specimens 1 to 58 prior to the routine tests of the main testing programme commencing with specimen 59.

Hot rolled asphalt - Prior to the delivery of the Instron testing machine exploratory studies were performed on nine specimens of hot rolled asphalt in an Instron testing machine already available in the Department. This

original Instron was not situated in a temperature controlled room but proved invaluable in the development of testing equipment and techniques. Once end caps and adaptors had been designed and manufactured, the results of load and crosshead limit controlled tests indicated the basic behaviour pattern of this type of material. The significance of load cell deflection and its influence on specimen strain and frequency was manifest in these early tests.

After delivery of the Instron testing machine used for the testing of roadbase materials described in this thesis, a further 13 specimens of hot rolled asphalt were tested in this new machine at room temperature. These specimens were tested in load-controlled cycling, the specimen deformation being monitored by a single LVDT and the output recorded on either a digital voltmeter or an X-Y plotter. Specimens 10 to 16 were each tested between load limits of 25 lb/in^2 compression and 25 lb/in^2 tension nominal settings and the load and deformation recorded on the X-Y plotter. Traces of the last complete cycle of specimens 11 and 15 shown in Figure 49 illustrate the extremes of loop shape encountered in this set of tests. The final loop of specimen 11 suggests that the specimen has cracked in contrast to that of specimen 15. It is pertinent to note that whatever the loop shape of the last complete cycle in this set of tests, the deformation range of the loops are of the same order. If the loop shape exhibited by specimen 11 indicates a cracked specimen, then the stress in the bitumen at failure will be very much greater than that of the bitumen in an uncracked specimen. Since the deformations at maximum (failure) load are similar, then these results suggest a constant strain criterion of failure.

Due to difficulties in recording specimen deformations at early stages in tests, the deformations of the final six specimens of hot rolled asphalt were recorded from a digital voltmeter. Figures 50 and 51 show the deformation curves of typical specimens tested in load controlled testing at equal loads about zero. In all such tests the specimens ultimately failed in tension despite the fact that compressive loads were often higher, as will be seen in Figure 51. Although the deformations at maximum (failure) load could not be recorded using a digital voltmeter, the maximum tensile deformation of the last complete cycle in each case was similar, irrespective of stress level or number of cycles, adding weight to the critical strain criterion of failure theory. Heukelom (133) has produced nomographs for the maximum tensile strain bitumens will withstand which are dependent upon the bitumen stiffness and independent of stress level.

This nomograph is reproduced in Figure 12. These critical strains, are however, applicable to single shot tests and it may well be that a further nomograph might be produced for the ultimate tensile strains of bitumens subjected to repeated applications of load.

One of the above specimens was subjected to 2000 cycles of alternating stress testing at a nominal setting of 25 lb/in^2. After a 64 hour rest period at zero load the test was resumed and the specimen cycled to failure. In this case the tensile deformation of the last complete cycle was significantly greater than those of continuous tests, as shown by the deformation curves in Figure 52. This indicates a recovery in the bitumen during the rest period which may well be complete. After separation at failure the specimen was reunited at a load of a few pounds, sufficient to ensure contact of a large area of the fractured surface. Further testing after a 66 hour rest period resulted in a temporary recovery sufficient to withstand a further 183 cycles. Although clearly the specimen was undergoing considerable consolidation during this retest period, it did withstand 183 tensile loadings of 25 lb/in^2. This small demonstration supports accepted healing theories and also the work of Bazin and Saunier (114).

Dense bitumen macadam - Following these exploratory tests on hot rolled asphalt material, 10 specimens of dense bitumen macadam roadbase material were tested under various conditions of load controlled testing. The first six specimens were tested at a temperature of +20°C and all subsequent exploratory tests leading up to the main testing programme were tested at a temperature of +10°C.

The deformation curves of a specimen of dense bitumen macadam tested at a temperature of +10°C are shown in Figure 53. Here, the specimen was subjected to three runs of compressive load cycling with a nominal stress of 25 lb/in^2. These were followed by a compressive stress of 12½ lb/in^2. The final two runs were tensile loading first of 12½ lb/in^2 and finally of 5 lb/in^2. The first three compressive repeated loading tests illustrate the temporary beneficial effect of rest periods although the overall behaviour suggests that the total deformation after 20,000 cycles is not reduced. The lower stress level of the final compressive repeated loading test indicates a final limit to the deformation due probably to the particle interaction of the aggregate. It is likely that a limit to the deformation would occur at the 25 lb/in^2 stress level. A threshold stress would exist at a higher stress level beyond which the specimen would either develop shear

failure planes or vertical tensile cracks resulting, in either case, in catastrophic failure. Tensile repeated loading tests indicate no threshold stress, in tension, compatible with viscous theory.

The subsequent 20 specimens of dense bitumen were subjected to deformation-controlled cyclic loading referred to hereafter as strain-cycling. All strain-controlled tests were performed with deformation limits set symmetrically about the zero position. This procedure was adopted since the results shown in Figure 54 indicate that the stiffness of dense bitumen macadam, defined as the stress range divided by the strain range, is independent of the mean deformation, providing the deformation passes through the original zero. This phenomenon applies only to the strain range examined and the extension limit settings studied.

In the production of dense bitumen macadam test specimens it was apparent from visual and practical observations that specimens were being produced with a significant volume of surface voids. These surface voids are attributed to the effect of the compaction moulds and it was felt that these might have an adverse effect on the performance of the specimens under test. One specimen of dense bitumen macadam was produced in the standard manner and scanned on the radioactive scanner described previously. All surface voids were then filled with a hot fines matrix of similar composition to the specimen and the cylinder rescanned. The resultant density traces were identical indicating that this scanning technique was insensitive to (small) surface voids. This modified specimen was then tested under conditions of strain controlled cycling at a temperature of $+10^{\circ}C$. The results shown in Figure 55 indicate that there is no apparent advantage to be gained from filling the surface voids. Either the filled material did not key to the specimen, resulting in similar specimens being compared, or the reduced stresses in the modified specimen have little effect on its performance. If the latter be the case then this supports the premise that it is strain amplitude that defines specimen behaviour under repeated application of load. The higher stiffness of the specimen with filled surface voids is not considered significant and no further specimens were modified in this or any other manner.

Tests to establish a criterion of service life - The above mentioned exploratory tests on both hot rolled asphalt base course and dense bitumen macadam roadbase materials led to a basic appreciation of the trends in behaviour of bitumen-bound materials in this form of test. It was apparent that the results of strain-controlled tests were easier than load controlled tests to monitor and record and that strain might have a greater influence

on performance. These factors and comments made at the beginning of Chapter 6 led to the adoption of the strain-controlled form of test on all subsequent bituminous roadbase material specimens.

Once the final form of the frequency modulator had been developed and tested it was employed on all subsequent work on bituminous roadbase material specimens unless otherwise stated.

As part of attempts to establish a criterion for service life a specimen was tested, without frequency control, over 78,000 cycles. This specimen was subjected to 7 rest periods of varying duration and the resulting stiffness/cycles plot is shown in Figure 56. The temporary beneficial effects of rest periods for this type of material determines that routine testing should be performed on a continuous basis. Since a maximum testing frequency of 40 cycles/minute is determined by the testing machine, and since it was not felt desirable to leave the testing machine in operation unattended for any length of time, tests would be restricted to some 30,000 cycles at the most. It was, therefore, necessary to determine some form of criterion for service life which would result in lives of less than 30,000 cycles at the lowest strain level examined.

Figure 57 shows the effect of repeated applications of load on the stiffness of dense bitumen macadam under strain-controlled testing at a temperature of $+10^{\circ}C$. It will be seen that the stiffness falls with increasing number of load cycles in a regular curve. In this case there is no evidence of a well defined "failure" point, although the stiffness is reduced to below 40% of its initial value. Four aspects of material behaviour were studied in order to define a failure point for service life. If one aspect rendered a repeatable failure criterion then this aspect would have to be studied with each routine test, unless the service life could be related to the material stiffness. These four aspects of material behaviour consisted of visual assessment of condition, reduction in stiffness during test, hysteresis losses and changes in internal temperatures of specimens under test. The recording equipment did not permit a study of material phase angle to be made.

Certain specimens of dense bitumen macadam tested at high strain levels in strain controlled cycling showed evidence of surface cracking. This cracking was of either a single or multiple nature and propagated around the circumference of the specimen under test. Multiple cracks either propagated independently or joined together to form fewer propagation paths.

Figure 55 shows the stages in strain-controlled tests when cracks

propagated by certain amounts. Although the degree of cracking may very roughly be related to the shape of the stiffness/cycles curve, cracking was not considered a good criterion of failure for the following reasons. First, cracking is only evident (at the temperature studied) on higher strain level tests. Secondly, cracking may be of a single or multiple nature and is difficult to define especially if cracking does not propagate near horizontally. Thirdly, crack propagation has to be monitored frequently either by visual or automatic means rendering an accurate determination of life impossible. Finally, cracking can only be examined on the surface of the specimen. Whereas it is likely that dominant cracking will occur at the surface of the specimen, due to inhomogenuities in the system, internal cracking may render the material unserviceable before it manifests itself on the surface. Cracking is not, therefore, considered a suitable criterion of failure in this form of test.

At this stage in studies into the behaviour of dense bitumen macadam specimens subjected to strain-controlled testing, practice had been to evaluate the stiffness of the specimen at various stages during the test and plot these on a stiffness/cycles graph. The possibility of employing some function of the reduction in stiffness during a test was studied by calculating the average fall in stiffness per cycle at various points in the test. This was done by averaging the fall in stiffness between stiffness calculations over the appropriate number of cycles and expressing the result as a fraction of the initial stiffness. This resulted in the evaluation of the "percentage fall in stiffness per cycle" which could be plotted against the appropriate cycle, on logarithmic paper, as shown in Figures 113 and 114. Here it will be seen that the relationship is linear for both low and medium strain levels although the initial stiffness has been reduced by up to 60%. Service life might possibly be defined as that number of cycles at which the fall in stiffness is reduced to a value of, say, 0.01% but this is rather a negative approach to the problem. Also, a special value would have to be considered together with the slope of the relationship. This aspect was not considered a good criterion for specimen failure, although it is considered in greater depth in Chapter 10 with regard to a mathematical approach to the analysis of specimen behaviour.

The third aspect of specimen behaviour to be studied with a view to the establishment of a criterion of failure was that of hysteresis losses. The hysteresis loops of a number of specimens were taken on the X-Y plotter at the same stages as stiffness calculations were made. The areas of these loops were then measured with a planimeter and plotted against the

appropriate cycle as shown in Figure 57. As each test proceeds and the specimen becomes progressively more damaged the hysteresis losses increase. When specimen damage is complete the hysteresis losses would decrease and the maximum hysteresis loss would therefore indicate the ultimate failure point of the specimen under test.

Reference to Figure 57 will show that at a strain level of $1.51.10^{-4}$ in/in. the maximum hysteresis losses occur at a stiffness 51.5% of the initial value whilst at a strain level of $1.08.10^{-4}$ in/in it occurs at 62.7% of the initial stiffness. In tests where the strain level was less than 1.10^{-4} in/in no maximum hysteresis loss was achieved during the test. Whereas the measurements of hysteresis loop areas is difficult, tedious and inaccurate, it was considered possible to produce a relationship between the proportion of the initial stiffness at which the maximum hysteresis losses occurred and strain level. From this relationship the lives of other test specimens might be determined from the stiffness/cycles plots. However, the relationship between the proportion of the initial stiffness at which maximum hysteresis losses occur and strain level might be expected to differ for each material, test temperature and, possibly, test frequency. Hysteresis loops would, therefore, need to be recorded for all specimens tested and would therefore be used to determine service life directly for each specimen.

Due to difficulties in the recording and measuring of hysteresis loop areas and the fact that service lives would exceed the facilities of the testing system reducing the range of strain levels studied to one decade, hysteresis losses were not considered suitable criterion of failure in this form of test.

The final aspect of material behaviour studied was that of internal temperature variations. It was felt that internal temperature rises and hysteresis losses might be inter-related. A study of the internal temperature variations of specimens might either confirm the findings of the hysteresis work or assist in the determination of a failure criterion.

A specimen of dense bitumen macadam was drilled with 5/32 inch masonry drill radially at the centre to radial a depth of 1 inch. A previously calibrated copper-constantan thermocouple, coated with bitumen was then placed in the specimen and the hole filled with bitumen. The specimen was finally tested in the standard manner under strain-controlled testing at a temperature of $+10^{o}C.$, a frequency of 40 cycles/minute and a strain level of approximately 3.10^{-4} in/in. The specimen was subjected to 15,000 applications of load which reduced the stiffness to less than

40% of its initial value. Throughout this test no change in internal temperature was recorded although the measuring equipment was capable of detecting temperature variations of $\frac{1}{4}^{o}C$.

It was felt that the inhomogenuities of the dense bitumen macadam specimen would result in local deteriorations of the material possibly remote from the thermocouple. In consequence, six sand asphalt specimens were produced with a thermocouple, already embedded in a small block of sand asphalt for protection under compaction, placed in the centre of each specimen. It was hoped that the potentially greater homogenuity of these sand asphalt specimens might result in more meaningful thermocouple outputs. These sand asphalt specimens were tested in strain-controlled cycling at temperatures of $+10^{o}C$ and $+20^{o}C$ and typical results are shown in Figure 58. Here it will be seen that internal temperature rises are evident at high strain levels but it is difficult to relate these to the stiffness/cycles relationship. Since the temperature rises are small service life cannot be related to internal temperature rises with any confidence. This aspect was not therefore pursued.

At this stage in the testing programme no suitable criterion of failure had been found from which to determine service life of specimens subjected to strain-controlled cyclic loading. It has been suggested by Monismith and others that service life might be defined as that number of load cycles required to reduce the stiffness of a material by a certain amount. This would appear to be a sound engineering compromise in the present situation and it was felt that a reduction in stiffness of 40% may render the material unserviceable in situ.

It was therefore decided that service life would be defined as that number of load cycles required to reduce the stiffness to 60% of its initial value.

DYNAMIC TESTS ON CONCRETE SPECIMENS

The first trial specimen of dry lean concrete was produced, during mix design work, with an aggregate cement ratio of 17.5:1. After bonding into the end caps it was sealed with wax and mounted in the testing machine for exploratory dynamic testing. It was mounted by the same method as employed for the bituminous specimens and did not appear to suffer any damage when clamped to the rigid end cap adaptors.

Stiffness tests were performed on the specimen at a temperature of $+10^{o}C$ in order to assess the effect of frequency of test, or rate of application of strain, on specimen stiffness. The results of these strain-

controlled tests, shown in Figure 59, confirm the findings of other investigators that the frequency of test over the range 2 to 50 cycles/minute has no detectable effect on the stiffness of dry lean concrete.

After these stiffness measurements, the specimen was subjected to repeated applications of load in strain-controlled cycling at a strain level of some $6.5.10^{-4}$ in/in and a frequency of 43 cycles/minute. The change in stiffness over the test period is shown in Figure 60. Here it will be seen that although the stiffness falls during the first 50 cycles of testing it increases with subsequent load applications. The test was terminated since it was then felt that the rigid end cap adaptors might be having an adverse effect on the specimen and its performance under dynamic loading.

Subsequent tests on dry lean concrete specimens with an aggregate cement ratio of 15:1 and tested between adjustable end cap adaptors revealed a similar pattern in specimen behaviour. A considerable amount of time was devoted to a study of this phenomenon and the results are presented in the following Chapter.

CHAPTER TEN

EXPERIMENTAL RESULTS OF MAIN TEST PROGRAMME

VOIDS IN SPECIMENS

The results of void determinations on a typical batch of dense bitumen macadam specimens produced with a 90/110 pen. bitumen are shown in Table 10. The method of calculation is set out in Appendix 2 and has been used for both bituminous and cement bound materials. In studying all void results it should be remembered that the internal voids refer to the voids in the material and may be compared both to other materials and to practice. Surface and total voids relate to the particular specimen size used in this investigation and may be used in conjunction with the test results of dynamic loading. It is emphasised that the results of total void determinations are not equal to the sums of the corresponding internal and surface void determinations since internal voids are expressed as a percentage of the volume of the material rather than the specimen.

At first sight the volumes of surface voids appear to be excessive, an average value being represented by almost a 10 cm cube. It should be remembered, however, that by virtue of the method of determination, the volume of surface voids is that volume of the surface of the specimen, less than the basic 4 inch diameter cylinder, into which water can penetrate. It therefore includes those internal voids continuous with the surface of the specimen.

The average results of void determinations on each batch of 90/110 dense bitumen macadam specimens are set out in Table 11a and those for 190/210 dense bitumen macadam, dense tar macadam and hot rolled asphalt in Tables 11b, 11c and 11d respectively. Standard deviations have been calculated using the computer program shown in Appendix 4 assuming that the average result is also subject to error (i.e. S.D. $= \sqrt{\frac{(x-\bar{x})^2}{n-1}}$). The implications of these results are discussed in Chapter 11.

STIFFNESS MEASUREMENTS

The results of a stiffness measurements test on a specimen of 90/110 dense bitumen macadam tested at a temperature of $+10^{\circ}C$ are shown in Figure 62. The rate of application of strain (strain rate) rather than frequency, has been taken as a basic parameter which, together with the strain range,

defines specimen stiffness. At a particular strain level, stiffness increases with increase in strain rate. Also, over the range of strain rates considered, the relationship between stiffness and strain rate at any strain level approximates to logarithmic.

These two basic phenomena conform with the nomograph for the determination of bitumen stiffness presented by Van der Poel (83). Reference to this nomograph, shown in Figure 8, will indicate that, for a specific binder and temperature, each tenfold increase in testing frequency does not result in a constant increase in bitumen stiffness. Rather, the increase in bitumen stiffness is greater at lower stiffness values. However, when converting the bitumen stiffness to mixture stiffness using the nomograph of Heukelom and Klomp (86) (Figures 11 and 66) this effect is reduced. Figure 67 shows the theoretical stiffness values of the pure bitumen and those of its mixture. Here it will be seen that for the mixture the increase in stiffness per decade increase in frequency is less affected by absolute frequency than in the pure bitumen. These effects are plotted for comparison in Figure 68. For the purposes of this study, therefore, it has been assumed that the relationship between stiffness and strain rate, at a particular strain level, is logarithmic. This assumption will lead only to very small errors, as shown in Figure 67, since test frequencies were well within the range 0.01 to 1 cycle/second.

With this basic assumption, stiffness increases by a constant factor with each uniform multiple increase in strain rate. Since this stiffness factor is sensibly constant for all strain levels over the range of strains examined it is possible to establish parallel stiffness/strain lines for various strain rates. The relationship between stiffness and strain rate, which is independent of strain level, has been defined by the parameter "rate effect." This rate effect is defined as the increase in stiffness per decade increase in strain rate at a specific strain level within the range examined.

The rate effects evaluated from stiffness measurement tests on all the types of bituminous roadbase materials studied are tabulated, together with the slopes of the stiffness/strain lines, in Table 12.

The stiffness/strain lines for various strain rates were sensibly parallel within each test on the three types of macadam specimens. However, reference to Figure 63 will show that this was not the case with the hot rolled asphalt specimens tested at $+30^{\circ}C$. Here the rate effect was found to increase at higher strain levels. This might be accounted for by the fact that the lower volume concentration of aggregate in this type of

mixture renders the mixture more susceptible to changes in binder characteristics. This aspect will be considered in more detail in Chapter 11. For the purposes of this study the rate effect of hot rolled asphalt is taken as that at a strain level of 5.10^{-4} in/in corresponding to the average strain level of repeated loading tests at this temperature.

The trend of increasing rate effect with an increase in strain level found for the richer hot rolled asphalt specimens has also been found in stiffness tests on pure bitumen. Results shown in Figure 92 indicate that this trend is certainly a function of the binder rather than the mixture and confirms a linear stiffness/strain relationship for pure bitumen over the strain range considered.

Results of stiffness measurement tests on a dry lean concrete specimen, shown in Figure 64, confirm that the strain rate has no detectable effect on the stiffness/strain relationship.

In all stiffness measurement tests good agreement was found between experimental results and the estimated stiffness/strain lines. At strain levels in excess of 5.10^{-5} in/in lines could be drawn such that stiffnesses were within at worst 5% of the estimated position. At lower strain values errors were greater due to inaccuracies in measuring specimen deformation (less than 0.3 thou-inch). Errors throughout the entire strain ranges examined were random suggesting linear rather than curved stiffness/strain relationships at constant rates of application of strain.

STIFFNESS/STRAIN RELATIONSHIPS

From the results of repeated loading tests on all the roadbase material specimens tested during the main testing programme, the results of the first loading cycle of each specimen have been used to establish stiffness/strain relationships for each material type and testing temperature. These relationships provide basic information which has subsequently been used in the Shell Bistro computer programme for the analysis of layered systems.

It has been shown both in theory and in practice that the stiffness of bituminous materials depends both upon the strain level (or time of loading) and the strain rate. Since the repeated loading work has been performed at a variety of strain rates, it has been found necessary to reduce all results to a common basis. This enables a direct comparison to be made of the stiffness/strain characteristics of different materials over a range of temperatures.

The results of the stiffness measurement tests described above showed that stiffness was related to the strain rate by the rate effect. The appropriate values of rate effect determined by the stiffness measurement tests have therefore been used to reduce all stiffness/strain results to a common strain rate of 100$\mu\varepsilon$/sec. The strain rate is given by:

$$\text{Strain rate} = (2.\varepsilon.f)\mu\varepsilon/\text{sec.}$$

where ε = strain in $\mu\varepsilon$

f = frequency in cycles/sec

assuming a triangular wave form. The stiffness determined from the first cycle of each repeated loading test is then reduced to the common strain rate by:

$$S_{R2} = S_{R1}.R^{\log_{10}\left(\frac{R_2}{R_1}\right)}$$

(by definition, see Appendix 3), and these stiffness corrections have been performed using part of the computer programme reproduced in Appendix 5. This programme also provides a best fit line for each stiffness/strain relationship based upon the method of least squares, assuming that the stiffness is the dependent variable.

In the case of dry lean concrete, since the rate effect is unity, no stiffness corrections were necessary.

The stiffness/strain relationship for the 90/110 dense bitumen macadam series of specimens tested at a temperature of +10°C is shown in Figure 75.

The range of strain rates at any strain level is not as large as would be desired since these results represent only the first cycle of a repeated loading test. At low strain levels the maximum strain rate is determined by the frequency limitations of the testing machine (40 cycles/min at $\varepsilon = 5.10^{-5}$ in/in defines maximum strain rate of 66.7$\mu\varepsilon$/sec). A significant reduction in frequency, and hence strain rate, would result in excessively long testing periods which were limited to 12 hours. At high strain levels a greater range in strain rates is possible but maximum values are restricted by the loading rate capacity of the testing machine. Loading rates were also kept down at low temperatures to avoid the possibility of brittle fracture of the binder. In general, there is at least a threefold increase in strain rate at each strain level.

There is generally good agreement between adjusted stiffness values at similar strain levels, the results being within the range of experimental error thus validifying the strain rate correction technique. Some 95% of results are within a factor of two of the best fit line.

In calculations of specimen strain and stiffness, the total dynamic deformation has been used to define the average strain over the free length of the specimen. Due to inhomogenuities of the material it is unlikely that the strain will be uniform over the entire length of the specimen. The total deformation will therefore represent the movement over a limited length of the specimen. The majority of experimental error is attributed to high local strains which would result in apparently low values of stiffness of the specimen as a whole. Assuming no other cause of experimental error, the true stiffness/strain, would lie above the experimental results as shown in Figure 65. Thus, the experimental point "P"-strain is $1.55.10^{-4}$ in/in, stiffness = $2.24.10^{5}$ lb/in^2, would represent a local strain of $1.10.10^{-3}$ in/in. This means that the total deformation would occur over 14.1% of the total free length of the specimen either continuously or discontinuously. Local strains would be caused by inhomogenuities in the specimen and movement occurring over only 14.1% (the worst case in Figure 65) is not unreasonable. Whereas other factors such as stress concentrations due to the bonded end caps and eccentricity of loading would also affect specimen stiffness, the order of local strain illustrated by this example supports the theory of inhomogenuity for a large proportion of experimental error. The phenomenon of local strain also applies to roadbase materials in their practical application. The best fit line of the adjusted experimental results should therefore prove a reasonable guide to the average stiffness/strain characteristics of this material at this temperature.

The results of stiffness/strain determinations for this 90/110 dense bitumen macadam tested at temperatures of 0°C, +10°C, +30°C and +40°C are shown in Figures 74 to 77. Again the majority of results lie within a factor of two of the best fit lines there being no indication of non-linear stiffness/strain relationships.

The softer 190/210 dense bitumen macadam has been tested at temperatures of 0°C, +10°C and +40°C and the resulting stiffness/strain relationships are shown in Figures 78 to 80 respectively. The results of these stiffness plots show remarkably little deviation from the best fit lines indicating very reproducable specimens and accurate rate effects. However, since the standard deviations of internal and surface voids are only some 25% and 35% lower than those of the harder 90/110 dense bitumen madadam specimens and, in the latter case, since low stiffness values cannot be associated with high voids, the general agreement of results cannot be ascribed to variations in void contents. It may well be that the distribution of internal and surface voids is more uniform with this type

of mix, thus resulting in better agreement of results, although no practical explanation of this phenomena can be offered. It is likely that the close proximity of results to the best fit lines is more fortuitous than logical.

Figures 81 to 84 show the stiffness/strain relationships of dense tar macadam for temperatures 0°C, +10°C, +30°C and +40°C and Figures 85 and 86 those for hot rolled asphalt at +10°C and +30°C respectively. As was the case with the softer dense bitumen macadam specimens a surprisingly low deviation of test results from the best fit lines is evident. In view of the increasingly good agreement of experimental results within themselves during the testing period it is possible that the distribution of specimen voids did, in fact, improve with practice in specimen manufacturing and testing techniques.

In the case of the dry lean concrete roadbase material specimens tested at a temperature of +20°C, it has been assumed that the difference between the stiffnesses of the first cycle of loading under stress-and strain-controlled testing is relatively insignificant. Since the stiffnesses of specimens tested either wet or dry is similar, the results of initial stiffness values shown in Figure 87 include all those specimens tested. Again, it will be seen that all results approximate closely to a straight line.

These stiffness/strain relationships for all the bituminous roadbase materials studied are summarised in Figures 88 to 91, together with the relationship for a frequency of 1 cycle/second. The dashed portions of the 100$\mu\varepsilon$/sec relationships indicate extrapolated values. Figure 87 shows the stiffness/strain relationship for dry lean concrete specimens tested both wet and dry. In this case there is no frequency or temperature effect.

On certain stiffness/strain graphs a line of maximum stiffness has been shown. These maximum stiffness values have been calculated using the maximum bitumen stiffness value quoted by Van der Poel (84), the aggregate content void correction of Van Draat and Sommer (92) and the mixture factors of Heukelom and Klomp (86), In the case of tar-bound mixtures the maximum stiffness of the tar is calculated by using the void content correction and mixture factors as before. It should be remembered that these maximum stiffness values represent the elastic asymptotes of stiffness and will never be achieved in practice. It should also be borne in mind that these maximum stiffness values take no account of strain level.

REPEATED LOADING TESTS ON BITUMINOUS MATERIALS

All repeated loading tests on the bituminous roadbase materials tested as part of the main testing programme were performed under conditions of controlled strain. As has been explained in Chapter 9, no definite failure point is evident in these types of materials and service life has been defined as the number of cycles required to reduce the specimen to 60% of its value in the first cycle.

90/110 dense bitumen macadam - The reductions in material stiffness with increasing number of applications of load are shown for a typical batch of 90/110 dense bitumen macadam specimens, tested under nominally identical conditions, in Figure 93. Here it will be seen that although the initial stiffness values vary within a range of two the service lives are relatively close to one another. The service lives, together with the average strain over the test are as follows:-

Specimen	59	61	62	60	63	64
Strain	$1.44.10^{-4}$	$1.22.10^{-4}$	$1.18.10^{-4}$	$1.16.10^{-4}$	$1.08.10^{-4}$	$9.50.10^{-5}$
Service life	$6.1.10^{3}$	$4.0.10^{4}$	$2.1.10^{4}$	$3.5.10^{4}$	$1.6.10^{4}$	$4.0.10^{4}$

Here it will be seen that the service lives lie within a range of 6.5 but the range of strain is 1.5. If allowance is made for the fact that a higher strain results in a shorter service life, a fact which will be evident in due course, the adjusted service lives become:-

Specimen	59	61	62	60	63	64
Corrected service life	$3.5.10^{4}$	$1.1.10^{5}$	$4.7.10^{4}$	$7.5.10^{4}$	$2.2.10^{4}$	$2.8.10^{4}$

This reduces the range of lives to within a factor of 5, the scatter being accounted for as with specimen stiffness, by high local strains within the specimen.

The variation in strain level, despite the identical extensometer limit settings, is attributed to the different visco-elastic responses of the individual specimens again due to high local strains. At specimen turn-round a load is sustained by the specimen and the deformation undergone at this time will depend upon the viscous and/or delayed elastic character of the specimen. Thus at a specific strain setting a greater strain range is due to the greater deformation of a more viscous material at turn-round and is generally associated with a lower stiffness (indicative of a high local

strain). This lower stiffness due to increased flow at turn-round should not be confused with lower stiffness values at higher strain settings although the mechanism may well be the same.

The foregoing comments are applicable to all bituminous roadbase materials tested under repeated loading over the entire range of temperatures considered.

It was explained in Chapter 7 that as the stiffness of a specimen falls under the repeated applications of load so the crosshead speed is reduced by the frequency modulator. This is to retain a constant testing frequency, compensating the reduction in load cell deformation. The reduction of crosshead speed also reduces the amount of overshoot at the reversal positions, which in turn, reduces the strain range of the specimen. In certain cases, the increase in viscous and/or delayed elastic deformation at turn-round causes an apparent increase in specimen strain range during a test. In either case a change in strain range deviates from a strain-controlled test and alters the potential service life of the specimen. It was therefore found necessary in certain tests to make allowance for a change in strain range and adjust the corresponding stiffness accordingly. It is shown in Appendix 3 that a change of 5% in strain would, at worst, alter the stiffness by 1%, Thus any strain deviating from the average value by more than 5% would have its appropriate stiffness corrected using the relationships

$$S_c = \left(\frac{\varepsilon_A}{\varepsilon_N}\right)^{(m+\log R)} \cdot S_N$$

where S_c = corrected stiffness

ε_A = average strain

S_N = stiffness at cycle N

ε_N = strain at cycle N

m = slope of $\log S/\log \varepsilon$ (from stiffness measurements)

R = rate effect (assumed constant throughout test)

The service life is then determined from the stiffness/cycles relationship using the strain-corrected stiffness values.

Results of two further groups of stiffness/cycles curves are shown in Figure 94. These represent extremes of strain levels investigated at a temperature of $+10^{\circ}C$ and will be seen, in either case, to give reproducable service lines.

The testing of specimens has been performed over as wide a range of strains and strain rates as possible. It was endeavoured to produce service lives for both high and low strain rates both at high and low strain levels. As explained previously, practical limitations of the testing facilities (time and loading capacity of the testing machine) restricted the range of results but nevertheless sufficient data was obtained to define material behaviour with confidence.

At a test temperature of $+10^{\circ}C$, 61 specimens of 90/110 dense bitumen macadam were tested and the service lives are shown plotted against the average strain level in Figure 99. Here, as is the case with all test results, service lives in excess of $3.0.10^{4}$ cycles have been extrapolated. It will be seen that all results approximate to a smooth curve and that the service life at any strain level is independent of the rate of application of strain. A best fit line has been determined for these results using the computer programme reproduced in Appendix 5 where it has been assumed that the service life is the dependent variable. This best fit line defines service life as:

$$\log_e N_s = \frac{135}{\mu\varepsilon^{0.56}}$$

This form of relationship will be seen to give an acceptable best fit line to the experimental results and has been selected in preference to the more complex, and less meaningful polynomial type expression. In the expression above the indices of the strain defines the shape of the curve and the constant term defines the position of the curve. The constant is the logarithm (to the base e) of the service life at a strain of 1.10^{-6} in/in. In general, service lives above a strain level of 5.10^{-4} in/in lie within a factor of 3 and below 5.10^{-4} in/in within a factor of 5. Of the 61 specimens tested only 4 results lie outside these scatter bands.

Further repeated loading tests were performed on the 90/110 dense bitumen macadam material to establish the service life/strain relationships at other temperatures. At a test temperature of $+30^{\circ}C$ a further 24 specimens were tested again covering as wide a range of strain levels and rates of application of strain as practicable. When plotted against strain level, service lives were found to fall within the scatter of the results at $+10^{\circ}C$, the service lives again being independent of strain rate. Additional tests at temperatures of $0^{\circ}C$ (11 specimens) and $+40^{\circ}C$ (12 specimens) confirmed the common relationship between service life and strain level, independent of rate of application of strain and temperature within the ranges examined. All service lives for this material are shown in Figure 103.

A best fit line for all the results of the 90/110 dense bitumen macadam specimens tested under repeated loading is given by:

$$\log_e N_s = \frac{118}{\mu\varepsilon^{0.53}}$$

Scatter of all experimental results about this best fit line is within a factor of 4 above a strain level of 5.10^{-4} in/in and within a factor of 7 below this strain level.

In order to establish whether, or not, the shapes of individual stiffness/cycles curves are similar at common strain levels but different temperatures and strain rates, the number of cycles required to reduce the specimen stiffness to 90% and 75% of its initial value have been determined as shown in Figures 101 and 102 respectively. Again, for each stiffness reduction, all results suggest common curves confirming that the shapes of all stiffness/cycles curves at common strain levels are similar. The best fit curves for cycles to a particular stiffness are:

$$\text{cycles to } 90\% S_I : \log_e C_{90} = \frac{62.1}{\mu\varepsilon^{0.65}}$$

$$\text{cycles to } 75\% S_I : \log_e C_{75} = \frac{112}{\mu\varepsilon^{0.60}}$$

It may thus be concluded that for the 90/110 dense bitumen macadam roadbase material, tested over a temperature range of $0^{\circ}C$ to $+40^{\circ}C$ and frequencies of 5 to 40 cycles/minute (within practical limitations), the shapes of the stiffness/cycles relationships are identical at common strain levels and independent of test temperature and strain rate.

<u>190/210 dense bitumen macadam</u> - The softer dense bitumen macadam was tested in a manner identical to that described above, corrections, where appropriate, being made to stiffness values during each test. In practice, only some one in ten results required adjustment. At a temperature of $+10^{\circ}C$, 27 specimens were tested good parallel stiffness/cycles relationships being obtained at common strain levels.

When service lives were plotted against strain level it was found that points lay within the scatter of the 90/110 dense bitumen macadam results. Further tests on 14 specimens at temperatures of $0^{\circ}C$ and $+40^{\circ}C$ confirmed the fact that, irrespective of test temperature and strain rate, the service lives of the softer dense bitumen macadam were the same as those of the harder dense bitumen macadam at similar strain levels. The results for both dense bitumen macadams are shown in Figure 106 and the best fit line is given by the equation:

$$\log_e N_s = \frac{111}{\mu\varepsilon^{0.52}}$$

Scatter of service lives for both dense bitumen macadams is within a factor of 5 for strain levels above 5.10^{-4} in/in and within a factor of 10 for strain levels below 5.10^{-4} in/in.

Reference to Figures 104 and 105 will show that since the relationship between strain and cycles to either 90% or 75% of the initial stiffness are common for both dense bitumen macadams, then the shapes of the stiffness/cycles curves are also common for both dense bitumen macadams at common strain levels. The shapes of these relationships for both materials are given by:

$$\text{cycles to } 90\%\ S_I \ :\ \log_e C_{90} = \frac{69.7}{\mu\varepsilon^{0.66}}$$

$$\text{cycles to } 75\%\ S_I \ :\ \log_e C_{75} = \frac{112}{\mu\varepsilon^{0.60}}$$

The constant term of the latter expression should clearly be between the constant terms for the expressions for cycles to 90% and 60% stiffness. The discrepancy in these constants is attributed to the fact that over a large strain range the form of expression is invalid. However, over the range of strains considered, these expressions provide curves well within the range of experimental results.

It is, therefore, concluded that both types of dense bitumen macadam roadbase materials studied, having identical aggregate type and grading, equal volumes of binder and similar void characteristics, differing only in binder hardness (with similar penetration indices) have identical stiffness/cycles characteristics at common strain levels, which are independent of test temperature and strain rate.

Dense tar macadam - The composition of the dense tar macadam differs from that of the dense bitumen macadams only in the binder type. Aggregate type and grading, binder volume and void characteristics of all three types of dense macadams are similar.

Initial tests on the dense tar macadam roadbase material were performed at a temperature of $+10^{\circ}C$. Figure 95 shows the results of a batch of six specimens tested under identical strain settings and frequencies. Although variations in initial stiffness are considerably less than the 90/110 dense bitumen macadam, as will be seen, in general, in Figure 95, the drops in stiffnesses with repeated applications of load are not as reproducable. The results of this batch of specimens, tested under

identical conditions are:

Specimen	435	434	431	436	433	432
Strain	$4.69.10^{-5}$	$4.50.10^{-5}$	$4.36.10^{-5}$	$4.35.10^{-5}$	$4.31.10^{-5}$	$3.74.10^{-5}$
Service life	$6.7.10^{3}$	$2.9.10^{3}$	$5.2.10^{3}$	$9.5.10^{3}$	$1.7.10^{4}$	$2.7.10^{3}$
Corrected service life	$6.7.10^{3}$	$3.1.10^{3}$	$5.5.10^{3}$	$1.0.10^{4}$	$1.8.10^{4}$	$2.8.10^{3}$

The corrections to service lives will be seen to be less than 6% which represents only 2% of the range of service lives recorded. Since in all cases service life corrections represented on extremely low proportion of the variations in service life scatter it is doubtful whether this correction is necessary. However, since this only became apparent after the majority of repeated loading tests in which corrections were necessary had been performed, corrections were carried out in all cases where the strain level deviated by more than 5% of the average value. In future it is suggested that these corrections should be confined to much wider strain variations, possibly in excess of 10%. In practice such large variations are unlikely to occur unless the range of interest is extended beyond a 40% drop in initial stiffness.

The results shown in Figure 96 are for the highest strain level studied at this temperature. Higher levels were not performed due to the low service lives at this setting. The root mean square service life in this case is 3.8 cycles but the tests have been run to less than 10% of the initial stiffnesses. Results indicate that a lower stiffness level of some 5% of the initial stiffness might exist. This would be due to the elastic component of the material, suggesting some form of Burger's model with no dashpot, as shown in Figure 3, might be appropriate for this macadam. The significance of the close proximity of the stiffness/cycles relationships even over this extended range of stiffness change will be discussed in Chapter 11.

Service lives of the 30 specimens tested at a temperatire of $+10^{\circ}C$ have been plotted against the appropriate strain levels in Figure 100. As was the case with the previous types of dense macadam materials studied, the strain rate appears to have no significant effect on service life over the range considered. The scatter in results is a little greater than that of the 90/110 dense bitumen macadam shown in Figure 99 although the best fit line appears to be a reasonable representation of the results. The best

fit line for the dense tar macadam roadbase material tested at a temperature of +10°C is given by:

$$\log_e N_s = \frac{111}{\mu\varepsilon^{0.65}}$$

The higher indices show that the dense tar macadam has shorter service lives than the 90/110 dense bitumen macadam at lower strain levels. At a service life of 100 cycles the dense bitumen macadam strain is $4.4.10^{-4}$ in/in whereas the dense tar macadam strain is $1.3.10^{-4}$ in/in. However, reference to Figure 75 and 82 will show that at these strain levels the corresponding stress levels at a rate of application of strain of 100$\mu\varepsilon$/sec are 123 lb/in^2 for the dense bitumen macadam and 221 lb/in^2 for the dense tar macadam. Thus, at this service life, although the dense bitumen macadam will withstand a higher strain than the dense tar macadam, the dense tar macadam will withstand a higher stress.

A further 35 specimens of dense tar macadam have been tested at a temperature of +30°C. In this case, although the strain/rate had no significant effect on the service life, the service life curve was not similar to the curve obtained at +10°C. The results of the 15 specimens tested at a temperature of +40°C also indicated service lives independent of rate of application of strain. Further, the service lives appeared to be within the scatter band of those at +30°C. In this case, the best fit line shown in Figure 109 is:

$$\log_e N_s = \frac{116}{\mu\varepsilon^{0.56}}$$

Scatter is within a factor of 2 at strain levels above 5.10^{-4} in/in and within a factor of 10 below this strain level. In comparing these with previous figures it should be remembered that the results of only 50 specimens have been produced compared with the 149 dense bitumen macadam type specimens tested over a wider range of temperatures.

Common relationships for cycles to 90% initial stiffness and cycles to 75% initial stiffness indicate that for test temperatures of +30°C and +40°C the shapes of the stiffness curves are similar for common strain settings.

Tests performed on dense tar macadam specimens at a temperature of 0°C were limited to strain levels below 2.10^{-4} in/in. This was due to the high stiffness of the material and the loading restrictions of the testing machine. At strain levels in excess of 1.10^{-4} in/in a few specimens pulled out of one or other of their end caps in tensile loading in excess of 3000 lb due to a bond failure of the epoxy resin adhesive.

Also, six specimens fractured under the first application of tensile load, even at low stress levels. This is attributed to brittle fracture of the binder during setting up due to slight (although unacceptable) eccentricities in the end caps. In two cases a positive crack was heard during tightening of an end cap screw suggesting brittle fracture of the binder. This was not fracture of the adhesive since the specimens did not subsequently pull out of their end caps.

Over the limited range of strain levels performed on the 10 specimens of dense tar macadam tested at a temperature of $0^{\circ}C$ it was again found that the strain rate had no significant effect on service life. Service lives obtained appeared to lie within the scatter of those achieved at a temperature of $+10^{\circ}C$. Figure 109 shows the results of the dense tar macadams tested at these two temperatures where the best fit line is given by:

$$\log_e N_s = \frac{108}{\mu\varepsilon^{0.63}}$$

Figures 107 and 108 show that, again, the shapes of the stiffness/cycles curves for common strain levels are similar.

Although the service life curves of results of tests at temperatures of $0^{\circ}C$ and $+10^{\circ}C$, and $+30^{\circ}C$ and $+40^{\circ}C$ cannot be considered similar, and neither can the curves of cycles to 90% initial stiffness, Figure 108 shows that the curves of cycles to 75% initial stiffness are coincident for all temperatures. The fact that stiffness curves at different temperatures intersect at the same proportion of the initial stiffness is noteworthy, although the fact that this value is 75% is purely fortuitous.

Hot rolled asphalt - As with the three previously described bituminous roadbase materials initial tests on hot rolled asphalt were performed at a temperature of $+10^{\circ}C$. Tests at this temperature were restricted to strain levels below 3.10^{-4} in/in since specimens were pulling out of one or other of their end caps at tensile loads greater than those at this strain level. In order to overcome this problem some specimens were stuck into their end caps in the testing machine with the end caps secured in the testing positions. This procedure did not help at all and it was felt that the problem might be that of air being trapped between the smooth specimen end and the end cap, reducing the bonded area. Certain techniques were employed to reduce the possibility of trapped air but to no avail. It was considered that the previously employed method of specimen fixing was not suitable for this type of rich, smooth surfaced material. In view of the

previous temperature non-dependency of the bitumen macadams, it was hoped that tests at higher temperatures, and hence lower loads, would enable a service life curve to be established despite the practical difficulties of the present system.

Of the 21 specimens of hot rolled asphalt tested at a temperature of +10°C only 13 produced service life values. Five specimens pulled out of one or other end cap and with three specimens the stiffness ceased to continue to fall with increasing number of load applications. Figure 97 shows the results of an original batch of 6 specimens tested at the highest strain level permitted by the adhesive, and results of low strain level tests. Specimen 804 will be seen to rise after 2000 load applications but service life has been determined from the extrapolation of the regular portion of the curve. This rise in stiffness occurred only once at this temperature and once each at test temperatures of +30°C and +40°C. This stiffness rise may be due to a redistribution of stresses within the specimen but more likely some drift in either the load measuring or extension controlling electronic circuitry. The problem did not persist and the aspect was not therefore pursued.

Tests on 33 specimens of hot rolled asphalt were performed at a temperature of +30°C covering a wide range of strain levels and strain rates. Shown in Figure 98 are the results of tests performed at the extremes of strain limits studied. The upper limit resulted in service lives of some 6 cycles whilst the lower limit was defined by the testing time available. It will be seen that specimen 842 experiences a temporary increase in stiffness between 200 and 1000 cycles but then resumes its predicted path. This was the only specimen tested at this temperature which exhibited this effect and as suggested earlier, is probably due to some drift in the electronic circuits.

The stiffness curves of the 3 macadam roadbase materials previously described all showed a convex form of curve on a log/log. basis indicating a continual fall in stiffness to beyond the service life stiffness. The curves of the hot rolled asphalt, however, are concave and may well reach minimum stiffness values. This would suggest the equivalent of a "fatigue limit" although this analogy ends at the shapes of the two types of curves. This aspect pursued in Chapter 11.

Results of service lives for all hot rolled asphalt specimens tested at temperatures of +10°C and +30°C, together with the results of 6 specimens tested at +40°C are shown in Figure 112. Results of tests at temperatures of +30°C and +40°C indicate, again, a lack of sensitivity of service life to

strain rate. Although the results of repeated loading tests at temperatures of +10°C and +30°C are relatively close, the lives at the higher temperature are consistently higher than those at the lower temperature. This may be significant, although it is felt that, in view of the difficulties experienced in loading the specimens into their end caps and testing at the lower temperature, the apparently shorter lives may be a phenomenon of the adhesive bond rather than the specimen material.

The best fit line for all the hot rolled asphalt specimens is given by $\log_e N_s = \frac{110}{\mu\varepsilon^{0.49}}$. Without the +10°C results: $\log_e N_s = \frac{207}{\mu\varepsilon^{0.58}}$.

Assuming a common service life curve for all temperatures the scatter in service lives is a factor of 10 at strain levels in excess of 5.10^{-5} in/in and 20 below this strain level. If the results of tests at a temperature of +10°C are excluded these scatter bands are reduced to a factor of 4 throughout.

Relationships between strain and cycles to 90% and 75% initial stiffness, shown in Figures 110 and 111 respectively, indicate the possibility that, like the dense tar macadam test results, the tests at higher temperatures reach a 10% drop in initial stiffness sooner than the lower temperature results, but the service lives later. Practical and rheological limitations did not permit a sufficient overlap in test results at different temperatures to be made in order to answer this probability more fully. Had time been available an alternative method of fixing specimens to their end caps might have been attempted in order to clarify the position. However, pressure of other commitments did not permit this aspect to be further pursued.

Footnote - The trends in all results of repeated loading tests presented above have been based upon the limited data acquired and have not been subjected to any statistical analysis to assess their significance. The limitations in the test equipment and the desire to cover as wide a range of materials and testing conditions as possible have precluded any form of statistical analysis being made, thus rendering the results indicative of trends rather than being quantitavely accurate.

MATHEMATICAL EXPRESSIONS FOR STIFFNESS/CYCLES CURVES

Mathematical expressions have been evaluated for various types of bituminous roadbase material specimens to define the shapes of the curves of both strain/service life and strain/cycles to both 90% and 75% initial

stiffness. Some of these expressions have been referred to above and all are summarised in Tables 13a to 13d. Although these relationships are of considerable value in defining the behaviour of the various materials tested under a variety of conditions, a description of the shapes of the stiffness/cycles curves would be of more general value.

Figure 113 shows the logarithmic relationship between the percentage stiffness drop/cycle and the appropriate cycle for three dense bitumen macadam specimens. For each specimen analysed, the stiffness drop/cycle has been taken as the ratio of the fall in stiffness between two consecutive stiffness calculations, expressed as a percentage of the stiffness in cycle 1, and the number of cycles between these two calculations. This average drop in stiffness per cycle has been plotted against the logarithmic mean of the range of cycles considered (i.e. the R.M.S. cycle). It will be seen that the points of three specimens of 90/110 dense bitumen macadam, tested at nominally similar strain levels, fall about a straight line which has been located by eye in Figure 113. This relationship may be defined by:

$$P = \frac{K}{N^m}$$

where P = percentage drop in stiffness/cycle

N = cycle number

m = arithmetic slope of line

K = percentage drop in stiffness in cycle 1

In Appendix 6 it is shown that this may be integrated to give:

$$D = \frac{K}{1-m}(N^{1-m} - 1) \qquad \text{when } m \neq 1$$

where D = drop in stiffness over N cycles

Further relationships for higher strain settings shown in Figure 114 suggest a similar slope of line up to the service lives but with a higher percentage stiffness drop/cycle, the latter indicating shorter service lives. Since the strain/service life relationship has been found to be common for both 90/110 and 190/210 dense bitumen macadams for all test temperatures and strain rates considered, these parallel relationships have been assumed to apply to all stiffness/cycles curves of the dense bitumen macadam specimens tested.

Appendix 3 shows how the constants "K" and "1-m" have been evaluated from the best fit line curves of strain level against cycles to 90%, 75% and 60% of the initial stiffness. Assuming that the constant "K" is a function of strain level and "1-m" a material and temperature constant, the stiffness/cycles relationship for the dense bitumen macadams

studied is found to be:

$$D = 1.64\varepsilon^{0.71}(N^{0.0622} - 1)$$

This relationship defines the shapes of the stiffness/cycles curves and is independent of test temperature and strain rate. Reference to the table of cycles to 90%, 75% and 60% of initial stiffness, in Appendix 6, will show that lives computed by the above expression are within a factor of 1.65 of the best fit line value at a corresponding strain level over the range of strains examined. Although this correlation is considered quite satisfactory it should be remembered that the basic curves from which the expression has been determined are themselves best fit lines and are not necessarily in themselves precisely indicative of material behaviour.

The other bituminous roadbase materials have beenanalysed in a similar manner. Figures 115 and 119 show that the assumption of linear logarithmic relationships between the percentage drop in stiffness/cycle and cycle number up to the service lives is well founded. In these cases, the slopes and positions of the linear lines are those calculated in Appendix 6. The shapes of the stiffness/cycles curves may therefore be defined as follows:

90/110 DBM, 190/210 DBM	all temps.	$D = 1.64\varepsilon^{0.71}(N^{0.0622} - 1)$
DTM	0°C and +10°C	$D = 0.0412\varepsilon^{1.07}(N^{0.365} - 1)$
DTM	+30°C and +40°C	$D = 8.87\varepsilon^{0.428}(1 - N^{-0132})$
HRA	+10°C and +30°C	$D = 3.90\varepsilon^{0.662}(N^{0.0354} - 1)$

Relationships between strain and cycles to 90%, 75% and 60% initial stiffness for the dense bitumen macadams are shown plotted with the corresponding experimental results in Figures 120 to 122. Good agreement is found for all materials studied between the calculated and determined results indicating the validity of the above expressions.

In Figure 123 theoretical stiffness/cycles curves have been plotted at two strain levels for each of the above expressions to illustrate material behaviour under repeated applications of load.

SHAPES OF LOAD AND DEFORMATION TRACES DURING TESTING

During repeated loading tests on bituminous roadbase materials it was found that the load and deformation traces varied in behaviour. Figure 124 shows the load and deformation shapes typical of the trace patterns

achieved during tests.

In Figure 124, three load trace shapes are shown. In tests of type A the "tensile" and "compressive" components of load, relative to the initial load zero position, fall off roughly evenly during the course of the test. Type B traces show a greater fall in "tensile" load and type C a greater fall in "compressive" load during the test. These latter two types of trace represent either an uneven fall in load or a shift in the load zero, or possibly a combination of the two.

The four various shapes of the deformation traces are also shown in Figure 124. Type 1 traces show negligible signs of varying extension limits and are the ideal test shapes. In traces approximately to type 2 there is a slight increase in the strain level over the first few cycles followed by a gradual reduction to a constant level. Type 3 represent a more significant rise in strain level over the first 50 or so cycles again followed by a reduction in level to a constant value. In these types 2 and 3 the increase in strain level is attributed to an increase in the deformation under load at turn-round which is subsequently offset by the reduction in crosshead speed. Finally, deformation traces approximating to the shape of trace 4 show a gradual increase in strain level throughout the course of the test. This is attributed, as in types 2 and 3, to the increase in deformation under load at the stationary points in the test but in this case the frequency correction is either negligible or at least insufficient to offset this effect completely.

In certain cases the load at the very first stationary point was significantly less than those loads at subsequent turn-round positions in the first few cycles. Such cases are identified subsequently with an asterisk and are caused by the delay in the development of a constant phase difference between the load and deformation components. This effect is purely a result of the commencement of test from a zero load, zero deformation, position but does indicate a characteristic of material property.

Each load and deformation trace of the 336 bituminous roadbase material specimens tested under repeated loading has been classified by a combination of the above trace shape letter and digit. Thus type A1 represents the "ideal" behaviour with constant strain level and uniformly diminishing load. The results are grouped in low, medium and high strain levels for each material and test temperature and are set out in Table 14. The rate of application of strain was also found to influence the shape of the load and deformation traces to some extent and therefore made trace

shape classification by strain level more difficult. However, it was found that a low strain rate at a low level tended to produce trace shapes more typical of the medium strain level group. Also a high strain rate at a high strain level produced medium strain level trace shapes. Therefore, when preparing the much simplified summary of trace shapes shown in Table 14, the effect of strain rate was taken into account when categorizing trace shapes in strain level groups.

Also included in Table 14 are the trends in changes in the ratio of compressive to tensile stiffness, assuming no shift in the load and deformation zeros, during each repeated loading test. The strain rate did not appear to have any significant effect on this categorization by strain level. It should be remembered that the contents of Table 14 are of a very general nature and serve only to illustrate the rough trends in material behaviour which will be discussed in Chapter 11.

NON-ROUTINE TESTS

During the course of the repeated loading tests on the bituminous roadbase material specimens described above, certain non-routine tests were performed in order to investigate certain aspects of material behaviour more fully. Since the results of these non-routine tests have little value out of context they will be presented together with the discussion and interpretation of experimental results in Chapter 11.

REPEATED LOADING TESTS ON DRY LEAN CONCRETE

It was stated in Chapter 9 that, due to the lack of sensitivity of stiffness to either test temperature or strain rate, all repeated loading tests on dry lean concrete have been performed at any convenient test frequency at a temperature of $+20^{\circ}C$.

Initial tests were performed on saturated specimens under conditions of controlled strain, in order to compare the behaviour of dry lean concrete with the bituminous materials described above. Figure 125 shows the results of specimen 615 tested at a strain range being symmetrical about the deformation zero position. For the first 3000 cycles, stiffness will be seen to fall linearly with increasing number of cycles, on logarithmic scales, after which it rises apparently beyond the initial value. This trend was found in other dry lean concrete specimens tested in strain-controlled cycling about the deformation zero.

In order to study this phenomena tests were performed on specimens either in tensile or compressive strain-controlled cycling and the results of one such test on specimen 618 are also shown in Figure 125. Here it

will be seen that in the tension cycling test the specimen stiffness first falls and then rises subsequently to excess of its initial value. The compression test, however, indicates a steady fall in stiffness with repeated applications of load, the relationship being slightly concave. These trends were further confirmed by tests performing either mode of cycling first.

At the end of the tensile strain-controlled test on specimen 618 described above it was found that at zero deformation a compressive load of some 1900 lb was indicated. At the end of the compressive strain-controlled test which was started in a stress free state, no residual load was found. This finding indicates a gradual build-up of compressive load in a tensile strain-controlled test attributed to tensile creep and the formation of microcracking within the concrete. Particle reorientation at these cracks might well prevent them from closing thus resulting in an apparent build-up in compressive load. Any cracks forming during a compressive strain controlled test would not open up and would not, therefore, result in any increase in compressive load.

This apparent build-up of compressive load in either a tension-compression or a tension strain-controlled repeated loading test is illustrated in Figures 126 and 128. The former is a hysteresis loop determined from the load and deformation traces of a reversed strain test and the latter from a tensile strain-controlled test. Figure 127 shows the stiffness/cycle curve of specimen 622, from which the hysteresis loops in Figure 128 are taken, together with the maximum tensile and compressive loads during the course of the test. Confirming the previous observations, Figures 127 and 128 show a reduction in tensile load throughout the duration of the test and a decrease in compressive load followed by an increase to excess of the initial value.

It was felt that this phenomenon of increasing compressive component of load might possibly be some characteristic of dry lean concrete peculiar to testing in a saturated condition. Six specimens were therefore left to dry out in the temperature controlled laboratory at a temperature of $+42^{\circ}C$ for a period of 21 days. During this time an average of 115 gm of water was lost compared with 148 gm from similar concrete specimens left for 24 hours in an oven at a temperature of $+135^{\circ}C$. The hysteresis loops of specimen 631, tested in tensile strain-controlled cycling, are shown in Figure 129. Again it will be seen that the loops revert to the compressive segment showing, ultimately, no tensile deformation

whatsoever. The stiffness/cycles relationship for this specimen is shown in Figure 127. This, and the other results of tests on dry lean concrete in a 78% dry state, show results similar to those specimens tested saturated and indicate that the degree of saturation has little effect upon the material behaviour under repeated application of load.

A final aspect of dry lean concrete under strain-controlled repeated loading which was considered was whether, or not, the repeated applications of compressive load had any effect on the static properties of the material. To this end a few saturated specimens were subjected to direct tensile loading to fracture and the results compared with those of specimens previously tested under repeated loading. Figure 131 shows typical results of tensile loading to fracture for a specimen (623) subjected to 14,000 cycles of compressive loading and for a specimen (630) with no previous loading history. Specimens with previous loading histories, whether tensile, compressive or a combination of the two, possessed lower tensile strengths with the ultimate tensile strength occurring at a lower strain level. It will be seen from Figure 131 that the specimen fails slowly unlike the previously unloaded specimen which fails abruptly. These phenomena clearly indicate that a change in specimen properties takes place during the repeated application of compressive load which although barely manifest in stiffness values, reduces the ultimate tensile properties significantly. This aspect is pursued in Chapter 11.

From the foregoing observations it became apparent that the only way to assess the behaviour of dry lean concrete under strain-controlled loading would be to perform the repeated loading tests and then compare the tensile properties with unloaded standards. This would require a large number of test results to extract any statistical significance and to embark upon such a programme of work was impracticable. For a roadbase material such as dry lean concrete, however, it was felt that since the tensile plastic properties of the material were so limited and so critical, a stress-controlled repeated loading test might be of significant value. To this end the remaining 30 specimens were tested wet under conditions of controlled stress.

In Figure 132 is shown the results of a stress-controlled repeated loading test on fully saturated dry lean concrete. The stress is repeated between zero and 57 lb/in^2 tension resulting in a continual increase in both the dynamic and total strain. The total and dynamic strains will be seen to increase in a regular manner up to some 400 cycles after which they increase to ultimate failure at 1002 cycles.

This test procedure was repeated over a range of tensile stress levels although the range of stresses examined was severely restricted by practical limitations. The ultimate tensile strength of the dry lean concrete roadbase material was found to be in the order of 90 lb/in^2, thus restricting repeated loading stresses to below 75 lb/in^2. At stresses below 45 lb/in^2 fracture did not occur within the testing time available; after in excess of 25,000 loading applications. The range of stresses examined was therefore limited to 45 lb/in^2 to 75 lb/in^2.

The results of all stress-controlled repeated loading tests on dry lean concrete are set out in Table 15. In Figure 136 the maximum total tensile strain has been plotted against the appropriate stress level, on logarithmic scales. Despite the large amount of scatter results indicate a trend of an increase in the maximum tensile strain at fracture with a decrease in the applied stress level. Figure 137 shows the relationship between the applied stress level and the number of cycles of load to failure. Over the limited range of stress levels examined there would appear to be a scatter in fracture lives of a factor of 50. A linear relationship has been assumed between the logarithms of stress level and service life and the line passed through the ultimate tensile stress at 1 cycle. The form of the relationship is tentatively offered at:-

$$N_f = \left(\frac{89}{\sigma}\right)^{13.7}$$

The strain/cycles results of a specimen tested between zero and 37½ lb/in^2 tension, where failure did not occur during the testing time available are shown in Figure 133. Here on day 1 the test was run for 25,000 cycles and the specimen left in a state of zero stress overnight. Upon resumption of the test on day 2, the total strain was found to continue the trend of day 1 and the dynamic strain to show slight, although temporary, signs of benefit from the rest period. This effect was confirmed by a few other specimens.

A few final tests on dry lean concrete were performed to assess the effect of both alternating and fluctuating stress on its behaviour. Figure 134 shows the results of a specimen (665) tested over a stress amplitude of 66 lb/in^2 which failed at a total tensile strain of $1.10.10^{-3}$ in/in at 10 cycles. The results of two tests of fluctuating stress 24½ lb/in^2 compression to 46½ lb/in^2 tension (specimen 663) and 62 lb/in^2 tension to 72 lb/in^2 tension (specimen 666) are shown in Figures 135 and 134 respectively. The corresponding tensile strains at failure are $1.50.10^{-3}$ in/in and $1.27.10^{-3}$ in/in respectively and the fracture lives

2500 and 65 cycles. These three fracture lives will be seen from Figure 137 to bear close agreement with those of specimens tested from zero to the same maximum tensile stress. Further, the tensile strains at failure are shown in Figure 136 to agree, within experimental error, with the tensile strains of tests at corresponding maximum tensile stresses. These two factors, supported by further alternating and fluctuating tests shown in Figures 136 and 137, indicate that the fracture life and the maximum tensile strain sustained by this material are dependent upon the maximum repeated tensile stress applied.

In all dry lean concrete roadbase material specimens tested, whether under strain-controlled cycling, stress-controlled cycling or direct tension, ultimate failure occurred in the vicinity of one or other end cap. Fractures were never more than $\frac{3}{8}$ inch from an end cap and failed surface conditions ranged from horizontal to concave into the end cap with a maximum depression in certain instances of $\frac{1}{2}$ inch. Generally fractures were clean although a few loose particles of aggregate or sand/cement matrix were occasionally encountered. The significance of these failure conditions is considered in the next Chapter.

BINDER VISCOSITY TESTS

The prime object of the binder viscosity tests was to determine the Newtonian viscosities of the binders in the bituminous roadbase material specimens tested in repeated loading. These results would enable the theoretical mixture stiffnesses to be determined at the test temperatures examined and hence any non-Newtonian characteristics of the binders or non-linear inducing effects of the aggregates, to be detected. In view of the difficulty of obtaining sufficient quantities of recovered binders to perform binder viscosity tests over the range of test temperatures examined, the viscosity/temperature characteristics of unheated binders have been established. It is hoped that the shapes of the viscosity/temperature curves of the recovered binders will be the same as those of the corresponding unheated binders. If so, then the measured recovered binder viscosity at any known temperature can be used to determine the position of the viscosity/temperature relationship. Hence the Newtonian viscosity of the binder in the bituminous material at any test temperature.

Initial tests on the disc viscometers, described in Chapter 8, were performed using a 90/110 pen. bitumen at test temperatures of $+30^{\circ}C$ and $+40^{\circ}C$. These tests were performed in order to assess the accuracy of the test equipment by comparing results with published figures. It was

hoped to procure a liquid of known viscosity in the order of 10^7 poise, or to measure the viscosity of the bitumens tested on another type of viscometer, such as the cone and plate viscometer, but neither of these alternatives proved possible.

The results of a viscosity test on an unheated 90/110 pen. bitumen tested at a temperature of $+30^{\circ}C$ are shown in Figure 138. Here the relationship between the reciprocal of the square of the plate separation and time will be seen to be linear up to 30 minutes and then level out at long loading times. The initial linear portion is the relationship predicted in theory and the curved portion is attributed to plate interaction restricting free volume flow at lower plate separations. Also shown in Figure 138 is the initial linear relationship plotted on an enlarged scale which is used to determine the Newtonian component of viscosity. The close proximity of experimental results to a straight line indicates the accuracy within which the test may be performed.

The results of viscosity tests on 11 specimens of 90/110 pen. bitumen tested at a temperature of $+30^{\circ}C$ using a variety of loadings and initial plate separations are set out in Table 16. All results lie within a scatter band of $1\frac{1}{2}$. The variation of individual results is attributed to inhomogenuities in the samples due to small particles or air bubbles and to errors in starting the test at zero time and exact plate separation. Results at a test temperature of $+40^{\circ}C$, also shown in Table 16, are of the same order of scatter.

Binder viscosity tests have been performed on each binder type used in the bituminous roadbase materials examined and tested, where practicable, at temperatures between $0^{\circ}C$ and $+40^{\circ}C$ in $10^{\circ}C$ increments. Tests have also been performed on these binders after being subjected to heating prior to mixing. These tests were performed in the hope that results would indicate both the effect of this initial heating on the binder properties and also the effect of a change in penetration index on the viscosity characteristics. The results of all tests are set out in Table 17 where it will be seen that the initial heating has no significant effect on the binder viscosities. The second objective of this aspect cannot, therefore, be assessed.

The average results of all binder viscosity tests are shown graphically in Figure 139 where the double logarithm of the binder viscosity has been plotted against the logarithm of the test temperature. These relationships would appear to be slightly curved although straight lines have been drawn in accordance with accepted figures (eg. ref. 70).

The experimentally determined results of viscosity tests on the recovered bitumens are also shown in Figure 139 together with the assumed viscosity/temperature relationships.

STATIC TESTS ON BINDERS

Standard penetration and ring and ball softening point tests have been performed on unheated, heated and recovered binders in order to determine their penetration indices. Test results are shown in Table 18 where it will be noticed that the penetration indices are little affected by initial heating. The increase in the penetration indices of the recovered bitumens is greater than would normally be encountered in practice indicating excessive binder hardening during mixing. This aspect is considered in more detail in Chapter 11. No process of binder recovery from the dense tar macadam roadbase material specimens was readily available and this aspect was not pursued since the temperature susceptibility characteristics of tar, and hence the shape of the viscosity/temperature relationship, is known to change with oxidation upon heating.

An attempt was made to determine the stiffness of unheated 90/110 pen. bitumen at high frequency and low temperature test conditions. This was to establish a binder stiffness approaching the maximum theoretical (elastic) stiffness of all bitumens which forms the asymptote to which practical stiffness curves approach.

Initial tests were performed using a standard electro-dynamic tester. This was used in preference to an ultrasonic tester since a knowledge of the Poisson's ratio of the material under study is not required to evaluate the stiffness, or complex modulus. Two metal specimens, one of steel and one of aluminium, each $1\frac{1}{2}$ x $1\frac{1}{2}$ x 12 inches in size, were first tested to calibrate the test equipment. Resonant frequencies of 8560 and 8330 cycles/second produced modulus values of 31.10^6 and 10.10^6 lb/in^2 respectively. The testing of a 2 x 2 x 12 inch specimen of bitumen taken from a deep freeze at a temperature of -17.5°C was found to flow under the clamp. This reduced the resonant frequency of the specimen and also led to spurious harmonics not in the standard ratios 1:2.7:5. The highest resonant frequency recorded was 2515 cycles/second indicating a stiffness of $3.50.10^5$ lb/in^2 but this was not considered satisfactory.

Attention was then transferred to the ultrasonic testing system using a standard unit for measuring the modulus of concrete. Initial tests on the metal specimens referred to above rendered pulse times of

54.0 μ seconds and 50.9 μ seconds for the steel and aluminium respectively. Assuming Poisson's ratio values of 0.25 for steel and 0.33 for aluminium (220) the resulting modulus values were found to be $30.2.10^6$ lb/in^2 and 9.43×10^6 lb/in^2 respectively. These were considered satisfactory, and a test on 90/110 pen. bitumen produced a pulse time of 140.0 seconds. Taking a value for Poisson's ratio of 0.35 (77) the resulting stiffness is found to be $4.44.10^5$ lb/in^2. Van der Poel (83) has quoted the elastic asymptote of bitumen stiffness as approximately 3.10^4 kg/cm^2 ($4.35.10^5$ lb/in^2).

A few basic tests were also performed on the time-dependence properties of bitumens but since results are qualitative rather than quantitative, they will be presented in context with the discussion of experimental results in the following chapter.

CHAPTER ELEVEN

DISCUSSION OF EXPERIMENTAL RESULTS

VOIDS IN SPECIMENS

The results of void determinations and standard deviations on the various types of roadbase material specimens produced are set out in Tables 11a to 11e.

The volume of binder in each of the three types of bituminous macadam roadbase material specimens produced was kept constant, and the temperatures of the aggregate and binders selected such that the binder viscosity at mixing was also constant. This procedure was adopted in order to produce specimens of similar void properties.

The average internal voids of the 90/110 dense bitumen macadam specimens was 6.9% (S.D. = 0.58%, i.e 6.9% $\pm$ 0.6%), the 190/210 dense bitumen macadam 6.6% (S.D. = 0.43%) and the dense tar macadam 7.0% (S.D. = 0.56%). These values indicate no significant difference in the average internal void contents. The average surface voids of the 90/110 dense bitumen macadam specimens was 6.2% (S.D. = 0.96%) compared with 5.1% (S.D. = 0.53%) for the softer bitumen macadam and 5.1% (S.D. = 0.65%) for the dense tar macadam. The higher surface voids of the harder bitumen macadam are attributed to the greater heat losses from the compaction mould due to higher mixture temperatures. This would reduce the surface temperature of the material, increasing the binder viscosity and reducing workability and resulting in higher surface voids. It may, therefore, be concluded that the above test results confirm the fact that, for a particular aggregate type, size and grading, binder volume content and mixing (hence compaction), viscosity and compactive effort, the degree of compaction in all materials is similar. The binder may, therefore, be considered purely as a lubricant during compaction. Also, the similar internal void characteristics enable the behaviour patterns of the dense bituminous macadam specimens tested under dynamic loading to be attributed to the binder type and any variation (if significant) in surface void characteristics.

It will be seen that in the case of all four types of bituminous specimens produced the absolute standard deviations of surface voids are much in excess of the standard deviations of internal voids. This is due to the degree of operator variable when hand rodding the materials in the compaction moulds during specimen manufacture.

A comparison of the void results of all four types of bituminous specimens set out in Tables 11a to 11d will show that the absolute standard deviation of the total specimen voids in each batch of specimens is generally less than either the standard deviations of the internal voids or the standard deviations of the surface voids. This indicates that high internal voids are associated with low surface voids and vice versa, the distinction between surface and internal voids being simply those voids connected to the surface and those not so connected.

It is generally accepted that similar specimen compactions are more easily obtained during a single mixing session than on separate occasions. The results of all specimens produced, including the comparative void determinations of the dry lean concrete, show that the standard deviations of the voids of all similar material specimens produced is greater than the average standard deviation of each individual batch. Further, when the absolute standard deviations are expressed graphically, as shown in Figure 61, there would appear to be a definite relationship between the standard deviations of voids in each batch and that of all specimens of a similar type. It may, therefore, be concluded that the standard deviation of voids in a large number of specimens produced in batches on separate occasions will be some 1.3 times the standard deviation of the voids in each batch. This applies for internal, surface and total voids for all the roadbase material specimens studied.

STIFFNESS MEASUREMENTS

Stiffness measurements have been performed on all the roadbase materials investigated at each of the temperatures at which repeated loading tests were carried out. These stiffness measurement tests were performed primarily to determine the rate effects of the materials, in order that the initial stiffness values of repeated loading tests might be reduced to a common datum.

It was stated earlier that in stiffness measurement tests care was taken to ensure that the rate effect was only measured over a strain range in which no permanent damage was sustained by the specimen. Each specimen was assumed to be undamaged so long as an early stiffness value could be repeated under similar testing conditions. This meant that the specimen had "fully recovered" after a few cycles of loading and results have shown that the rate effect is constant over the strain range examined. It should be stressed, however, that this "recovery" may be only temporary and that

subsequent loadings may result in stiffness values different from those if the specimen had had no loading history.

The slopes of the stiffness/strain relationships of specimens used for stiffness measurement tests will be seen from Table 12 to lie within a scatter band of at worst 20% about their mean values. The slopes of the stiffness/strain relationships of the first cycle of specimens tested under repeated loading are set out in Table 13. A comparison of the results of corresponding materials and testing temperatures in Tables 12 and 13 will show that the slopes of stiffness measurement tests generally lie within $\pm$10% of the slopes of the cycle 1 repeated loading test specimens. This indicates two significant points. First, the recovery of stiffness during a rest period in stiffness measurement tests is permanent, rather than temporary, for all strain levels examined. This is exemplified by the fact that if a low strain level stiffness can be reproduced after a previous loading history and rest period, then a high strain level stiffness can also be reproduced. This high level stiffness determined after a previous loading history followed by recovery during a rest period will be the same as that determined with no previous loading history. Secondly, the rate effects determined during stiffness measurement tests would appear to be applicable to the correction of stiffness results to a common datum over the range of strains examined. Thus the assumption of parallel and linear stiffness/strain relationships for different strain rates (or frequencies) is valid, or at least the inaccuracies arising from this assumption are considerably less than inaccuracies arising from experimental error, again over the strain range examined.

These conclusions are based on the general trends of tests on bituminous roadbase materials. A detailed comparison of Tables 12 and 13, however, will show that the slopes of the stiffness/strain relationships of the two dense bitumen macadam materials tested at a temperature of 0°C are less than the corresponding materials tested in repeated loading and reduced to a common datum. This would indicate either that the rate effects used to reduce the repeated loading results are too high, since strain rates at low strain levels are generally less than the datum strain rate and those at high strain levels are greater, or alternatively that the assumption of a constant rate effect over the strain range examined is invalid.

It was shown in Chapter 4 that, in theory, the stiffness/time relationship for a bituminous material over a wide range of loading times is convex, i.e. stiffness is reduced with increasing loading time. Now if stiffness values are expressed at a datum strain rate then the effects

of time of loading and strain level are interchangeable. Therefore if the material is considered as a simple Maxwell liquid it is possible to calculate the relationship between the slope of the stiffness/strain curve at any strain level and the corresponding rate effect. This relationship, which applies in fact to any number of Maxwell models in parallel and embraces the theoretical models of Secor and Monismith (76,77) is shown graphically in Figure 143b. Also shown in Figure 143b is the theoretical relationship between slope and rate effect for one or any number of series Kelvin models representing visco-elastic solids, as suggested by Papizan (78). All slope/rate effect factors for linear visco-elastic materials should lie within this envelope their positions relative to the bisecting line defining their state as either a visco-elastic solid or a visco-elastic liquid. If a convex stiffness stiffness/strain relationship is assumed, then as the slope is reduced, so is the rate effect. Thus at low strain levels the rate effect would be less than at high strain levels. If the rate effects at low strain levels are taken as less than the assumed constant values then the slopes of the reduced stiffness/strain relationships of the dense bitumen macadam materials at low test temperatures will approach those slopes of the stiffness measurement stiffness/strain relationships. Thus it may be concluded that at low test temperatures, where the bituminous materials are more elastic and the slopes of the stiffness/strain relationships are less than at higher temperatures, the errors in assuming a linear stiffness/strain relationship with a constant rate effect outweigh the errors due to experimental inaccuracies.

A final observation is to be made from a comparison of the slopes of the stiffness/strain relationships of stiffness measurement and reduced repeated loading test results. This is that at a test temperature of $+40^{\circ}C$ the slopes of the individual stiffness measurement results of the 90/110 dense bitumen macadam are considerably greater than the slope of the reduced repeated loading tests relationship. Two factors which would cause this effect are that the recovery between individual stiffness measurement tests is not permanent, resulting in reduced stiffnesses at higher strain levels, and that the rate effect is too low. The former factor would not appear logical since the recovery of bituminous materials at equivalent strain levels would be expected to be greater at higher temperatures. This has been confirmed by Bazin and Saunier (114). The cause of an apparently low rate effect could well be due to the converse of the high rate effect described above suggesting a concave stiffness/strain relationship. This supposition is supported by other rate effect phenomena

and is of considerable significance in the selection of suitable stiffness values for bituminous materials in the analysis of layered systems.

The theoretical stiffnesses of the 90/110 dense bitumen macadam material have been calculated, over a range of temperatures and frequencies, using the Van der Poel nomograph shown in Figure 8 and the mix factor nomograph shown in Figure 11. These theoretical stiffness curves, shown in Figure 70, indicate that (in theory) the rate effect increases with increase in temperature. The rate effect/temperature relationship, together with those determined from the stiffness measurement tests, is illustrated in Figure 143a. Here it will be seen that the rate effects of those bituminous materials do not increase continuously with temperature, as do the theoretical values, but rather increase to an optimum value and then decrease.

A visco-elastic liquid has a convex stiffness/time (or strain, or temperature) relationship as shown in Figure 144, and a visco-elastic solid has a concave relationship as shown in Figure 145. Complex models, however, consisting of Maxwell and Kelvin elements, as the simple Burger model with no series dashpot, behave as visco-elastic solids at high loading times, large strains and high temperatures. Thus the maximum rate effects determined from stiffness measurement tests, shown in Figure 143a, indicate the transition from convex to concave stiffness curves.

The behaviour of a bituminous bound aggregate mixture approximating to a simple Burgers model with no series dashpot may be attributed to the model behaviour of the binder or, alternatively, some non-linear effect of the mixture.

Figure 143b shows the envelope of the slope/rate effect relationship for linear visco-elastic materials. The results of slopes and corresponding rate effects for all the bituminous roadbase material specimens used in stiffness measurement tests are also shown. These values, rather than the average values of the first cycles of repeated loading test specimens, have been used since the slope/rate effect relationship is peculiar to each individual specimen tested. The average results are therefore less meaningful. In Figure 143b it will be seen that at low test temperatures ($0^{\circ}C$ and $+10^{\circ}C$) all bituminous materials behave as linear liquids and are therefore on the convex portion of the stiffness/time curve. As the test temperature is increased results tend to fall to the right of the linear model envelope. This indicates that the concave portion of the stiffness curve is due to a non-linear effect of the material and not a result of the analogous model behaviour of the binder. This conforms with the findings of Van der Poel whose nomograph

values indicate the behaviour of pure bitumen as a liquid.

In summary results of stiffness measurement tests on bituminous materials indicate that a complete recovery of stiffness during a rest period following repeated loading is not only complete but permanent. The behaviour of rate effects show that the stiffness curve has a minimum value due to non-linearity of the material.

Only one specimen of dry lean concrete has been employed for stiffness measurement tests since the prime object was to ascertain whether, or not, the material was time-dependent. As this single specimen confirmed that it was not time-dependent, a further study of the recoverable properties was not made.

It will be evident from Figure 64 and also from the stiffness/strain relationship built up from the results of the first loading cycle of repeated loading tests, that the dry lean concrete roadbase material studied exhibits marked non-linearity characteristics. In the absence of documented evidence of non-linearity in cement crystals, non-linearity of dry lean concrete is attributed to creep phenomenon.

It is well established that creep rate is accelerated by increasing load and therefore the induced load will not increase linearly with increasing strains applied at greater than creep rate speeds. It was reported in Chapter 5 that creep was attributed by many investigators to viscous flow of the cement paste, movements of water within the material and microcrack propagation. Since it was found possible to measure the stiffness of dry lean concrete at a relatively high strain level and then repeat a previously measured stiffness at a lower strain level, progressive microcracking cannot be considered a contributory factor to non-linear behaviour. The mobility of free water creep theory of Glucklich (174) is proffered as an explanation for the non-linearity of dry lean concrete.

Illston (176), among others, has found creep rate to be significantly greater in tension than in compression. This would result in the development of a residual compressive load during stiffness measurement tests. During the one stiffness measurement test performed on dry lean concrete no significant residual load was observed, probably due to the relatively few loading cycles applied to the specimen.

STIFFNESS/STRAIN RELATIONSHIPS

The stiffness/strain relationships of the bituminous roadbase material specimens studied are shown graphically in Figures 88 to 91.

Stiffness values are shown reduced to a strain rate of 100$\mu\varepsilon$/sec and also at a test frequency of 1 cy/sec. As stated previously, a triangular deformation wave form has been assumed in the calculation of strain rate from actual test frequency.

Parallel plate viscometer tests on the recovered bitumens have enabled the theoretical material viscous asymptotes to be derived. These have been calculated by applying the mix coversion factors of Heukelom and Klomp (86) to the bitumen viscous asymptote calculated from $S = 2.\frac{\lambda}{t}$ (See Appendix 1). The derived material viscous asymptotes for the 90/110 dense bitumen macadam presented with the measured stiffness/strain relationships in Figures 74-77 show that at low temperatures of 0°C and +10°C the slopes of derived and measured relationships are almost identical. The lower magnitude of the measured values is attributed to high local strains within the specimens. (See Figure 65). At higher temperatures the slopes of the measured relationships are less than the derived viscous asymptotes and stiffnesses are higher. These findings further support the theory of elastico-viscous material behaviour at low temperatures and non-linear firmo-viscous behaviour at higher temperatures.

The establishment of apparently non-linear behaviour of all bituminous materials studied (i.e. stiffness being strain-dependent) does not concur with the results of many investigators who report linear material behaviour for strains up to at least 1.10^{-4} in/in. (74,78,94,116-119,123-126), although non-linear behaviour has been found at high temperatures and low frequencies (118,121,122). The majority of these tests have been performed on specimens in bending and it may well be the case that non-linear effects at low strains are masked by the distribution of stresses across the specimens and the low values of measured deformations. There would appear to be no reason why non-linear behaviour should be initiated at strains in the order of 1.10^{-4} since the corresponding bitumen strain would be well in excess of its yield value and well below its fracture strain. Further, a purely Newtonian fluid is non-linear insomuch as stiffness at constant strain rate is strain-dependent.

Considering the stiffness/time curve of a material represented by a Burger model with no series dashpot as shown in Figure 145, there is no linear portion between the convex and the concave portions of the curve. If, however, the concave portion of the curve is caused by a non-linear effect of the material, then the laws of deformation and flow governing the Burger model need not necessarily apply to these non-linear materials. It is therefore postulated that since there is no evidence of a curved stiffness/strain relationship at medium test temperatures (+10°C to +30°C) for

any of the bituminous materials tested, then these stiffness determinations have been performed in the linear portion of the compound stiffness curve. Low temperature stiffness measurements fall around the transition from convex to linear and high temperature stiffness measurements around the transition from linear to concave.

The non-linear stiffness/strain relationship of the bituminous materials studied, indicating a lower limit to the reduction in stiffness with increasing strain, is attributed to the presence of the aggregate particles in the mixture.

The stiffness of a bituminous mixture is equal to the stiffness of the binder, defined by the temperature and the strain rate, and the concentration of aggregate in the material. As the material is compressed the aggregate particles become more intimately associated in the direction of application of load, thus increasing the effective aggregate concentration. This increases the viscosity of the binder and therefore increases the instantaneous mixture stiffness.

The complete stiffness/strain curve for a particular bituminous material at a specific temperature and strain rate is therefore explained as follows. Consider a simple, linear Maxwell binder as the continuous phase in a binder-aggregate mixture. At an infinitely small strain the frequency of loading is infinitely high and the viscosity of the binder approaches its maximum, near elastic, value. The stiffness of the mixture is also near its maximum, the increase over the binder stiffness being defined by the concentration of aggregate in the mixture. As the strain level is increased the stiffness of the binder and hence of the mixture is reduced since at a constant rate of strain the induced stress in the binder is a constant value. The stiffness curve of the mixture would then tend towards the viscous asymptote. This asymptote would have a slope of 45° to the horizontal axis in the case of pure Newtonian binder but its angle is reduced due to the greater contribution of the aggregate to the mixture stiffness at lower binder stiffnesses. The slope of the viscous asymptote is further reduced by the apparent increase in effective aggregate concentration increasing the instantaneous mixture stiffness and thus reducing the rate of reduction of mixture stiffness with increasing strain level. This non-linear strain dependent effect will dominate the stiffness/strain relationship until the effective aggregate concentration increases to such an extent that the aggregate particles themselves begin to form a more stable structure. The stiffness/strain curve will then tend to approach the lower stiffness asymptote which will be equal in

magnitude to that of the unbound, but laterally restrained, aggregate. The magnitude of this lower stiffness asymptote will depend upon the aggregate type, size and grading but may well, to a close approximation, be defined simply by the aggregate concentration in the mixture.

It is a well established fact that the effects of time and temperature on the stiffness of bituminous binders are interchangeable. Thus the stiffness of a binder at any temperature and time of loading may be determined by applying a suitable shift factor to the stiffness curve in the time axis. The slope of the linear portion of the stiffness/strain relationship for a bituminous material has been accounted for in terms of the non-linear strain-dependent behaviour of the material. It might therefore be expected that for a specific material composition and strain rate, strain and temperature might be interchangeable.

The stiffness/strain results of both types of dense bitumen macadam materials tested, shown in Figures 88 and 89, indicate a reduction in slope with increase in temperature. This is simply accounted for by two factors. First, at medium temperatures, as the temperature is increased the viscosity of the binder falls and the contribution of the aggregate increases. Thus the increase in material stiffness due to the increasing effective aggregate concentration upon increasing the strain (which partially offsets the reduction in stiffness due to the increase in strain, common for all temperatures) is more significant at higher temperatures where the basic bitumen stiffness is less. Second, at high temperatures the material stiffness at high strains is nearer the lower stiffness limit and therefore the stiffness/strain relationship may be partially or totally on the concave portion of the curve. By a similar argument the slopes of the stiffness/strain relationships at low temperatures would be expected to decrease as the upper stiffness asymptote is approached.

The foregoing explanations have been presented in terms of compressive loading although they apply equally well to tension-compression stress reversals.

The results of tests on dense tar macadam, shown in Figure 90, confirm the above postulations and illustrate the complete process described. The results of hot rolled asphalt specimens, shown in Figure 91, only cover two test temperatures and therefore, although they cannot support the above theory they can at least be explained by it.

It is therefore concluded that a temperature shift factor cannot be applied to the stiffness/strain curve of a specific bituminous

composition at a specific strain rate whereas it can be applied to the binder on its own.

The foregoing discussion indicates that, whereas the stiffness/time relationships for various bitumens established from the nomograph of Van der Poel (83) are undoubtedly quite valid, the application of the aggregate mixture factor of Heukelom and Klomp (86) in conjunction with the void correction of Van Draat and Sommer (92) is only applicable in the region of linear material behaviour. The effect of increasing the strains beyond the linear range of the material could easily be included in the form of a further nomograph. Its application might, however, be limited to static creep behaviour since other factors may well preclude the use of such high strain levels in situations where a large number of stress reversals is expected.

The stiffness/strain relationship for dry lean concrete is shown in Figure 87. It will be remembered that repeated loading tests were performed on both wet and dry specimens in conditions of controlled strain and wet specimens in controlled stress. The stiffness/strain relationship is built up from the initial stiffness values of all three test conditions.

It was suggested previously that the well established non-linearity of this material is due to some of the factors causing creep. The mobility of free water theory of Glucklich (174) accounting for creep would explain the somewhat higher stiffness values of the strain-controlled dry specimens tested. The reduced free water content of these specimens would reduce the creep flow resulting in higher stiffness values.

No significant difference is evident in the stiffness values of the wet stress-and strain-controlled test specimens. This suggests that it is the direction of application of load and not the physical position of the specimen relative to its initial state which defines the compressive load in the first application. Stress-controlled testing did not compress the specimen beyond its initial length whereas in strain controlled deformation the compressive strain was half the strain range.

The similarity of slope between the stiffness/strain relationship obtained from the initial cycles of repeated loading tests and that from the stiffness measurement test further confirms the lack of damage to the stiffness measurement specimen. Thus it is improbable that, in this case, non-linearity of the stress/strain relationship is due to microcracking as suggested by Barnard (180) and Popovics (181). Non-linearity is therefore

attributed to creep phenomena excluding that of microcracking.

REPEATED LOADING TESTS IN BITUMINOUS MATERIALS

It was established in Chapter 10 that for the two types of dense bitumen macadam roadbase material specimens, each bitumen with a penetration index of about -0.5, for the entire range of temperatures and strain rates examined, the drop in stiffness with repeated applications of strain-controlled loading is given by:-

$$D = 1.64\varepsilon^{0.71}(N^{0.0622} - 1)$$

where D = percentage drop in stiffness

ε = strain level in $\mu\varepsilon$

N = number of cycles

This common relationship clearly indicates a progressive reduction in material stiffness. The lack of sensitivity of stiffness reduction due to such factors such as test temperature and speed of loading suggests that the progressive reduction in stiffness is due mainly to the cumulative effect of continually straining the material. To double the strain level and half the number of cycles of loading would result in the same cumulative strain on the material and thus might be expected to have the same reduction in stiffness. However, if a certain amount of recovery takes place at the stationary points in stress reversals, and the rate of recovery while stationary is less than the rate of damage while mobile, then for lower strain levels with similar waveforms, the damage accumulated over the same number of loading cycles will be less.

The value of unity in the above relationship has been employed to provide an expression for the drop in stiffness expressed as a proportion of the first complete cycle. However, in view of the theory of cumulative strain, it was felt that since stiffness is measured over the middle two quarters of the loading cycle a more fundamental relationship might be achieved by taking the fall in stiffness in the first cycle as occurring over the first three quarters of the cycle. The value of unity was therefore replaced by 0.75 and a fresh general expression determined. The degree of agreement of predicted and experimentally determined service lives was far worse than when the above expression using unity was employed. This is attributed to the fact that each cycle is preceded by the last quarter of the previous cycle whereas the first cycle is not, thus invalidating the expression.

A second effect of the progressive-damage-due-to-cumulative-strain theory is that the first cycle of loading, taken as the reference zero, is

itself reduced due to progressive damage. In the relationships between the average percentage drop in stiffness/cycle and the number of applications of load as shown in Figures 113 to 119, the intercept with the ordinate at cycle 1 represents the damage sustained by the material during the first cycle of loading. Taken to its logical (?) conclusion this argument suggests that the potential stiffness of a bituminous material is significantly higher than that recorded during the first application of load although, in practice, it is impossible to achieve this. The fact that the damage sustained during the first cycle of loading is a function of strain alone at a given temperature for each material further supports the theory of progressive failure from the initiation of deformation.

Thus it is concluded that the reduction in stiffness of the bituminous materials tested in this investigation is due to a progressive reduction in material stiffness throughout the test and that this factor alone determines the service life. The mechanism of failure by fatigue (a failure due to the initiation and propagation of a structural defect during repeated loading) is not, therefore, present in these bituminous materials in this form of test. This aspect is pursued later in this Chapter.

A progressive reduction stiffness of a bituminous material may be due to two distinct factors. First, macroscopic damage either in the form of a crack propagation within the binder, or a degeneration in the adhesion properties of the binder/aggregate interface. Second, microscopic changes in the binder itself. Due to the ratio of aggregate stiffness to binder stiffness, changes in the aggregate properties can be discounted.

It is felt that a progressive reduction in stiffness due to any macroscopic crack propagation is unlikely. The main reason being that the rate of crack propagation would depend to a very significant extent upon the internal stress distributions within the specimen. The inhomogeneous nature of the bituminous materials studied, due to the random positioning of the aggregate particles and the consequent variability in void content and structure, would lead to localised stress concentrations and semi random crack patterns. This would in turn lead to a high degree of scatter in service lives far in excess of those encountered. Further, strain-controlled repeated loading work by other investigators (94), where crack propagation has led to ultimate failure by complete fracture, has shown that the test temperature and speed of loading has a significant influence on the fracture life of a bituminous material. These factors, together with a distinct absence of visual cracks in all but a very few isolated

instances, indicate strongly that crack propagation is not the cause of the progressive reduction in material stiffness. This concurs with the findings of Monismith (147) who has shown that the service lives of beams subjected to strain-controlled 3-point bending is unaffected if the lower face is flexed in tension, compression or reversed strain of equal amplitude. Clearly, the rate of crack propagation would depend upon the maximum fibre stress rather than the strain amplitude and any stress relieving due to plastic flow would take a finite time thus affecting the value of service life.

It is therefore concluded that the progressive reduction in the stiffness of the bituminous roadbase materials studied under the repeated applications of load is due to a microscopic change in the binders themselves. The most logical binder property to account for this phenomenon is that of thixotropy.

It will be remembered that thixotropy was defined as that property of a substance which causes its viscosity to be reduced under the continual application of shear and to be regained, either in part or in whole, when the shearing is terminated. Although the term thixotropy is generally considered to apply to a complete gel-sol-gel transformation (97,101), it is used in this context to identify the shear thinning phenomena rather than the complete reversible cycle. This concurs with the definition of thixotropic behaviour of bitumens employed by Traxler (102) and is synonomous with Pryce Jones's false body (103) in the case of visco-elastic solids.

The behaviour of the bituminous materials studied under repeated loading can be easily explained using the thixotropic theory as follows.

In strain-controlled testing, as soon as the binder is subjected to increasing deformation thixotropic shear-thinning takes place. Thus the stiffness of the binder, and hence the stiffness of the mixture, is reduced not only by the increasing strain but also by its reducing viscosity. This progressive reduction will continue to take place until deformation is terminated. At the stationary point thixotropic recovery and stress relaxation due to delayed elastic effects will commence. Once deformation is recommenced, in the reverse direction, the above procedure will be repeated.

Clearly, thixotropy will not be manifest in repeated loading behaviour only if the period of stationary positions is sufficiently long to permit complete thixotropic recovery. The degree of thixotropic recovery at each stationary point will depend upon its duration, the rate at which the delayed elastic effects are dissipated and the rate of thixotropic recovery. It may well be that thixotropic recovery and the delayed elastic effect of

of a bituminous binder are interrelated. If the shape of the trapezoidal wave form is such that the thixotropic recovery is less than the thixotropic damage then cumulative damage will result. The stiffness of the binder will then decrease until some factor determines otherwise.

In stress-controlled testing the instantaneous stiffness will decrease during the first tensile loading due to both the increasing strain and the thixotropic decrease in binder viscosity. During the first tensile stationary point the material will continue to flow under the action of the tensile stress and thixotropic damage will continue at a reduced rate, due to the continued deformation. This reduced rate of thixotropic damage may either be reduced or offset by the thixotropic recovery resulting from the damage during the increasing tensile loading, Upon reversing the stress to an equal compressive level the deformation and consequently the thixotropic damage will depend upon the compressive properties of the material. If these exceed the tensile properties of the material then, upon repeated applications of loading, a permanent tensile deformation will develop until such time as it exceeds the ultimate value of the material, resulting in fracture and complete failure. In this case the thixotropic properties of the binder will not be the sole cause of failure but will hasten its inception.

Clearly the above hypotheses can be used to explain the experimental phenomena but the experimental phenomena cannot be used to establish the hypotheses.

In an attempt to establish whether, or not, the binders used in this investigation exhibit thixotropic behaviour, simple rotating shear tests were performed as described in Chapter 8.

The results of two continuous shear tests on unheated 40/50 penetration bitumen at a temperature of $+30^{\circ}C$ are shown in Figure 140. Although the torque spring used was the stiffest spring available with the standard shear vane apparatus, a considerable time was taken for it to wind up to indicate the actual torque exerted by the binder under test. The recorded torque/time curves have therefore been extrapolated backwards towards the commencement of the tests as represented by the dashed lines. These tests are not strictly constant shear rate tests, again due to the finite stiffness of the spring but results do indicate a definite drop in torque and hence binder viscosity with continual shear. The fall in torque at the end of the first test reached zero after 10 minutes indicating that the equilibrium state between breakdown and reformation of the miceller structure, described by Wilkinson (98), has been reached. These

viscosity
factors being so, then the reduction in binder/due to continual shear is due to thixotropy.

A further constant shear test was carried out on some unheated 90/110 penetration bitumen at a temperature of +15°C. The viscosity of this binder at this temperature is similar to that of the 40/50 penetration bitumen at +30°C. The results of this test, using the same torque spring as before, are also shown in Figure 140. Again thixotropic behaviour is indicated. In this case the binder tended to spiral up the inner cylinder resulting in a sharp fall in torque after 50 minutes of shear. This portion of the torque curve has no practical significance but does indicate that the viscosity of the binder in this test is the lowest that can be studied with these boundary conditions.

The results of a third test on the unheated 90/110 penetration bitumen at a temperature of +20°C are also illustrated in Figure 140. It was hoped that the effect of temperature on the reduction in binder torque might be assessed but the restrictions of the apparatus did not permit this aspect to be pursued.

Clearly, these coaxial cylinder viscosity tests are rather unsophisticated and provide only a rough qualitative indication of binder behaviour. The torque curves could be equally well explained in terms of pseudoplastic behaviour under non-isothermal conditions. However, a simple test based on the method of illustrating thixotropic behaviour suggested by Pryce Jones (221) has been found to apply to the binders studied. If a specimen of binder is sheared continuously until a state of equilibrium is obtained and the shearing then terminated, the torque in the inner cylinder will decay with time as shown in Figure 140. By restraining the inner cylinder from rotating when shearing is terminated for a fixed period of time. The shear rate is then increased by a given increment and the specimen sheared at that rate for the same fixed period. This procedure is repeated in increasing and subsequently decreasing increments of shear rate and the resulting shear stress loop plotted. If the decreasing portion of the loop is linear this indicates a thixotropic "Newtonian" material. A non-linear portion indicates either a thixotropic pseudoplastic or Bingham plastic, the latter being distinguished by not passing through the origin. Materials which have common increasing and decreasing relationships have no shear rate memory and are not, therefore, thixotropic. This test method will clearly distinguish thixotropic and pseudoplastic behaviour.

Dahlgren (224) has employed the test method of Green and Weltmann to ascribe a coefficient of thixotropic breakdown and Goodeve and Whitfield (225) have employed this test method to determine a coefficient of thixotropy.

Either coefficient would prove most useful in a quantitative study into thixotropic behaviour of bituminous materials.

Unfortunately, time did not permit a variable speed drive and necessary improvements to the coaxial cylinder viscometer to be made so that these quantitative approaches could not be pursued.

Further experimental evidence of thixotropic behaviour is offered in the form of results from repeated loading tests performed on the bituminous roadbase materials studied in the main testing programme. Set out in Table 19 are the results of specimens which were retested after their service lives had been determined. In the majority of cases of specimens rested at least overnight, the second run showed a log stiffness/log cycles relationship parallel to that of the preceding run over the total number of cycles re-run. This indicates that the thixotropic reduction in binder stiffness is the same for both first and second runs, where the second run exhibits either complete recovery, or where the recovery still occurring during the second run is obscured by the thixotropic damage. This is in accordance with results of the main testing programme, which showed that the rate of thixotropic damage occurring during a strain -controlled test is a function only of the strain level and not of the magnitude of the initial stiffness.

Rests re-run after only 1 hour, or less, rest exhibited significant recovery, and in these cases the log. stiffness/ log. cycles relationships were not parallel to the first runs when plotted from the beginning of each case. This is easily explained by the fact that since the rate of thixotropic shear thinning decreases with time, if a test resumed before complete recovery has taken place then the rate of fall in stiffness will be less than the original test.

Time did not permit a more detailed study to be made of the recovery of stiffness during rest periods after repeated loading. Had this been possible attention would certainly have been concentrated upon the recovery properties after small groups of cycles representing batches of traffic in practice. It may well be possible to predict the behaviour of a bituminous material by establishing a model for the recovery after one load application (the damage during the first application of load has now been established) and applying or establishing some law for cumulative damage.

Accepting the hypothesis of recoverable damage being caused to bituminous materials being subjected to repeated applications of load by

thixotropy, certain experimental phenomena require to be explained. First, is it reasonable to expect a particular material to have a thixotropic strain-dependency which is independent of test temperature and strain rate and over what range of strains, test temperatures and strain rates would this be expected to apply? Secondly, why have certain materials at high temperatures indicated minimum values to the reductions in material stiffness? Having satisfied these questions it will be possible to find ways in which roadbase materials may be designed to reduce the distress causes by this thixotropic phenomenon.

Consider a gel-type bitumen, or a sol-type bitumen with an asphaltene content which is sufficiently high such that the miceller disperse phase of the binder forms a partially flocculated long chain polymer system. Upon shearing, low energy inputs cause a partial uncoiling of the polymer chains resulting in elastic deformations of the flocculated disperse phase. Only when the applied stress exceeds the force of flocculation will deformation occur. This force of flocculation, manifest as yield stress in macroscopic terms, is the result of the intermolecular attraction between the polymer chains. As these bonds are broken under the action of shear they quickly reform with adjacent newly released chains. It will be remembered from Chapter 4 that only a small section of each chain will become unbonded from an adjacent chain and jump to another free chain, bonding to reform the structure. No fundamental change is experienced in the structure so long as no polymer chains are broken.

Under constant shear the breaking and forming of bonds eventually reaches a state of equilibrium and this can only be destroyed by changing the rate of shear. To reduce the shear rate reduces the rate of bond breaking resulting in an increased equilibrium viscosity. Hence, at zero rate, no reduction in viscosity occurs at rest.

The thixotropic (false body) effect will only become non-reversible if some of the polymer chains are fractured. A fracture will result in increased loading in adjacent chains which may in turn fracture due to overloading. In this case a microcrack is formed which may propagate, possibly linking with other microcracks leading to macroscopic cracking in the binder. This is a logical application of the theory on cross-linked polymers proffered by Beuche (226).

In microscopic terms the above mechanism is independent of direction of shear but it may well be influenced by external effects.

From the foregoing it will be apparent that the viscosities of bitumens with high asphaltene contents, whilst being less susceptible to

changes in test temperatures and strain rates, will be more prone to thixotropic effects. This has been observed in practice by Coombs and Traxler (93) and by Saal and Labout (61) who have found marked thixotropic effects in air blown, gel-type, bitumens. As the bitumen type passes through the gel and sol to the pitch type categories, the reduction in micelle content reduces viscosity reduction due to thixotropy. Tars and pitch type bitumens which exhibit marked Newtonian characteristics would be expected to be relatively insensitive to thixotropic effects.

Reference to Figure 141 will show the trend of increasing thixotropic breakdown with shear rate for colloidal systems. The coaxial cylinder viscosity tests described previously did not permit the breakdown and recovery properties of the various binders used in the roadbase materials studied to be made. Had this been possible then the rate of reduction in material stiffness under repeated applications of load might have been calculated thus verifying, or otherwise the thixotropic hypothesis.

To assess the effect of a reduction in the viscous component of a visco-elastic material on the overall stiffness requires the use of a mathematical model. It has been suggested that to a first approximation, a simple Burger model with no series dashpot serves well to illustrate the rheological behaviour of bitumens. In Figure 146 a dimensionless plot has been presented of the stiffness of this model for varying values of $\frac{\lambda}{Emt}$, assuming linear elements. The ratio of E_k to E_M (=n) has been varied from zero, representing a Maxwell model, to infinity, representing a single elastic component. Considering the curve $n = 1.10^{-3}$, for a repeated loading test under conditions of controlled strain at constant strain rate, or t, as the coefficient of viscous traction, λ, is reduced, due to thixotropic effects, then so is the model stiffness reduced. To reduce the model stiffness by 40% requires reductions in viscosity, the magnitude of which depends upon the initial model stiffness. For example, at $\frac{\lambda}{Emt} = 1.10^{1}$ then to reduce the model stiffness by 40% required a reduction (in) of 87%, whereas, at $\frac{\lambda}{Emt} = 1.10^{-1}$ a reduction of only 40% is required. Due to the Kelvin elastic component, at $\frac{\lambda}{Emt} = 10^{-3}$ the reduction (in) required to produce a 40% reduction in model stiffness is increased to 82%.

The dimensionless plot of bitumen stiffness calculated from the Van der Poel nomograph (see Figure 8) is shown in Figure 147. Here it will be seen that the absence of a lower elastic limit to stiffness within the range of loading times examined suggests a ratio $\frac{E_k}{E_M}$ of much less than 1.10^{-3}. It is therefore reasonable to consider the Maxwell curve shown in Figure 146, where n = 0, to assess the effect of thixotropic changes in the binder

viscosity on stiffness.

In a strain-controlled repeated loading test at constant strain rate, hence constant time, it is evident that for higher strain rates, or higher frequencies, the reduction in binder viscosity required to reduce the overall binder stiffness by a set amount is greater than at lower frequencies. Only when all frequencies correspond to initial $\frac{\lambda}{Emt}$ values lying on the sensibly linear portion of the stiffness curve will test frequency have no effect on the magnitude of thixotropic breakdown required to reduce the stiffness by a set amount. In practice the initial values of $\frac{\lambda}{Emt}$ for 90/110 penetration bitumen are shown in Figure 147 to depend upon strain rate. However, it should be remembered that these values themselves include a certain amount of thixotropic damage being derived from varying strain range tests and do not, therefore, correspond to the theoretical nomograph values of Van der Poel for small linear strains.

Relating these theoretical considerations to practical results on strain-controlled constant strain rate tests on bituminous roadbase materials: at high strain rates and low strain levels resulting in high initial binder, hence mixture, stiffness values, dynamic tests are performed in the convex region of the stiffness curve shown in Figure 146. (It should also be borne in mind that since the binder accounts for only some 10% to 20% of the material volume then the value of $\frac{\lambda}{Emt}$ for the binder will be some 3 to 5 times greater than that value of the mixture). Therefore, as the test frequency is increased so is the required reduction in binder viscosity increased for a specified net reduction in binder stiffness. Taken to its extreme case this conforms with the findings of Heukelom (133) that when bitumen stiffness approaches the elastic asymptote value then "fatigue" phenomena almost disappears. Now it was stated previously that the rate of thixotropic breakdown of colloidal systems was greater at higher strain rates. Therefore rate effect on thixotropic breakdown will partially offset the greater breakdown in binder viscosity required for a specified reduction in binder stiffness at higher test frequencies. Whereas it is not suggested that these two opposing effects exactly counteract one another, it is clearly possible that a unique relationship exists between the shear rate and the rates of thixotropic breakdown and recovery, and the shape of the stiffness curve which would result in the effect of frequency on the net rate of stiffness breakdown being minimal. In view of the limited range of strain rates examined in the practical work reported previously it would appear that any frequency effect is masked by the degree of experimental error.

At higher strain levels and lower strain rates where binder stiffnesses lie on the sensibly linear portion of the stiffness curve, the effect of test frequency on the overall rate of stiffness breakdown is minimal. At the same time the effect of strain rate on the rate of thixotropic breakdown of binder viscosity is reduded. Therefore, whereas the effect of strain rate defining the time required for a specified reduction in binder viscosity will result in some frequency effect, this is masked in practice by the experimental errors over the small frequency range considered.

Experimental results on the stiffness characteristics of pure bitumen, shown in Figures 92 and 147, do not indicate any lower stiffness value, suggesting a Burger type model might be used to illustrate binder behaviour. It is likely, therefore, that as the time of loading is increased and hence the reducing strain rate has relatively less effect on the rate of thixotropic breakdown of the viscous component of the binder the effect of test frequency on service life will be minimal.

The experimental results of all tests on the four types of bituminous roadbase materials studied, ranging from high frequency tests at low temperature to low frequency tests at high temperature, have shown no dependence of test frequency on service life. This fact, substantiated by the findings of Kirk (151), indicates that the two factors defining the time taken to reduce mixture stiffness by 40% offset each other. In the absence of experimental results or published data on thixotropic breakdown it is not possible to say whether this condition has been approached. However, since the range of strain rates examined under repeated loading was relatively small and the loading times only a very small fraction of the equilibrium shear time, any variations in net rates of thixotropic breakdown are probably outweighed by the degree of experimental scatter.

The time/temperature interchangeability characteristics of tars and bitumens may be applied to the dimensionless stiffness curves of Figure 146 but not necessarily to the strain rate dependency of thixotropic breakdown. As the test temperature is increased the micellar density is reduced thus not only reducing the resistance to shear but also reducing the number of bonds available for breaking. An increased shear rate may well compensate for the increase in test temperature, resulting in similar thixotropic characteristics but this has not been determined. The temperature susceptibility of thixotropy might be expected to be of the same order as the temperature susceptibility of viscosity since lower viscosities exhibit lower rates of thixotropic breakdown. Thus with the binders

employed in the roadbase materials studied, the tar would be expected to show a greater susceptibility to test temperature than the bitumens. Since the range of strain rates employed in the experimental work was similar for all test temperatures, it might be expected that larger service lives, due to the reduced rate of thixotropic breakdown, would be associated with higher temperatures. This situation would be counteracted to some extent by the fact as test temperature is increased the coefficient of viscous traction is reduced thus reducing the initial value of $\frac{\lambda}{Emt}$.

No significant trend in service life with temperature could be detected in the two types of dense bitumen macadam roadbase materials examined. This is attributed to the relatively small range in temperatures and again the fact that any possible trend may well have been outweighed by the experimental scatter. The limited number of results from the repeated loading tests performed on the hot rolled asphalt roadbase material did suggest some temperature effect. At test temperatures of $+10^{o}C$ and $+30^{o}C$ longer lives were recorded at the higher temperature where the rate of thixotropic breakdown would be expected to be less. This effect has been reported by other investigators (139, 148-150) testing low void content materials at frequencies much in excess of those studied in this investigation. The greater temperature sensitivity of the 40/50 penetration bitumen used in the hot rolled asphalt over the softer bitumens used in the dense macadams is due to its more gel like, higher asphaltene content, structure indicated by the higher penetration index of +0.4 compared with some -0.5 of the softer bitumens.

Further confirming the thixotropic temperature susceptibility theory, the service lives of the dense tar macadam specimens tested were larger at higher test temperatures. At lower test temperatures the number of cycles required reduce the initial stiffness values by 10% was greater than at higher test temperatures for similar strain levels. This indicates that at these low temperatures the initial value of $\frac{\lambda}{Emt}$ were on the convex portion of the stiffness curves shown in Figure 146.

From the experimental results on the four types of roadbase materials investigated it would appear that the effect of strain rate on the rate of thixotropic breakdown in binder viscosity is compensated by the effect of strain rate on stiffness as shown in Figure 146. The effect of test temperature the rate of thixotropic breakdown in binder viscosity is not compensated for by a shift in the time scale of the stiffness curve of Figure 146. This means that the time and temperature interchangeability

characteristics of bituminous binders in stiffness calculations cannot be applied to the rates of thixotropic breakdown. The fact that test temperature has no significant effect on the service lives of the dense bitumen macadam specimens indicates that the initial $\frac{\lambda}{Emt}$ values of the binder lay upon the sensibly linear portion of the stiffness curve.

Considering briefly limitations to the above conclusions: at normal roadbase temperatures within the range $0^{\circ}C$ to $+30^{\circ}C$ the effect of temperature on the rate of fall in stiffness will depend upon the initial value of $\frac{\lambda}{Emt}$. If this value falls upon the high stiffness convex portion of the stiffness curve then a large reduction in binder viscosity will be required to reduce the stiffness by a preset amount. This would appear to be offset by the increased rate of thixotropic breakdown at lower temperatures resulting in no detectable effect of low temperature testing on service life. At high temperatures where initial values of $\frac{\lambda}{Emt}$ are on the concave portion of stiffness curve of Figure 146, the time taken to reduce the binder stiffness by a preset amount will increase thus significantly increasing the service lives. There may come a time when the initial value of $\frac{\lambda}{Emt}$ is such that stiffness cannot fall by the specified amount due to the lower stiffness value of the material.

The lack of evidence of any strain rate, or frequency, effect upon service life and the lack of quantitative information on the effect of strain rate on the rate of thixotropic breakdown precludes any conclusions to be drawn on the effect of frequency upon service life.

So far only the progressive thixotropic reduction in material stiffness has been considered and this is not a true fatigue phenomenon in the strict definition of the word. The fatigue of metals should technically originate from the initiation of cracking from a fatiguing crystal but is usually considered as the rate of crack propagation from inherent flaws either in the material or in the crystal lattice structure. Similarly, in strain-controlled testing of bituminous materials, cracks may propagate from flaws resulting in stress concentrations, and lead to cracking. The rate of crack propagation at low temperatures will be much greater than that at high temperatures due to the higher level of energy input to the material. Crack propagation may be arrested by plastic flow, inhomogenuities such as air voids and foreign bodies, or by other cracks running perpendicular to the crack in question.

Failure of a specimen resulting from the propagation of cracks,

originating from flaws, to catastrophic proportions is not strictly a fatigue phenomenon. Andrews (155), however, has suggested that flaws can themselves develop into potential crack initiation sources even if the energy input per cycle is less than that required for propagation. Thus the repeated application of load can distort a flaw until such time as it becomes capable of propagation. Clearly, it would be extremely difficult to differentiate between cracks propagating from flaws and flaws propagating into cracks in practice and the likelihood of either at high stiffness conditions is quite probable.

Another factor which might account for true fatigue failure in bituminous materials is that of strain hardening. Since the yield stress of bitumen is extremely low a continual strain hardening process takes place during the repeated application of load. The yield stress of bitumen is increased as its stiffness increases. Therefore, at high stiffness conditions, the resulting increase in stress for a set strain range may well exceed the fracture strength of the binder. In the case of polymers, strain hardening is the result of preferential orientation of the chains along the axis of strain thus offering a greater inter-mollecular cross-link bond. As the chains are drawn more parallel the fracture strength is also increased but an exceedence of the fracture stress will result in bond slippage and fracture. Clearly the fracture strength depends upon the density of the micellar chains and will be greater for higher asphaltene content bitumens.

Certain of the bituminous materials tested at low temperature and high frequency showed external signs of cracking during test. It is not possible to state categorically whether this cracking was the result of propagation from a flaw or local strain hardening. The extreme inhomogeneity of the materials studied, however, suggests the former explanation to be more likely. The possibility of fatigue failure by strain hardening at low temperatures and high loading rates is unlikely in roadbase but possible in richer, more homogeneous, basecourse and wearing course materials. The possibility of fatigue cracking by strain hardening on the surface of undressed rich, stiff, dense bituminous surfacing materials at low temperatures is quite possible and may account for the "typical" alligator cracking on road surfaces frequently referred to as a fatigue phenomenon.

Much of the above discussion is the result of an extension of the implications of the limited experimental work reported earlier in this

thesis. It is regretted that time did not permit a closer study of these hypotheses to be made. It is felt, however, that the experimental results have provided a stimulus for discussion which may lead to a better appreciation of the behaviour of bituminous roadbase materials under low frequency repeated loading.

REPEATED LOADING TESTS ON DRY LEAN CONCRETE

Repeated strain-controlled tests on dry lean concrete in both wet and dry states were performed on specimens where deformation was either symmetrical about the original position or tensile relative to the original position. In either case, with repeated applications of load, the stiffness fell slightly then increased often to levels greater than the original stiffness values. At the termination of each test a considerable residual compressive load was recorded when the specimen was rested at its original deformation position. Conversely, when specimens were tested in compressive strain-controlled cycling, a very slight fall in stiffness was recorded with the repeated applications of load and no residual load was found on rest.

It was suggested earlier in this chapter that the non-linearity of dry lean concrete might be attributed solely to the non-microcracking component of creep, probably the internal movement of free water. Creep phenomena would also adequately explain the behaviour of dry lean concrete subjected to strain-controlled repeated loading. When deforming a specimen in a tensile direction relative to its initial position the resulting creep effectively increases the gauge length. Thus, in cycling the specimen between fixed positions, the gauge length would be expected to approach the most tensile deformation limit resulting in a gradual build up of residual compressive load during the process. If this residual compressive load is purely a creep phenomenon then at any stage during the course of a test it would be expected to be the same as that load resulting from a single application of a compressive deformation equal to the effective increase in gauge length.

The residual compressive load resulting from 7,000 applications of what was initially a tensile strain-controlled repeated loading test at a strain level of approximately 2.10^{-4} in/in was found with specimen 618 to be 1900 lb. (Figure 125). Performing a compressive strain-controlled repeated loading test on the same specimen at a nominally similar strain level resulted in no residual load after a further 10,000 cycles. Now it will be seen from Figure 130 that in a simple compression test the strain level at which the compressive load is 1900 lb is only $2.04.10^{-5}$ in/in.

This stiffness of $7.40.10^6$ lb/in^2 is a factor of 2 higher than the best fit line value of stiffness at corresponding strain shown in Figure 87 whereas the initial stiffness of specimen 618 agrees closely with the corresponding best fit line value. Making allowance for this variation, it is evident that the residual compressive load resulting from tensile repeated loading tests on specimen 618 is far less than the compressive load resulting from a single application at a deformation equal to the creep deformation. Since stiffness measurements before and after creep have resulted in similar stiffness values at constant strain level, the low value of residual load is indicative of structural damage within the specimen.

Structural damage resulting from the repeated applications of load in compression is also evidenced in pure compressive repeated loading tests. The results of the compressive repeated loading tests, e.g. specimen 618 (Figure 125), show clearly a gradual fall in stiffness under the repeated applications of compressive load. Final confirmation of structural damage after compressive loading is illustrated in the different ultimate tensile properties discussed in Chapter 10.

The most logical explanation of the gradual reduction in stiffness, not accompanied by any evidence of creep, is that of microcracking. The relatively irregular shapes of the stiffness/cycles curves of compressive repeated loading tests, in contrast to the regular shapes of tensile curves, further supports the microcracking theory. These microcracks, probably propagating from the abundance of potential flaws, would be expected to run in an anxial direction, although transverse cracking resulting in the relief of internal tensile stresses would also reduce compressive stiffness.

The strain/cycles curves of dry lean concrete tested in tensile stress-controlled conditions of repeated loading, typically illustrated in Figure 132, show two distinct portions to the curve. The major portion of the curve indicates a regular increase in strain with repeated applications of load attributed mainly to creep with an increasing contribution of microcracking. Ultimately, microcracking becomes the dominant factor resulting in a rapid increase in the rate of increase in strain leading quickly to catastrophic failure.

The trend of smaller strain levels to failure resulting from higher tensile stress levels shown in Figure 136 indicates clearly that the rate of crack propagation, defined by the energy input during loading, is the parameter defining fracture strain and fracture life. This also accounts for the dependence of ultimate strain and fracture life upon the maximum

tensile stress, irrespective of the other stress limit under both fluctuating and alternating test conditions.

It will be remembered from Chapter 5 that the static failure mechanism of concrete has been described by all authors as that of microcracking. Further, the majority of references consider that the microcracking originates and generally propagates in bond failure between the coarse aggregate and the sand/cement matrix. A study of the failure surfaces of all specimens tested in this investigation showed nothing to refute these findings.

Without exception, dry lean concrete specimens tested wet and dry in stress and strain-controlled cycling and direct tension failed within $\frac{3}{8}$" of one or other of their end caps. Since there was no statistical evidence of preferential end failure these end failures are the result of either uneven compaction or end cap stress concentrations. Due to the method of the compaction during specimen production each specimen end tended to be rather dry in sand/cement matrix resulting in lower strength characteristics. Although this would encourage end failures the lean portions were generally within the confines of the end caps and therefore impregnated with epoxy resin. These end cap failures are more likely to be the result of stress concentrations set up by the resin adhesive, partly due to its bonding to the end caps and partly to its impregnation into the concrete ends.

Although all dry lean concrete specimens ultimately failed at one or other end cap this does not dictate that all damage during repeated loading also took place in these regions. A "Demec"-type strain gauge was employed to study the variation in dynamic strain throughout the lengths of a few specimens and this confirmed that there was little variation in strain over the free lengths of the specimens. This procedure was not adopted as routine due to the rubber membranes on wet-tested specimens. Considering that the ultimate tensile strength of the specimens was found to be in the order of $^1/_{10}$ of the cube strength, as would be expected, it is felt that the results of the strain-controlled repeated loading tests are relatively meaningful. Also, since a large proportion of the permanent extension of specimens during tensile stress-controlled cyclic loading has been attributed to creep, stress concentrations at the end caps may only become sufficiently high to cause distress when the Poisson's ratio effect creates high radial tensile stresses after considerable longitudinal extension. Therefore although the results of tests on dry lean concrete should be

viewed with caution it is felt that they cannot be considered invalidated by the ultimate failure conditions.

Time did not permit alternative methods of gripping or testing of dry lean concrete to be pursued. The possibility of using shaped concrete specimens and dry gripping as employed by Elvery (227) would reduce stress concentrations but would require considerable modifications to the method of specimen preparation. Johnson (178,194) has applied axial tensile loads of up to 12 tons by using lever grips to apply compressive restraint to the specimen whilst under axial tension. This method of gripping would require a considerable amount of modification for use in reversed-stress testing.

No reference has been made to "fatigue" in dry lean concrete. Due to the obvious inhomogeneity and anisotropy of this material stress concentrations within a specimen could be many orders of magnitude greater than the externally applied stress. This will result in local ruptures on the first application of load and the subsequent propagation of microcracks. Although fatigue is possible in the form of flaws in, or work hardening (see Taylor's theory (228)) of the cement crystal lattice, or stress concentrations, it is probable that with dry lean concrete fatigue would seldom develop due to premature failure arising from initial crack propagation. This view is supported by virtually all the papers reviewed in Chapter 5.

In summary, the experimental results of tests on dry lean concrete reported earlier in this thesis indicate that in strain-controlled cyclic loading tensile loads are progressively relieved due to creep phenomenon. Although the propagation of microcracking during tensile loading is likely, it contributes far less to material behaviour than does creep. In compressive strain-controlled testing a very gradual reduction in stiffness with repeated applications of load is the result of microcracking but these cracks may become wedged by fine loose particles resulting sometimes in an increase in stiffness. In stress-controlled tension cycling dry lean concrete undergoes a continual increase in length caused partly by creep and partly by microcracking. The overall increase in strain at failure is dependent upon the value of the maximum tensile stress limit, the lower the stress the higher the strain at failure.

Fatigue in the form of crack initiation is not considered a relevant factor in the performance of dry lean concrete roadbases.

CHAPTER TWELVE

EFFECT OF ROADBASE STIFFNESS ON THE THEORETICAL PAVEMENT STRENGTH

The stiffness/strain relationships of all the roadbase materials tested and presented earlier in this thesis have been used to study the effect of roadbase material on the theoretical stresses and strains in a road pavement structure. The theoretical analysis has been performed using the Shell Bistro computer programme (229) which evaluates the stresses, strains and displacements in elastic layered systems.

For the purposes of this study constant sub-base and subgrade properties have been employed. The modulus of elasticity of the subgrade has been taken as $1.0.10^4$ lb/in^2 which, according to Seed, Chan and Lee (230), is a typical value for clays subjected to a deviator stress of about 5 lb/in^2. This modulus might be expected from a C.B.R. value of some 7% (231,232) and such a subgrade would, according to Road Note 29 for Chart 1 roads (2), require a minimum sub-base thickness of 6 inches. The clay subgrade has been assumed saturated and so a Poisson's ratio of 0.5 has been taken.

It has been suggested (231,233) that where initially the modulus of the sub-base material greatly exceeds that of the subgrade material, then the induced tensile strains in the sub-base result in decompaction and a subsequent reduction in effective modulus. This process generally produces a modular ratio of between 1.5 and 4 for these two layers. A value of 2.5, as suggested by Edwards (233), has been assumed for the purposes of this study to provide a sub-base modulus of $2.5.10^4$ lb/in^2. Poisson's ratio of this unbound sub-base material has been taken as 0.2.

Taylor (124) has reported similar stiffness characteristics for wearing course and base-course hot rolled asphalt mixtures despite the richer, filled nature of the former. In view of this both the wearing course and base-course layers have been considered as a single surfacing layer of 4 inch thickness. Whereas it was intended to employ the stiffness values of surfacing materials presented by Taylor, it was found that results of the hot rolled asphalt base-course material were far less than those reported earlier in this thesis for a similar roadbase material. The maximum stiffness values found by Taylor, determined by cantilever testing of rotating bending specimens, were temperature dependent. This was considered a phenomenon of the method of test and so the stiffness values determined by simple uniaxial testing reported earlier in this thesis have

been employed for surfacing stiffnesses.

The values of Poisson's ratio for bituminous road paving materials has been generally found to lie within the range 0.3 at high stiffness conditions to 0.5 at low stiffness conditions (78,88,118,234,235). Sayegh (120), however, has reported values as low as 0.22. Ashton and Moavenzadeh (104) have shown that a change in Poisson's ratio from 0.2 to 0.4 will only affect the theoretical surface deflection by 8% and Peattie (28) has found an increase in vertical stresses of only 10% and horizontal strains by 19% when increasing the value for all bituminous bound layers from 0.35 to 0.5. In consequence, a value of Poisson's ratio of 0.35 has been taken for all the theoretical work. This is considered quite representative for frequencies of 1 and 10 cycles/second at an ambient temperature of $+10^{o}C$ at which much of the theoretical work has been performed.

The Poisson's ratio of concrete has been quoted by Simmons (236) as being between 0.22 at a modulus of 7.10^{6} lb/in^2 and 0.3 at $3.5.10^{6}$ lb/in^2. These results were from ultrasonic tests and the static value is generally considered to be in the order of $^1/6$ (179). For this study a value of 0.2 has been adopted.

Table 20 sets out details of the main systems studied, each with rough layer interfaces and a single 9,000 lb wheel load applied over a 6 inch radius circular area. In system 1 a surfacing stiffness of $6.0.10^{6}$ lb/in^2 has been employed with a roadbase stiffness of $1.0.10^{6}$ lb/in^2. The load position has been varied to assess the change in load wavelength throughout the structure. The results shown in Figures 148 and 149 indicate that, if wavelength is defined as the distance between points where the strain is 5% of the maximum, then that at the top of the roadbase is some three times that at the bottom. The surfacing, however, is subject to much higher frequency effects due partly to stress reversals and partly to dynamic effects. In consequence, at ambient temperatures below $+10^{o}C$ and frequencies above 1 cycle/second, the maximum theoretical surfacing stiffness of $6.0.10^{6}$ lb/in^2 has been taken in this analysis. For ambient temperatures of $+30^{o}C$ and a frequency of loading of 1 cycle/second a surface stiffness of $6.0.10^{5}$ lb/in^2 has been employed. For simplicity, a common frequency of loading has been considered to apply throughout the depth of the roadbase. Klomp and Niesman (24) have found experimentally that the frequency of loading in the roadbase is in the order of 0.3 times the velocity of the vehicle in Km/hr. Thus a test frequency of 1 cycle/second would correspond to a creep vehicle speed of some 2 m.p.h. From Figure 148 the average wavelength of horizontal strains is in the order of 6 ft suggesting a frequency of 1 cycle/second corresponds to a vehicle speed of approximately 4 m.p.h.

Hveem and Carmany (48) have found that a creep vehicle speed of 4 m.p.h. generates in the structure a wave time of 1.8 seconds, i.e. 1 cycle/second corresponding to 7 m.p.h.

Figures 150 and 151 show the effect of roadbase stiffness on the stresses and strains in the bituminous bound layers of systems 2a to 2e. Here the ratio of surfacing to roadbase stiffness has been varied from $\frac{1}{2}$ to 8. In subsequent systems only the effective roadbase stiffness and selected stressed and strains are presented, but the overall stress and strain distributions may be interpolated from these curves.

Shown in Table 21 are the results of reiterations performed on structures with varying types of roadbase materials and prevailing conditions. In system 3 the roadbase material is 90/110 dense bitumen macadam and the temperature and loading frequency $+10^{\circ}C$ and 1 cycle/second. In the first instance the average strain in the roadbase, being the average of the strains at depths of 1, 3, 5 and 7 inches in the roadbase, is assumed to be $1.0.10^{-5}$ in/in and the corresponding stiffness from Figure 88 used to compute the strains in the system. The corresponding stiffness at this average roadbase strain has been used to recompute the strains. After two repetitions of this procedure the resulting average strain will be seen to correspond to the average strain of the preceding reiteration.

In subsequent systems where the surfacing stiffness is the same as system 3 the initial average strain has been selected by assuming that, in all cases, the product of stress and strains is constant. Thus in system "n" the stiffness S_n is determined, from the appropriate stiffness/strain relationship at the equilibrium strain ε_3. The appropriate strain is then $\varepsilon_n = \frac{S_3}{S_n}$, ε_3, and the corresponding stiffness at this strain used in the computations. Reference to Table 21 will show that this operation often results straight away in the equilibrium state. In all cases, the process of reiteration was continued until the computed strain was within 5% of the assumed strain.

System 4 was a repetition of system 3 but with the single layer roadbase replaced 4 x 2 inch layers each with the appropriate stiffness. It will be seen from the results in Table 22 that there is no significant difference in the results and subsequent computations were all performed on a single roadbase layer.

The effect of reducing the roadbase stiffness to 60% of its initial value is illustrated in the results of system 12 set out in Table 22. Although the tensile strain on the underside of the surfacing is almost

doubled from $1.1.10^{-5}$ in/in in system 3 to $1.9.10^{-5}$ in/in, the latter value is still extremely low and should not show signs of thixotropic damage in its lifetime. Vertical stresses on the subgrade are increased by some 25% but are again very low. Likewise the increased surface deflection and horizontal roadbase strains are unlikely to provide cause for concern.

From the foregoing results of the stresses, strains and deflections before and after a 40% drop in roadbase stiffness it should not be concluded that the definition of service life is unreasonably conservative. At other temperatures and loading times it is likely that a 40% drop in roadbase stiffness would have a more pronounced effect on pavement performance. Even where surface deflections are small a localised fall in roadbase stiffness along high axle load wheel paths may result in local compaction and subsequent rutting.

The results of all computations are presented in abridged form in Table 22. In all cases the vertical stress on the subgrade is minimal, certainly well below the bearing capacity of typical clays (approx 4 x cohesion), and probably insufficient to cause distress under repeated applications. Surface deflections are also very low. Hveem (49) has found that for a 15,000 lb. axle load surface deflections less than 20 thou inch generally indicated satisfactory pavement performance whereas those above 25 thou inch were often associated with cracked and failed sections. The many results of the AASHO road test (15) revealed satisfactory structural performances with surface deflections of 30 to 40 thou inch under 12,000 to 30,000 lb axle loads. This aspect is further pursued by Peattie (41).

Also shown in Table 22 are the number of continuously applied repetitions of loading which the bituminous materials will withstand. These thixotropic lives are the results of tests reported earlier in this thesis on uniaxially stressed systems. Gardner and Shook (117) have found that lateral (in this case vertical) stresses of up to 20 lb/in^2 have no effect on stiffness. Since the average vertical roadbase stresses seldom exceed this value it has been assumed that the insensitivity of stiffness to lateral stress is also applicable to the behaviour of those roadbase materials under repeated loading.

Results indicate very low lives for the dense tar macadam roadbase both at low and high stiffness conditions. Also the dense bitumen macadam at low stiffness conditions, although it is stressed that no account has been made of any thixotropic recovery.

The results of system 8 indicate that the stiffness of dry lean concrete roadbase material is so high that the predicted stress under

loading exceeds the ultimate tensile strength of the material. Serafim and Guerreiro (215) have quoted the thermal coefficient of expansion of mass concrete as being $7.6.10^{-6}/^{o}C$ corresponding to a strain of $3.04.10^{-4}$ in/in during a $40^{o}C$ change in temperature. Thus if the dry lean concrete roadbase does not crack under repeated vehicular loading it is likely to crack under thermal cyclic stressing. The use of some bituminous material in the concrete as suggested by Williams and Patanker (195) may well go a long way to solving these problems deriving from the brittle nature of dry lean concrete. The rate at which concrete cracking will propagate depends upon the stiffness of the overlying bituminous layers. System 13 results show that when the concrete has completely failed surface deflections are increased almost threefold (whilst still being quite acceptable), although the highest hot rolled asphalt strain still has a thixotropic life at some $4.4.10^{6}$ cycles. With recovery the life would be quite acceptable at this temperature.

It will be remembered that, for convenience, a constant stiffness of 6.10^{6} lb/in^{2} was taken for the surfacing at temperatures of 0 and $+10^{o}C$ and 6.10^{5} lb/in^{2} at $+30^{o}C$. These values may well be too high resulting in low stresses and strains within the structure and on the subgrade, and computed values, therefore, should be viewed with caution.

Stiffness values of dry lean concrete taken from Figure 87 are far higher than would normally be expected. The Young's modulus of steel, determined in the concrete testing apparatus using the steel dumbell shown in Figure 22 is found from Figure 43 to be $2.56.10^{7}$ lb/in^{2}, the 15% error being attributed to the free hanging LVDT supporting rods. This suggests that the high dry lean concrete stiffness values are a characteristic of the material rather than the testing apparatus. Although high tensile creep would account for increases in stiffness of up to a factor of 3, no simple explanation of these very high stiffness values can be offered. Results of computations using the dry lean concrete stiffness values determined experimentally should, therefore, also be viewed with caution.

CHAPTER THIRTEEN

CONCLUSIONS

From the experimental results reported in this thesis and from the ensuing discussion the following main conclusions are drawn. The void characteristics of laboratory prepared hot mixed bituminous materials are dependent, for identical aggregate type and grading and binder volume, entirely upon the viscosity of the binder at compaction. The binder may therefore be considered purely as a lubricant during compaction. Those materials compacted at higher temperatures generally exhibit slightly higher surface voids due to the higher rate of heat loss to the atmosphere. Internal voids are unaffected by compaction temperature, at equivalent binder viscosities and are representative of material voids achieved under rolling compaction in the field. Higher internal voids are associated with lower surface voids and vice versa suggesting that their distinction by the water displacement method is not satisfactory. The overall percentage standard deviation of similar material specimens produced in batches over a long period of time is some 1.3 times the percentage standard deviation of specimens produced in one batch in one single mixing session. This applies to both the bituminous and cementitious bound roadbase material specimens produced.

The dynamic stiffness of all the roadbase materials studied is independent of the mean strain level provided that the specimen is cycled up to or through the no load position. This was found true for strain levels of up to some 1.10^{-4} in/in for bituminous materials and up to 1.10^{-5} in/in for dry lean concrete.

To a first approximation the relationship between stiffness and strain for all the roadbase materials studied is logarithmic, indicating non-linear behaviour. The rate effect of bituminous materials at a constant strain level is sensibly constant over the strain ranges considered and is also logarithmic. Thus the change in stiffness caused by change in strain level and strain rate for all the materials studied is given by:

$$\frac{S_2}{S_1} = \left(\frac{\varepsilon_2}{\varepsilon_1}\right)^m \cdot \left(\frac{R_2}{R_1}\right)^{\log_{10} R}$$

where S_1 = stiffness at ε_1 and R_1

S_2 = stiffness at ε_2 and R_2

ε_1 = strain level at strain rate R_1

ε_2 = strain level at strain rate R_2

m = slope of stiffness/strain relationship for constant strain rate

R = rate effect

For linear materials m = 0, for elastic materials R = 1 and for Newtonian materials R = 10. For the roadbase materials studied the values of "m" and "R" were found to be as follows:

Material	Temp.	Slope "m"	Rate effect "R"	Stiffness at $= 1.10^{-4}$ and $100\mu\varepsilon$/sec	Strain range (in/in)
90/110 DBM	0°C	-0.592	1.85	$2.12.10^{6}$	1.10^{-5}-4.10^{-4}
	+10°C	-0.630	2.60	$7.10.10^{5}$	4.10^{-5}-3.10^{-4}
	+30°C	-0.573	2.89	$1.53.10^{5}$	1.10^{-5}-2.10^{-3}
	+40°C	-0.337	1.95	$6.92.10^{4}$	5.10^{-6}-8.10^{-4}
190/210 DBM	0°C	-0.773	2.42	$1.02.10^{6}$	2.10^{-5}-1.10^{-4}
	+10°C	-0.752	2.95	$3.80.10^{5}$	3.10^{-5}-2.10^{-3}
	+40°C	-0.576	1.33	$1.18.10^{4}$	5.10^{-6}-5.10^{-4}
DTM	0°C	-0.384	1.57	$4.08.10^{6}$	7.10^{-6}-2.10^{-4}
	+10°C	-0.611	2.65	$2.01.10^{6}$	2.10^{-5}-1.10^{-3}
	+30°C	-0.736	3.07	$7.57.10^{4}$	2.10^{-5}-3.10^{-3}
	+40°C	-0.606	1.80	$1.86.10^{4}$	1.10^{-5}-7.10^{-4}
HRA	+10°C	-0.567	2.22	$1.07.10^{6}$	1.10^{-5}-3.10^{-4}
	+30°C	-0.642	2.84	$8.28.10^{4}$	1.10^{-5}-4.10^{-3}
DLC	+20°C	-0.635	1.00	$1.39.10^{6}$	-

Measured rate effects and non-linear characteristics show that at high stiffness conditions the bituminous materials approximate in behaviour to visco-elastic liquids and at low stiffness conditions to firmo-viscous solids. The former effect is attributed to the characteristics of the binder and the latter to the non-linearity of the material due to the concentration of the aggregate. Although a simple Burger model with no series dashpot has been used to illustrate the stiffness/time characteristics, the model's mathematical laws of time and temperature interchangeability are not applicable to these bituminous materials. Under normal roadbase conditions bituminous and cementitious roadbase materials may, for the purposes of pavement analysis, be considered as having their stiffness related to strain level and strain rate as shown above.

The non-linearity of dry lean concrete roadbase material stiffness is attributed to free water migration and viscous creep phenomena. This non-linearity is due mainly to non-reversible non-linear tensile characteristics of the material. Over the normal range of roadbase conditions the stiffness properties of dry lean concrete are independent of temperature and strain rate although the former is based upon documented evidence rather than experimental results.

Under repeated applications of strain-controlled loading the dynamic stiffness of all four types of bituminous materials studied falls progressively to beyond the value of 60% of the initial stiffness at which most tests were terminated. Since service life is defined as a fraction of the initial stiffness of a specimen, the magnitude of surface and internal voids within nominally identical specimens will have no direct effect upon service life. The percentage drop in stiffness, D, after N repetitions of loading at a strain level ε is given for each material by:-

$D = 1.64\,\varepsilon^{0.71}\,(N^{0.0622}-1)$ for 90/110 and 190/210 dense bitumen macadams at 0°C, +10°C, +30°C and +40°C.

$D = 0.0412\,\varepsilon^{1.07}\,(N^{0.365}-1)$ for dense tar macadam at high stiffness conditions (0 and +10°C)

$D = 8.87\,\varepsilon^{0.428}\,(1-N^{-0.132})$ for dense tar macadam at low stiffness conditions (+30 and +40°C)

$D = 3.90\,\varepsilon^{0.662}\,(N^{0.0354}-1)$ for hot rolled asphalt at +10, +30 and +40°C

All these progressive falls in stiffness with repeated applications of load are independent of strain rate and are attributed to the thixotropic breakdown of the binders. Other tests have shown that this thixotropic phenomena is evident in pure bitumen and that recovery, when complete is permanent. Thus a material whose stiffness has been significantly reduced under the action of repeated loading will, after having fully recovered over a period of rest, follow a similar pattern of fall in stiffness when loaded for a second time. This has been found true for all the bituminous materials studied. No evidence of fatigue in the form of crack initiation was found although crack propagation was detected in low temperature, high strain level tests. It is felt that fatigue arising from strain hardening of the binder, whilst possible in rich surfacing materials, is unlikely in roadbase applications.

Repeated applications of strain-controlled loads on dry lean concrete, be the strain range either symmetrical about the initial no load position or tensile relative to it, result in a progressive build up in a compressive residual load. After a slight fall in dynamic stiffness the stiffness rises, often to beyond its initial value as the residual load increases. Equilibrium is reached when the rate of build up in residual load, caused by the predominantly tensile creep properties of the material, is exceeded by the rate of increase of internal damage due to microcracking. A steady reduction in stiffness then ensues with further repeated applications of load due to microcracking. This reduction in stiffness follows no set pattern due to the ingress of fine particles wedging open microcracks and the non-uniform rate of crack propagation. It has not been found possible to define this behaviour quantitavely.

The dynamic and permanent strains of tensile stress-controlled testing of dry lean concrete increase with increasing number of load applications. The initial steady rise in strains with number of load applications is attributed to tensile creep phenomena and ultimate failure to the rapid growth of microcracks. The total strain at failure and the number of load applications required to induce failure are greater with smaller maximum tensile stresses. Therefore, the rate of crack propagation, defined purely by the energy input derived from the maximum imposed tensile stress, irrespective of the other stress reversal limit, is the sole parameter defining fracture strain and fracture life. Microcracking appears to propagate as bond breakdown between the coarse aggregate and the sand-cement matrix. The ultimate crack network is the linking of these bond cracks across the matrix and so fatigue failure within the matrix is discounted.

The fracture life for dry lean concrete under stress-controlled repeated loading is given by:-

$$N = \left(\frac{89}{\sigma}\right)^{13\cdot7}$$

where N is the fracture life under a maximum tensile stress of σ, although the fracture of all dry lean concrete roadbase material specimens in the vicinity of one or other end cap renders general findings of a qualitative rather than quantitative nature.

Theoretical stresses, strains and deflections of road pavement structures computed, using the experimentally determined stiffness/strain relationships of the roadbase materials studied, are of a magnitude unlikely to cause distress of the structure. Only at high ambient temperatures are

the thixotropic lives of certain bituminous roadbase materials quite low but no account has been taken of the recovery properties of these materials. The brittle nature of dry lean concrete is such that a concrete roadbase is likely to crack very soon after installation and for practical purposes should, in its present form, be considered as an extension of the unbonded dry granular sub-base material.

In view of the experimental results presented in this thesis, it is felt that more economic use could be made of the bituminous bound roadbase materials studied if their stiffness and repeated loading characteristics would be put to greater advantage. This could be effected either in reduced roadbase thickness or better, if satisfactory frost protection to the sub-grade can be retained, in the replacement of equivalent quantities of sub-base material. The use of dry lean concrete as a roadbase material in its present form would appear to have only short-term advantages over dry granular material.

CHAPTER FOURTEEN

APPLICATION OF EXPERIMENTAL RESULTS TO PRACTICE

The work reported in this thesis forms part of a long term research programme being undertaken at Nottingham University to study the behaviour of flexible road pavement materials subjected to dynamic loading. The results of previous Nottingham investigators, together with other theoretical and practical work on the analysis of layered systems, is being incorporated into a proposed pavement thickness design method. It is hoped that the work reported in this thesis will not only provide useful practical information about the materials studied, but will also make some small contribution towards a better understanding of the behaviour of bound flexible road pavement materials in general.

Results of dynamic tests on the roadbase material studied indicate their high magnitudes of stiffness at low strains and, in the case of the bituminous bound materials, low temperatures. These stiffness values, which are higher than is generally appreciated, have the advantage of considerable load spreading capabilities but the associated high maximum tensile stresses may be sufficient to cause brittle fracture. Lee and Rigden (238) have found the fracture strength of both tars and bitumens to reduce as binder stiffness is increased and it is significantly reduced, by up to a factor of five, as the stress is changed from uniaxial to hydrostatic tension. To reduce the occurrence of brittle fracture in bituminous roadbase materials at high stiffness conditions, the use of a rich low void content material should be avoided. The inclusion of a significant volume of voids (up to, say 8%) is a desirable feature since it reduces the intensity of hydrostatic tensile stressing and provides greater facility for the flow of local highly stressed binder. The brittleness of dry lean concrete may be reduced by increasing the tensile creep properties (see Chapter 4) but this would be of limited benefit under high frequency loading conditions. In this case the addition of a bituminous admixture during mixing as used by Williams and Patankar (195) would increase its ductility.

As ambient temperature is increased the brittle properties of bituminous roadbase materials become less important. However, experimental results show that by increasing material temperature from $0^{\circ}C$ to $+40^{\circ}C$ the stiffness of 90/110 dense bitumen macadam roadbase material at a strain level of 1.10^{-4} in/in decreases by a factor of 30.6, that of 190/210 dense bitumen macadam by 86.5 and that of dense tar macadam by 219. These reduced road-

base stiffnesses result in higher surface and roadbase stresses and strains which may lead to distress under the action of repeated loading. The use of a less temperature sensitive bituminous roadbase binder would be advantageous suggesting a gel-type binder with correspondingly high molecular weight. Apart from the poorer aggregate adhesion properties of this type of binder, experimental results have led to the suggestion that gel-type binders are more susceptible to thixotropic softening under repeated loading. A compromise has therefore to be reached between temperature and thixotropic susceptibility.

Over 3000 patents have been taken out on methods of reducing the temperature susceptibility of bituminous binders, mainly by the use of admixtures, but none has proved completely successful. The most promising method of temperature stabilisation is the addition of sulphur to hot bitumen prior to mixing. Considerable care has to be taken with temperature control prior to placing since the sulphur is irrevocably damaged at temperatures above +150°C and cross linking commences at a temperature below 120°C. A successful sulphur-bitumen mixture has good workability characteristics when hot and when cool transforms the binder, by random intermolecular cross-links, from a thermoplastic into a less temperature sensitive thermosetting material. The cross-links reduce the amount of molecular slippage and would therefore be expected to greatly reduce thixotropic softening. The addition of sulphur, or any cross-link additive such as S.B.S. or epoxy resin, takes a bituminous binder out of the amorphous category. It is therefore suggested that, whereas temperature susceptibility and thixotropy would undoubtedly be reduced, the possibility of crystal lattice fatigue should be carefully considered. In view of the ever increasing density of high magnitude axle loads in concentrated wheel paths it may well prove economical to utilise relatively thin high quality roadbases and the use of modified binders cannot be precluded.

In Chapter 5 most of the published methods of testing the behaviour of bituminous road paving materials have been reviewed. In almost all cases, of both stress-and strain-controlled testing, the thixotropic theory can be employed to explain experimental results. In cases where test specimens are subjected to a uniform bending strain over a large portion of their lengths, experimental phenomena concur with the findings reported in this thesis. The thixotropic theory can be employed to explain these phenomena and the findings of other investigators are compatible with predicted thixotropic effects. In cases where specimens are subjected to localized maximum stresses, a localized thixotropic shear thinning resulting in a redistribution of stresses

producing further localized softening will result ultimately in specimen fracture. It is therefore suggested that the term "fatigue", implying crack initiation, not preceded by any change in material properties , be reconsidered in view of the conclusions reached in this thesis. If the thixotropic theory is accepted as the main cause of loss in serviceability of road pavement profiles, due to changes in material properties, then basic work on binder behaviour under continual sher and its recoverable properties may be employed to assess the suitability of binders and bituminous materials to road pavement structures.

CHAPTER FIFTEEN

RECOMMENDATIONS FOR FURTHER WORK

The main conclusion drawn from the results of tests on bituminous roadbase materials is that under repeated applications of load the dynamic stiffness falls in a regular manner and recovers upon resting. It has been suggested that this phenomena is due to the thixotropic nature of the binder but this has not been irrefutably established.

Thixotropy can be quantitatively established in pure binders by using the coaxial cylinder viscometer method developed by Green and Weltmann (222,223). The coefficients of thixotropic breakdown of Dahlgren (224) or Goodeve and Whitfield (225) may (the) be used to relate the thixotropic properties of pure binders to the behaviour of bitumen aggregate mixtures under repeated loading. It is suggested that these tests be employed to determine the existence and degree of thixotropic breakdown in bituminous road pavement materials.

Before the results of continuously applied repeated applications of load on roadbase materials can be applied to practice it is necessary to determine the degree of recovery during rest periods. A considerable saving in experimental effort could be made if such work on pure binders, performed using the coaxial cylinder viscometer described above, could be theoretically applied to roadbase materials. Thus the effect of intermittent compound loading on the in-situ performance of bituminous roadbase materials could be assessed. A few confirmatory tests on roadbase materials would, of course, be necessary and these could easily be performed using the apparatus developed for the experimental work reported in this thesis.

If the experimental work on pure binders cannot, for some reason, be applied to the mixed roadbase materials, then it is strongly recommended that the effect of cumulative damage and rest periods be studied using the apparatus described in this thesis. With the fall in stiffness under repeated loading already defined, a theoretical model for cumulative damage can easily be established (as shown in Appendix 7) and confirmed by a few laboratory tests.

The results of the effect of rest periods on a few well chosen tests should be sufficient to predict in-situ behaviour.

It is possible that the thixotropic breakdown of a binder may result in permanent damage of a bituminous material. This aspect may be profitably

pursued by taking samples of binder after various times of shearing either from the coaxial cylinder viscometer or from test specimens of binder or mixture. By measuring the viscosity of a (say 5%) solution of this recovered binder in paraffin, a reduction in viscosity will indicate a breakdown of the polymer chains indicative of permanent damage. Care should be taken to perform this test in an oxygen free atmosphere since oxygen will break down the polymer chains and result in erroneous conclusions.

The stiffness characteristics of the bituminous materials studied in this investigation and those theoretically derived values all suggest a continual fall in stiffness with increasing strain level or time of loading. Clearly there are some physical lower limits to these stiffness curves due to the inherent aggregate structure within the material. A determination of these values would merit further investigation. Not only would this provide useful information regarding the static properties of these materials under creep or standing loads, but it would also enable a suitable model to be derived from which to estimate the behaviour of other bituminous materials. Static or dynamic uniaxial compressive loading tests are considered most appropriate for this study and advantage of the simplicity of test method might be taken in determining the values of Poisson's ratio for specific loading conditions.

Finally, in view of the experimental results on dry lean concrete, the practice of adding a bituminous binder to dry lean concrete roadbase materials initiated by Williams and Patankar (195) would merit further investigation. In view of the reduced stiffness of the modified concrete the apparatus used in the experimental work described in this thesis should prove most appropriate.

If the experimental work suggested above is successfully completed, then this, together with the basic work reported in the thesis, will enable a better understanding of the behaviour of bound roadbase materials to be achieved. When applied to practice this understanding should lead to a more efficient use of roadbase materials thus effecting a significant economy in road pavement construction.

BIBLIOGRAPHY

1 MINISTRY OF TRANSPORT, Specification for Road and Bridge Works - Technical Memorandum No. T4/66 (London 1966).

2 MINISTRY OF TRANSPORT, Road Note 29, A Guide to the Structural Design of Flexible and Rigid Pavements for New Roads - Second Edition H.M.S.O. 1965.

3 * STATE OF CALIFORNIA DIVISION OF HIGHWAYS, Test Method No. 304D - Materials Manual No. 1, 1963.

4 MARSHALL TESTING AND CONSULTING LABORATORY, The Marshall Method for the Design and Control of Bituminous Paving Mixtures - Third Revision (Mississippi, March 1957).

5 NIJBOER, L.W., Plasticity as a Factor in the Design of Dense Bituminous Carpets - Elsevier Pub. Co. (New York, 1948).

6 * SMITH, V.R., - Proc. Assoc. Asph. Pav. Tech. Vol 18,82-224 (Detroit, Feb. 1949).

7 BRITISH STANDARDS INSTITUTION, B.S.S. 594:1961, Specification for Rolled Asphalt (Hot Process) - B.S.I. (London, May 1962).

8 BECKER, W., Development and Structural Design of Asphalt Pavements in Germany - Proc.Int. Conf. on Struct. Design of Asphalt Pavements, 839-850 (Univ. of Mich., August 1962).

9 * U.S. DEPARTMENT OF COMMERCE. CIVIL AERONAUTICS ADMINISTRATION, Design Manual for Airport Pavements - U.S. Dept. of Commerce (Washington 1944 and 1946).

10 HICKS, L.D., Structural Design of Flexible Pavements in North Carolina - Proc. Int. Conf. on Struct.Design of Asphalt Pavements, 802-811. (Univ. of Mich., August 1962).

11 * PORTER, O.J., Foundations for Flexible Pavements - Proc. High. Res. Bd. Vol 22 (1) 100-136 (Washington, Jan. 1942).

12 STEELE, D.J. (Chairman of Committee), Classification of Highway Subgrade Materials - Proc. High. Res. Bd., Vol 25, 376-384 and 388-392 (Washington, 1945).

13 DAVIS, E.H., Pavement Design for Roads and Airfields - Rd. Res. Tech. Paper No. 20 H.M.S.O. (London 1951).

14 HUBBARD, P. and FIELD, F.C., A Direct Method for Determining Thickness of Asphalt Pavement with Reference to Subgrade Support - Ashp. Inst. Res. Series No. 7 (April 1941).

---

* Bibliography not read by the author.

15 * HIGHWAY RESEARCH BOARD, The AASHO Road Test: Report 51 - Pavement Research - High. Res. Bd. Special Report 61 - E (Washington, 1961-2).

16 LIDDLE, W.J., Application of AASHO Road Test Results to the Design of Flexible Pavement Structures - Proc. Int. Conf. on Struct. Design of Asphalt Pavements, 42-51 (Univ. of Mich. August 1962).

17 SHOOK, J.F. and FINN, F.N., Thickness Design Relationships for Asphalt Pavements - Proc. Int. Conf. on Struct. Design of Asphalt Pavements, 52-83 (Univ. of Mich. August 1962).

18 BEATON, J.L., ZUBE, E. and FORSYTH, R., Field Application of the Resilience Design Procedure for Flexible Pavements - Proc. 2nd. Int. Conf. on Struct. Design of Asphalt Pavements, 355-366 (Univ. of Mich. August 1967).

19 BURMISTER, D.M., Proc. High. Res. Bd. Vol 23, 126-159. (Washington, Jan. 1943).

20 BARKSDALE, R.D. and LEONARDS, G.A., Predicting Performance of Bituminous Surfaced Pavements. Proc. 2nd Int. Conf. on Struct. Design of Asphalt Pavements, 321-340 (Univ. of Mich. August 1967).

21 PISTER, K.S. and WESTMANN, R.A., Analysis of Visco-elastic Pavements Subjected to Moving Loads - Proc. Int. Conf. on Struct. Design of Asphalt Pavements, 522-529 (Univ. of Mich. August 1962).

22 THROWER, E.N., Calculations of Stresses and Displacements in a Layed Elastic Structure - Report L R 160, R.R.L. (Crowthorne 1968).

23 WIFFIN, A.C. and LISTER, N.W., The Application of Elastic Theory to Flexible Pavements - Proc. Int. Conf. on Struct. Design of Asphalt Pavements, 499-521 (Univ. of Mich. August 1962).

24 KLOMP, A.J.G. and NIESMAN, T.W., Observed and Calculated Strains at Various Depths in Asphalt Pavements - Proc. 2nd. Int. Conf. on Struct. Design of Asphalt Pavements, 671-688 (Univ. of Mich. August 1967).

25 GUSFELDT, K.H. and DEMPWOLFF, K.R., Stress and Strain Measurements in Experimental Road Sections under Controlled Loading Conditions - Proc. 2nd. Int. Conf. on Struct. Design of Asphalt Pavements, 663-669 (Univ. of Mich. August 1967).

26 MONISMITH, C.L., SEED, H.B., MITRY, F.G. and CHAN, C.K., Prediction of Pavement Deflections from Laboratory Tests - Proc. 2nd. Int. Conf. on Struct. Design of Asphalt Pavements, 109-140 (Univ. of Mich. August 1967).

27 DORMON, G.M. and METCALF, T.C., Design Curves for Flexible Pavements Based on Layered System Theory - High Res. Bd. Record 71, 69-87 (Washington, Jan. 1964).

28 PEATTIE, K.R., A Fundamental Approach to the Design of Flexible Pavements. Proc. Int. Conf. on Struct. Design of Asphalt Pavements, 403-411 (Univ. of Mich. August 1962).

29 DORMAN, G.M., The Extension to Practice of a Fundamental Procedure for The Design of Flexible Pavements - Proc. Int. Conf. on Struct. Design of Asphalt Pavements 785-793 (Univ. of Mich. August 1962).

30 SHELL INTERNATIONAL PETROLEUM COMPANY, Shell 1963 Design Charts for Flexible Pavements - 2nd Reprint, June 1966.

31 BROWN, S.F. and PELL, P.S., Developments in the Structural Design of Flexible Pavements - Rds. and Rd. Const. Vol 48 (569) 141-156 (London, May 1970).

32 LEE, A.R., Recent Research on some Problems in the Construction and Maintenance of Roads - Rds. and Rd. Const. (London, March, April, May 1958).

33 NICHOLS, F.P., A Practical Approach to Flexible Pavement Design - Proc. 2nd Int. Conf. on Struct. Design of Asphalt Pavements 769-779 (Univ. of Mich. August 1967).

34 COFFMAN, B.S., ILVES, G. and EDWARDS, W., Theoretical Asphaltic Concrete Equivalences - High. Res. Record No. 239, 95-119 (Washington, 1968).

35 MONISMITH, C.L., TERREL, R.L. and CHAN, C.K., Load Transmission Characteristics of Asphalt Treated Base Courses - Proc. 2nd. Int. Conf. on Struct. Design of Asphalt Pavements 883-907 (Univ. of Mich. August 1967).

36 WILKINS, E.B. (Chairman of Committee), Pavement Evaluation Studies in Canada, Special Committee on Pavement Design and Evaluation, Canadian Good Roads Association - Proc. Int. Conf. on Struct. Design of Asphalt Pavements 137-218 (Univ. of Mich. August 1962).

37 PRANDI, E., The Lacroix - O.C.P.C. Deflectograph - Proc. Int. Conf. on Struct. Design of Asphalt Pavements 1059-1069 (Univ. of Mich. August 1967).

38 CRONEY, D. and LOE, J.A., Full-scale Pavement Experiment on the A1 at Alconbury Hill, Hunts. - Proc. Inst. Civ. Eng. Vol 30, 225-270 (London, Feb. 1965).

39 ROAD RESEARCH LABORATORY, The deflection beam - LF3 - Rd. Res. Lab. (Crowthorne May 1970).

40 * HVEEM, F.N., Devices for Recording and Evaluating Road Roughness - High. Res. Bd. Bulletin No. 264 (Washington, 1960).

41 PEATTIE, K.R., Surface Deflection in the Performance and Evaluation of Flexible Pavements - The Queen's Highway Vol 32 (1) p 3 (London, Jan. 1966).

42 HUTCHINSON, B.B., The Measurement of Highway Pavement Performance - Proc. 2nd. Int. Conf. on Struct. Design of Asphalt Pavements 39-52 (Univ. of Mich. August 1967).

43 DEHLEN, G.L., An Investigation of Flexure Cracking on a Major Highway - Proc. Int. Conf. on Struct. Design of Asphalt Pavements 812-820 (Univ. of Mich. August 1962).

44 KUNG, K.Y., A New Method of Correlation Study on Pavement Deflection and Cracking - Proc. 2nd. Int. Conf. on Struct. Design of Asphalt Pavements 1037-1046 (Univ. of Mich. August 1967).

45 BENKLEMANN - The Benklemann Beam (1953). Equipment now in common use but original reference unknown.

46 PEATTIE, K.R., Structural Performance of Pavements - Lecture Q Bituminous Materials for Flexible Pavements (Univ. of Nottingham, April 1970).

47 ROAD RESEARCH LABORATORY, Measurements of the Changes in the Dynamic Elastic Properties of the Experimental Flexible Road at Alconbury Hill between 1957 and 1960 - Draft Res. Memo No. 7/RJ.

48 HVEEM, F.N. and CARMANY, R.M., The Factors Underlying the Rational Design of Pavements - Proc. High. Res. Bd. 28, 101-136 (Washington, Jan. 1948).

49 HVEEM, F.N., Pavement Deflections and Fatigue Failure - High.Res. Bd. Bulletin 114, 43-73 (Washington, 1955).

50 HVEEM, F.N., The WASHO Road Test, Part 2, Test Data Analysis, Findings - High. Res. Bd. Special Report No. 22 (Washington, 1955).

51 FINN, F.N., Factors Involved in the Design of Asphalt Pavement Surfaces - Nat. Co-op. High. Res. Programme Report No. 39, High. Res. Bd. (1967).

52 SCHMIDT, R.J. and SANTUCCI, L.E., The Effect of Asphalt Properties on the Fatigue Cracking of Asphalt Concrete on the Zaca - Wigmore Test Project - Proc. Assoc. Asph. Pav. Tech. Vol 38, 39-64 (Los Angeles, Feb. 1969).

53 SPEER, T.L., Progress Report on Laboratory Traffic Tests of Miniature Bituminous Highways - Proc. Assoc. Asph. Pav. Tech. Vol 29, 316-361 (Memphis, Jan. 1960).

54 * NIJBOER, L.W., Some observations on the Properties of Bitumen/ Mineral Aggregate Mixtures in Relation to their Application in Hydraulic Works - De Ingenieur No. 29 (1952).

55 NIJBOER, L.W. and VAN DER POEL, C., A Study of Vibration Phenomena in Asphaltic Road Construction - Proc. Assoc. Asph. Pav. Tech. Vol 22, 197-231 (Houston, Feb. 1953).

56 NIJBOER, L.W., Mechanical Properties of Asphalt Materials and Structural Design of Asphalt Roads - Proc. High. Res. Bd. Vol 33, 185-200 (Washington, Jan. 1954).

57 DICKINSON, E.J., The Constitution of Road Tar - J. Soc. of Chem. Ind. Vol 64 (5) 121-130 (London, June 1940).

58 * NELLENSTEYN, F.J., - J. Inst. Petroleum Tech. 10, P.311 (Dallas, 1924).

59 * NELLENSTEYN, F.J., The Structure of the Nucleus of the Micelle of Bitumen and Coal Tar and Related Problems - Chem. Weekblad 46 P. 362 (1939).

60 WOOD, L.J. and PHILLIPS, G., Constitution and Structure of Coal Tar Pitch - J. Appl Chem. Vol 5, 326-338 (London, July 1955).

61 SAAL, R.N.J. and LABOUT, J.W.A., Rheological Properties of Asphalts - Chapter 9 of Rheology, Theory and Application - Vol 2 Academic Press (New York, 1958).

62 * WILLIAMS, M.L., LANDEL, R.F. and FERRY, J.D., - J. of American Chem-Soc. 77 P.3701 (1955).

63 PFEIFFER, L.J.P. and VAN DOORMAAL, P.M., The Rheological Properties of Asphaltic Bitumen - J. Inst. Petroleum Tech. Vol 22 (152) 414-440 (Dallas, 1936).

64 * MACK, C. - J. Physical Chem. Vol 36 P.2901 (1932). Also Proc. Assoc. of Asph. Pav. Tech. 5 P.40 (Washington, Feb. 1933).

65 PFEIFFER, L.J.P. and SAAL, R.N.J. , Asphaltic Bitumen as a Colloid System - J. Physical Chem. Vol 44 139-149 (Baltimore, 1940).

66 PFEIFFER, L.J.P. (Ed.), The Properties of Asphaltic Bitumen With Reference to its Technical Applications - P.27 and P.163. Elsevier Pub. Co. (Amsterdam, 1950).

67 LABOUT, J.W.A., Chapter 4 of Ref. 66.

68 SAAL, R.N.J. and LABOUT, J.W.A., Rheological Properties of Bitumens - J. Physical Chem. Vol 44, 149-165 (Baltimore, 1940).

69 STANDARDIZATION OF TAR PRODUCTS TEST COMMITTEE, Standard Methods of Testing Tar and its Products - Gomersal Pub. Co. 74-80 (Leeds, 1957).

70 ROAD RESEARCH LABORATORY, Bituminous Materials in Road Construction - H.M.S.O. (London, 1960).

71 BRITISH STANDARDS INSTITUTION, B.S.S. 3235: Test Methods for Bitumen - Br.St.Inst. (London, 1964).

72 * VAN DER POEL, C., Representation of Rheological Properties of Bitumens over a Wide Range of Temperatures and Loading Times - 2nd Int. Congress on Rheology, 331-337 (Oxford, July 1953).

73 HEUKELOM, W., Observations on the Rheology and Fracture of Bitumens and Asphalt Mixes - Proc. Assoc. Asph. Pav. Tech. Vol 35, 358-396 (Minneapolis,Feb. 1966).

74 MONISMITH, C.L., ALEXANDER, R.L. and SECOR, K.E., Rheological Behaviour of Asphaltic Concrete - Proc. Assoc. Asph. Pav. Tech. (Minneapolis, Feb. 1966).

75 SAAL, R.N.J., Rheology and Applied Mechanics - Proc. 2nd. Int. Congress on Rheology 28-35 (Oxford, July 1953).

76 SECOR, K.E. and MONISMITH, C.L., Visco-elastic Properties of Asphaltic Concrete - Proc. High. Res. Bd. Vol 41, 199-320 (Washington, Jan. 1962).

77 MONISMITH, C.L. and SECOR, K.E., Visco-elastic Behaviour of Asphalt Concrete Pavements - Proc. Int. Conf. on Struct. Design of Asphalt Pavements 476-498 (Univ. of Mich. August 1962).

78 PAPIZAN, H.S., The Response of Linear Visco-elastic Materials in the Frequency Domain with Emphasis on Asphaltic Concrete - Proc. Int. Conf. on Struct. Design of Asphalt Pavements 454-463 (Univ. of Mich. August 1962).

79 FERRY, J.D., Discussion on Ref. 75 Page 36.

80 FERRY, J.D. and FITZGERALD, E.R., Dynamic Rheological Properties of Linear Polymers - Proc. 2nd. Int. Conf. on Rheology 140-147 (Oxford, July 1953).

81 SECOR, K.E. and MONISMITH, C.L., The Visco-elastic Response of Asphaltic Paving Slabs under Creep Loading: Bituminous Materials and Mixes - High. Res. Record No. 67, 84-97 High. Res. Bd. (Washington, 1965).

82 PAGEN, G.A., Rheological Response of Bituminous Concrete, Bituminous Materials and Mixes - High. Res. Record No. 67, 1-26 High. Res. Bd. (Washington, 1965).

83 VAN DER POEL, C., A General System Describing the Visco-Elastic Properties of Bitumens and its Relation to Routine Test Data - J. App. Chem. Vol 4 (5) 221-236 (London, May 1954).

84 VAN WAZER, J.R., LYONS, J.W., KIM, K.Y. and COLWELL, R.E., Viscosity and Flow Measurement - Intersciences Pub. (John Wiley & Sons) (New York, 1963).

85 TRELOAR, L.R.G., The Physics of Rubber Elasticity - Clarendon Press (Oxford, 1949).

86 HEUKELOM, W. and KLOMP, A.J.G., Road Design and Dynamic Loading - Proc. Assoc. Asph. Pav. Tech. Vol 33, 92-125 (Dallas, Feb. 1964).

87 THROWER, E.N., The Rheological Properties of Bitumens and Tars - J. Inst. Petroleum Tech. 80-93 (Dallas, March 1959).

88 * EINSTEIN, A., - Annal. Physik Vol 19, P.289 (1906).

89 * ARNSTEIN, A. and REINER, M., - Civ. Eng. (Sept. 1945) (?).

90 * ROSCOE, R., The Viscosity of Suspensions of Rigid Spheres (8) Brit. J. Applied Physics Vol.3 P.267-269 (London, August 1952).

91 VAN DER POEL, C., Time and Temperature Effects on the Deformation of Asphaltic Bitumens and Bitumen-Mineral Mixtures - S.P.E. J. Vol 11 (7) 47-64 (1955).

92 * VAN DRAAT, W.E.F. and SOMMER, P., Ein Gerat Zur Bestimmung Der Dynamischen Elastizitatsmodulu Von Asphalt - Strasse Autobahn Vol 6, 206-211 (1965).

93 * COOMBS, C.E. and TRAXLER, R.N., - Rheological properties of Asphalts IV - J. Applied Physics Vol 8 (4) 291-296 (New York, Apr. 1937).

94 PELL, P.S. and McCARTHY, P.F., Amplitude Effect on Stiffness of Bitumens and Bituminous Mixes under Dynamic Loading Conditions - Rheo. Acta Vol 2 (2) 174-179 (Darmstadt, June 1962).

95 * LEE, A.R., WARREN, J.B. and WATERS, D.B., The Flow Properties of Bituminous Materials - J. Inst. Petroleum Vol 26 (197) 101-128 (Dallas, 1940).

96 * EISENSCHITZ, Kolloid Zeitschrift 64 P.184 (1933).

97 SCOTT-BLAIR, G.W., Introduction to Industrial Rheology - J. and A. Churchill Ltd. (London, 1938).

98 WILKINSON, W.L., Non-Newtonian Fluids - Pergamon Press (London, 1960).

99 EDELMANN, K., Viscosity and Molecular Weight of Macromolecules - Proc. 2nd. Int. Congress on Rheology 107-113 (Oxford, July 1953).

100 MACDONALD, I.F., MARSH, B.D. and ASHARE, E., Rheological Behaviour for Large Amplitude Oscillatory Motion - Chem. Eng. Science Vol 24 (10) 1615-1625 (London, Oct. 1969).

101 WELTMAN, R.N., J. Applied Physics Vol 14, 343- (1943).

102 HOIBERG, A.J. (Ed.), Bituminous Materials, Vol 1., Asphalts, Tars and Pitches, Chapter 4 Rheology and Rheological Modifiers other than Elastomers: Structure and Time. (R.N. Traxler) - Inter Science Pub. (New York 1964).

103 * PRYCE-JONES, J., Kolloid Zeitschrift, 96 P.129 (1952).

104 LODGE, A.S., Elastic Liquids - Academic Press (New York, 1964).

105 WANKET, P.C., Flow During Axial Compression Testing of Materials - Ind. and Eng. Chem., Fundamentals Vol 8 (3) 598 (Washington, Aug.1969).

106 HANSON, J.M., Particle Interaction and the Stability of Asphalt Mixes - M. Phil. Thesis (Univ. of London, 1967).

107 FINN, F.N., HICKS, R.G., KARI, W.J. and COYNE, L.D., Design of Emulsified Asphalt Treated Bases - High. Res. Record No.239, Hig. Res. Bd. (Washington, 1968).

108 SHOOK, J.F. and KALLAS, B.F., Factors Influencing Dynamic Modulus of Asphalt Concrete - Proc. Assoc. Asph. Pav. Tech. Vol 138, 140-166, (Atlanta, Feb. 1968).

109 * McLEOD, N.W., The Asphalt Institute's Layer Equivalency Programme - Research Series No. 15 P.18. The Asphalt Institute (Maryland, March 1967).

110 McLEOD, N.W., Influence of Viscosity of Asphalt-Cements on Compaction of Paving Mixtures in the Field - High. Res. Record No. 158, 76-111 (Washington, 1967).

111 SECOR, K.E. and MONISMITH, C.L., Analysis of Triaxial Test Data on Asphaltic Concrete using Visco-elastic Principles - Proc. High. Res. Bd. Vol 40, 295-314 (Washington, Jan. 1961).

112 GOETZ, W.H., Sonic Testing of Bituminous Mixes - Proc. Assoc. Pav. Tech., Vol 24 (New Orleans, Feb. 1955).

113 JIMENEZ, R.A. and GALLAWAY, B.M., Behaviour of Asphaltic Concrete Diaphragms to Repetitive Loadings - Proc. Int. Conf. on Struct. Design of Asphalt Pavements, 339-344, (Univ. of Mich. August 1962).

114 BAZIN, T. and SAUNIER, J.B., Deformability, Fatigue and Healing Properties of Asphalt Mixes - Proc. 2nd Int. Conf. on Struct. Design of Asphalt Pavements, 553-569, (Univ. of Mich. August 1967).

115 FINN, F.N., Factors Involved in the Design of Asphaltic Pavement Surfaces, Nat. Co-op. High. Res. Programme, Report 39 - High. Res. Bd. (1967).

116 PAGAN, C.A. and KU, B., Effect of Asphalt Viscosity on the Rheological Properties of Bituminous Concrete - High. Res. Record No. 104, 124-140, High. Res. Bd. (Washington, Jan. 1965).

117 GARDNER, L.J. and SKOK, E.L., Use of Visco-elastic Concepts to Evaluate Laboratory Test Results and Field Performance of some Minnesota Asphalt Mixtures - Proc. 2nd Int. Conf. on Struct.Design of Asphalt Pavements, 1005-1019 (Univ. of Mich. August 1967).

118 KALLAS, B.F. and RILEY, J.C., Mechanical Properties of Asphalt Pavement Materials - Proc. 2nd Int. Conf. on Struct. Design of Asphalt Pavements 931-952 (Univ. of Mich. August 1967).

119 COFFMAN, B.S., KRAFT, D.C. and TAMAYO, J., A Comparison of Calculated and Measured Deflections for the AASHO Test Road - Proc. Assoc. Asph. Pav. Tech. Vol 33, 54-91. (Dallas, Feb. 1964).

120 SAYEGH, G., Determinations of the Visco-elastic Properties of Bituminous Concrete by Longitudinal Vibrations - Brit. Soc. of Rheo. Conf. (Univ. of Sheffield, 1967).

121 DEACON, J.A. and MONISMITH, C.L., Laboratory Flexure-Fatigue Testing of Asphalt Concrete with Emphasis on Compound Loading Tests - High. Res. Record 158, 1-31. High. Res. Bd. (Washington 1967).

122 CRAGG, R., The Dynamic stiffness of bituminous road materials - M.Sc. Thesis, (University of Nottingham, May 1970).

123 PELL, P.S., Fatigue of Asphalt Pavement Mixes - Proc. 2nd Int. Conf. on Struct. Design of Asphalt Pavements 577-594 (Univ. of Mich. August 1967).

124 TAYLOR, I.F., Asphaltic Road Materials in Fatigue - Ph.D. Thesis (Univ. of Nottingham, 1968).

125 PELL, P.S. and TAYLOR, I.F., Asphaltic Road Materials in Fatigue - Proc. Assoc. Asph. Pav. Tech. Vol 38, 371-422 (Los Angeles, Feb.1969).

126 EISENMANN, J., On the Determination of Maximum Permissible Stresses in Bituminous Load Carrying Layers, in Particular Consideration of Repeated Loading Condition - Trans. Report No. 320, Tech. Univ. of Munich, Inst. of Railway and Road Building (June, 1966).

127 * ALEXANDER, R.L., Limits of Linear Visco-elastic Behaviour of an Asphalt Concrete in Tension and Compression - Dr. of Eng. Thesis (Univ. of California, 1964).

128 KALLAS, B.F., Dynamic Modulus of Asphalt Concrete in Tension and Tension-Compression - Proc. Assoc. Asph. Pav. Tech. Vol 39, 1-20, (Kansas, Feb. 1970).

129 HARGETT, E.R., Basic Material Properties for the Design of Bituminous Concrete Surfaces - Proc. Int. Conf. on Struct. Design of Asphalt Pavements 606-610 (Univ. of Mich., August 1962).

130 * PFEIFFER, J.P. and SAAL, R.N.J., Some Remarks on Ductility Determinations of Asphaltic Bitumen - 2nd World Petroleum Cong. (Paris, 1937).

131 EPPS, J.A., Influence of Mixture Variables on the Flexural Fatigue and Tensile Properties of Asphaltic Concrete - Ph.D. Thesis Inst. of Trans. and Traffic Engineering (Univ. of California, 1968).

132 PELL, P.S. and TAYLOR, I.F., Fatigue Phenomena in Bituminous Systems - Proc. Int. Conf. on Structure, Solid Mechanics and Engineering Design in Civ. Eng. Materials, (Univ. of Southampton, April 1969).

133 MONISMITH, C.L., Flexibility Characteristics of Asphaltic Paving Mixtures - Proc. Assoc. Asph. Pav. Tech. Vol 27, 74-106 (Montreal, Feb. 1958).

134 THOMAS, T.W., The Testing of Asphalt Paving Specimens upon a Flexible Spring Base - Proc. Assoc. Asph. Pav. Tech. Vol 17, (Chicago, Feb. 1948).

135 PAPIZAN, H.S. and BAKER, R.F., Analysis of Fatigue Type Properties of Bituminous Concrete - Proc. Assoc. Asph. Pav. Tech. Vol 18, 179-210 (Denver, Feb. 1959).

136 PELL, P.S., Fatigue characteristics of Bitumen-Sand Mixes - Ph.D. Thesis (Univ. of Nottingham, 1959).

137 SAAL, R.N.J. and PELL, P.S., Fatigue of Bituminous Road Mixes - Kolloid Zeitschrift Vol 171, 61 (1960).

138 PELL, P.S., McCARTHY, P.F. and BOYD, G., Fatigue of Bitumen and Bituminous Mixes - Int. J. Mech. Sciences, Vol 3 (4) 247-267 (Oxford, 1961).

139 PELL, P.S., Fatigue Characteristics of Bitumens and Bituminous Mixes - Proc. Int. Conf. on Struct. Design of Asphalt Pavements, 310-322 (Univ. of Mich., August 1962).

140 PELL, P.S. and BOYD, G., Fatigue of Asphalt Road Material - Civ. Eng. & Pub. Works Review, Vol 61 (717) 423 (London, April 1966).

141 DEACON, J.A., Fatigue of Asphaltic Concrete - Graduate Report, Inst. of Trans. and Traffic Eng. (Univ. of California, 1965).

142 * MONISMITH, C.L. and DEACON, J.A., Fatigue of Asphalt Paving Mixtures - American Soc. of Civ. Eng. (Dallas, Feb. 1967).

143 LUCAS, A.G., BAZIN, P. and SAUNIER, J.B., The Fatigue Testing of Bituminous Mixtures - Rev. Gen. Routes Aero. 404 (Nov. 1965).

144 MAJIDZADEH, K., RAMSAMOOJ, D.V. and FLETCHER, T.A., Analysis of Fatigue of a Sand Asphalt Mixture - Proc. Assoc. Asph. Pav. Tech. Vol 38, 495-518 (Los Angeles, Feb. 1969).

145 HENNES, R.G. and CHEN, H.H., Dynamic Design of Bituminous Pavements - The Trend in Engineering 22-25 (Univ. of Washington, 1950).

146 McCARTHY, P.F., Factors Effecting the Fatigue characteristics of Bitumen-Sand Mixes - Ph.D. Thesis (Univ. of Nottingham, 1960).

147 MONISMITH, C.L., SECOR, K.E. and BLACKMER, W., Asphalt Mixture Behaviour in Repeated Flexure - Proc. Assoc. Asph. Pav. Tech. Vol 30, 188-222 (Charleston, Feb. 1961).

148 * MONISMITH, C.L., Asphalt Mixture Behaviour in Repeated Flexure - Rep. TE - 63 - 2 (Univ. of California, Nov. 1963).

149 * MONISMITH, C.L., Asphalt Mixture Behaviour in Repeated Flexure - Rep. TE - 65 - 9 (Univ. of California, Nov. 1965).

150 MONISMITH, C.L., Asphalt Mixture Behaviour in Repeated Flexure - Rep. TE - 66 - 6 (Univ. of California, Dec. 1966).

151 KIRK, J.M., Results of Fatigue Tests on Different Types of Bituminous Materials - Proc. 2nd Int. Conf. on Struct. Design of Asphalt Pavements 571-575 (Univ. of Mich., August 1967).

152 JIMENEZ, R.A., An Apparatus for Laboratory Investigations of Asphaltic Concrete under Repeated Flexural Deformations - Rep. to Texas High. Dept., The Texas Trans. Inst. (1962).

153 * SHELLY, See Ref. 230 of Ref. 141.

154 * INGLES, E.C., Transactions Inst. Naval Arch. Vol 60, 219 (London, 1913).

155 ANDREWS, E.H., Fracture in Polymers - Oliver and Boyd (Edinburgh, 1968).

156 * BRADBURY, R.D., Reinforced Concrete Pavements - Wire Reinforcement Inst. Washington 1938.

157 VALLERGA, B.A., FINN, F.N. and HICKS, R.G., Effect of Asphalt Aging on the Fatigue Properties of Asphalt Concrete - Proc. 2nd Int. Conf. on the Design of Asph. Pavements 595-617 (Univ. of Mich., August 1967).

158 MONISMITH, C.L. and SECOR, K.E., Thixotropic Characteristics of Asphalt Paving Mixtures with Reference to Behaviour in Repeated Loading - Proc. Assoc. Asph. Pav. Tech. Vol 29, 114-135 (Memphis, Jan. 1960).

159 SLATE, F.O. and MEYERS, B.L., Some Physical Processes Involved in Creep of Concrete - Int. Conf. on Structures, Solid Mechanics and Eng. Design in Civil Eng. Mats. (Southampton, April 1969).

160 REINUS, E., A Theory of the Deformation and Failure of Concrete - Mag. Conc. Res. Vol 8 (24) (Slough, Nov. 1956).

161 POWERS, T.C. and BROWNYARD, T.L., Studies of the Physical Properties of Hardened Cement Paste - J. American Conc. Inst. Vol 43, 101-132 (Detroit, Oct. 1946) and Vol 44, 933-992 (Detroit, April 1947).

162 * LEA, F.M., Cement Research and the Future - 3rd Int. Symposium on the Chemistry of Cement, 31-38 (London, 1952).

163 FREYSSINET, E., The Deformation of Concrete - Mag. Conc. Res. Vol 3 (8), 49-56 (Slough, Dec. 1951).

164 NESSIM, A.P. and WAJDA, R.L., The Rheology of Cement Pastes and Fresh Mortars - Mag. Conc. Res. Vol 17 (51), 59-68 (Slough, June 1965).

165 GREENBERG, S.A. and MEYER, L.M., Rheology of Fresh Portland Cement Pastes - High. Res. Record No. 3, 9-29, High. Res. Bd. (Washington, Jan. 1963).

166 HANSEN, W.C., Anhydrous Minerals and Organic Materials as Sources of Distress in Concrete - High. Res. Record No. 43, 1-7, High. Res. Bd. (Washington, Jan. 1963).

167 RASHEEDUZZAFAR, The Mechanics of Autogenous Healing of Concrete - Ind. Conc. J. Vol 34 (1) 24-26 and 29 (Bombay, Sept. 1954).

168 MAYERS, B.L., SLATE, F.O. and WINTER, G., Relationship Between Time-Dependent Deformation and Microcracking of Plain Concrete - J. American Conc. Inst. Vol 66 (1) 60-68 (Detroit, Jan. 1969).

169 ILLSTON, J.M., The Components of Strain in Concrete under Sustained Compressive Stress - Mag. Conc. Res. Vol 17 (50), 21-29 (Slough, March 1965).

170 GLUCKLICH, J., Rheological Behaviour of Hardened Cement Paste under Low Stresses - J. American Conc. Inst. Vol 56, 327-337 and 1357. (Detroit, Oct. 1959).

171 FLUCK, P.J. and WASHA, G.W., Creep of Plain and Reinforced Concrete - J. American Conc. Inst. Vol 54, 879-895 (Detroit, April 1958).

172 WARD, M.A. and COOK, D.J., The Mechanism of Tensile Creep in Concrete - Mag. Conc. Res. Vol 21 (68), 151-158 (Slough, Sept.1969).

173 NEVILLE, A.M., Theories of Creep in Concrete - J. American Conc. Inst. Vol 51, 47-60(Detroit, Sept. 1955).

174 GLUCKLICH, J. and ISHAI, O., Rheological Behaviour of Hardened Cement Paste under Low Stresses - J. American Conc. Inst. Vol 57, 947-963, (Detroit, Feb. 1961).

175 * McHENRY, D., A New Aspect of Creep in Concrete and its Application to Design - Proc. American Soc. Testing Materials Vol 43, (1943).

176 ILLSTON, J.M., The Creep of Concrete under Uniaxial Tension - Mag. Conc. Res. Vol 17 (51), 77-84, (Slough, June 1965).

177 HANSEN, W.C., Influence of Aggregate and Voids on the Modulus of Elasticity of Concrete, Cement Mortar and Cement Paste - J. American Conc. Inst. Vol 62, 193-215 (Detroit, Feb. 1965).

178 JOHNSON, C.D., Testing Concrete in Tension and Compression - Mag. Conc. Res. Vol 20 (65), 221-228 (Slough, Dec. 1968).

179 PLOWMAN, J.M., Young's Modulus and Poisson's Ratio of Concrete Cured at Various Humidities - Mag. Conc. Res. Vol 15 (44) 77-82 (Slough, July 1963).

180 BARNARD, P.R., Researches into the Complete Stress-Strain Curve for Concrete - Mag. Conc. Res. Vol 16 (49), 203-210 (Slough, Dec. 1964).

181 POPOVICS, S., A Review of Stress - Strain Relationships for Concrete - J. American Conc. Inst. Vol 67 (3), 243-248. (Detroit, March 1970).

182 GRIMER, F.J. and HEWITT, R.C., The Form of the Stress - Strain Curve of Concrete Interpreted with a Diphase Concept of Material Behaviour. Bldg. Res. Str., Min. of Pub. Bldg. & Wks. Nov. 1968.

183 NEVILLE, A.M., Properties of Concrete - Pitman (London, 1963).

184 OLADIPO, I.O., Cracking and Failure in Plain Concrete Beams - Mag. Conc. Res. Vol 16 (47), 103-110 (Slough, June 1964).

185 BAKER, A.L.L., An Analysis of Deformation and Failure Characteristics of Concrete - Mag. Conc. Res. Vol 11 (33), 119-128 (Slough, November 1959).

186 ANSON, M., An Investigation into a Hypothetical Deformation and Failure Mechanism for Concrete - Mag. Conc. Res. Vol 16 (47), 73-82. (Slough, June 1964).

187 AKROYD, T.N.W., Concrete under Triaxial Stress - Mag. Conc. Res. Vol 13 (39), 111-118 (Slough, Nov. 1961).

188 JONES, R. and KAPLAN, M.F., The Effect of Coarse Aggregate on the Mode of Failure of Concrete in Compression and Flexure - Mag. Conc. Res. Vol 9 (26), 89-94 (Slough, Aug. 1957).

189 BRESLER, B. and PISTER, K.S., Strength of Concrete under Combined Stresses - J. American Conc. Inst. Vol 55, 321-345 (Detroit, Sept. 1958).

190 KRISHNASWAMY, K.T., Strength and Microcracking of Plain Concrete - J. American Conc. Inst. Vol 65 (10) 856-862 (Detroit, Oct. 1968).

191 KUPFER, H., HILSDORF, H.K. and RUSCH, H., Behaviour of Concrete under Biaxial Stresses - J. American Conc. Inst. Vol 66 (8), 656-666 (Detroit, Aug. 1969).

192 CLEMMER, H.F., Fatigue of Concrete - Proc. American Soc. for Testing Materials Vol 22 (11), 408-419. (Atlantic City, June 1922).

193 DOYLE, J.N., KUNG, S.H.L., MURDOCH, J.W. and KESLER, C.E., Second Progress Report - Mechanism of Fatigue Failure in Concrete T & AM Report No. 623 (Univ. of Illinois, Aug. 1962).

194 JOHNSTON, C.D., Strength and Deformation of Concrete in Uniaxial Tension and Compression - Mag. Conc. Res. Vol 22 (70), 5-16, (Slough, March 1970).

195 WILLIAMS, R.I.T. and PATANKAR, V.D., The Effect of Cement Type, Aggregate Type and Mix Water Content on the Properties of Lean Concrete Mixes - Rds. and Rd. Const. (London, Feb./March 1968).

196 * WEIBULL, W., Fatigue Testing and Analysis of Results - Pergamon (Oxford, 1961).

197 NORDBY, G.M., Fatigue of Concrete - A Review of Research - J. American Conc. Inst. Vol 55, 321-345, (Detroit, Sept. 1958).

198 * De JOLY, La Resistance et L'Elasticite des Ciments Portland - Annals des Ponts et Chaussees, Memoirs V 16 Series 7, 198-244 (1898).

199 MURDOCH, J.W., A Critical Review of Research on Fatigue of Plain Concrete, Univ. of Illinois, Eng. Exp. Station, Bulletin 475 (Feb. 1965).

200 RAITHBY, K.D. and WIFFIN, A.C., Failure of Plain Concrete under Fatigue Loading - A Review of Current Knowledge - R.R.L. Report LR 231. (Crowthorne, 1968).

201 * VAN ORNUM, J.L., Fatigue of Cement Products - Transactions American Soc. Civ. Eng. Vol 51, P.443 (1903).

202 BENNETT, E.W., Some Fatigue Tests of High-Strength Concrete in Axial Compression - Mag. Conc. Res. Vol 19 (59), 113-117 (Slough, June 1967).

203 RAJU, N.K., Fatigue of High Strength Concrete in Compression - Ph.D. Thesis (Univ. of Leeds, 1968).

204 TROTT, J.J. and FOX, E.N., Comparison of the Behaviour of Concrete Beams under Static and Dynamic Loads - Mag. Conc. Res. Vol 11 (31), 15-24 (Slough, March 1959).

205 LINGER, D.A. and GILLESPIE, H.A., A Study of the Mechanism of Concrete Fatigue and Fracture - Research News No. 22, 40-51, High. Res. Bd. (Feb. 1966).

206 * KESLER, C.E., Effect of Speed of Testing on Fatigue Strength of Plain Concrete - Proc. High. Res. Bd. Vol 32, 251-258 (Washington, Jan. 1953).

207 * HATT, W.K., Fatigue of Concrete - Proc. 4th Annual Meeting 47-60 High. Res. Bd. (Dec. 1924). Also 5th Annual Meeting 112-118 (Dec. 1925).

208 ASSIMICOPOULOS, M., WARNER, R.F. and EKBERG, C.E., High Speed Fatigue Tests on Small Specimens of Plain Concrete - J. Prestressed Conc. Inst. Vol 4 (2), 53-70 (Sept. 1959).

209 OPLE, F.S. and HULSBOS, C.L., Probable Fatigue Life of Plain Concrete with Stress Gradient - J. American Conc. Inst. Vol 63, 59-80 (Detroit, Jan. 1966).

210 ANTRIM, J.D., The Mechanism of Fatigue in Cement Paste and Plain Concrete - High. Res. Record No. 210, 95-107 (Washington, 1967).

211 HILSDORF, H.K. and KESLER, C.E., Fatigue Strength of Concrete under Varying Flexural Stresses - J. American Conc. Inst. Vol 63, 1057-1076 (Detroit, Oct. 1966).

212 * HATT, W.K., Note on Fatigue of Mortar - Proc. American Conc. Inst. Vol 18, 167-173 (1922).

213 WHITLAM, E.F., Autogenous Healing of Concrete in Compression - Struct. Eng. Vol 32 (9), 235-243 (London, Sept. 1954).

214 MENON, R.G., Autogenous Healing of Concrete - Indian Concrete Journal Vol 33 (5), 161-162 and 178 (Bombay, May 1959).

215 SERAFIN, J.L. and GUERREIRO, M., Autogenous and Hygrometric Expansion of Mass Concrete - J. American Conc. Inst. Vol 66 (9), 716-719 (Detroit, Sept. 1969).

216 MONISMITH, C.L., The Function of Asphalt Layers in Pavements with Regard to Performance - PD 41 (1967).

217 MINISTRY OF TRANSPORT, The Resistance to Deformation of Dense Tar Macadam and Bitumen Macadam Base Courses - R.R.L. LN163 (August 1962).

218 HARLAND, D.G., A Radio-active Method of Measuring Variations in the Density of Concrete Cores, Cubes and Beams - Mag. Conc. Res. Vol 18 (55), 95-101 (Slough, June 1966).

219 DIENES, G.J. and KLEMM, H.F., Theory and Application of the Parallel Plate Viscometer - J. App. Phy. Vol 17 (6), 458-471. (London, 1946).

220 NADAI, A., Theory of Flow and Fracture of Solids - Vol 1, 2nd Ed., McGraw-Hill Book Co. (New York, 1950).

221 * PRYCE-JONES, J., J. Oil and Colloidal Chem. Assoc. Vol 19 P.295 (1938).

222 * GREEN and WELTMANN, Ind. Eng. Chem. Vol 18 (67), (1946) (Quoted from McKennell, R., Measurement and Control of Viscosity and related flow properties in Instrument Manual 1960 Section XI).

223 * GREEN - , Industrial Rheology and Rheological Structures - Chapman and Hall (London, 1949).

224 * DAHLGREN -, Transactions Chalmers Univ. Tech. Gothenburg No. 159, Vol 1 (1959).

225 GOODEVE and WHITFIELD, Transactions Faraday Soc. Vol 34, P.511 (1938).

226 BUECHE, F., Tensile Strength of Plastics above the Glass Transition - J. App. Phy. Vol 26 (9), 1133-1140 (New York, Sept. 1955).

227 ELVERY, R.H., A Direct Tensile Test for Concrete under Long and Short Term Loading - Mag. Conc. Res. Vol 20 (63), 111-116 (Slough, June 1968).

228 * TAYLOR, G.I., Proc. Royal Soc. A145 P.362 (London, 1934).

229 PEUTZ, M.G.F., JONES, A. and van KEMPEN, H.P.M., Layered Systems under normal surface loads - Computer Programme BISTRO - KONINKLIJKE/SHELL-LABORATORIUM. (May 1968).

230 SEED, H.B., CHAN, C.K. and LEE, C.E., Resilience Characteristics of Subgrade Soils and their Relation to Fatigue Failures in Asphalt Pavements - Proc. Int. Conf. on Struct. Design of Asphalt Pavements, 611-636 (Univ. of Mich., August 1962).

231 HEUKELOM, W. and KLOMP, A.J.G., Dynamic Testing as a Means of Controlling Pavements During and After Construction - Proc. Int. Conf. on Struct. Design of Asphalt Pavements, 667-679 (Univ. of Mich., August 1962).

232 * HEUKELOM, W. and FOSTER, C.R., Proc. Am. Soc. Civil Eng. Vol 86, 1-28 (1960).

233 DORMON, G.M., The Extension to Practice of a Fundamental Procedure for the Design of Flexible Pavements - Int. Conf. on the Struct. Design of Asphalt Pavements, 785-801 (Univ. of Mich., August 1962).

234 PAGAN, C.A., Rheological Properties of Bituminous Concrete - High. Res. Record No. 67. High. Res. Bed. (Washington, 1965).

235 MONISMITH, C.L., KASIANCHUK, D.A. and EPPS, J.A., Asphalt Mixture Behaviour in Repeated Flexure: A Study of an In-Service Pavement Near Morrow Bay, California - Report No. TE67 - 4 to Mats. and Res. Dept., Div. of High. State of California - Dept. of Civ. Eng., Univ. of California (Dec. 1967).

236 SIMMONS, J.C., Poisson's Ratio of Concrete: A Comparison of Dynamic and Site Measurements - Mag. Conc. Res. Vol 7 (2), 61-67 (Slough, July 1955).

237 ZUBE, E. and CECHETINI, J., Expansion and Contraction of asphalt concrete mixes - High. Res. Record No. 104, 141-163 (Washington, Jan. 1965).

238 RIGDEN, P.J. and LEE, A.R., The Brittle Fracture of Tars and Bitumens - J. App. Chem. Vol 3 (2), 62-70 (London, Feb. 1953).

239 TROUTON, F.T., On the viscosity of pitch-like substances - Proc. Phy. Soc. Vol 19, p.47 (1905).

240 TROUTON, F.T., On the coefficient of viscous traction - Proc. Royal Soc. A77, p.326 (1906).

PLATES

Plate	
1	Compaction moulds and base plates.
2	Modified automatic Proctor compactor.
3	Extruder.
4	Hydraulic jacks.
5	Specimen end caps.
6	End cap fixing jig.
7	Bituminous specimen mounted for testing.
8	Dry lean concrete specimen mounted for testing.
9	Steel dumbell mounted in testing machine.
10	Modified control console for Instron testing machine.
11	Mechanical unit of frequency modulator.
12	Frequency modulator.
13	General view of testing equipment.
14	Parallel plate viscometer.
15	Loading frame for low viscosity viscometer tests.
16	Loading frame for high viscosity viscometer tests.
17	Modified shear vane apparatus for coaxial cylinder viscometer tests.
18	Graded aggregates used in specimen preparation.
19	Sawn sample of dense bitumen macadam.
20	Sawn sample of hot rolled asphalt.
21	Sawn sample of dry lean concrete.
22	Fractured sample of dense bitumen macadam.

Plate 1 - Compaction Moulds and Base Plates.

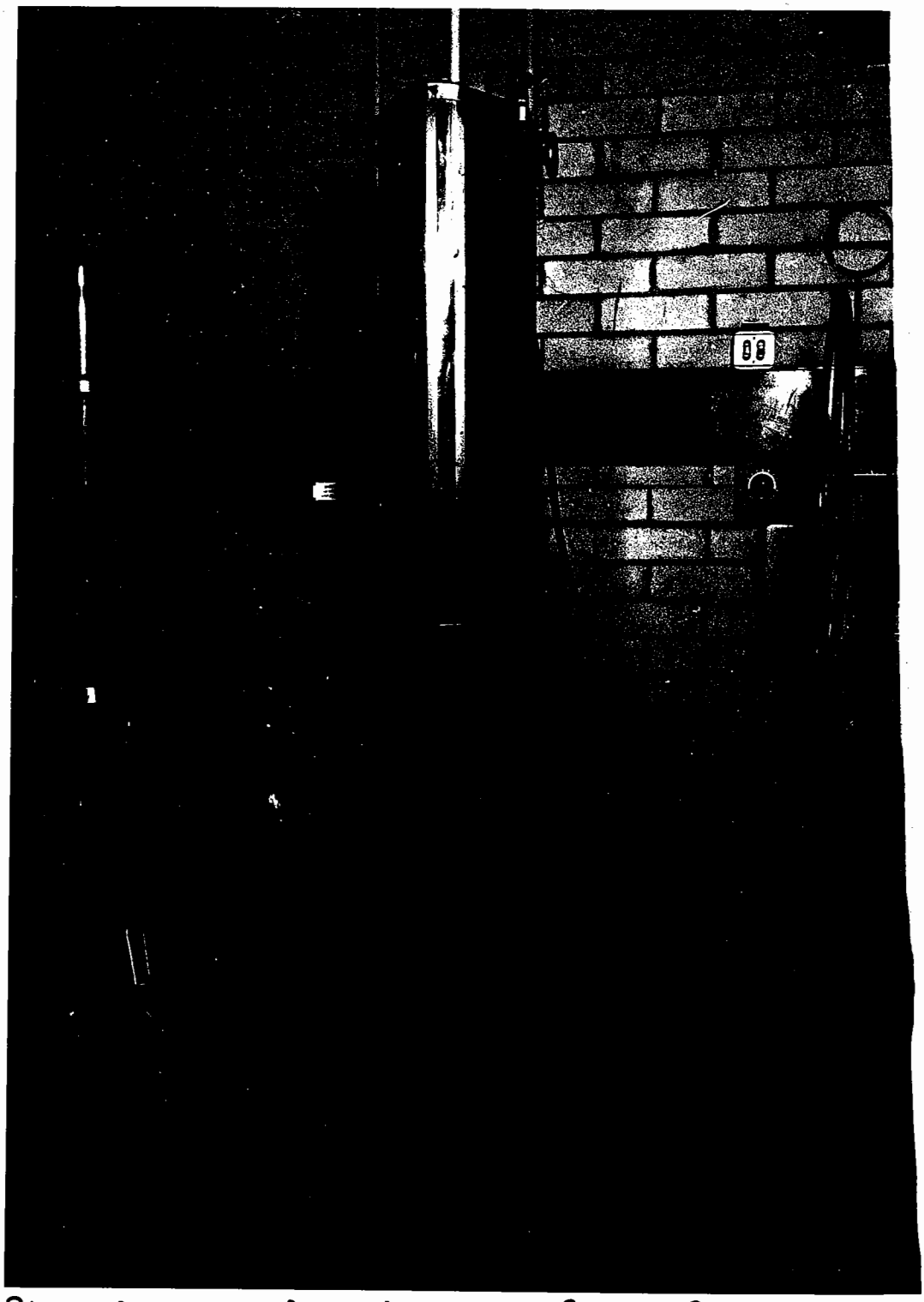

Plate 2 - Modified Automatic Proctor Compactor

Plate 2

Plate 3 - Extruder
Make ?

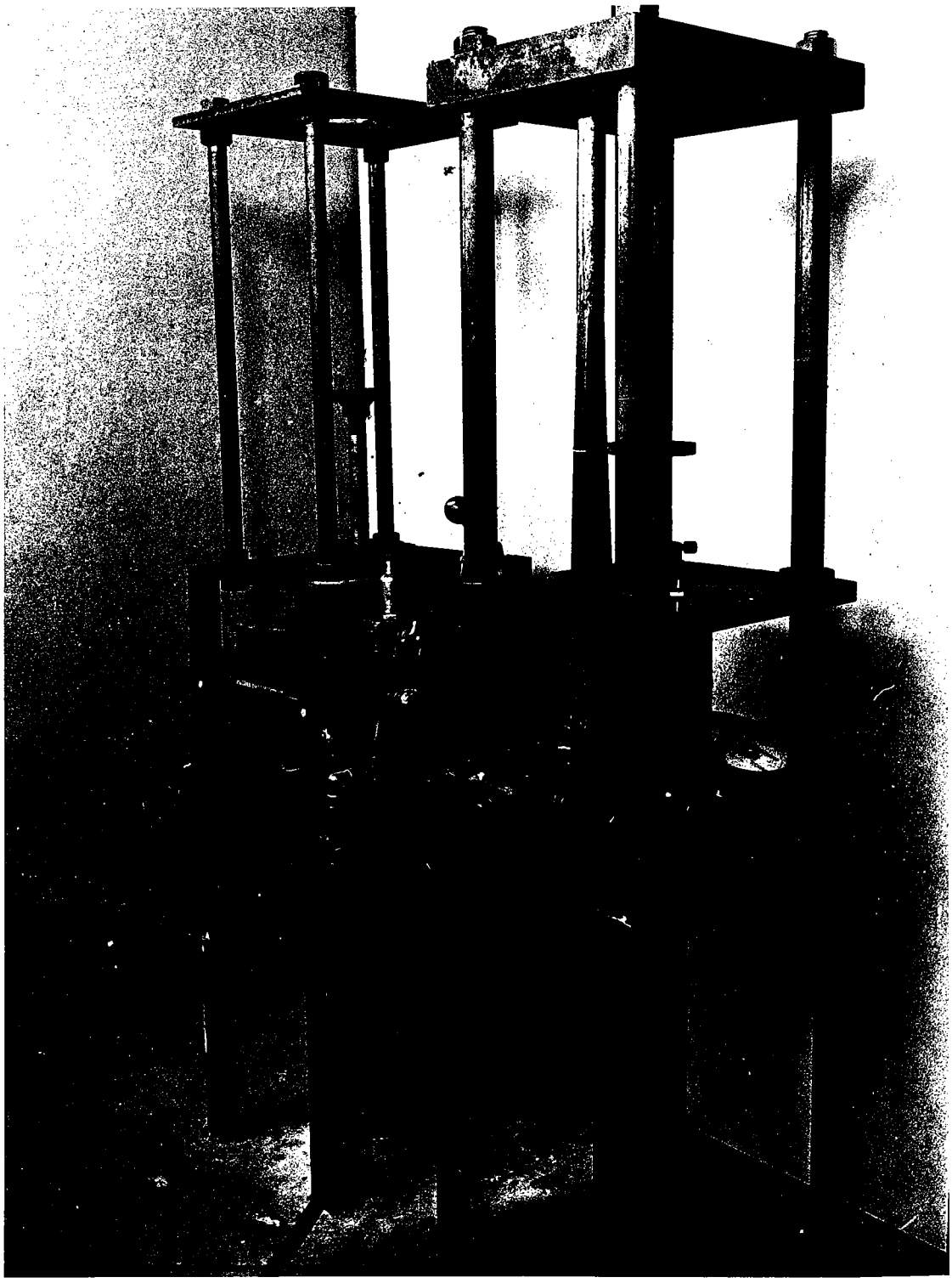

Plate 4 - Hydraulic Jacks

Plate 4

Plate 5 - Specimen End Caps

Plate 5

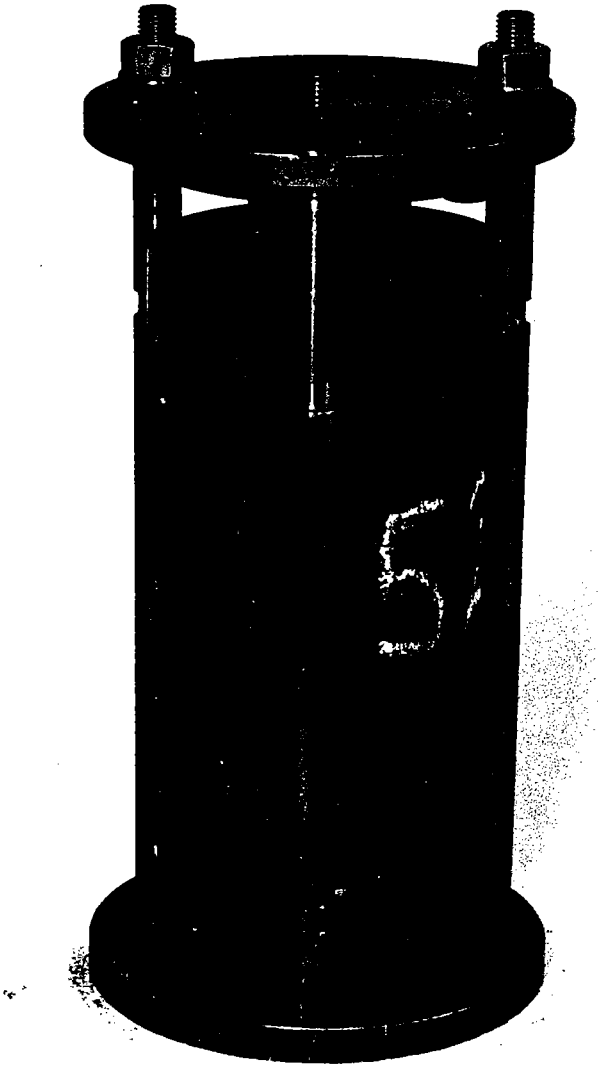

Plate 6- End Cap Fixing Jig

Plate 6

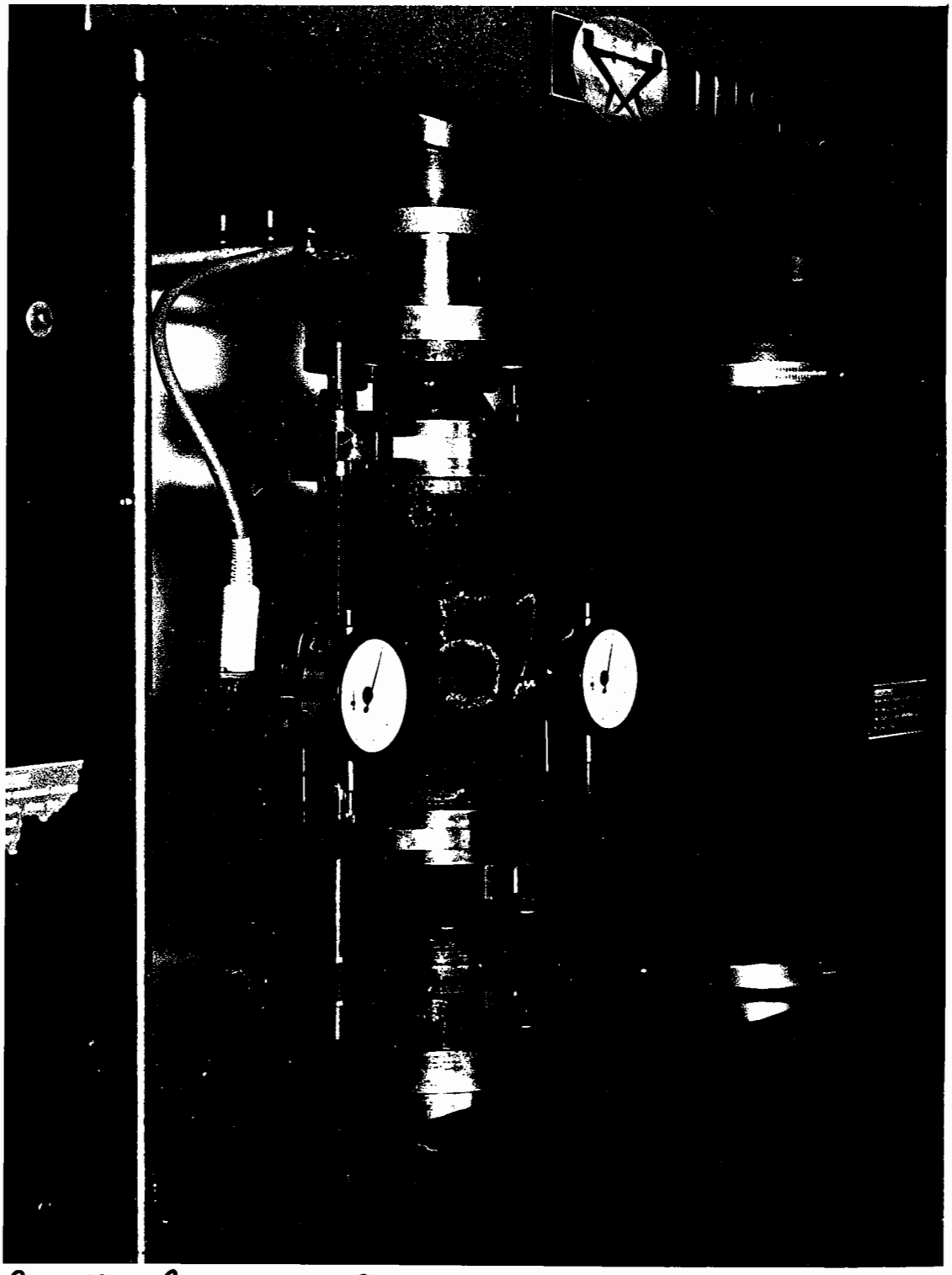

Plate 7 - Bituminous Specimen Mounted for Testing

Plate 7

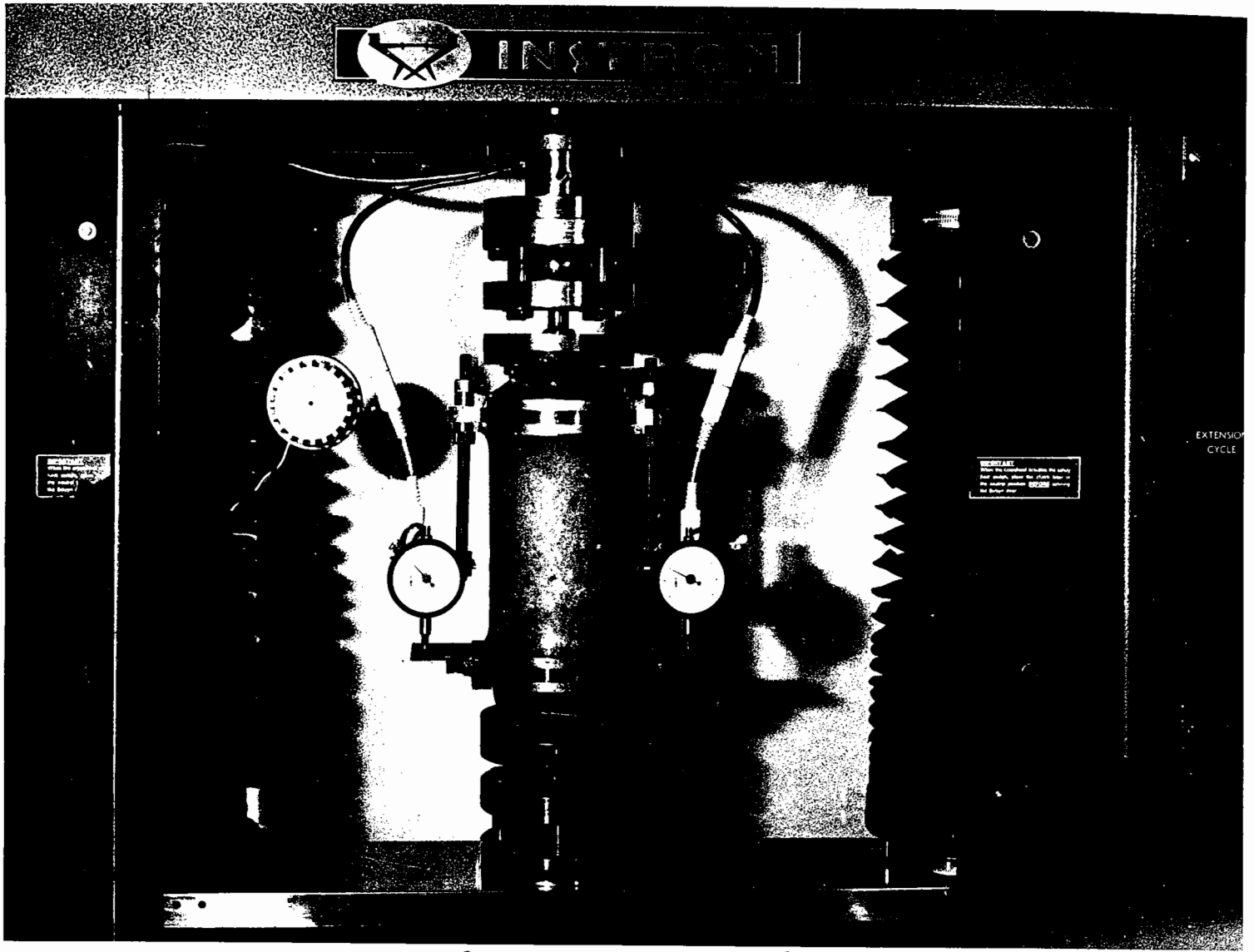

Plate 8 - Dry Lean Concrete Specimen Mounted for Testing.

Plate 8

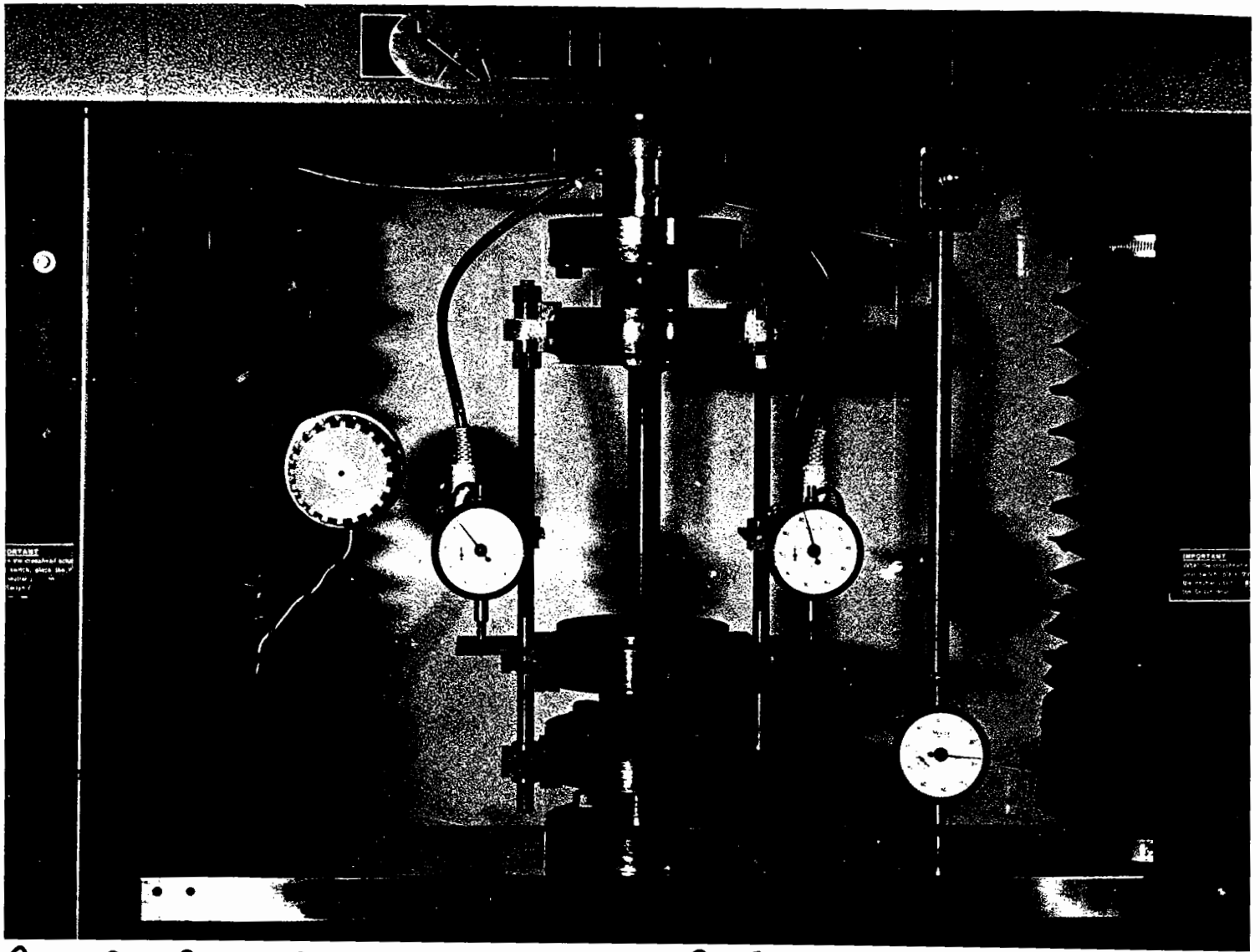

Plate 9 - Steel Dumbell Mounted in Testing Machine
Plate 9

Plate 10 · Modified Control Console for Instron Testing Machine.

Plate 10

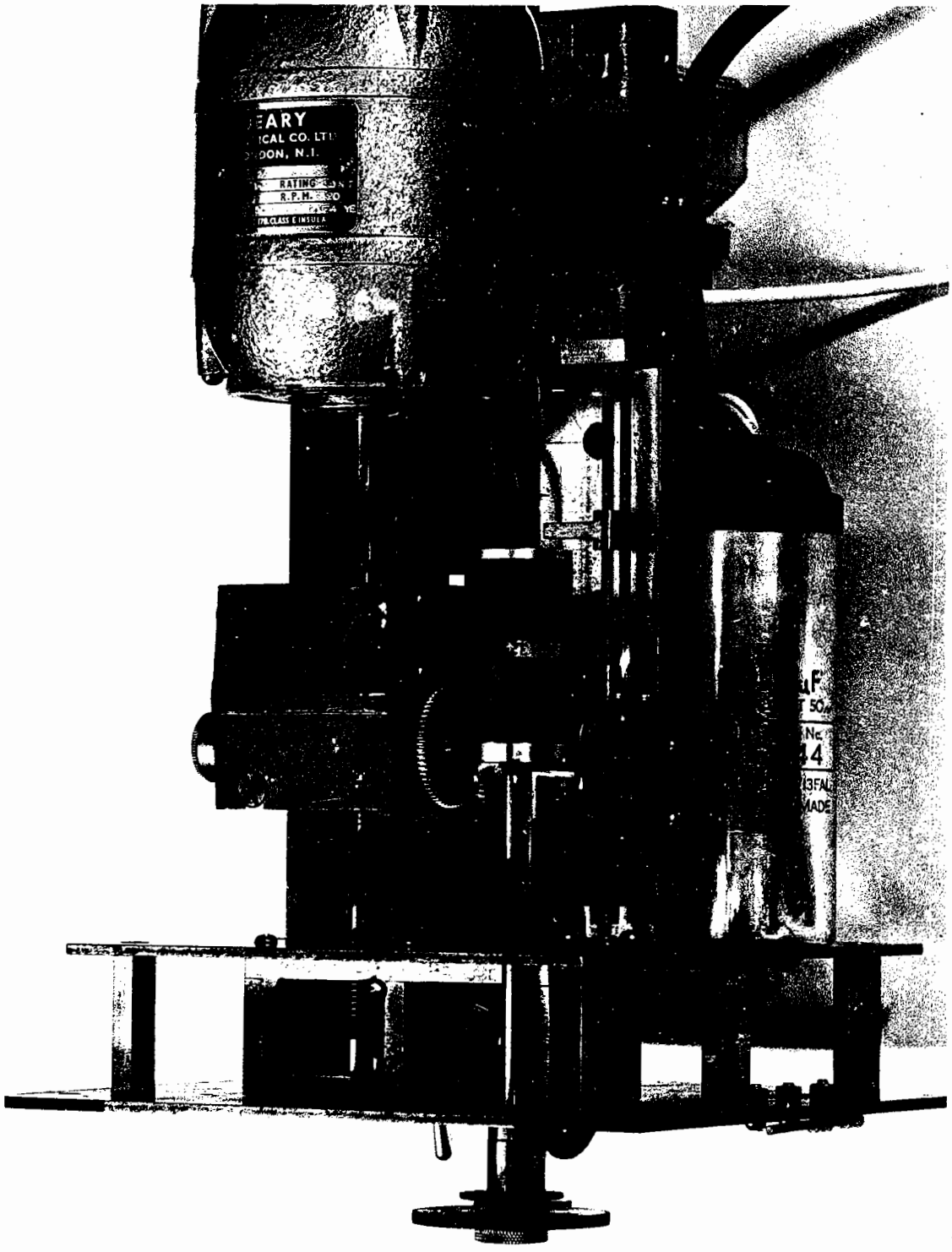

Plate 11 - Mechanical Unit of Frequency Modulator

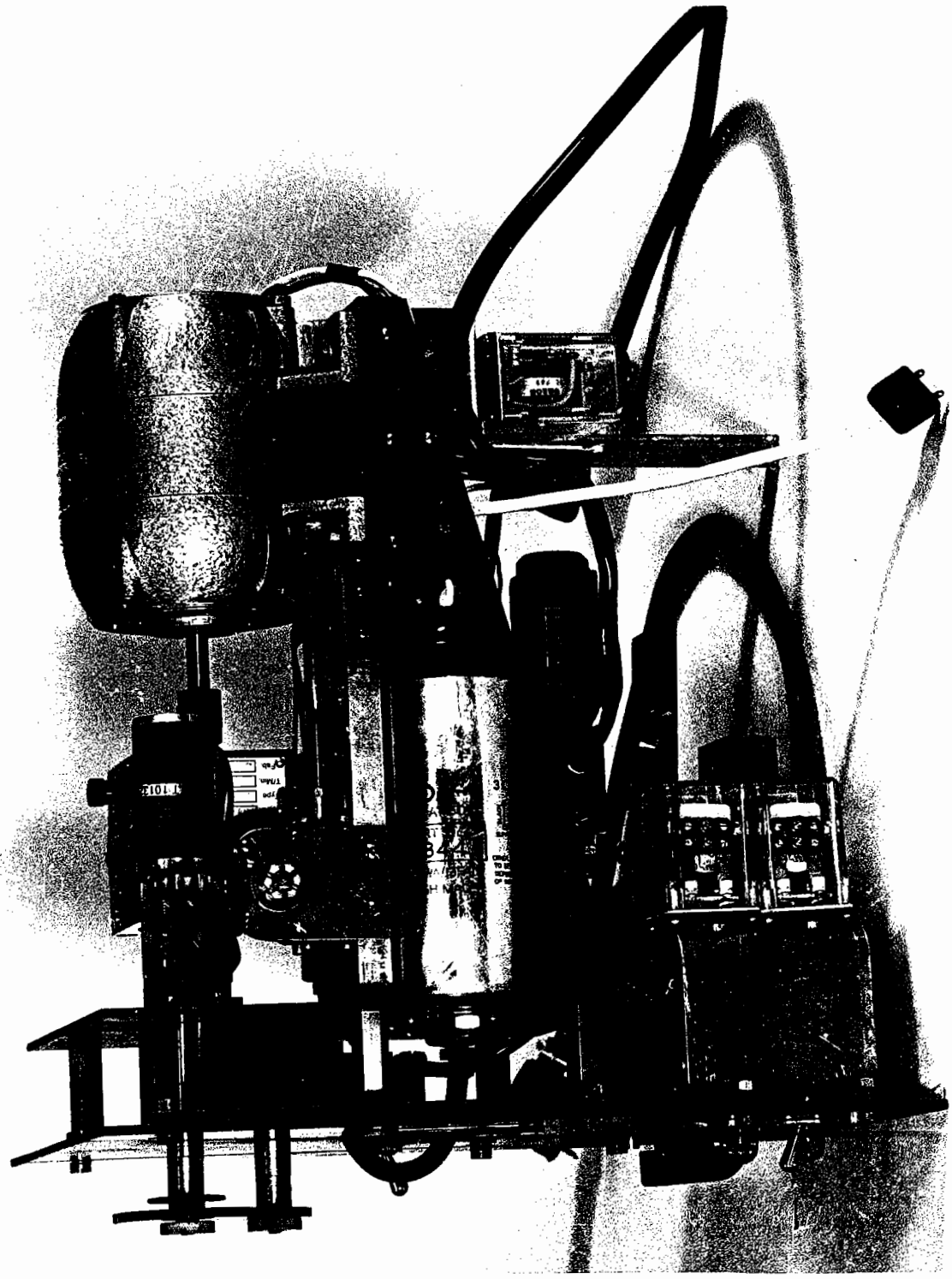

Plate 12 – Frequency Modulator

Plate 13 General View of Testing Equipment

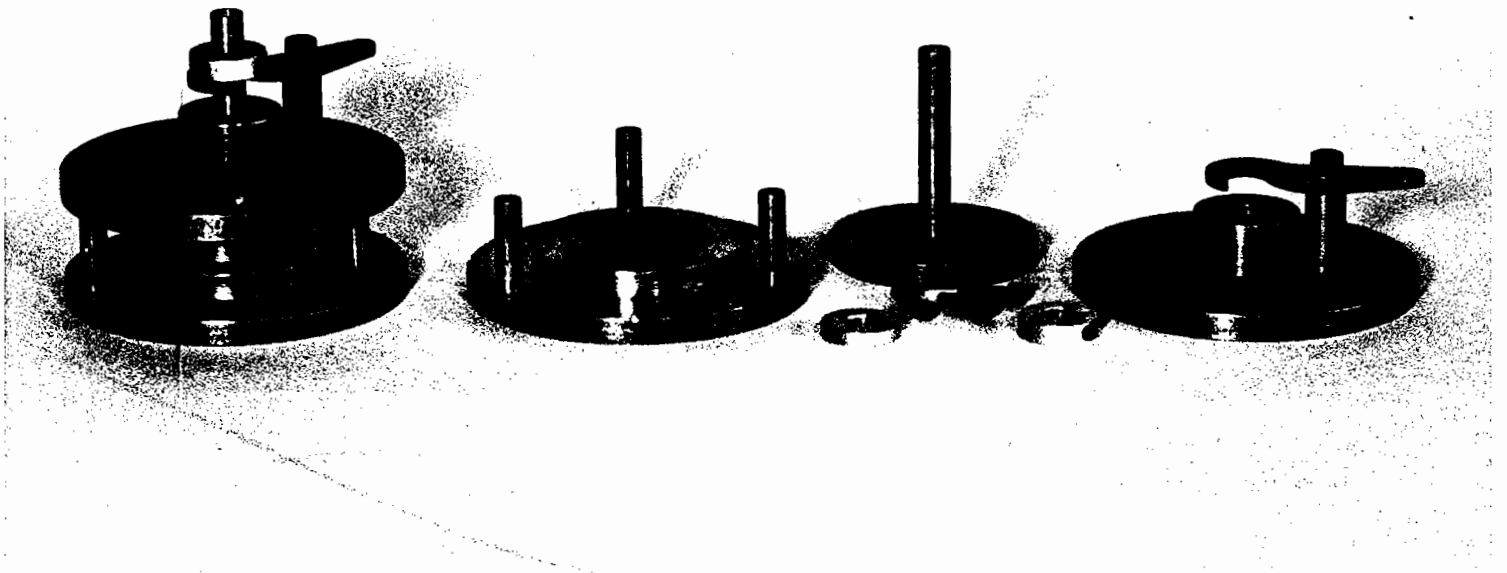

Plate 14 - Parallel Plate Viscometers

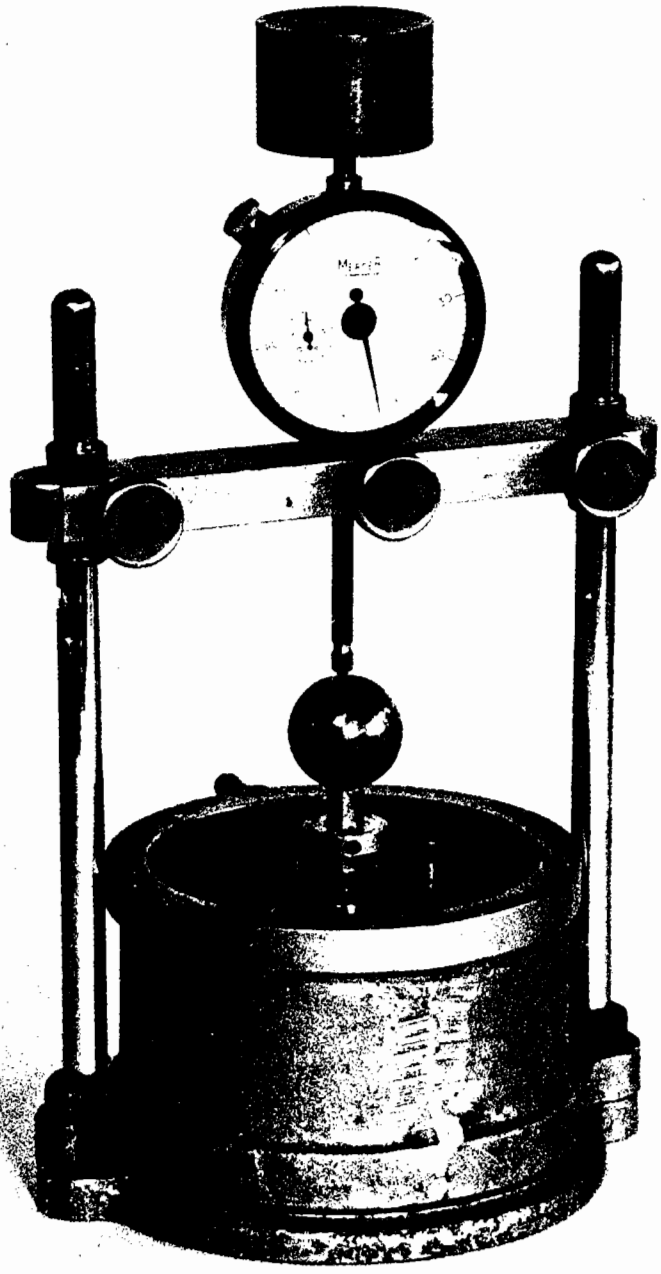

Plate 15 - Loading Frame for low Viscosity Viscometer Tests.

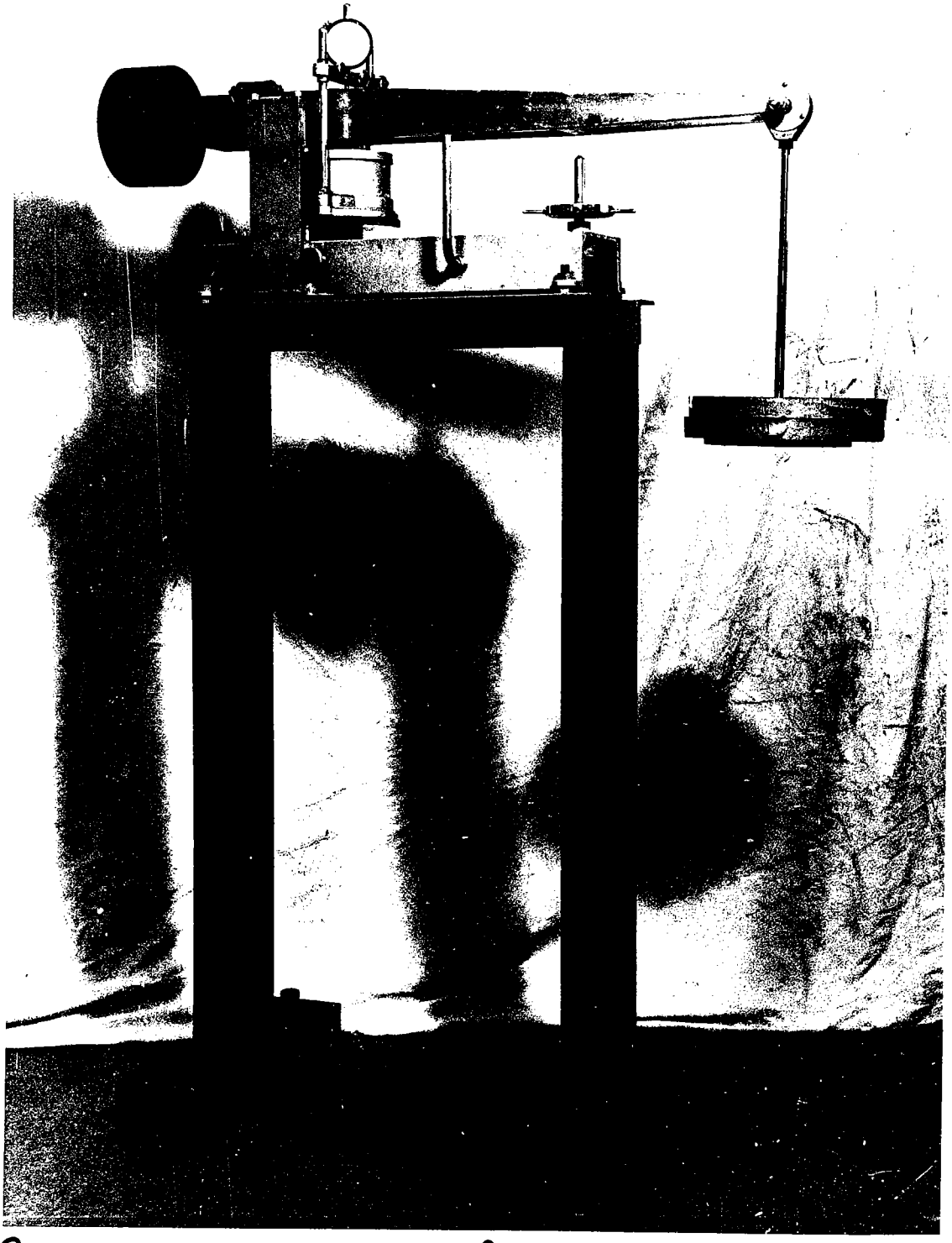

Plate 16 - Loading Frame for High Viscosity Viscometer Tests.

Plate 16

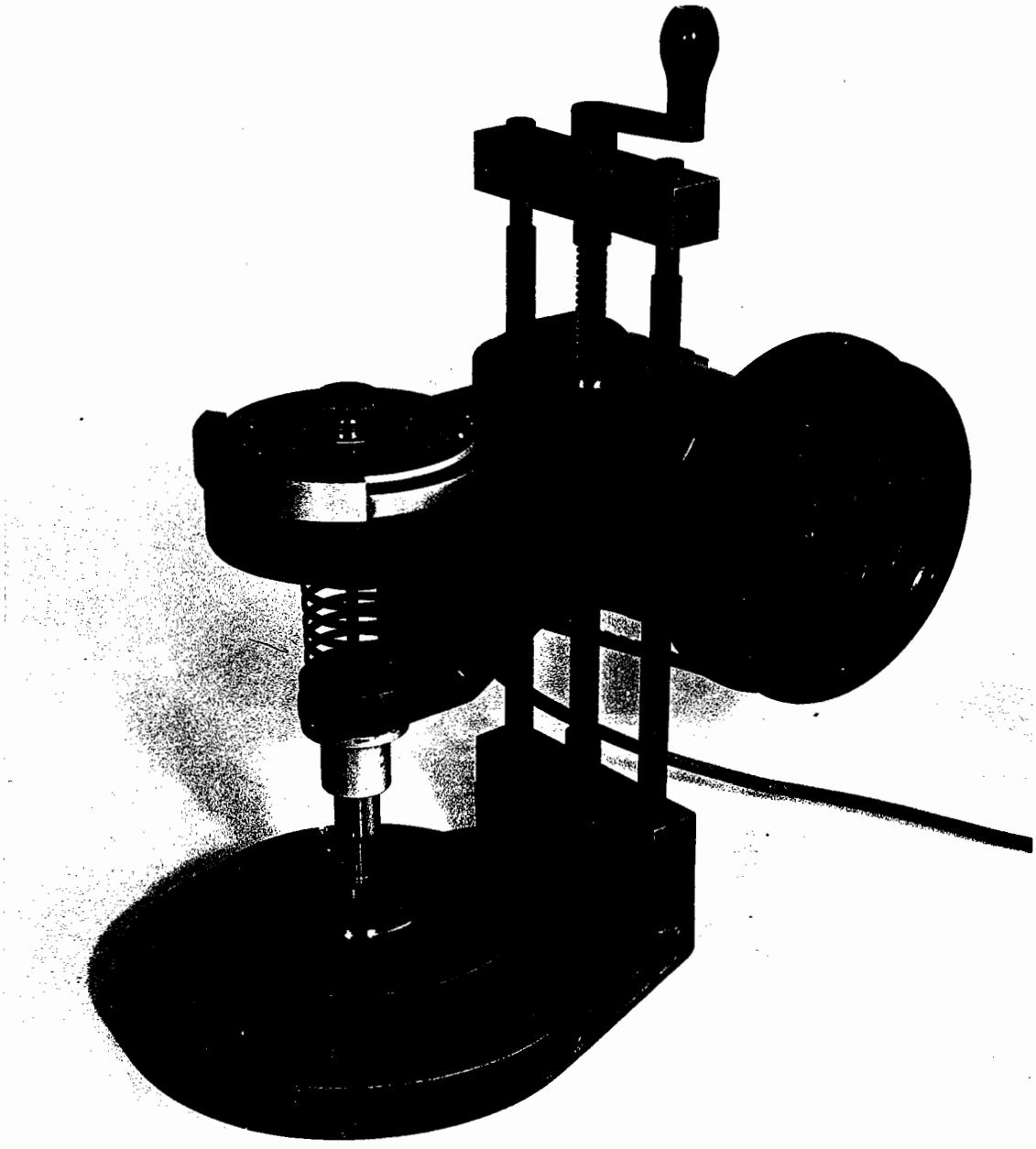

Plate 17 - Modified Shear Vane Apparatus for Coaxial Cylinder Viscometer Tests.

Plate 18 - Graded Aggregates Used In Specimen Preparation

Plate 18

Above - Dense Macadams.
Centre - Hot Rolled Asphalt.
Below - Dry Lean Concrete.

Plate 19 - Sawn Specimen of Dense Bitumen Macadam

Plate 19

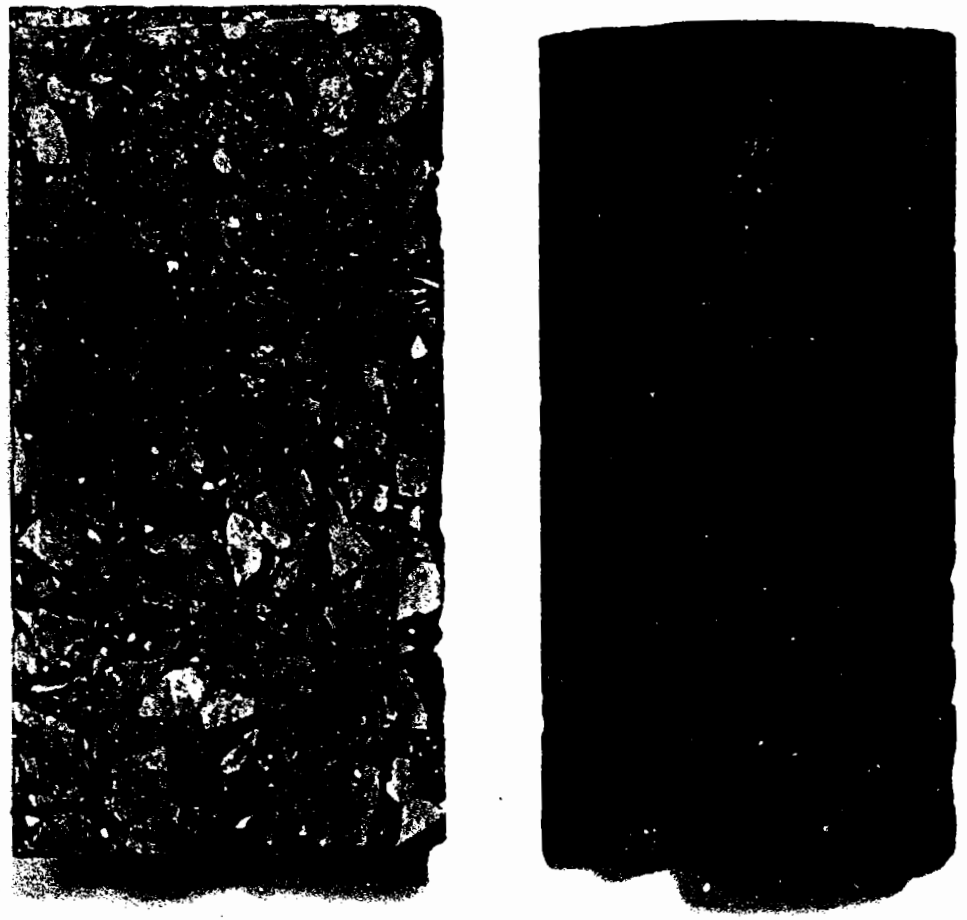

Plate 20 - Sawn Specimen of Hot Rolled Asphalt

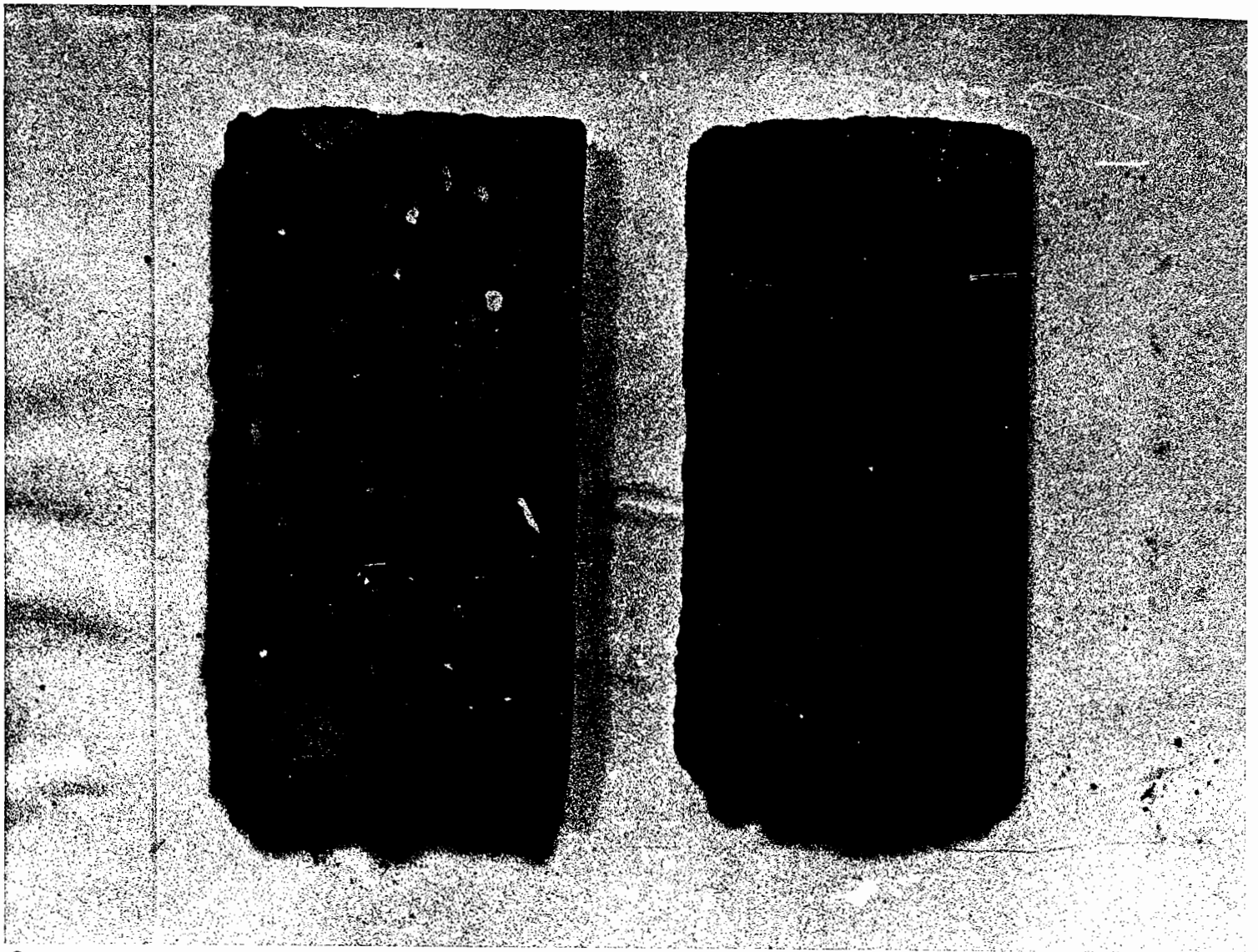

Plate 21 - Sawn Specimen of Dry Lean Concrete

Plate 21

Plate 22 - Fractured Specimen of Dense Bitumen Macadam

FIGURES

Figure

1 Structural details of flexible road pavement for heavily trafficked roads.

2 Basic rheological elements and models.

3 Rheological behaviour of bituminous binders.

4 Rheological behaviour of pitch-,sol-and gel-type bitumens.

5 Plastic flow indices of different types of bitumens.

6 Characteristics of non-linear elastic and viscous components of visco-elastic fluids.

7 Nomograph for determining the penetration index of bitumen.

8 Nomograph for determining the stiffness of bitumen (Van der Poel).

9 Nomograph for determining the stiffness of bitumen (Heukelom and Klomp).

10 Nomograph for determining the stiffness of bituminous mixtures (Van der Poel).

11 Nomograph for determining the stiffness of bituminous mixtures (Heukelom and Klomp).

12 Nomograph for determining the fracture strain of bitumen.

13 Modified Goodman diagram.

14 Variation of stress and strain on underside of asphalt for varying asphalt stiffness and depth.

15 Aggregate grading curves of materials tested.

16 Gamma-ray traces of single and three-layer compacted bituminous specimens.

17 Voids in bituminous roadbase specimen.

18 Specimen relative to crossheads and load cell.

19 Details of extrusion collar, compaction mould and baseplate.

20 Details of end caps and adaptors.

21 Details of end cap adaptors for use when testing concrete specimens.

22 Details of steel dumbell and dummy specimen.

23 Circuit diagram of $\overline{\Pi}$-type impedence and attenuation pad.

24 Circuit diagram of operational amplifier buffer/attenuator.

25 Circuit diagram from extensometer terminal strip.

26 Circuit diagram from bench terminal strip.

27 Diagrammatic layout of Instron crosshead control system.

28 Effect of dependent variables on change in stiffness of specimen under stress- and strain-controlled testing.

29 Block diagram of frequency modulator servo loop.

Figure

30 Block diagram of frequency modulator and cycle counting electronic components.

31 Cone drive layouts of original frequency modulator.

32 Epicyclic gearbox of modified frequency modulator.

33 Schematic layout of mechanical control of frequency modulator servo system.

34 Details of parallel plate viscometer.

35a Deformation of load cell and fittings over $\pm$ 4000 lb.

35b Deformation of load cell and fittings over $\pm$ 1000 lb.

36 Record of load cell calibration by dead weights.

37 Record of load waveform of steel dummy specimen in load cycling.

38 Record of load reversal of steel dummy specimen in load cycling.

39 Calibration of crosshead speeds with frequency modulator.

40 Record of load and deformation when load cycling steel dummy specimen with no baffles around specimen.

41 Record of load and deformation when load cycling steel dummy specimen with baffles around specimen.

42 Record of hysteresis loops of steel dumbell.

43 Hysteresis loops of steel dumbell in concrete testing fittings.

44 Effect of strain level and strain rate on stiffness of steel dumbell.

45 Change in stiffness of steel dumbell in stress-controlled repeated loading.

46 Climatization of sand asphalt specimen.

47 Frequency correction on bituminous specimen in strain-controlled repeated loading by means of cone frequency modulator.

48 Frequency correction on bituminous specimen in strain-controlled repeated loading by means of "variator" frequency modulator.

49 Records of last complete cycles of hot rolled asphalt in stress-controlled repeated loading.

50 Deformation curves of hot rolled asphalt in stress-controlled repeated loading.

51 Deformation curves of hot rolled asphalt in stress-controlled repeated loading.

52 Deformation curves of hot rolled asphalt in stress-controlled repeated loading with rest periods before and after fracture.

53 Deformation curves of dense bitumen macadam in various levels of stress-controlled repeated loading.

54 Effect of strain level and strain mode on stiffness of dense bitumen macadam.

55 Change in stiffness of dense bitumen macadam in strain-controlled repeated loading at $+10^{\circ}C$.

Figure

56 Effect of rest periods on change in stiffness of sand asphalt in strain-controlled repeated loading at +10°C.

57 Change in stiffness and hysteresis loop areas of dense bitumen macadam in strain-controlled repeated loading at +10°C.

58 Internal temperature changes of sand asphalts in strain-controlled repeated loading.

59 Effect of strain level and strain rate on stiffness of trial specimen of dry lean concrete with unmodified mountings at +10°C.

60 Change in stiffness of trial specimen of dry lean concrete in strain-controlled repeated loading at +10°C.

61 Standard deviation of voids in all specimens produced.

62 Effect of strain level and strain rate on specimen of 90/110 dense bitumen macadam at +10°C.

63 Effect of strain level and strain rate on specimen of hot rolled asphalt at +30°C.

64 Effect of strain level and strain rate on specimen of dry lean concrete at +20°C.

65 Maximum stiffness of 90/110 dense bitumen macadam at +10°C.

66 Mixture conversion factors of bitumen-bound materials studied.

67 Nomograph stiffnesses of 90/110 pen. bitumen and 90/110 dense bitumen macadam at +10°C.

68 Theoretical dependence of rate effect of 90/110 pen. bitumen and 90/110 dense bitumen macadam on frequency rage at +10°C.

69 Nomograph stiffness of 90/110 pen. bitumen at 0°C.

70 Nomograph stiffness of 90/110 dense bitumen macadam for internal voids only.

71 Nomograph stiffness of 90/110 dense bitumen macadam for total voids.

72 Nomograph stiffness of 190/210 dense bitumen macadam for internal voids only.

73 Nomograph stiffness of hot rolled asphalt for internal voids only.

74 Adjusted stiffnesses of 90/110 dense bitumen macadam at 0°C.

75 Adjusted stiffnesses of 90/110 dense bitumen macadam at +10°C.

76 Adjusted stiffnesses of 90/110 dense bitumen macadam at +30°C.

77 Adjusted stiffnesses of 90/110 dense bitumen macadam at +40°C.

78 Adjusted stiffnesses of 190/210 dense bitumen macadam at 0°C.

79 Adjusted stiffnesses of 190/210 dense bitumen macadam at +10°C.

80 Adjusted stiffnesses of 190/210 dense bitumen macadam at +40°C.

81 Adjusted stiffnesses of dense tar macadam at 0°C.

82 Adjusted stiffnesses of dense tar macadam at +10°C.

83 Adjusted stiffnesses of dense tar macadam at +30°C.

84 Adjusted stiffnesses of dense tar macadam at +40°C.

85 Adjusted stiffnesses of hot rolled asphalt at +10°C.

Figure

86 Adjusted stiffnesses of hot rolled asphalt at +30°C.

87 Stiffnesses of dry lean concrete at +20°C.

88 Summary of stiffnesses of 90/110 dense bitumen macadam.

89 Summary of stiffnesses of 190/210 dense bitumen macadam.

90 Summary of stiffnesses of dense tar macadam.

91 Summary of stiffnesses of hot rolled asphalt.

92 Stiffness of 90/110 pen. bitumen at 0°C.

93 Stiffness curves of batch of specimens of 90/110 dense bitumen macadam at medium strain level at +10°C.

94 Stiffness curves of 90/110 dense bitumen macadam at high and low strain levels at +10°C.

95 Stiffness curves of batch of specimens of dense tar macadam at medium strain level at +10°C.

96 Stiffness curves of dense tar macadam at low strain level at +10°C.

97 Stiffness curves of hot rolled asphalt at medium strain level at +10°C.

98 Stiffness curves of hot rolled asphalt at high and low strain levels at +30°C.

99 Cycles to 60% of initial stiffness of 90/110 dense bitumen macadam at +10°C.

100 Cycles to 60% of initial stiffness of dense tar macadam at +10°C.

101 Cycles to 90% of initial stiffness of 90/110 dense bitumen macadam at 0°C to +40°C.

102 Cycles to 75% of initial stiffness of 90/110 dense bitumen macadam at 0°C to +40°C.

103 Cycles to 60% of initial stiffness of 90/110 dense bitumen macadam at 0°C to +40°C.

104 Cycles to 90% of initial stiffness of 90/110 and 190/210 dense bitumen macadam at 0°C to +40°C.

105 Cycles to 75% of initial stiffness of 90/110 and 190/210 dense bitumen macadam at 0°C to +40°C.

106 Cycles to 60% of initial stiffness of 90/110 and 190/210 dense bitumen macadam at 0°C to +40°C.

107 Cycles to 90% of initial stiffness of dense tar macadam at 0°C to +40°C.

108 Cycles to 75% of initial stiffness of dense tar macadam at 0°C to +40°C.

109 Cycles to 60% of initial stiffness of dense tar macadam at 0°C to +40°C.

110 Cycles to 90% of initial stiffness of hot rolled asphalt at +10°C to +40°C.

111 Cycles to 75% of initial stiffness of hot rolled asphalt at +10°C to +40°C.

Figure

112 Cycles to 60% of initial stiffness of hot rolled asphalt at +10°C to +40°C.

113 Change in stiffness curves of 90/110 dense bitumen macadam at medium strain level at +10°C.

114 Change in stiffness curves of 90/110 dense bitumen macadam at high strain level at +10°C.

115 Change in stiffness curves of dense tar macadam at low strain level at +10°C.

116 Change in stiffness curves of dense tar macadam at medium strain level at +10°C.

117 Change in stiffness curves of dense tar macadam at low strain level at +30°C.

118 Change in stiffness curves of dense tar macadam at medium strain level at +30°C.

119 Change in stiffness curves of hot rolled asphalt at high strain level at +30°C.

120 Calculated cycles to 90% of initial stiffness of 90/110 and 190/210 dense bitumen macadam at 0°C to +40°C.

121 Calculated cycles to 75% of initial stiffness of 90/110 and 190/210 dense bitumen macadam at 0°C to +40°C.

122 Calculated cycles to 60% of initial stiffness of 90/110 and 190/210 dense bitumen macadam at 0°C to +40°C.

123 Calculated stiffness curves of all bituminous materials tested.

124 Shapes of load and deflection curves of bituminous materials during repeated loading tests.

125 Stiffness curves of dry lean concrete in strain-controlled repeated loading.

126 Hysteresis loop of specimen of dry lean concrete in first cycle of fluctuating strain-controlled repeated loading.

127 Stiffness curves of dry lean concrete in tensile strain-controlled repeated loading.

128 Hysteresis loops of specimen of dry lean concrete in tensile strain-controlled repeated loading.

129 Hysteresis loops of specimen of dry lean concrete in tensile strain-controlled repeated loading.

130 Hysteresis loop of specimen of dry lean concrete in first cycle of compressive strain-controlled repeated loading.

131 Deformation characteristics of typical specimens of dry lean concrete, with and without previous loading history, loaded to fracture.

132 Strain curves of specimen of dry lean concrete in tensile stress-controlled repeated loading.

133 Strain curves of specimen of dry lean concrete in low tensile stress-controlled repeated loading.

134 Strain curves of specimen of dry lean concrete in fluctuating and alternating stress-controlled repeated loading.

Figure

135 Strain curves of specimen of dry lean concrete in fluctuating stress-controlled repeated loading.

136 Fracture strain of dry lean concrete after all stress-controlled modes of repeated loading.

137 Fracture life of dry lean concrete after all stress-controlled modes of repeated loading.

138 Plate separations of parallel plate viscometer test on 90/110 pen. bitumen at +30°C.

139 Measured viscosities of unheated binders at 0°C to +40°C.

140 Torque curves of unheated bitumens in coaxial cylinder viscometer.

141 Illustration of thixotropy of fluid in steady shear.

142 Thixotropic recovery curves after equilibrium torque in steady shear.

143 Theoretical and practical rate effects for bituminous mixtures.

144 Effect of time of loading on stiffnesses of elastico-viscous fluids.

145 Effect of time of loading on stiffnesses of firmo-viscous fluids.

146 Effect of time of loading on stiffnesses of elastico-viscous fluids with various viscous components.

147 Nomograph and practical effect of time of loading on stiffness of 90/110 pen. bitumen at 0°C.

148 Theoretical horizontal strains in bituminous bound layers of flexible road pavement along path of travel.

149 Theoretical horizontal strains in bituminous bound layers of flexible road pavement perpendicular to path of travel.

150 Theoretical vertical and horizontal stresses in bituminous bound layers of flexible road pavement in vertical axis under load.

151 Theoretical vertical and horizontal strains in bituminous bound layers of flexible road pavement in vertical axis under load.

SURFACING	WEARING COURSE	1½" HRA
	BASE – COURSE	2½" of HRA or DBM or DTM
ROADBASE	7" HOT ROLLED ASPHALT or 8" DENSE BITUMEN MACADAM or 8" DENSE TAR MACADAM or 3" HRA or DBM or DTM on 7" DRY LEAN CONCRETE	
SUB-BASE	FOR THICKNESS SEE FIGURE BELOW 6" MINIMUM THICKNESS FOR FROST-SUSCEPTIBLE SUBGRADE MATERIAL	
SUBGRADE	REPLACE MATERIAL WITH C.B.R. VALUE < 2	

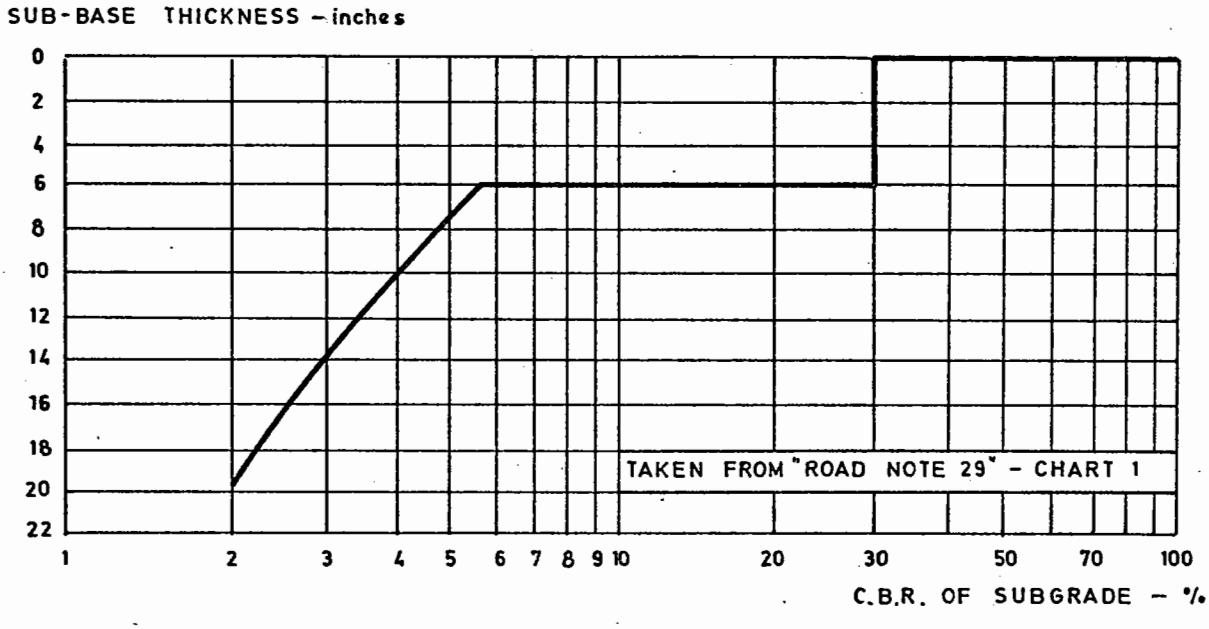

FIG. 1 STRUCTURAL DETAILS OF FLEXIBLE ROAD PAVEMENT FOR HEAVILY TRAFFICKED ROADS

a) ELEMENTS

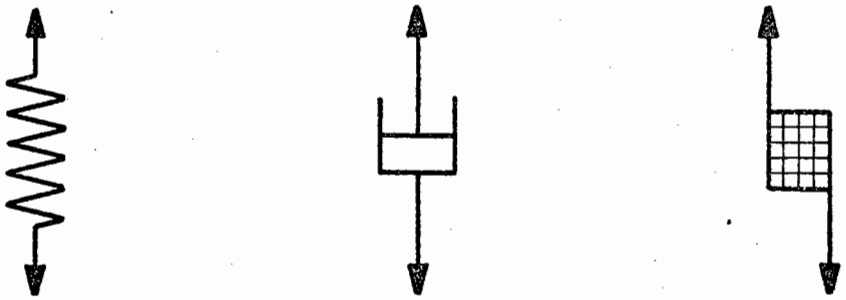

RHEOLOGICAL DIAGRAMS

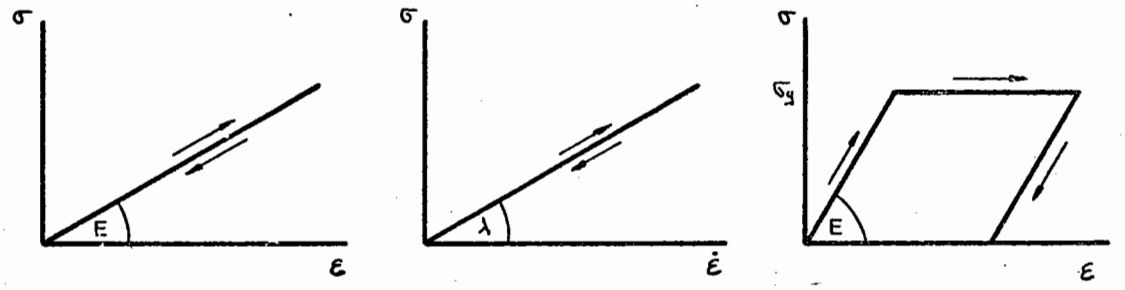

HOOKE – ELASTIC NEWTON – VISCOUS ST. VENANT – PLASTIC

---

b) MODELS

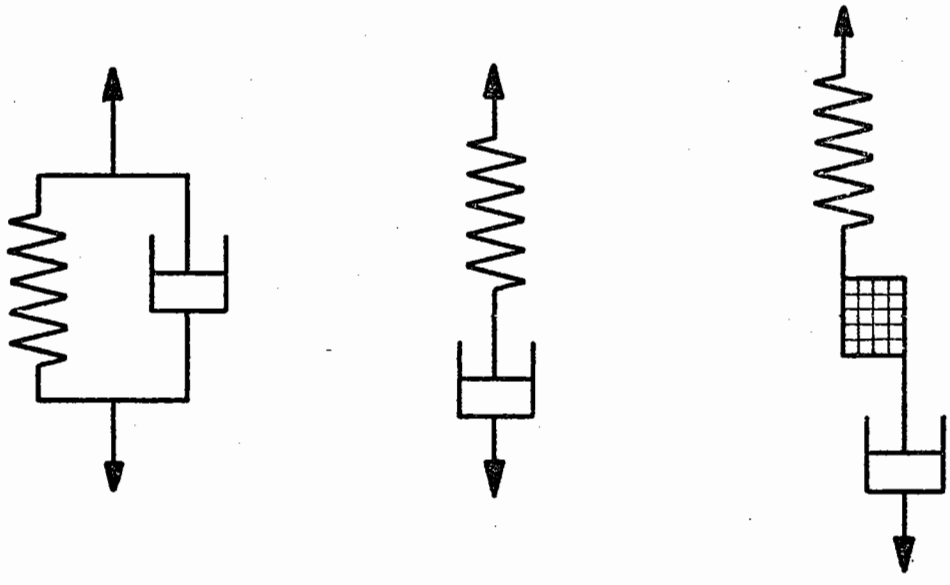

RHEOLOGICAL DIAGRAMS

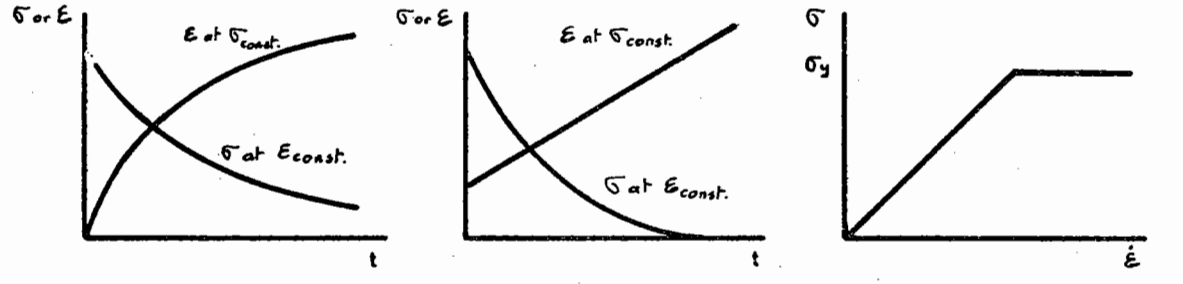

KELVIN (or VOIGT) – FIRMO-VISCOUS MAXWELL – ELASTICO-VISCOUS BINGHAM – PLASTICO-VISCOUS

FIG. 2 BASIC RHEOLOGICAL ELEMENTS AND MODELS

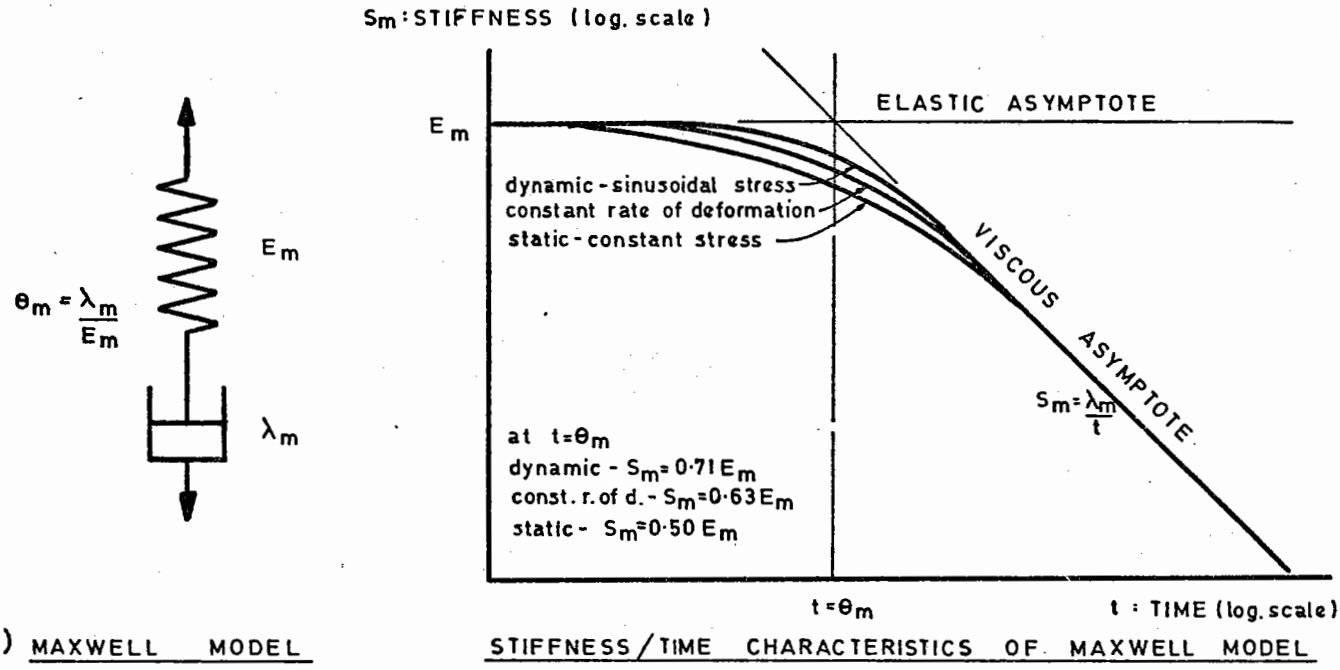

a) MAXWELL MODEL

STIFFNESS / TIME CHARACTERISTICS OF MAXWELL MODEL

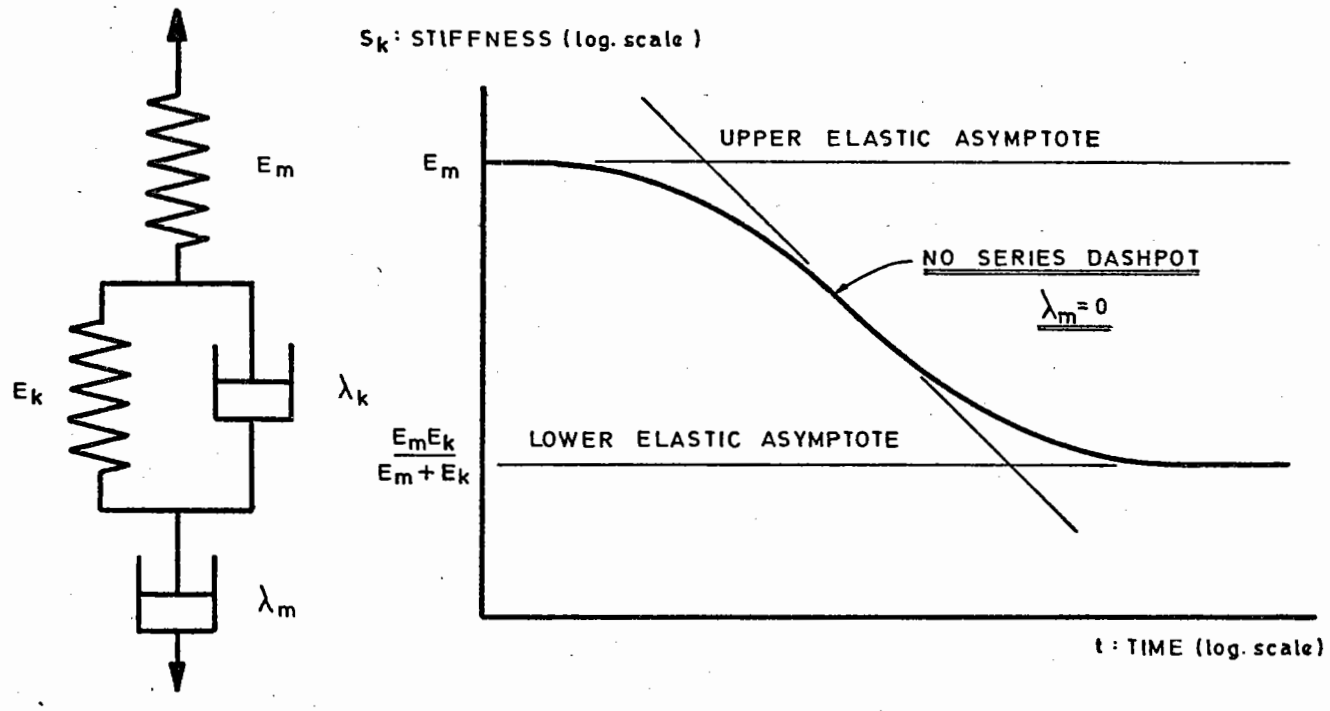

b) BURGER MODEL

STIFFNESS TIME CHARACTERISTICS OF BURGER MODEL WITH NO SERIES DASHPOT

FIG. 3 RHEOLOGICAL BEHAVIOUR OF BITUMINOUS BINDERS

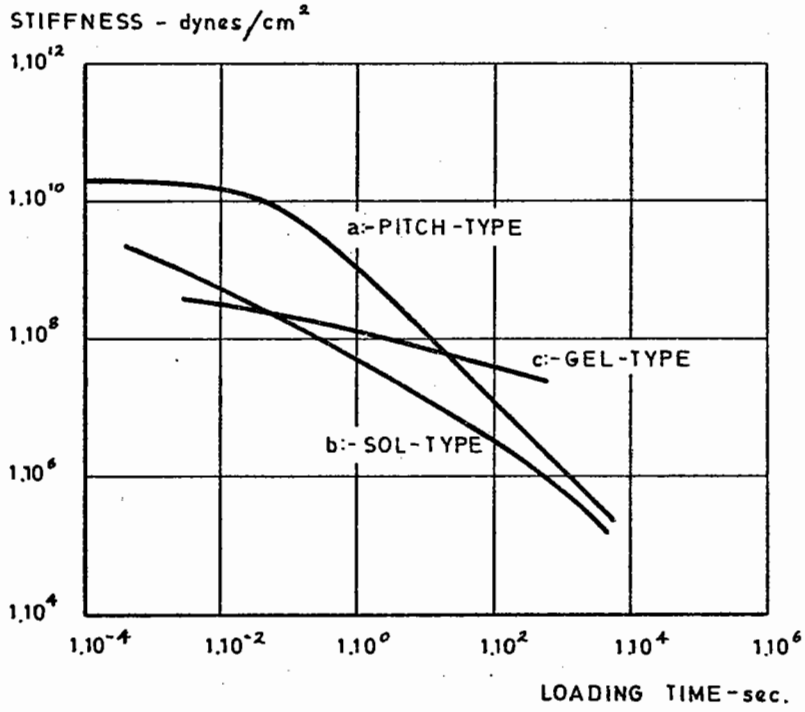

FIG. 4 RHEOLOGICAL BEHAVIOUR OF PITCH SOL- AND GEL-TYPE BITUMENS after Saal and Labout (61)

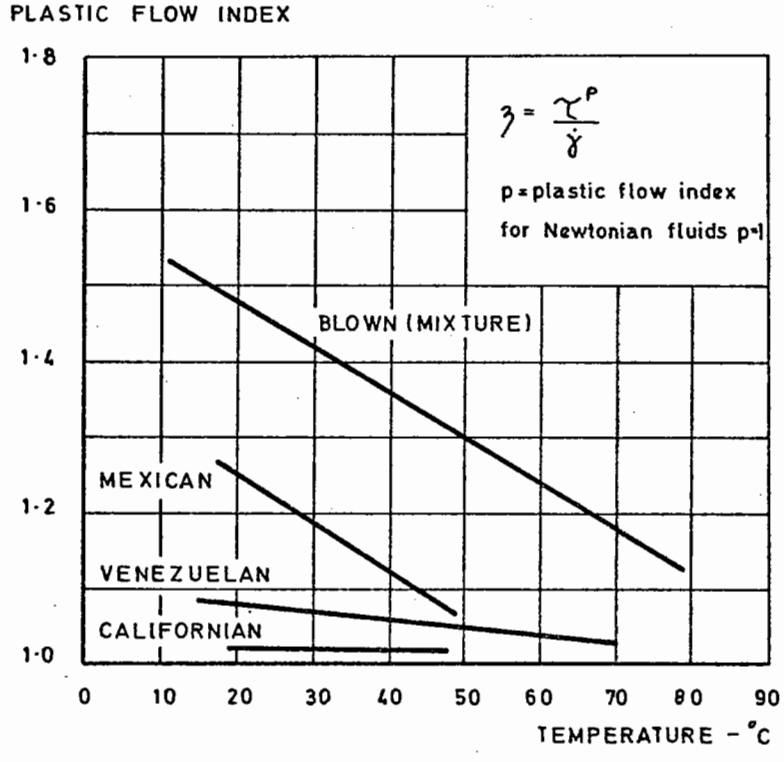

FIG. 5 PLASTIC FLOW INDICEES OF DIFFERENT TYPES OF BITUMENS after Lee (70)

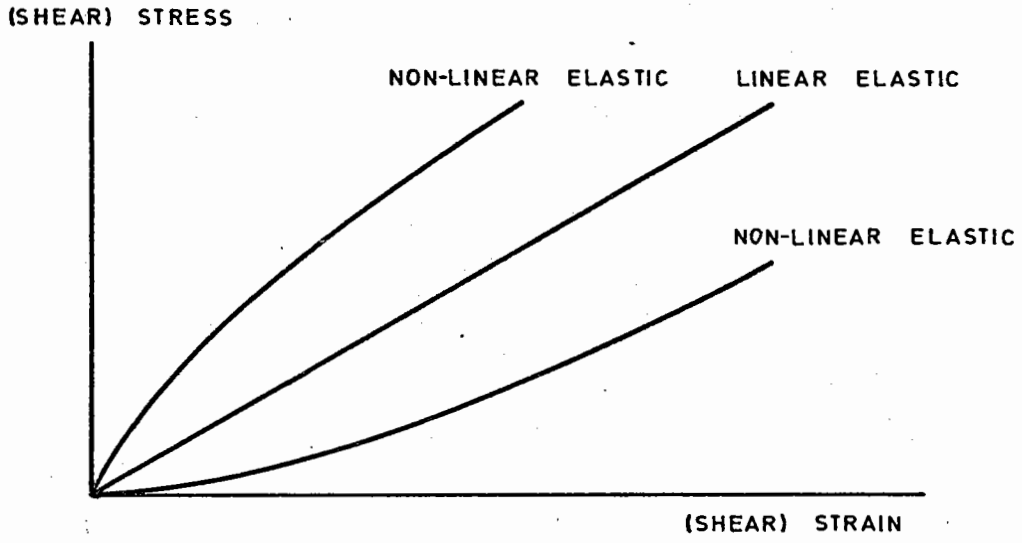

a) ELASTIC COMPONENT - STRAIN

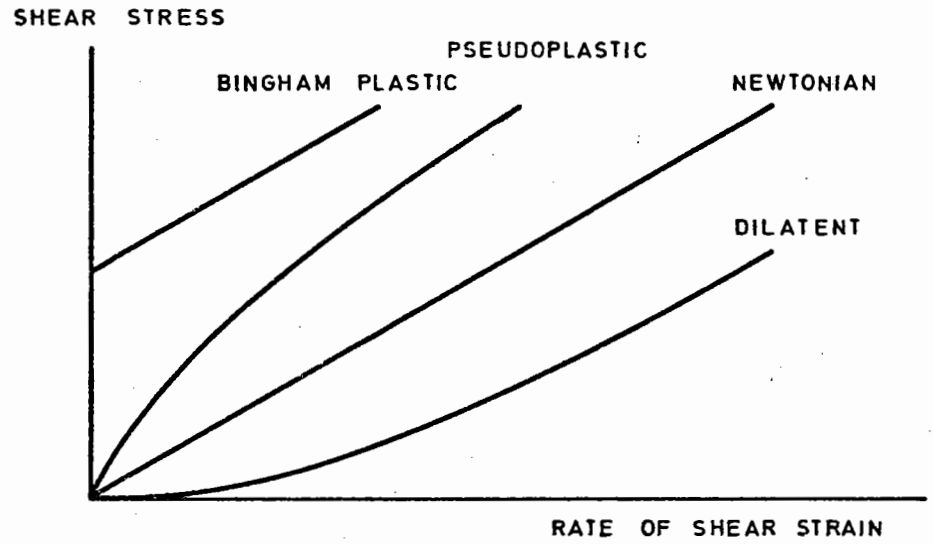

b) VISCOUS COMPONENT - STRAIN RATE

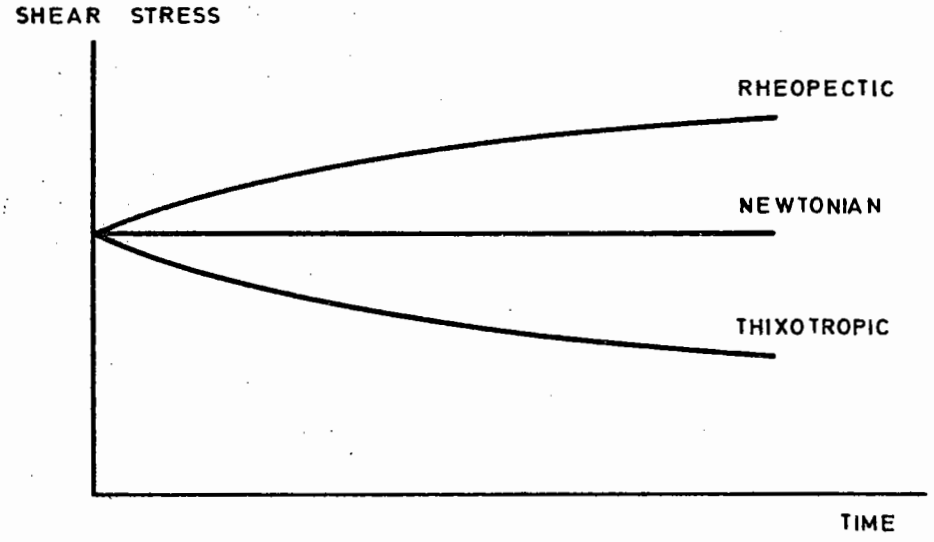

c) VISCOUS COMPONENT - TIME

FIG. 6 CHARACTERISTICS OF NON-LINEAR ELASTIC AND VISCOUS COMPONENTS OF VISCO-ELASTIC FLUIDS

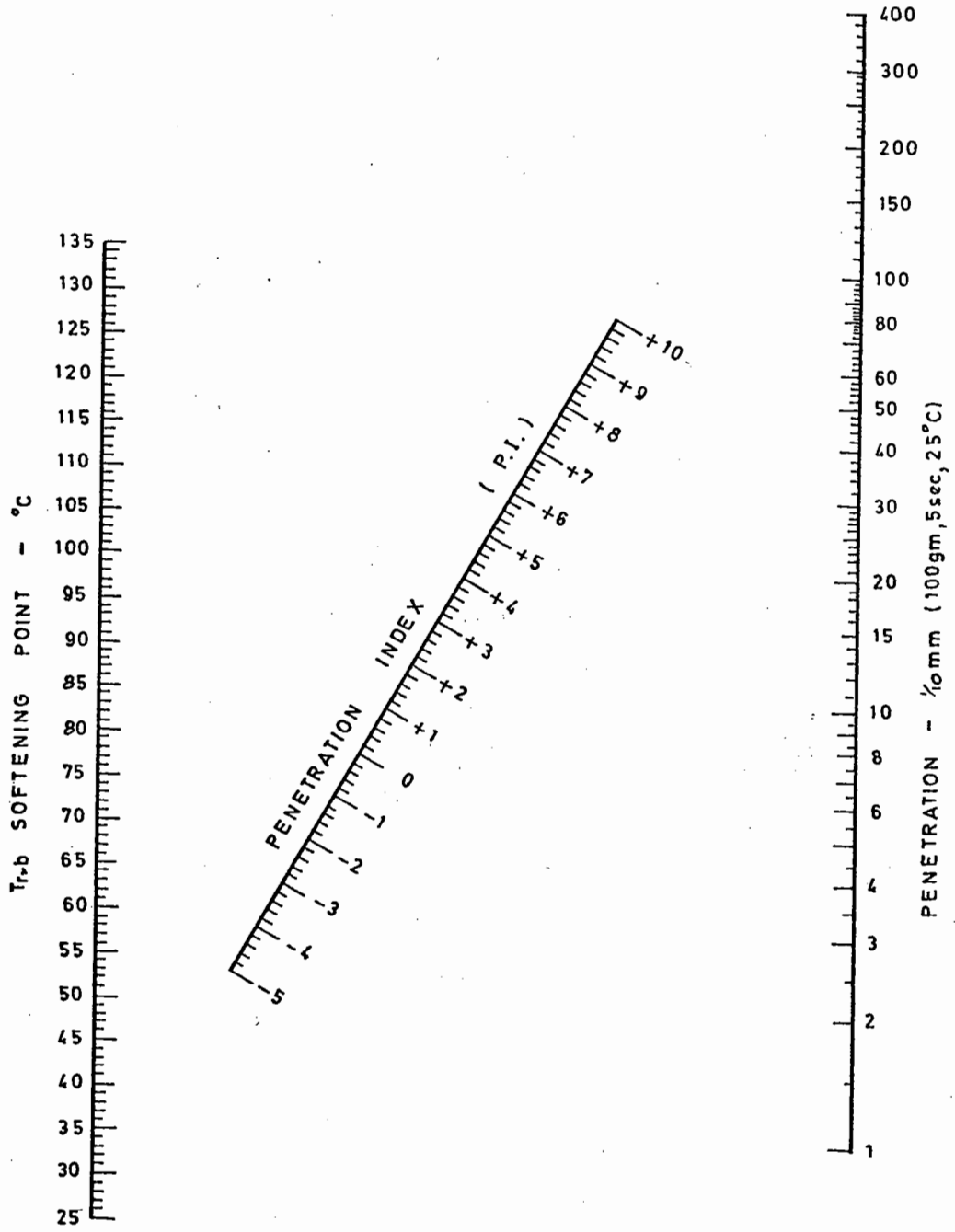

FIG. 7 NOMOGRAPH FOR DETERMINING THE PENETRATION INDEX OF BITUMEN after Pfeiffer and Van Doormaal (63)

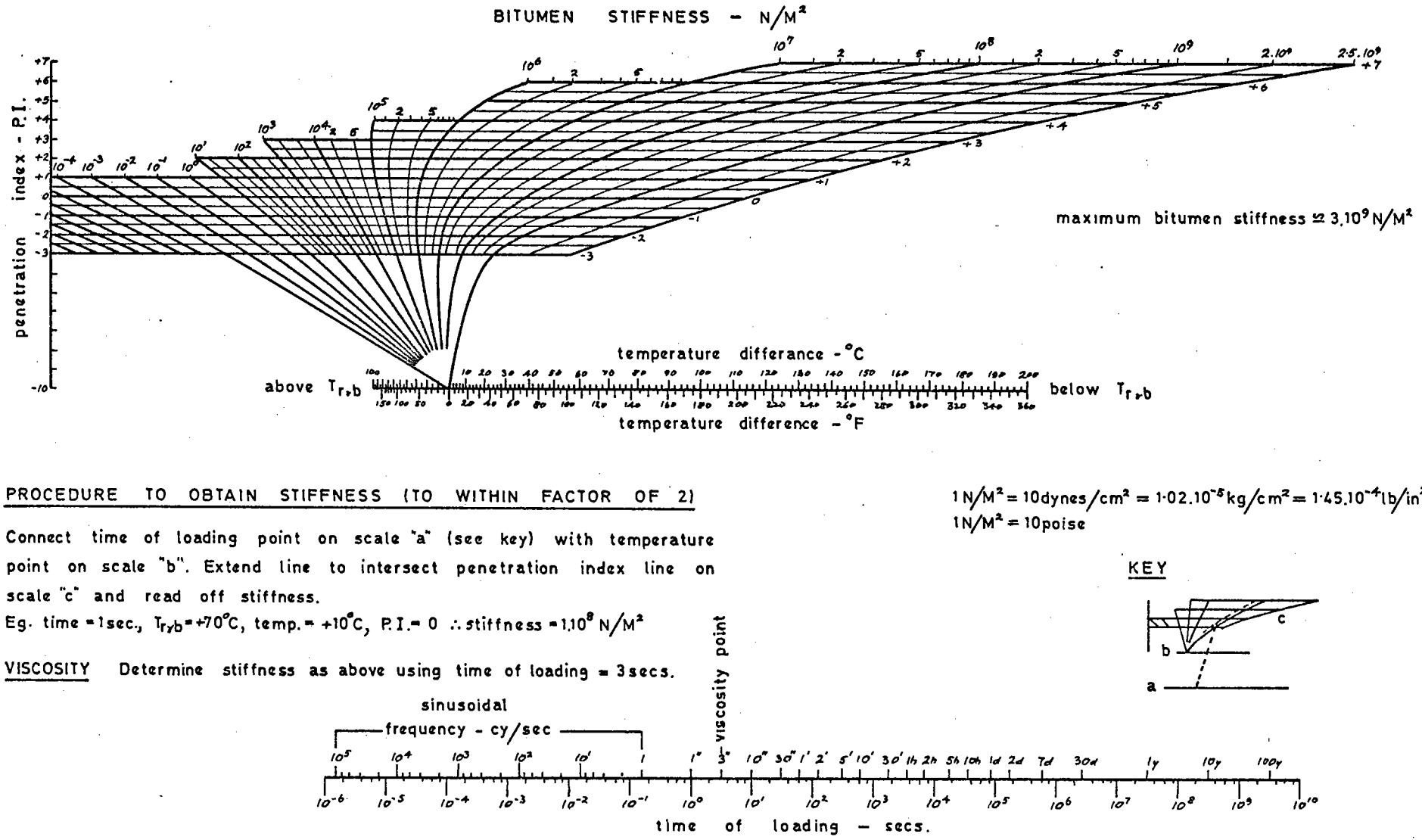

FIG. 8 NOMOGRAPH FOR DETERMINING THE STIFFNESS OF BITUMEN after Van der Poel (83)

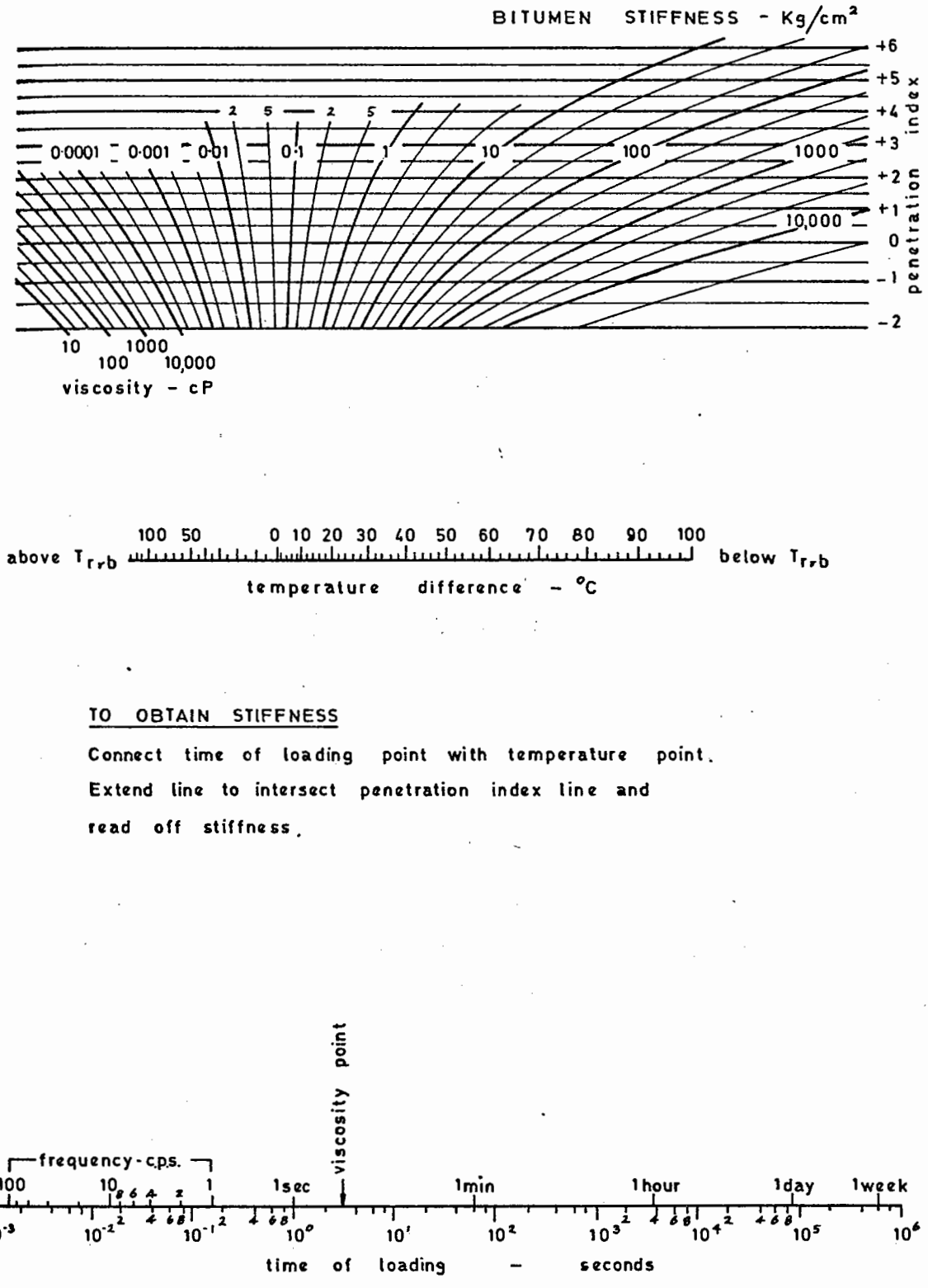

FIG. 9 NOMOGRAPH FOR DETERMINING THE STIFFNESS OF BITUMEN after Heukelom and Klomp (86)

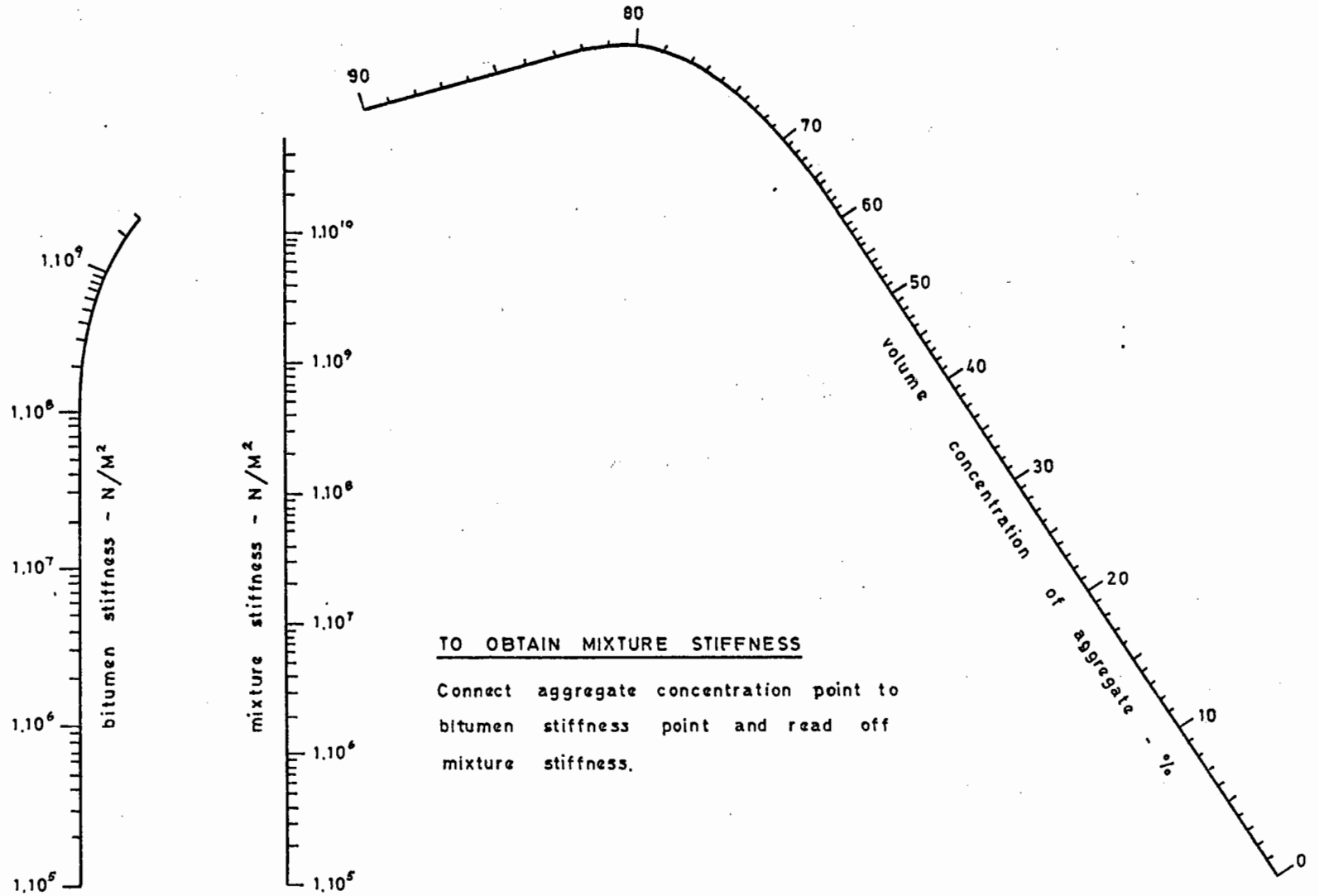

FIG. 10 NOMOGRAPH FOR DETERMINING THE STIFFNESS OF BITUMINOUS MIXTURES after Van der Poel (91)

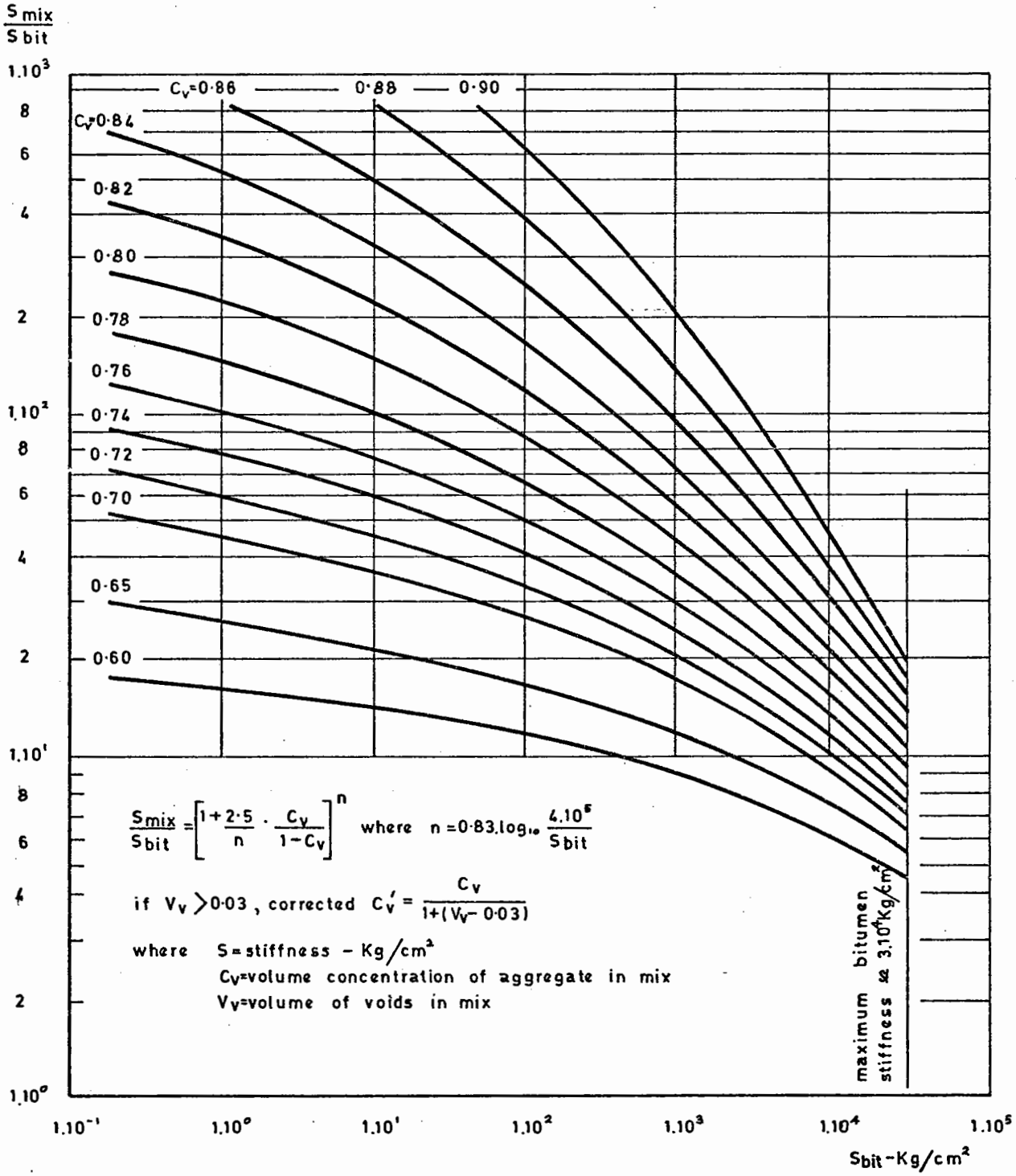

FIG. 11 NOMOGRAPH FOR DETERMINING THE STIFFNESS OF BITUMINOUS MIXTURES after Heukelom and Klomp (86)

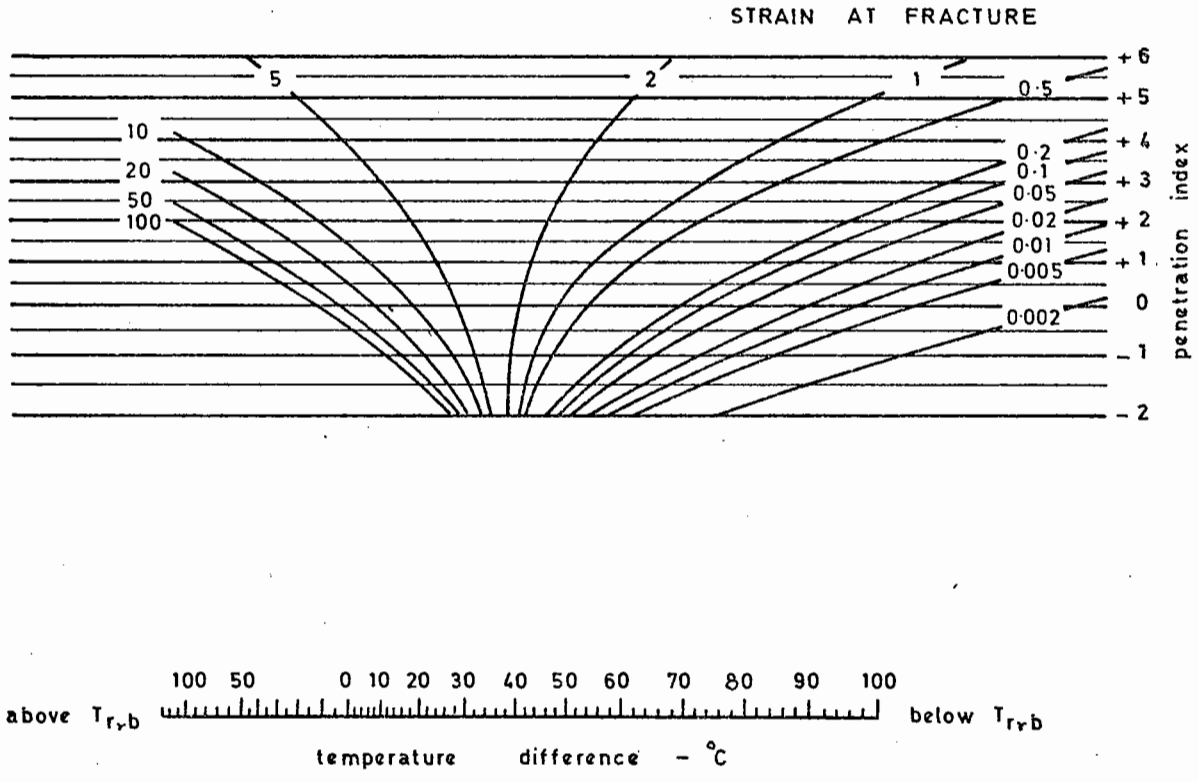

TO OBTAIN STRAIN AT FRACTURE

Connect time to fracture point with temperature point. Extend line to intersect penetration index line and read off strain at fracture.

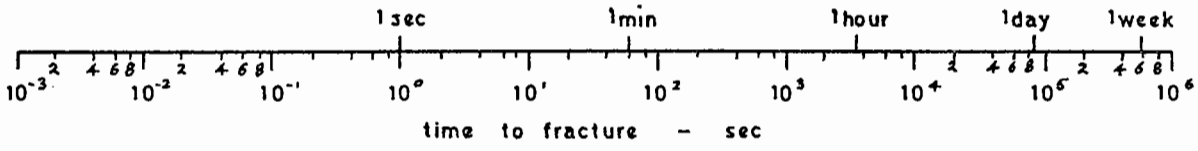

FIG. 12 NOMOGRAPH FOR DETERMINING THE FRACTURE STRAIN OF BITUMEN after Heukelom (73)

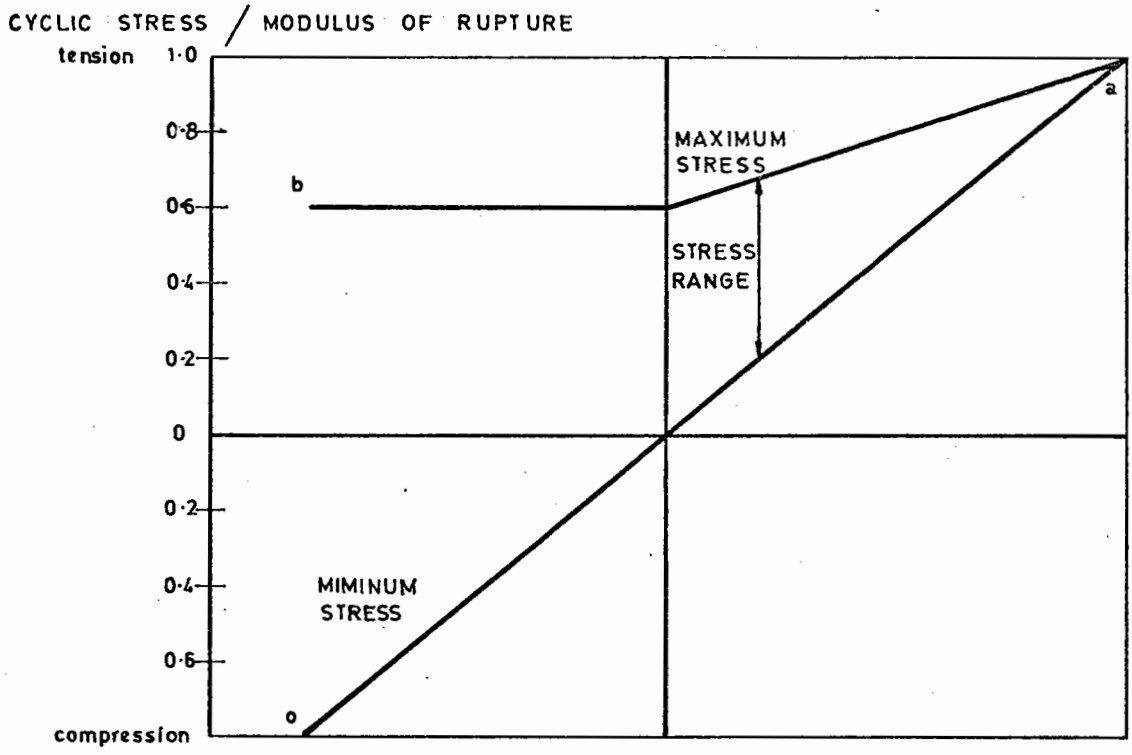

FIG. 13 MODIFIED GOODMAN DIAGRAM after Raithby & Miffin (200)

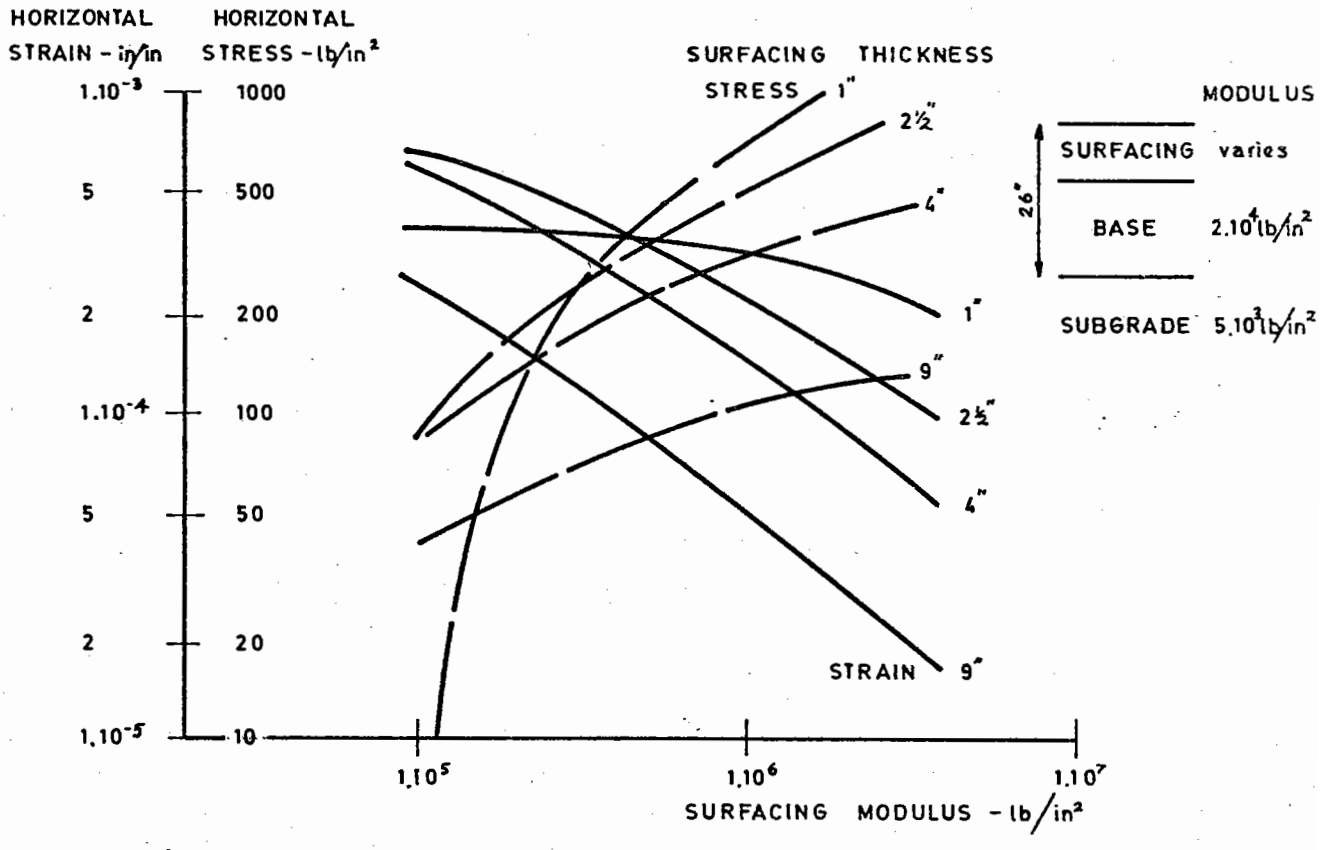

FIG. 14 VARIATION OF STRESS AND STRAIN ON UNDERSIDE OF ASPHALT FOR VARYING ASPHALT STIFFNESS AND DEPTH after Monismith (216)

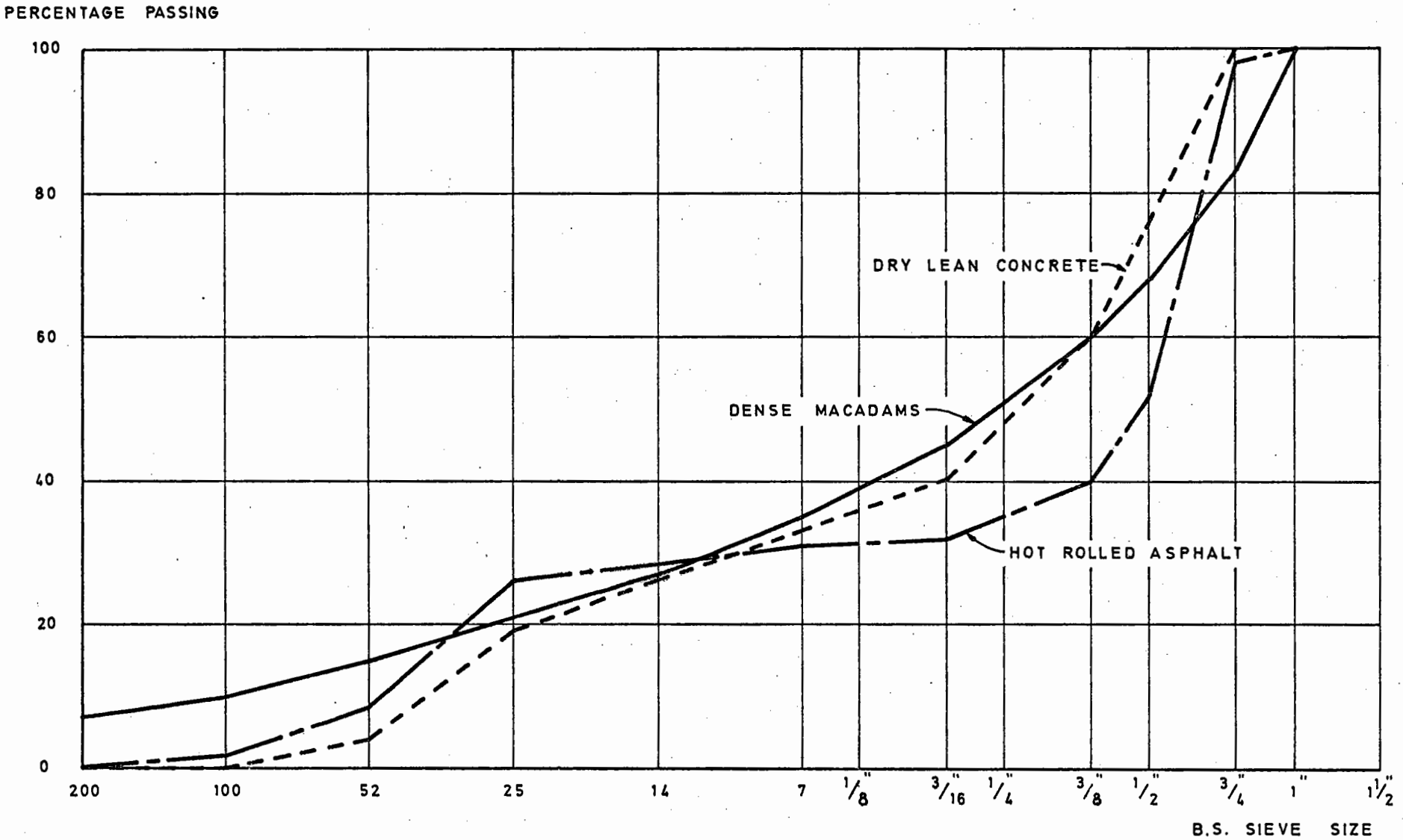

FIG. 15 AGGREGATE GRADING CURVES OF MATERIALS TESTED

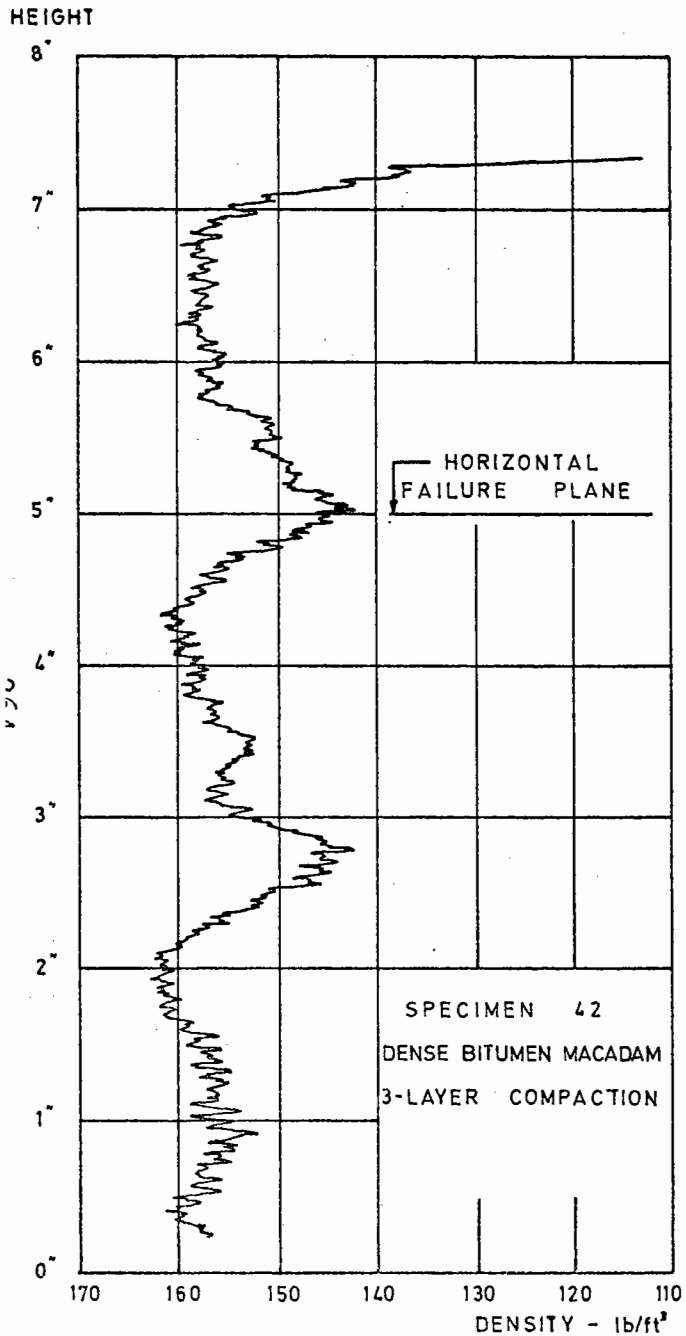

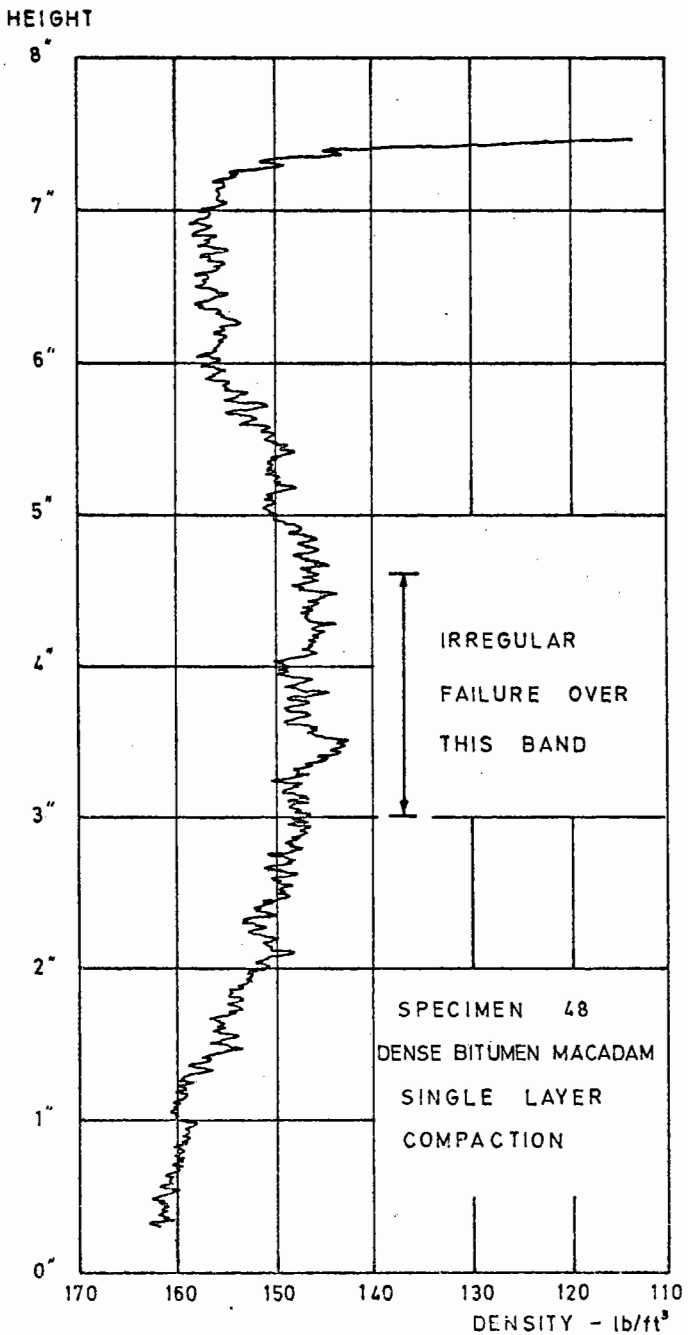

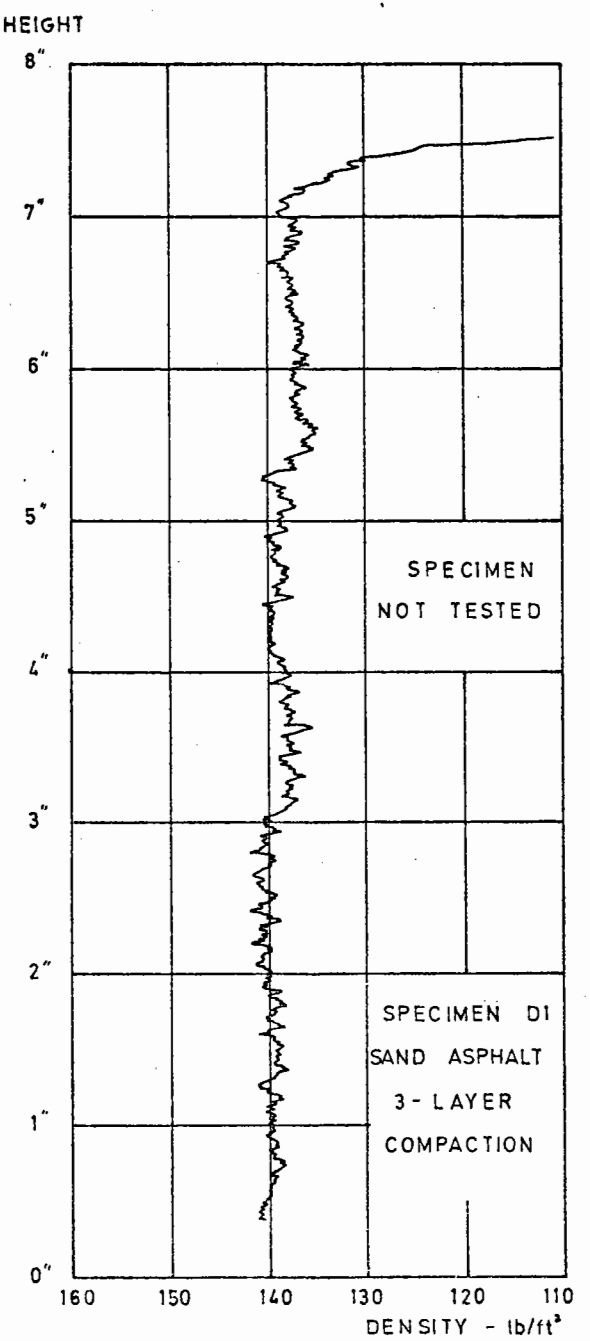

FIG. 16 GAMMA-RAY TRACES OF SINGLE AND THREE-LAYER COMPACTED BITUMINOUS SPECIMENS

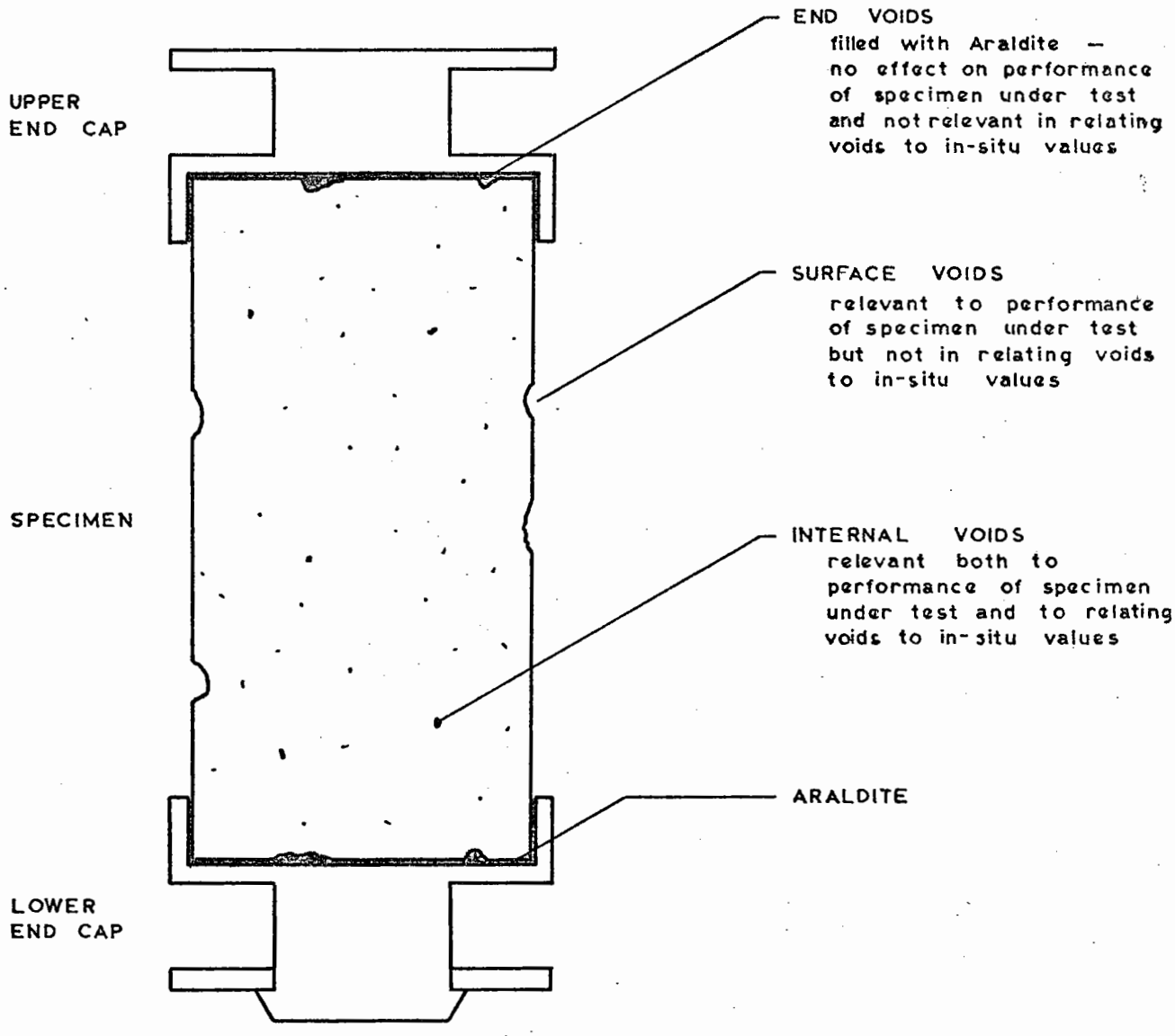

FIG. 17 VOIDS IN BITUMINOUS ROADBASE SPECIMEN

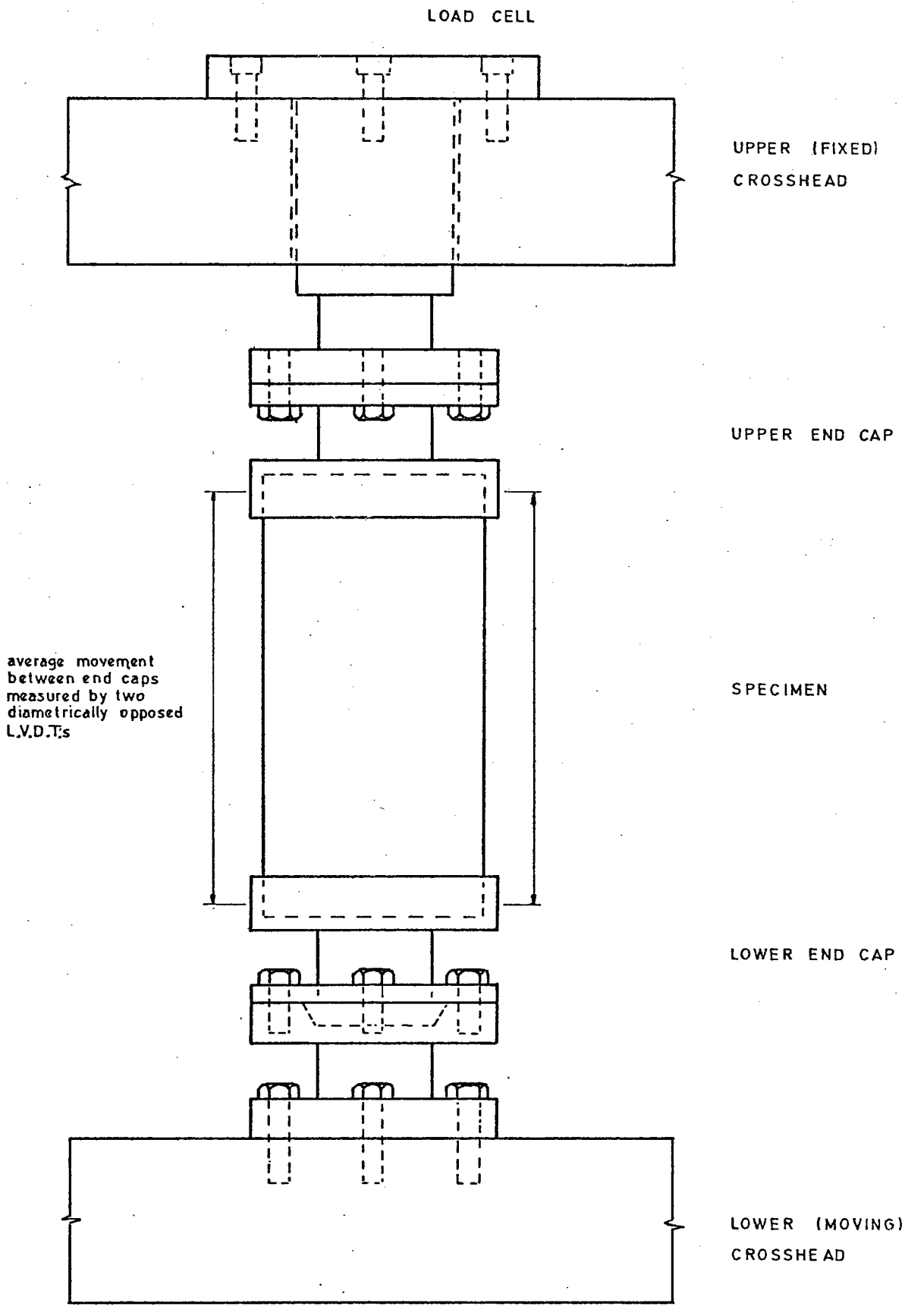

FIG. 18 SPECIMEN RELATIVE TO CROSSHEADS AND LOAD CELL

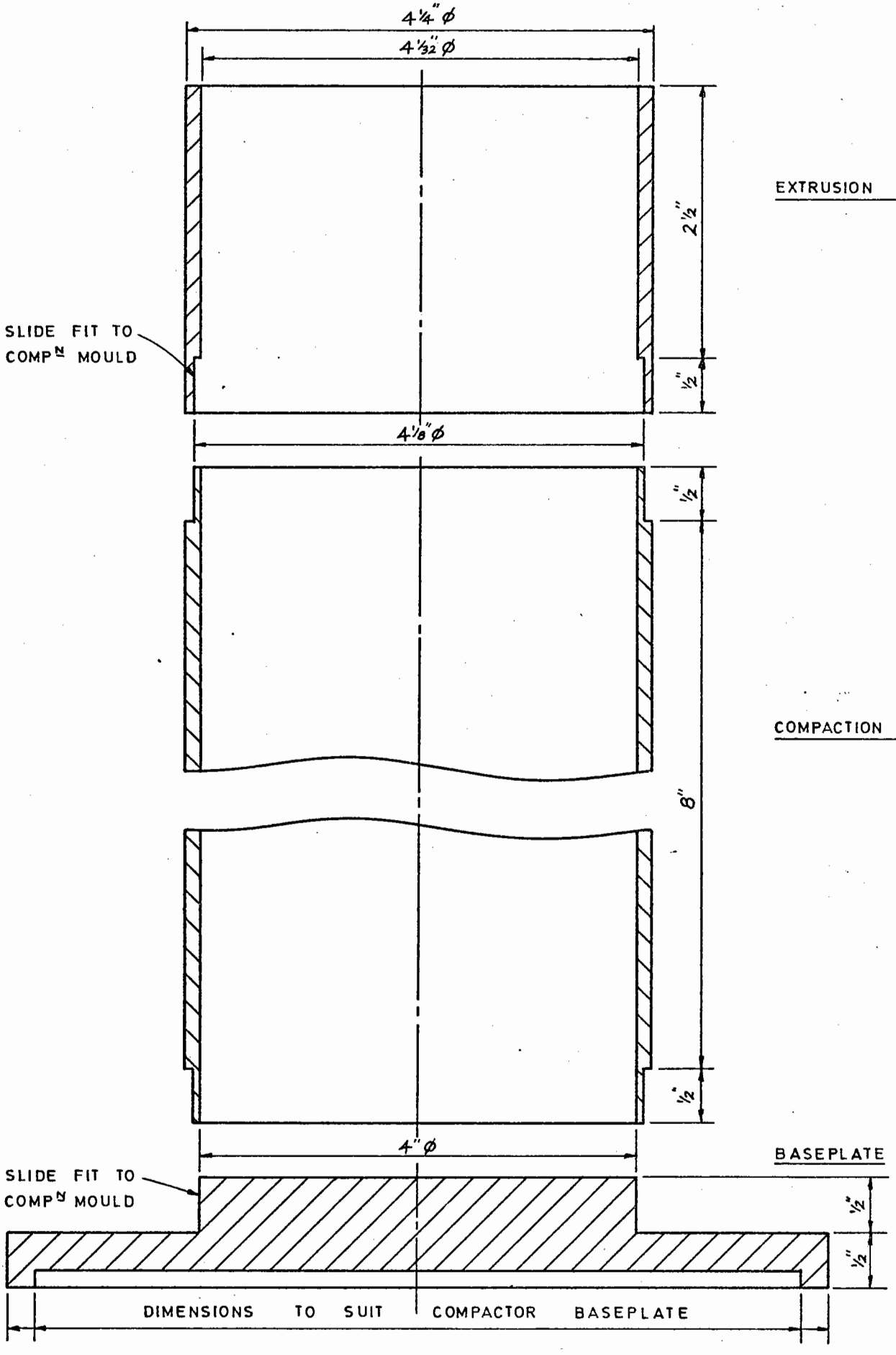

FIG. 19 DETAILS OF EXTRUSION COLLAR, COMPACTION MOULD AND BASEPLATE

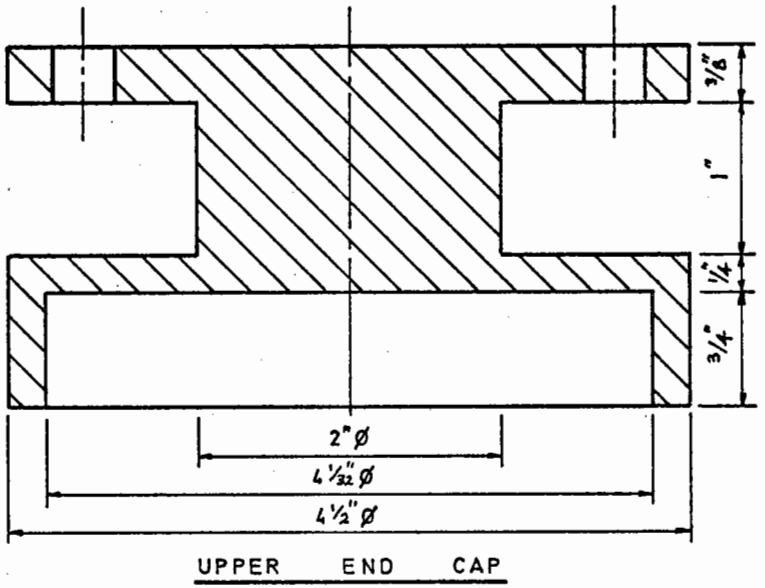

UPPER END CAP

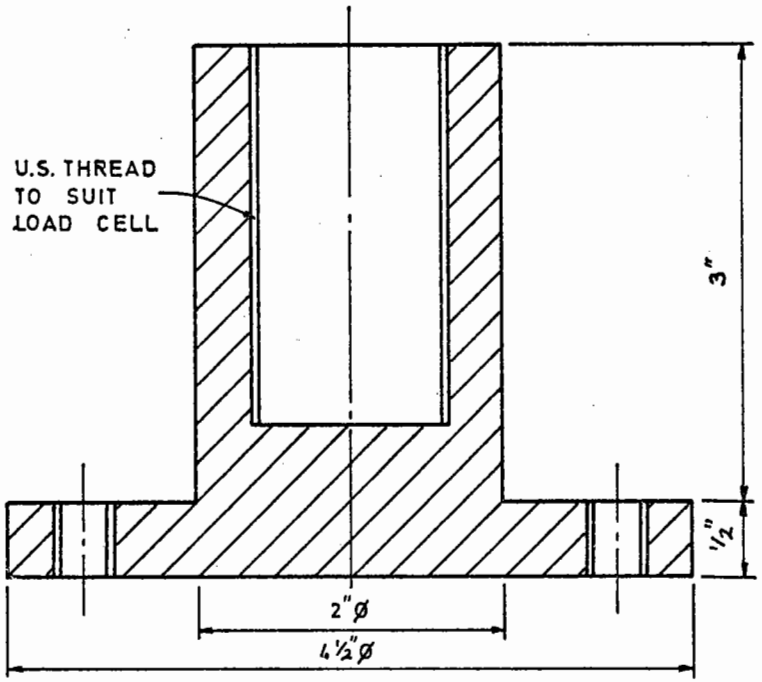

LOAD CELL ADAPTOR

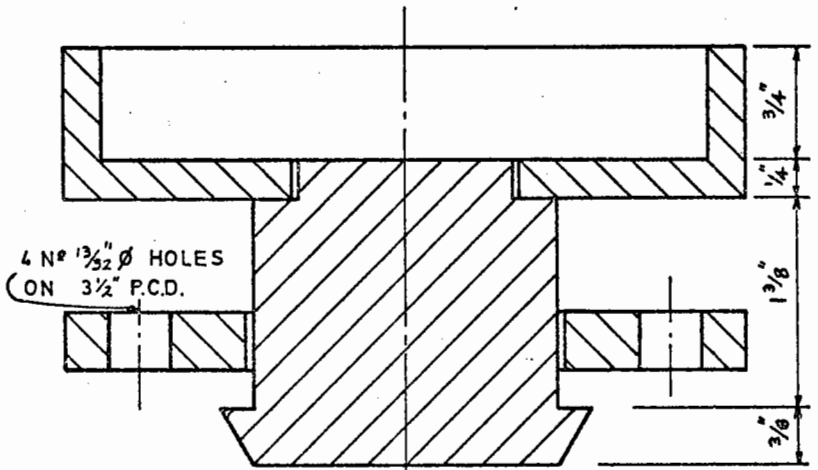

LOWER END CAP

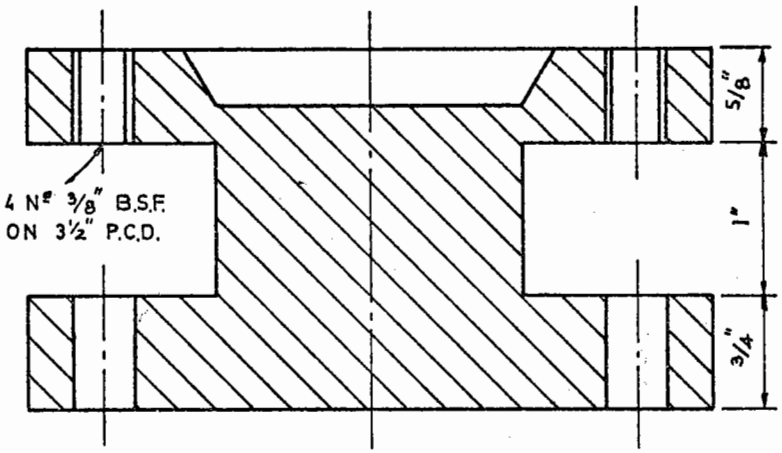

CROSSHEAD ADAPTOR

FIG. 20 DETAILS OF END CAPS AND ADAPTORS

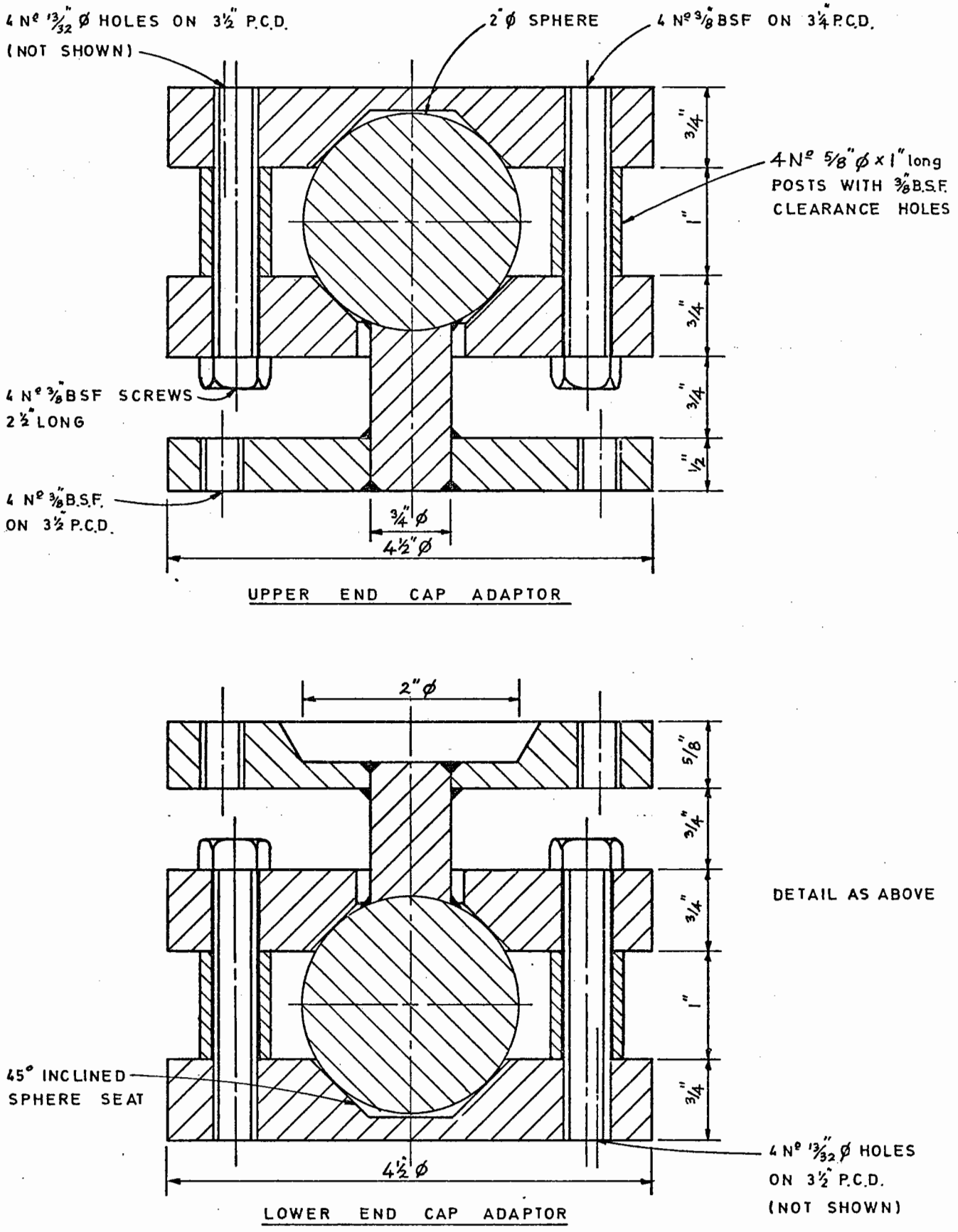

FIG. 21 DETAILS OF END CAP ADAPTORS FOR USE WHEN TESTING CONCRETE SPECIMENS

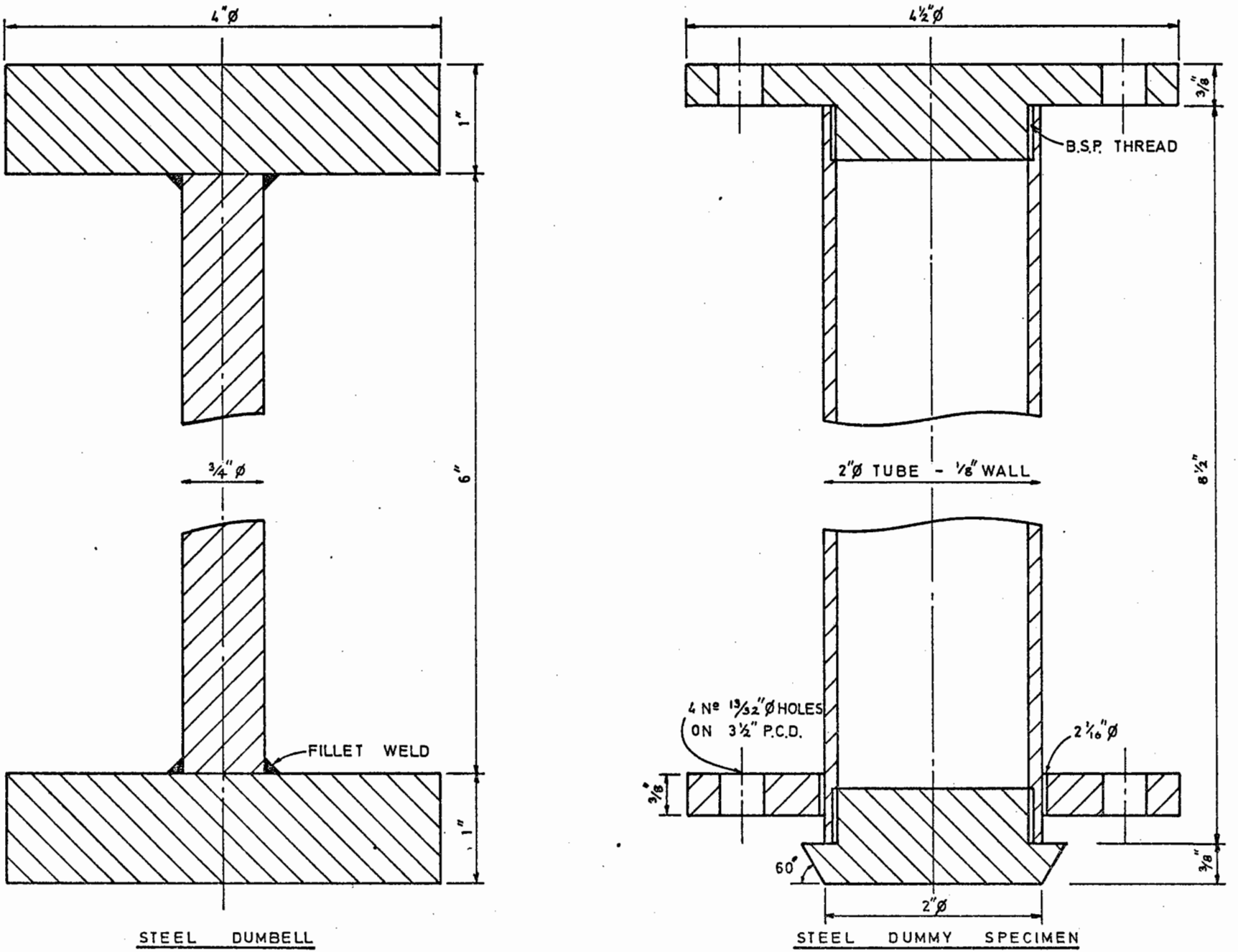

FIG. 22 DETAILS OF STEEL DUMBELL AND DUMMY SPECIMEN

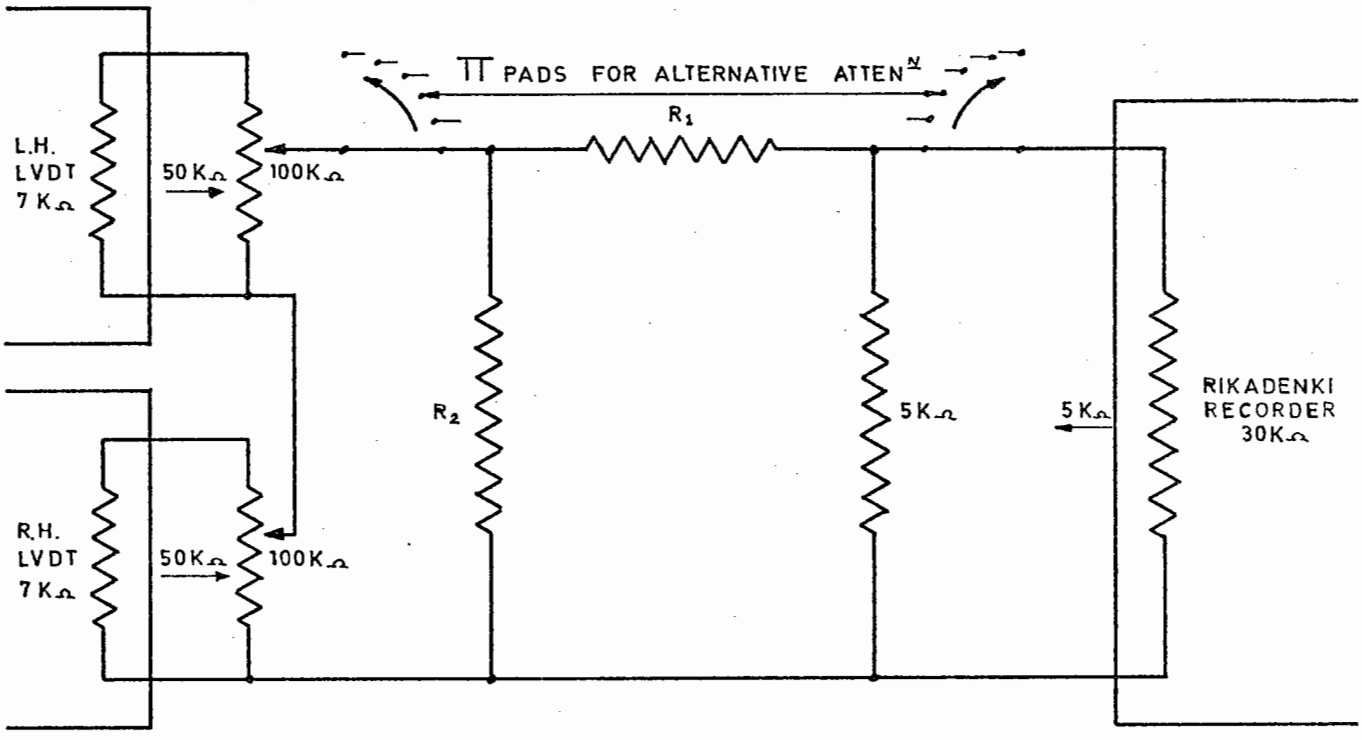

R_1 determines attenuation $\left(\frac{V_{in}}{V_{out}} = \frac{R_1 + 4{\cdot}3\,K}{4{\cdot}3K} \right)$

R_2 " load impedence

FIG. 23 CIRCUIT DIAGRAM OF π-TYPE IMPEDENCE AND ATTENUATION PAD

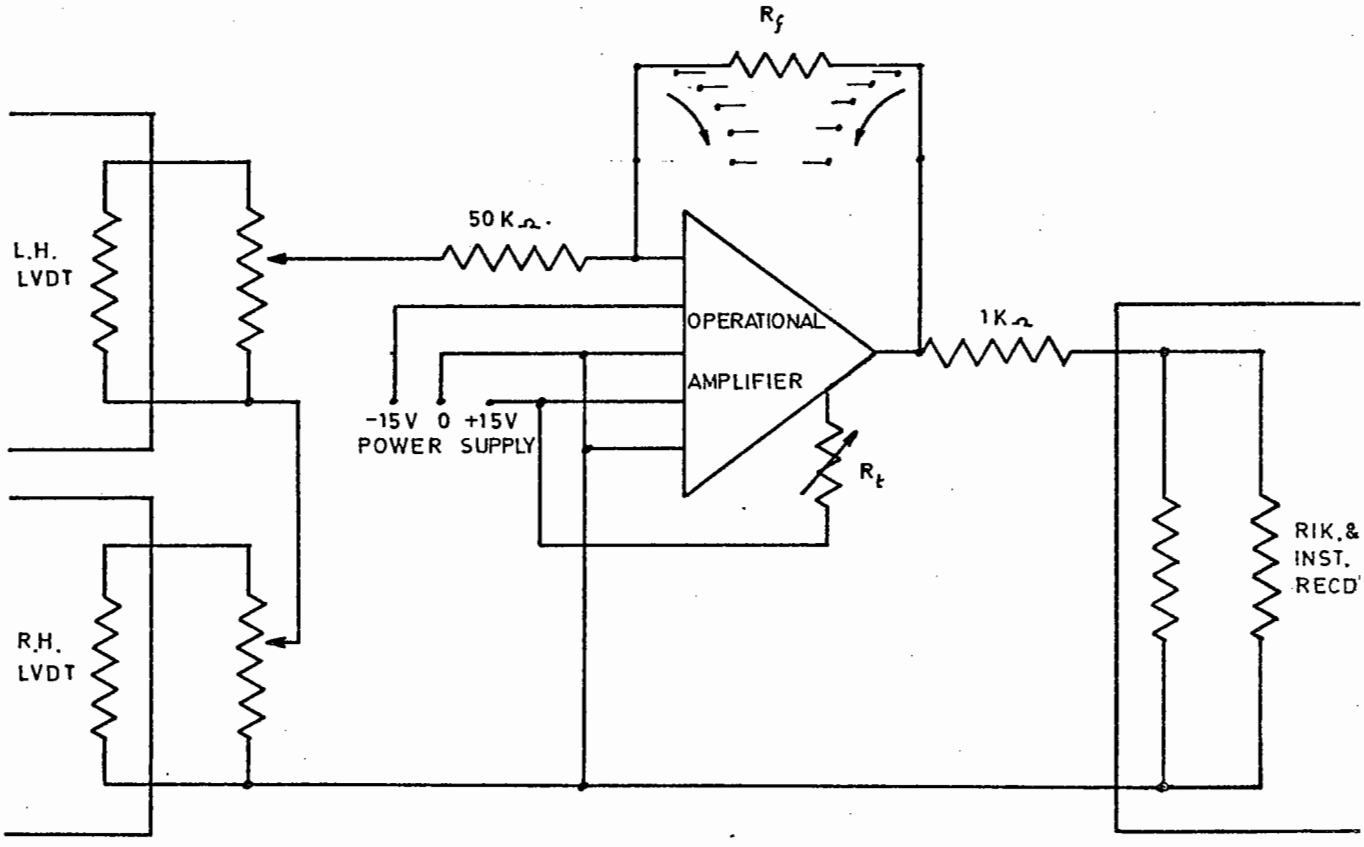

R_f determines attenuation $\left(\frac{V_{in}}{V_{out}} = \frac{50K}{R_f} \right)$

R_t " zero suppression

FIG. 24 CIRCUIT DIAGRAM OF OPERATIONAL AMPLIFIER BUFFER/ATTENUATOR

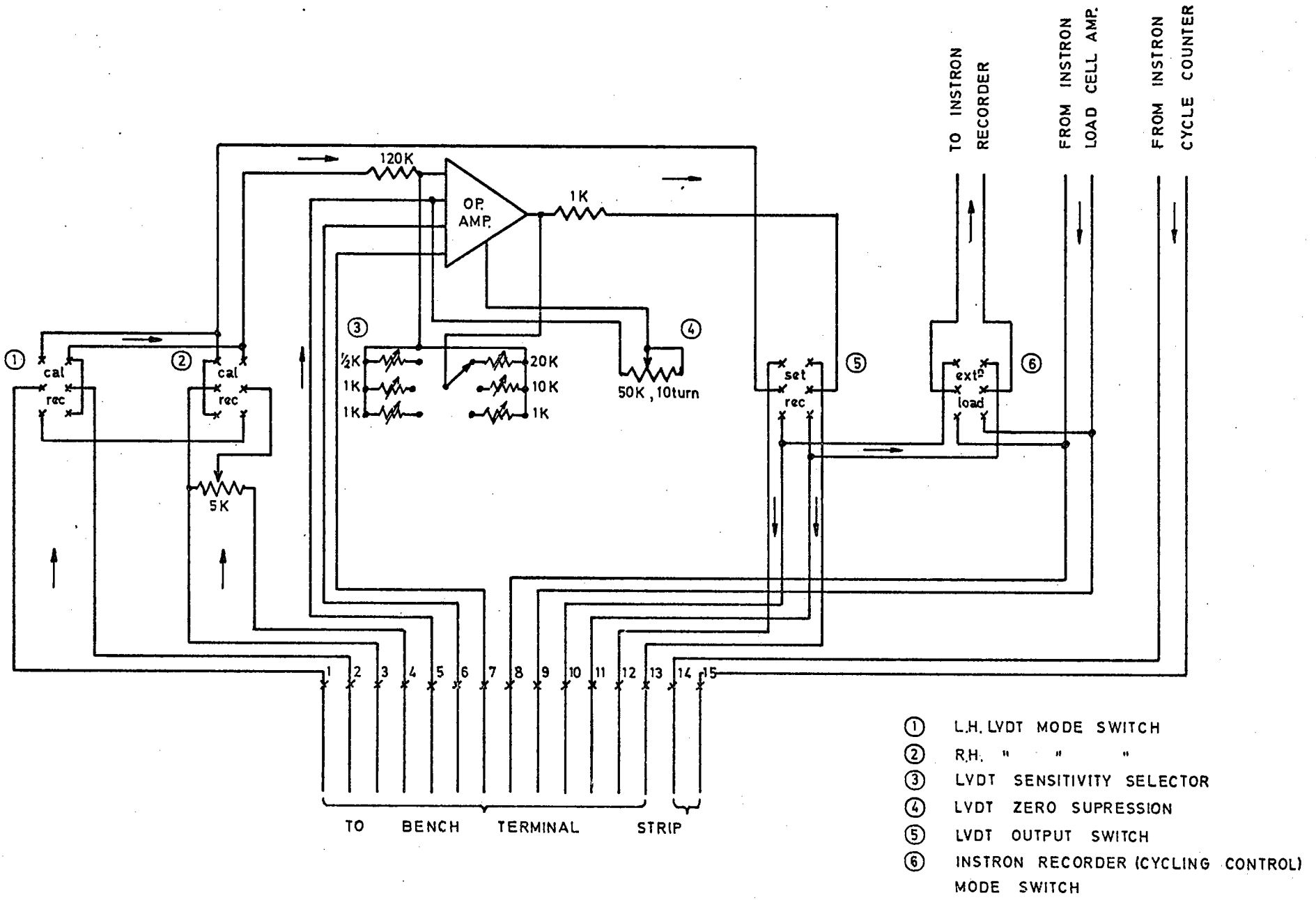

FIG. 25 CIRCUIT DIAGRAM FROM EXTENSOMETER TERMINAL STRIP

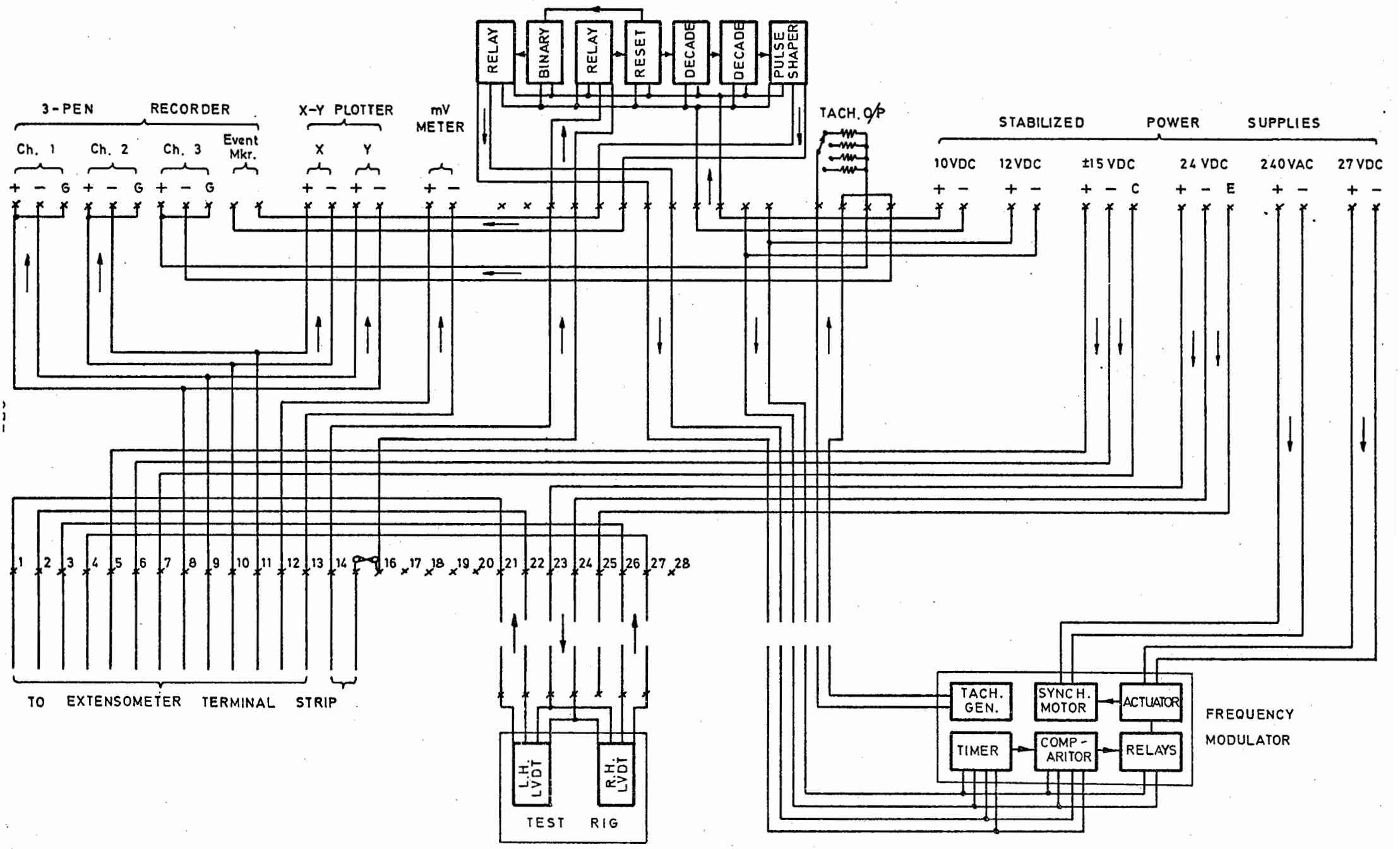

FIG. 26 CIRCUIT DIAGRAM FROM BENCH TERMINAL STRIP

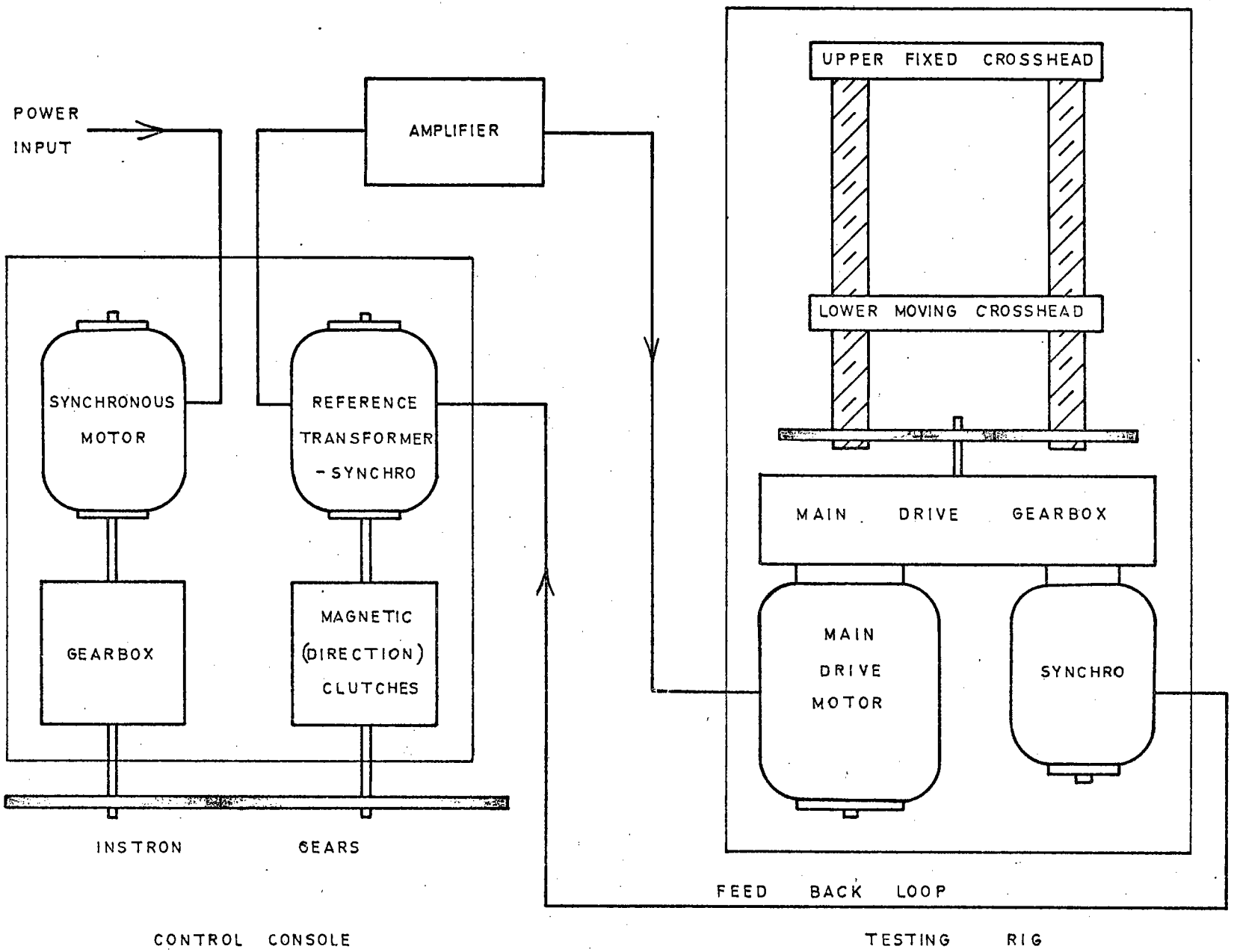

FIG. 27 DIAGRAMMATIC LAYOUT OF INSTRON CROSSHEAD CONTROL SYSTEM

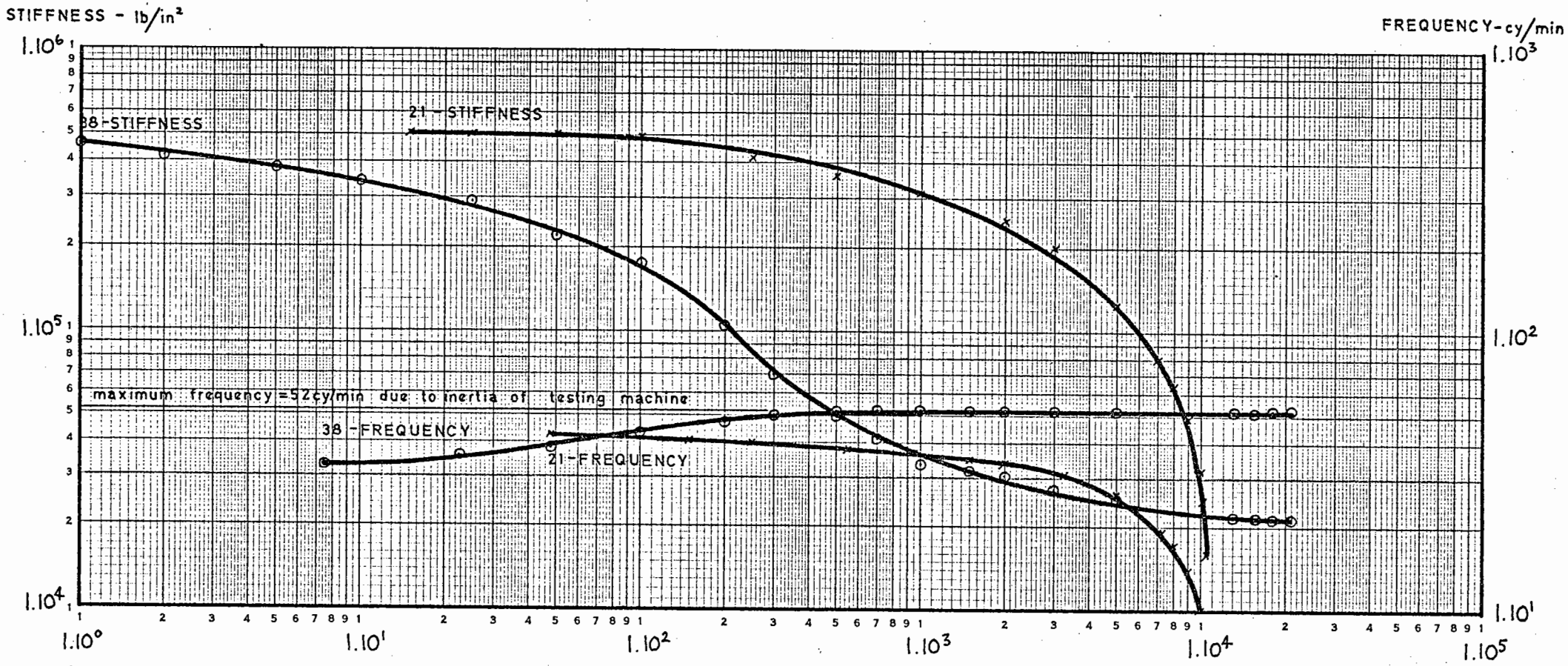

STRESS:	no initial readings due to lack of		122 lb/in²	116 lb/in²	105 lb/in²
STRAIN:	permanent recording facility at this time		2·48.10⁻⁴	3·73.10⁻⁴	3·26.10⁻³
STRAIN:	4·60.10⁻⁴	4·85.10⁻⁴	5·54.10⁻⁴	6·90.10⁻⁴	6·98.10⁻⁴
STRESS:	209 lb/in²	165 lb/in²	95·4 lb/in²	25·0 lb/in²	15·5 lb/in²

FIG. 28 EFFECT ON DEPENDENT VARIABLES OF CHANGE IN STIFFNESS OF SPECIMEN UNDER STRESS- AND STRAIN-CONTROLLED TESTING

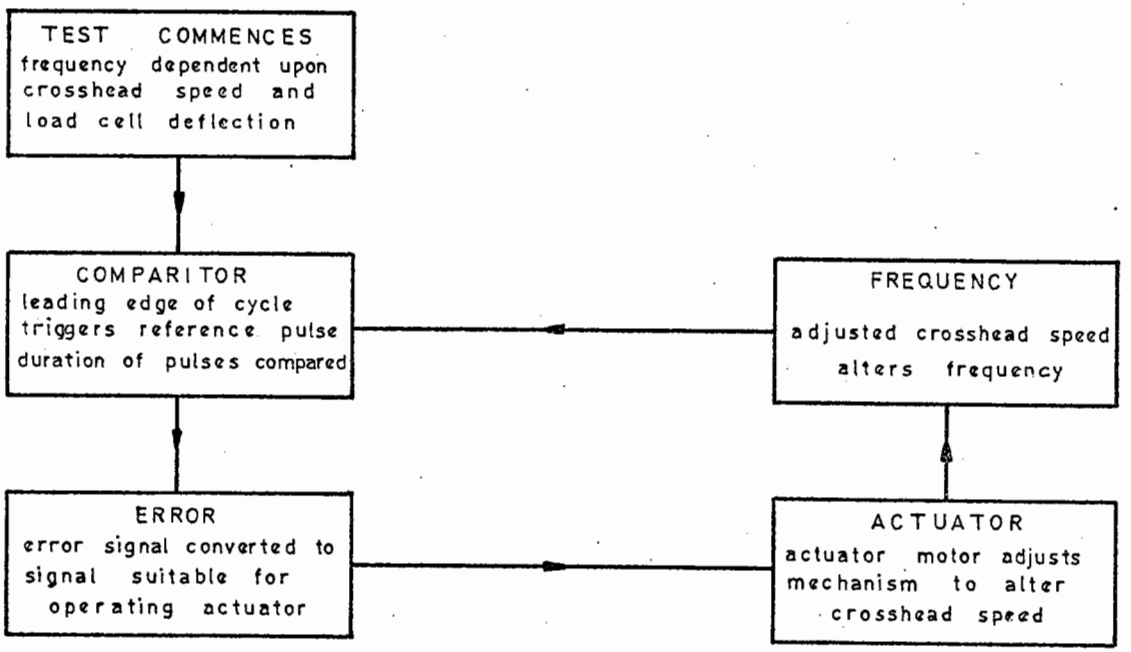

FIG. 29 BLOCK DIAGRAM OF FREQUENCY MODULATOR SERVO LOOP

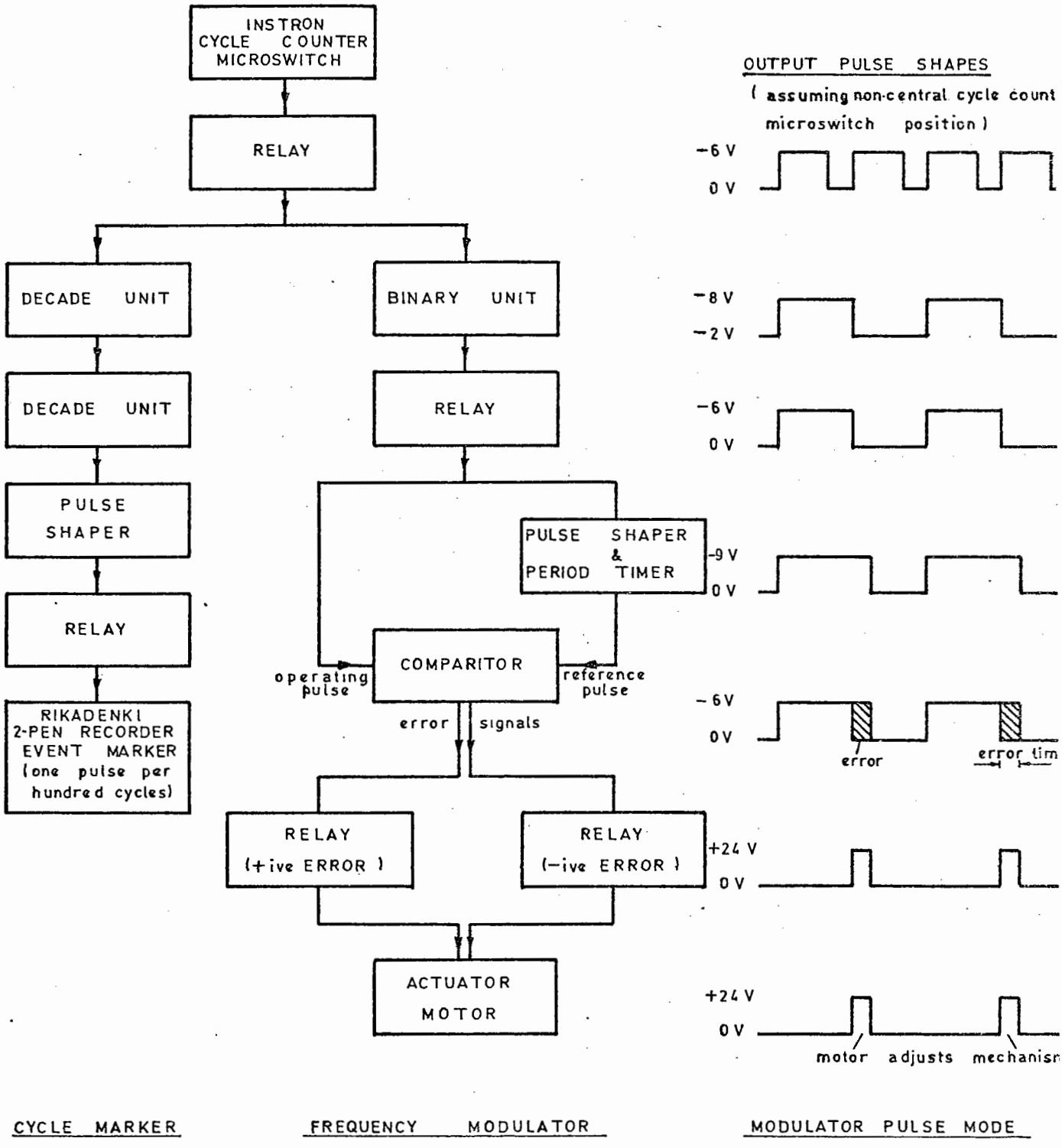

FIG. 30 BLOCK DIAGRAM OF FREQUENCY MODULATOR AND CYCLE COUNTING ELECTRONIC COMPONENTS

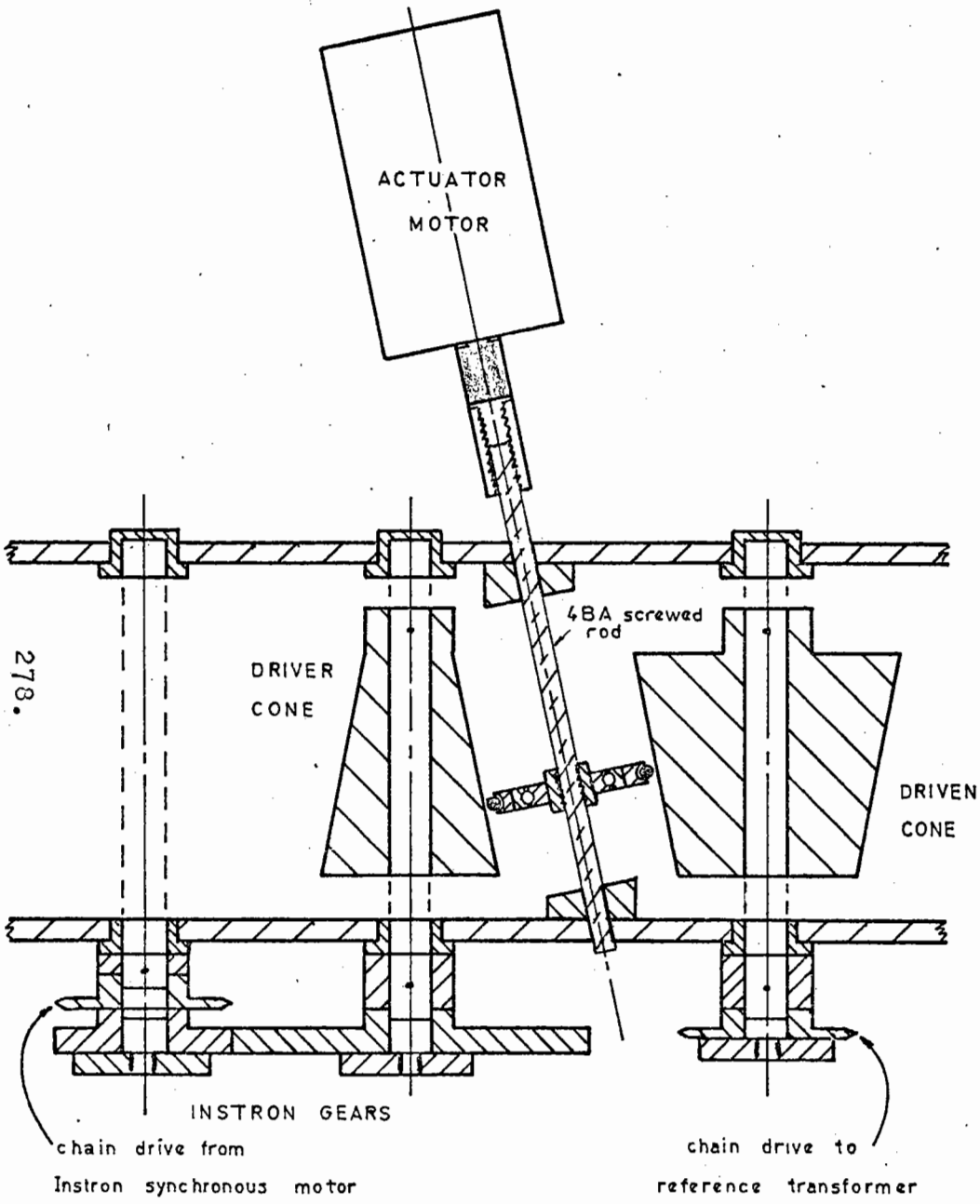

Fig. 6a original design – brass cones, rubber tyred jockey wheel

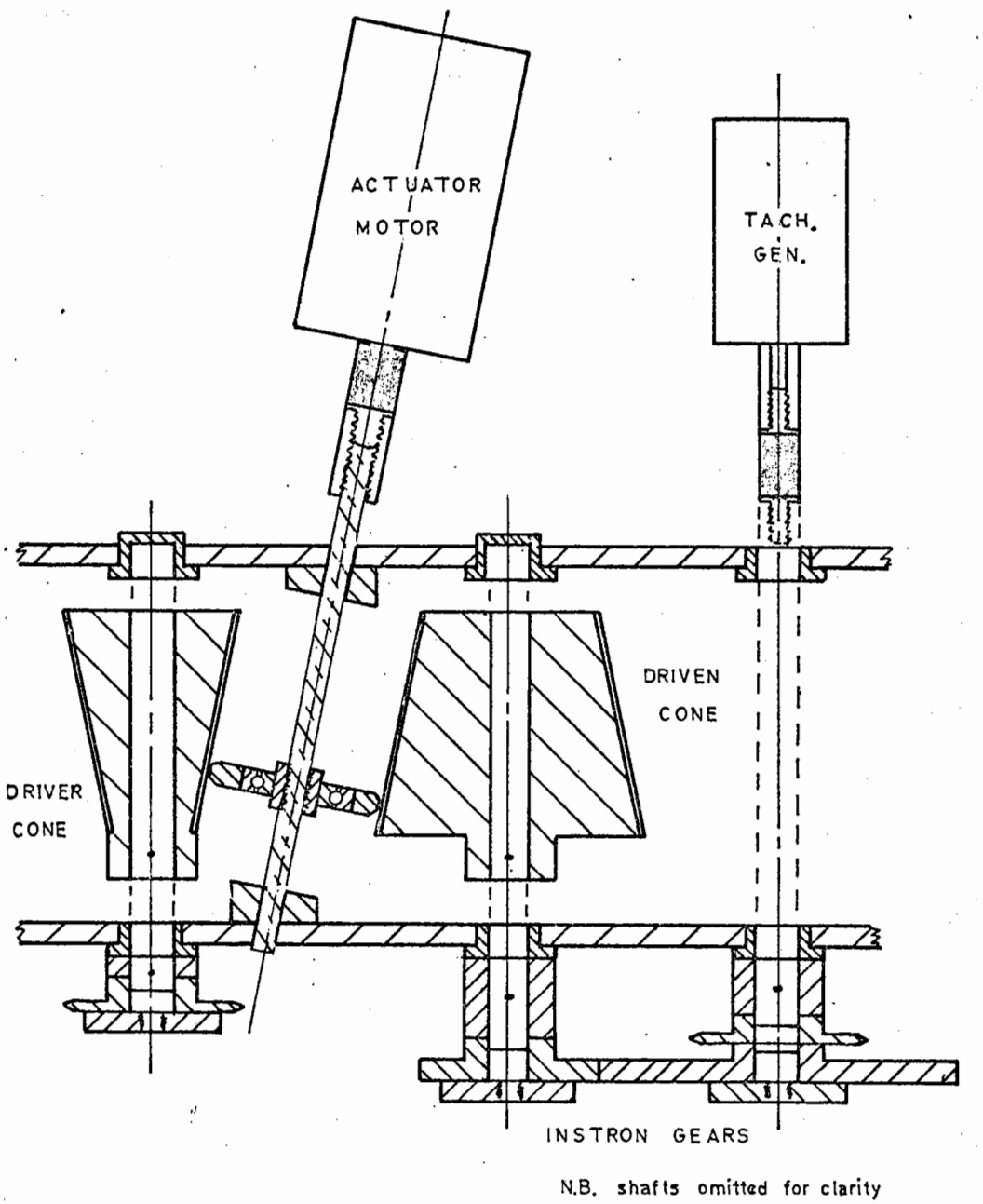

Fig. 6b modified design – silicone rubber covered cones, aluminium jockey wheel

FIG. 31 CONE DRIVE LAYOUTS OF ORIGINAL FREQUENCY MODULATOR

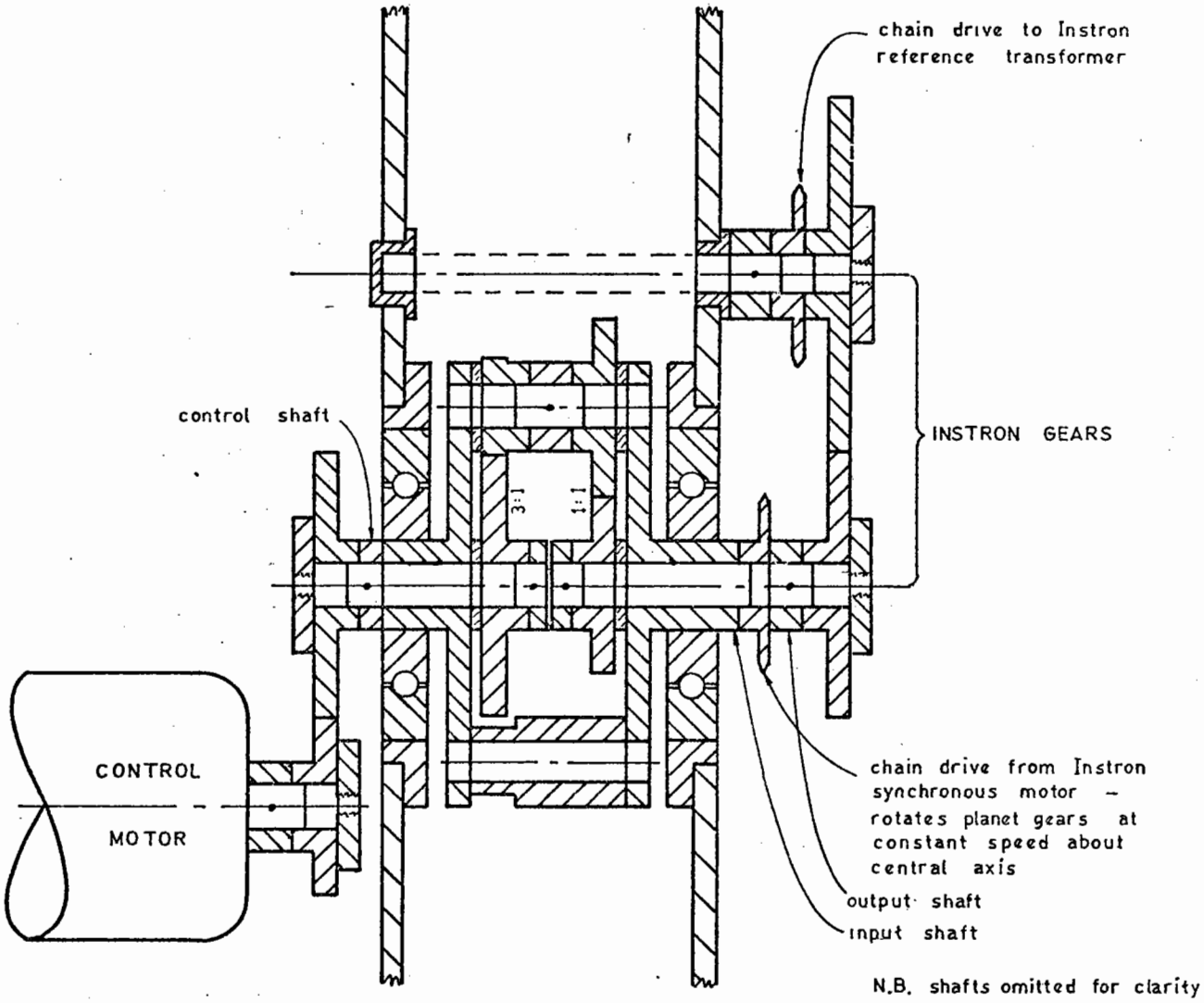

input shaft speed = $+R_i$ (+ive clockwise as viewed from right)

control " " = $+R_c$ " " " " " "

output " " = $3R_c - 2R_i$ " " " " " "

$\therefore$ for output range +7 to 525 r.p.m. control range = +25·7 to 40·8 r.p.m.

where input shaft speed = +35 r.p.m.

FIG. 32 EPICYCLIC GEARBOX OF MODIFIED FREQUENCY MODULATOR

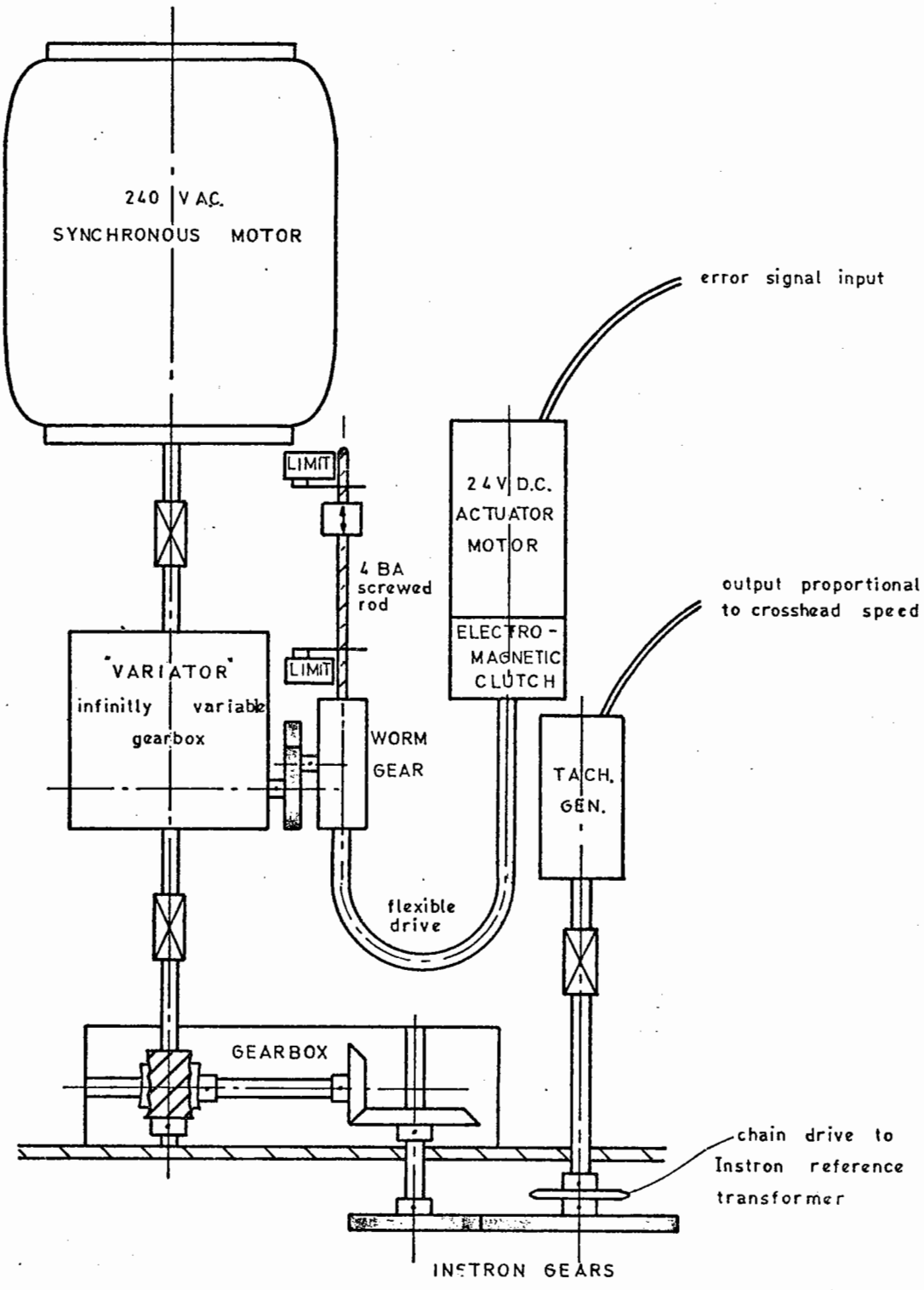

FIG. 33 SCHEMATIC LAYOUT OF MECHANICAL CONTROL OF FREQUENCY MODULATOR SERVO SYSTEM

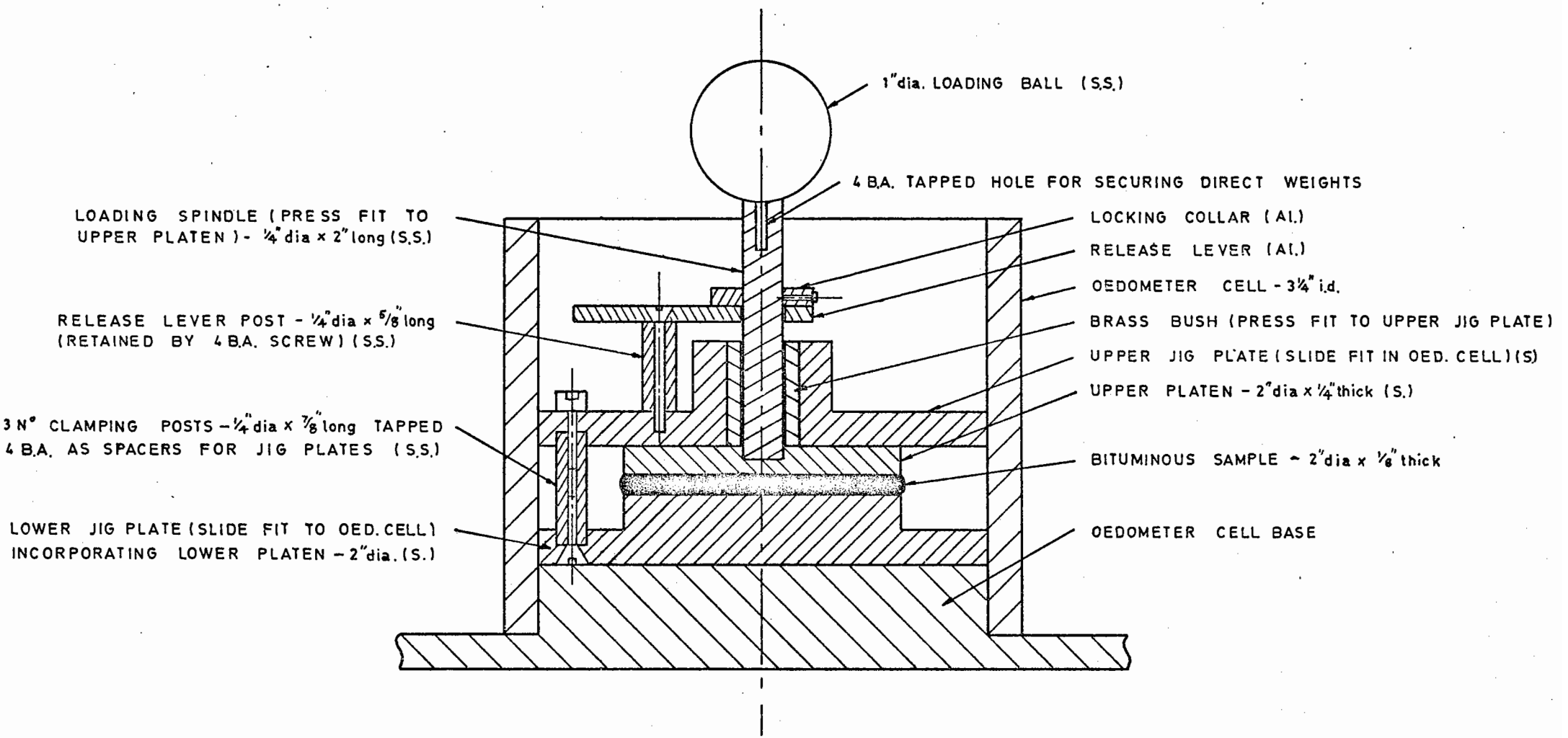

FIG. 34 DETAILS OF PARALLEL PLATE VISCOMETER

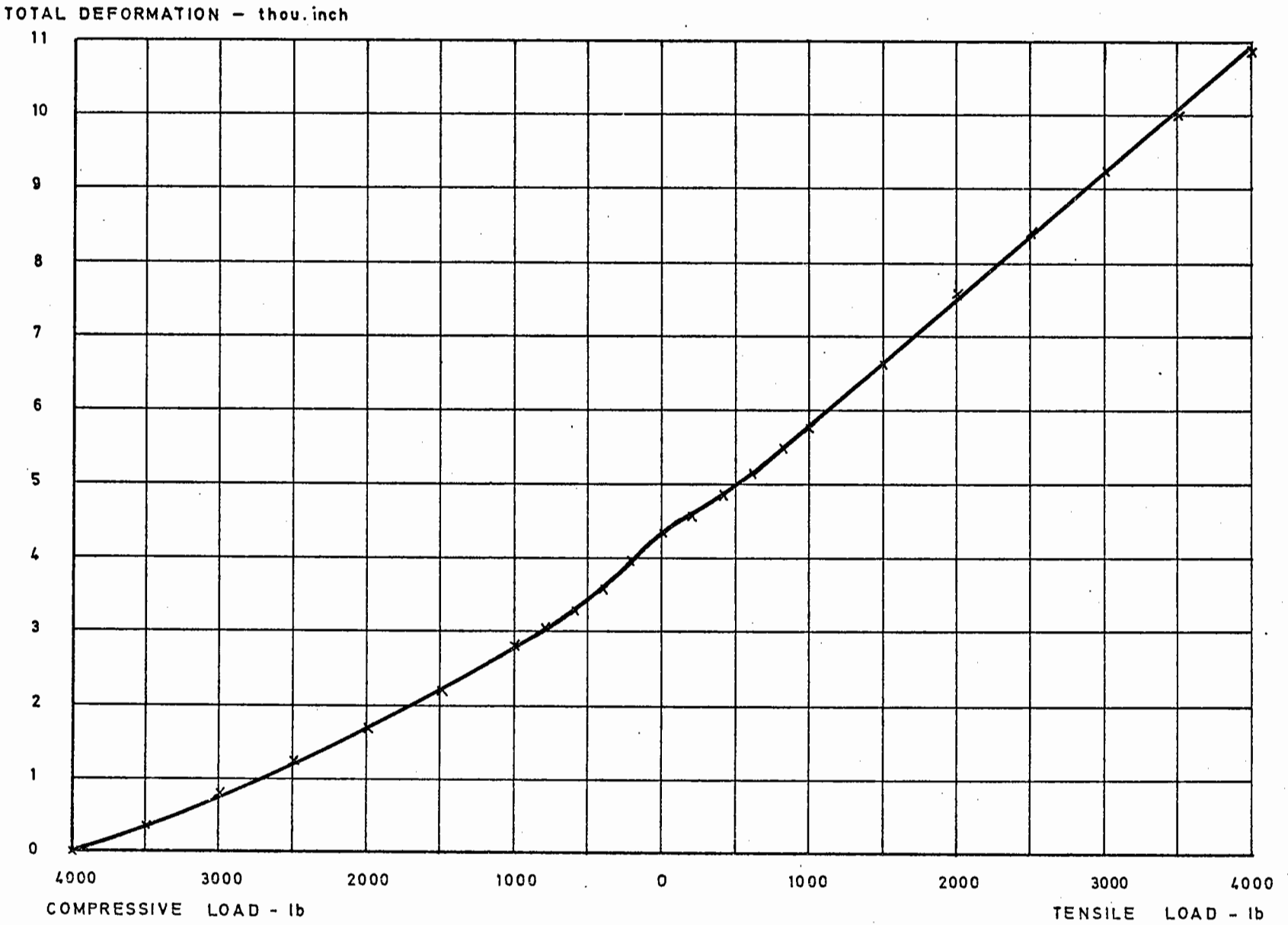

FIG. 35a DEFORMATION OF LOAD CELL AND FITTINGS OVER ± 4000 lb

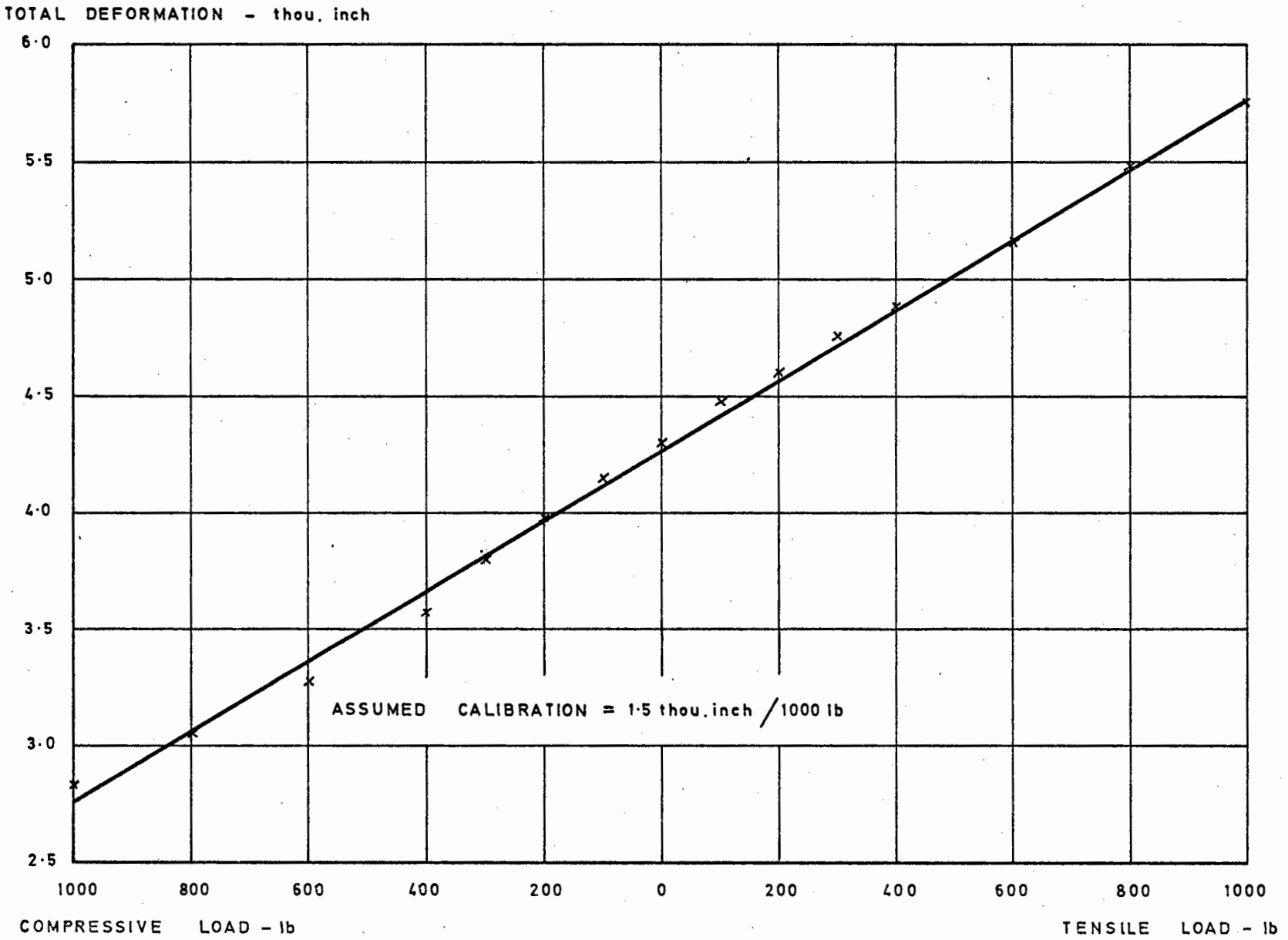

FIG. 35b DEFORMATION OF LOAD CELL AND FITTINGS OVER ± 1000 lb

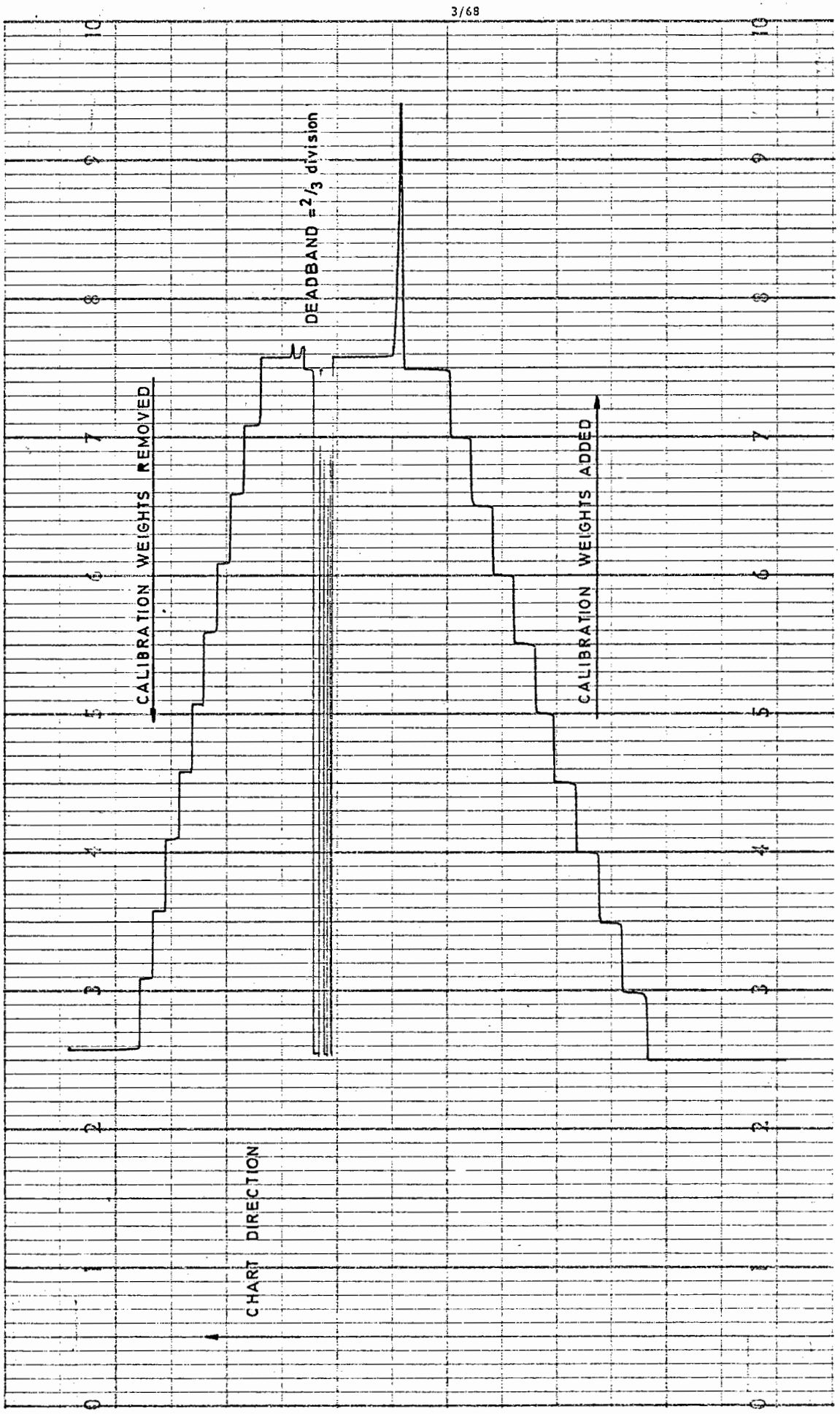

FIG. 36 RECORD OF LOAD CELL CALIBRATION BY DEAD WEIGHTS

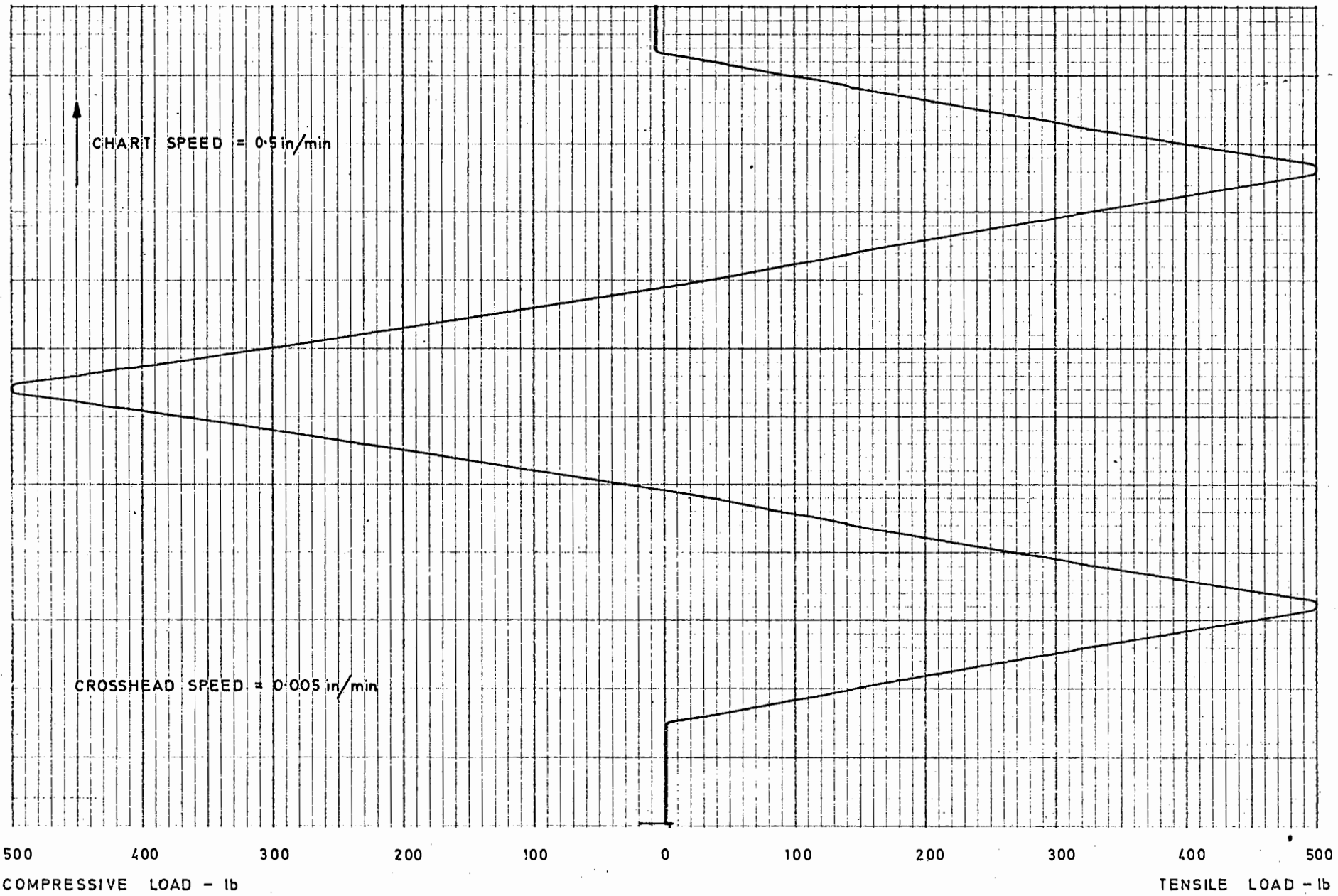

FIG. 37 RECORD OF LOAD WAVEFORM OF STEEL DUMMY SPECIMEN IN LOAD CYCLING

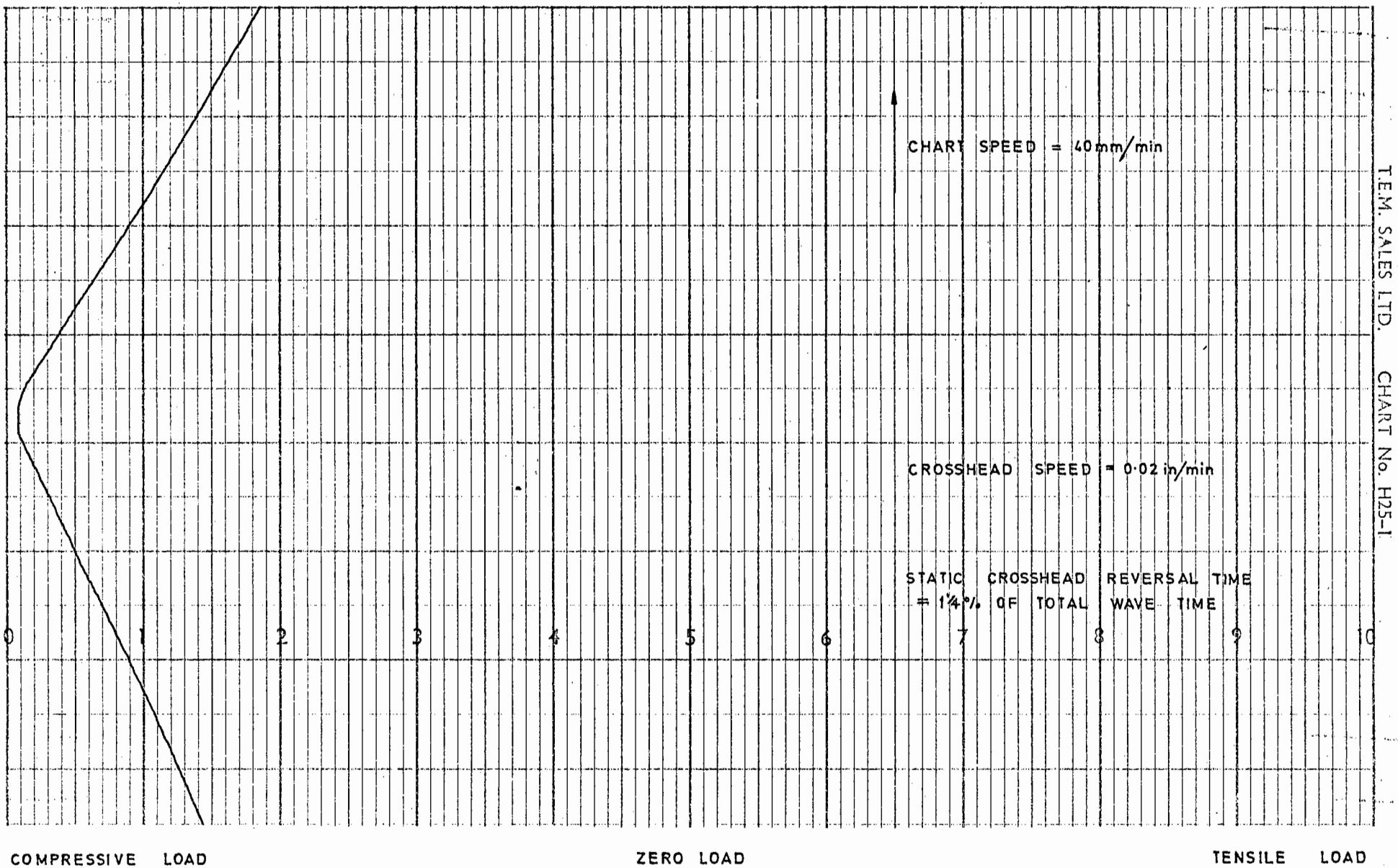

FIG. 38 RECORD OF LOAD REVERSAL OF STEEL DUMMY SPECIMEN IN LOAD CYCLING

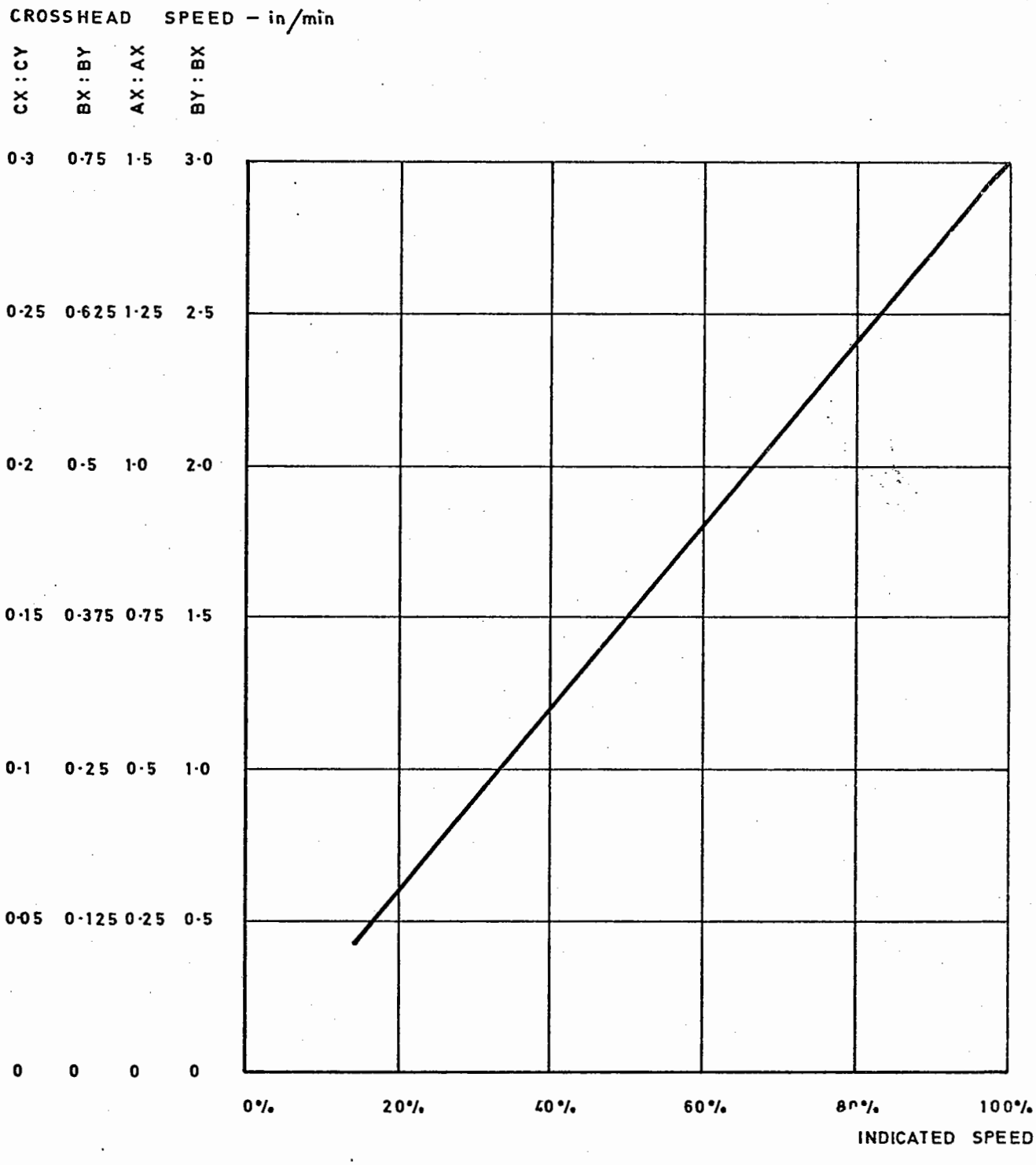

FIG. 39 CALIBRATION OF CROSSHEAD SPEEDS WITH FREQUENCY MODULATOR

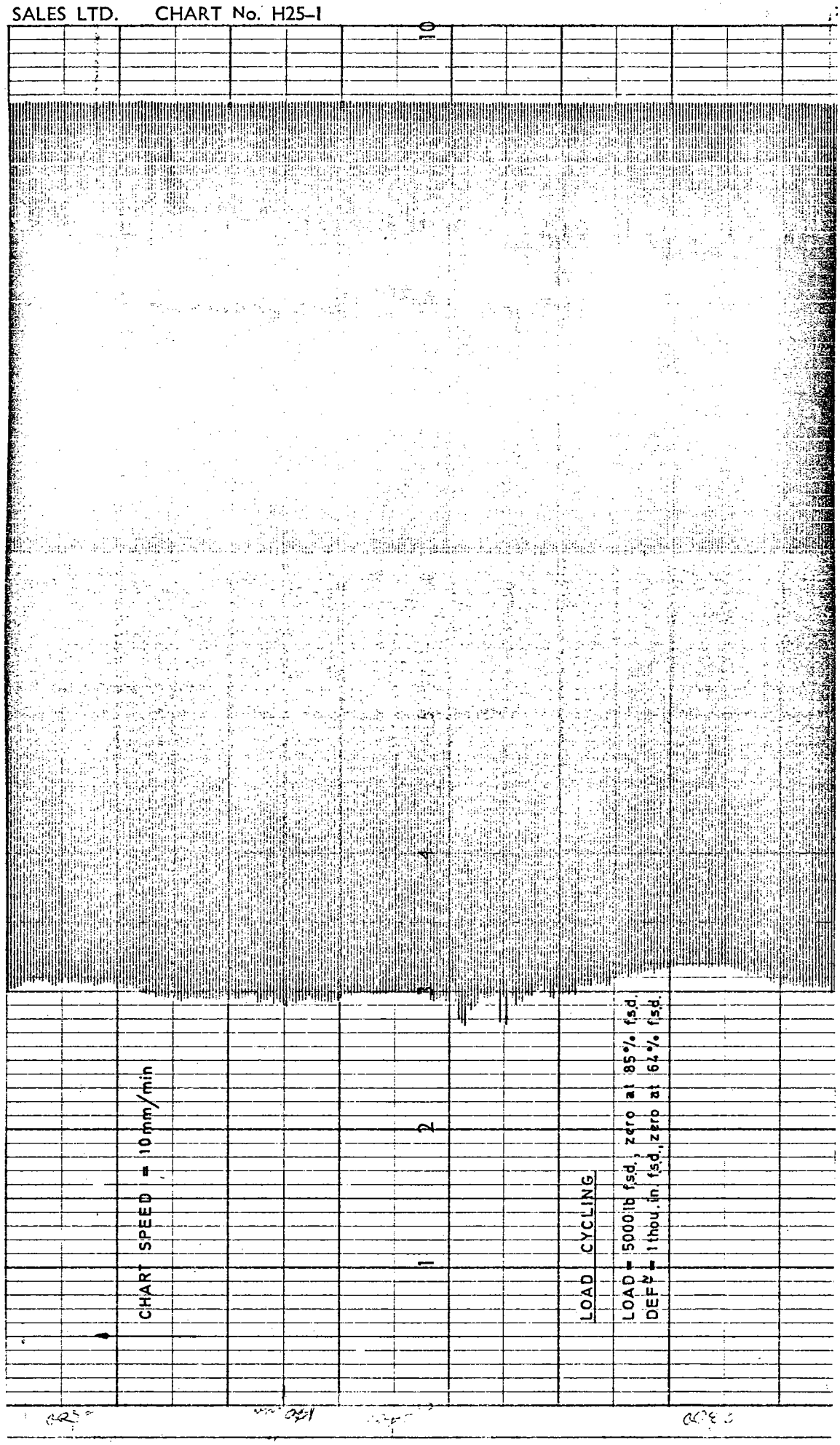

FIG. 40 RECORD OF LOAD AND DEFORMATION WHEN LOAD CYCLING STEEL DUMMY SPECIMEN WITH NO BAFFLES AROUND SPECIMEN

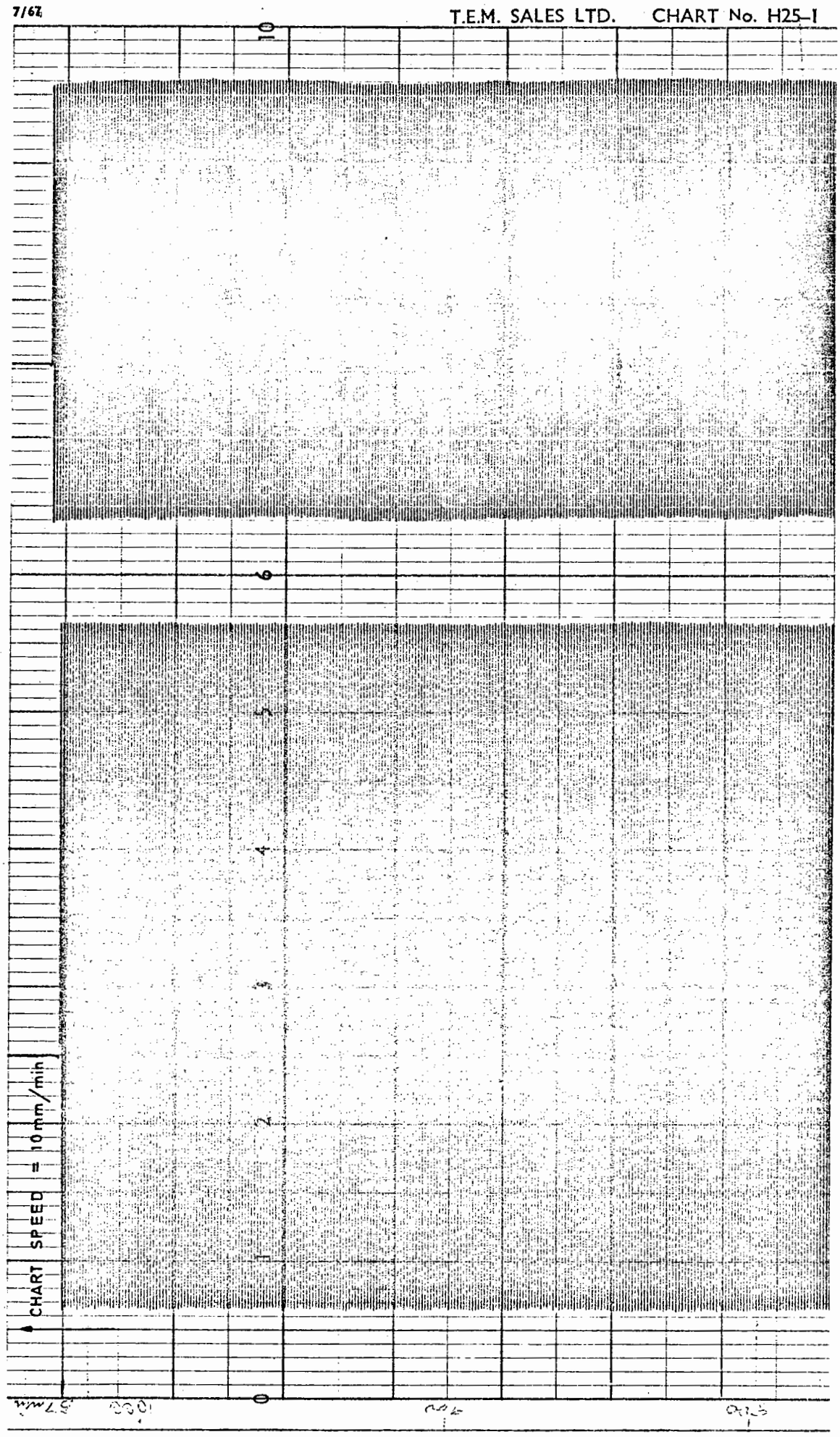

FIG. 41 RECORD OF LOAD AND DEFORMATION WHEN LOAD CYCLING STEEL DUMMY SPECIMEN WITH BAFFLES AROUND SPECIMEN

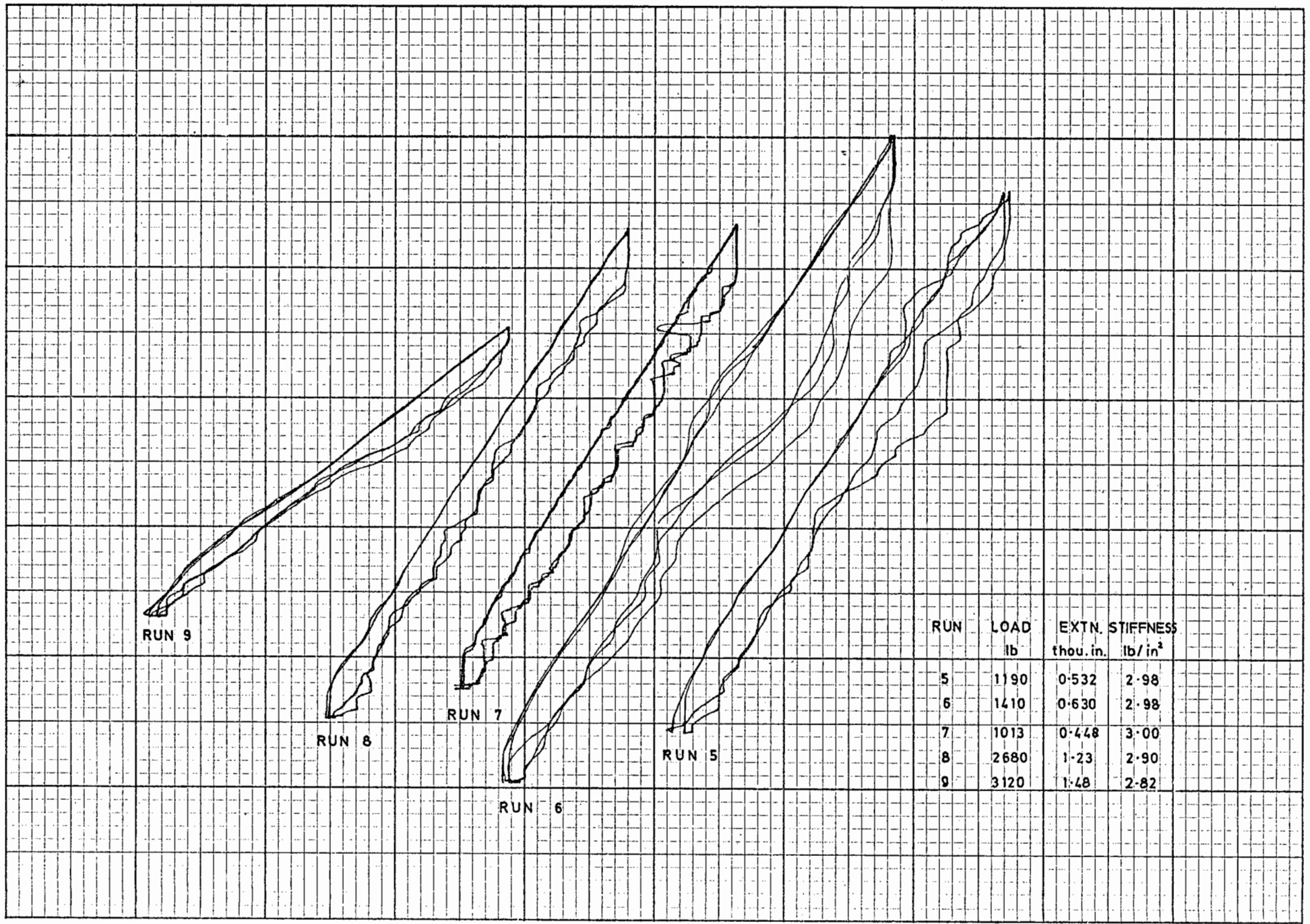

RUN	LOAD lb	EXTN. thou. in.	STIFFNESS lb/in²
5	1190	0·532	2·98
6	1410	0·630	2·98
7	1013	0·448	3·00
8	2680	1·23	2·90
9	3120	1·48	2·82

FIG. 42 RECORD OF HYSTERESIS LOOPS OF STEEL PIMPELL

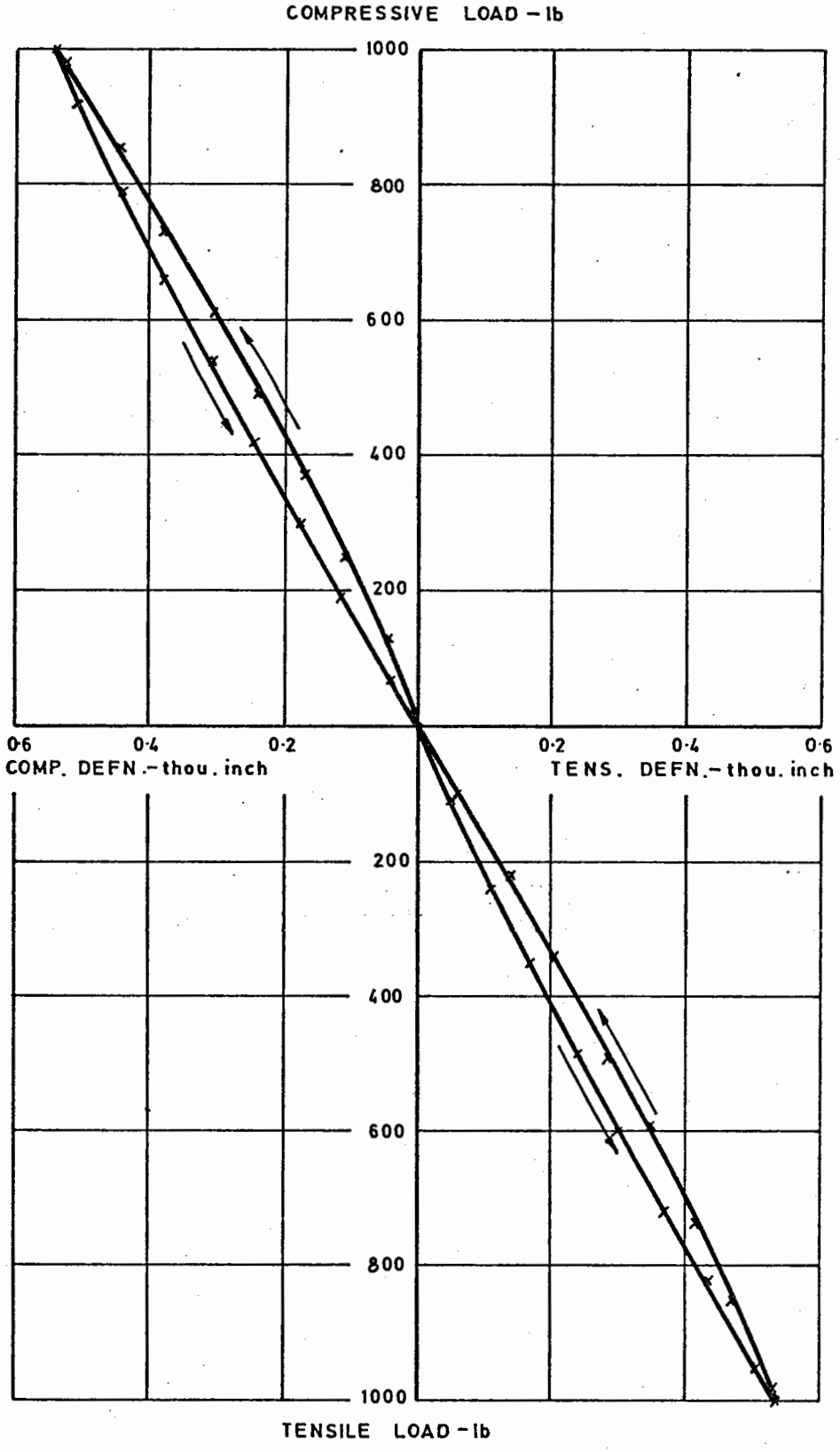

FIG. 43 HYSTERESIS LOOPS OF STEEL DUMBELL IN CONCRETE TESTING FITTINGS

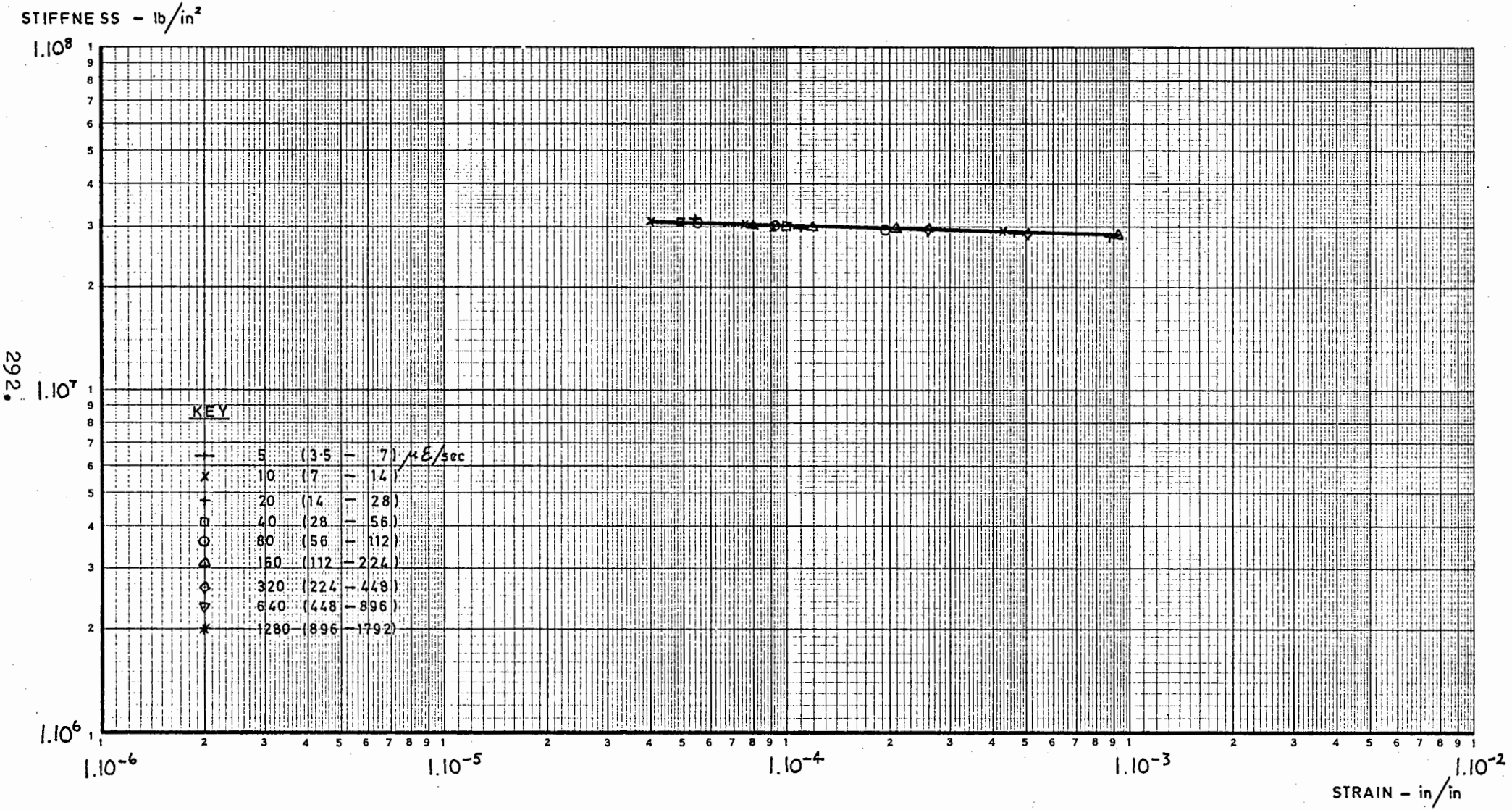

FIG. 44 EFFECT OF STRAIN LEVEL AND STRAIN RATE ON STIFFNESS OF STEEL DUMBELL

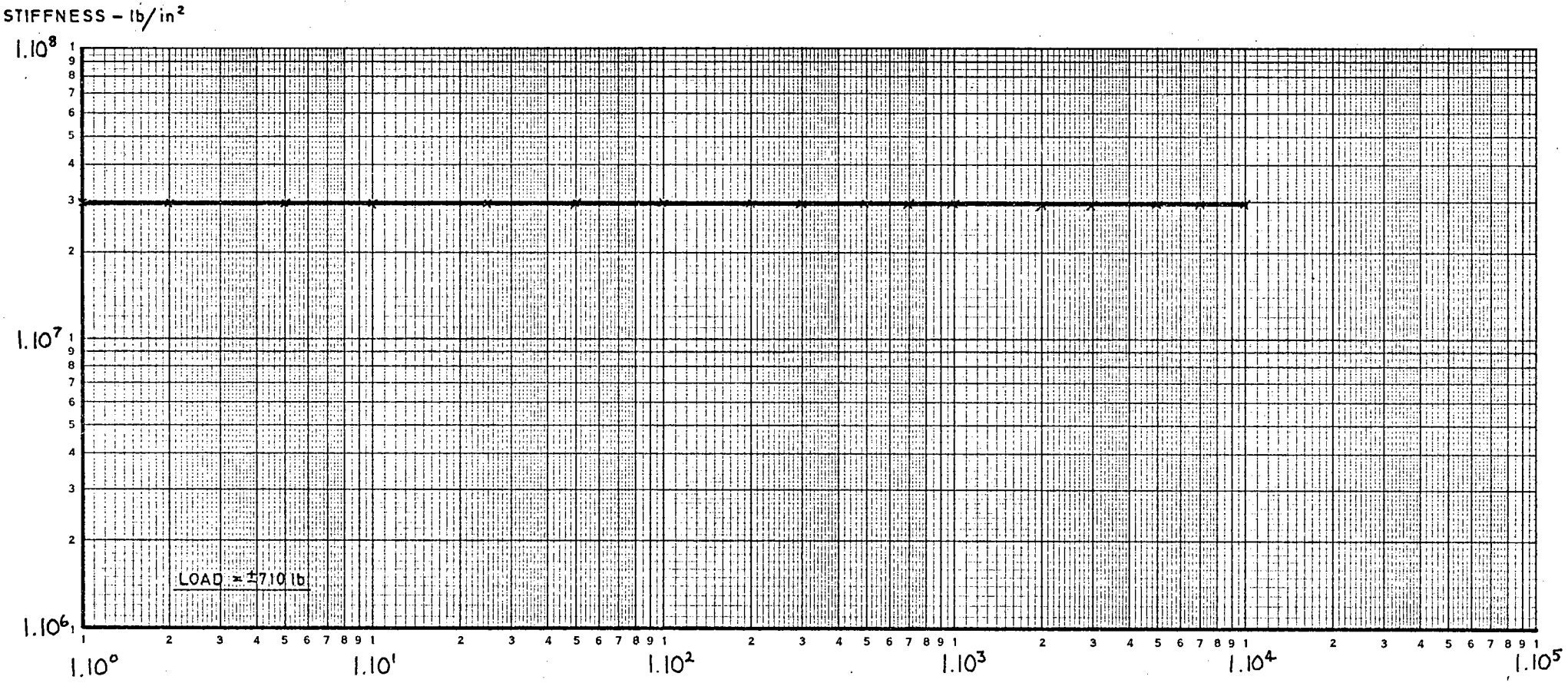

FIG. 45 CHANGE IN STIFFNESS OF STEEL DUMBELL IN STRESS-CONTROLLED REPEATED LOADING

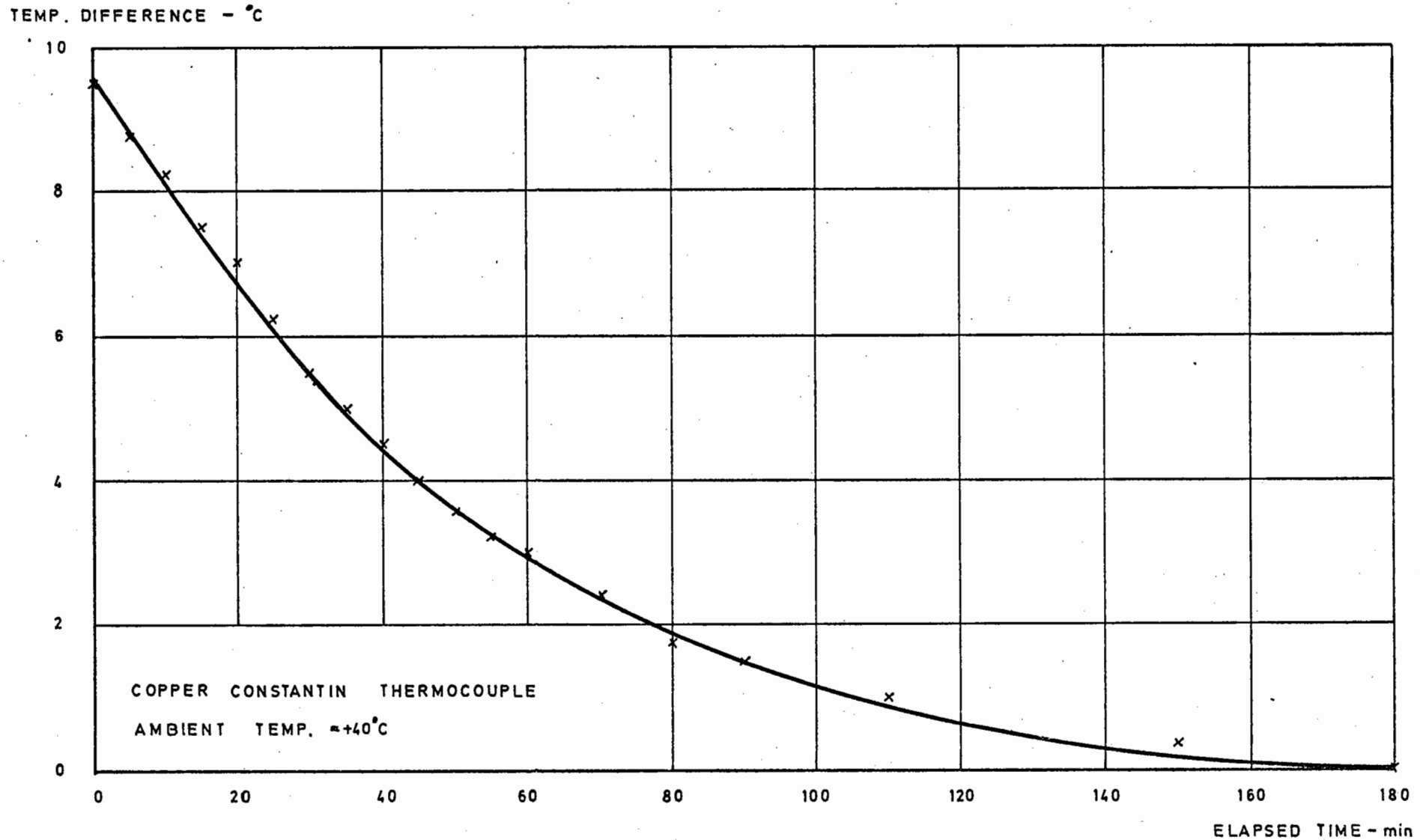

FIG. 46 CLIMATIZATION OF SAND ASPHALT SPECIMEN

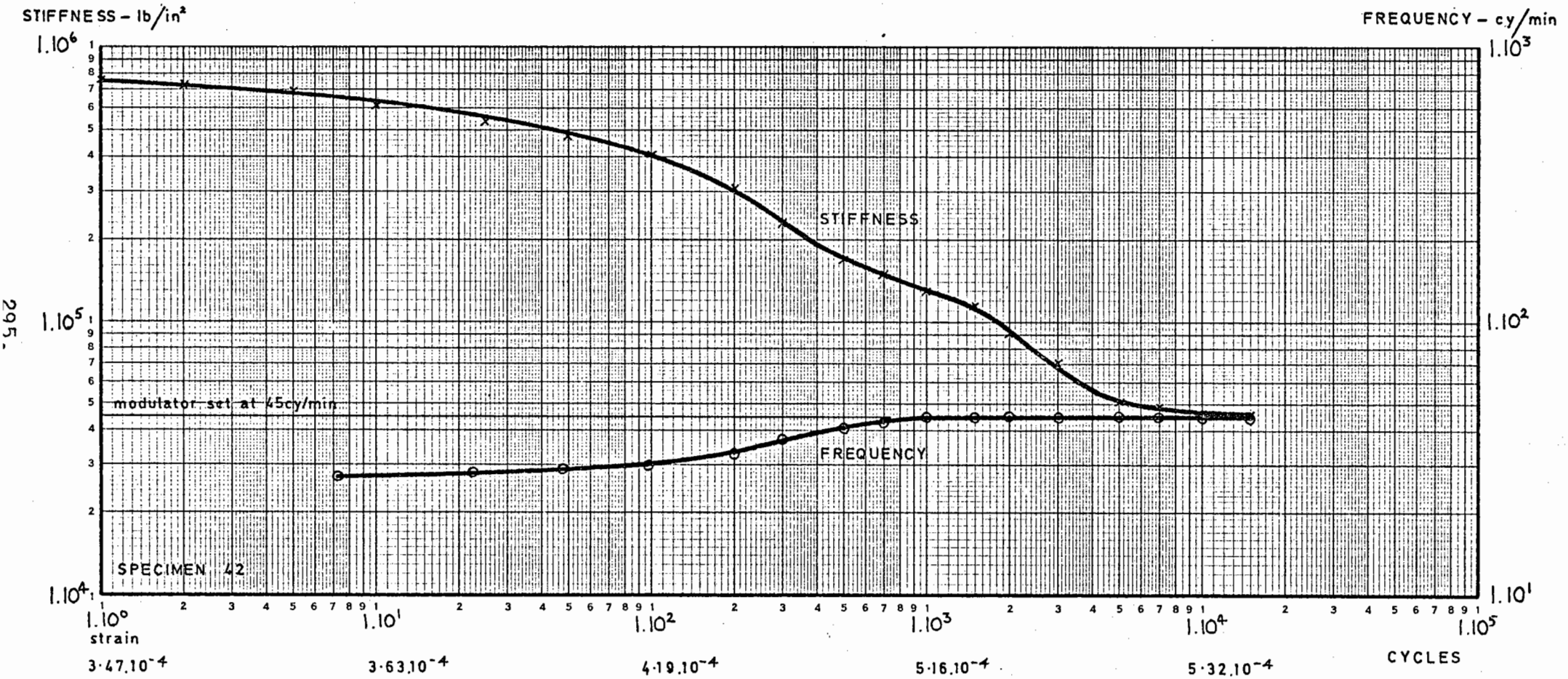

FIG. 47 FREQUENCY CORRECTION ON BITUMINOUS SPECIMEN IN STRAIN-CONTROLLED REPEATED LOADING BY MEANS OF CONE FREQUENCY MODULATOR

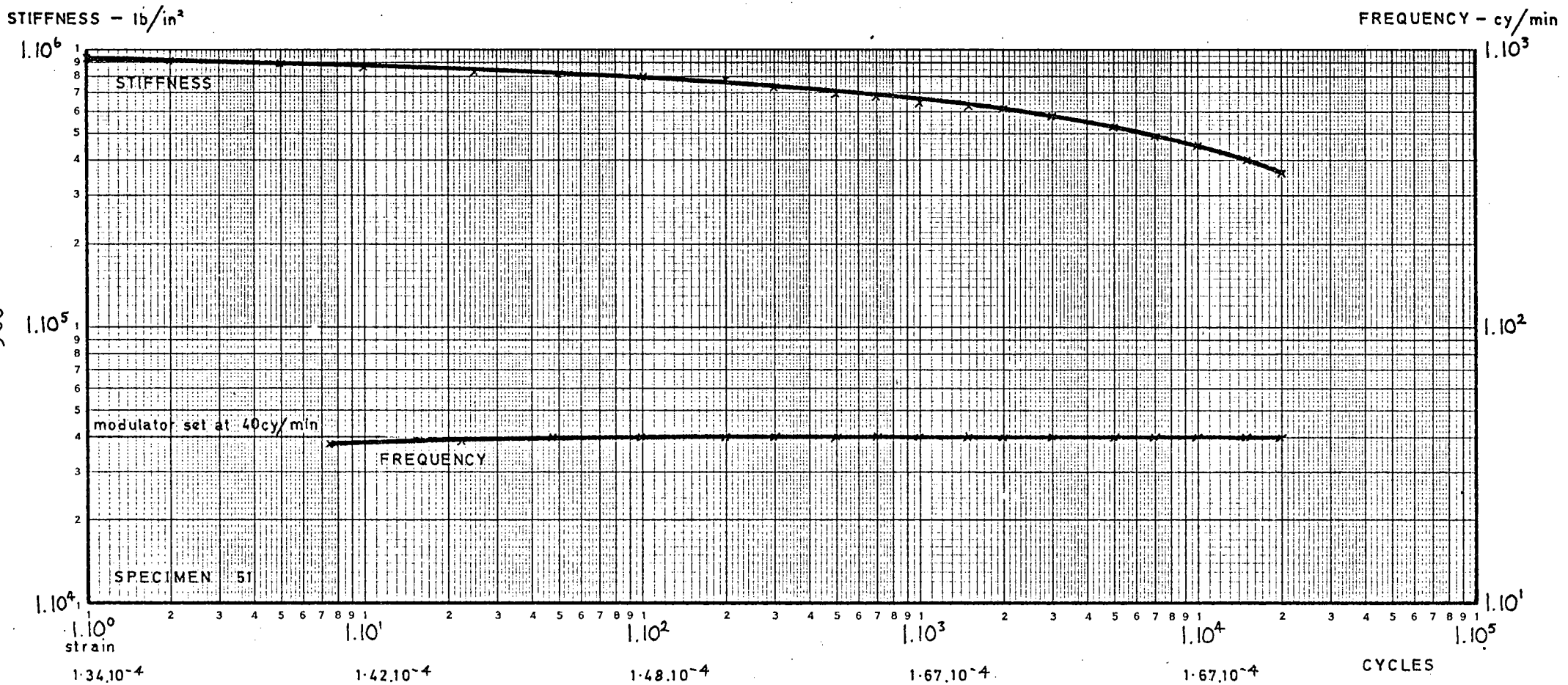

FIG. 48 FREQUENCY CORRECTION ON BITUMINOUS SPECIMEN IN STRAIN-CONTROLLED REPEATED LOADING BY MEANS OF "VARIATOR" FREQUENCY MODULATOR

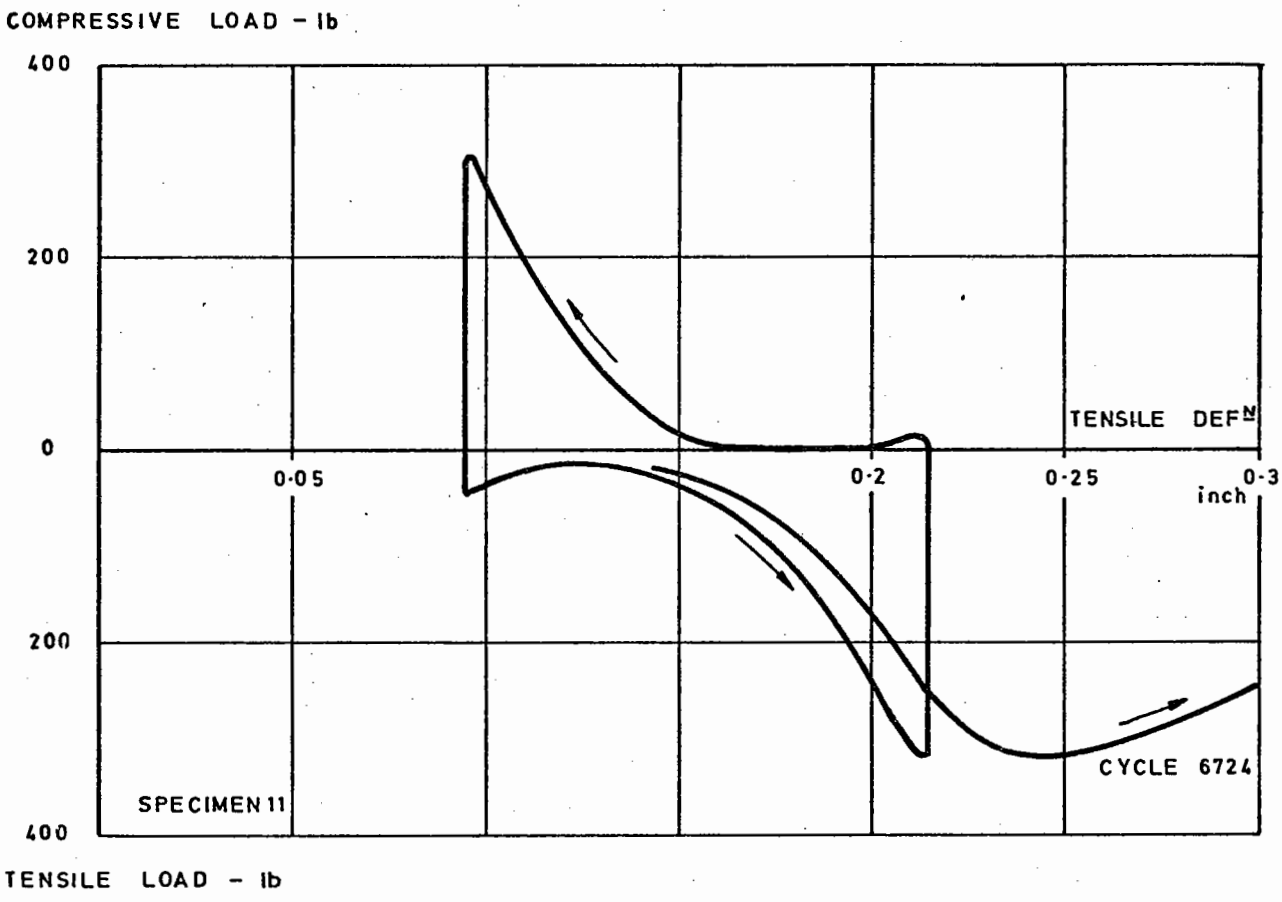

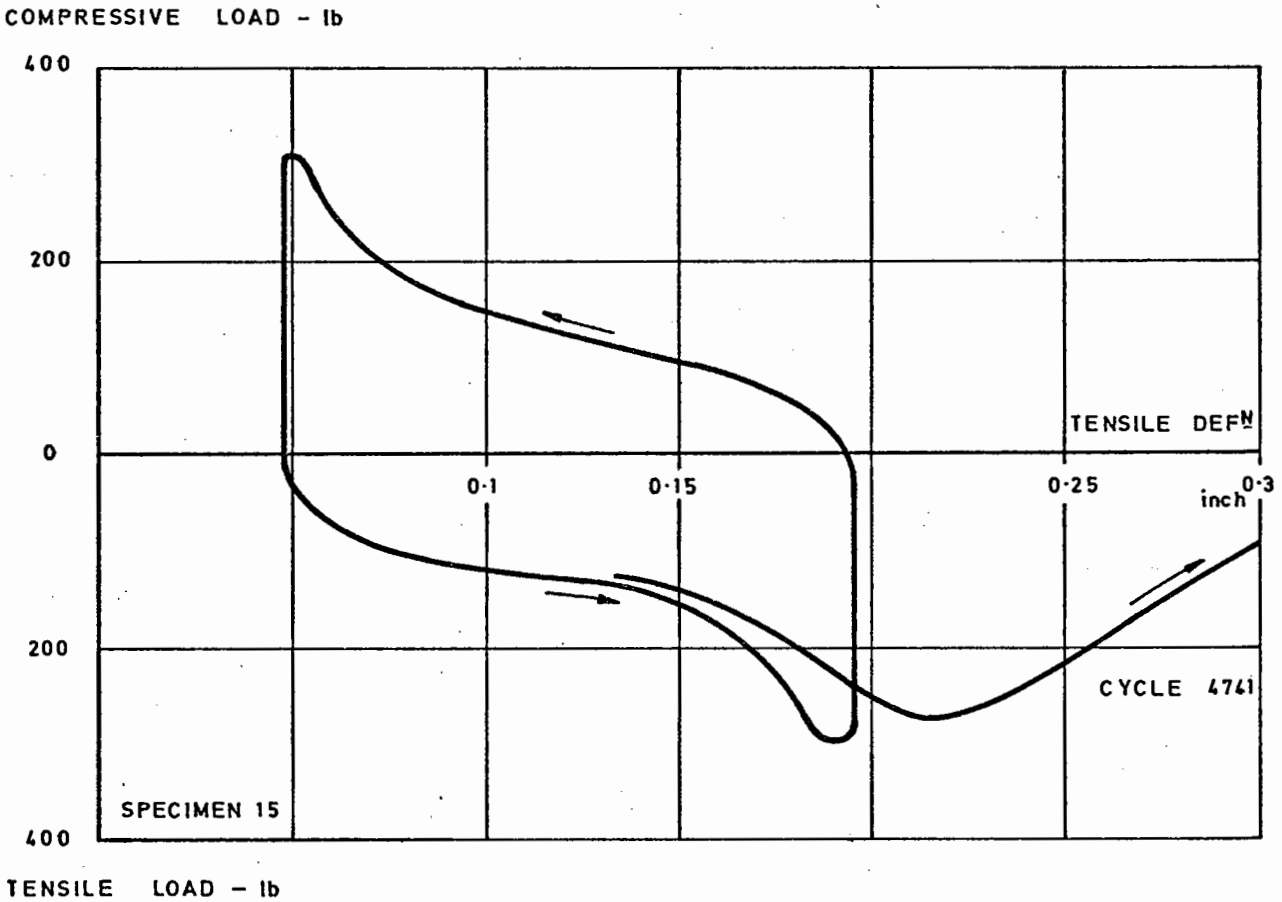

FIG. 49 RECORDS OF LAST COMPLETE CYCLES OF HOT ROLLED ASPHALT IN STRESS-CONTROLLED REPEATED LOADING

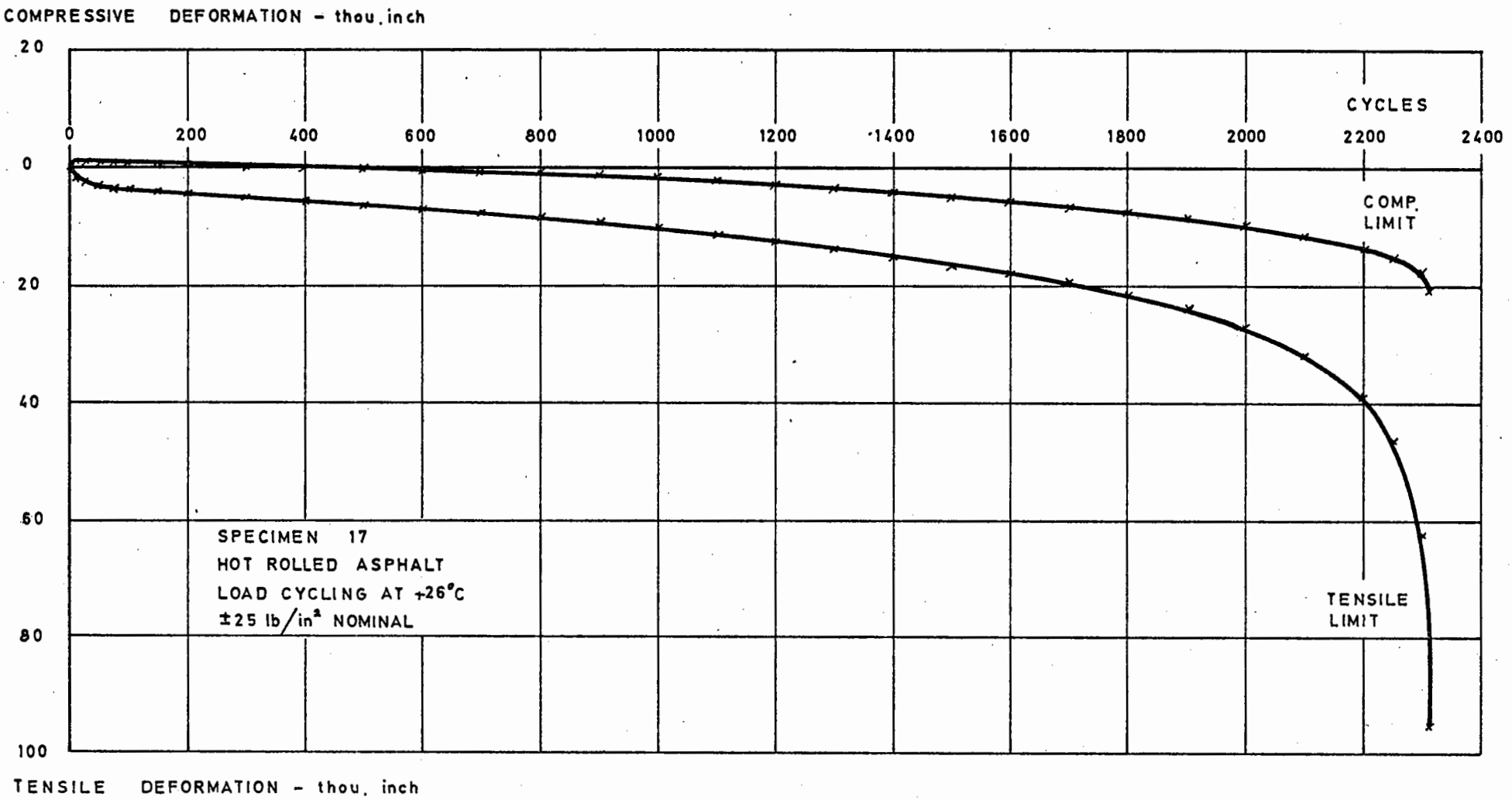

FIG. 50 DEFORMATION CURVES OF HOT ROLLED ASPHALT IN STRESS-CONTROLLED REPEATED LOADING

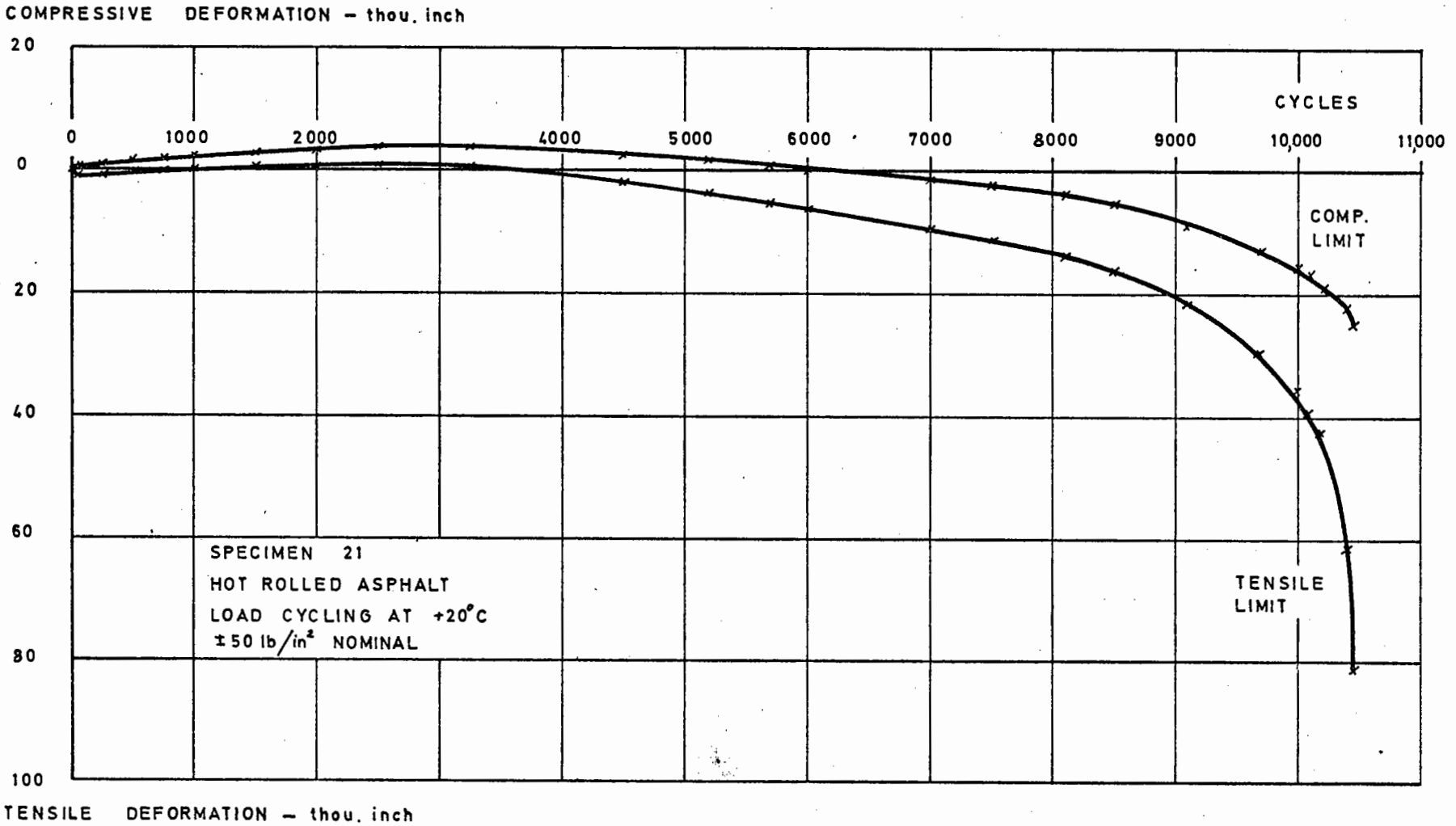

FIG. 51 DEFORMATION CURVES OF HOT ROLLED ASPHALT IN STRESS-CONTROLLED REPEATED LOADING

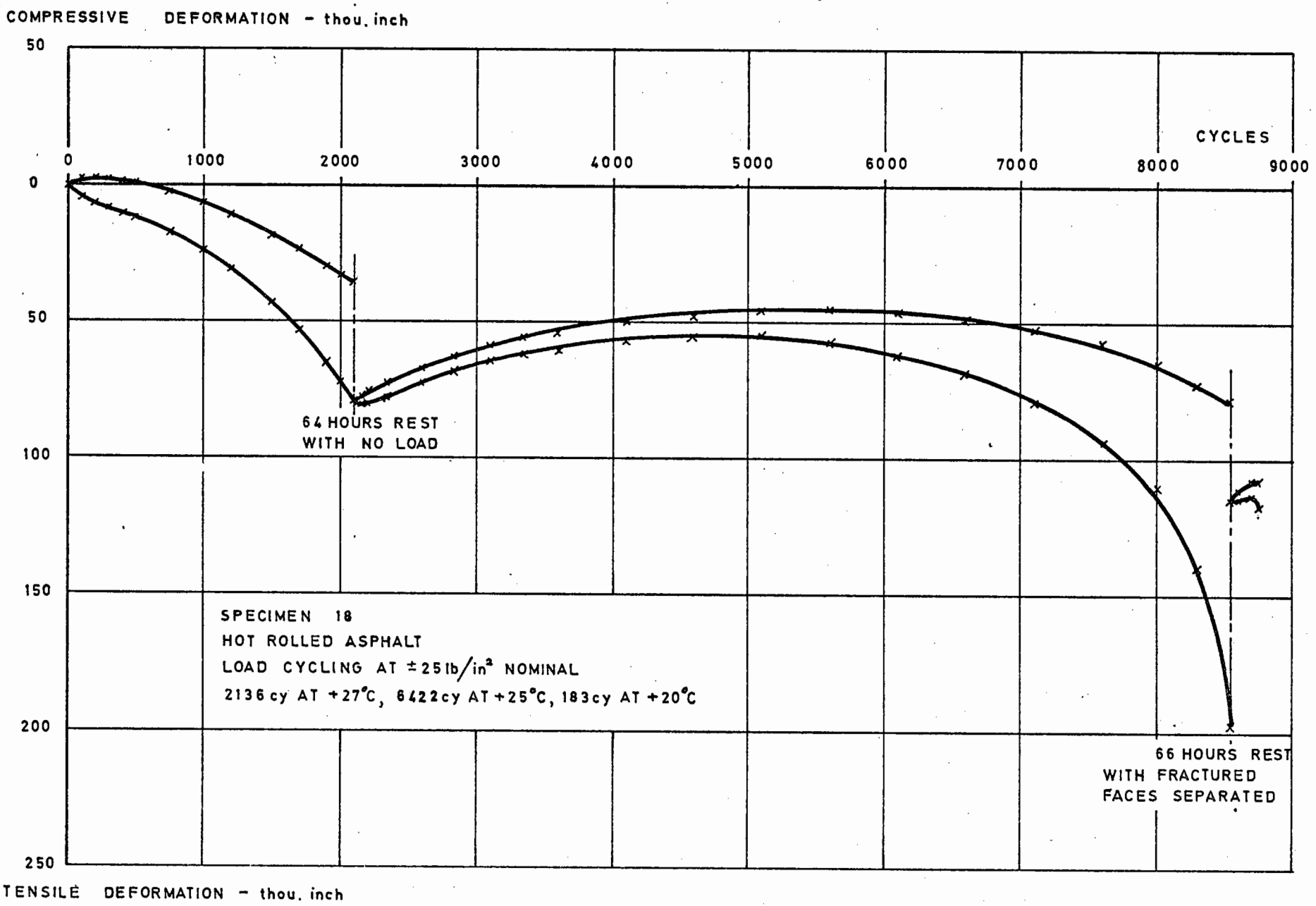

FIG. 52 DEFORMATION CURVES OF HOT ROLLED ASPHALT IN STRESS-CONTROLLED REPEATED LOADING WITH REST PERIODS BEFORE AND AFTER FRACTURE

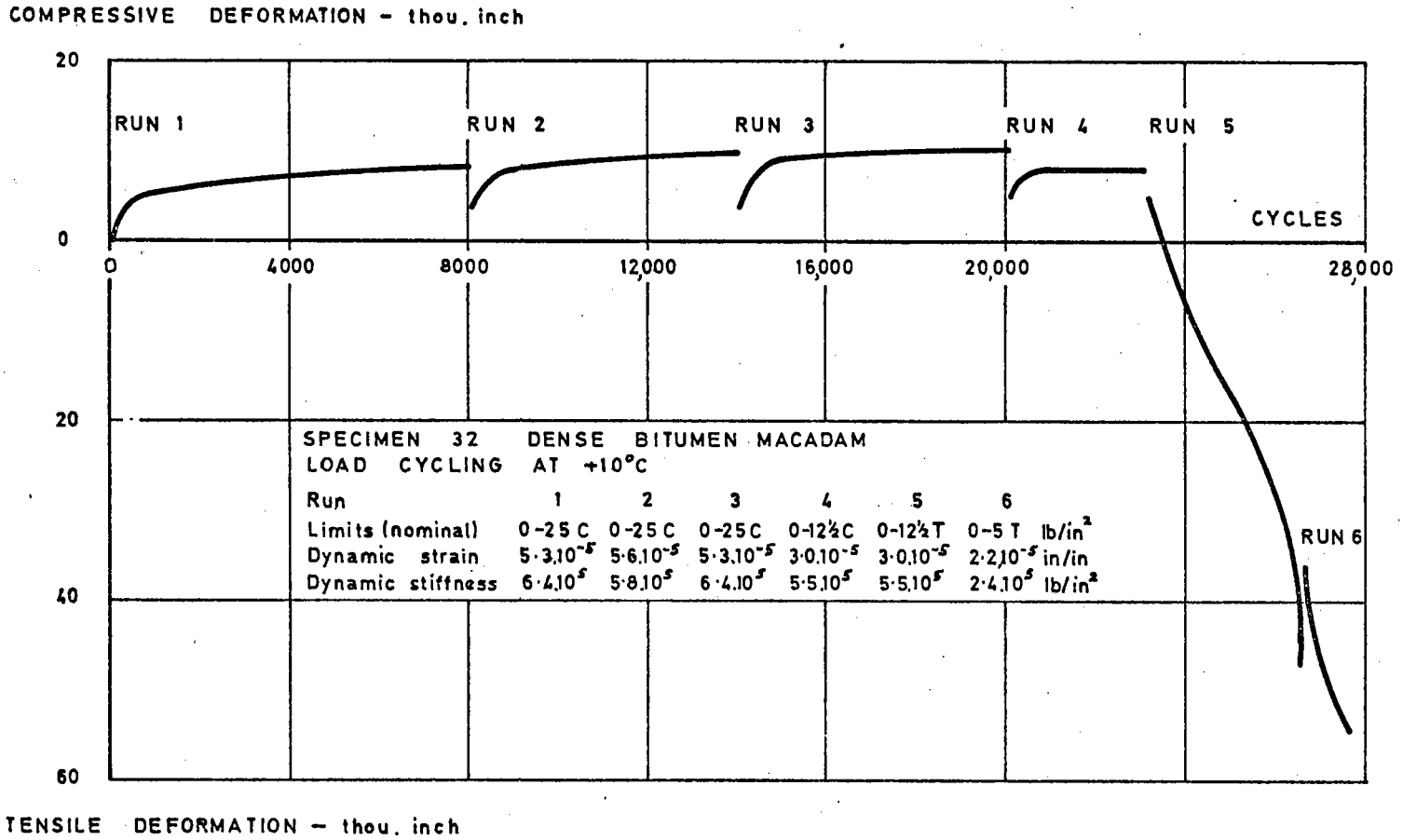

FIG. 53 DEFORMATION CURVES OF DENSE BITUMEN MACADAM IN VARIOUS LEVELS OF STRESS-CONTROLLED REPEATED LOADING

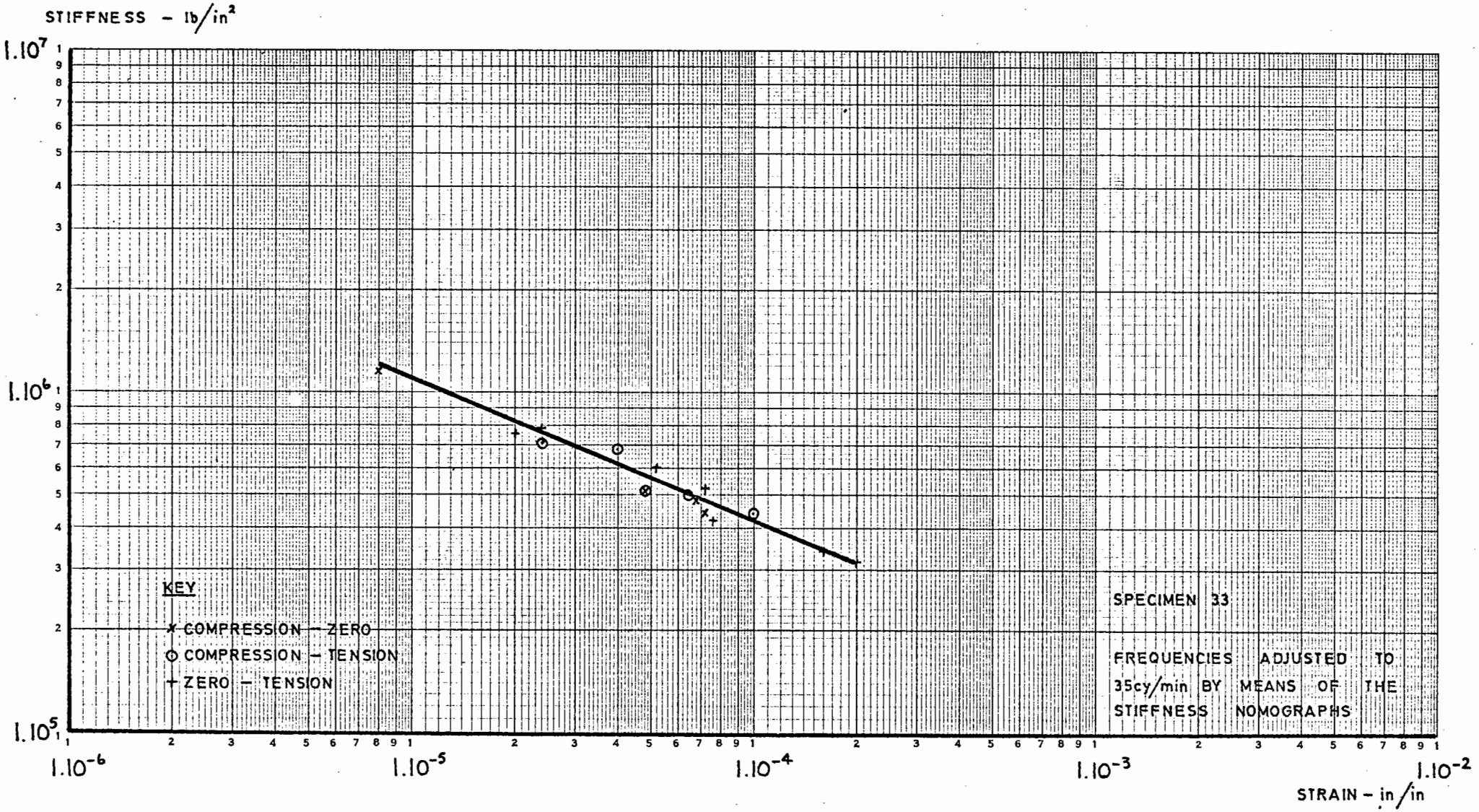

FIG. 54 EFFECT OF STRAIN LEVEL AND STRAIN MODE ON STIFFNESS OF DENSE BITUMEN MACADAM

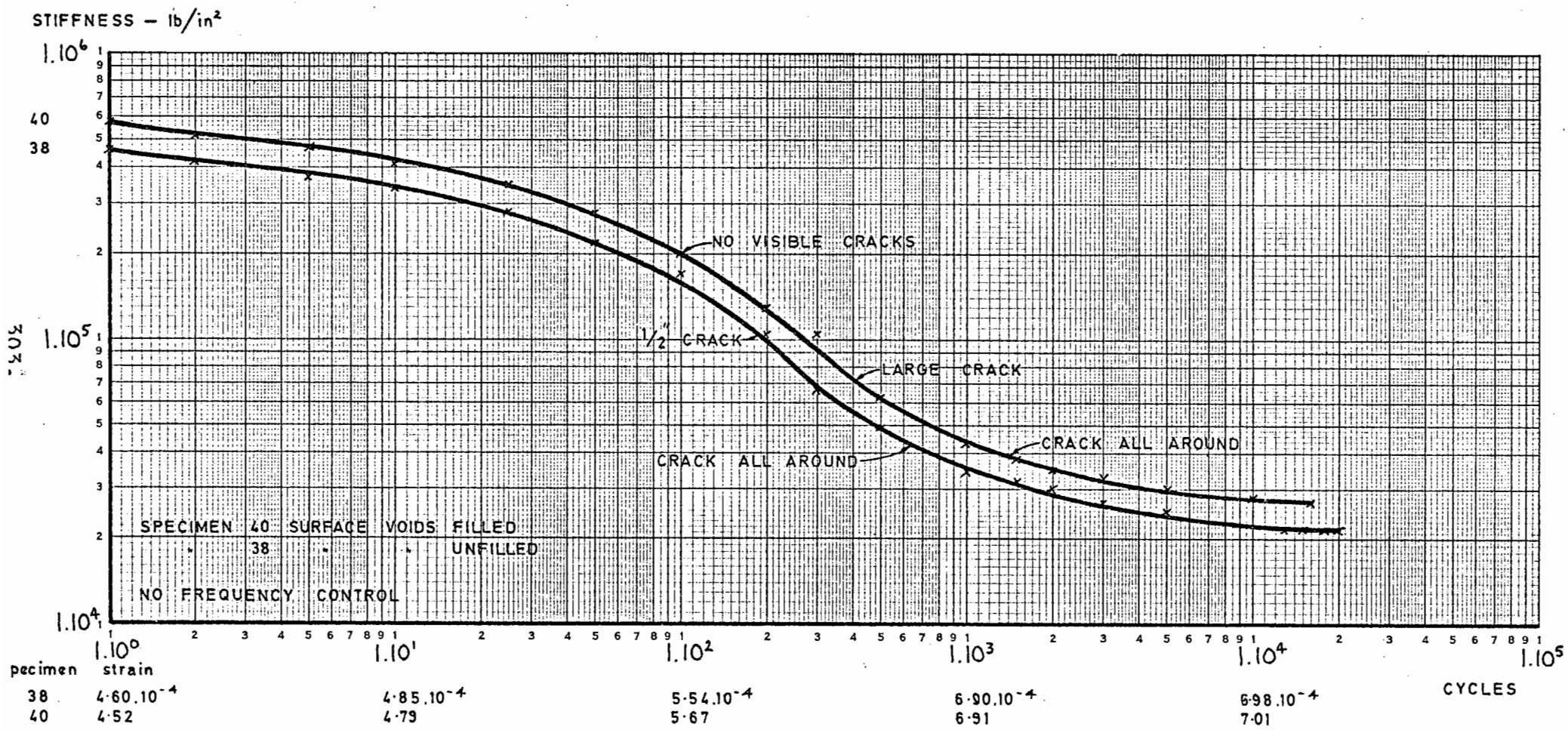

FIG. 55 CHANGE IN STIFFNESS OF DENSE BITUMEN MACADAM IN STRAIN-CONTROLLED REPEATED LOADING AT +10°C

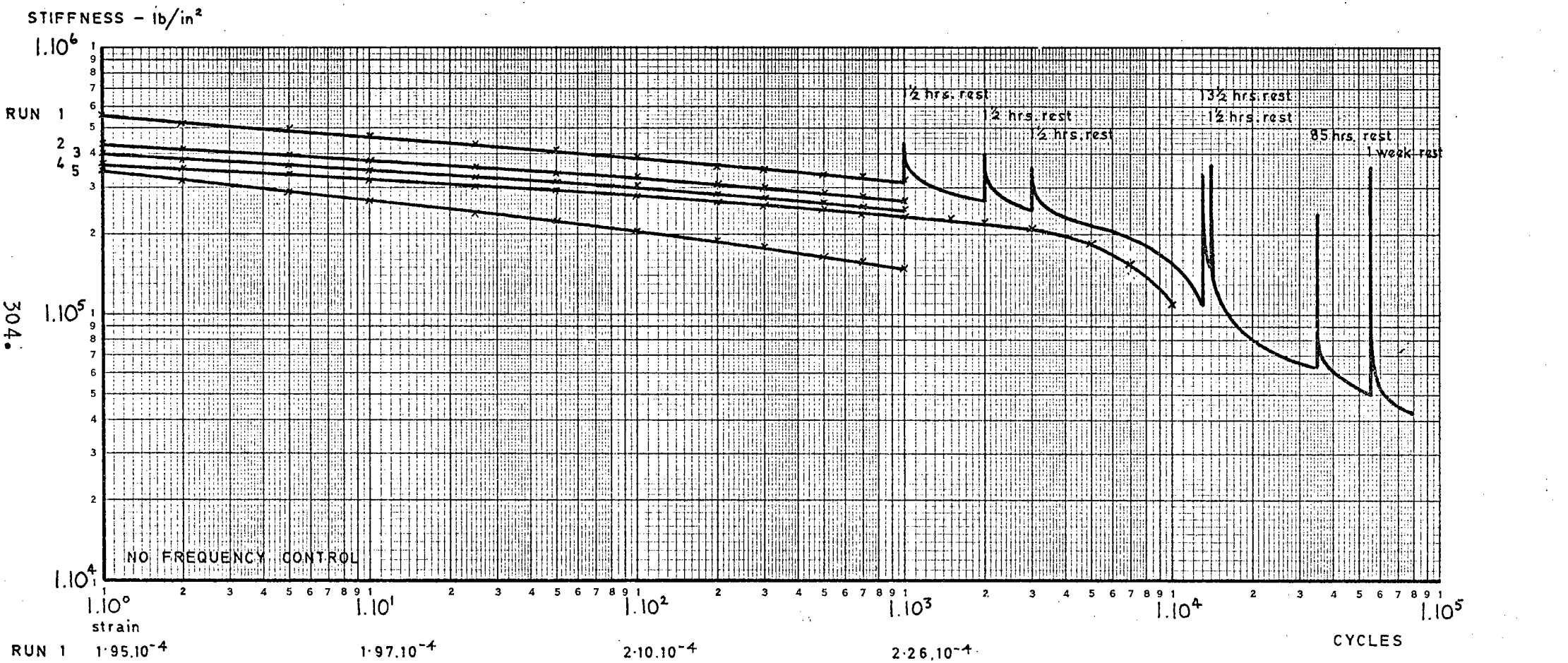

FIG. 56 EFFECT OF REST PERIODS ON CHANGE IN STIFFNESS OF SAND ASPHALT IN STRAIN-CONTROLLED REPEATED LOADING AT +10°C

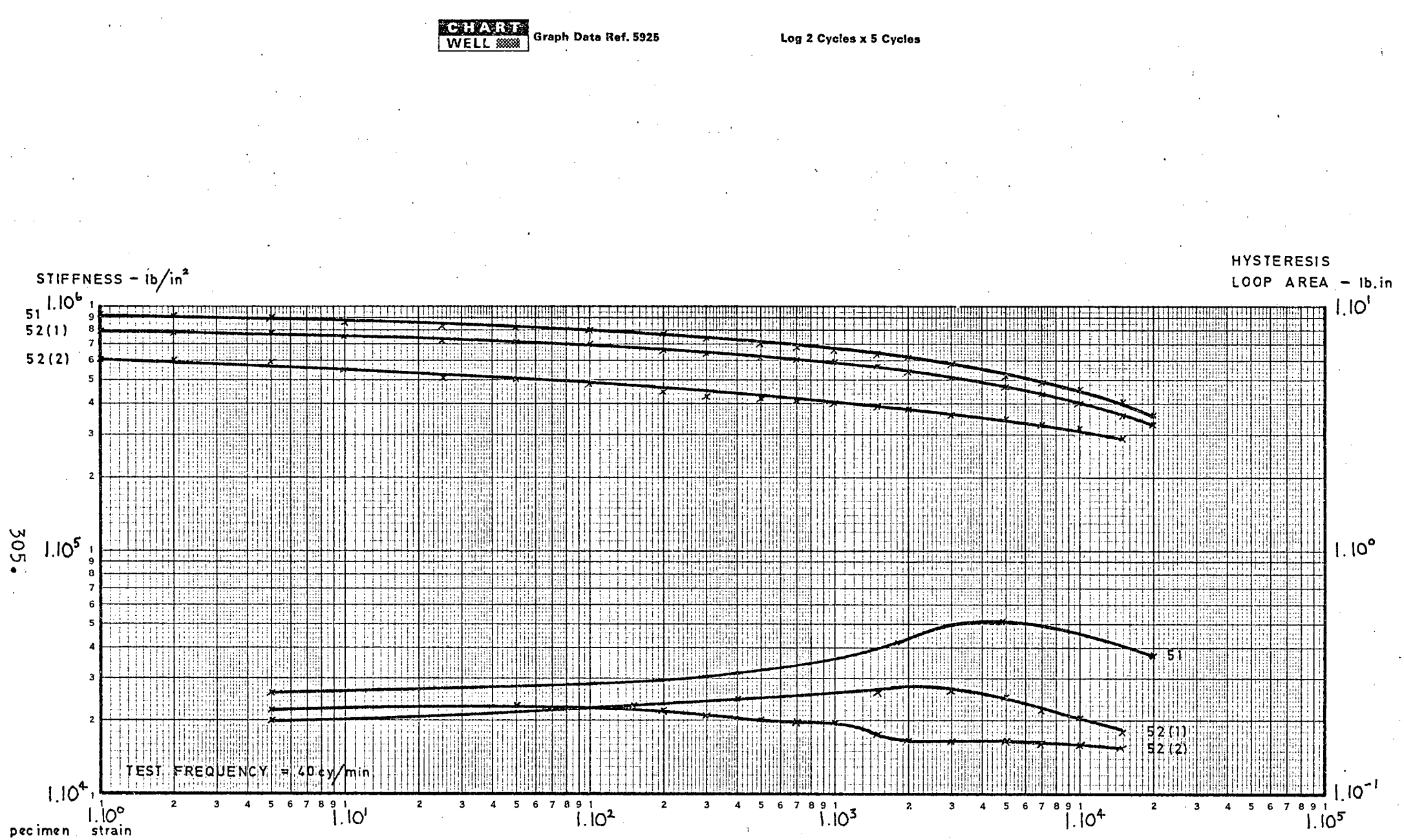

Specimen	strain				
51	$1 \cdot 34.10^{-4}$	$1 \cdot 42.10^{-4}$	$1 \cdot 48.10^{-4}$	$1 \cdot 67.10^{-4}$	$1 \cdot 67.10^{-4}$
52(1)	$9 \cdot 57.10^{-5}$	$9 \cdot 91.10^{-5}$	$1 \cdot 06.10^{-4}$	$1 \cdot 18.10^{-4}$	$1 \cdot 23.10^{-4}$
52(2)	$9 \cdot 78.10^{-5}$	$1 \cdot 04.10^{-4}$	$1 \cdot 27.10^{-4}$	$1 \cdot 37.10^{-4}$	$1 \cdot 49.10^{-4}$

FIG. 57 CHANGE IN STIFFNESS AND HYSTERESIS LOOP AREAS OF DENSE BITUMEN MACADAM IN STRAIN-CONTROLLED REPEATED LOADING AT +10°C

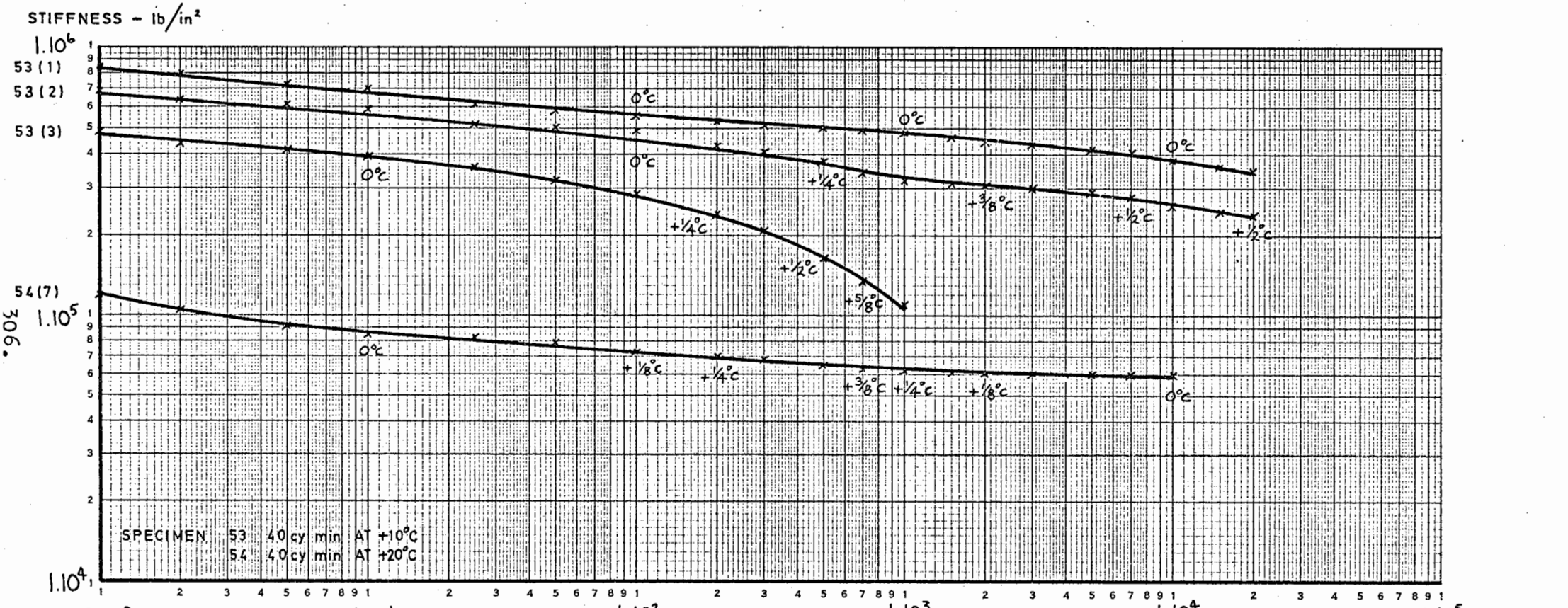

53 (1)	$2 \cdot 60.10^{-4}$	$2 \cdot 58.10^{-4}$	$2 \cdot 55.10^{-4}$	$2 \cdot 48.10^{-4}$	$2 \cdot 24.10^{-4}$
53 (2)	$5 \cdot 17$	$5 \cdot 25$	$5 \cdot 85$	$6 \cdot 98$	$5 \cdot 35$
53 (3)	$1 \cdot 10.10^{-3}$	$1 \cdot 05.10^{-3}$	$1 \cdot 27.10^{-3}$	$8 \cdot 48.10^{-3}$	—
54 (7)	$2 \cdot 10$	$2 \cdot 33$	$2 \cdot 36$	$2 \cdot 15$	$2 \cdot 07.10^{-3}$

FIG. 58 INTERNAL TEMPERATURE CHANGES OF SAND ASPHALTS IN STRAIN-CONTROLLED REPEATED LOADING

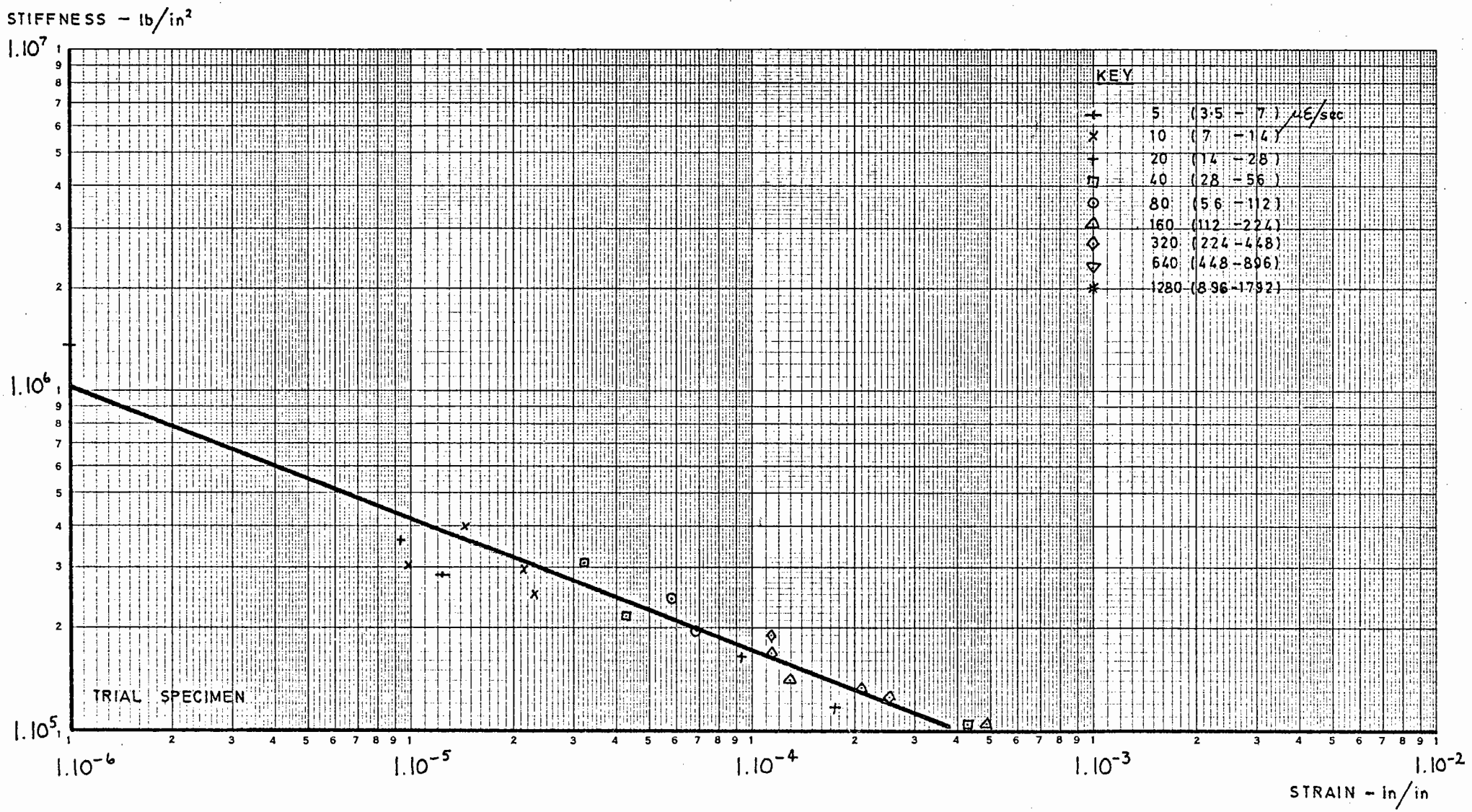

FIG. 59 EFFECT OF STRAIN LEVEL AND STRAIN RATE ON STIFFNESS OF TRIAL SPECIMEN OF DRY LEAN CONCRETE WITH UNMODIFIED MOUNTINGS AT +10°C

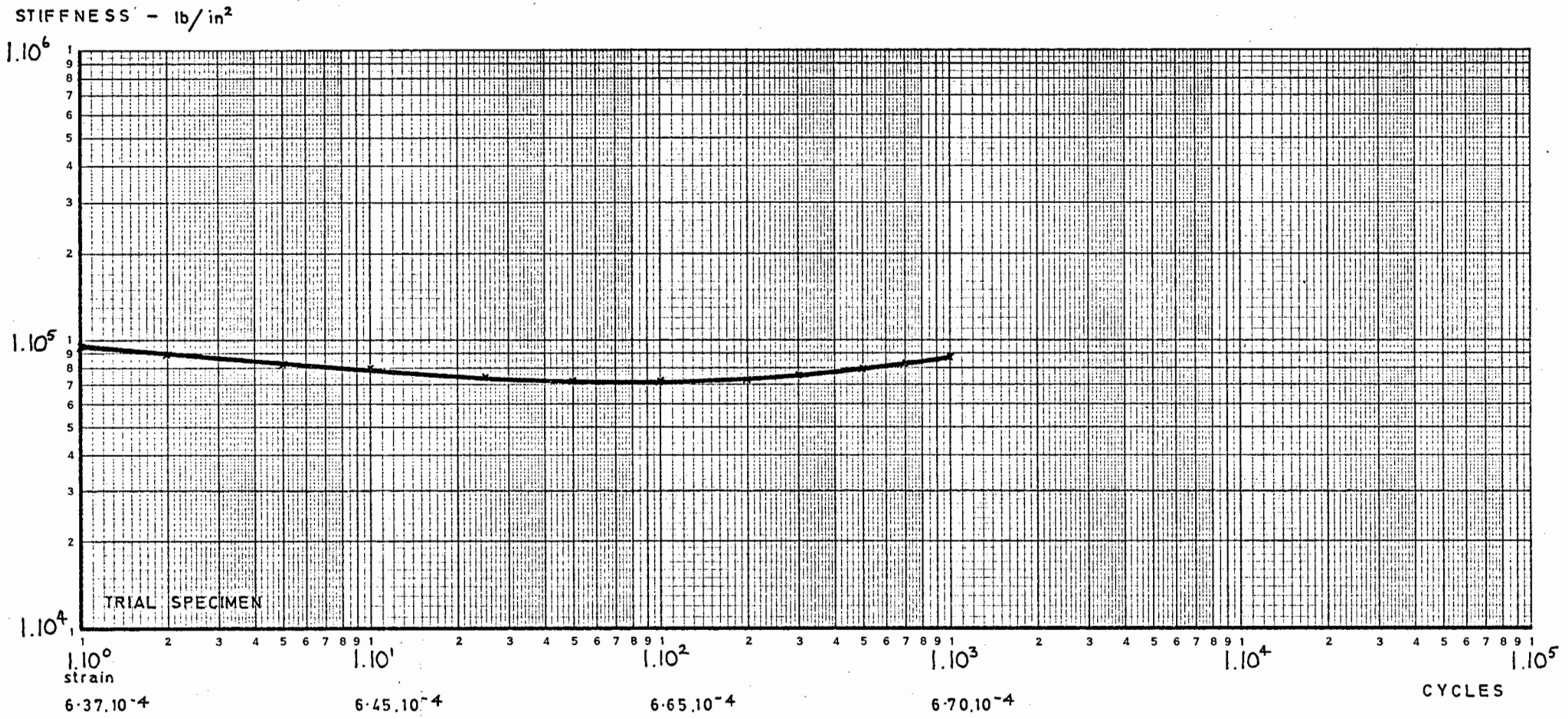

FIG. 60 CHANGE IN STIFFNESS OF TRIAL SPECIMEN OF DRY LEAN CONCRETE IN STRAIN-CONTROLLED REPEATED LOADING AT +10°C

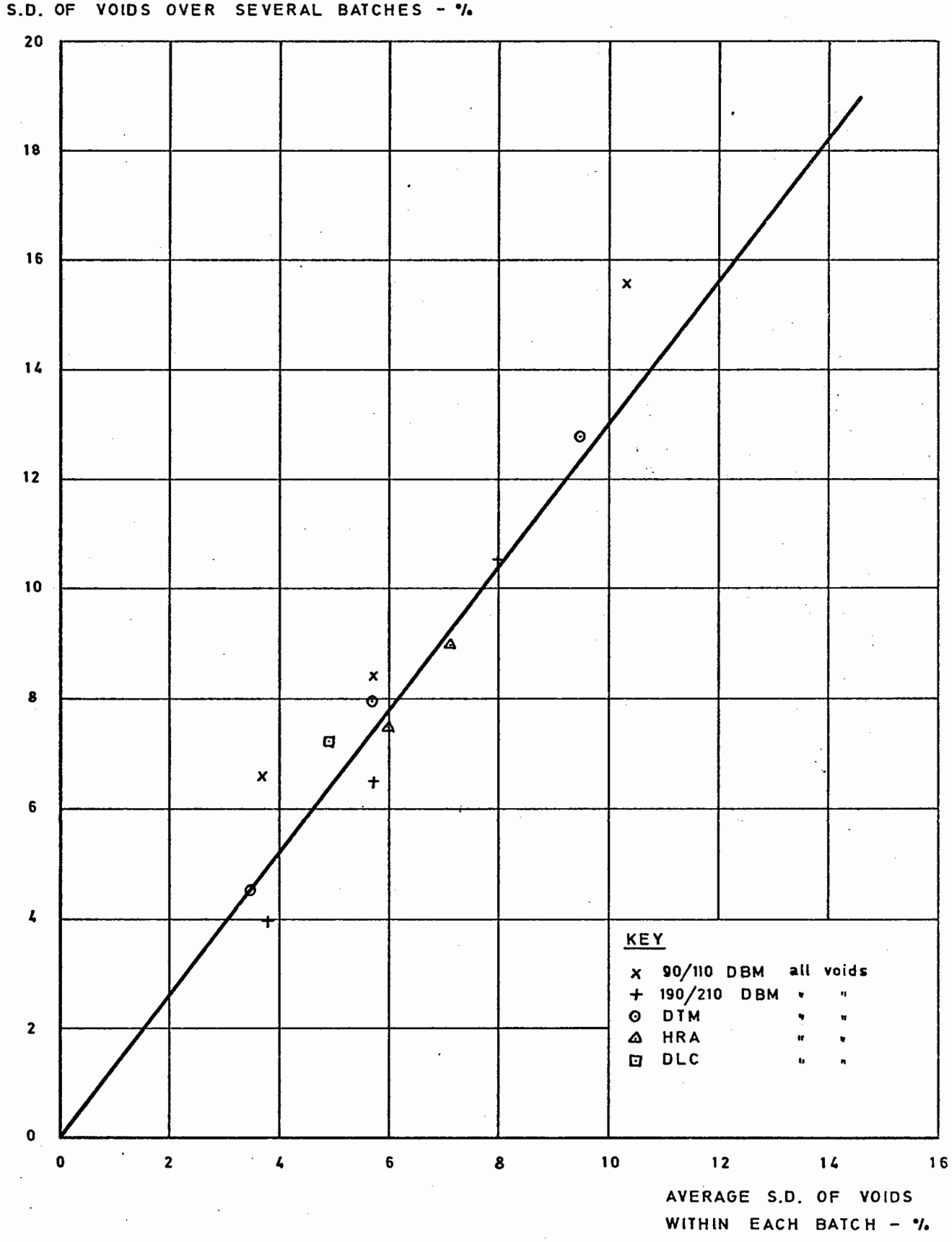

FIG. 61 STANDARD DEVIATION OF VOIDS IN ALL SPECIMENS PRODUCED

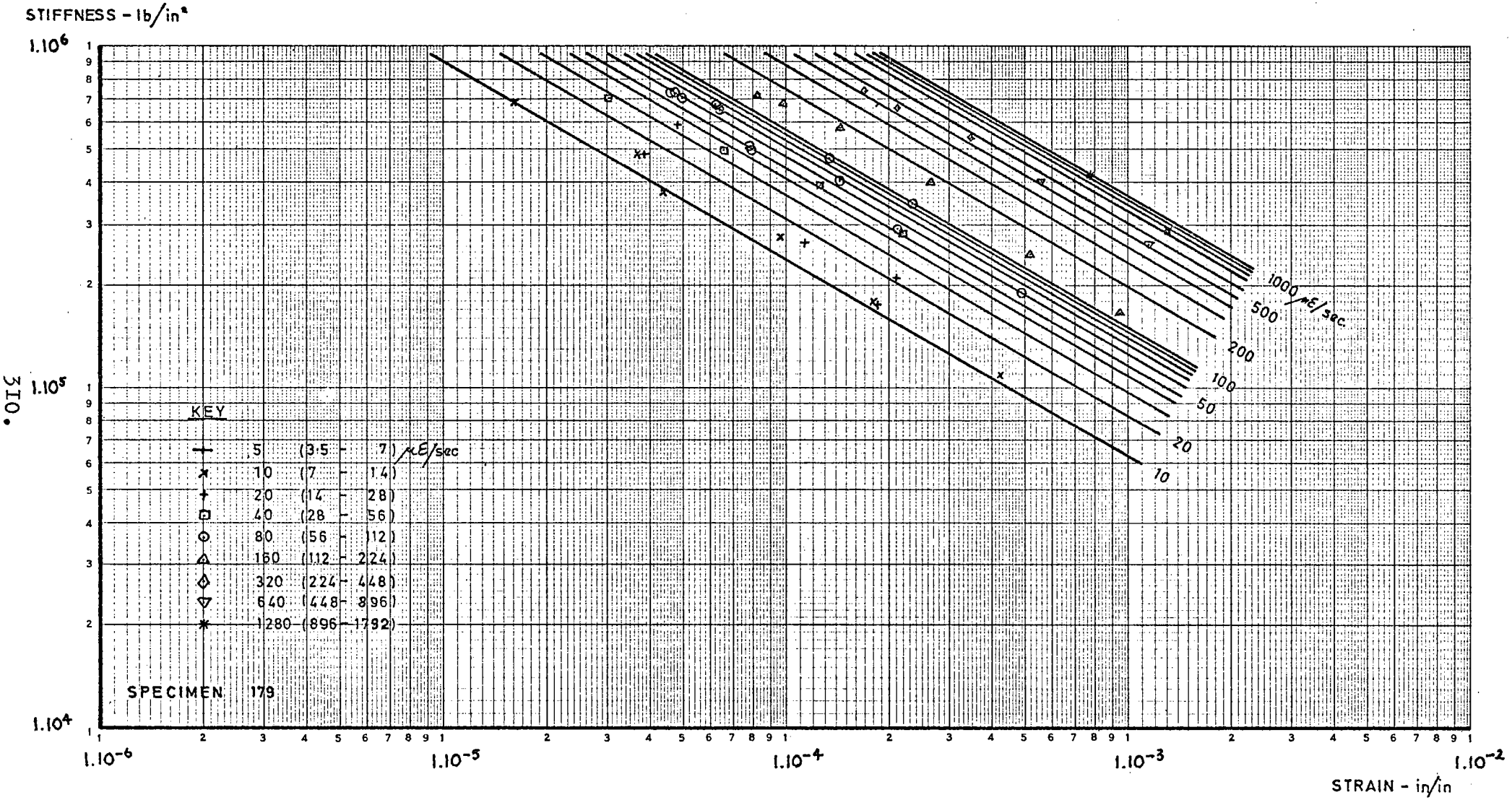

FIG. 62 EFFECT OF STRAIN LEVEL AND STRAIN RATE ON SPECIMEN OF 90/110 DENSE BITUMEN MACADAM AT +10°C

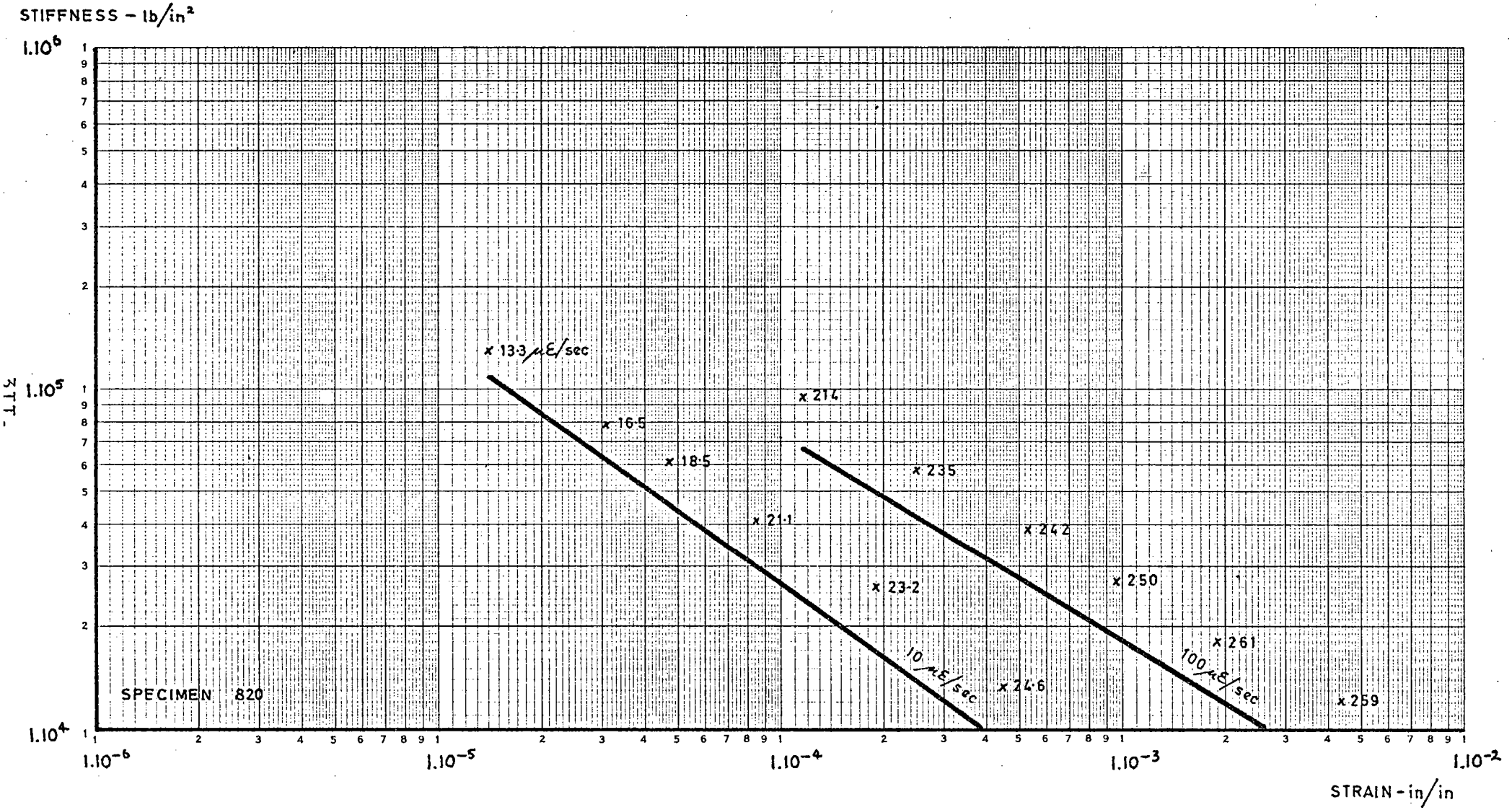

FIG. 63 EFFECT OF STRAIN LEVEL AND STRAIN RATE ON SPECIMEN OF HOT ROLLED ASPHALT AT +30°C

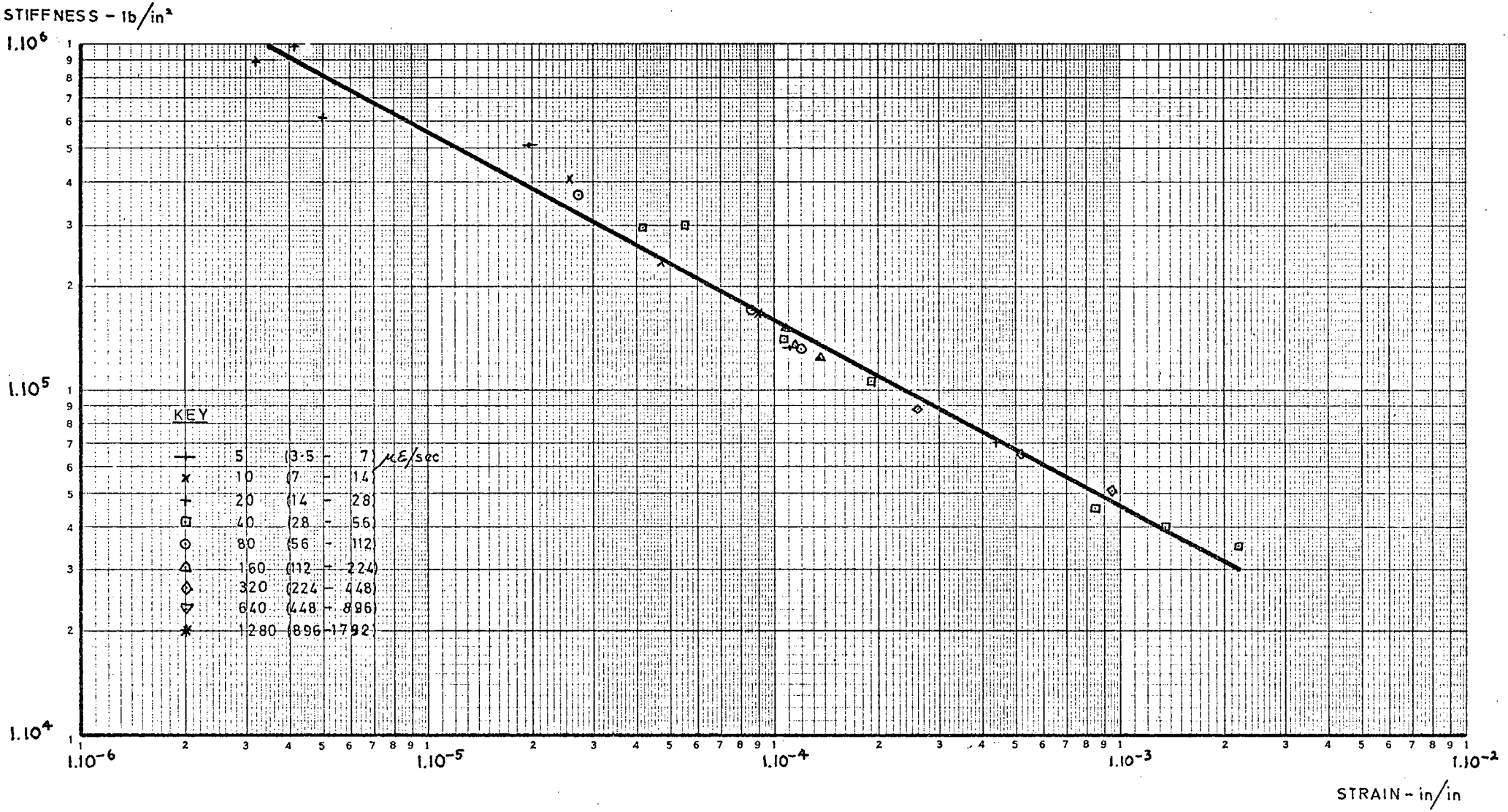

FIG. 64 EFFECT OF STRAIN LEVEL AND STRAIN RATE ON SPECIMEN OF DRY LEAN CONCRETE AT +20° C

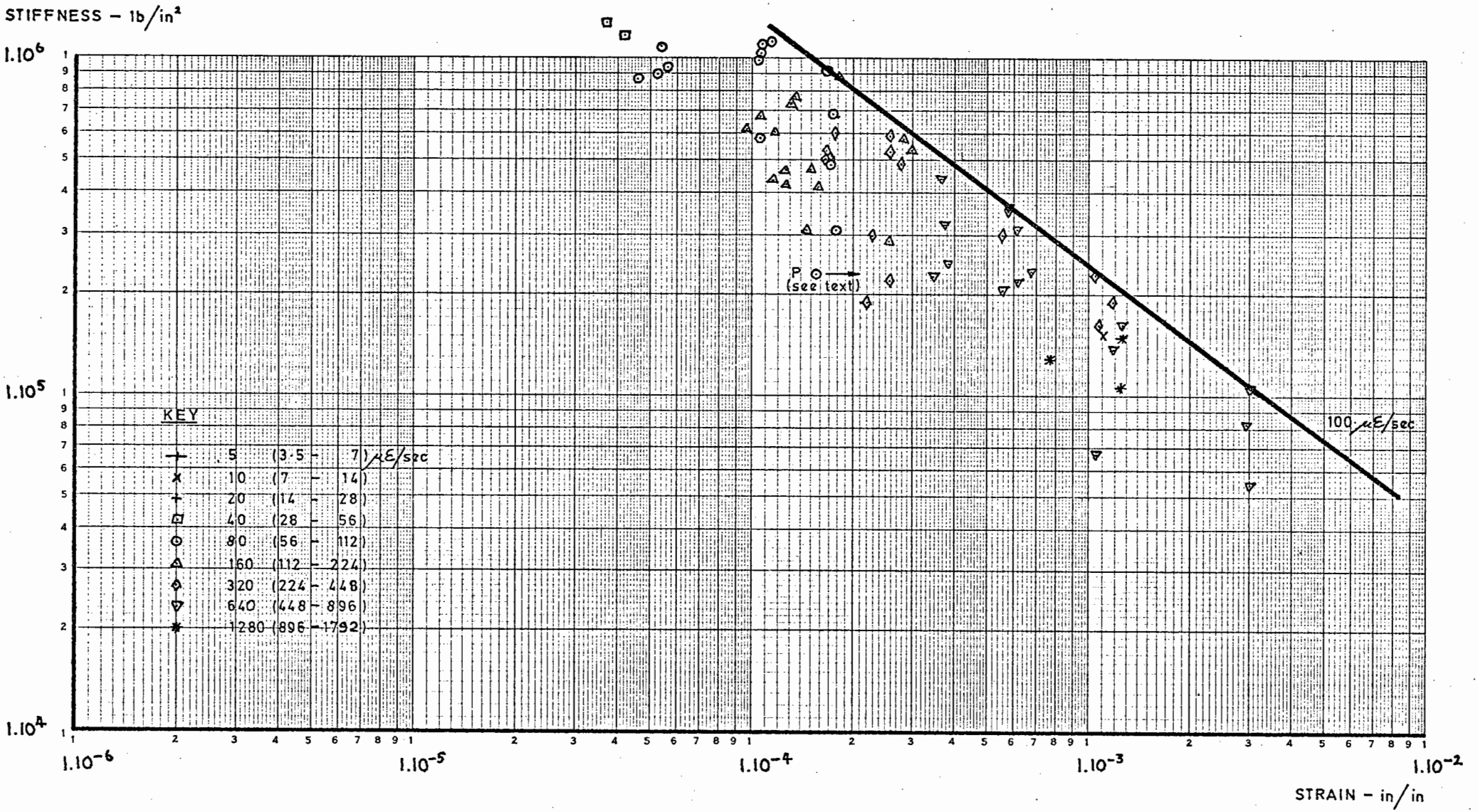

FIG. 65 MAXIMUM STIFFNESS OF 90/110 DENSE BITUMEN MACADAM AT +10°C

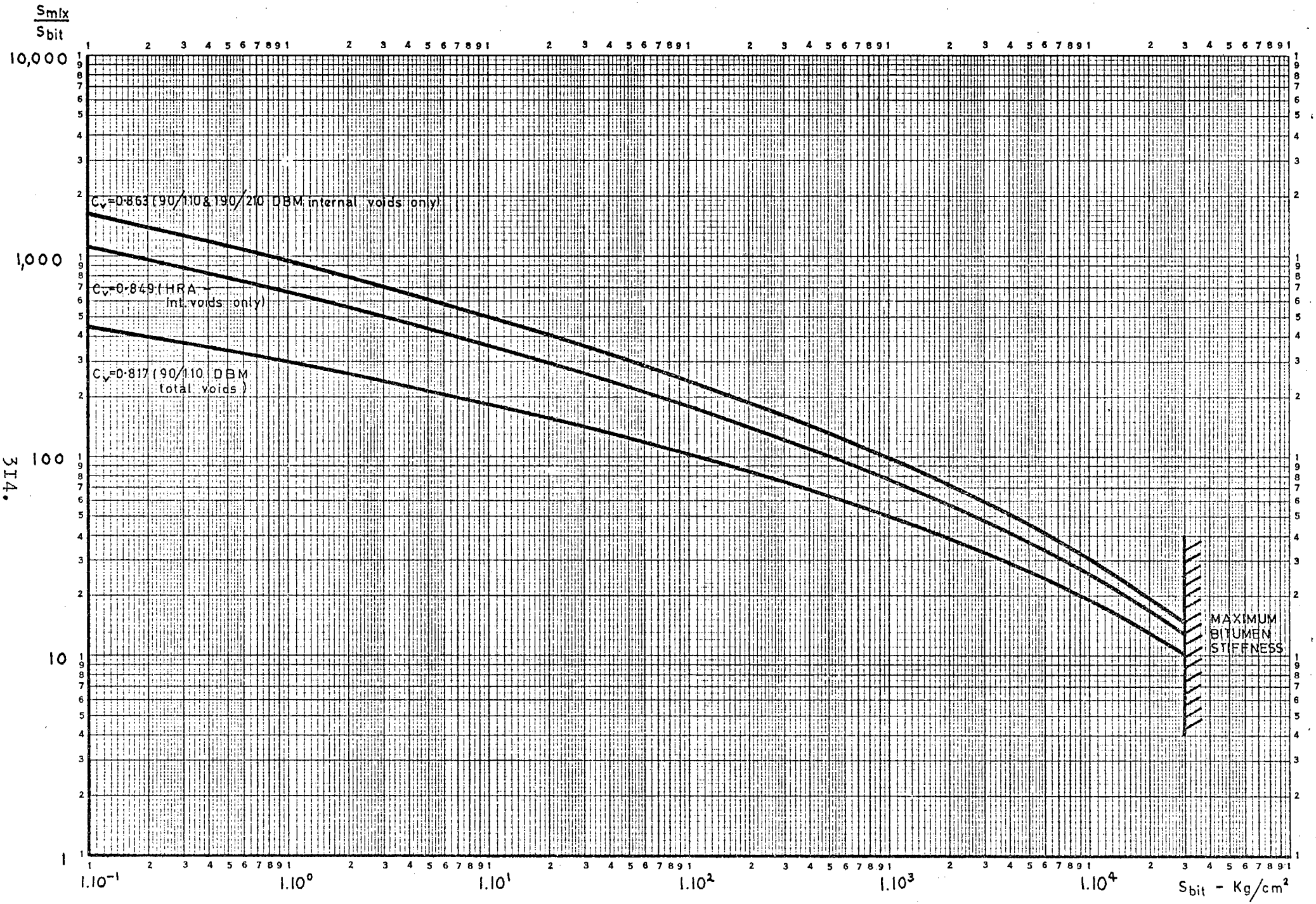

FIG. 66 MIXTURE CONFESTION FACTORS OF BITUMEN BOUND MATERIALS STUDIED

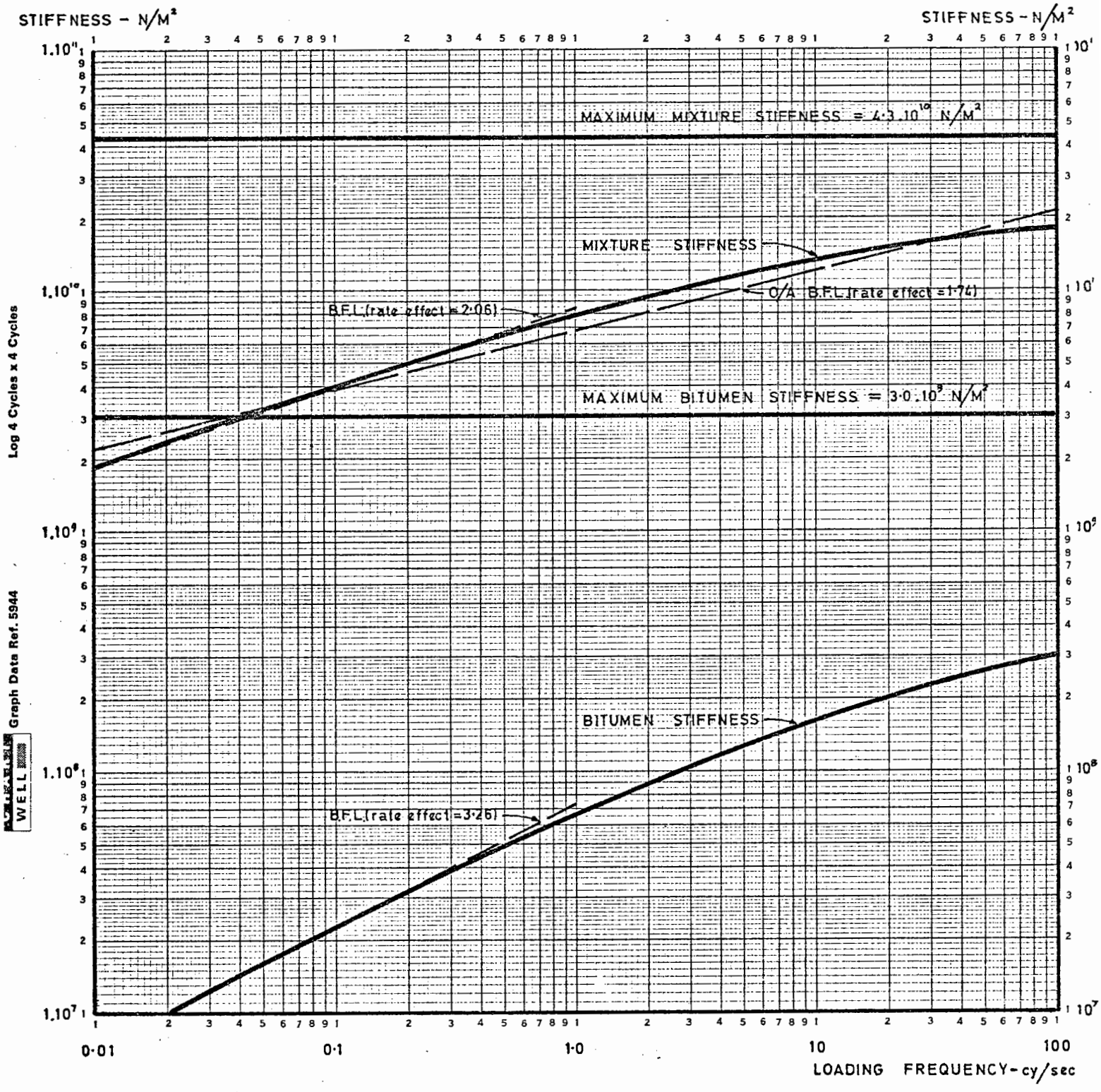

FIG. 67 NOMOGRAPH STIFFNESSES OF 90/110 pen. BITUMEN AND 90/110 DENSE BITUMEN MACADAM AT +10°C

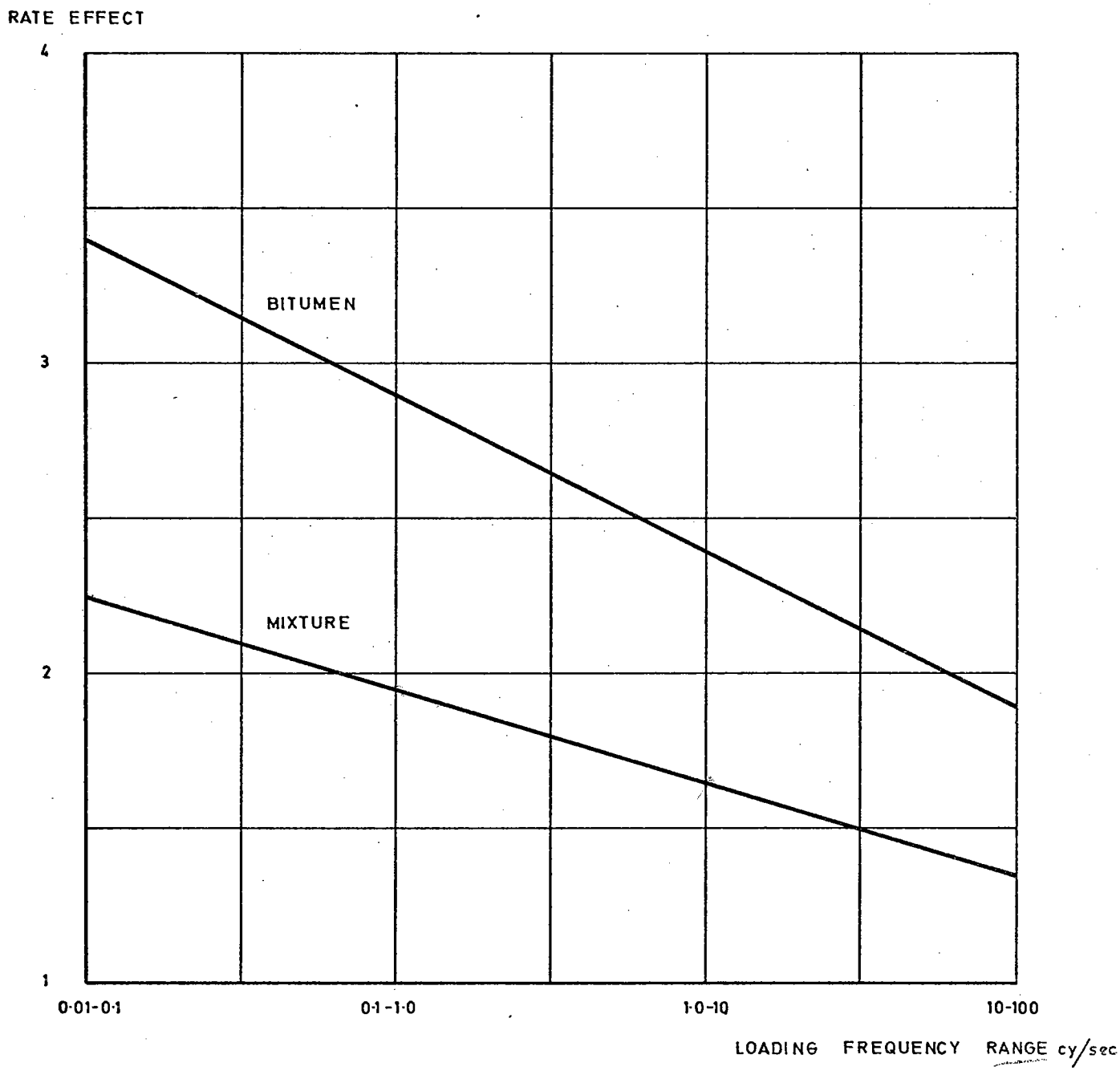

FIG. 68 THEORETICAL DEPENDENCE OF RATE EFFECT OF 90/110 pen. BITUMEN AND 90/110 DENSE BITUMEN MACADAM ON FREQUENCY RANGE AT +10° C

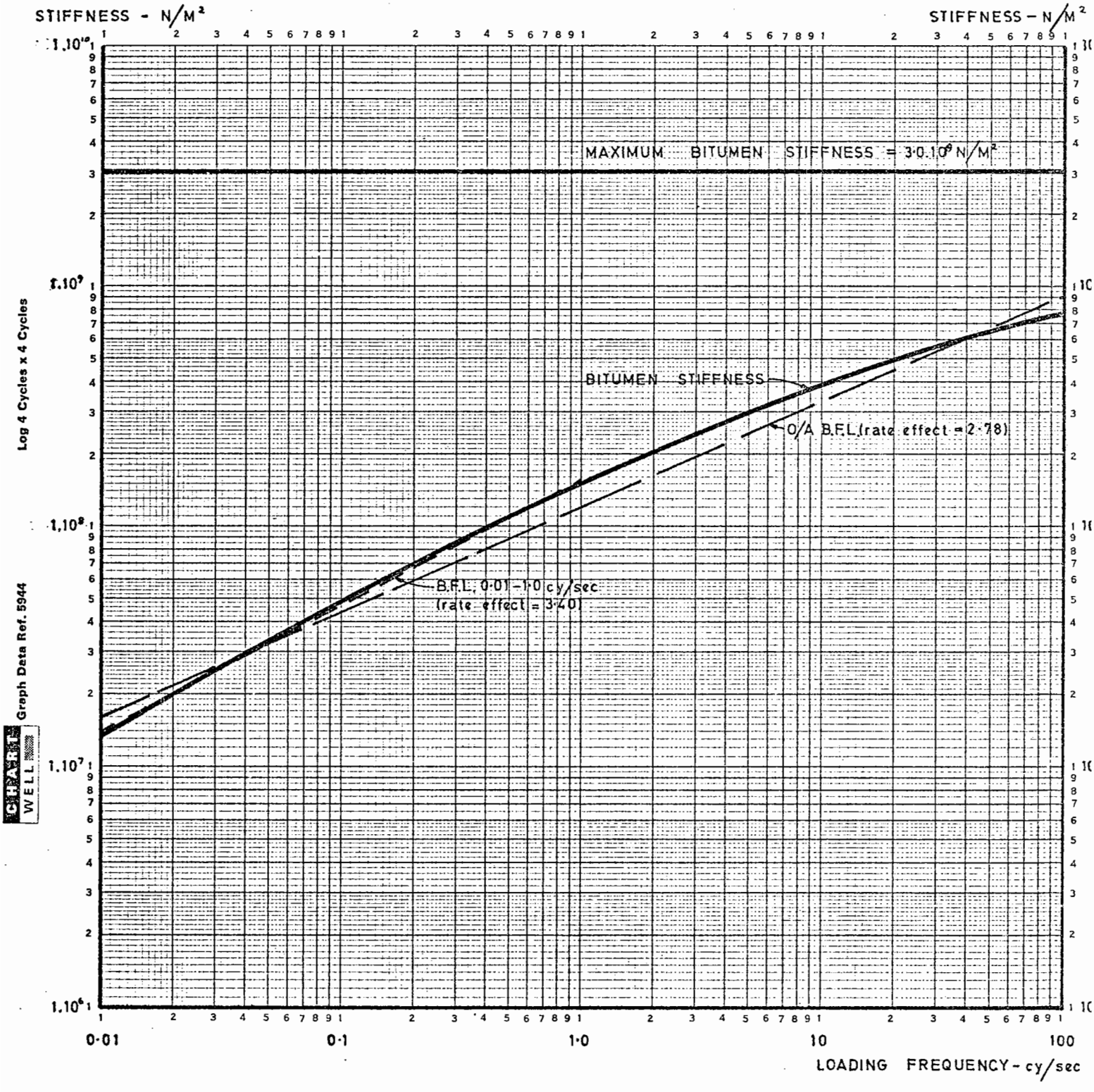

FIG. 69 NOMOGRAPH STIFFNESS OF 90/110 pen. BITUMEN AT 0°C

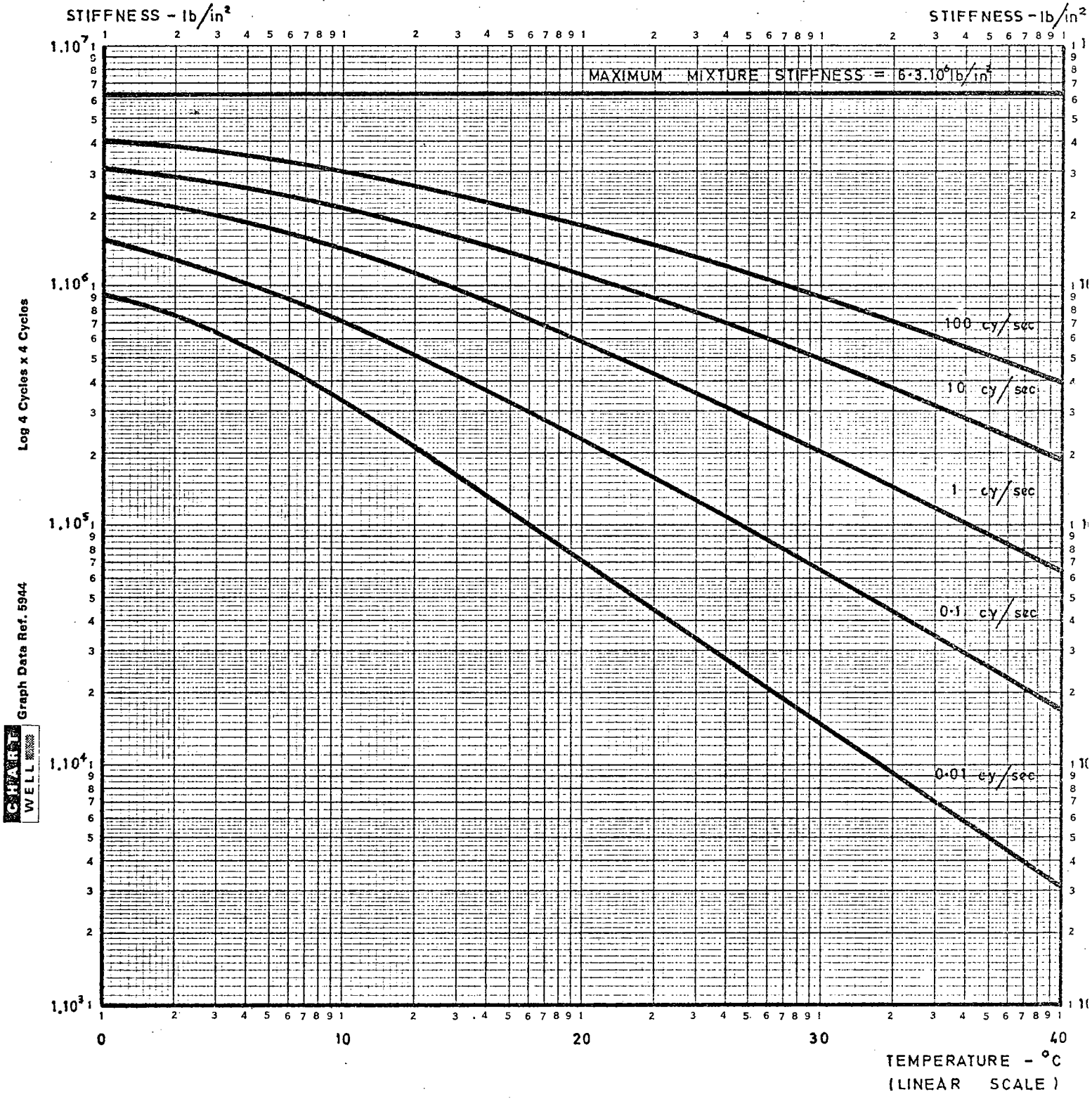

FIG. 70 NOMOGRAPH STIFFNESS OF 90/110 DENSE BITUMEN MACADAM FOR INTERNAL VOIDS ONLY

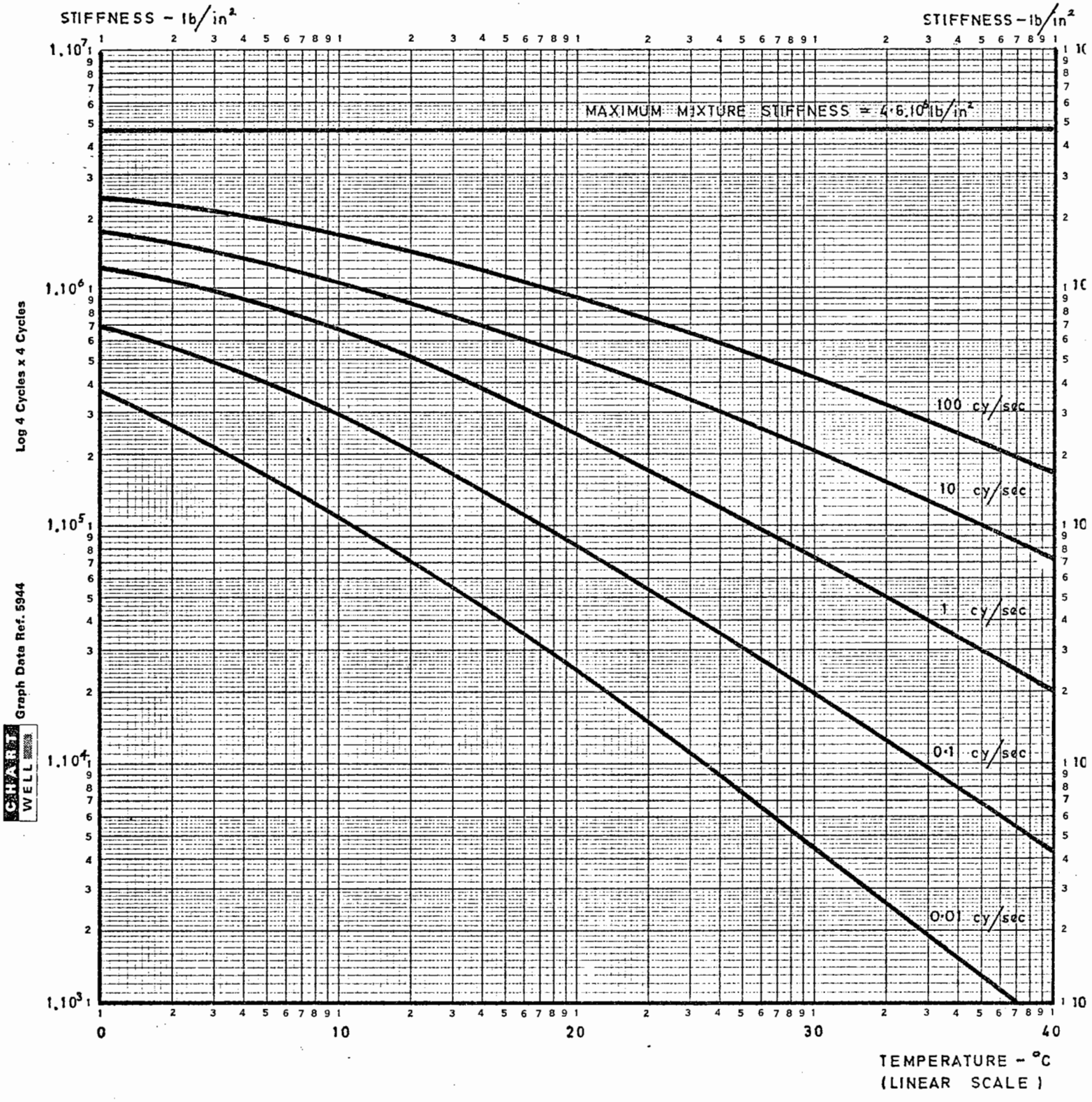

FIG. 71 NOMOGRAPH STIFFNESS OF 90/110 DENSE BITUMEN MACADAM FOR TOTAL VOIDS

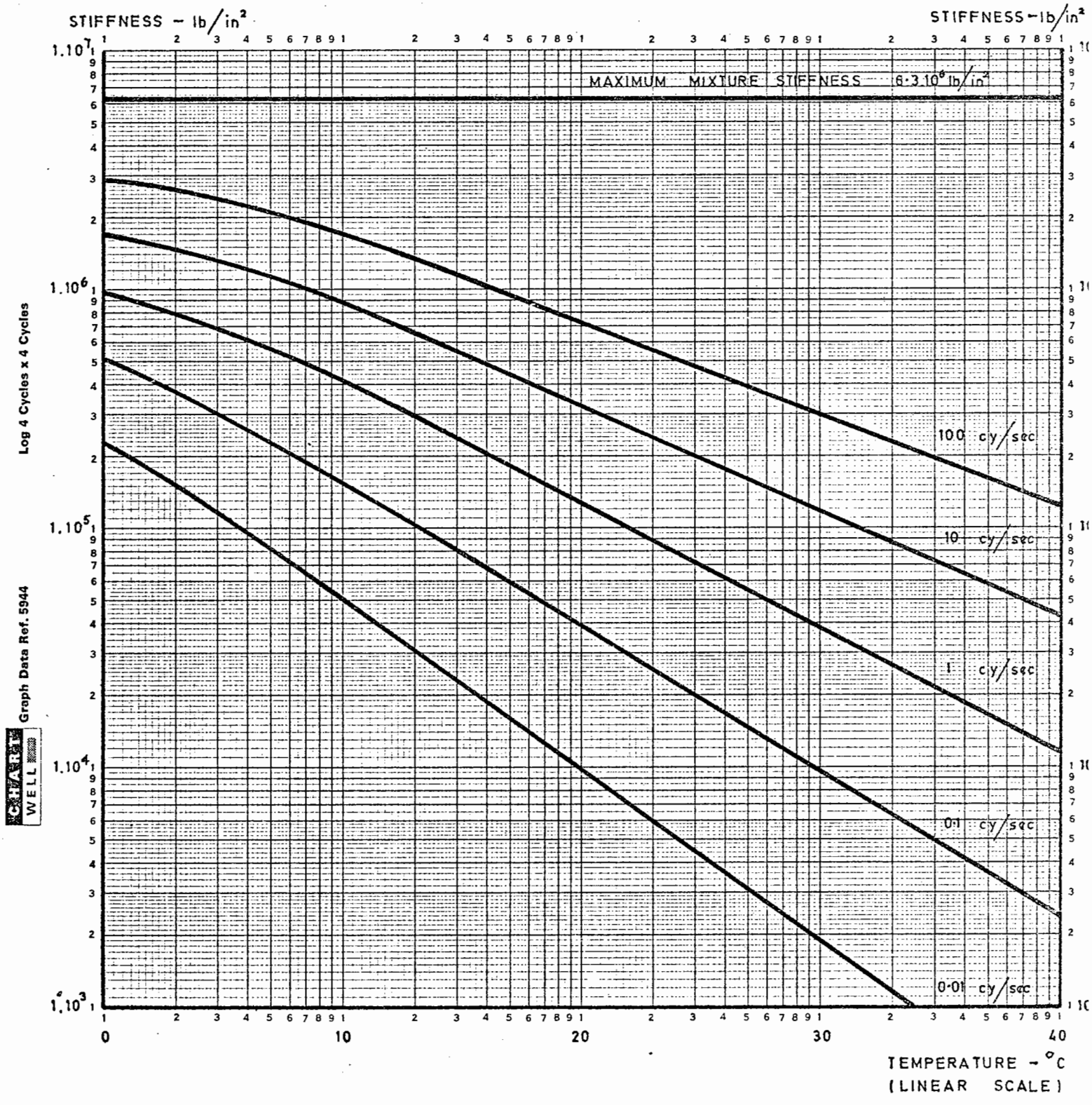

FIG. 72 NOMOGRAPH STIFFNESS OF 190/210 DENSE BITUMEN MACADAM FOR INTERNAL VOIDS ONLY

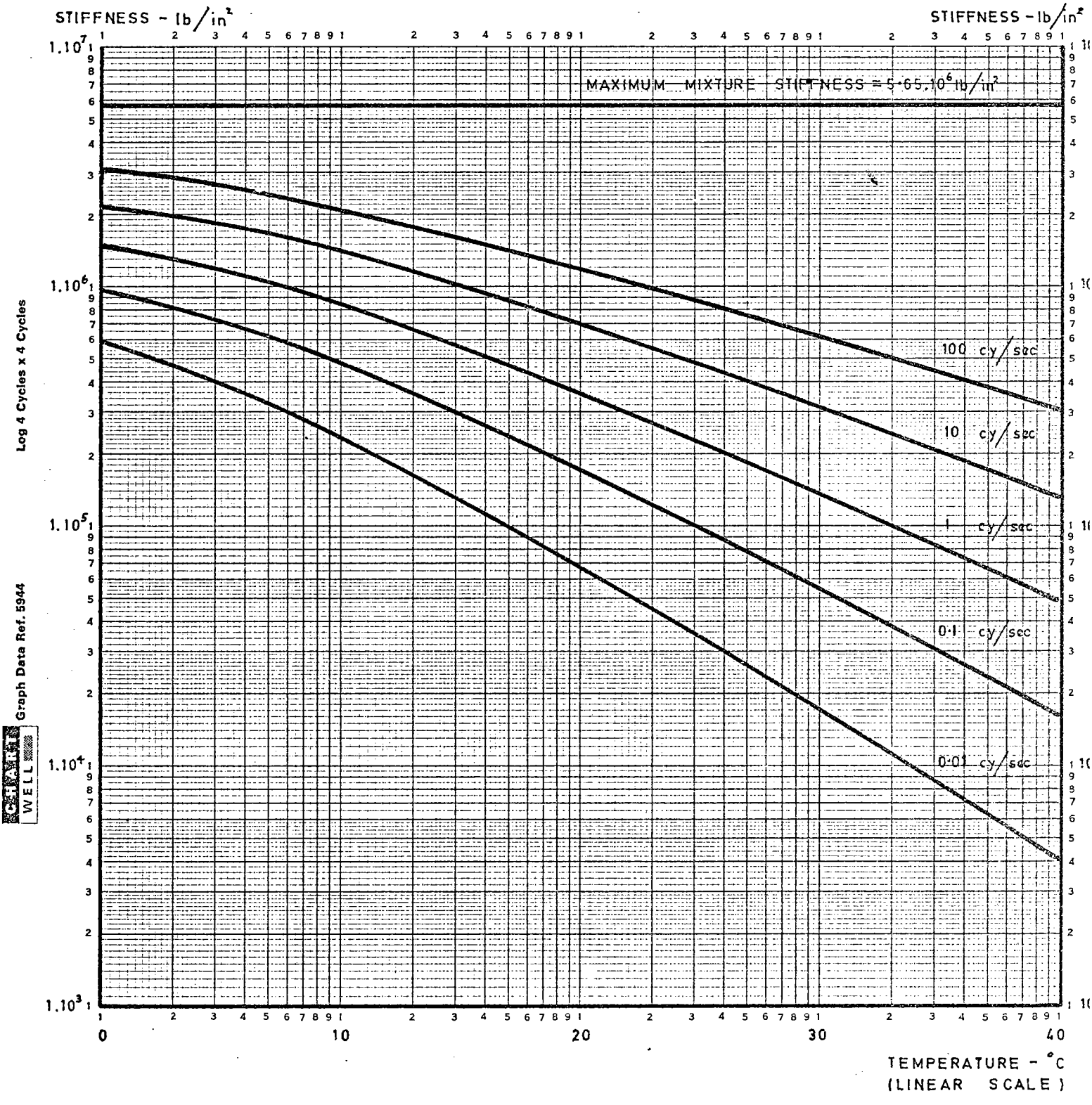

FIG. 73 NOMOGRAPH STIFFNESS OF HOT ROLLED ASPHALT FOR INTERNAL VOIDS ONLY

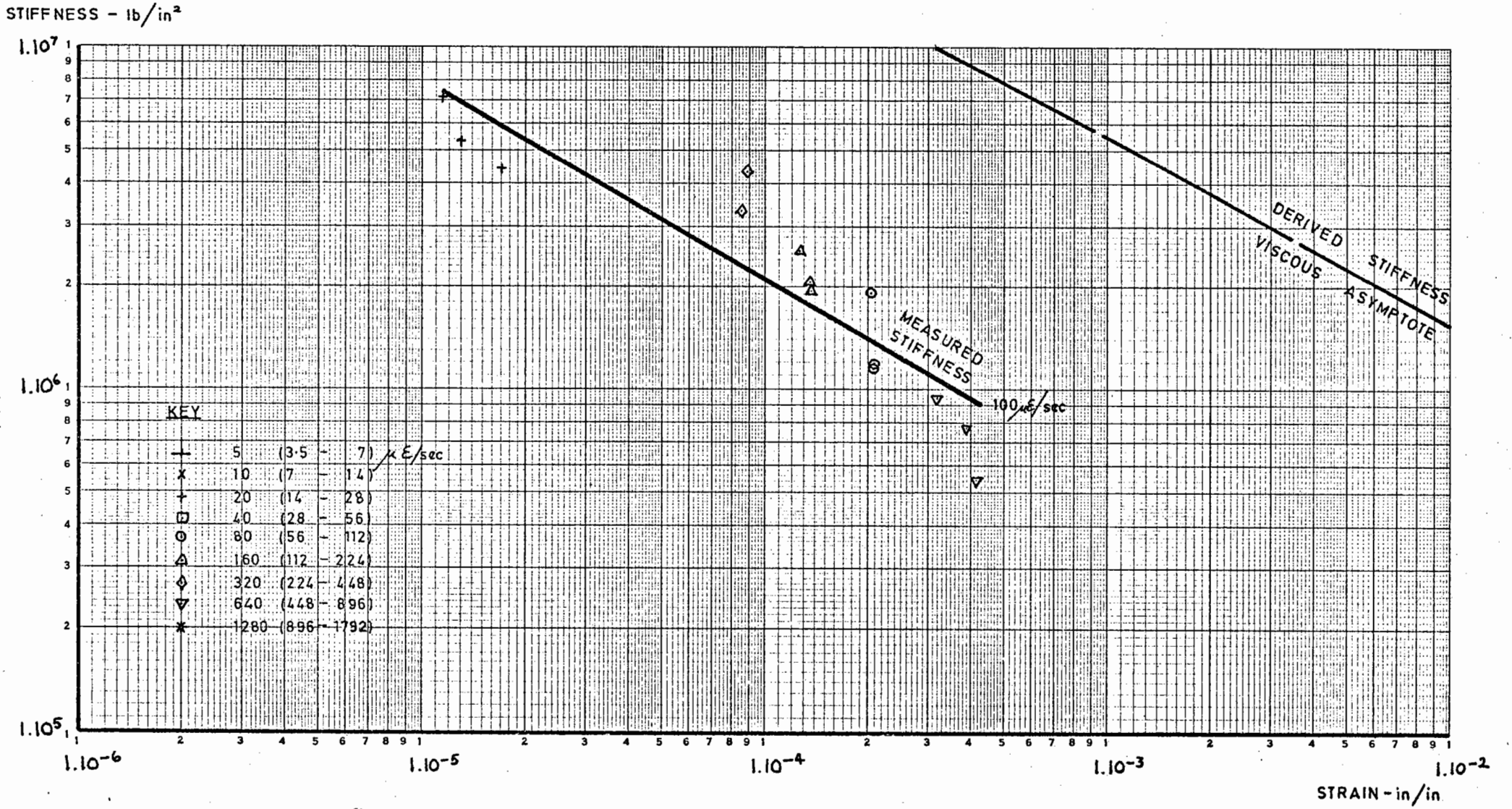

FIG. 74 ADJUSTED STIFFNESSES OF 90/110 DENSE BITUMEN MACADAM AT 0°C

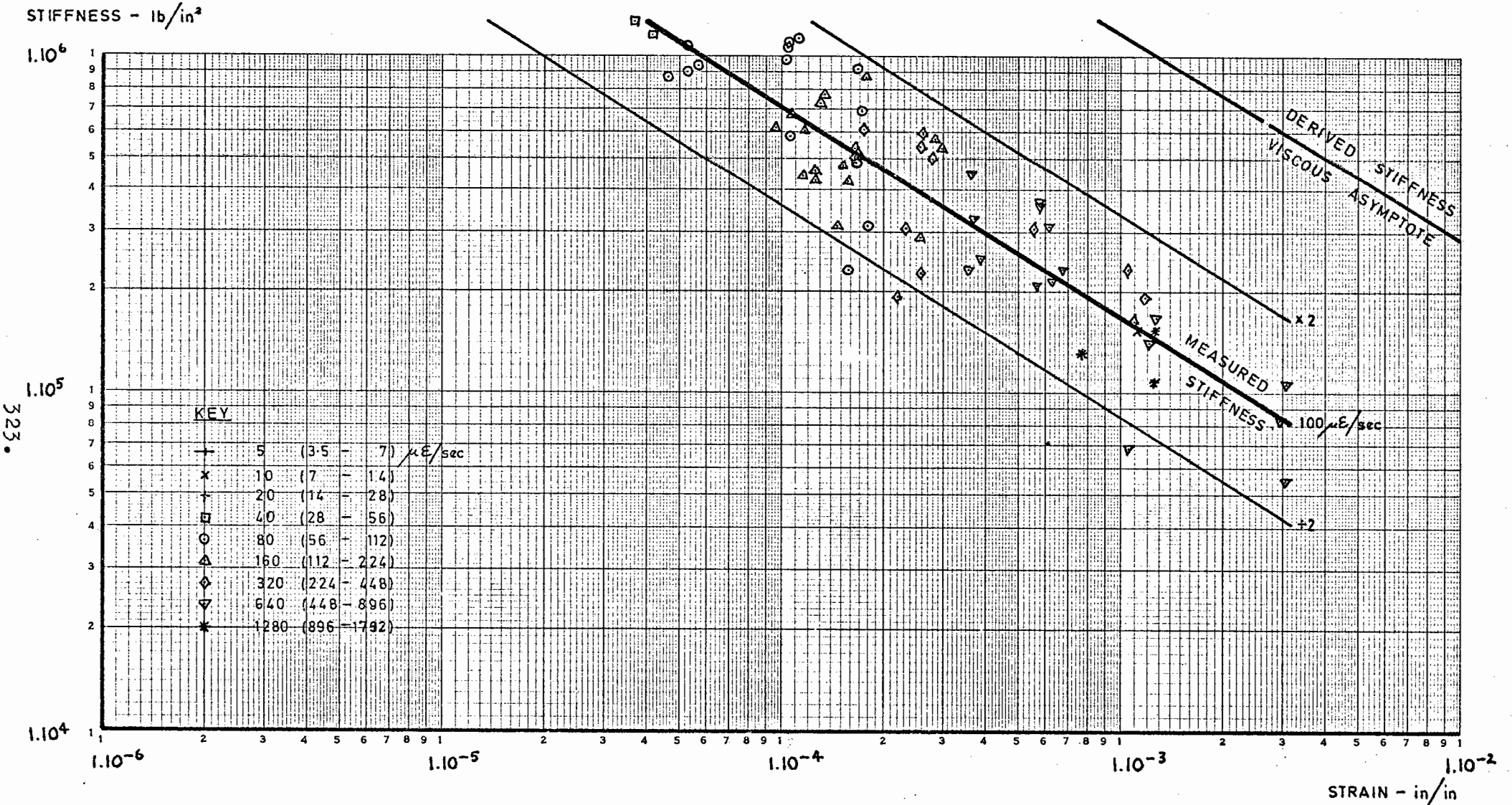

323.

FIG. 75 ADJUSTED STIFFNESSES OF 90/110 DENSE BITUMEN MACADAM AT +10°C

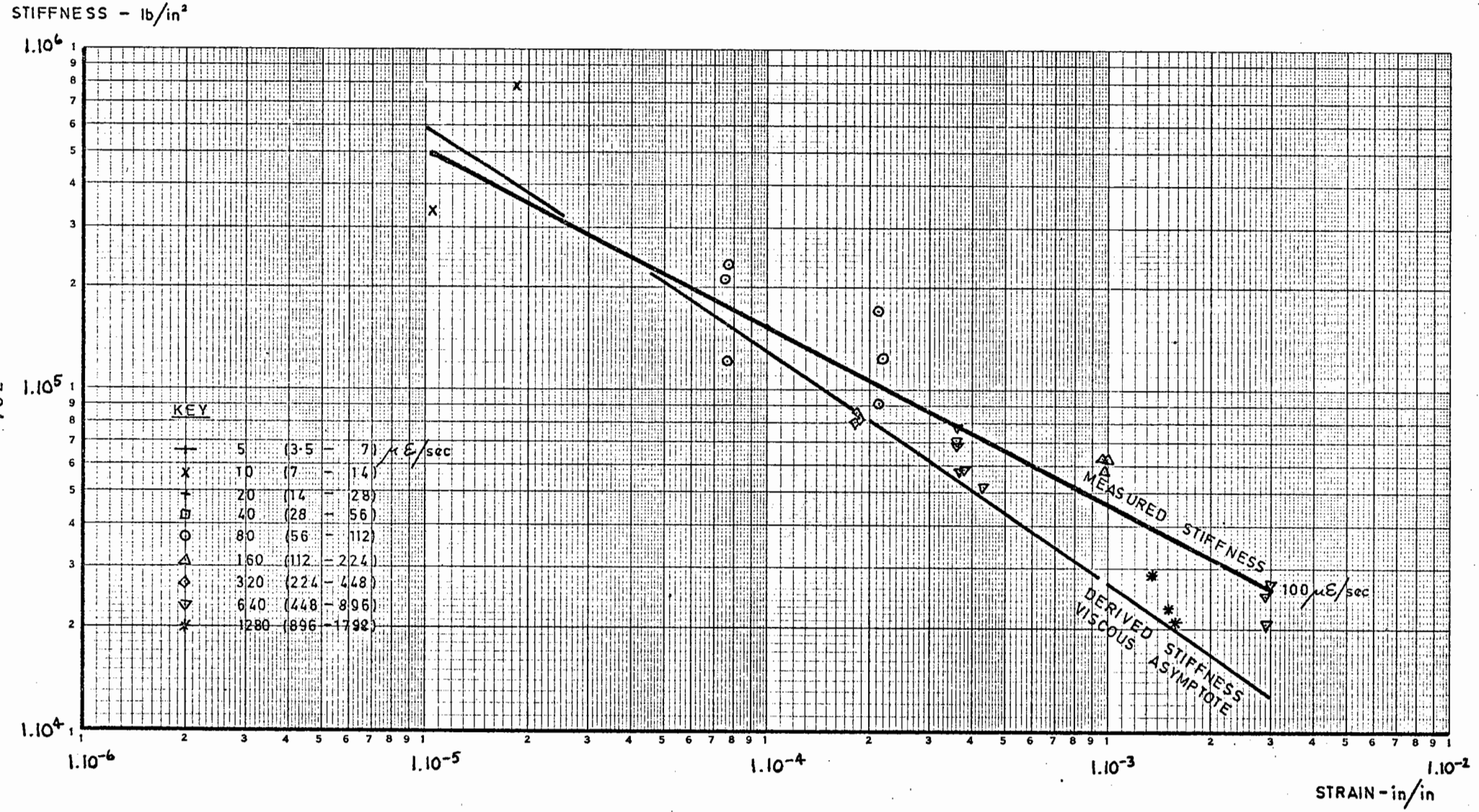

FIG. 76 ADJUSTED STIFFNESSES OF 90/110 DENSE BITUMEN MACADAM AT +30° C

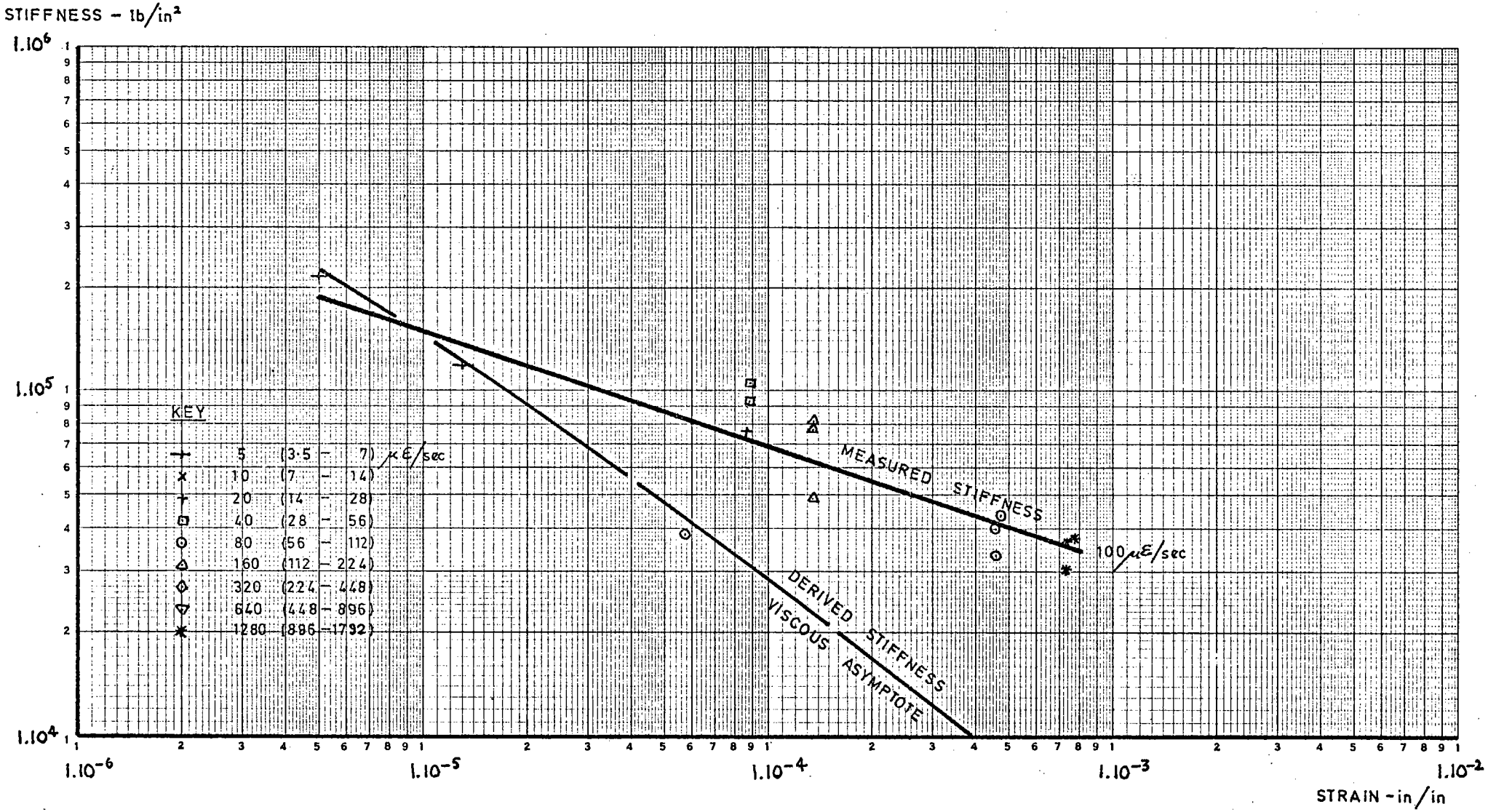

FIG. 77 ADJUSTED STIFFNESSES OF 90/110 DENSE BITUMEN MACADAM AT +40°C

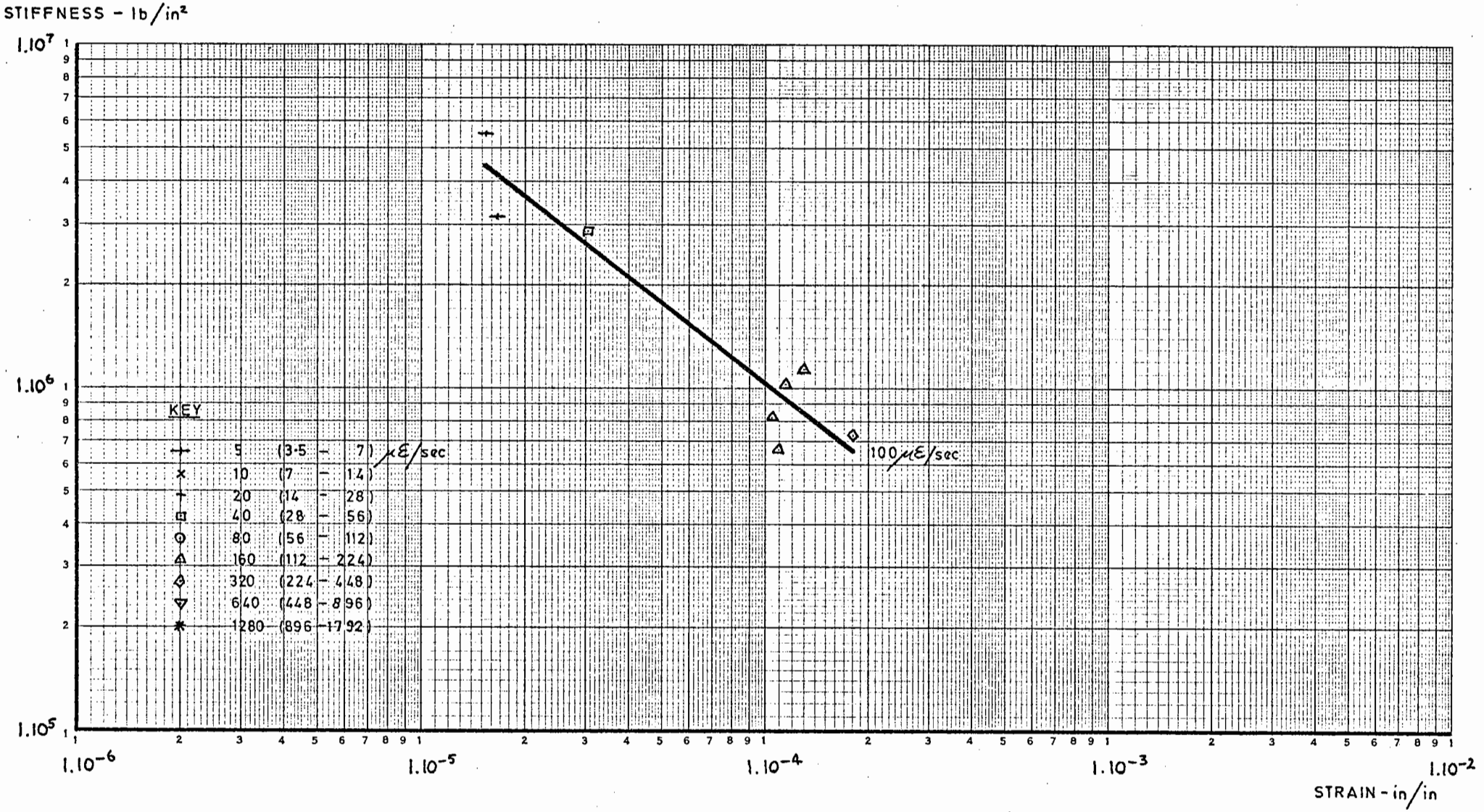

FIG. 78 ADJUSTED STIFFNESSES OF 190/210 DENSE BITUMEN MACADAM AT 0°C

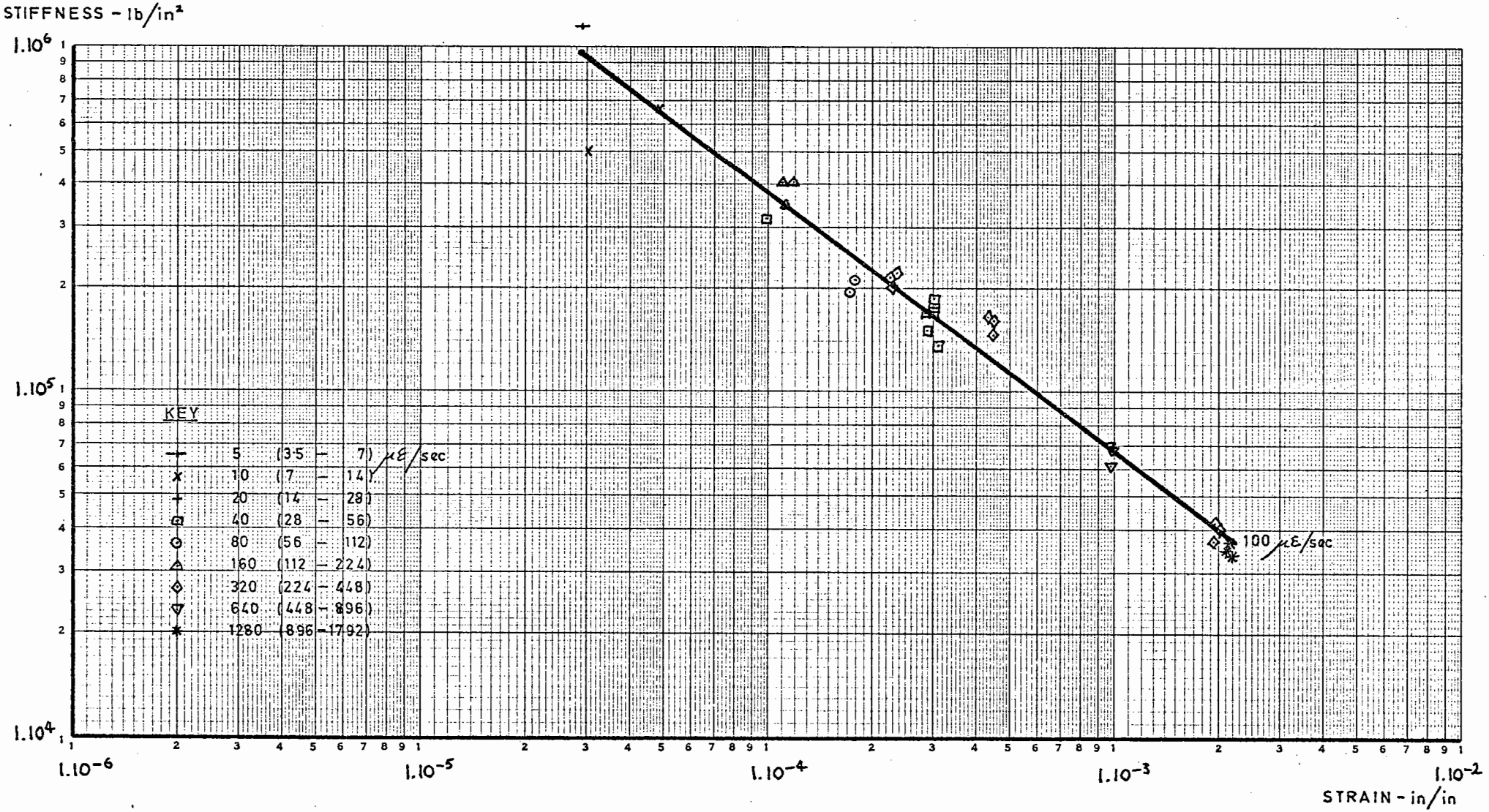

FIG. 79 ADJUSTED STIFFNESSES OF 190/210 DENSE BITUMEN MACADAM AT +10°C

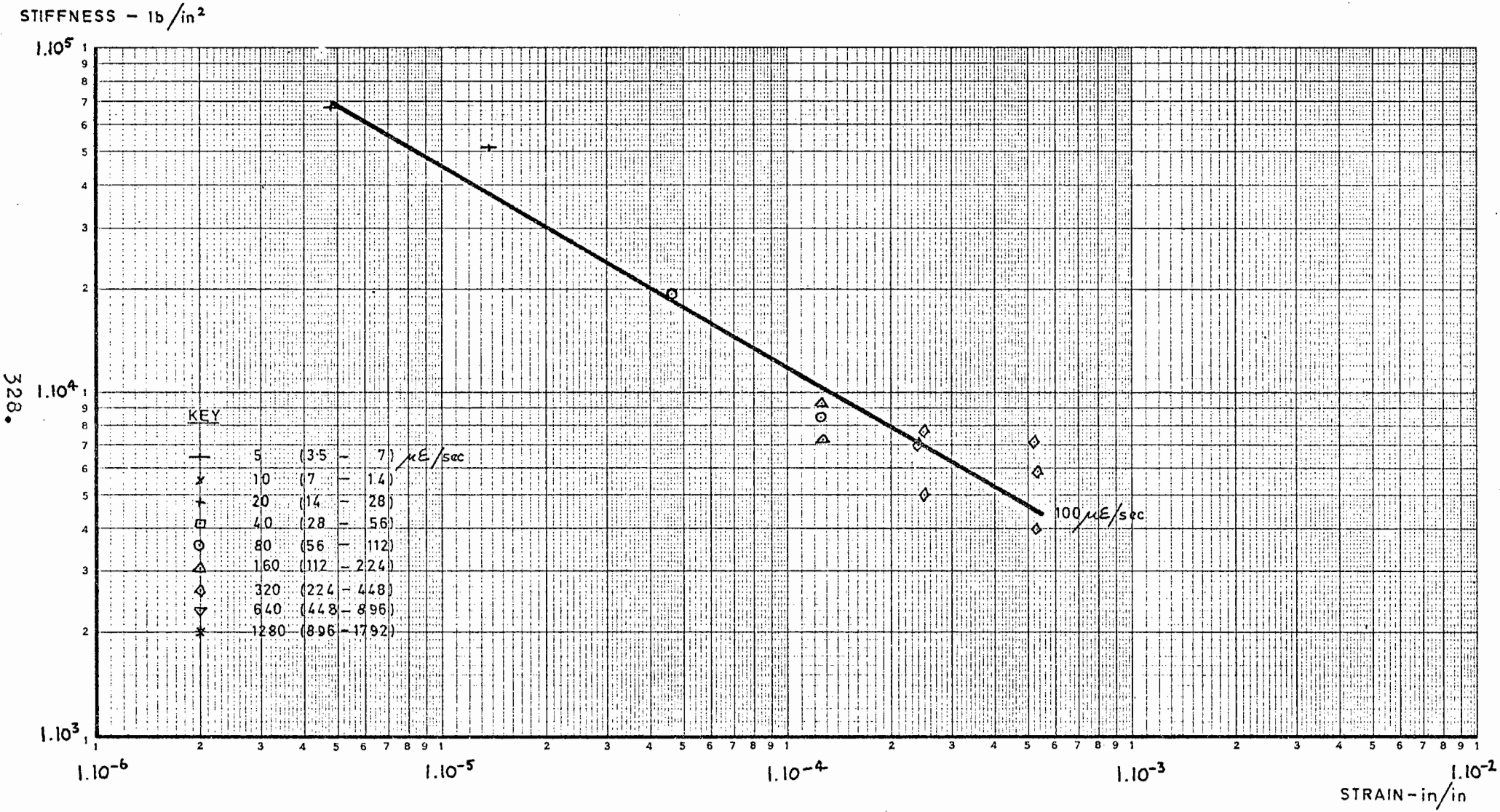

FIG. 80 ADJUSTED STIFFNESSES OF 190/210 DENSE BITUMEN MACADAM AT +40° C

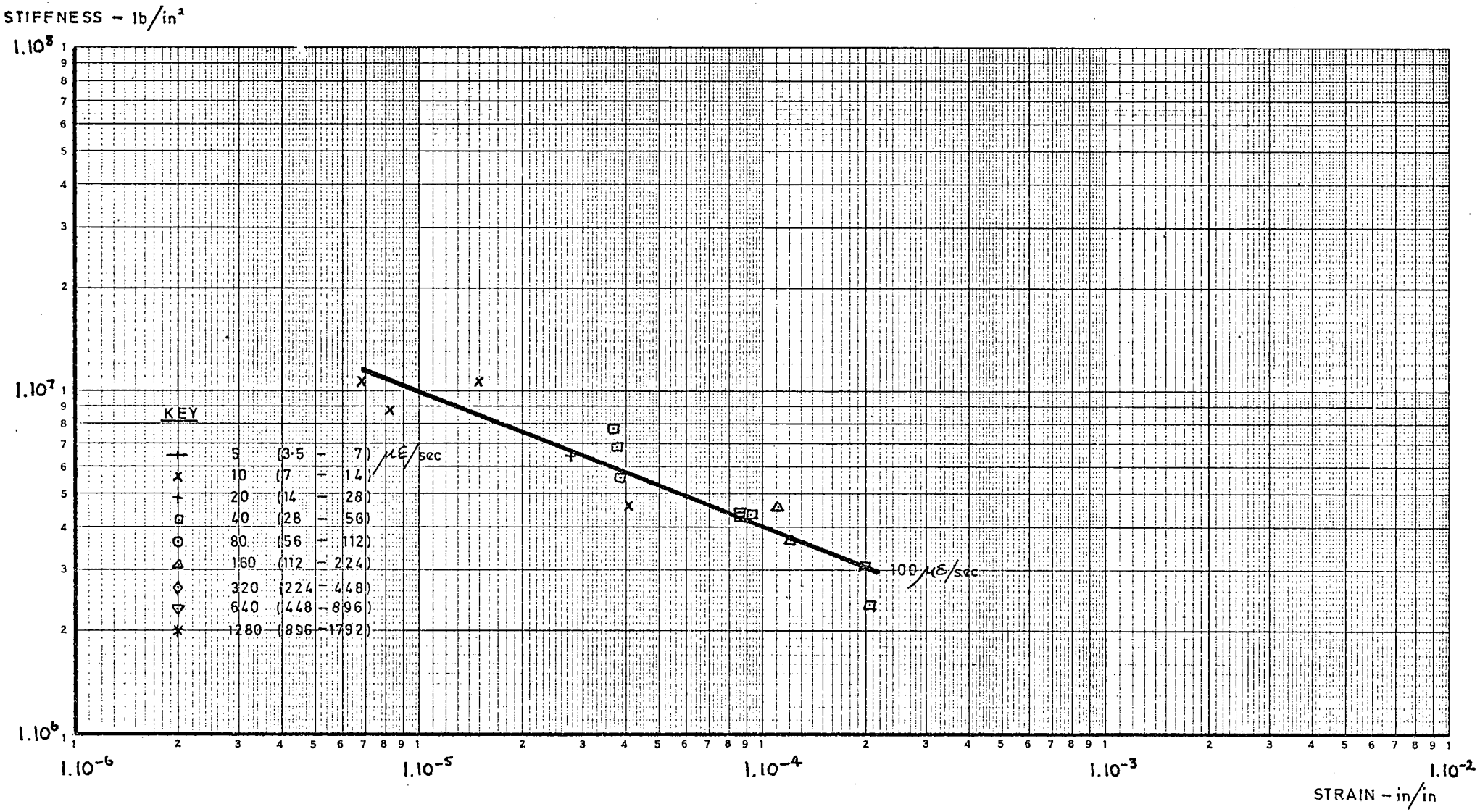

FIG. 81 ADJUSTED STIFFNESSES OF DENSE TAR MACADAM AT 0°C

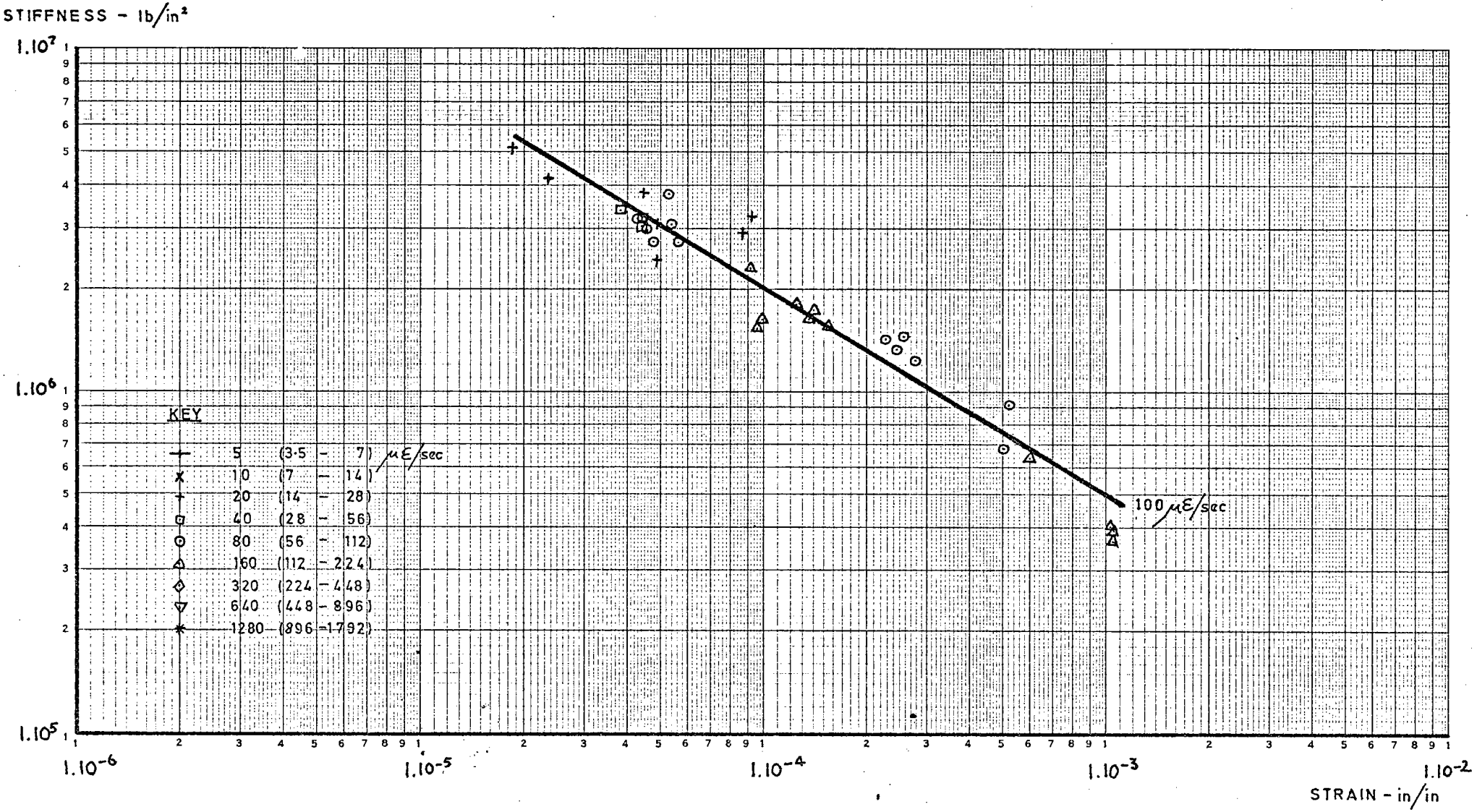

FIG. 82 ADJUSTED STIFFNESSES OF DENSE TAR MACADAM AT +10°C

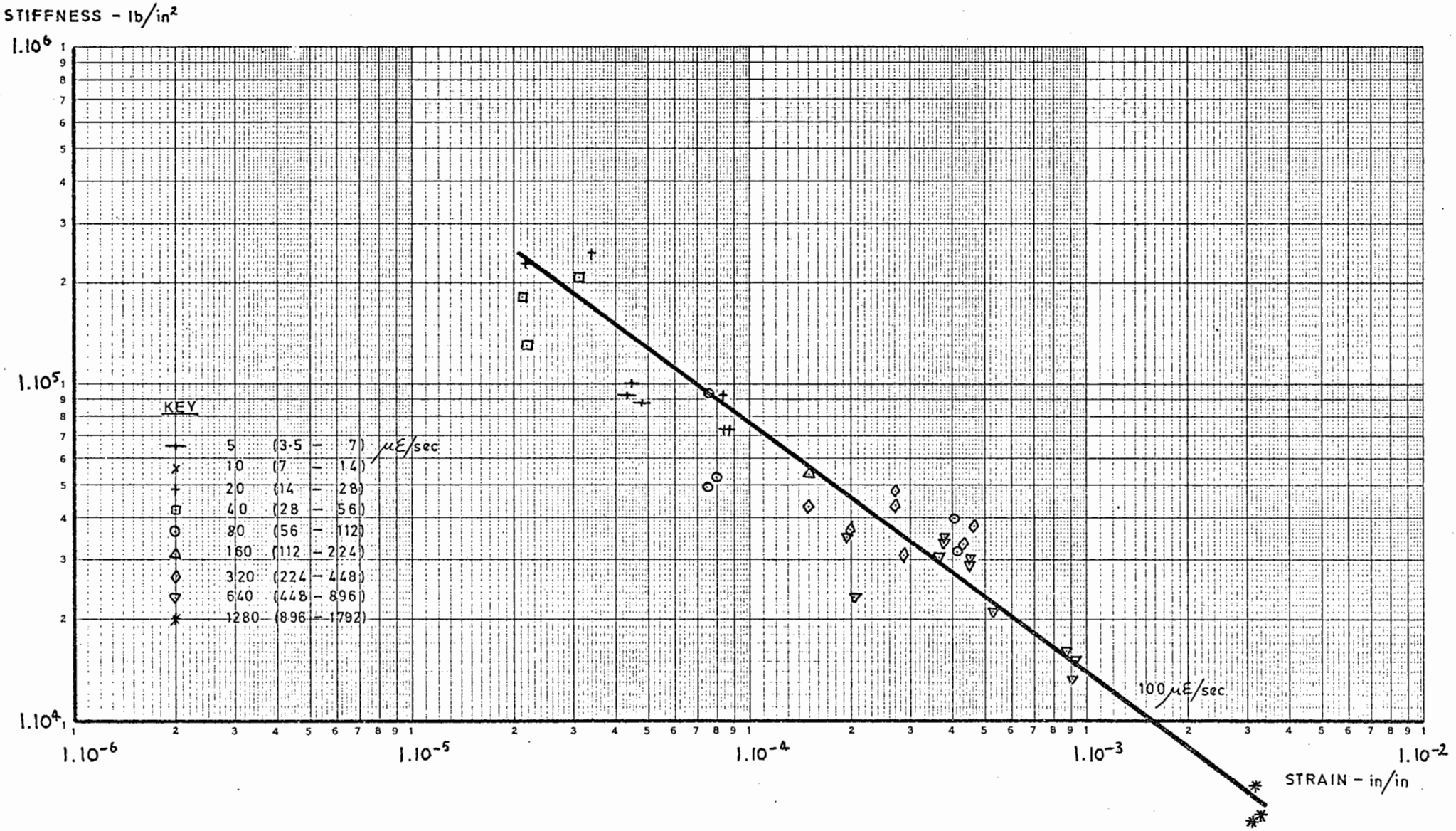

FIG. 83 ADJUSTED STIFFNESSES OF DENSE TAR MACADAM AT +30°C

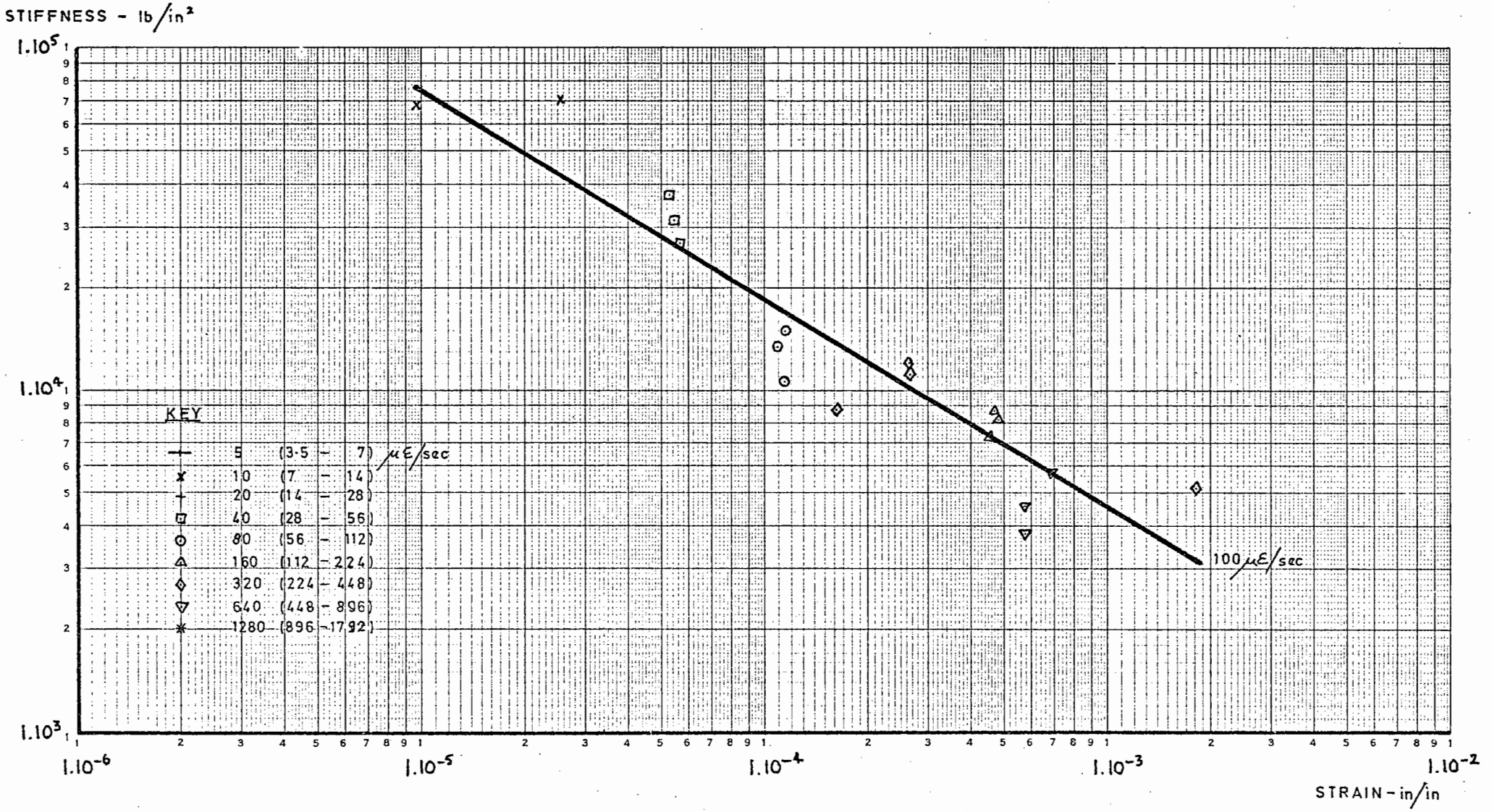

FIG. 84 ADJUSTED STIFFNESSES OF DENSE TAR MACADAM AT +40°C

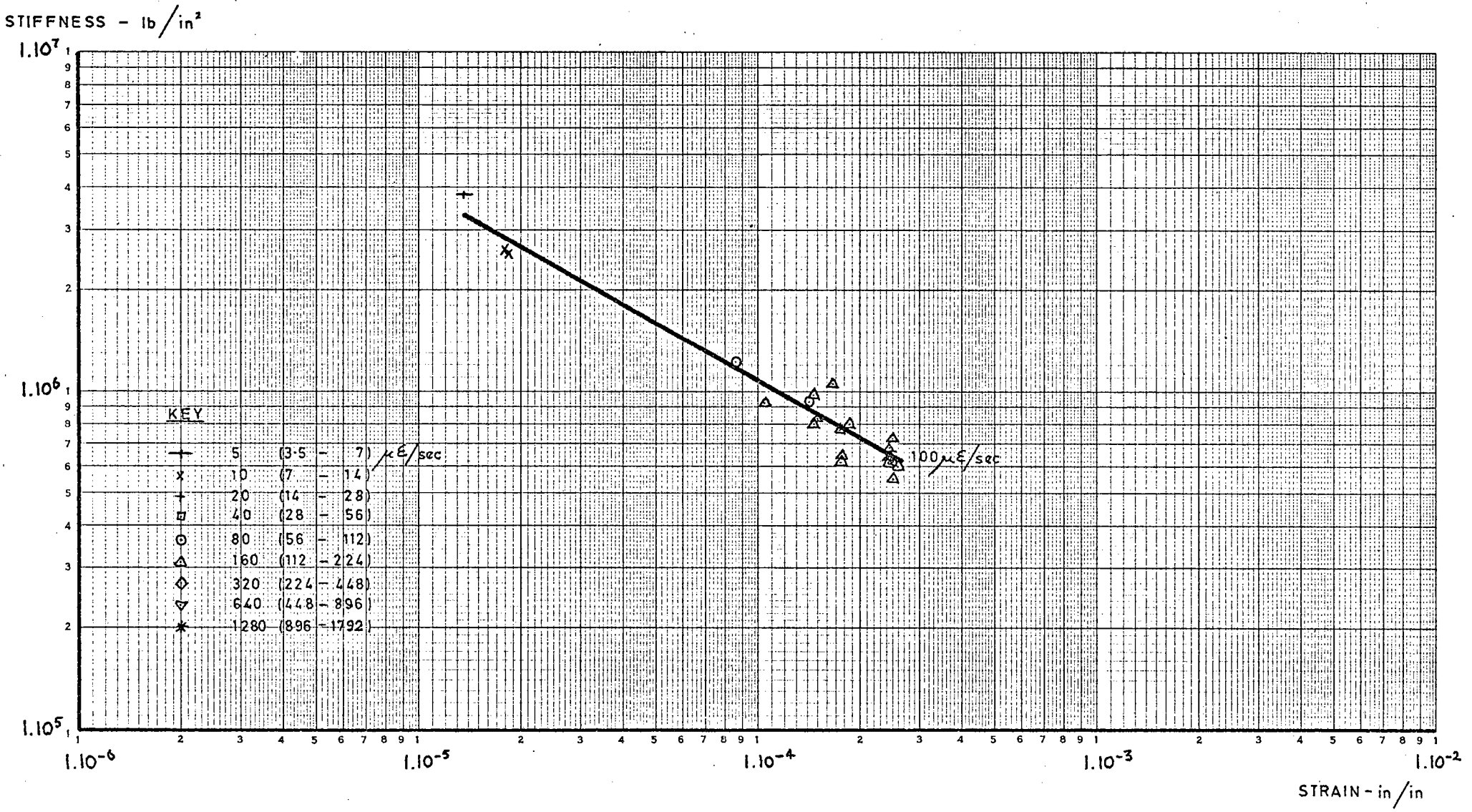

FIG. 85 ADJUSTED STIFFNESSES OF HOT ROLLED ASPHALT AT +10°C

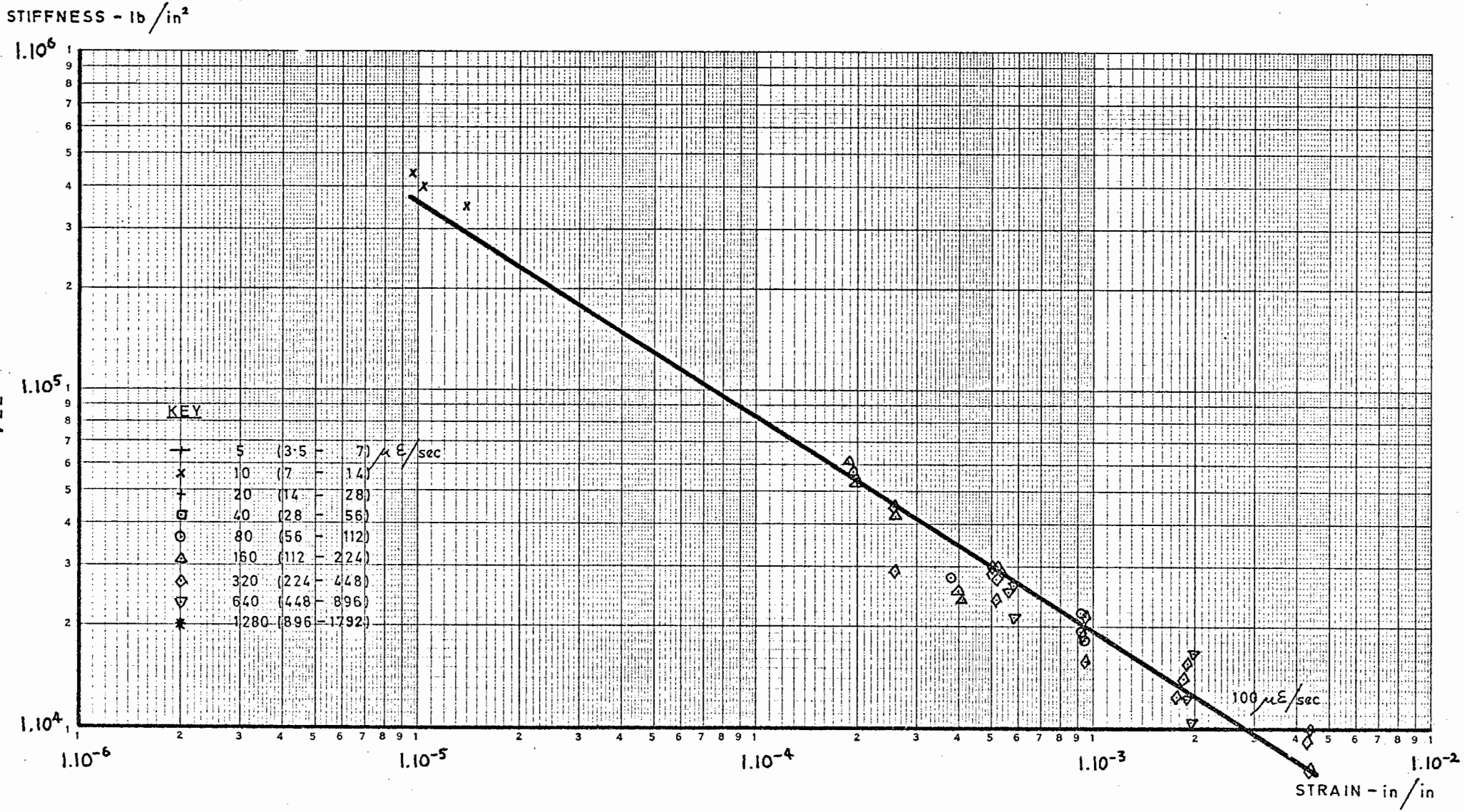

FIG. 86 ADJUSTED STIFFNESSES OF HOT ROLLED ASPHALT AT +30°C

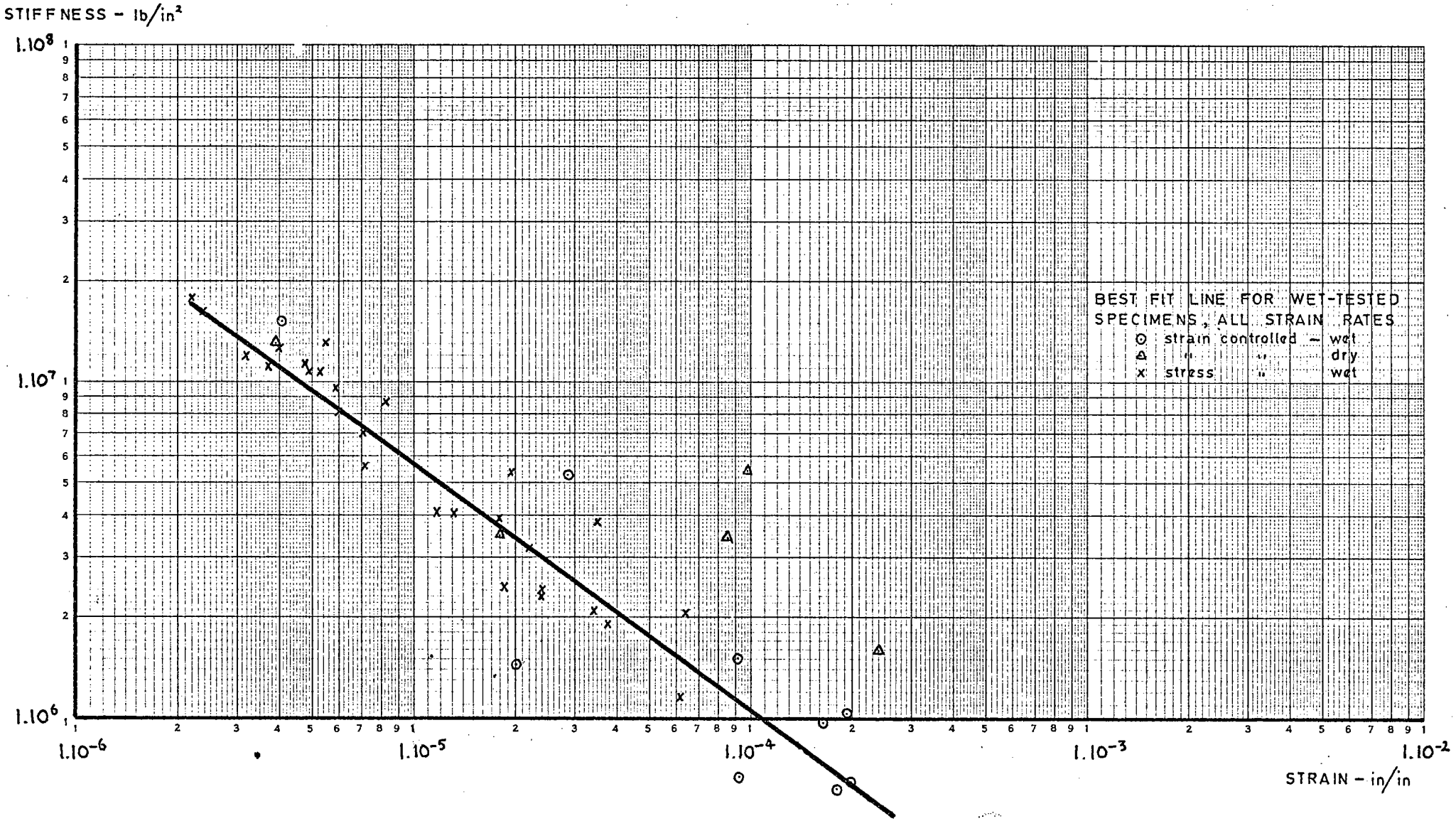

FIG. 87 STIFFNESSES OF DRY LEAN CONCRETE AT +20°C

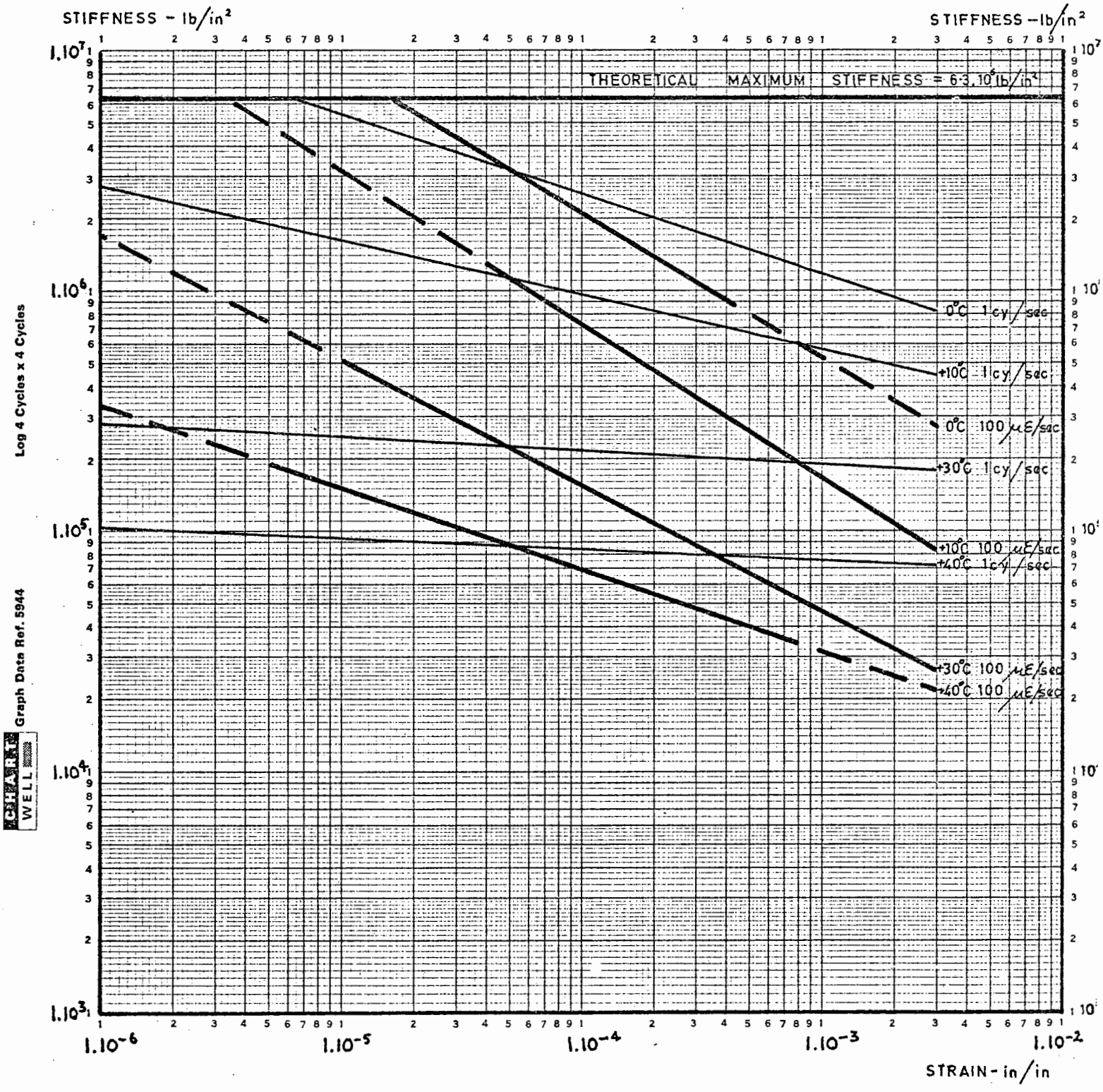

FIG. 88 SUMMARY OF STIFFNESSES OF 90/110 DENSE BITUMEN MACADAM

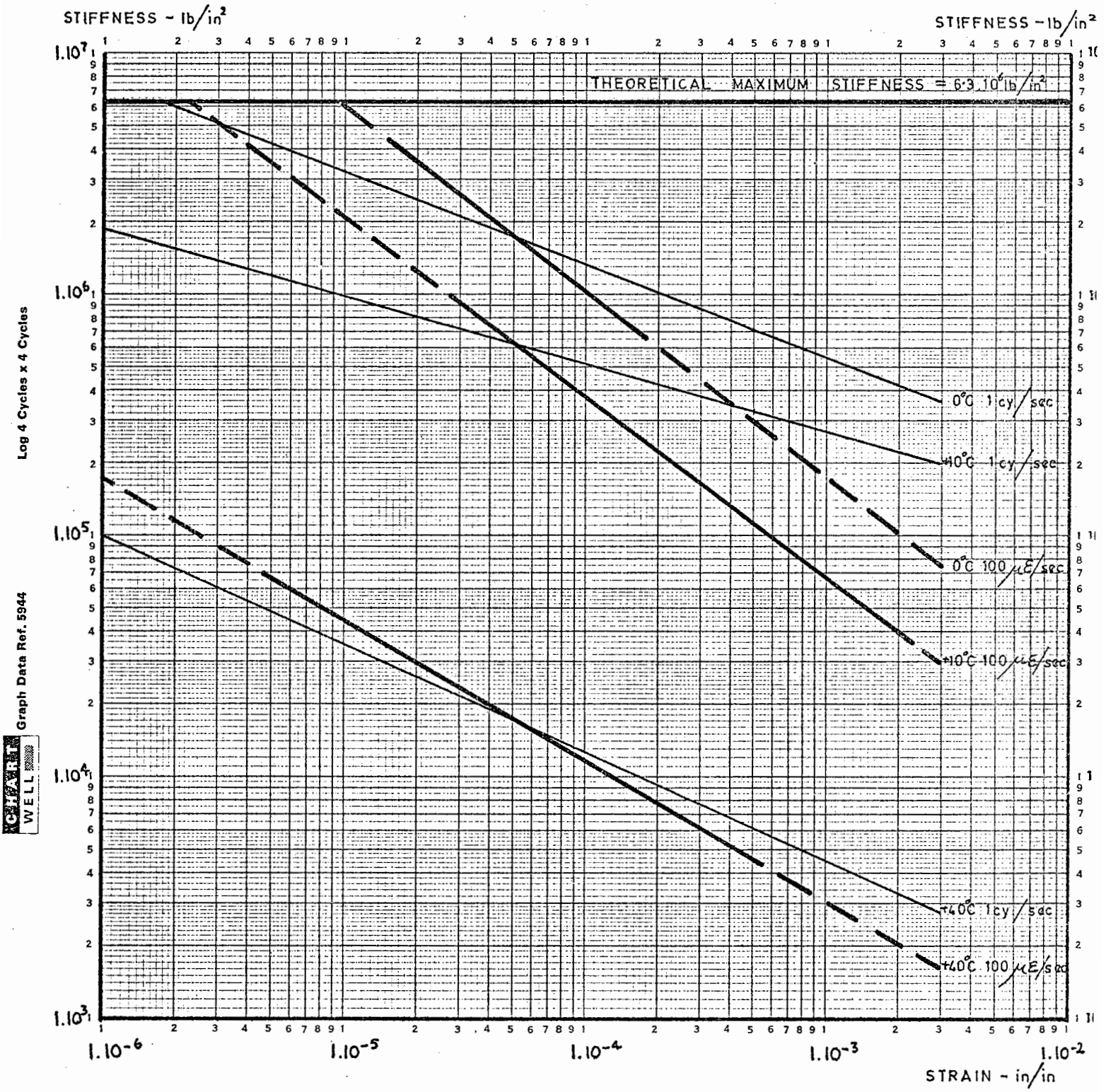

FIG. 89 SUMMARY OF STIFFNESSES OF 190/210 DENSE BITUMEN MACADAM

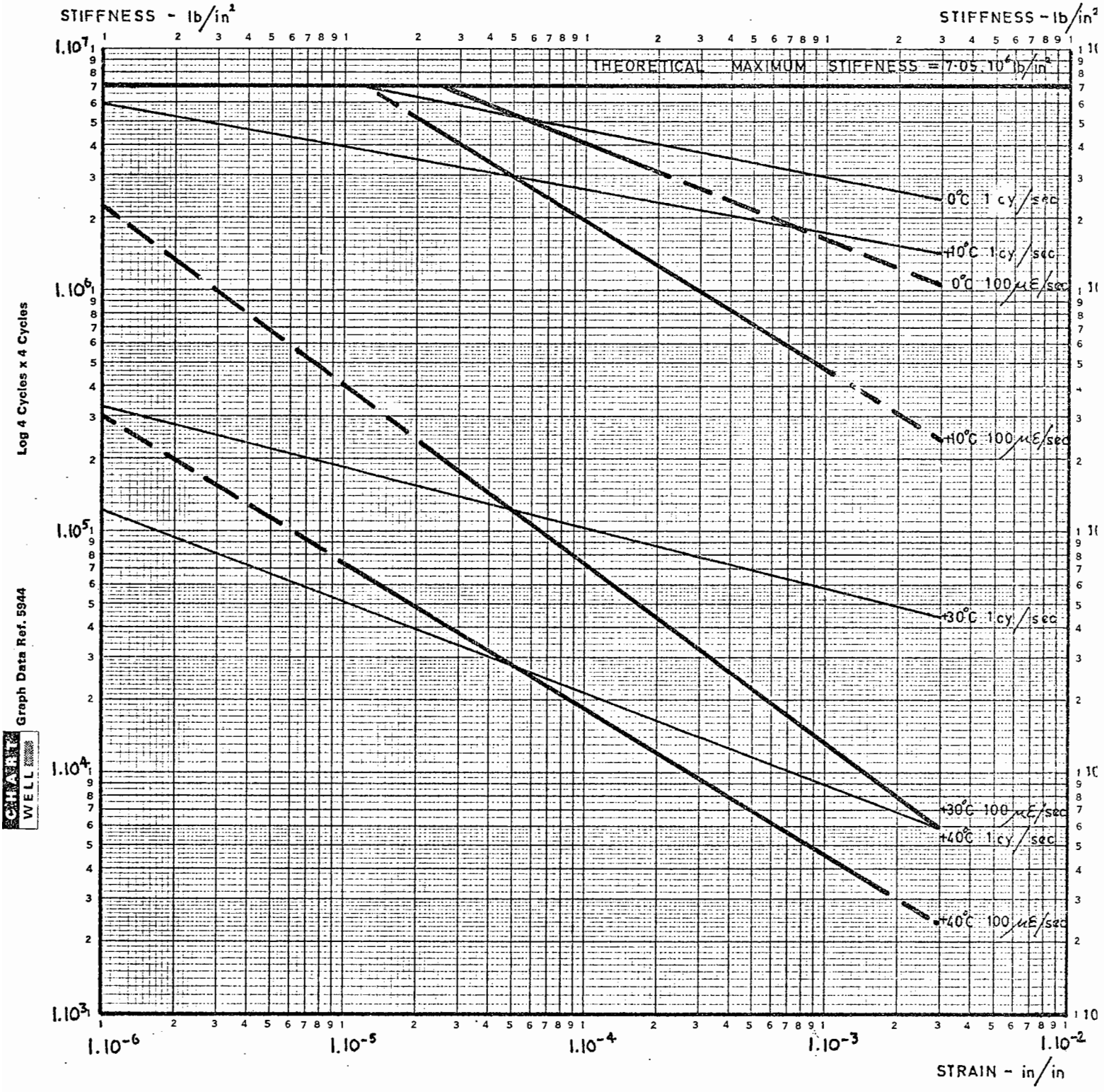

FIG. 90 SUMMARY OF STIFFNESSES OF DENSE TAR MACADAM

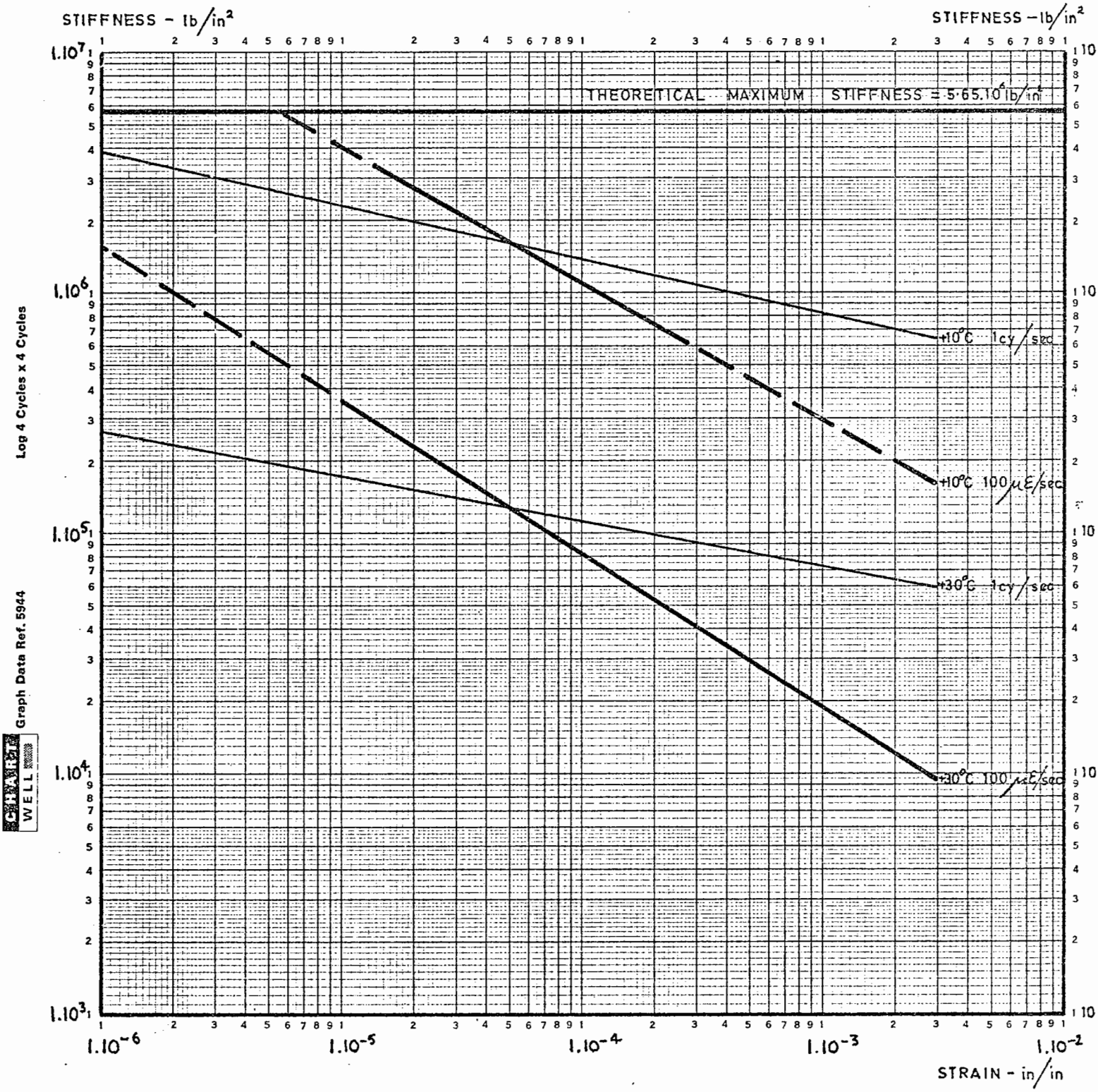

FIG. 91 SUMMARY OF STIFFNESSES OF HOT ROLLED ASPHALT

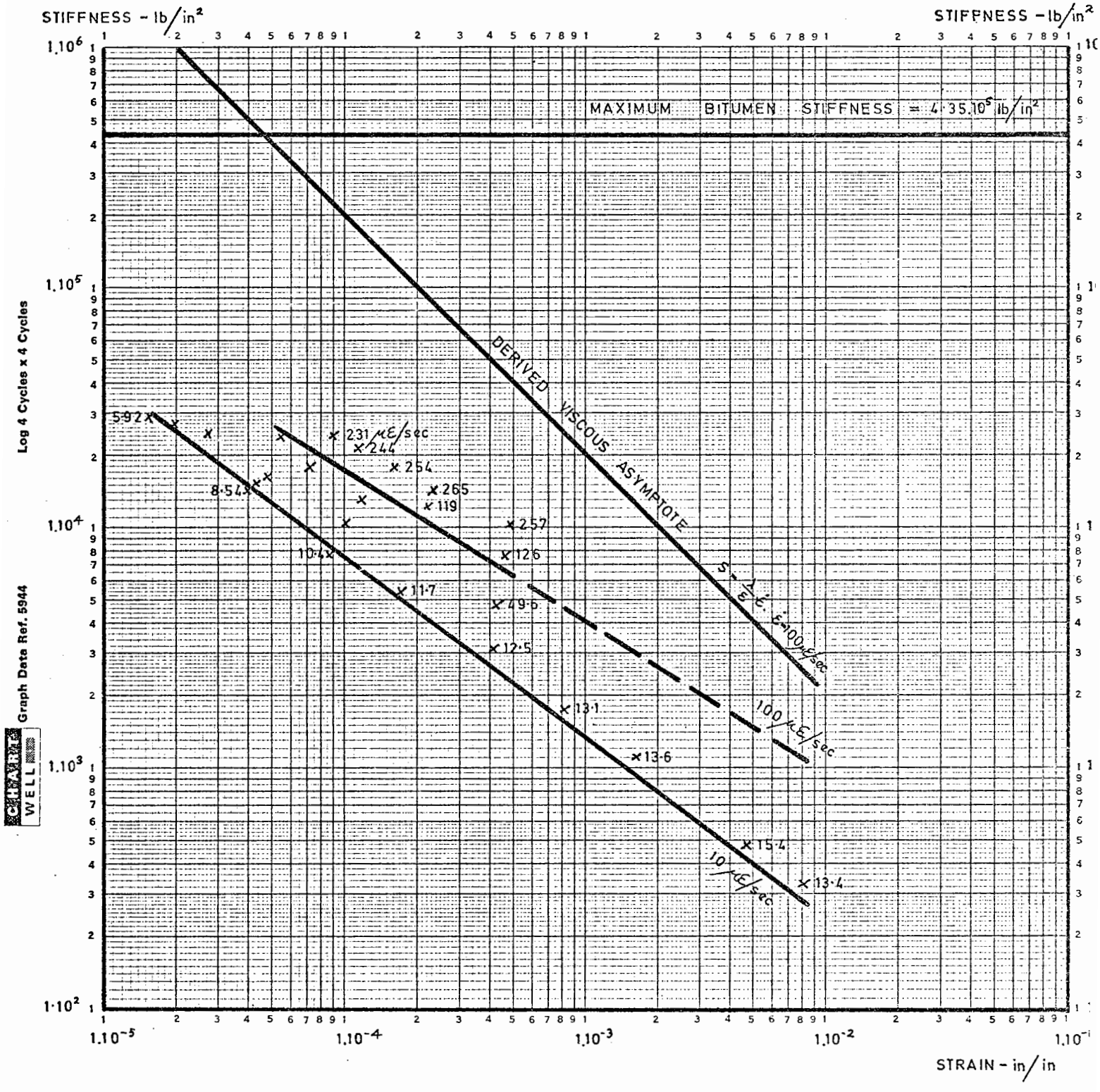

FIG. 92 STIFFNESS OF 90/110 pen. BITUMEN AT 0°C

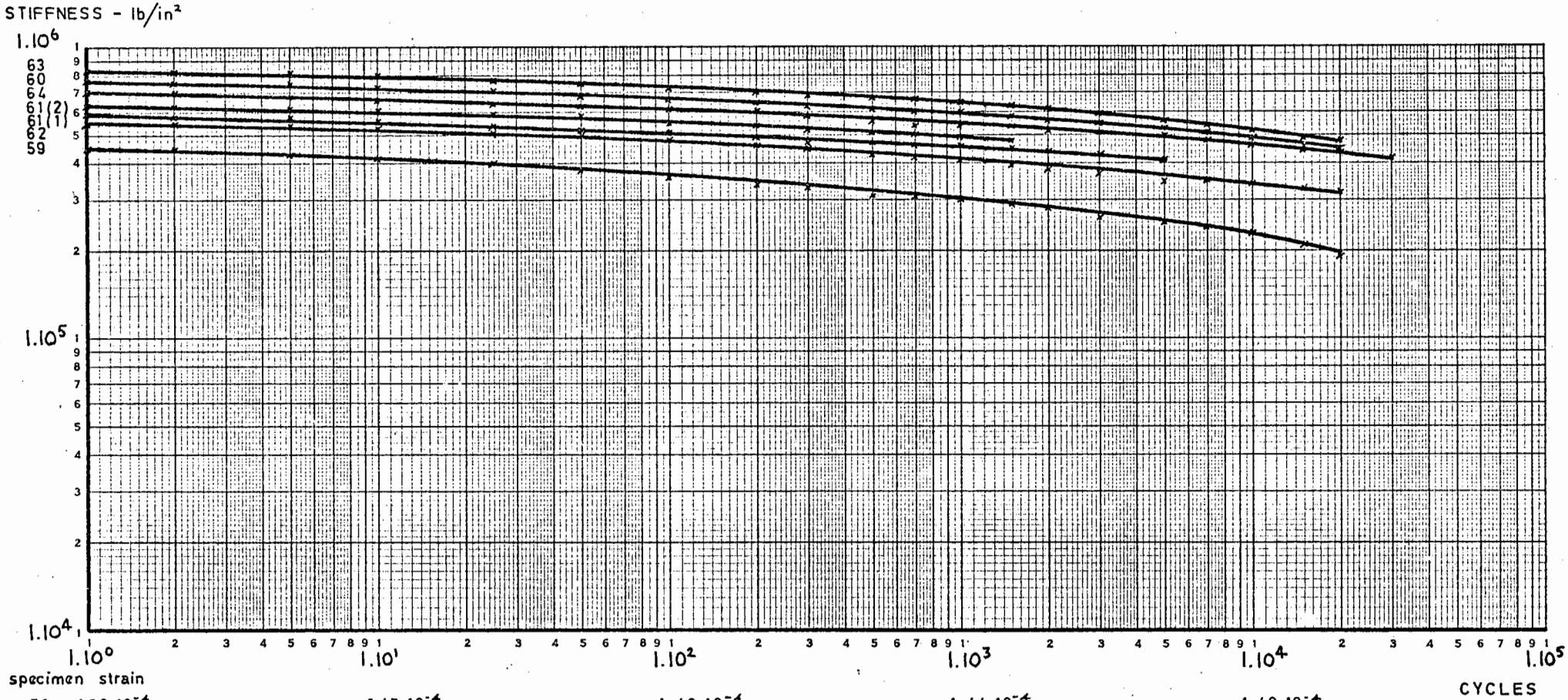

specimen	strain				
59	$1{\cdot}30.10^{-4}$	$1{\cdot}45.10^{-4}$	$1{\cdot}48.10^{-4}$	$1{\cdot}44.10^{-4}$	$1{\cdot}40.10^{-4}$
60	0·97	1·04	1·09	1·16	1·36
61(1)	1·11	1·19	1·24	1·27	—
61(2)	1·02	1·07	1·12	1·21	—
62	1·07	1·16	1·22	1·28	1·14
63	0·96	1·02	1·05	1·10	1·12
64	0·91	0·96	1·00	1·01	0·87

FIG. 93 STIFFNESS CURVES OF BATCH OF SPECIMENS OF 90/110 DENSE BITUMEN MACADAM AT MEDIUM STRAIN LEVEL AT +10° C.

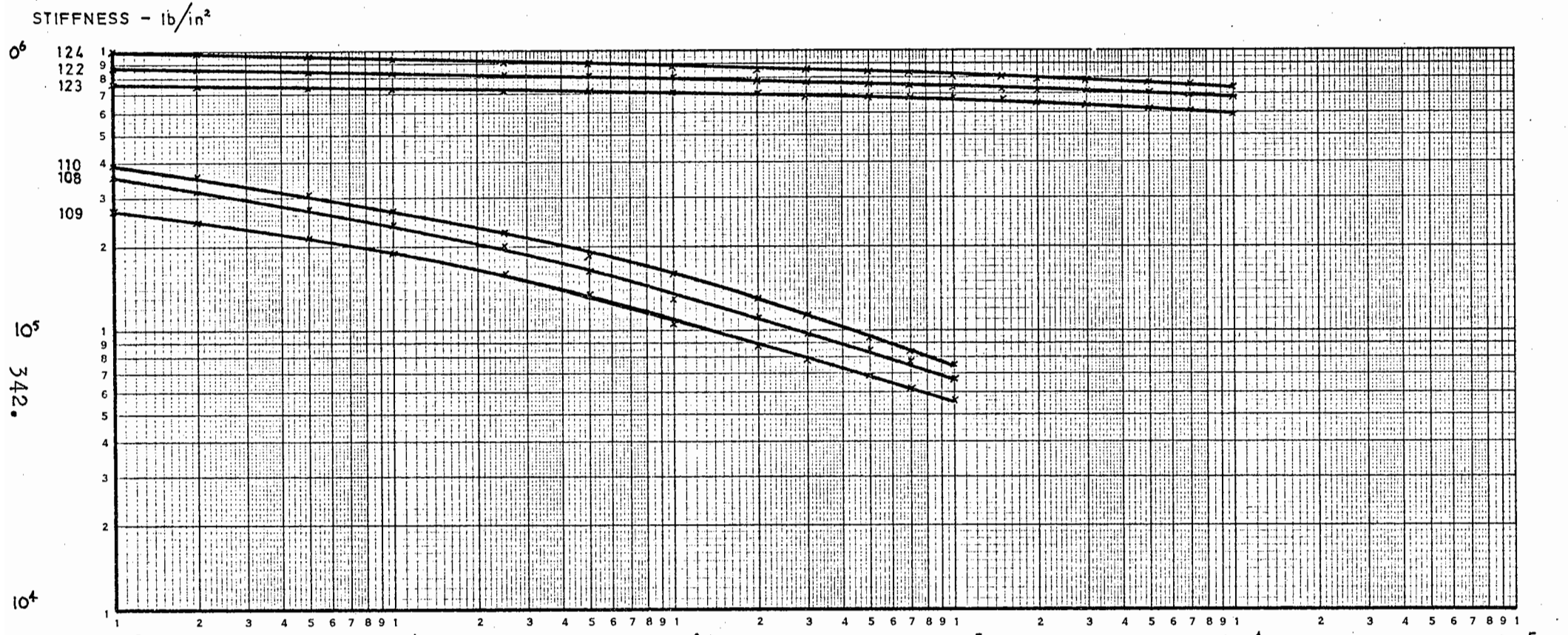

specimen	strain				
122	$5{\cdot}64.10^{-5}$	$5{\cdot}67.10^{-5}$	$5{\cdot}72.10^{-5}$	$5{\cdot}75.10^{-5}$	$5{\cdot}50.10^{-5}$
123	$5{\cdot}62$	$5{\cdot}62$	$5{\cdot}53$	$4{\cdot}94$	$5{\cdot}01$
124	$5{\cdot}49$	$5{\cdot}49$	$5{\cdot}49$	$5{\cdot}20$	$5{\cdot}17$
108	$1{\cdot}21.10^{-3}$	$1{\cdot}20.10^{-3}$	$1{\cdot}14.10^{-3}$	$1{\cdot}06.10^{-3}$	—
109	$1{\cdot}22$	$1{\cdot}22$	$1{\cdot}13$	$1{\cdot}06$	—
110	$1{\cdot}23$	$1{\cdot}22$	$1{\cdot}15$	$1{\cdot}06$	—

FIG. 94 STIFFNESS CURVES OF 90/110 DENSE BITUMEN MACADAM AT HIGH AND LOW STRAIN LEVELS AT +10°C

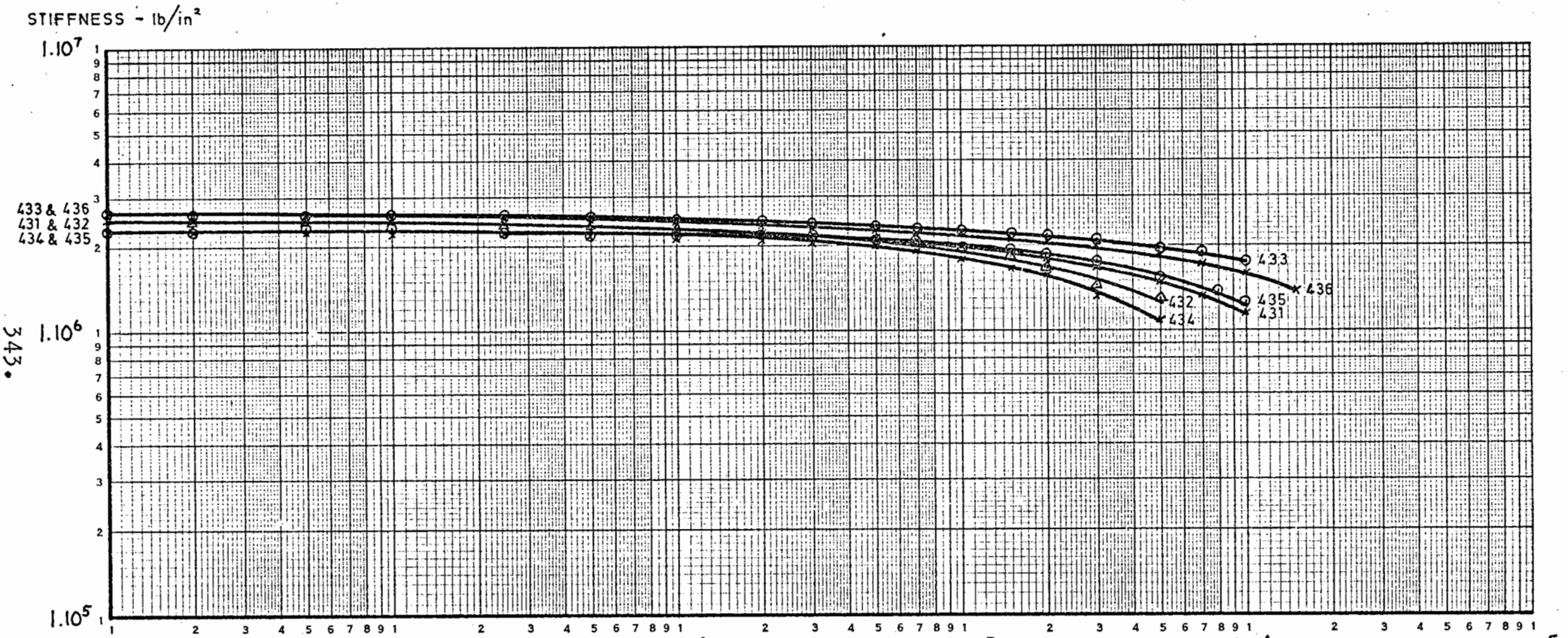

specimen	strain				
431	$3{\cdot}85.10^{-5}$	$3{\cdot}94.10^{-5}$	$4{\cdot}12.10^{-5}$	$4{\cdot}65.10^{-5}$	$5{\cdot}17.10^{-5}$
432	3·66	3·75	3·92	4·09	—
433	4·05	4·05	4·13	4·39	4·81
434	4·35	4·35	4·43	4·85	—
435	4·27	4·36	4·61	4·70	5·13
436	3·94	4·12	4·18	4·35	5·02

FIG. 95 STIFFNESS CURVES OF BATCH OF SPECIMENS OF DENSE TAR MACADAM AT MEDIUM STRAIN LEVEL AT +10° C

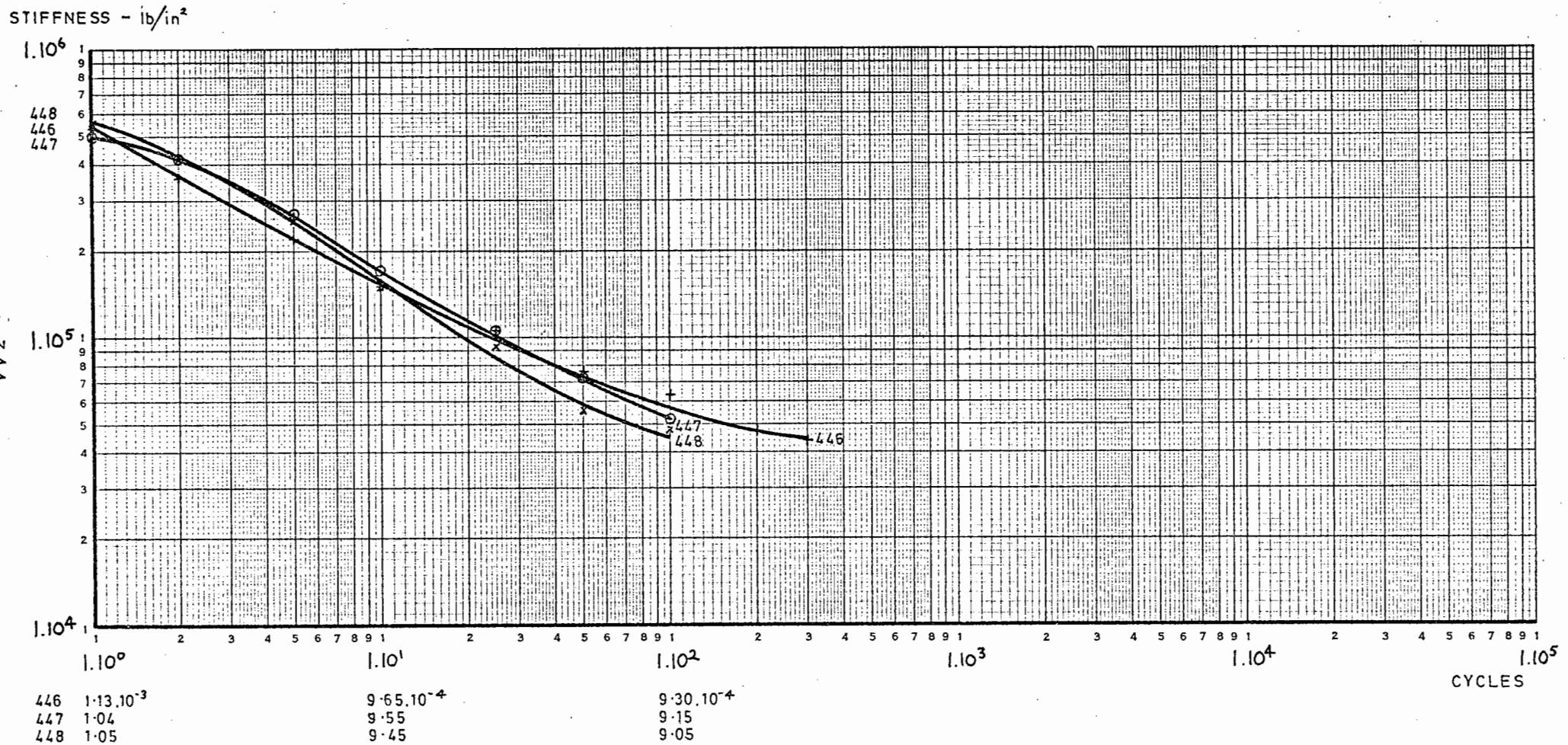

FIG. 96 STIFFNESS CURVES OF DENSE TAR MACADAM AT LOW STRAIN LEVEL AT +10°C

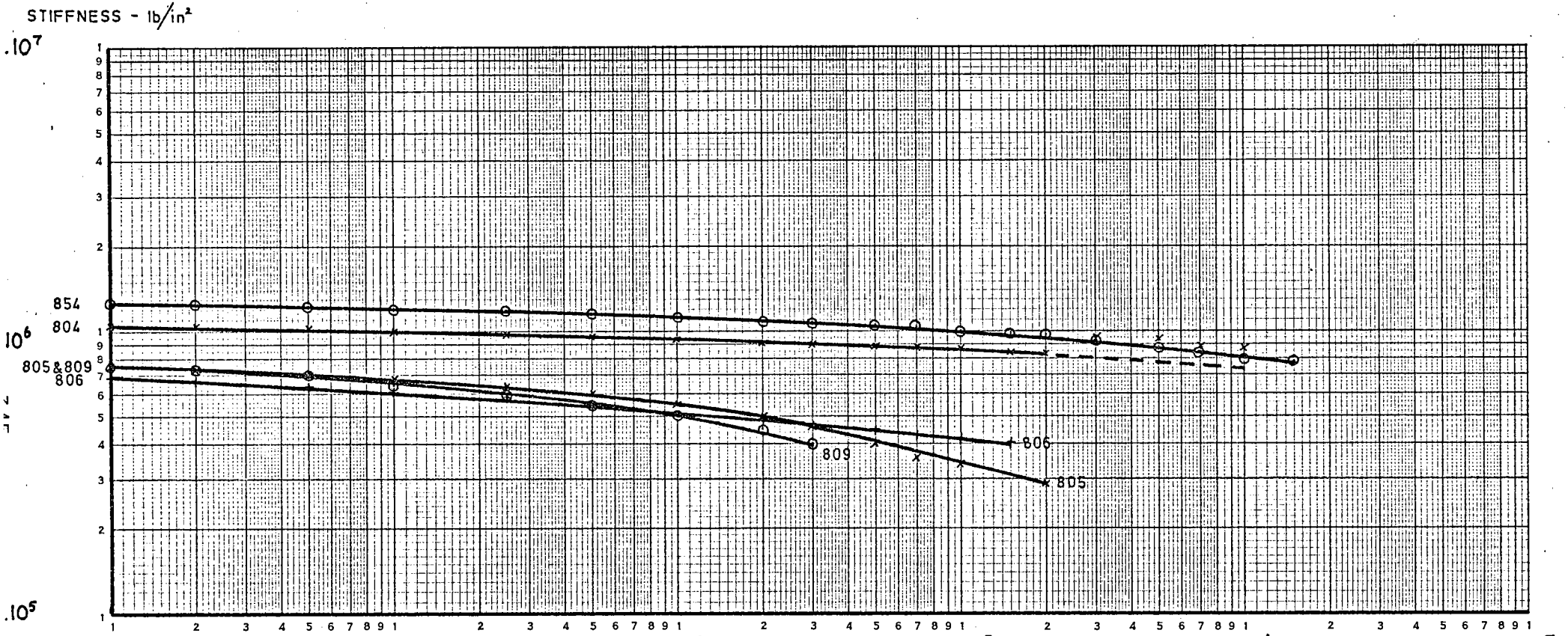

specimen	strain				
854	$7{\cdot}99.10^{-5}$	$8{\cdot}40.10^{-5}$	$8{\cdot}65.10^{-5}$	$9{\cdot}07.10^{-5}$	$9{\cdot}25.10^{-5}$
804	$1{\cdot}00.10^{-4}$	$1{\cdot}06.10^{-4}$	$1{\cdot}10.10^{-4}$	$1{\cdot}20.10^{-4}$	$1{\cdot}03.10^{-4}$
805	2·50	2·60	2·63	2·50	—
806	2·53	2·57	2·55	2·52	—
809	2·50	2·51	2·52	—	—

FIG. 97 STIFFNESS CURVES OF HOT ROLLED ASPHALT AT MEDIUM STRAIN LEVEL AT +10°C

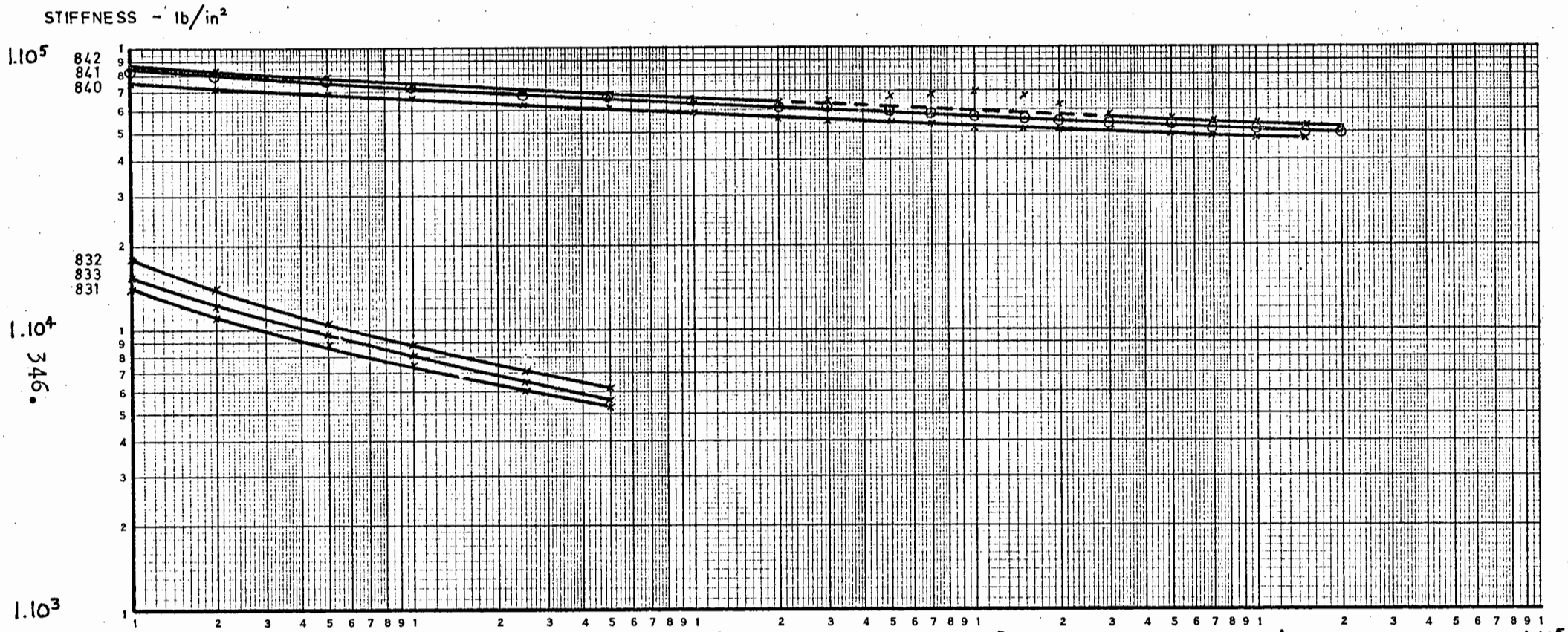

specimen	strain				
840	$1{\cdot}98.10^{-4}$	$1{\cdot}98.10^{-4}$	$1{\cdot}99.10^{-4}$	$2{\cdot}02.10^{-4}$	$2{\cdot}00.10^{-4}$
841	2·00	1·96	1·97	1·99	2·00
842	1·94	1·94	1·94	1·84	1·93
831	$4{\cdot}33.10^{-3}$	$4{\cdot}32.10^{-3}$	—	—	—
832	4·35	4·34	—	—	—
833	4·36	4·36	—	—	—

FIG. 98 STIFFNESS CURVES OF HOT ROLLED ASPHALT AT HIGH AND LOW STRAIN LEVELS AT +30°C

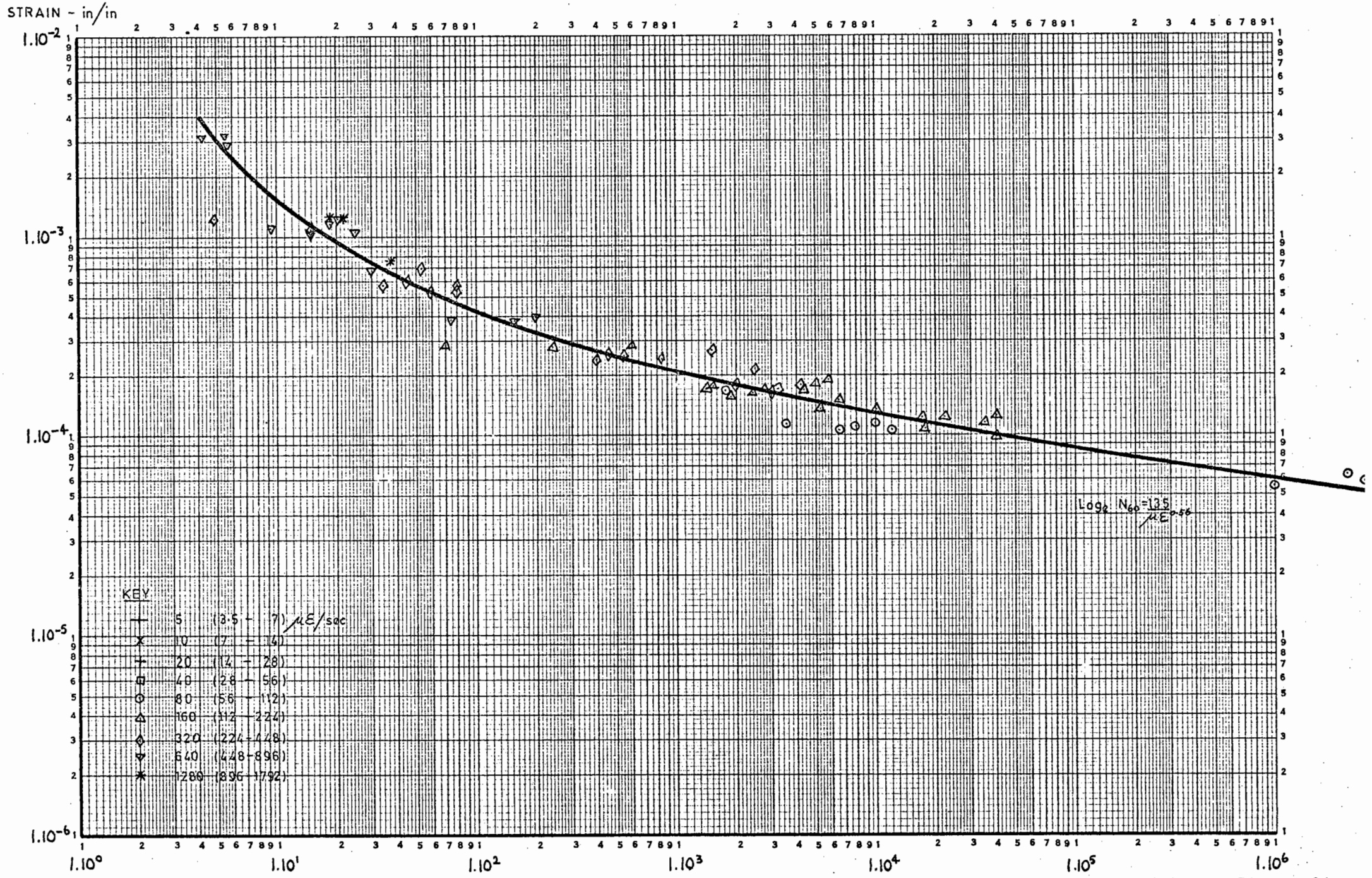

FIG. 99 CYCLES TO 60% OF INITIAL STIFFNESS OF 90/110 pen. R.B.M. AT +10° C

CHART WELL Graph Data Ref. 5946 Log 4 Cycles x 6 Cycles

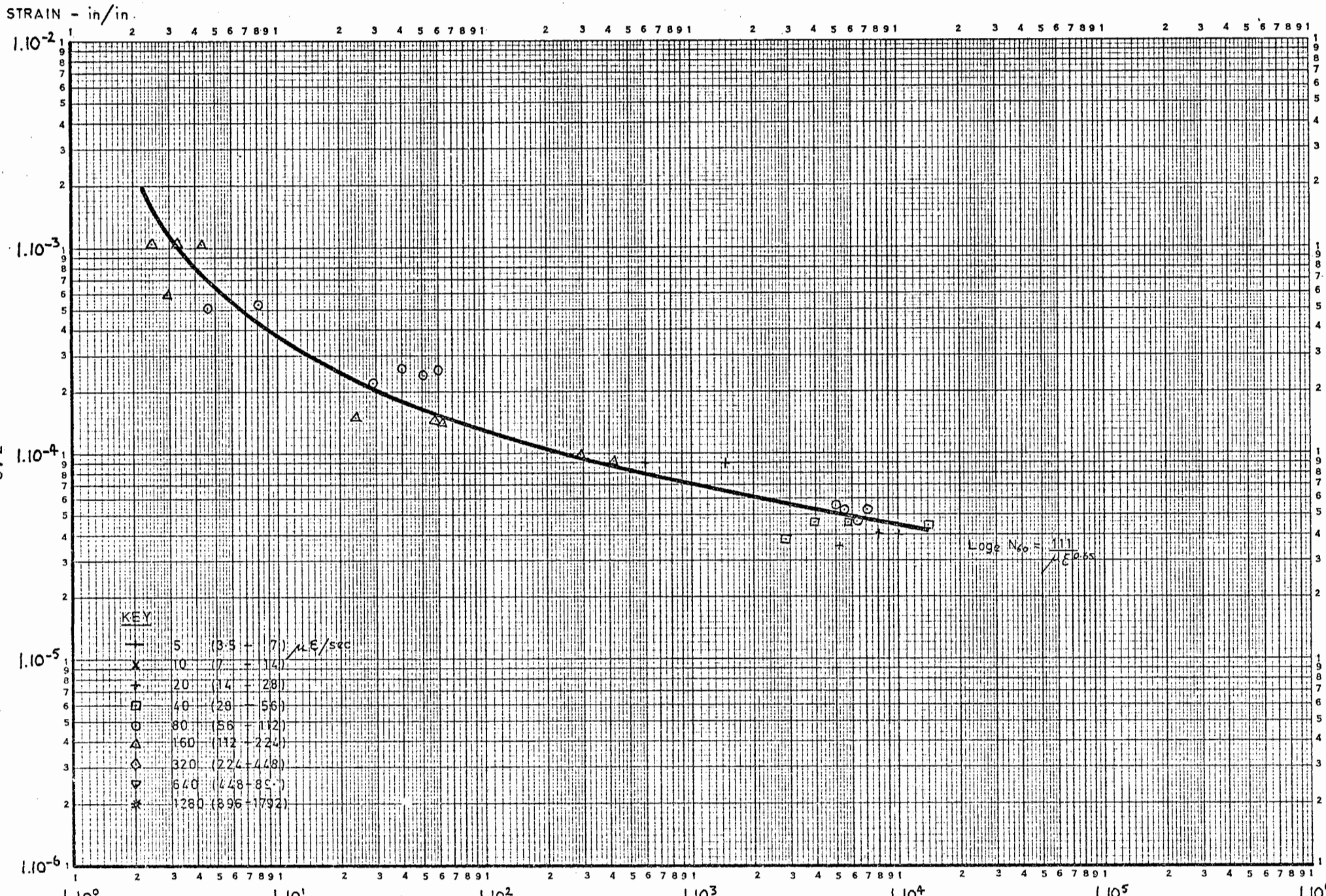

FIG. 100 CYCLES TO 60% OF INITIAL STIFFNESS OF D.T.M. AT +10° C

WELL Graph Data Ref. 5948 Log 4 Cycles x 6 Cycles

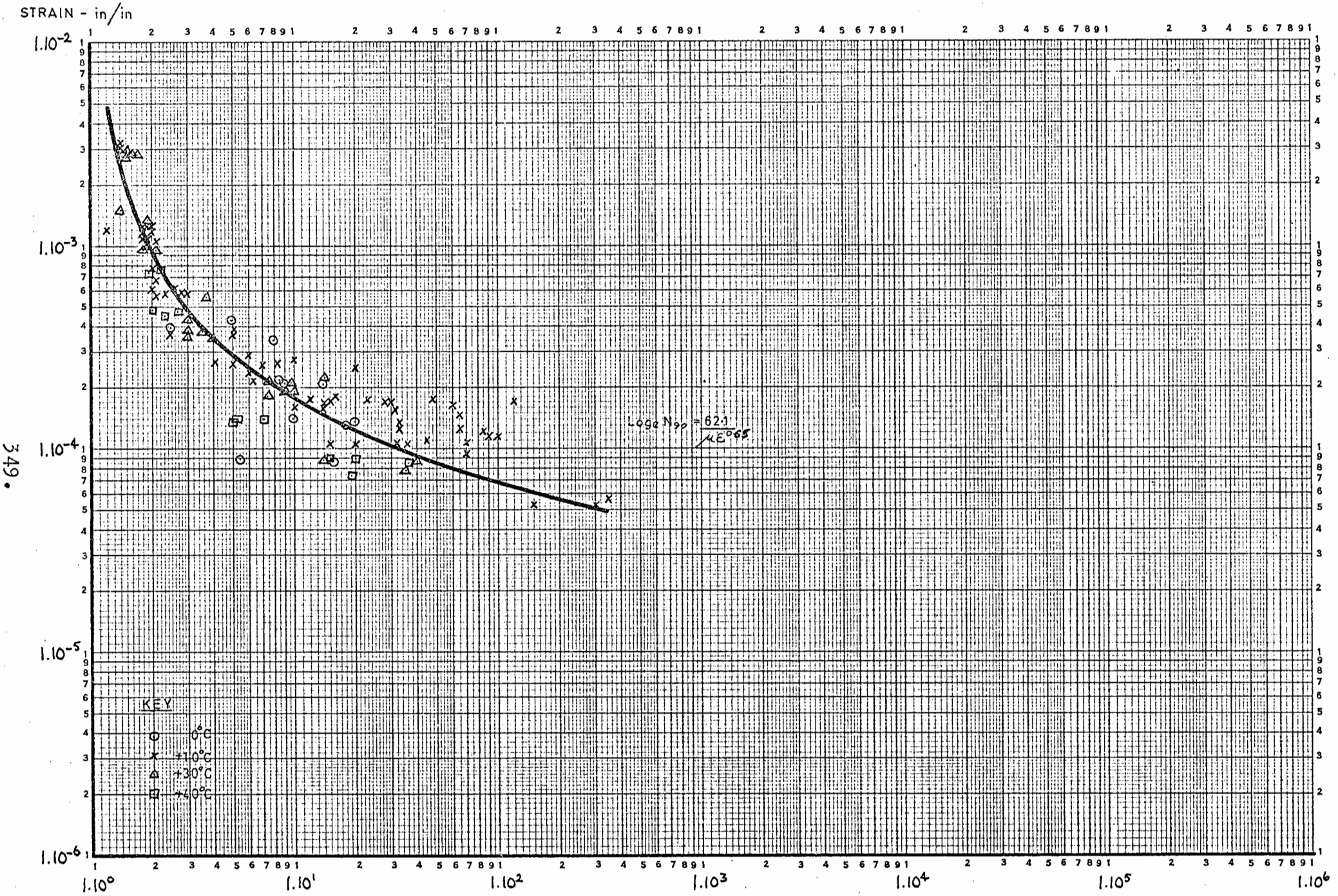

FIG. 101 CYCLES TO 90% OF INITIAL STIFFNESS OF 90/110 D.B.M. AT 0°C to +40°C

WELL DOC Graph Data Ref. 5946 Log 4 Cycles x 6 Cycles

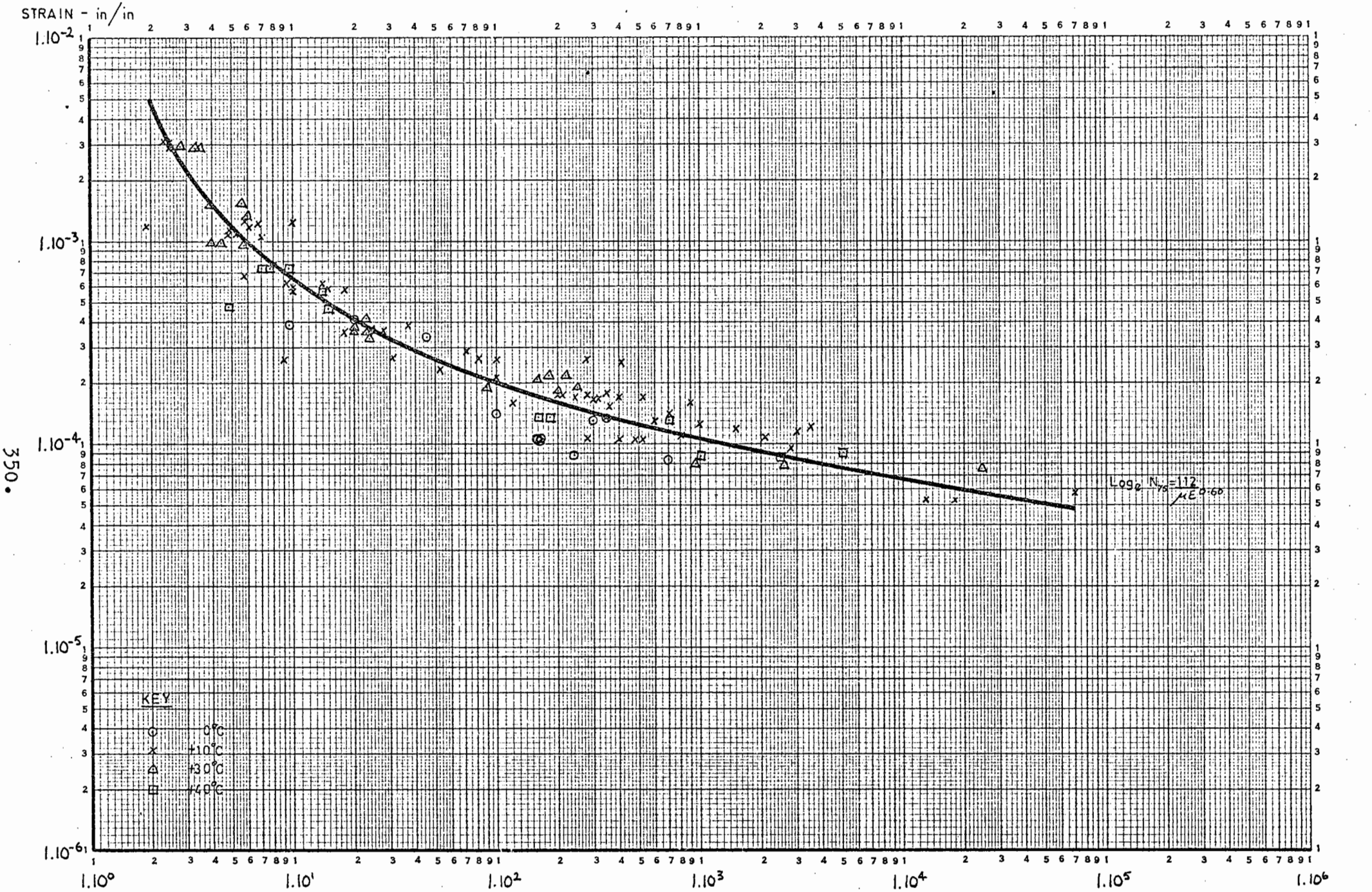

FIG. 102 CYCLES TO 75% OF INITIAL STIFFNESS OF 90/110 D.B.M. AT 0°C to +40°C

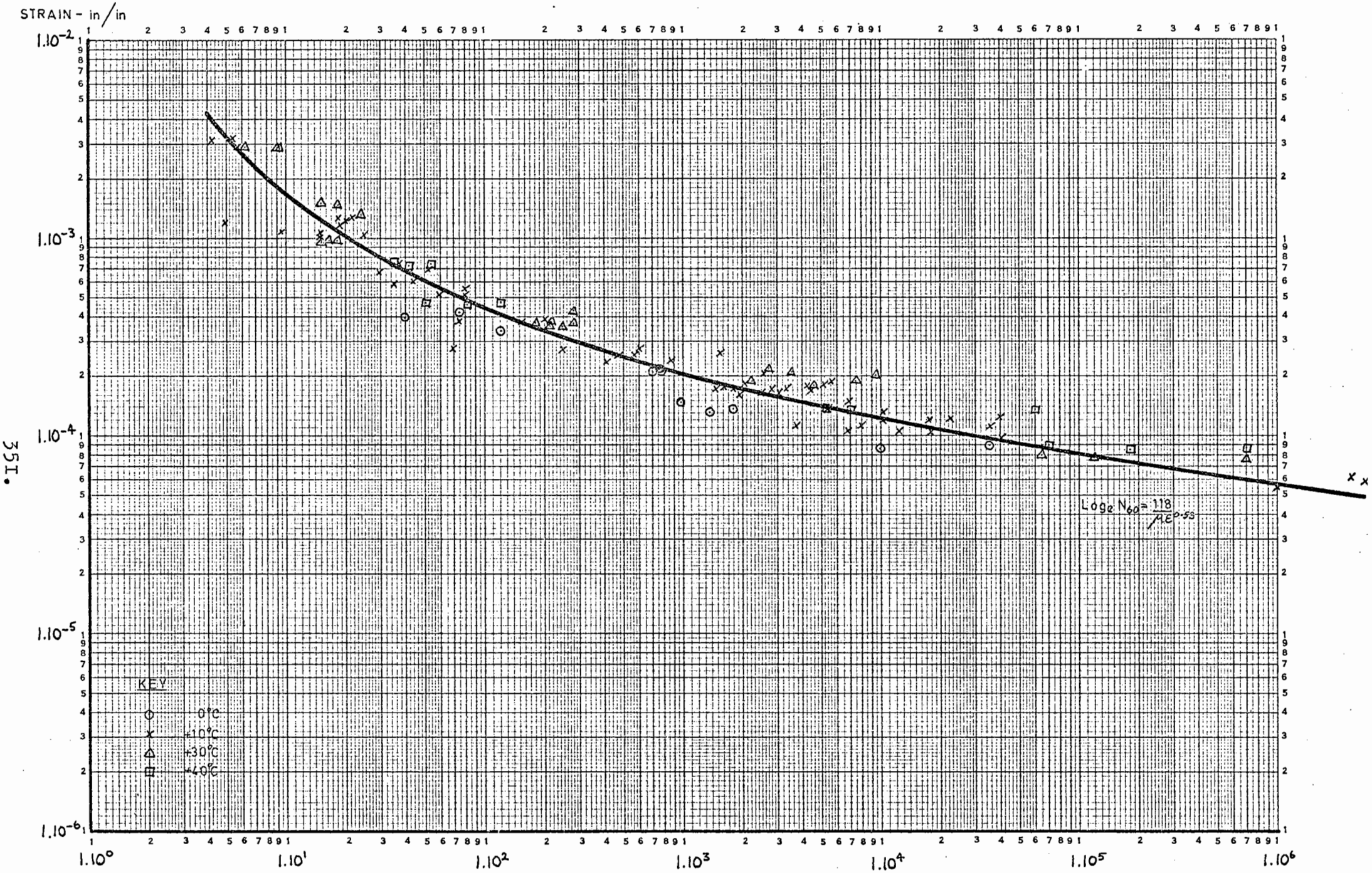

FIG. 103 CYCLES TO 60% OF INITIAL STIFFNESS OF 90/110 D.B.M. AT 0°C to +40°C SERVICE LIFE (CYCLES TO 60% S_I)

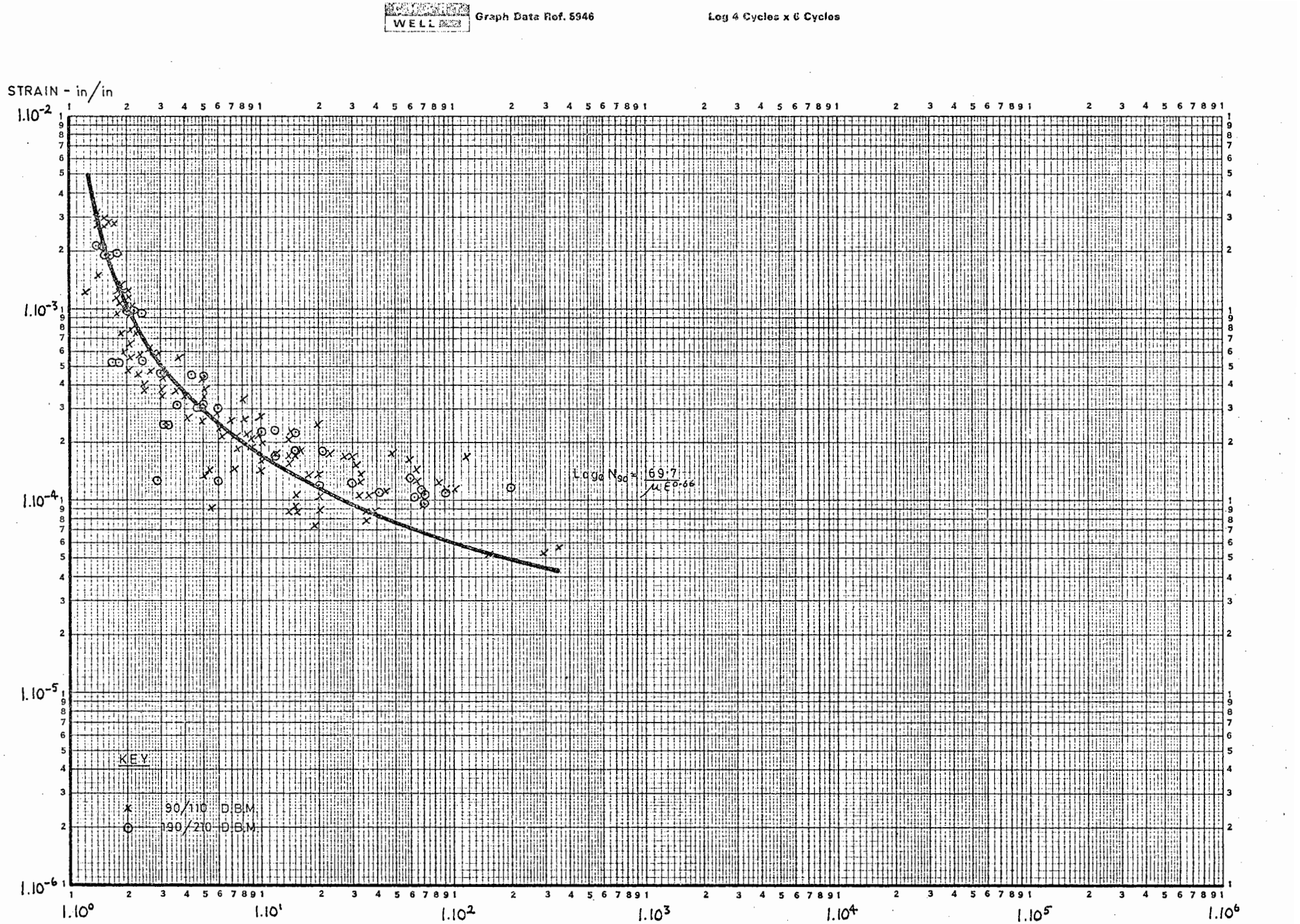

FIG. 104 CYCLES TO 90% OF INITIAL STIFFNESS OF 90/110 AND 190/210 D.B.M. AT 0°C to +40°C

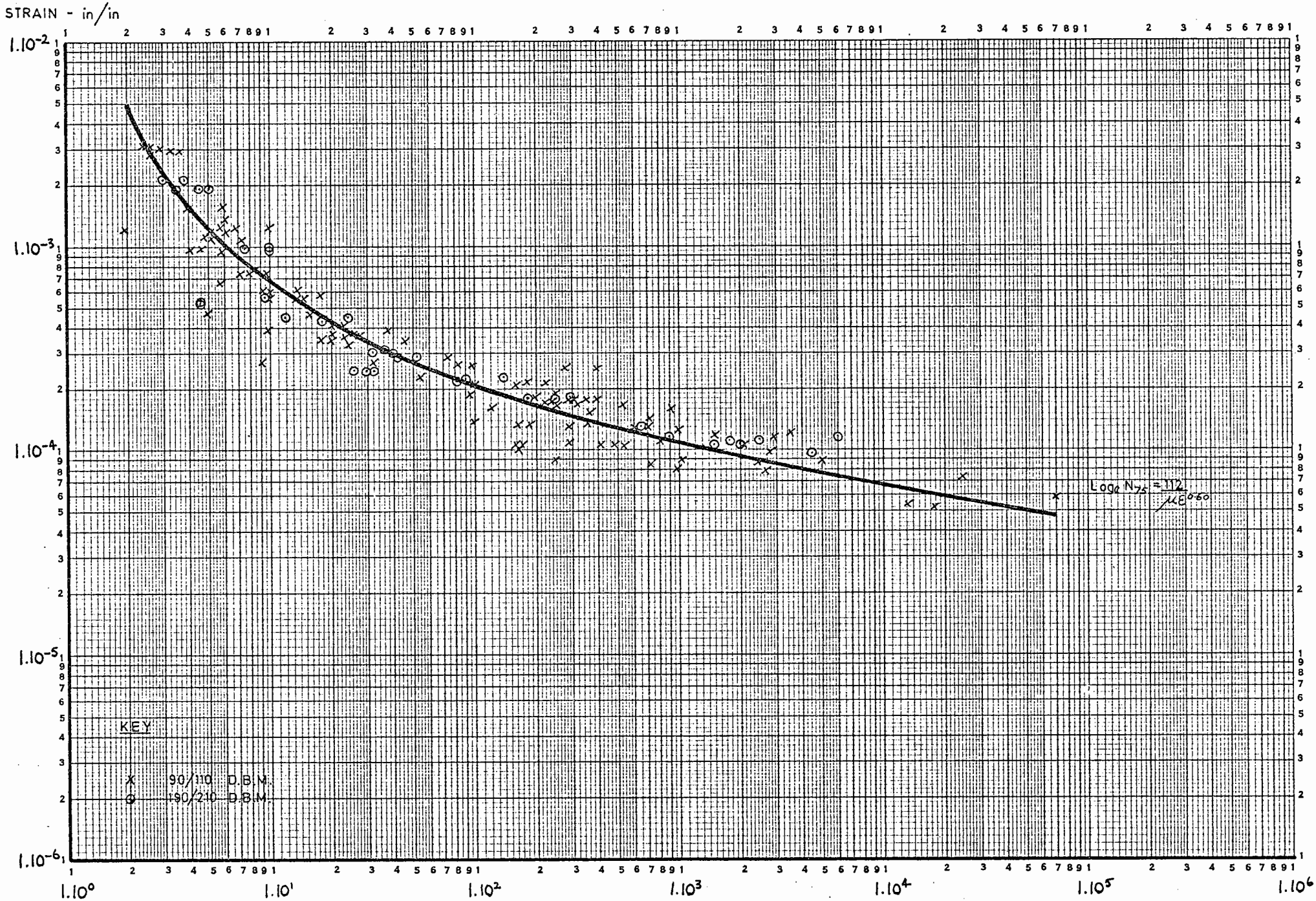

FIG. 105 CYCLES TO 75% OF INITIAL STIFFNESS OF 90/110 AND 190/210 D.B.M. AT 0°C to +40°C CYCLES TO 75% S_I

WELL Graph Data Ref. 5946 Log 4 Cycles x 6 Cycles

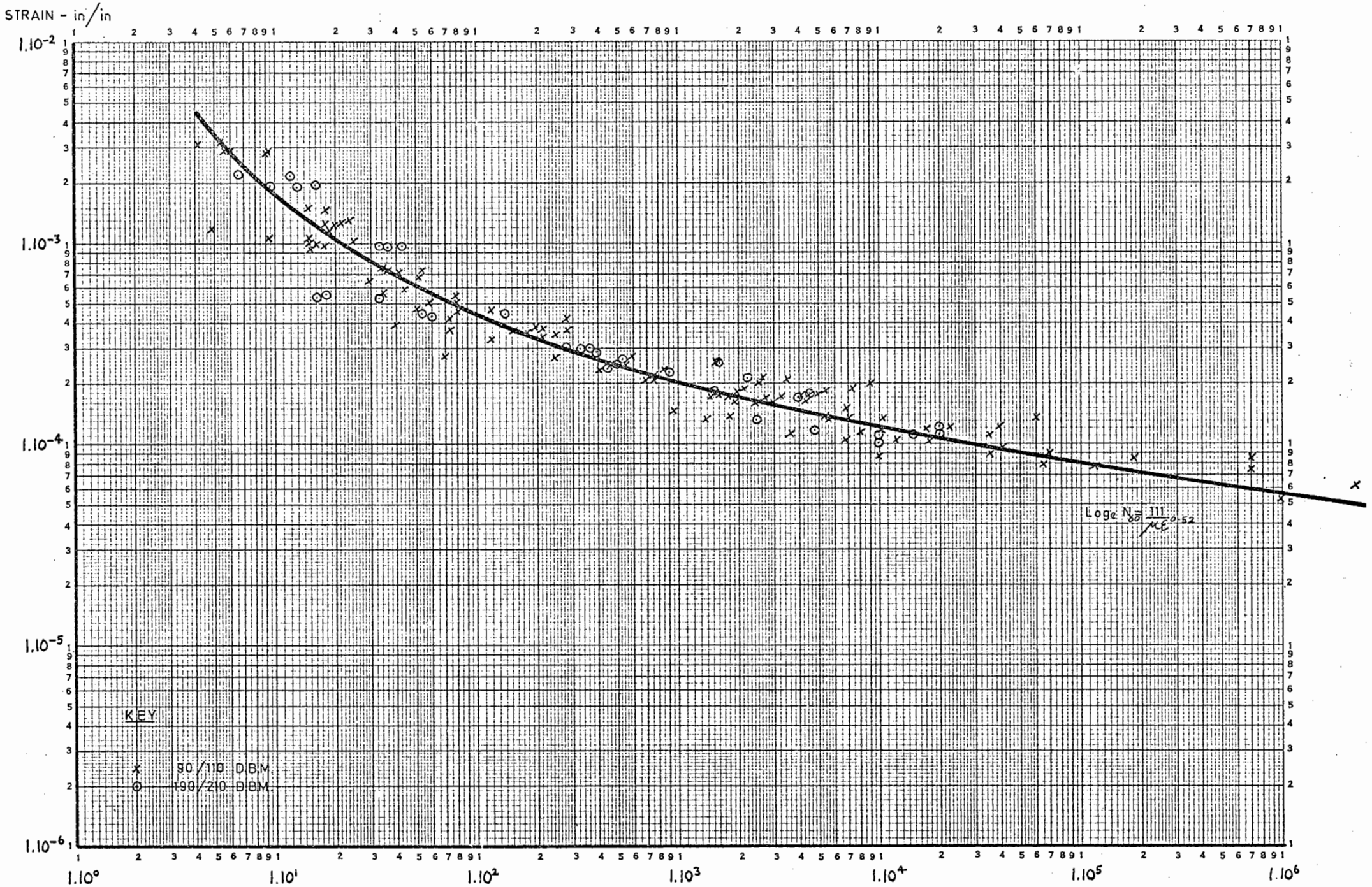

FIG. 106 CYCLES TO 60% OF INITIAL STIFFNESS OF 90/110 AND 190/210 D.B.M. AT SERVICE LIFE (CYCLES TO 60% S_t)

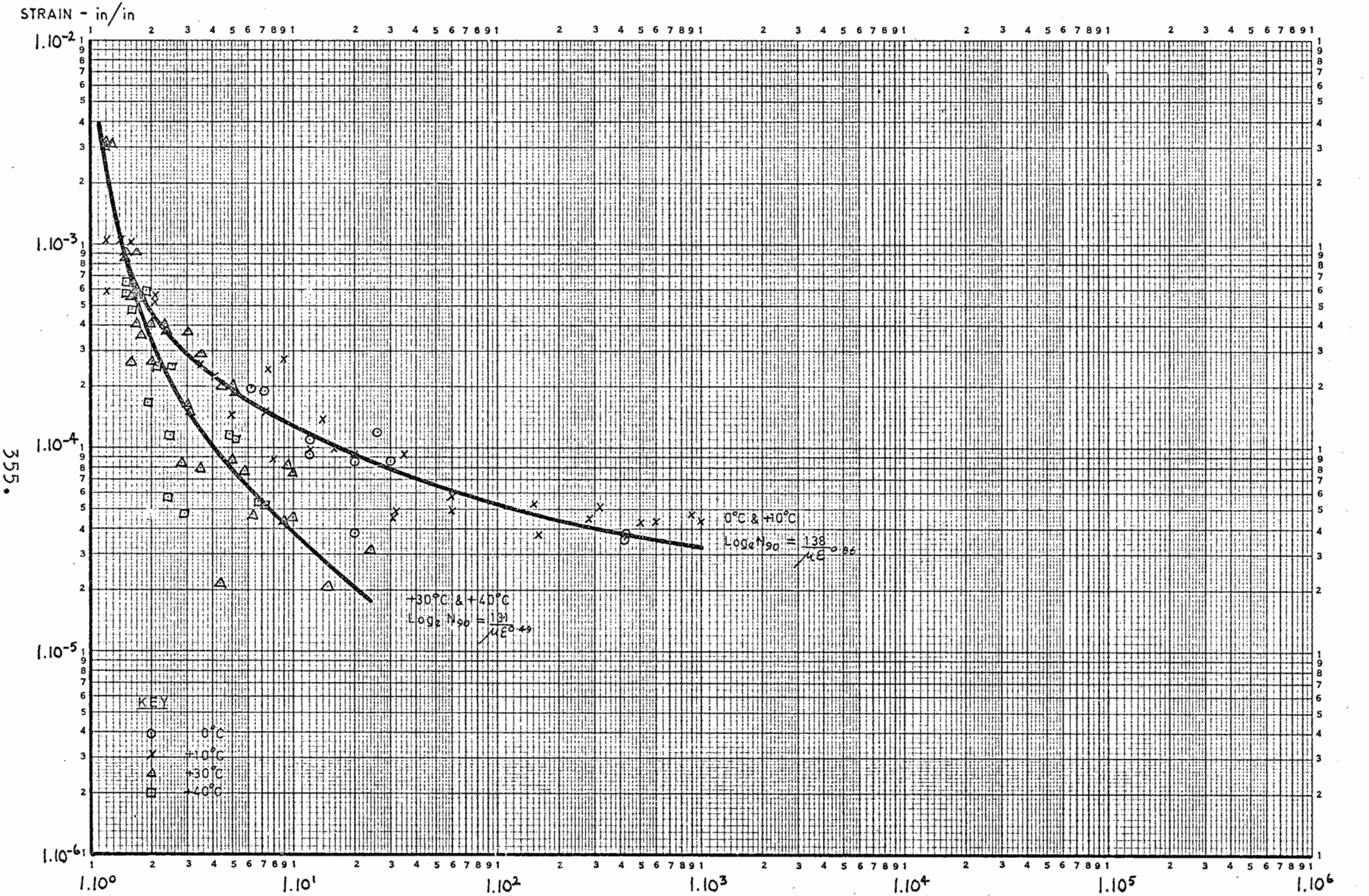

FIG. 107 CYCLES TO 90% OF INITIAL STIFFNESS OF D.T.M. AT 0°C to +40 C

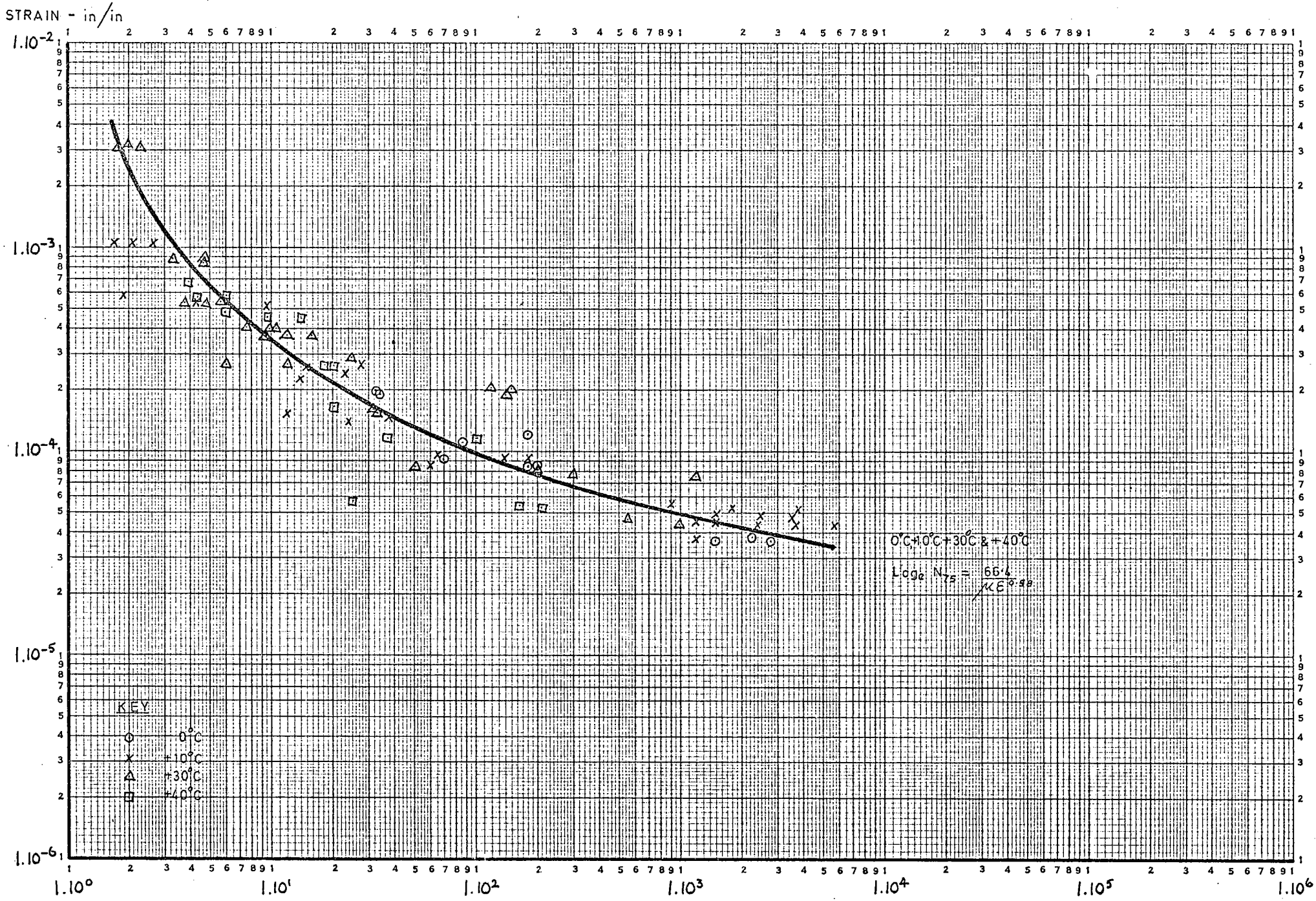

FIG. 108 CYCLES TO 75% OF INITIAL STIFFNESS OF D.T.M. AT 0°C to +40°C

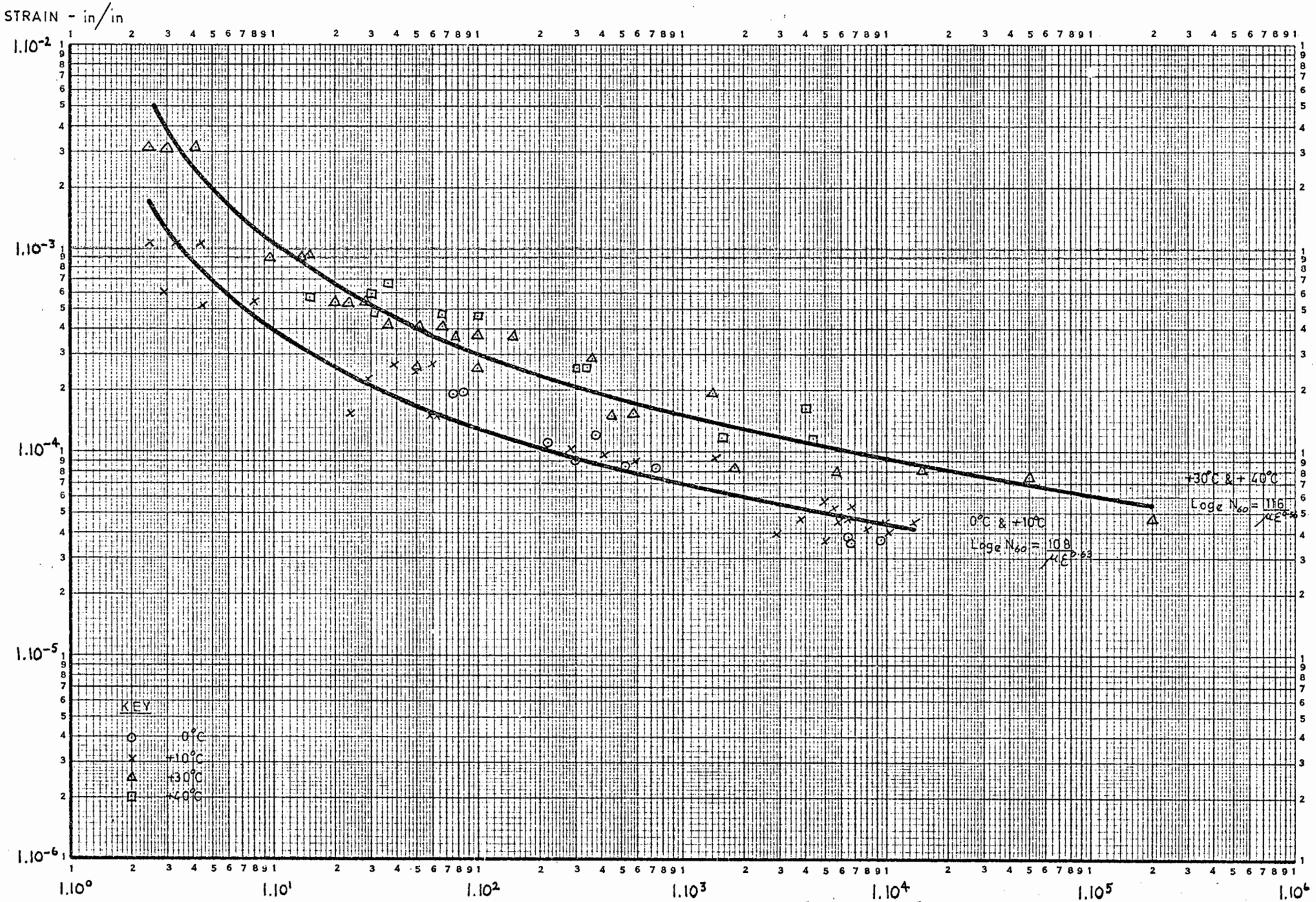

FIG. 109 CYCLES TO 60% OF INITIAL STIFFNESS OF D.T.M. AT 0°C to +40°C

SERVICE LIFE (CYCLES TO 60% S_I)

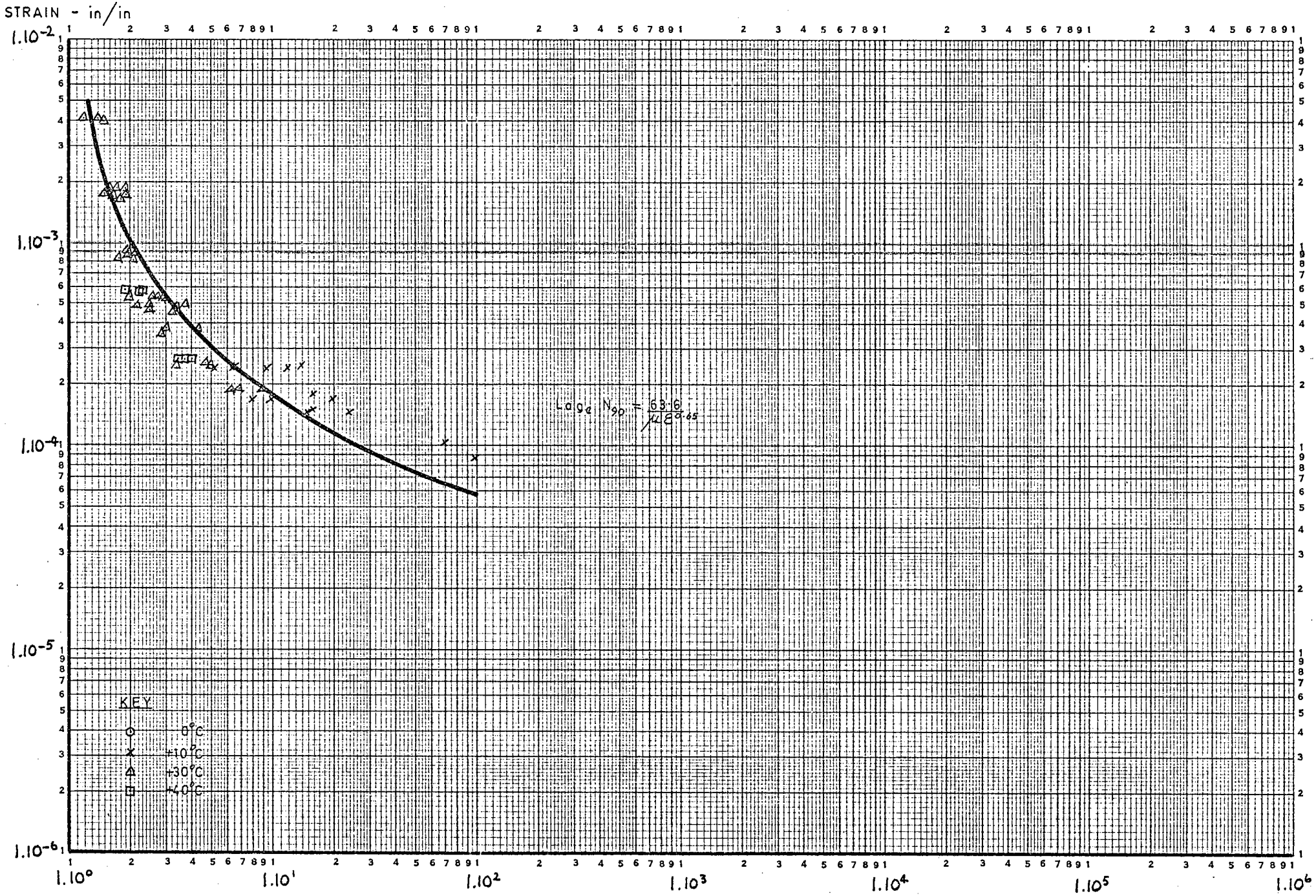

FIG. 110 CYCLES TO 90% OF INITIAL STIFFNESS OF H.R.A. AT +10°C to +40°C

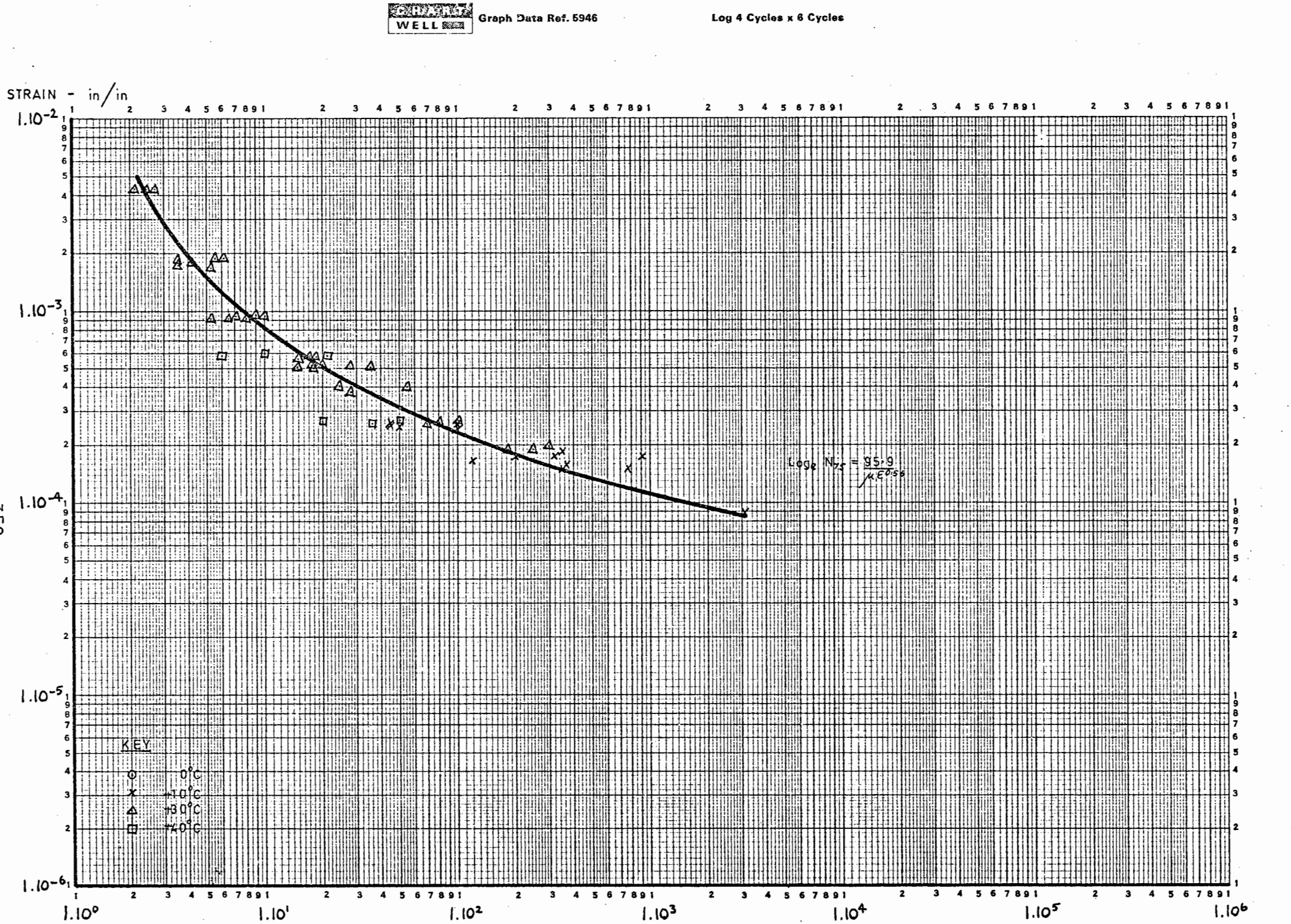

FIG. 111 CYCLES TO 75% OF INITIAL STIFFNESS OF H.R.A. AT +10°C to +40°C

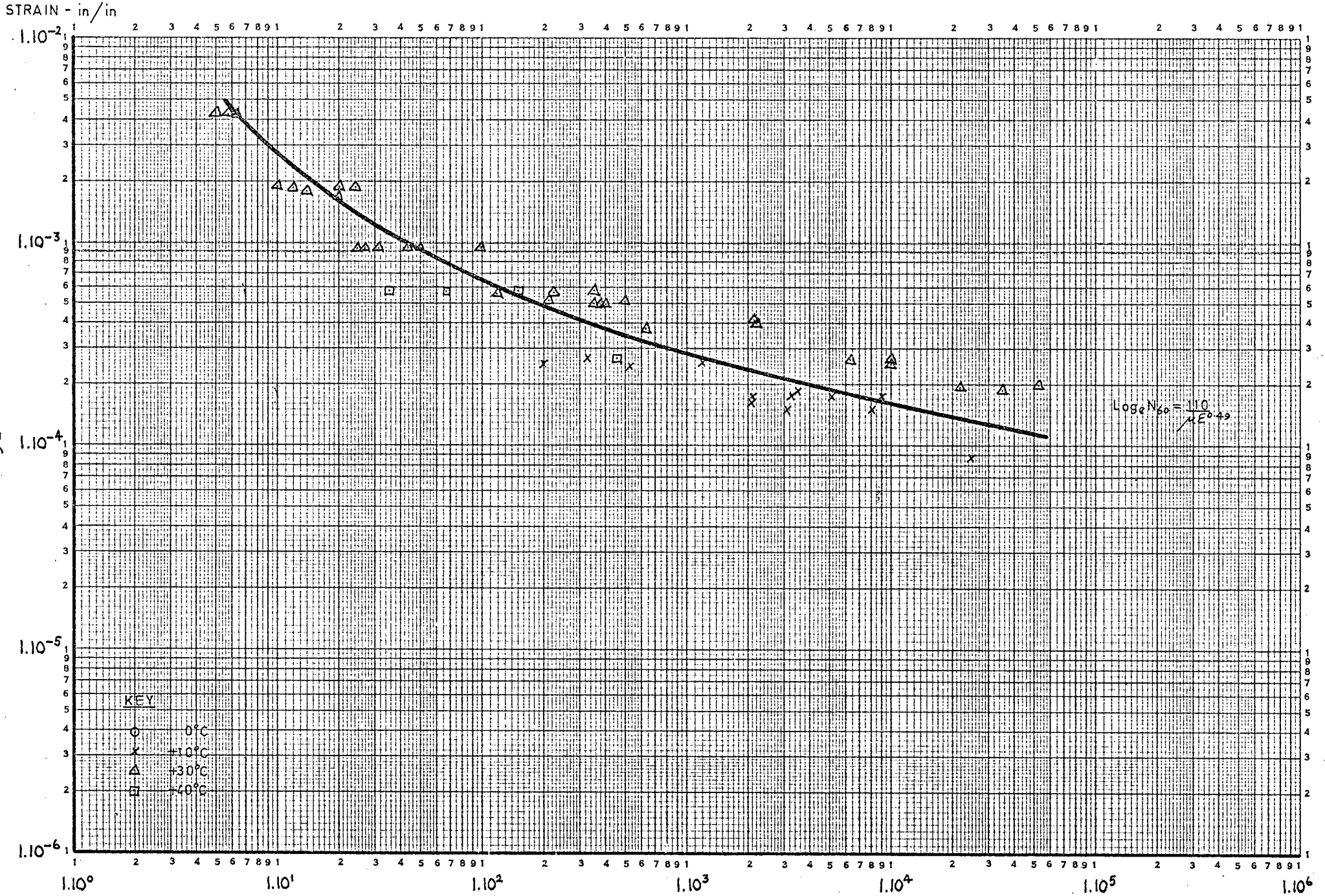

FIG. 112 CYCLES TO 60% OF INITIAL STIFFNESS OF H.R.A. AT +10°C to +40°C

SERVICE LIFE (CYCLES TO 60% S_i)

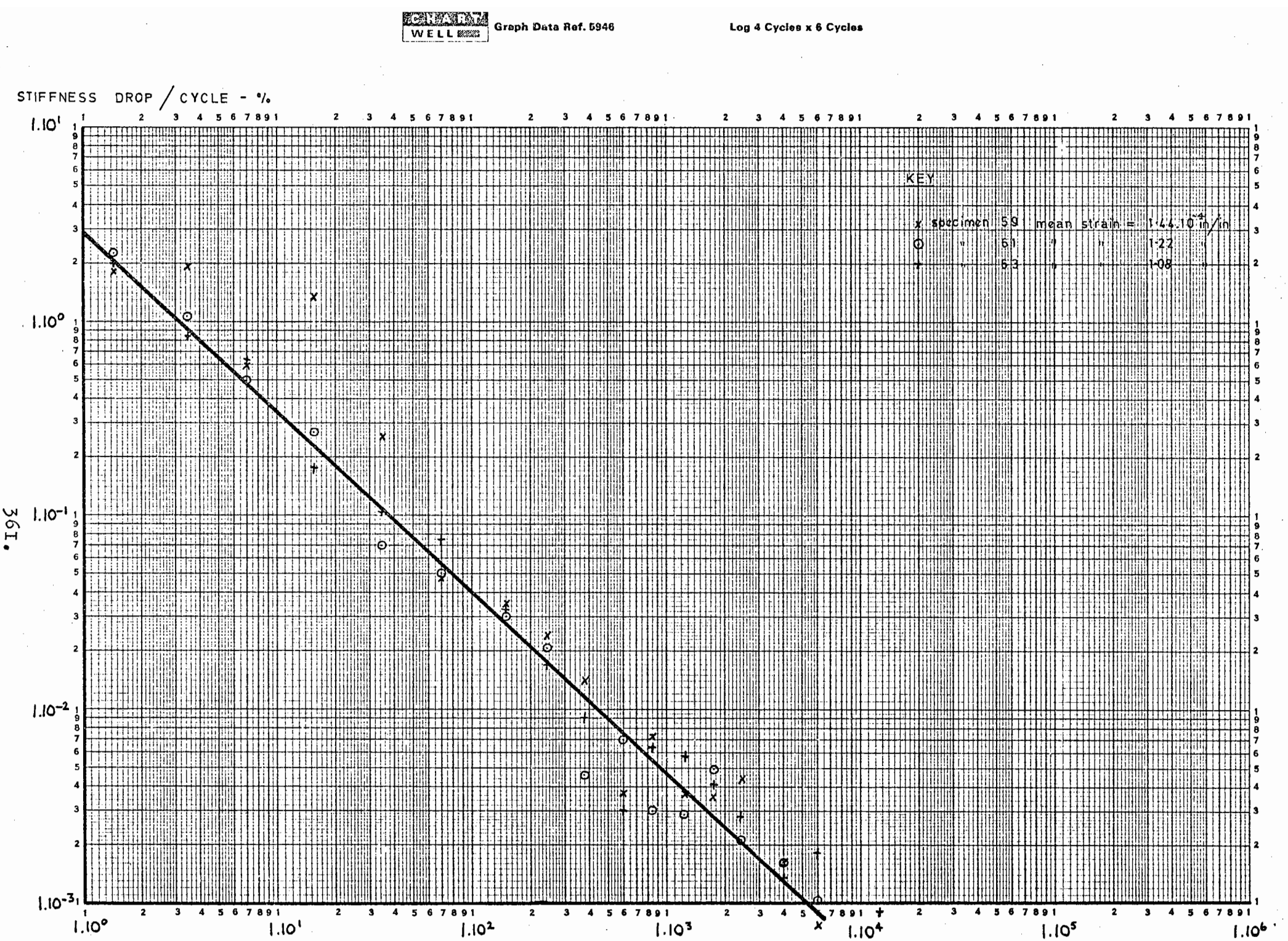

FIG. 113 CHANGE IN STIFFNESS CURVES OF 90/110 D.B.M. AT MEDIUM STRAIN LEVEL AT +10°C

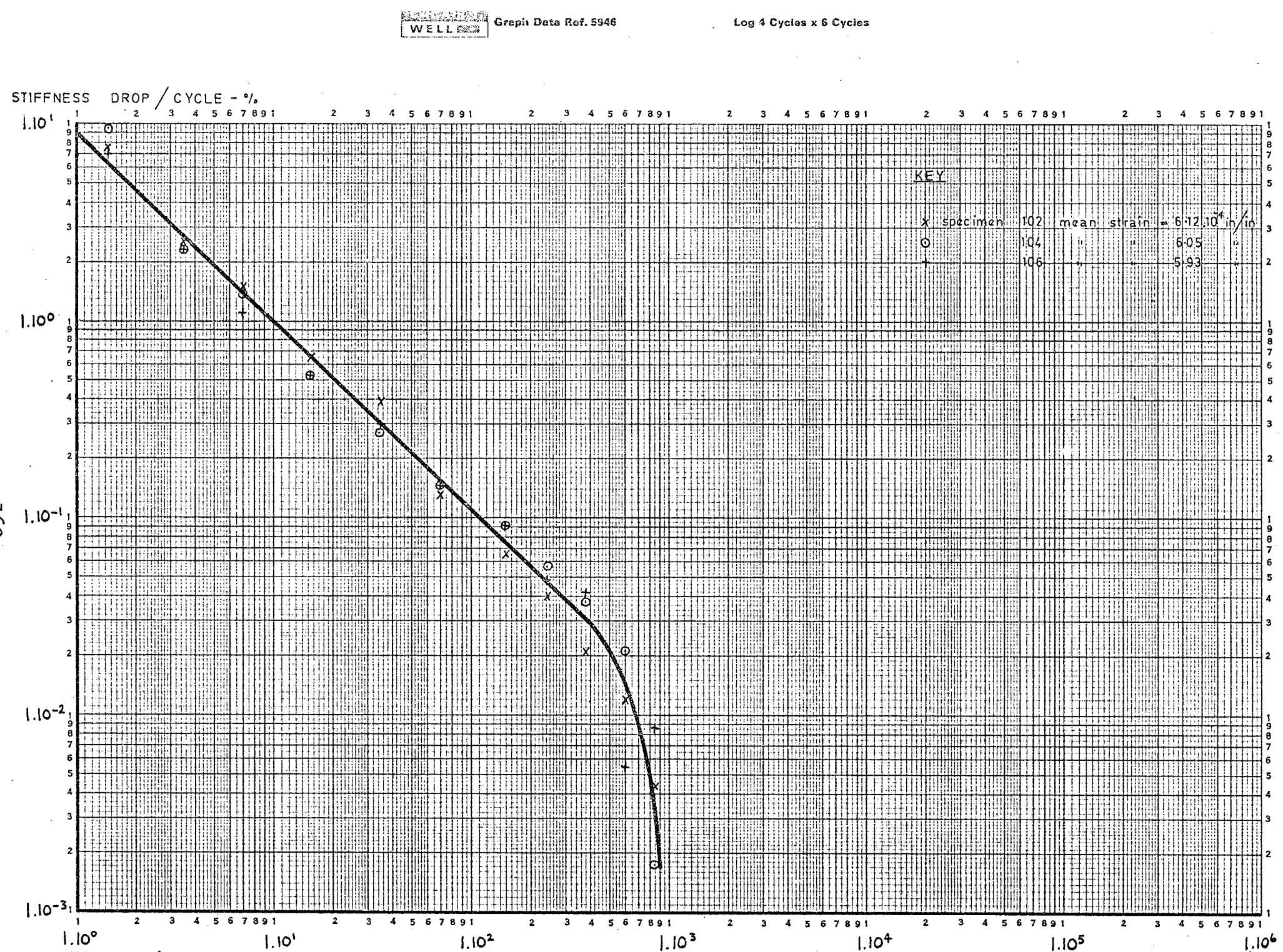

FIG. 114 CHANGE IN STIFFNESS CURVES OF 90/110 D.B.M. AT HIGH STRAIN LEVEL AT +10°C

Graph Data Ref. 5946

Log 4 Cycles x 6 Cycles

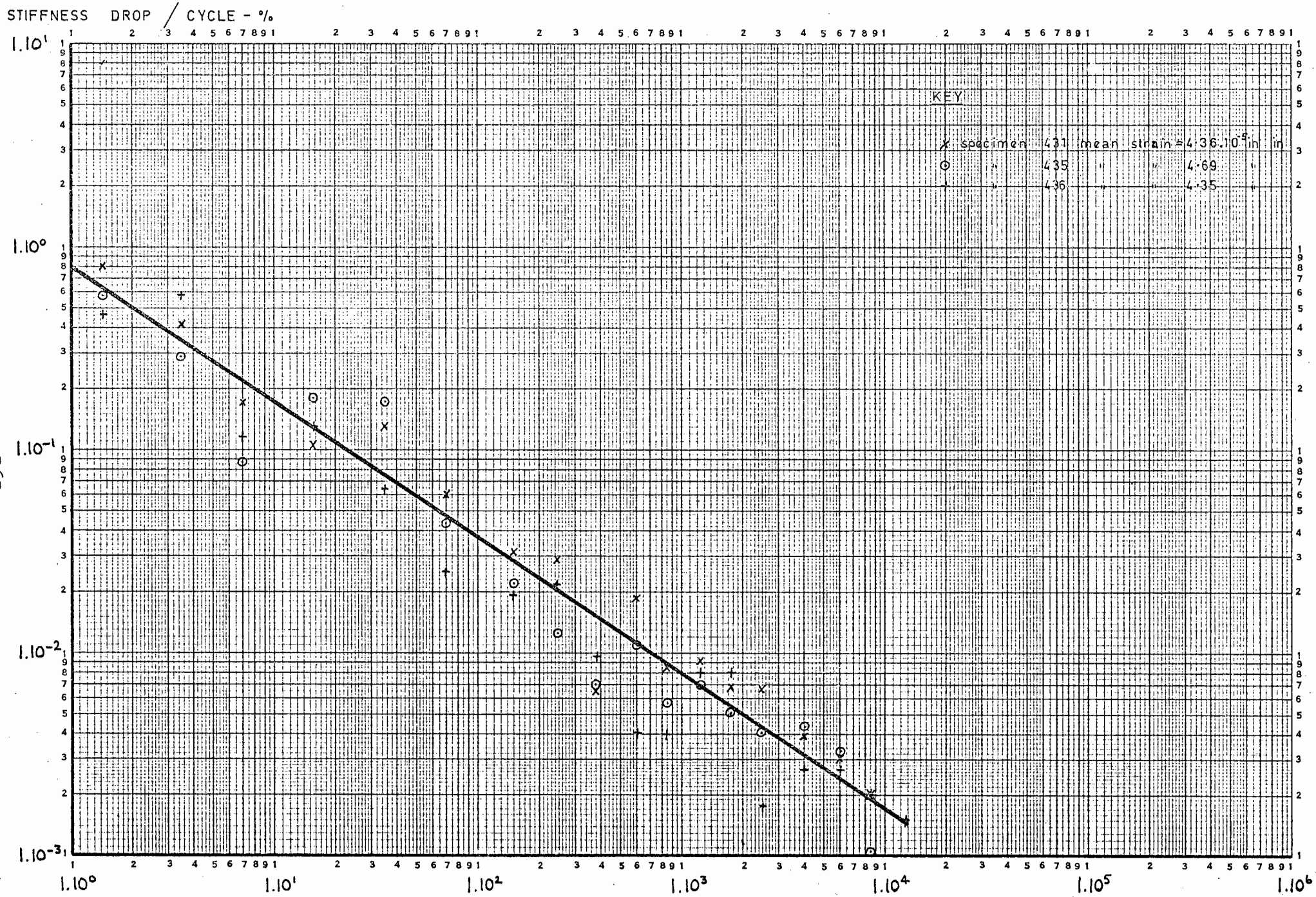

FIG. 115 CHANGE IN STIFFNESS CURVES OF D.T.M. AT LOW STRAIN LEVEL AT +10°C

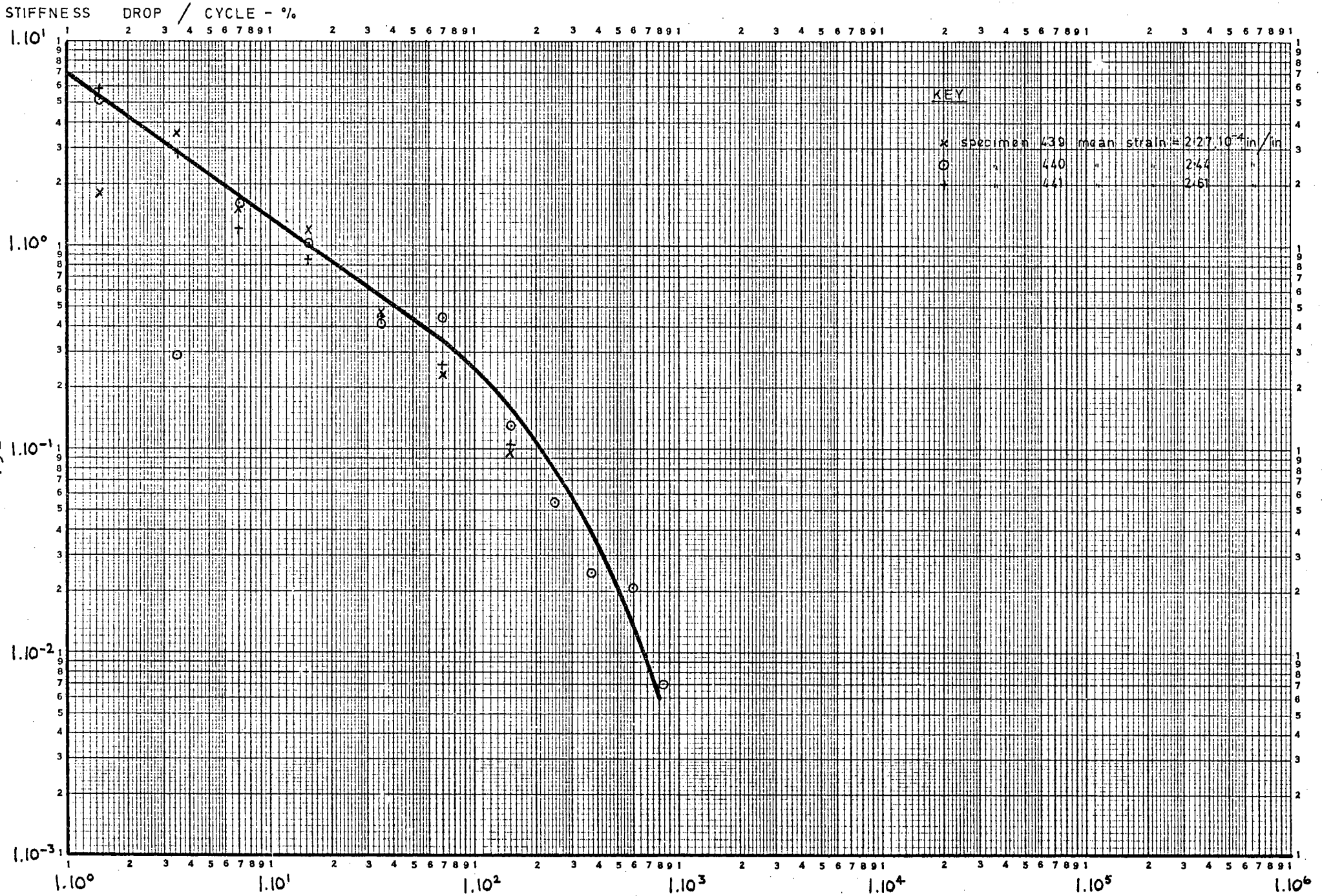

FIG. 116 CHANGE IN STIFFNESS CURVES OF D.T.M. AT MEDIUM STRAIN LEVEL AT +10°C

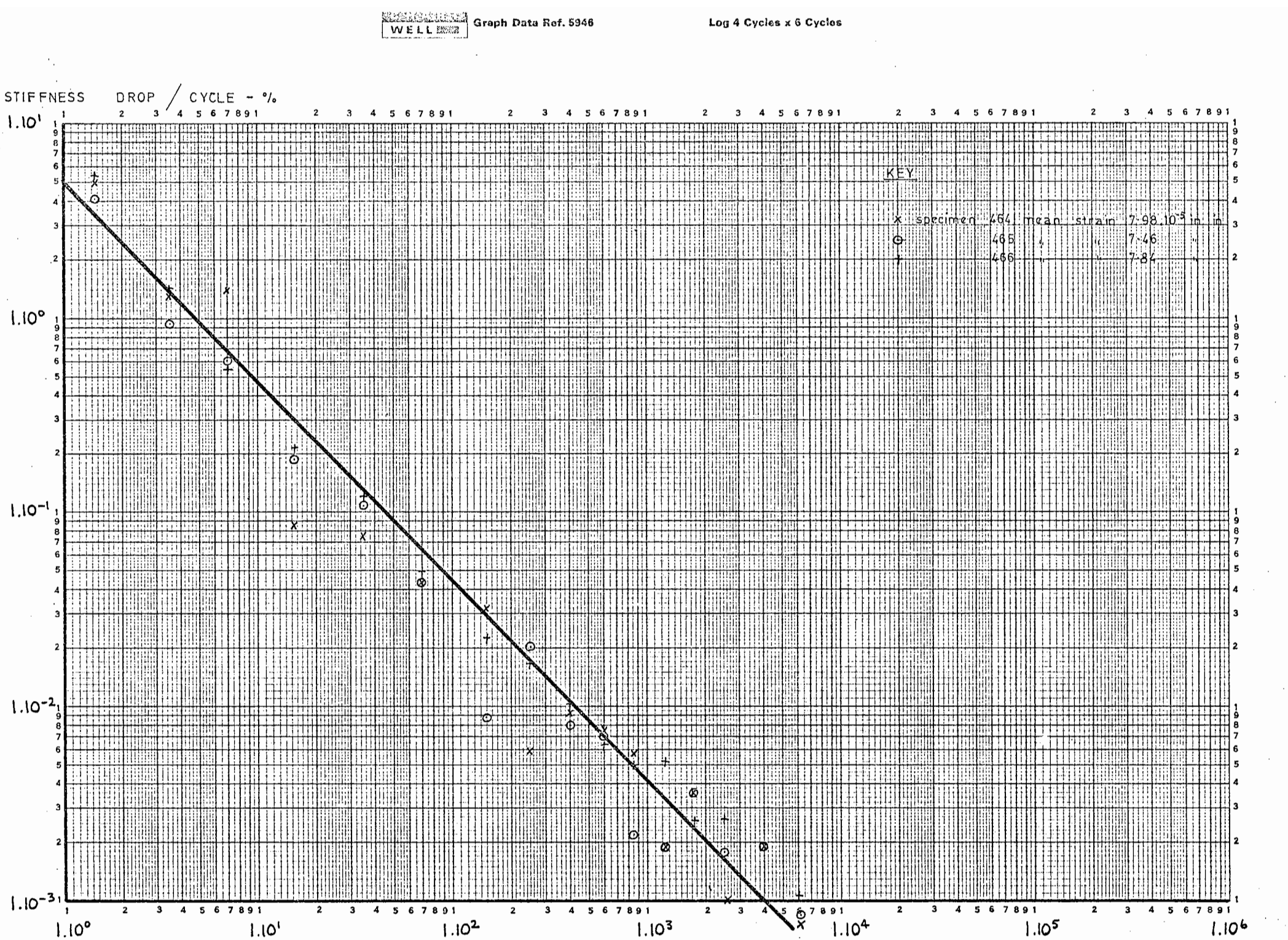

FIG. 117 CHANGE IN STIFFNESS CURVES OF D.T.M. AT LOW STRAIN LEVEL AT +30°C

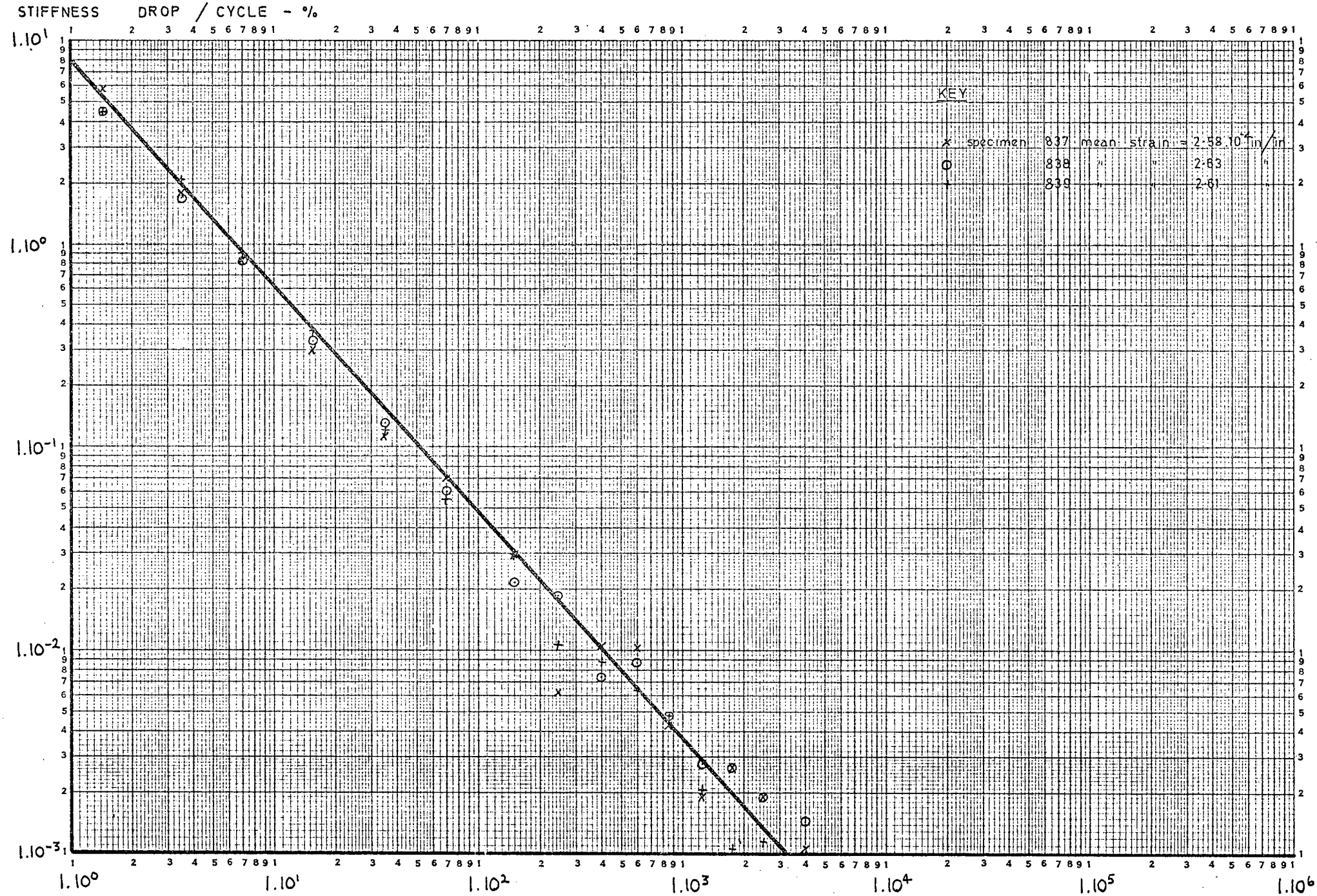

FIG. 118 CHANGE IN STIFFNESS CURVES OF D.T.M. AT MEDIUM STRAIN LEVEL AT +30°C

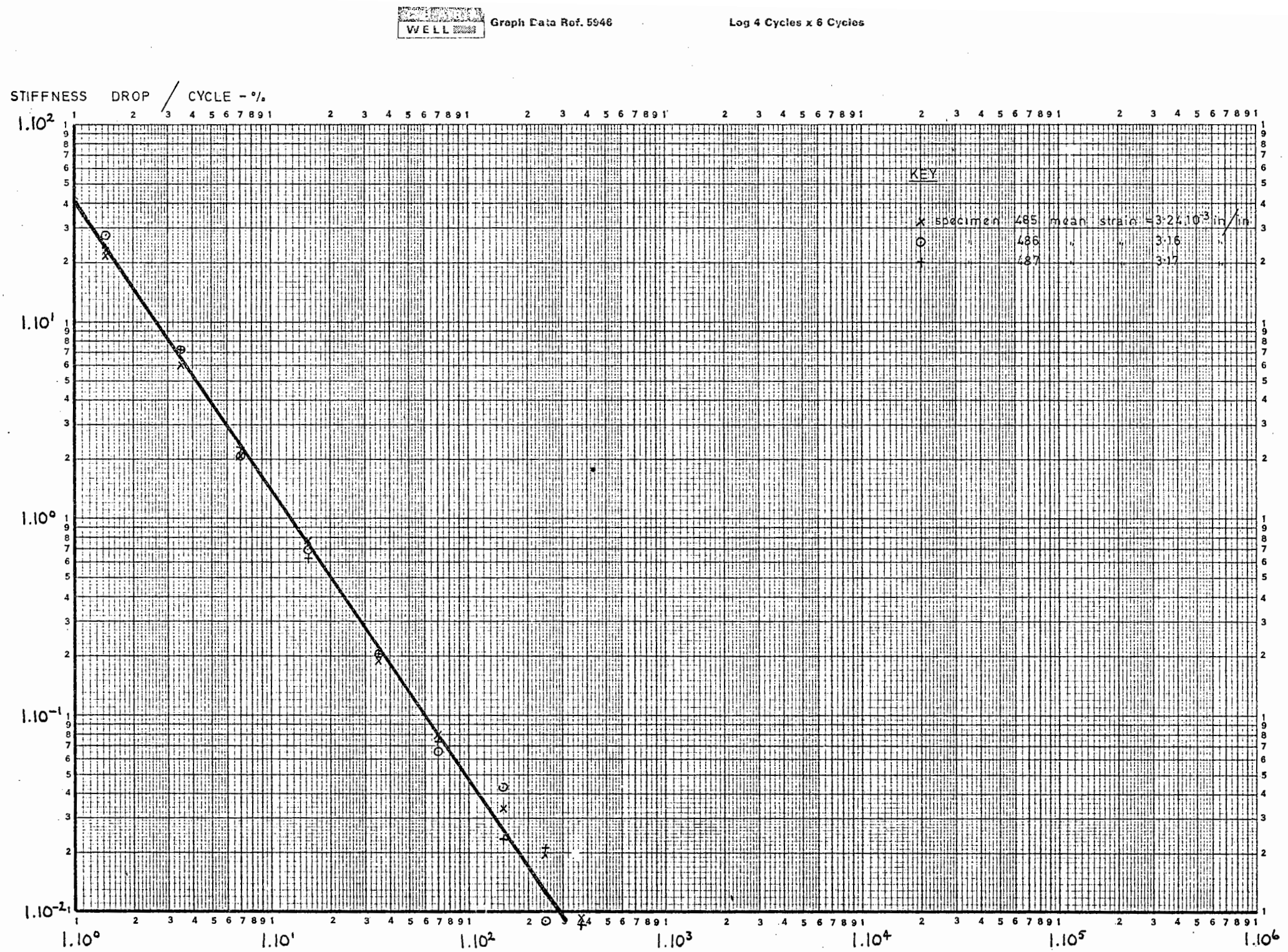

FIG. 119 CHANGE IN STIFFNESS CURVES OF H.R.A. AT HIGH STRAIN LEVEL AT +30°C

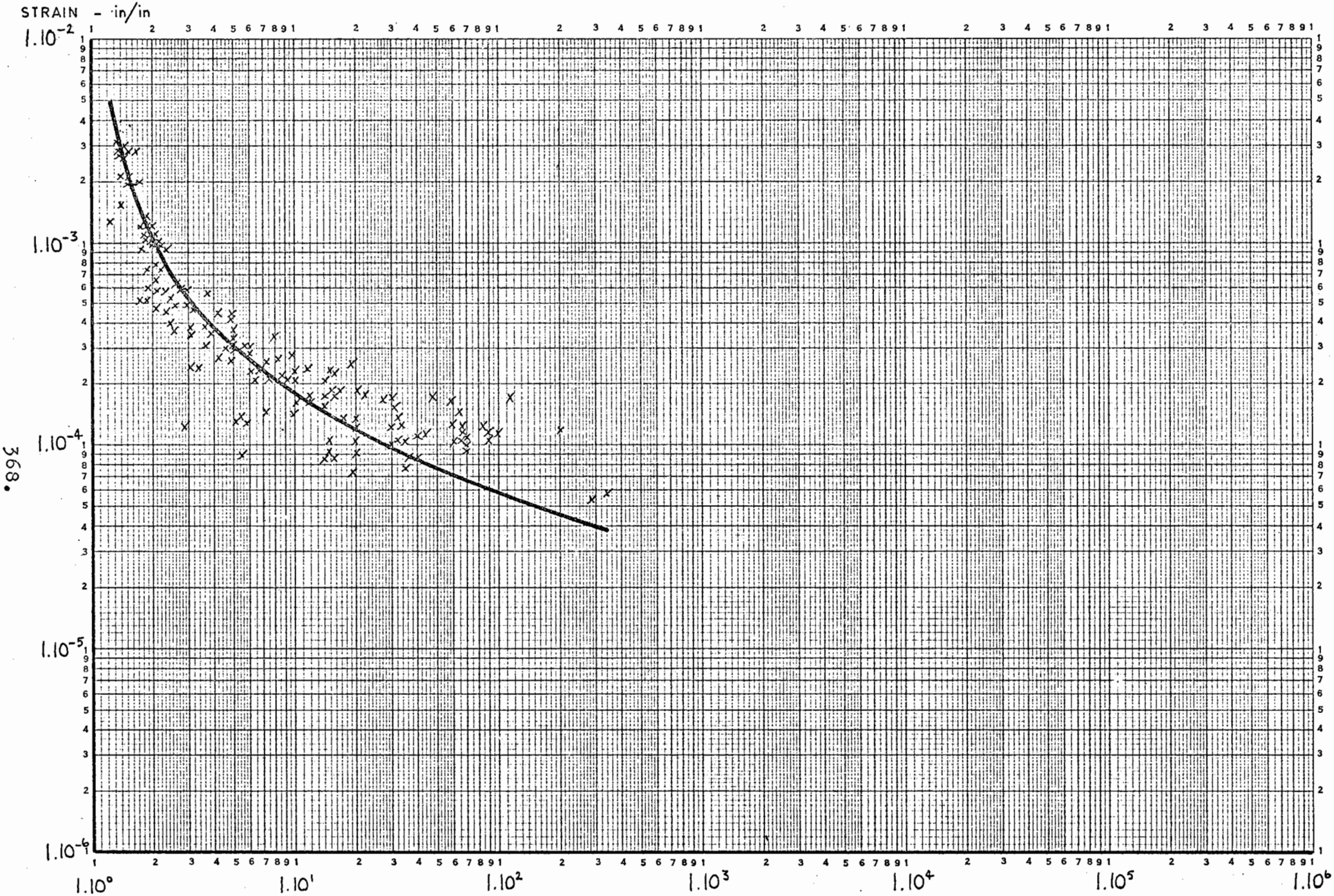

FIG. 120 CALCULATED CYCLES TO 90% OF INITIAL STIFFNESS OF 90/110 AND 190/210 D.B.M. at 0°C

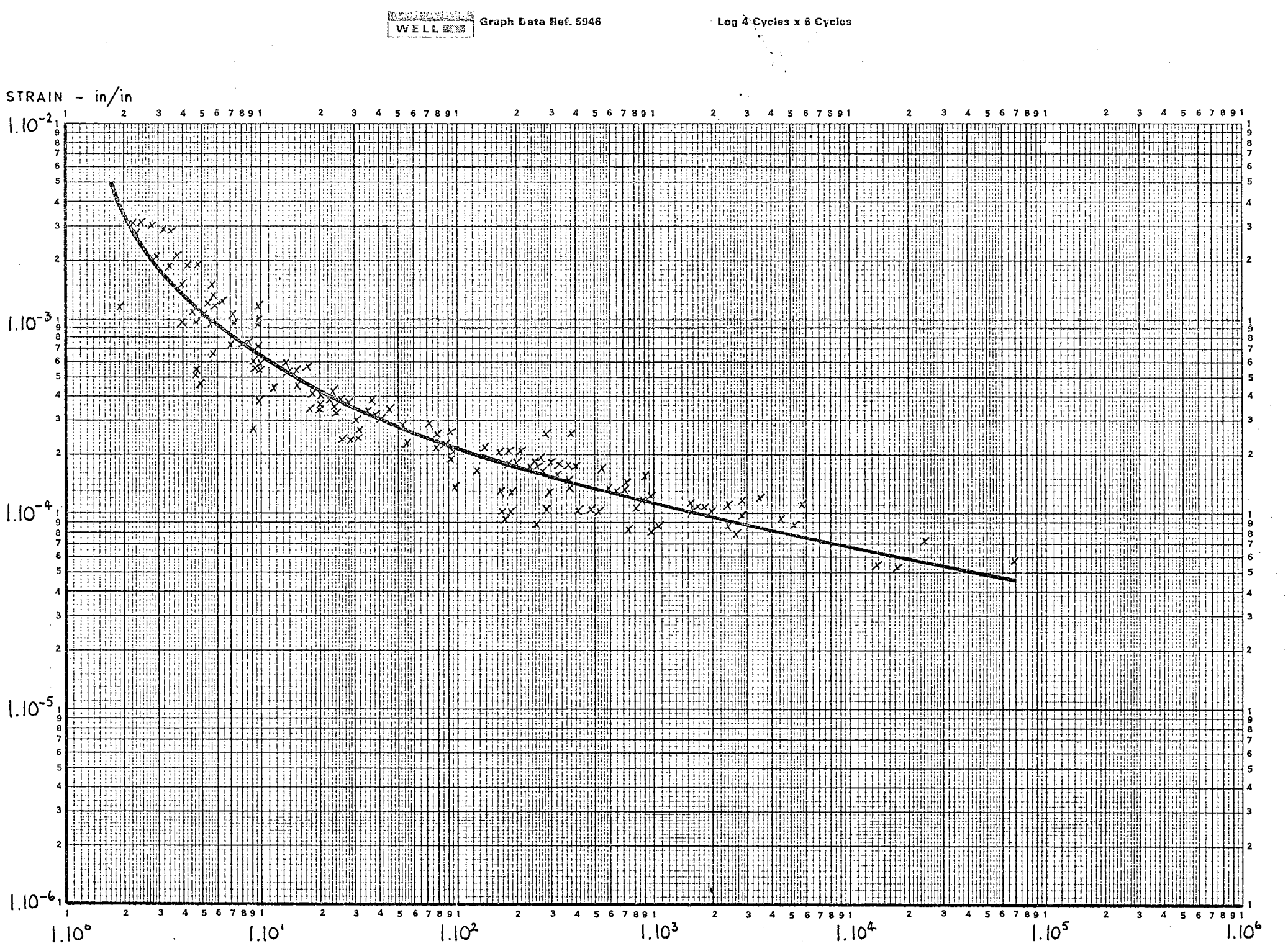

FIG. 121 CALCULATED CYCLES TO 75% OF INITIAL STIFFNESS OF 90/110 AND 190/210 D.B.M. AT 0°C to +40°C

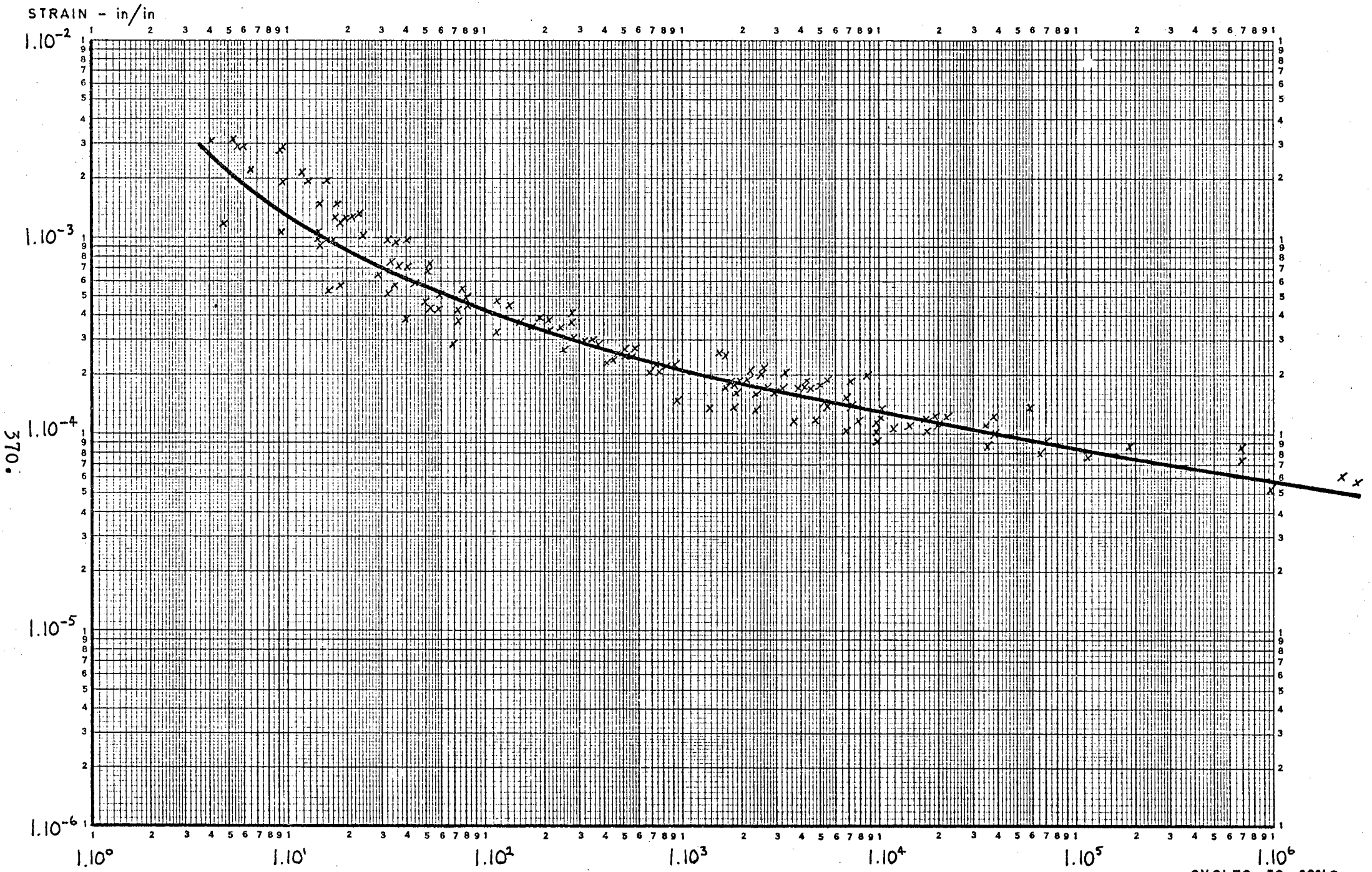

FIG. 122 CALCULATED CYCLES TO 60% OF INITIAL STIFFNESS OF 90/110 AND 190/210 D.B.M. AT 0°C to +40°C

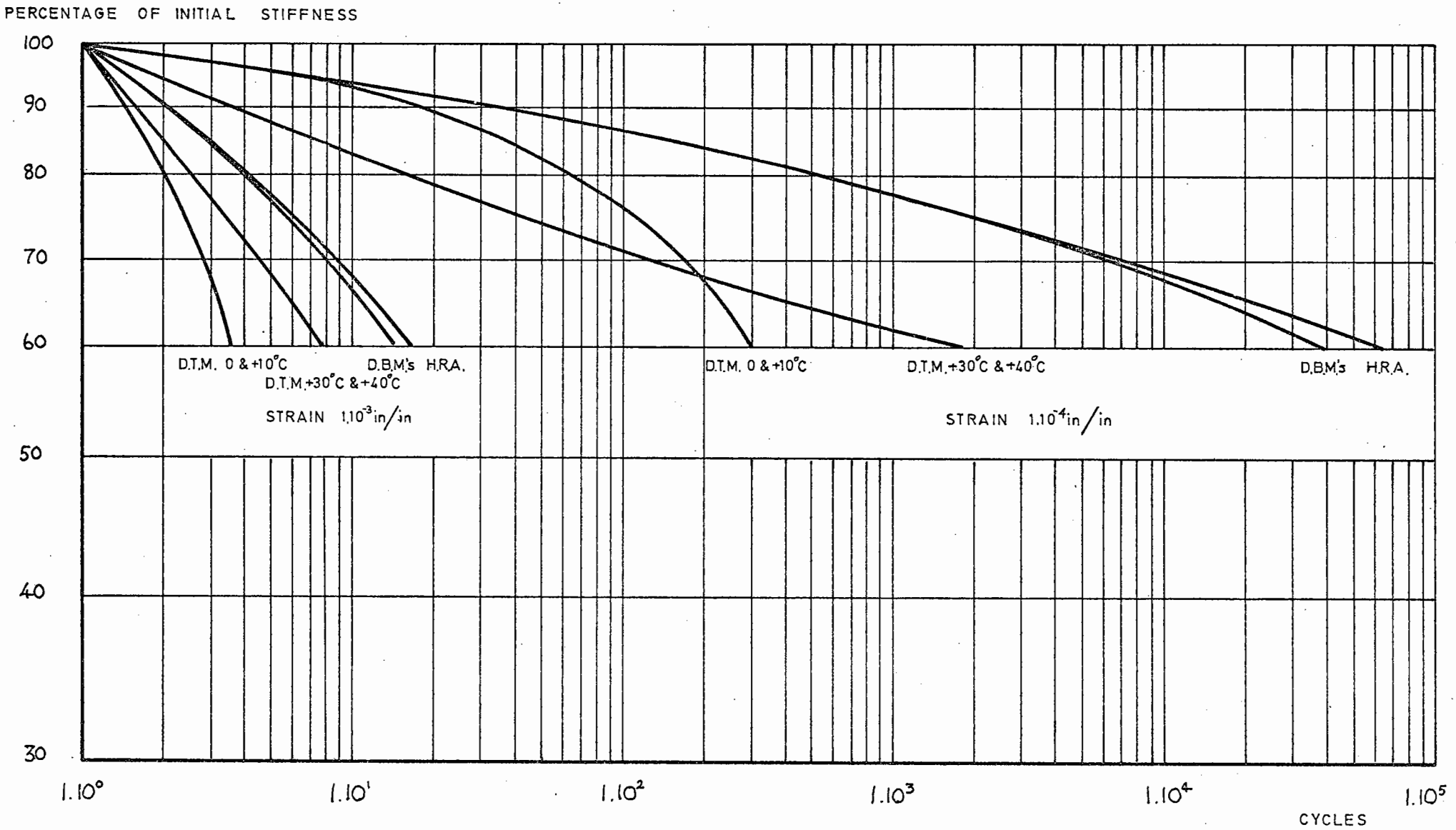

FIG. 123 CALCULATED STIFFNESS CURVES OF ALL BITUMINOUS MATERIALS STUDIED

LOAD CURVE SHAPES

TYPE A TENSILE AND COMPRESSIVE LOADS BOTH DECREASE ROUGHLY PROPORTIONALLY OVER DURATION OF TEST
B TENSILE LOAD DECREASES OVER DURATION OF TEST BUT COMPRESSIVE LOAD UNAFFECTED OVER FIRST FEW CYCLES
C COMPRESSIVE LOAD DECREASES OVER DURATION OF TEST BUT TENSILE LOAD SHOWS SLIGHT INCREASE OVER FIRST FEW CYCLES

DEFORMATION CURVE SHAPES

TYPE 1 TENSILE AND COMPRESSIVE DEFORMATIONS REMAIN CONSTANT OR DECREASE SLIGHTLY OVER DURATION OF TEST
2 TENSILE AND COMPRESSIVE DEFORMATIONS INCREASE OVER FIRST FEW CYCLES THEN DECREASE GRADUALLY FOR REMAINDER OF TEST
3 TENSILE AND COMPRESSIVE DEFORMATIONS INCREASE SIGNIFICANTLY FOR AT LEAST FIRST 50 CYCLES THEN DECREASE FOR REMAINDER OF TEST
4 TENSILE AND COMPRESSIVE DEFORMATIONS INCREASE OVER DURATION OF TEST

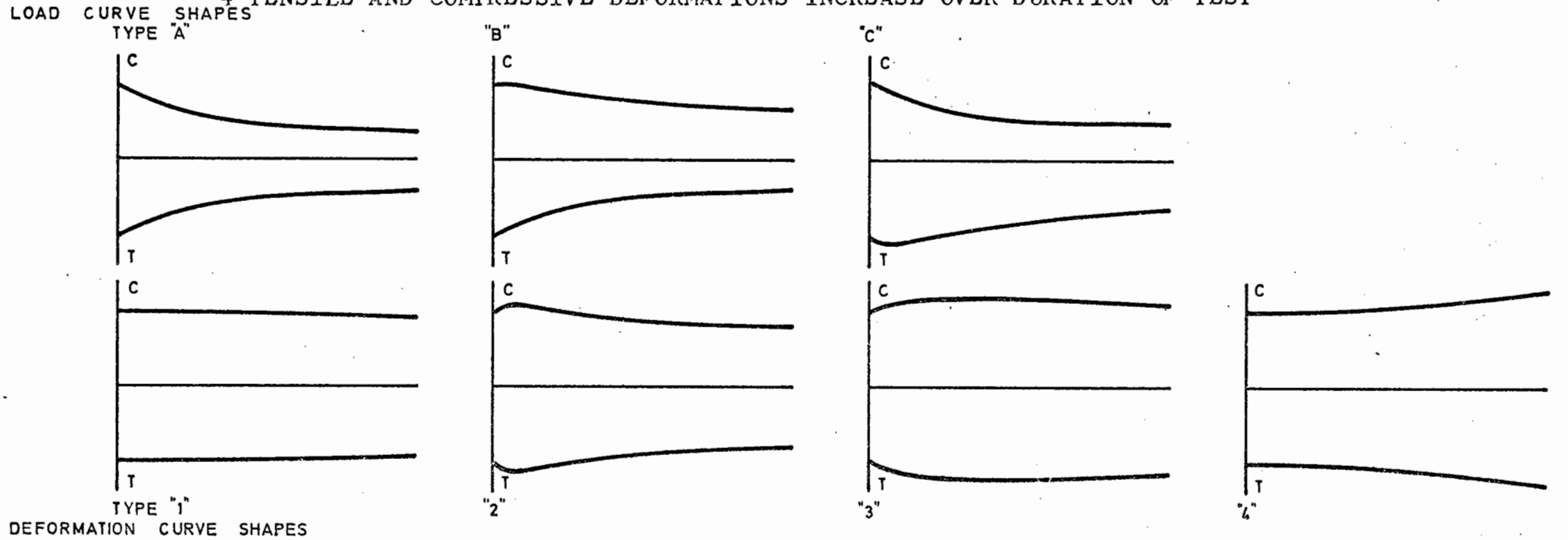

FIG. 124 SHAPES OF LOAD AND DEFLECTION CURVES OF BITUMINOUS MATERIALS DURING REPEATED LOADING TESTS

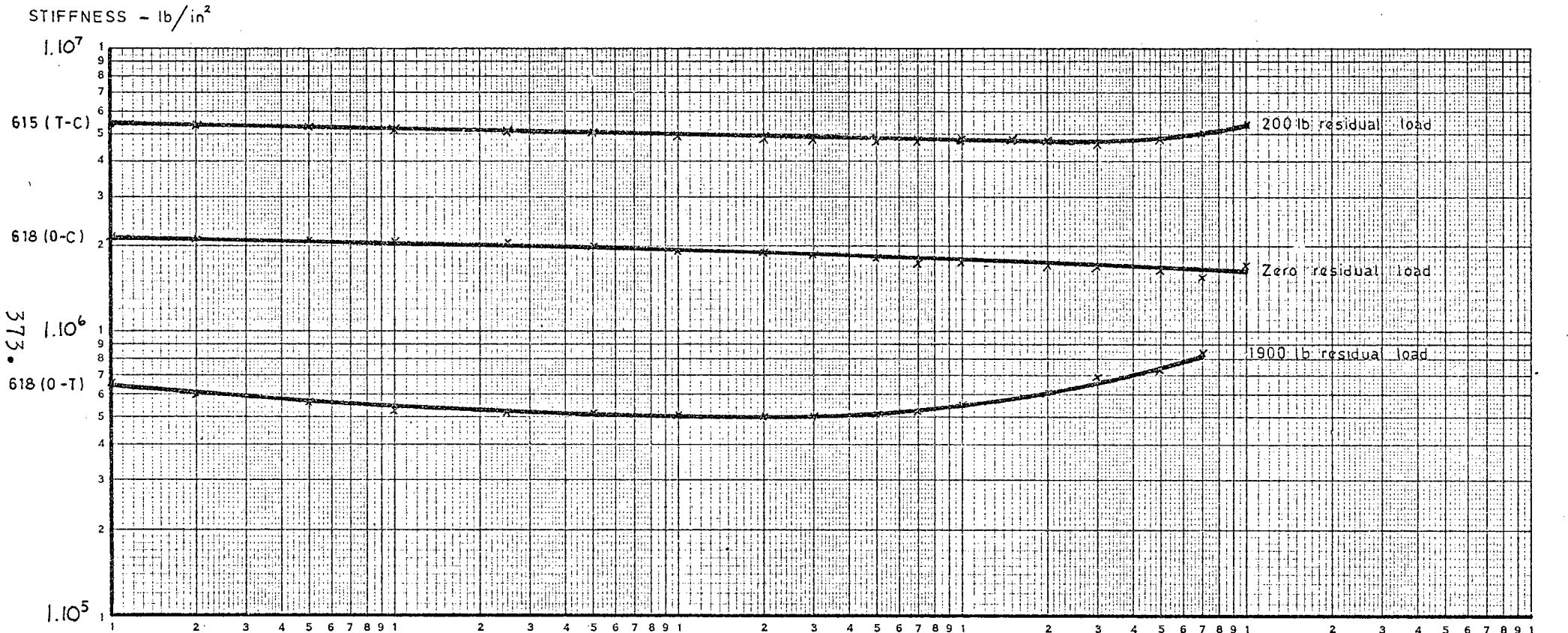

373.

specimen	strain				
615 (T-C)	$2{\cdot}88.10^{-5}$	$2{\cdot}74.10^{-5}$	$2{\cdot}76.10^{-5}$	$2{\cdot}70.10^{-5}$	$2{\cdot}90.10^{-5}$
618 (0-C)	$1{\cdot}94.10^{-4}$	$1{\cdot}94.10^{-4}$	$1{\cdot}94.10^{-4}$	$1{\cdot}92.10^{-4}$	$1{\cdot}92.10^{-4}$
618 (0-T)	$2{\cdot}02.10^{-4}$	$1{\cdot}96.10^{-4}$	$1{\cdot}94.10^{-4}$	$1{\cdot}94.10^{-4}$	—

FIG. 125 STIFFNESS CURVES OF DRY LEAN CONCRETE IN STRAIN-CONTROLLED REPEATED LOADING

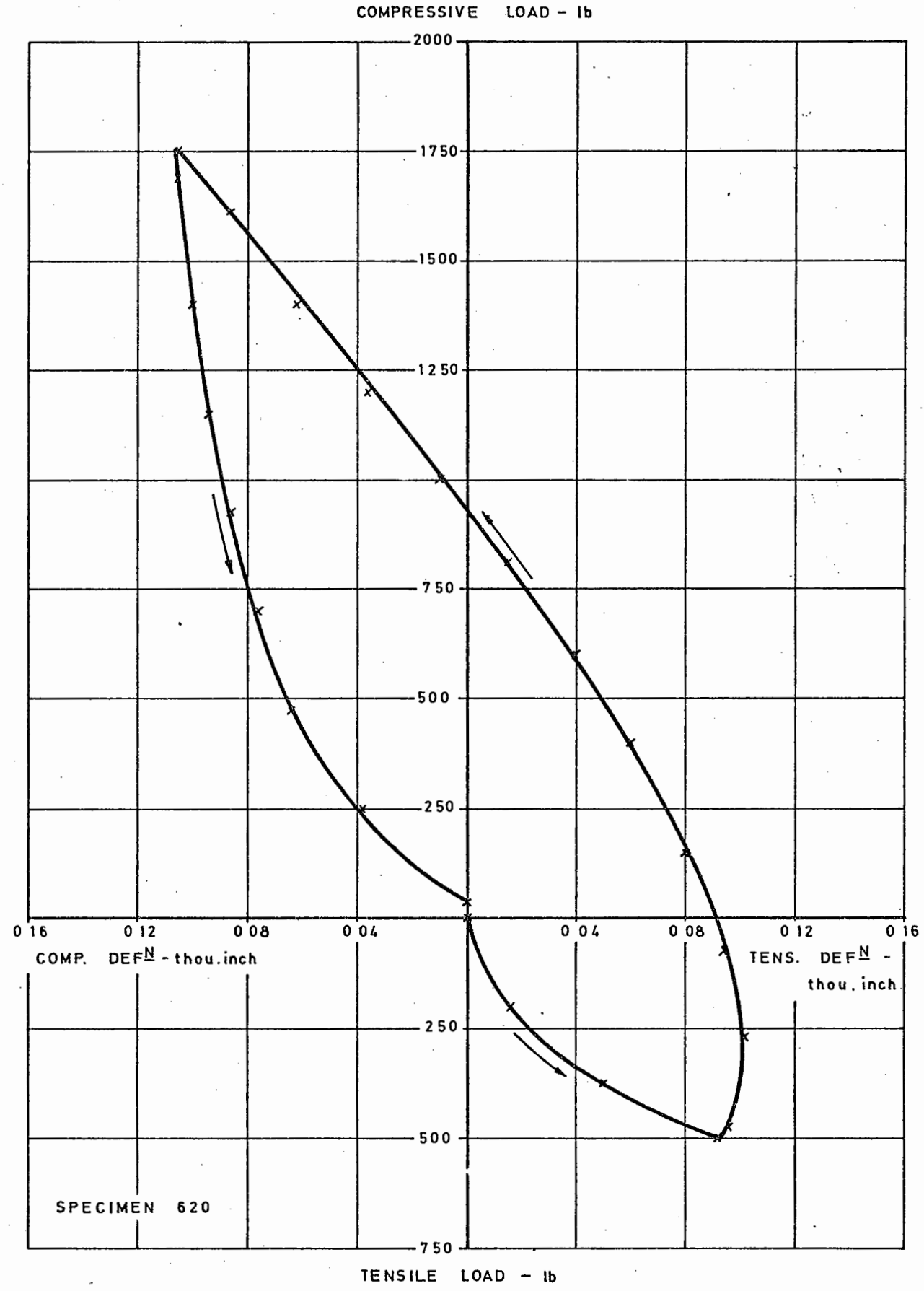

FIG. 126 HYSTERESIS LOOP OF SPECIMEN OF DRY LEAN CONCRETE IN FIRST CYCLE OF FLUCTUATING STRAIN-CONTROLLED REPEATED LOADING

Log 2 Cycles x 5 Cycles

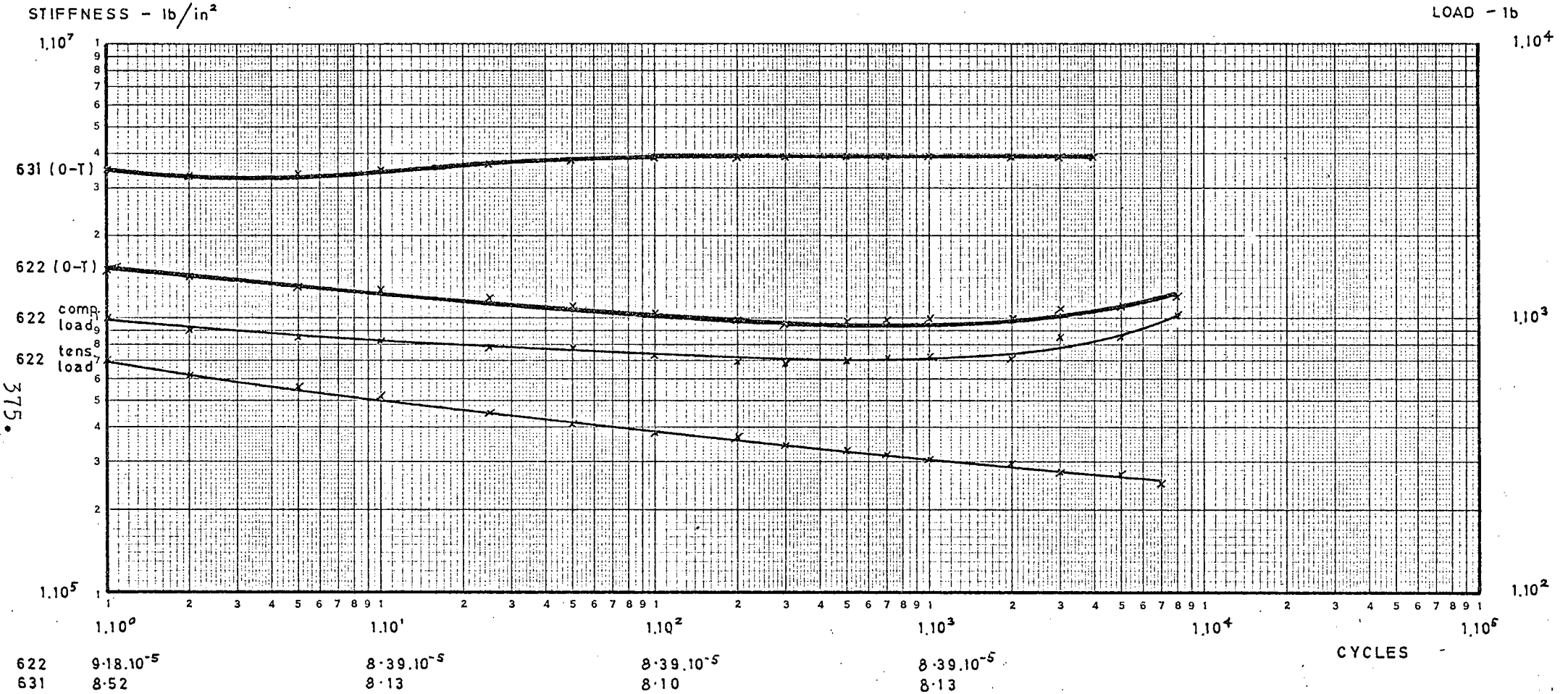

FIG. 127 STIFFNESS CURVES OF DRY LEAN CONCRETE IN TENSILE STRAIN-CONTROLLED REPEATED LOADING

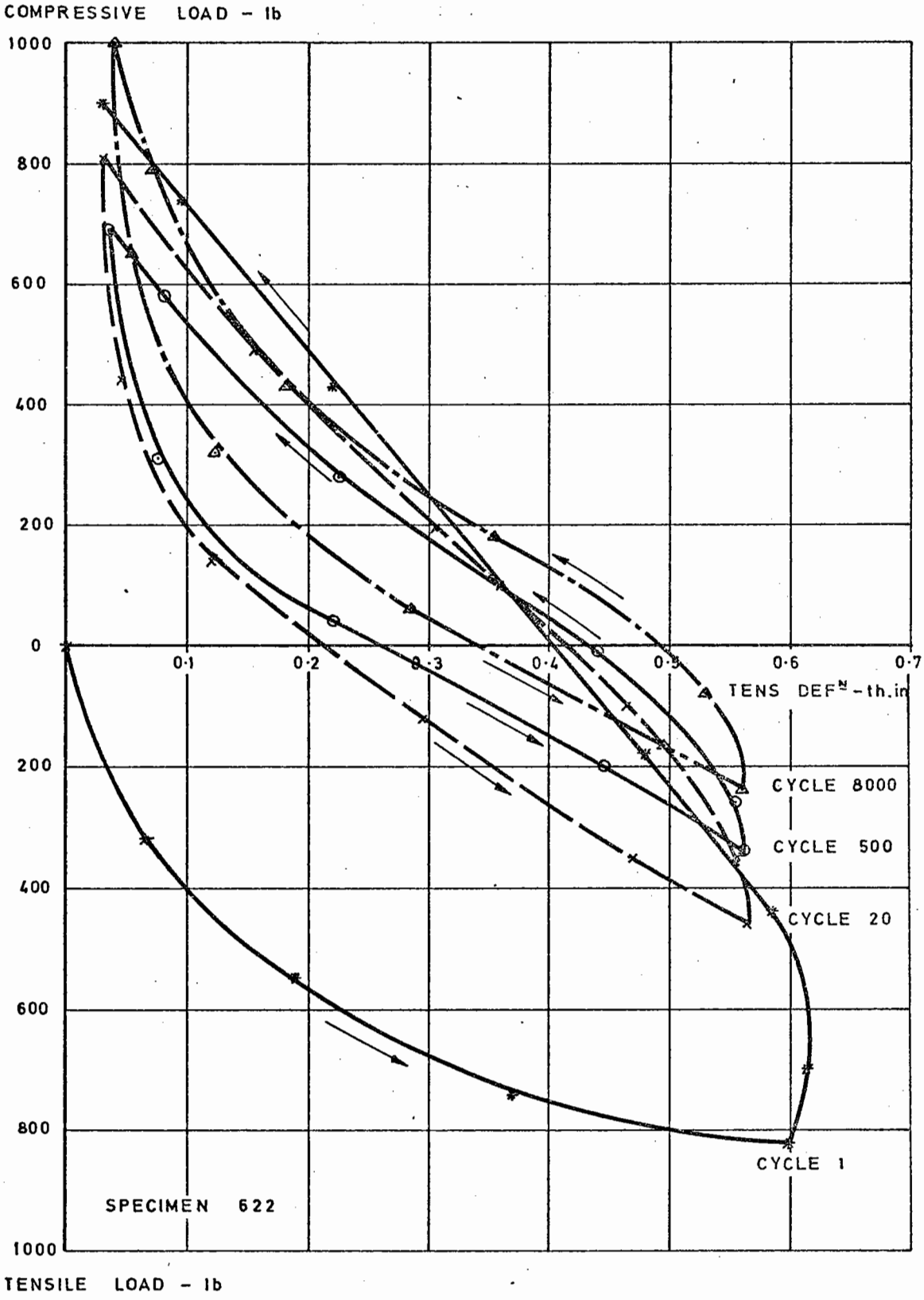

FIG. 128 HYSTERESIS LOOPS OF SPECIMEN OF DRY LEAN CONCRETE IN TENSILE STRAIN-CONTROLLED REPEATED LOADING

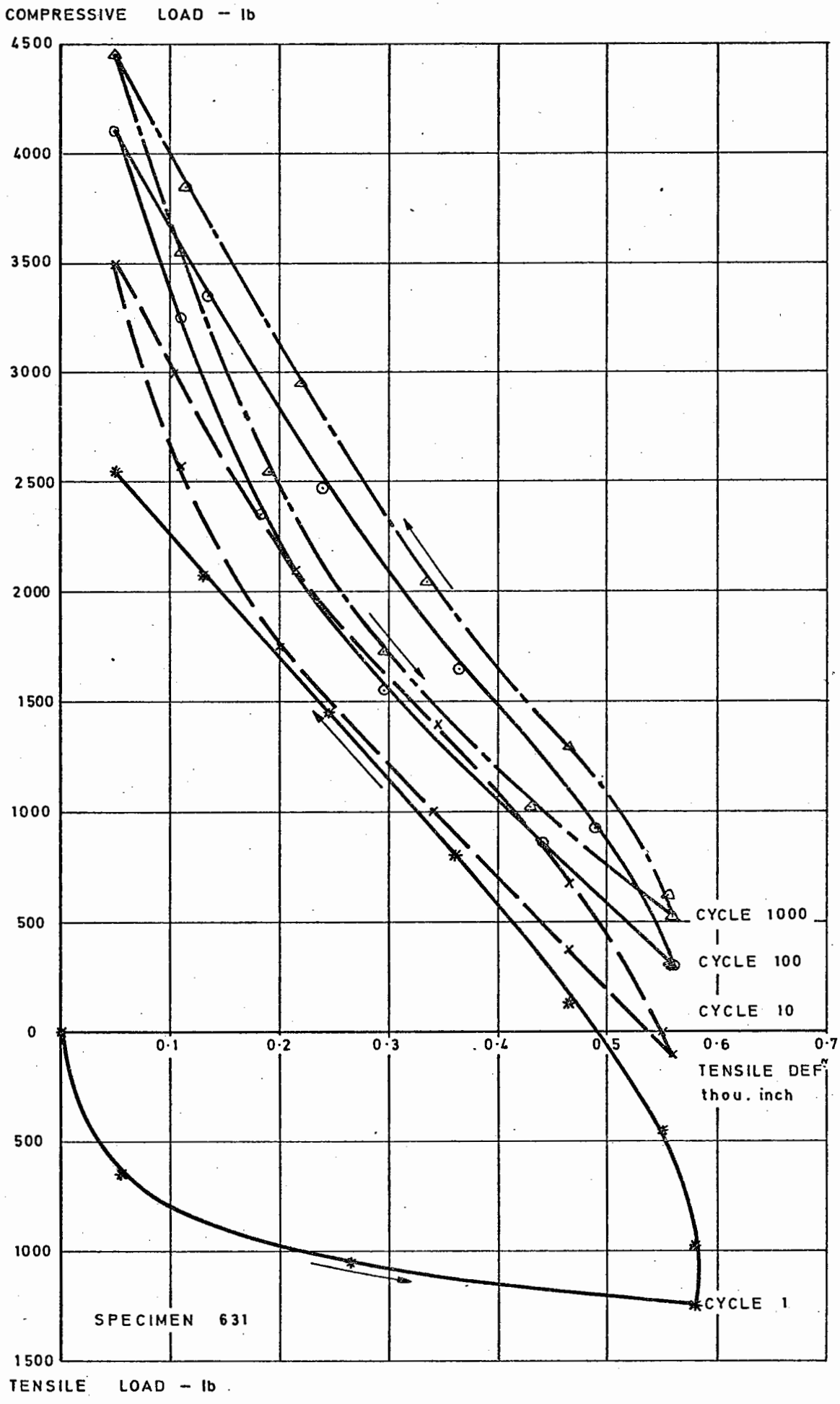

FIG. 129 HYSTERESIS LOOPS OF SPECIMEN OF DRY LEAN CONCRETE IN TENSILE STRAIN-CONTROLLED REPEATED LOADING

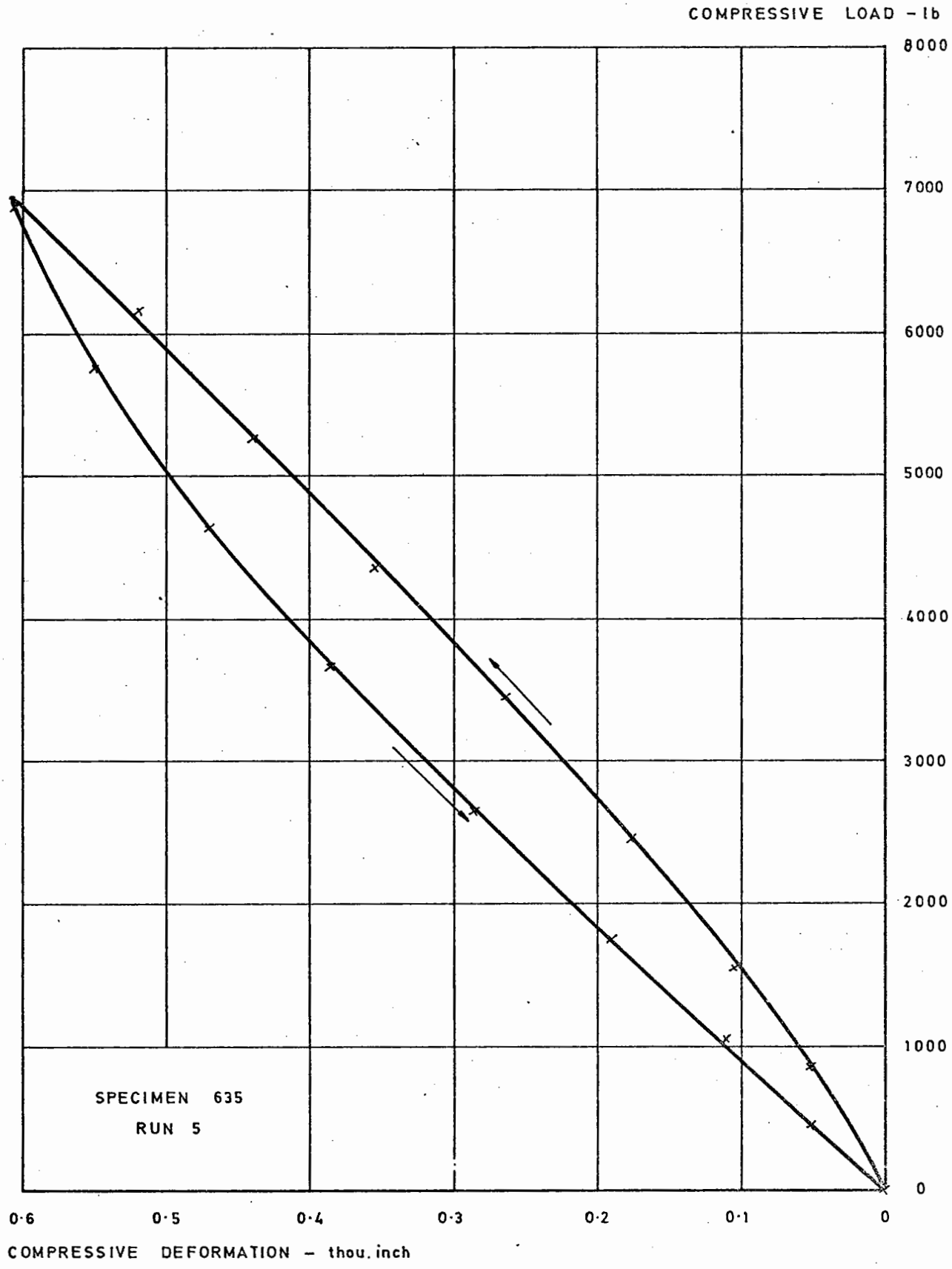

FIG. 130 HYSTERESIS LOOP OF SPECIMEN OF DRY LEAN CONCRETE IN FIRST CYCLE OF COMPRESSIVE STRAIN-CONTROLLED REPEATED LOADING

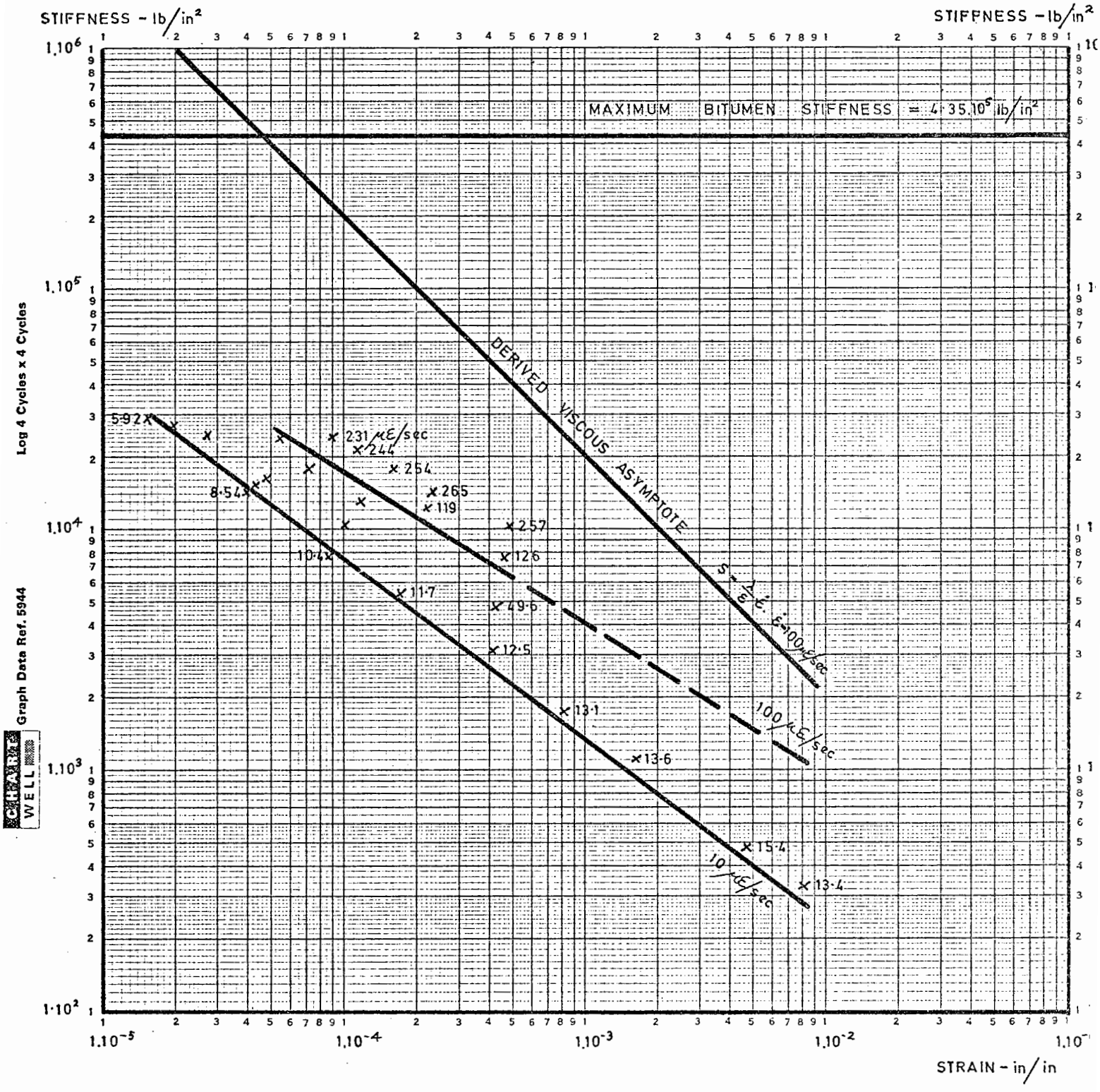

FIG. 92 STIFFNESS OF 90/110 pen. BITUMEN AT 0°C

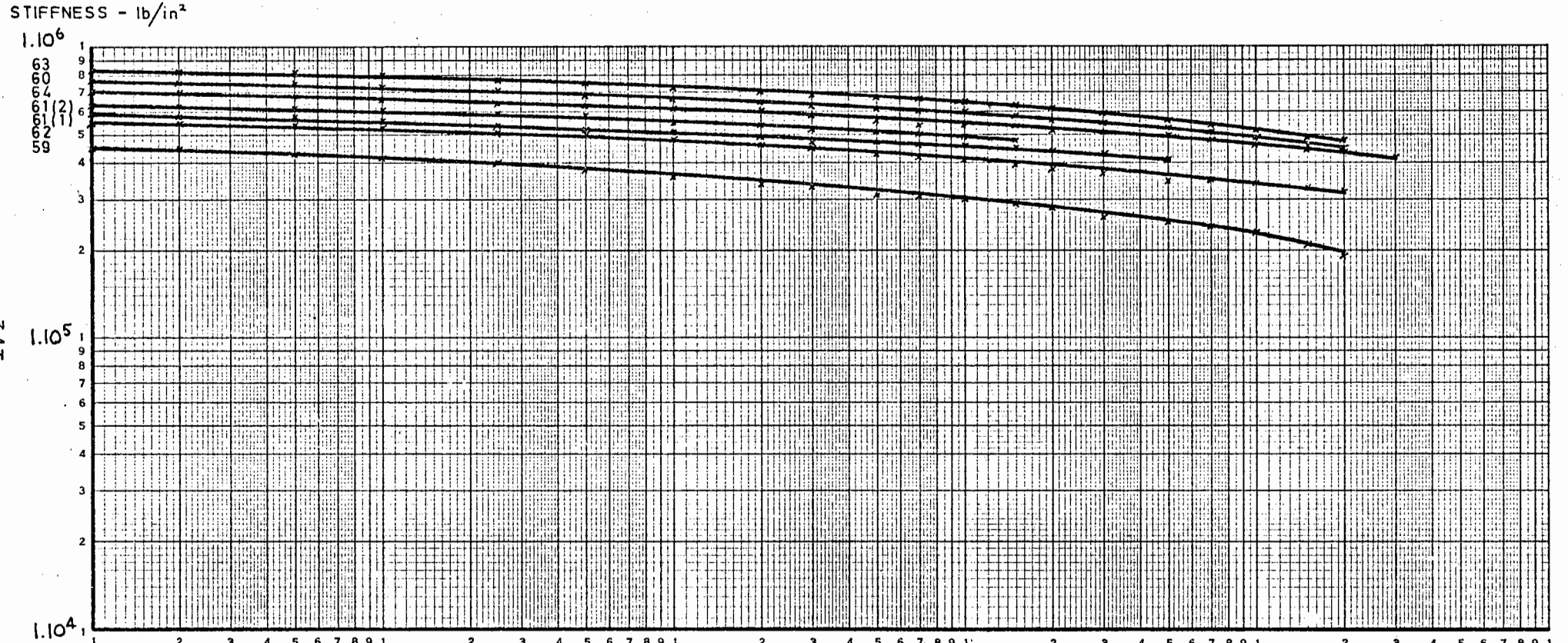

specimen	strain				
59	$1{\cdot}30.10^{-4}$	$1{\cdot}45.10^{-4}$	$1{\cdot}48.10^{-4}$	$1{\cdot}44.10^{-4}$	$1{\cdot}40.10^{-4}$
60	0·97	1·04	1·09	1·16	1·36
61(1)	1·11	1·19	1·24	1·27	—
61(2)	1·02	1·07	1·12	1·21	—
62	1·07	1·16	1·22	1·28	1·14
63	0·96	1·02	1·05	1·10	1·12
64	0·91	0·96	1·00	1·01	0·87

FIG. 93 STIFFNESS CURVES OF BATCH OF SPECIMENS OF 90/110 DENSE BITUMEN MACADAM AT MEDIUM STRAIN LEVEL AT +10°C

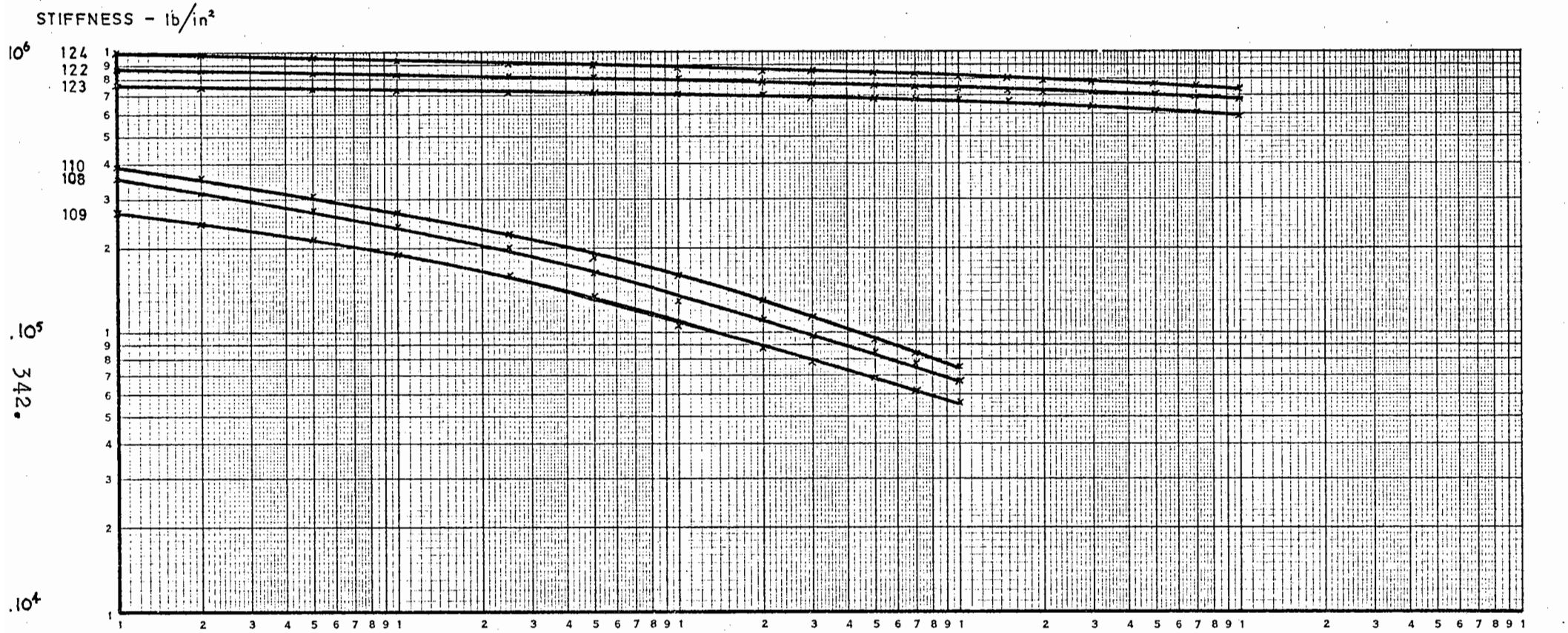

specimen	strain				
122	$5{\cdot}64.10^{-5}$	$5{\cdot}67.10^{-5}$	$5{\cdot}72.10^{-5}$	$5{\cdot}75.10^{-5}$	$5{\cdot}50.10^{-5}$
123	$5{\cdot}62$	$5{\cdot}62$	$5{\cdot}53$	$4{\cdot}94$	$5{\cdot}01$
124	$5{\cdot}49$	$5{\cdot}49$	$5{\cdot}49$	$5{\cdot}20$	$5{\cdot}17$
108	$1{\cdot}21.10^{-3}$	$1{\cdot}20.10^{-3}$	$1{\cdot}14.10^{-3}$	$1{\cdot}06.10^{-3}$	—
109	$1{\cdot}22$	$1{\cdot}22$	$1{\cdot}13$	$1{\cdot}06$	—
110	$1{\cdot}23$	$1{\cdot}22$	$1{\cdot}15$	$1{\cdot}06$	—

FIG. 94 STIFFNESS CURVES OF 90/110 DENSE BITUMEN MACADAM AT HIGH AND LOW STRAIN LEVELS AT +10°C

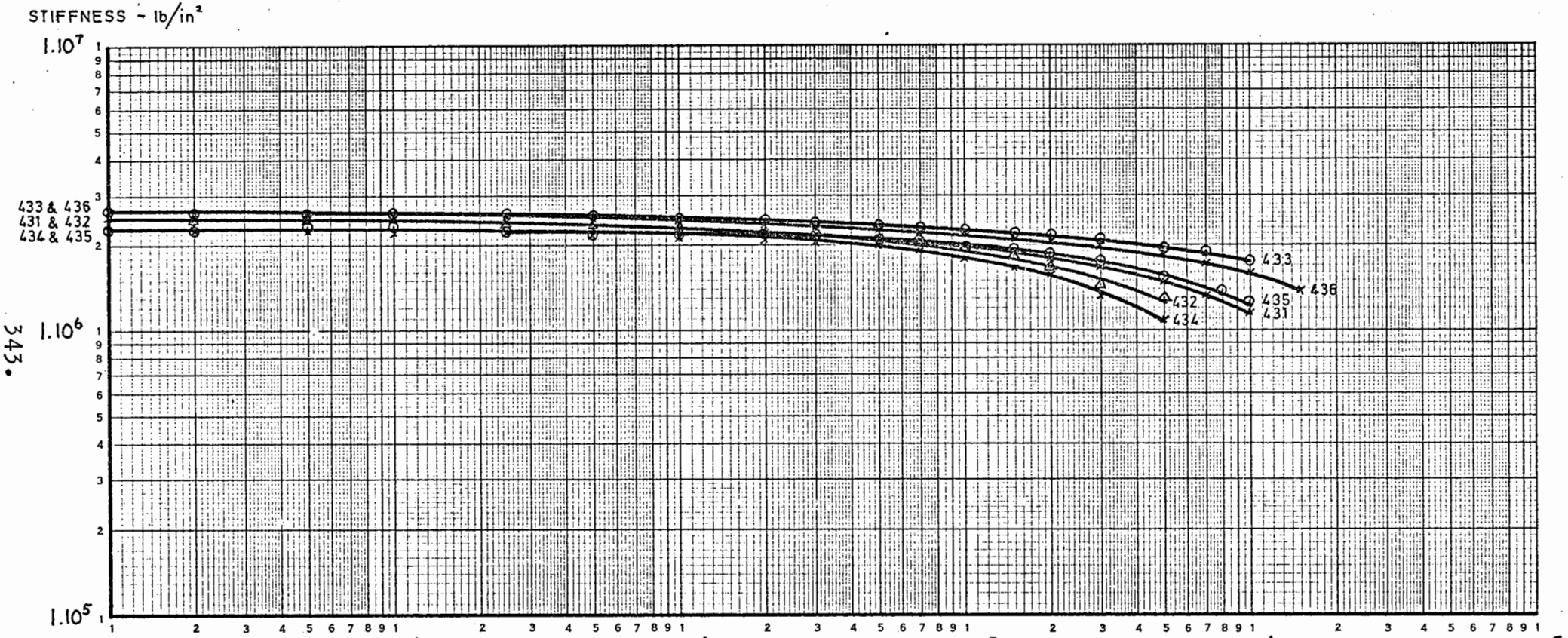

specimen	strain				
431	$3{\cdot}85.10^{-5}$	$3{\cdot}94.10^{-5}$	$4{\cdot}12.10^{-5}$	$4{\cdot}65.10^{-5}$	$5{\cdot}17.10^{-5}$
432	3·66	3·75	3·92	4·09	—
433	4·05	4·05	4·13	4·39	4·81
434	4·35	4·35	4·43	4·85	—
435	4·27	4·36	4·61	4·70	5·13
436	3·94	4·12	4·18	4·35	5·02

FIG. 95 STIFFNESS CURVES OF BATCH OF SPECIMENS OF DENSE TAR MACADAM AT MEDIUM STRAIN LEVEL AT +10° C

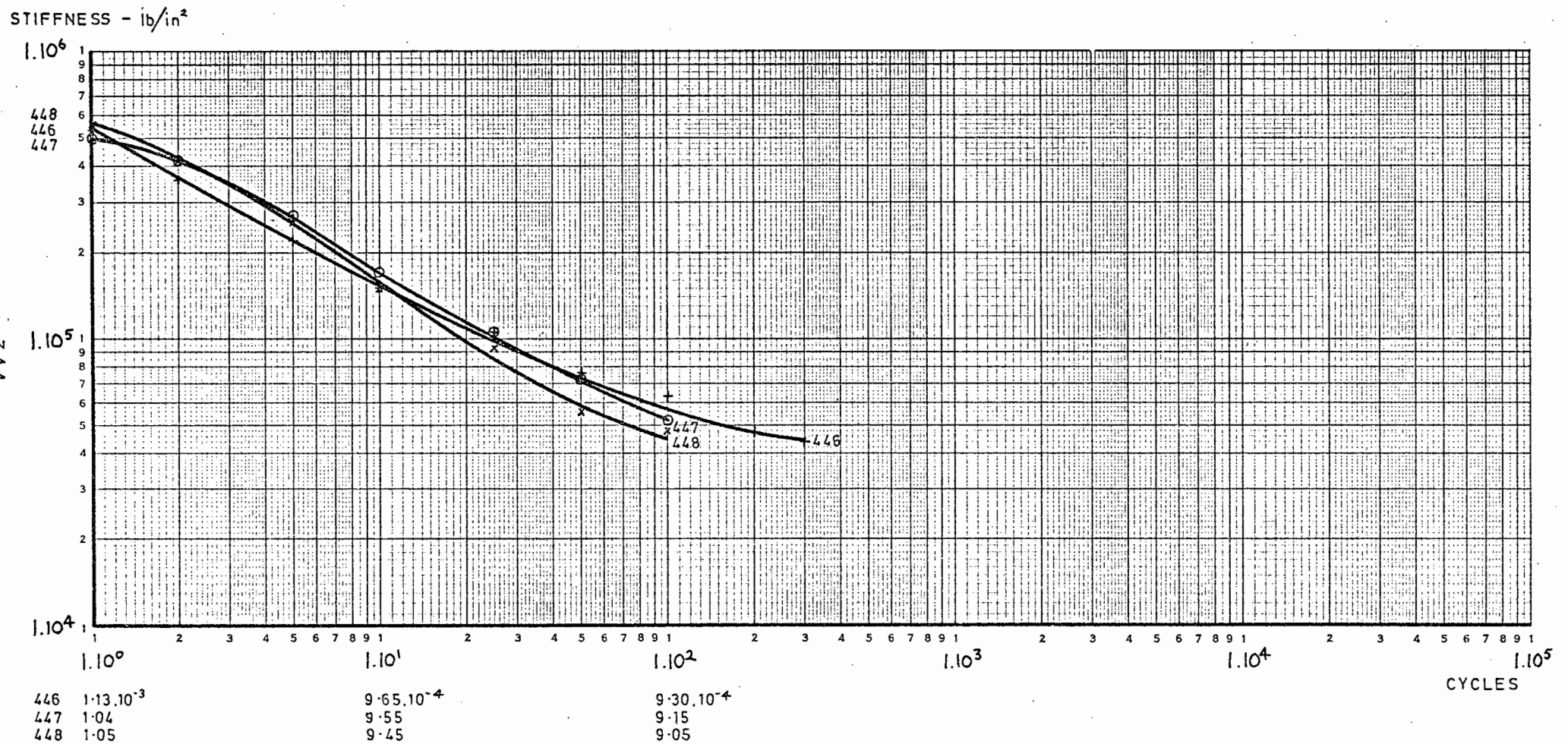

FIG. 96 STIFFNESS CURVES OF DENSE TAR MACADAM AT LOW STRAIN LEVEL AT +10°C

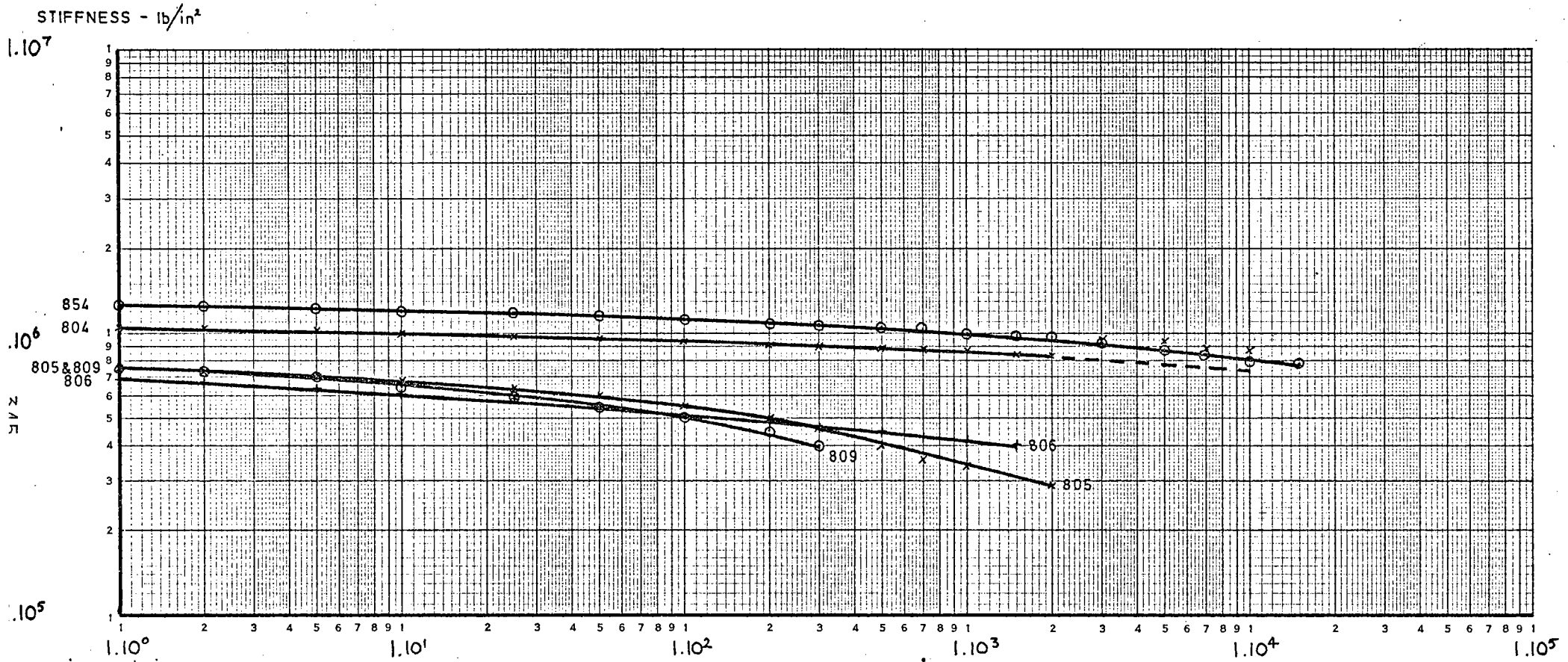

specimen	strain				
854	$7{\cdot}99.10^{-5}$	$8{\cdot}40.10^{-5}$	$8{\cdot}65.10^{-5}$	$9{\cdot}07.10^{-5}$	$9{\cdot}25.10^{-5}$
804	$1{\cdot}00.10^{-4}$	$1{\cdot}06.10^{-4}$	$1{\cdot}10.10^{-4}$	$1{\cdot}20.10^{-4}$	$1{\cdot}03.10^{-4}$
805	2·50	2·60	2·63	2·50	—
806	2·53	2·57	2·55	2·52	—
809	2·50	2·51	2·52	—	—

FIG. 97 STIFFNESS CURVES OF HOT ROLLED ASPHALT AT MEDIUM STRAIN LEVEL AT +10°C

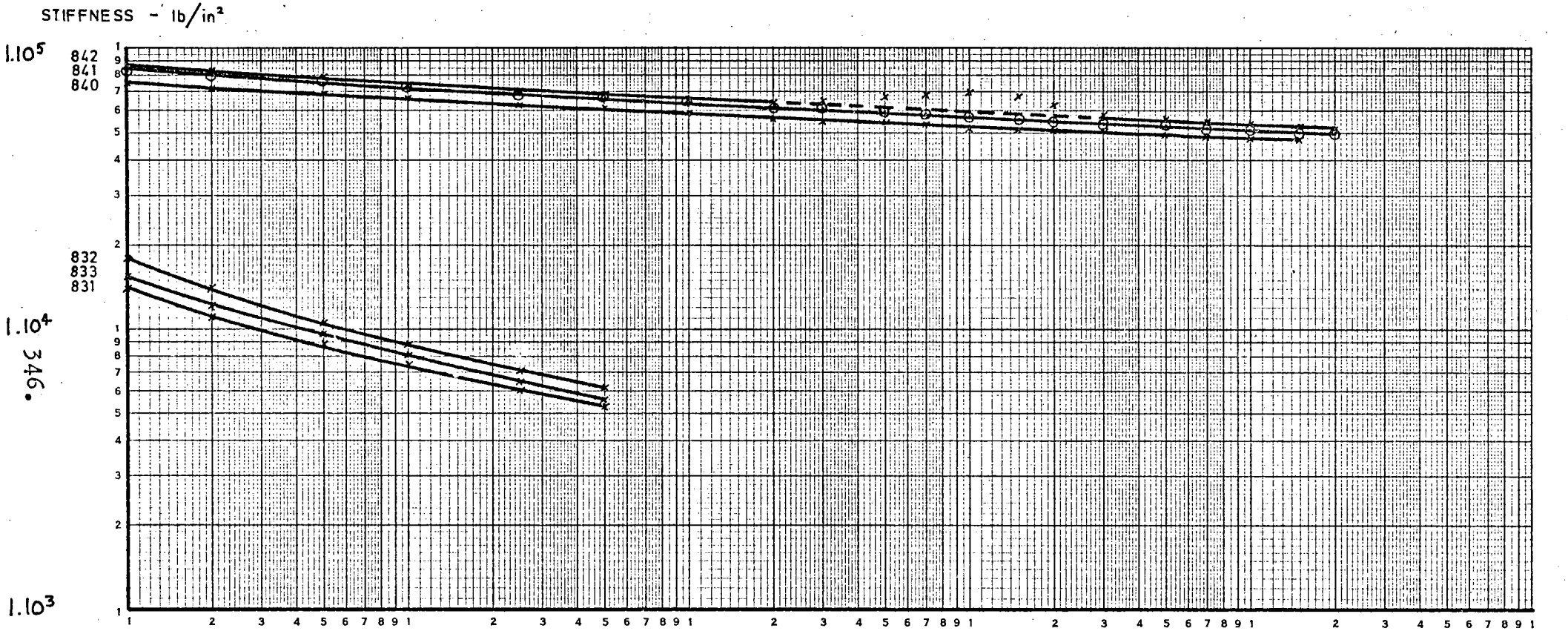

specimen	strain				
840	$1{\cdot}98.10^{-4}$	$1{\cdot}98.10^{-4}$	$1{\cdot}99.10^{-4}$	$2{\cdot}02.10^{-4}$	$2{\cdot}00.10^{-4}$
841	2·00	1·96	1·97	1·99	2·00
842	1·94	1·94	1·94	1·84	1·93
831	$4{\cdot}33.10^{-3}$	$4{\cdot}32.10^{-3}$	—	—	—
832	4·35	4·34	—	—	—
833	4·36	4·36	—	—	—

FIG. 98 STIFFNESS CURVES OF HOT ROLLED ASPHALT AT HIGH AND LOW STRAIN LEVELS AT +30°C

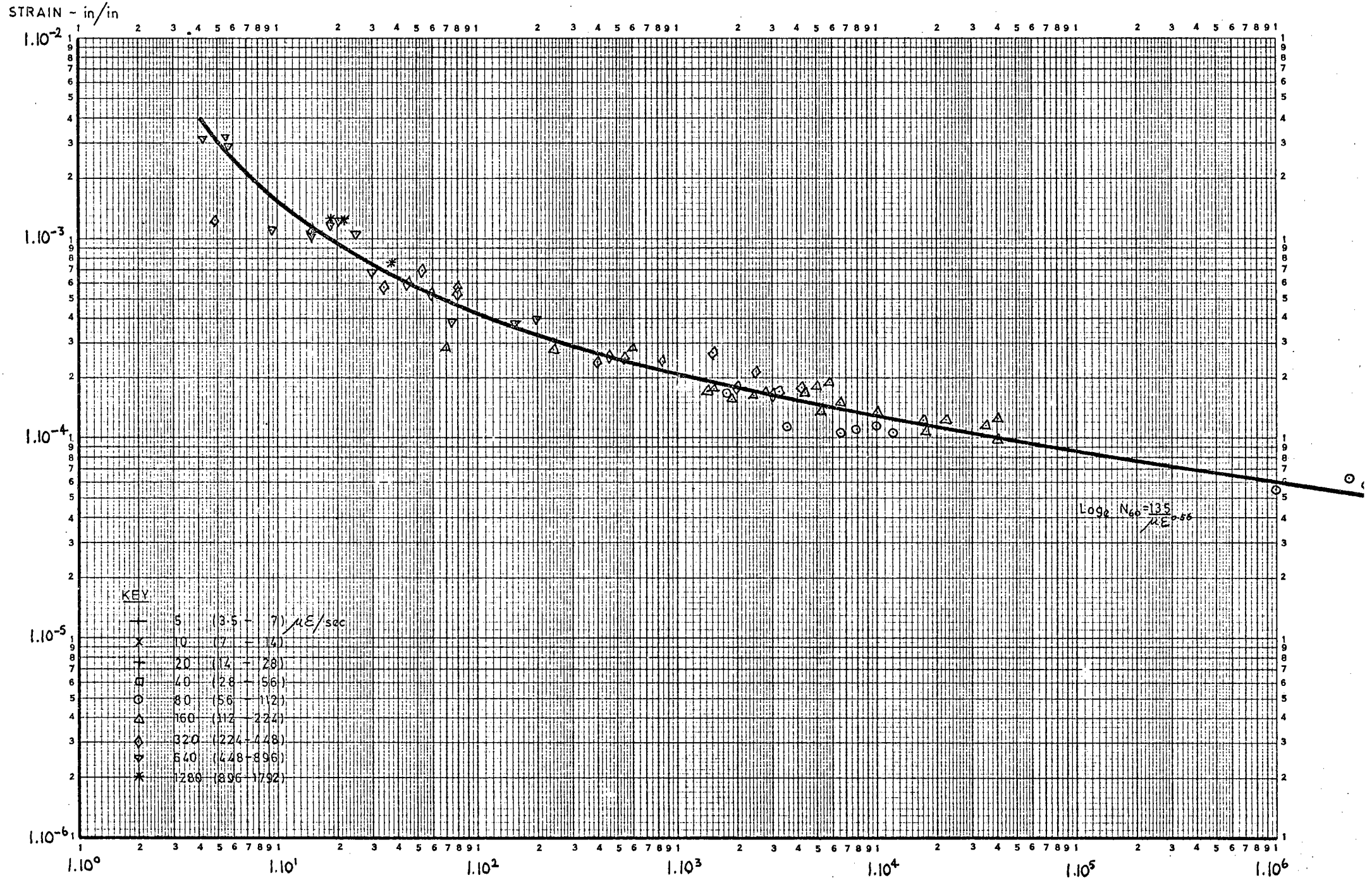

FIG. 99 CYCLES TO 60% OF INITIAL STIFFNESS OF 90/110 pen. R.B.M. AT +10° C

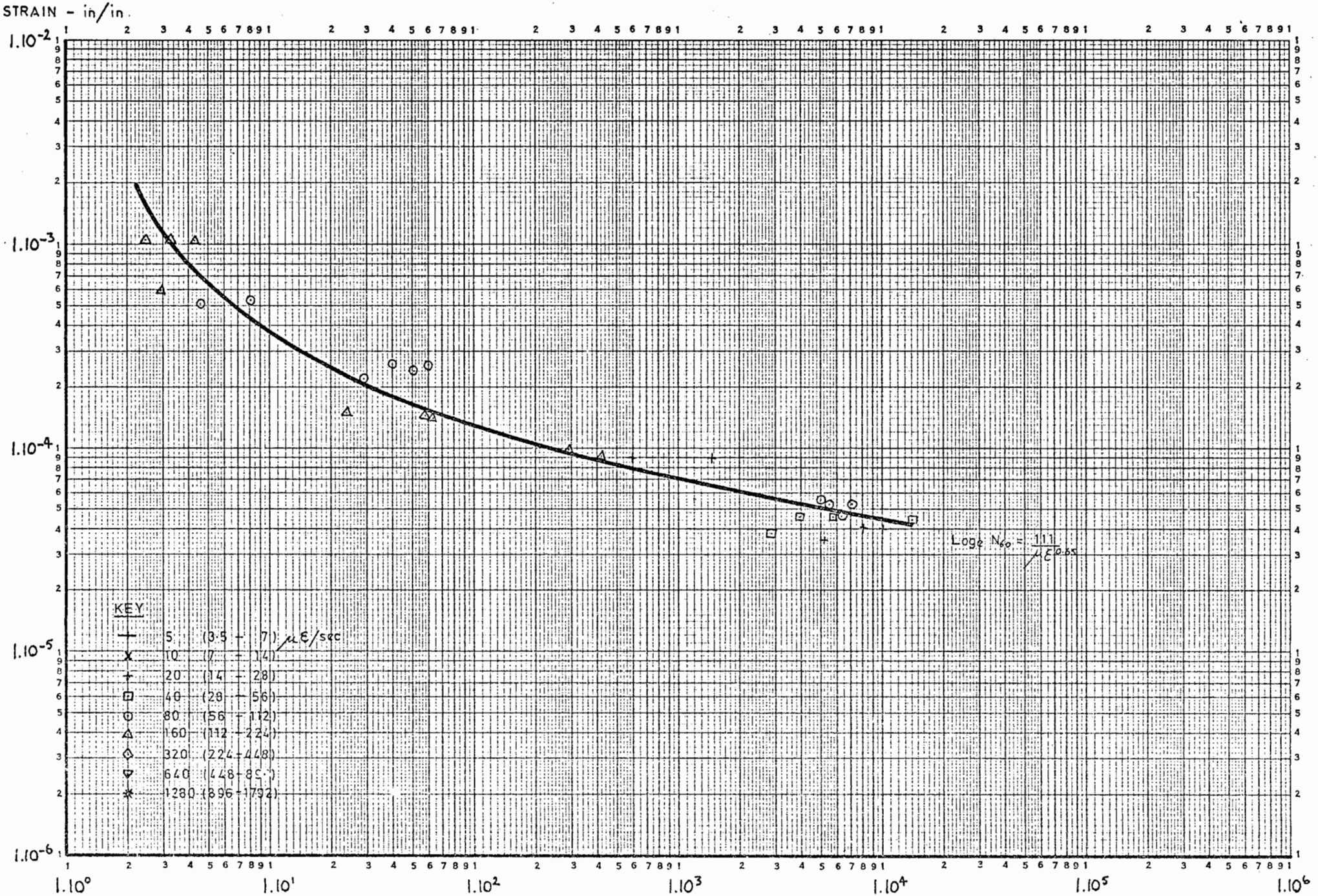

FIG. 100. CYCLES TO 60% OF INITIAL STIFFNESS OF D.T.M. AT +10° C

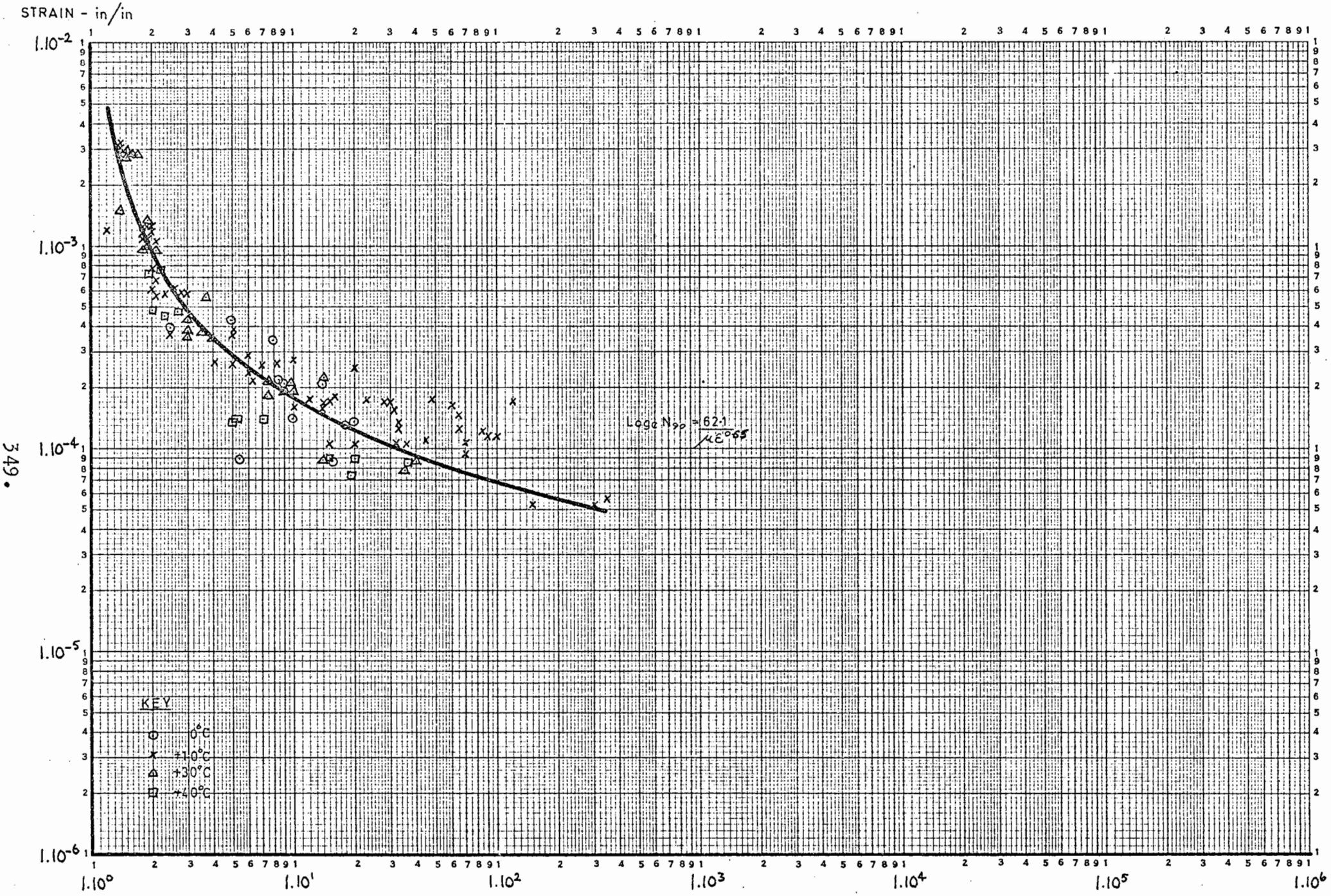

FIG. 101 CYCLES TO 90% OF INITIAL STIFFNESS OF 90/110 D.B.M. AT 0°C to +40°C

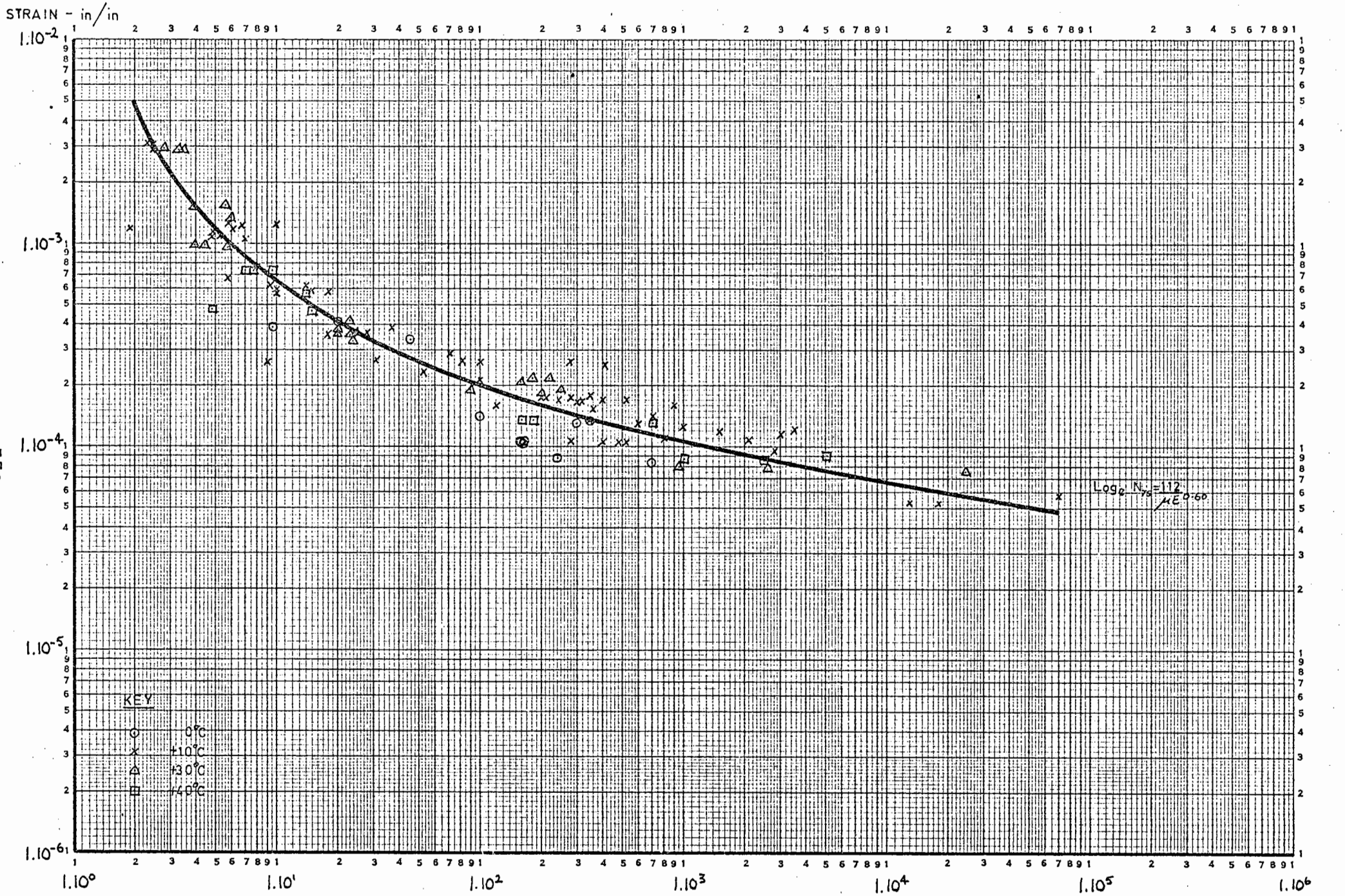

FIG. 102 CYCLES TO 75% OF INITIAL STIFFNESS OF 90/110 D.B.M. AT 0°C to +40°C

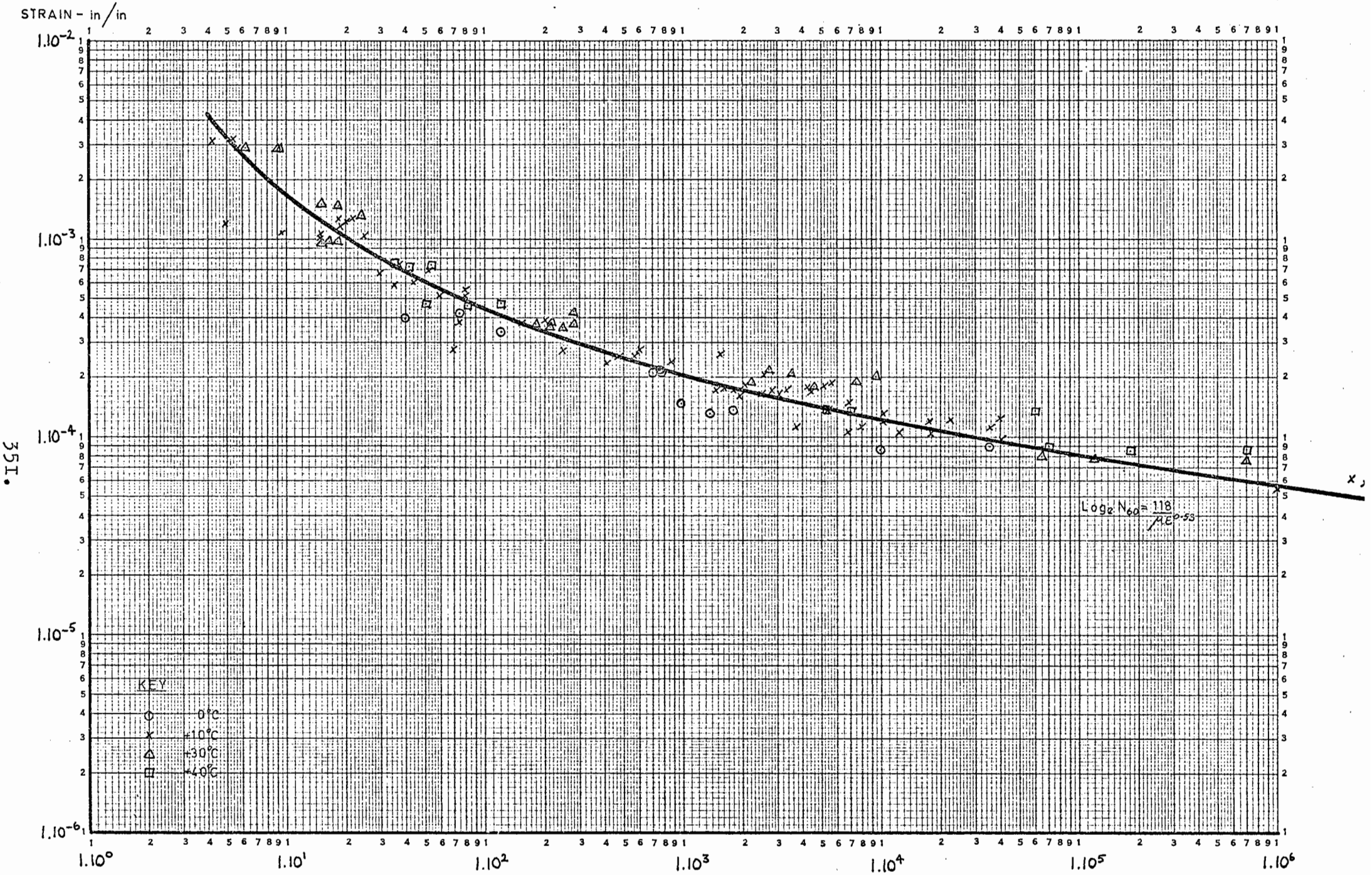

FIG. 103 CYCLES TO 60% OF INITIAL STIFFNESS OF 90/110 D.B.M. AT 0°C to +40°C SERVICE LIFE (CYCLES TO 60% S_I)

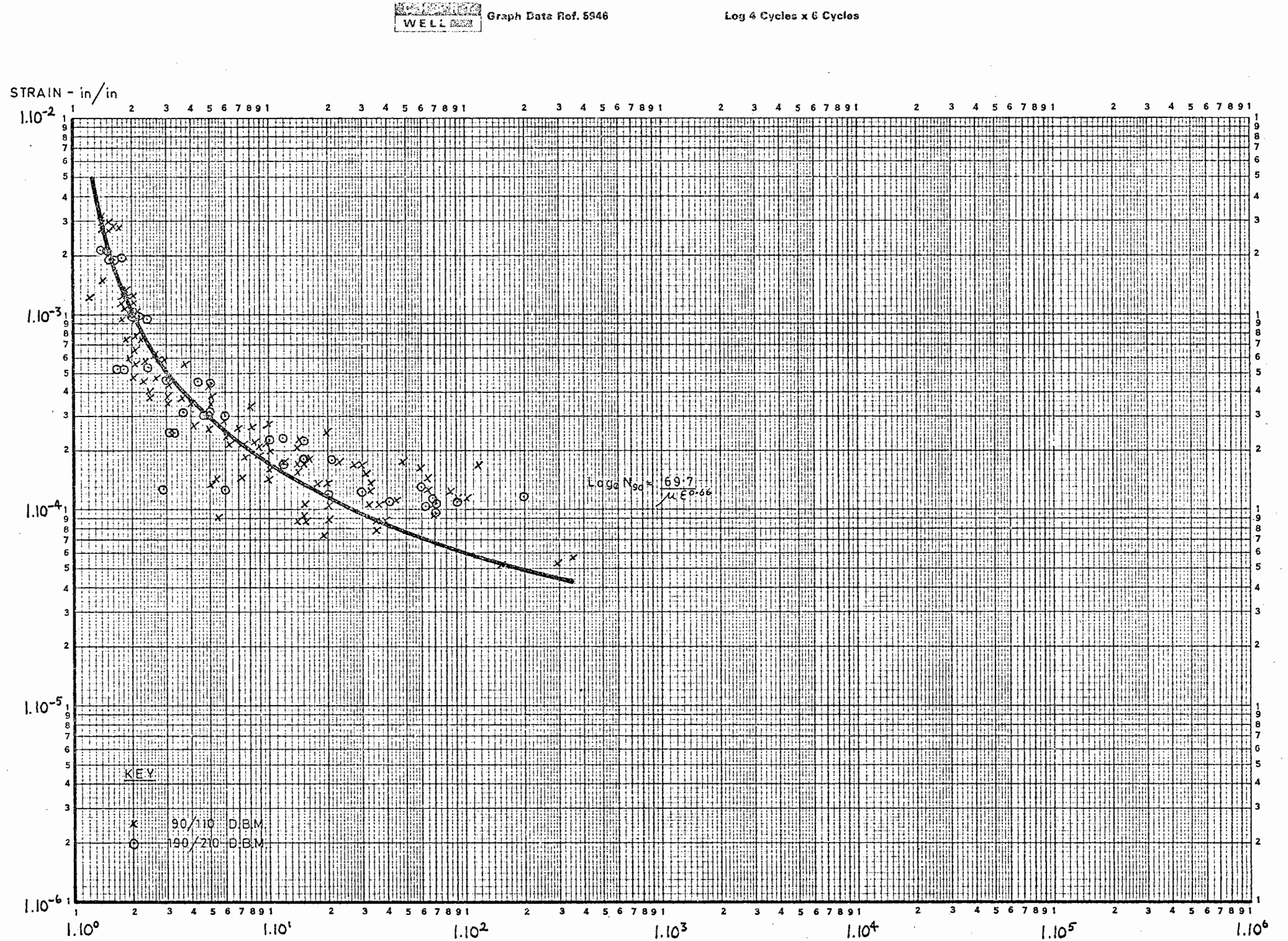

FIG. 104 CYCLES TO 90% OF INITIAL STIFFNESS OF 90/110 AND 190/210 D.B.M. AT 0°C to +40°C

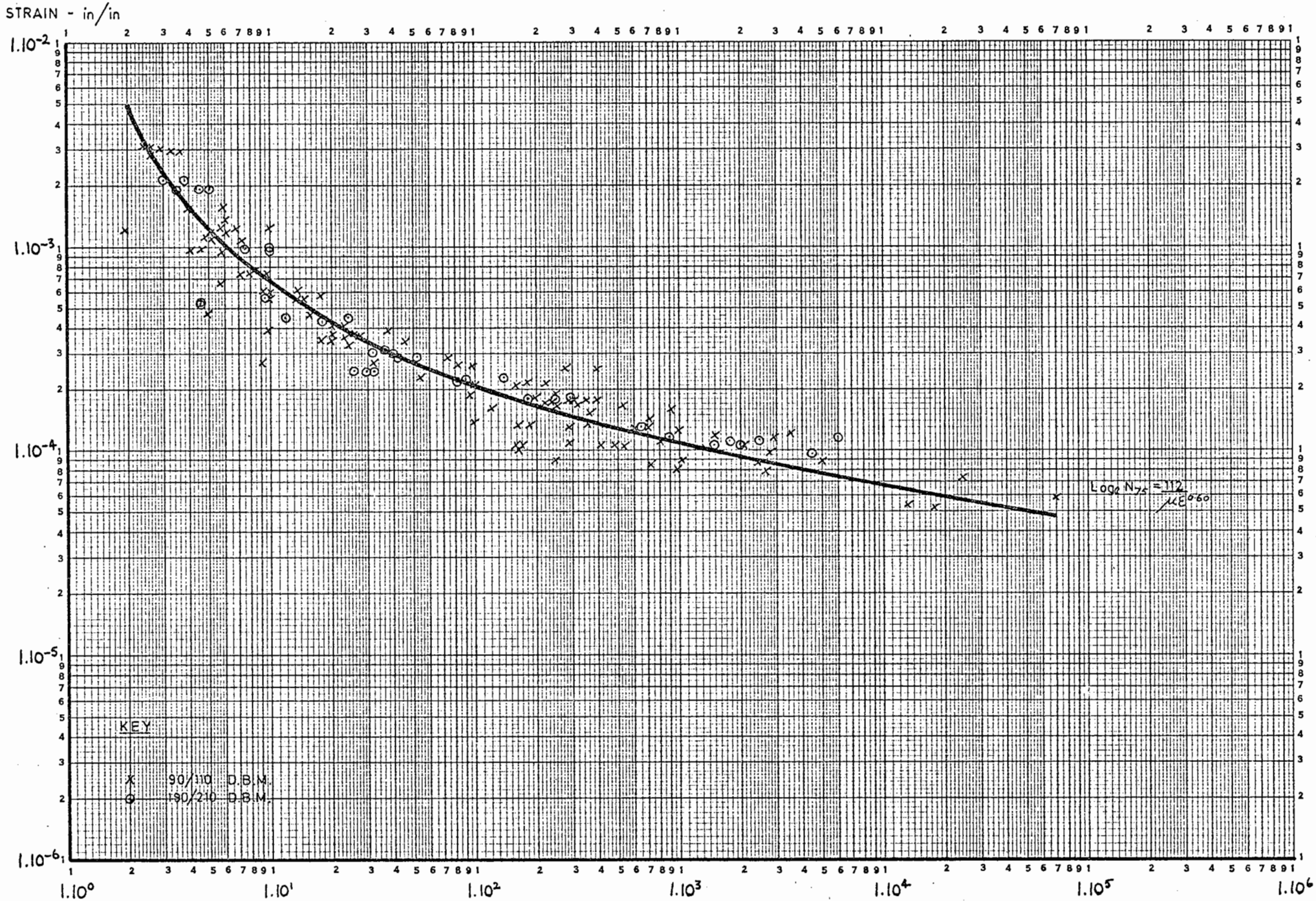

FIG. 105 CYCLES TO 75% OF INITIAL STIFFNESS OF 90/110 AND 190/210 D.B.M. AT 0°C to +40°C CYCLES TO 75% S_I

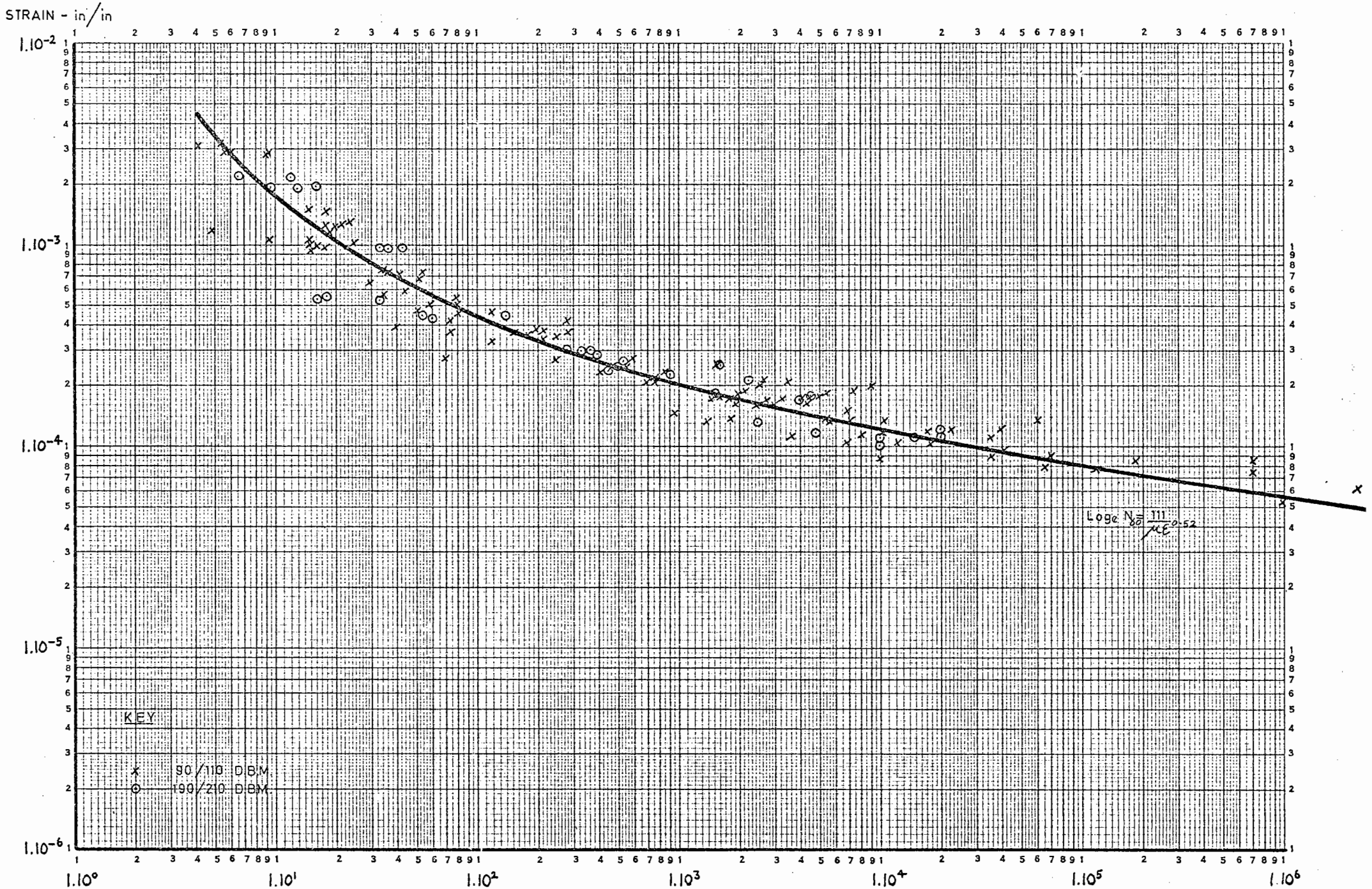

FIG. 106 CYCLES TO 60% OF INITIAL STIFFNESS OF 90/110 AND 190/210 D.B.M. AT SERVICE LIFE (CYCLES TO 60% S_t)

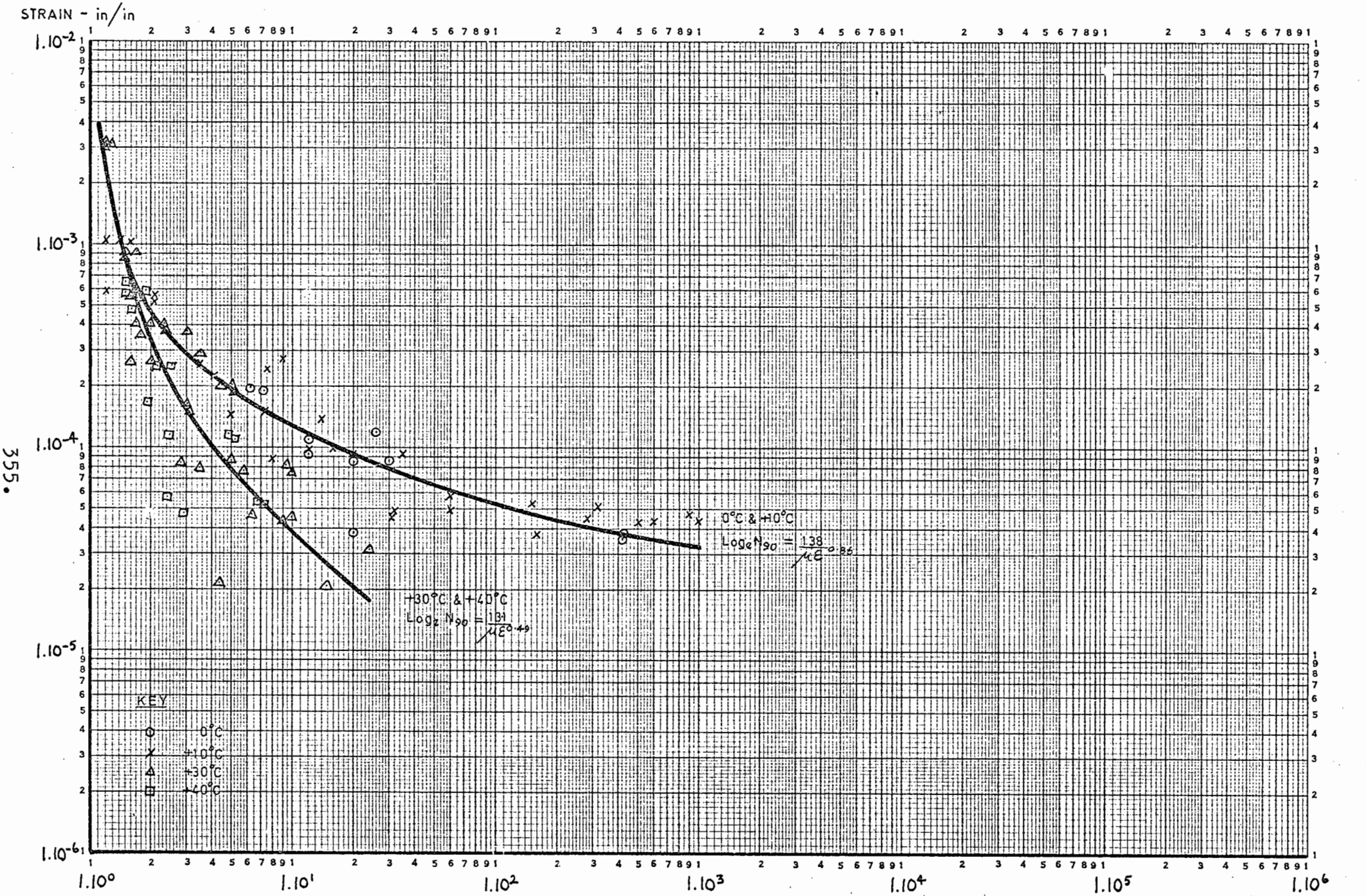

FIG. 107 CYCLES TO 90% OF INITIAL STIFFNESS OF D.T.M. AT 0°C to +40 C

CYCLES TO 90% S_I

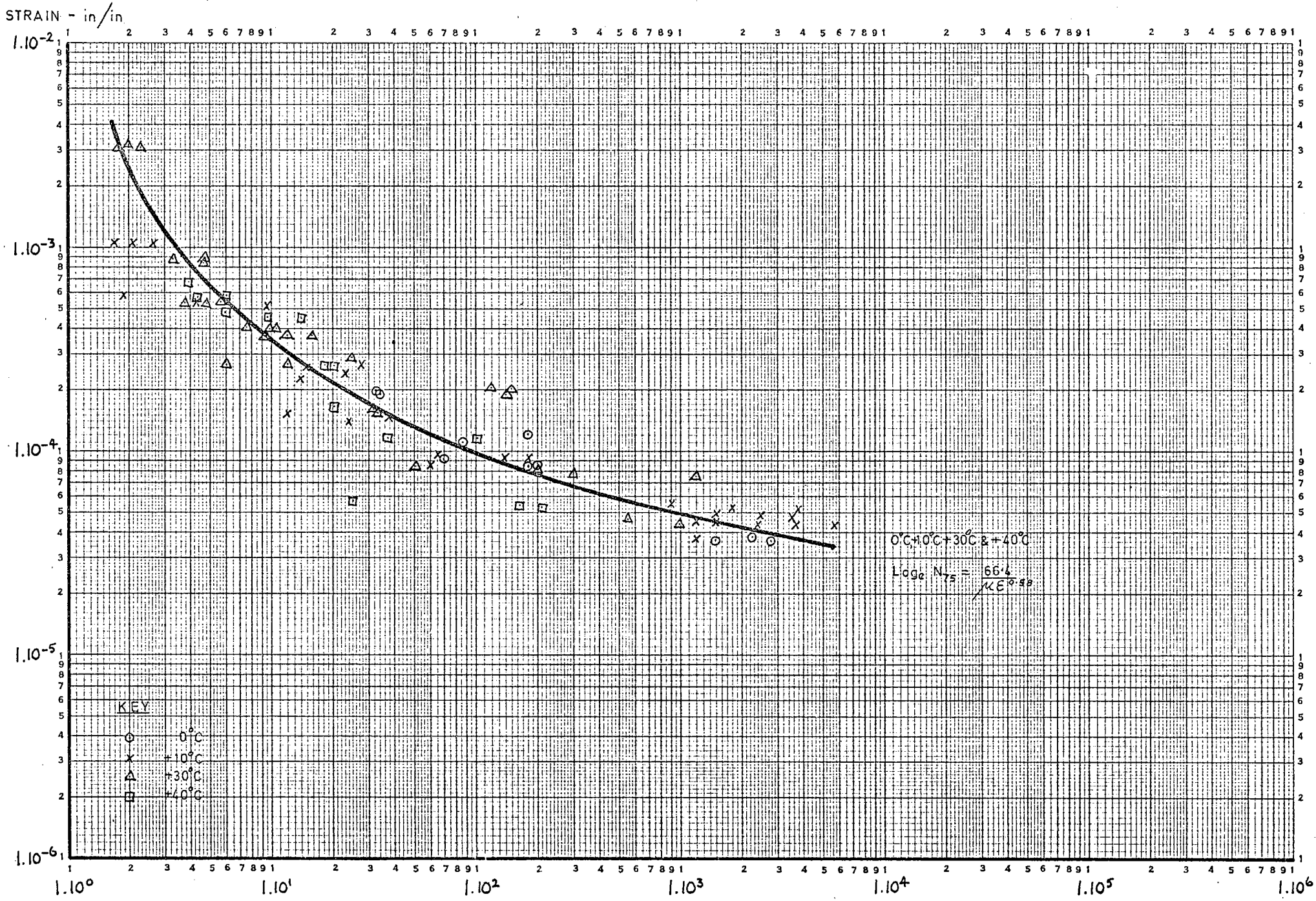

FIG. 108 CYCLES TO 75% OF INITIAL STIFFNESS OF D.T.M. AT 0°C to +40°C

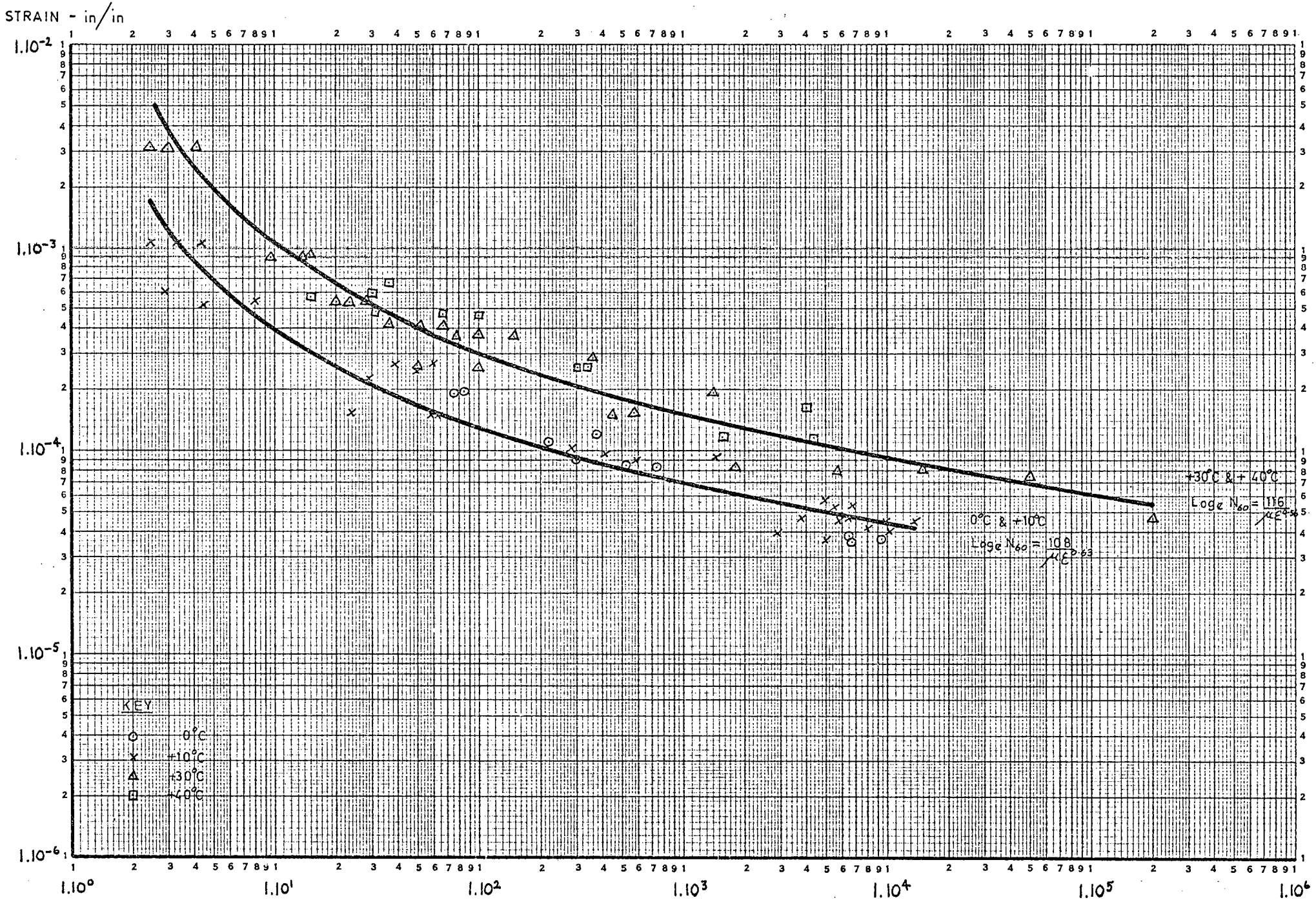

FIG. 109 CYCLES TO 60% OF INITIAL STIFFNESS OF D.T.M. AT 0°C to +40°C

SERVICE LIFE (CYCLES TO 60% S_I)

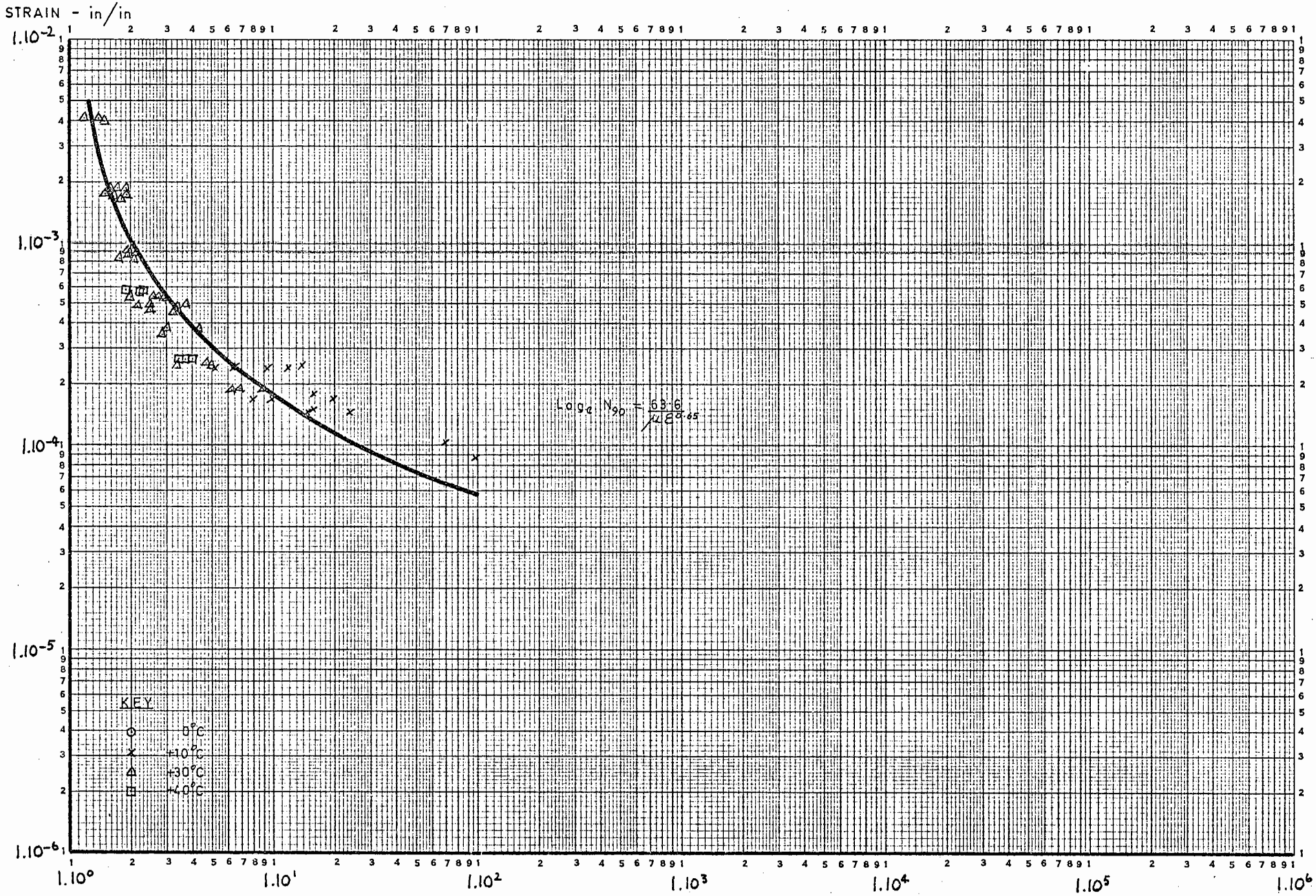

FIG. 110 CYCLES TO 90% OF INITIAL STIFFNESS OF H.R.A. AT +10°C to +40°C

WELL Graph Data Ref. 5946 Log 4 Cycles x 6 Cycles

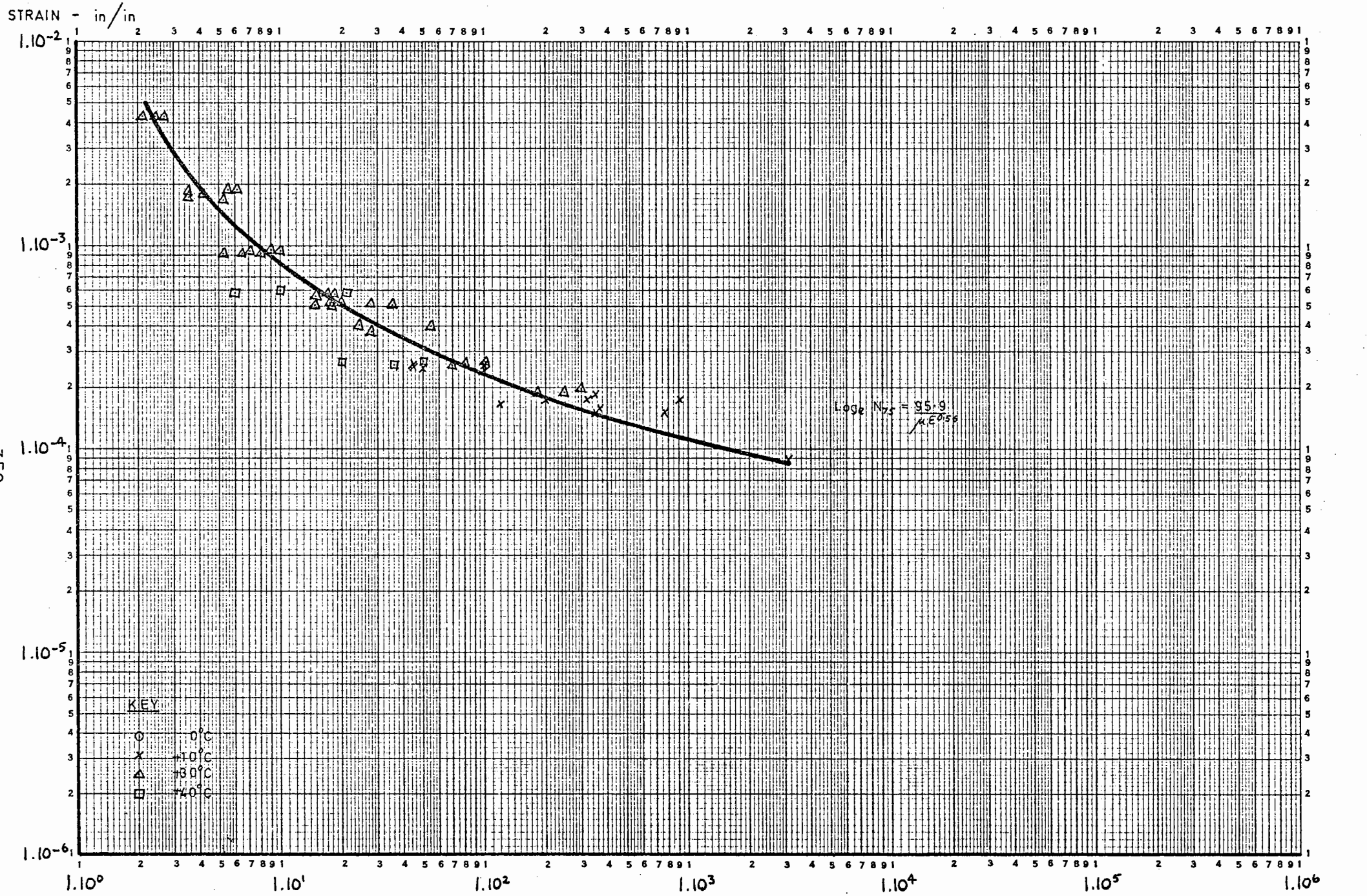

FIG. 111 CYCLES TO 75% OF INITIAL STIFFNESS OF H.R.A. AT +10°C to +40°C

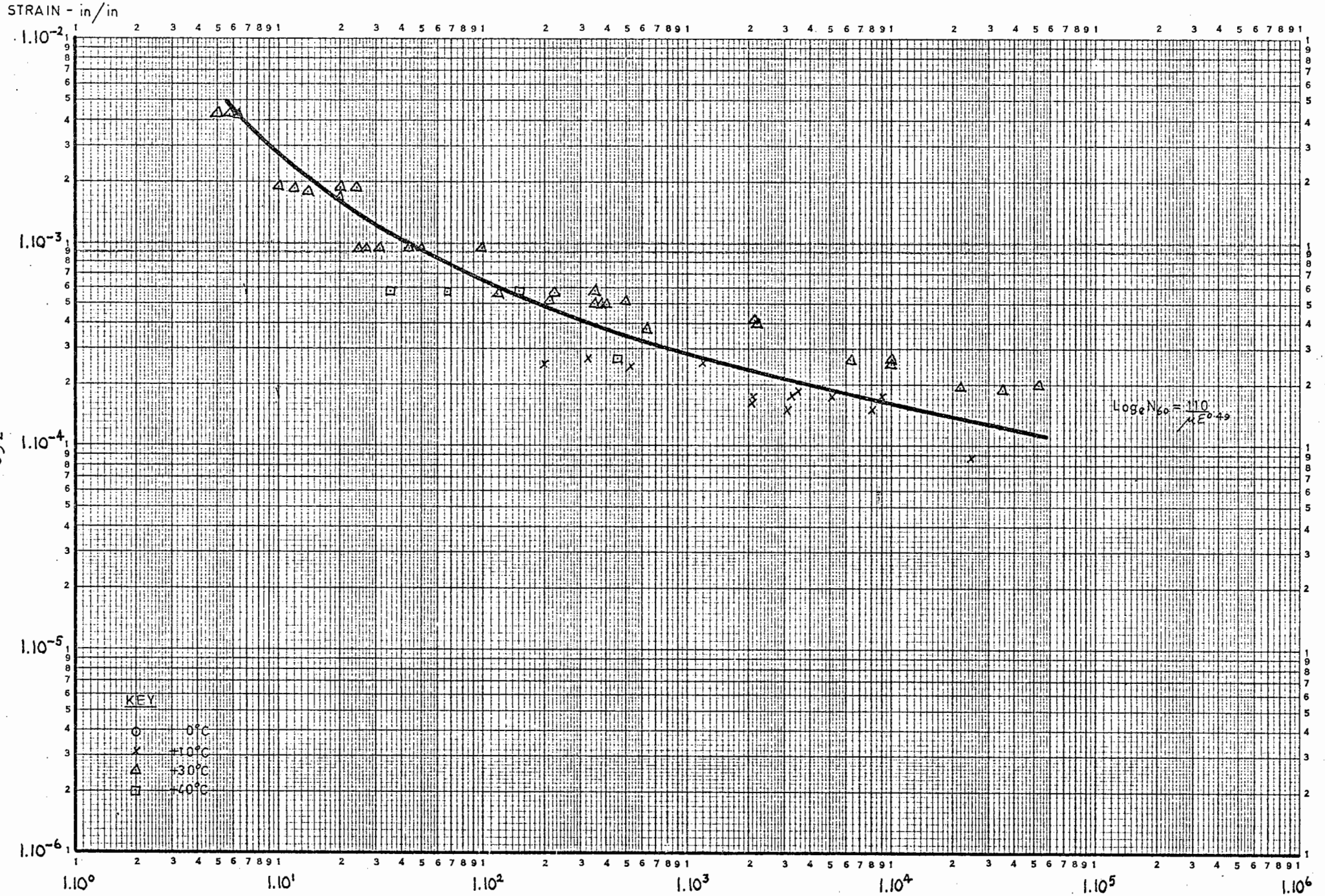

360.

FIG. 112 CYCLES TO 60% OF INITIAL STIFFNESS OF H.R.A. AT +10°C to +40°C

SERVICE LIFE (CYCLES TO 60%.S_I)

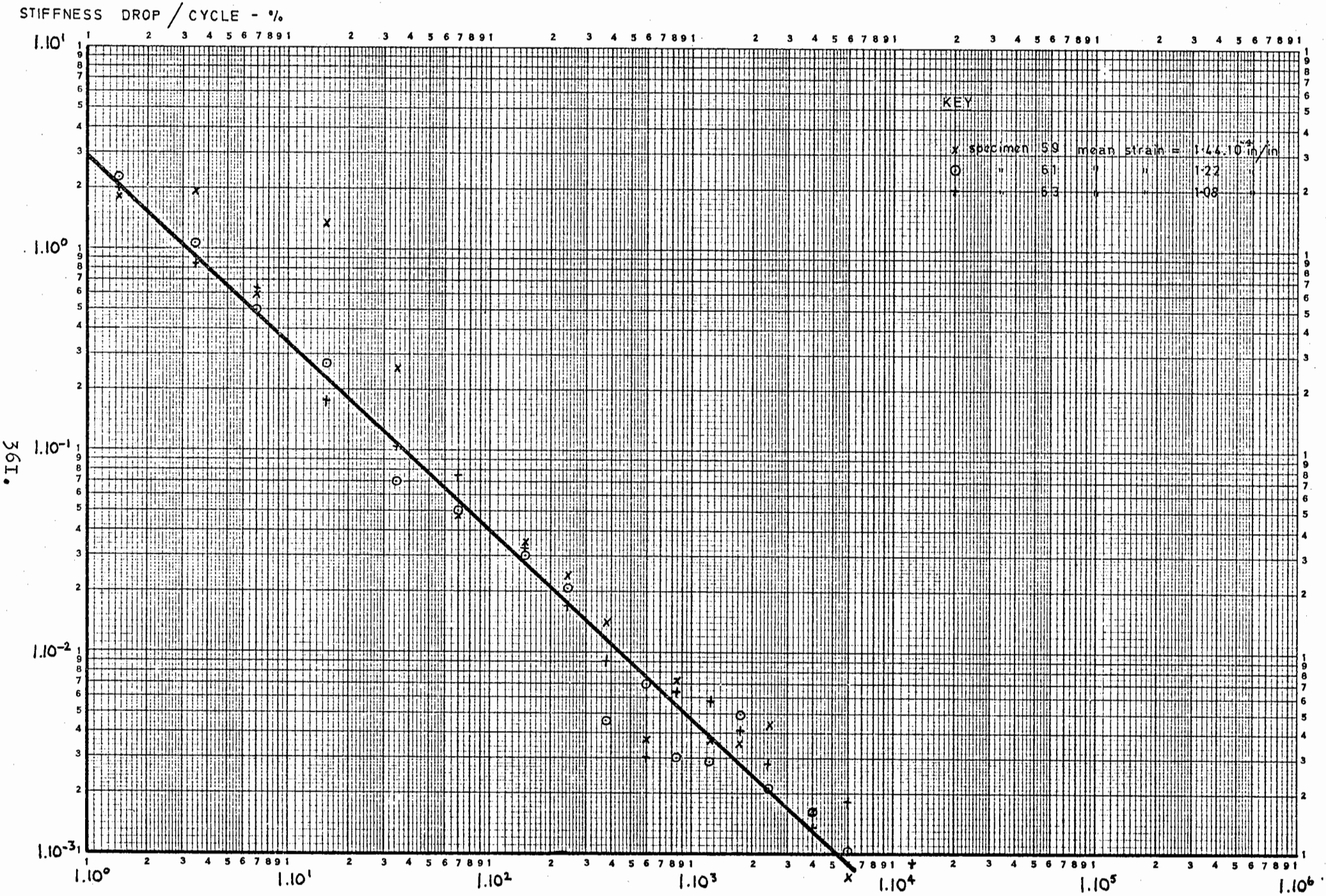

FIG. 113 CHANGE IN STIFFNESS CURVES OF 90/110 D.B.M. AT MEDIUM STRAIN LEVEL AT +10°C

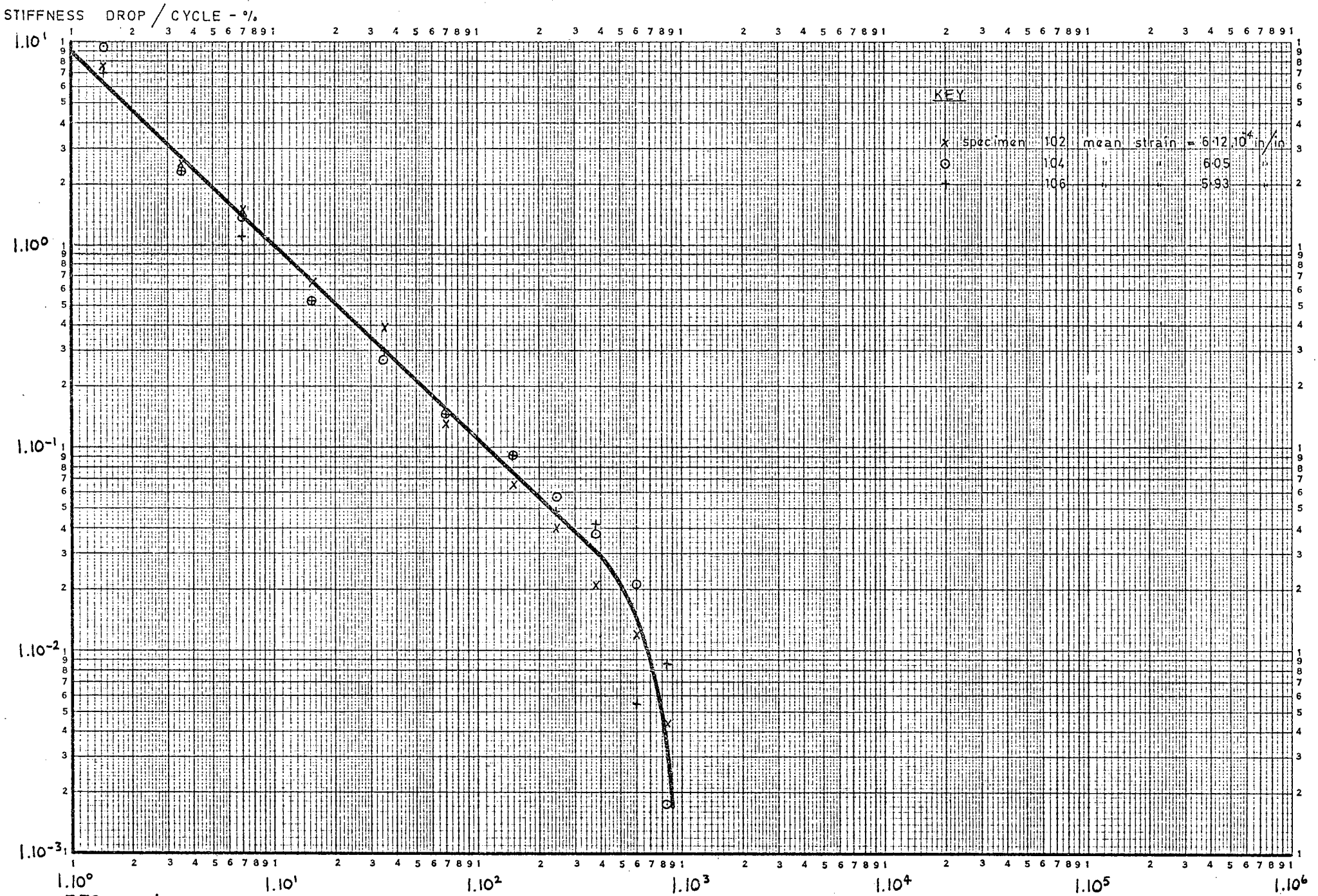

FIG. 114 CHANGE IN STIFFNESS CURVES OF 90/110 D.B.M. AT HIGH STRAIN LEVEL AT +10°C

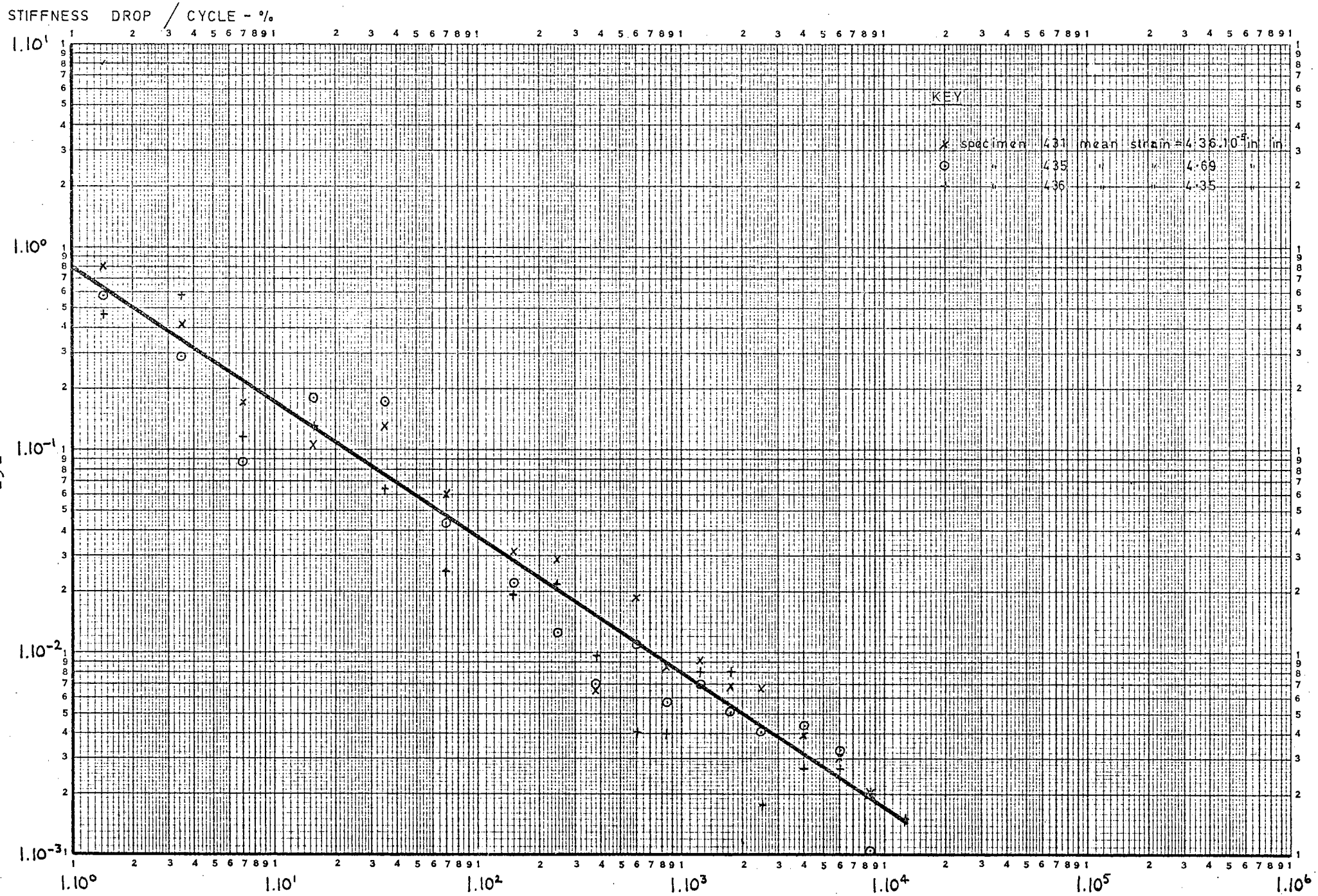

FIG. 115 CHANGE IN STIFFNESS CURVES OF D.T.M. AT LOW STRAIN LEVEL AT +10°C

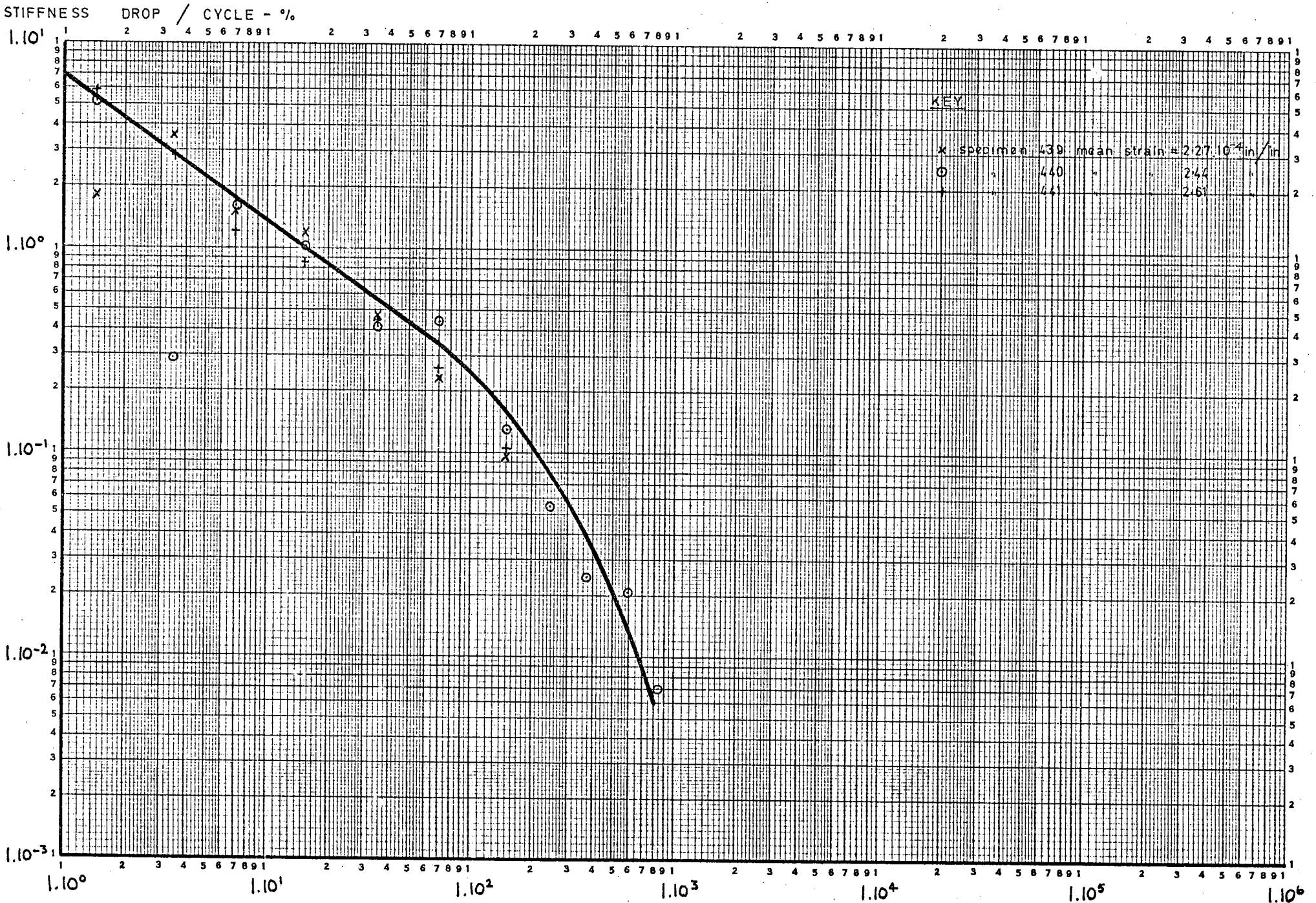

FIG. 116 CHANGE IN STIFFNESS CURVES OF D.T.M. AT MEDIUM STRAIN LEVEL AT +10°C

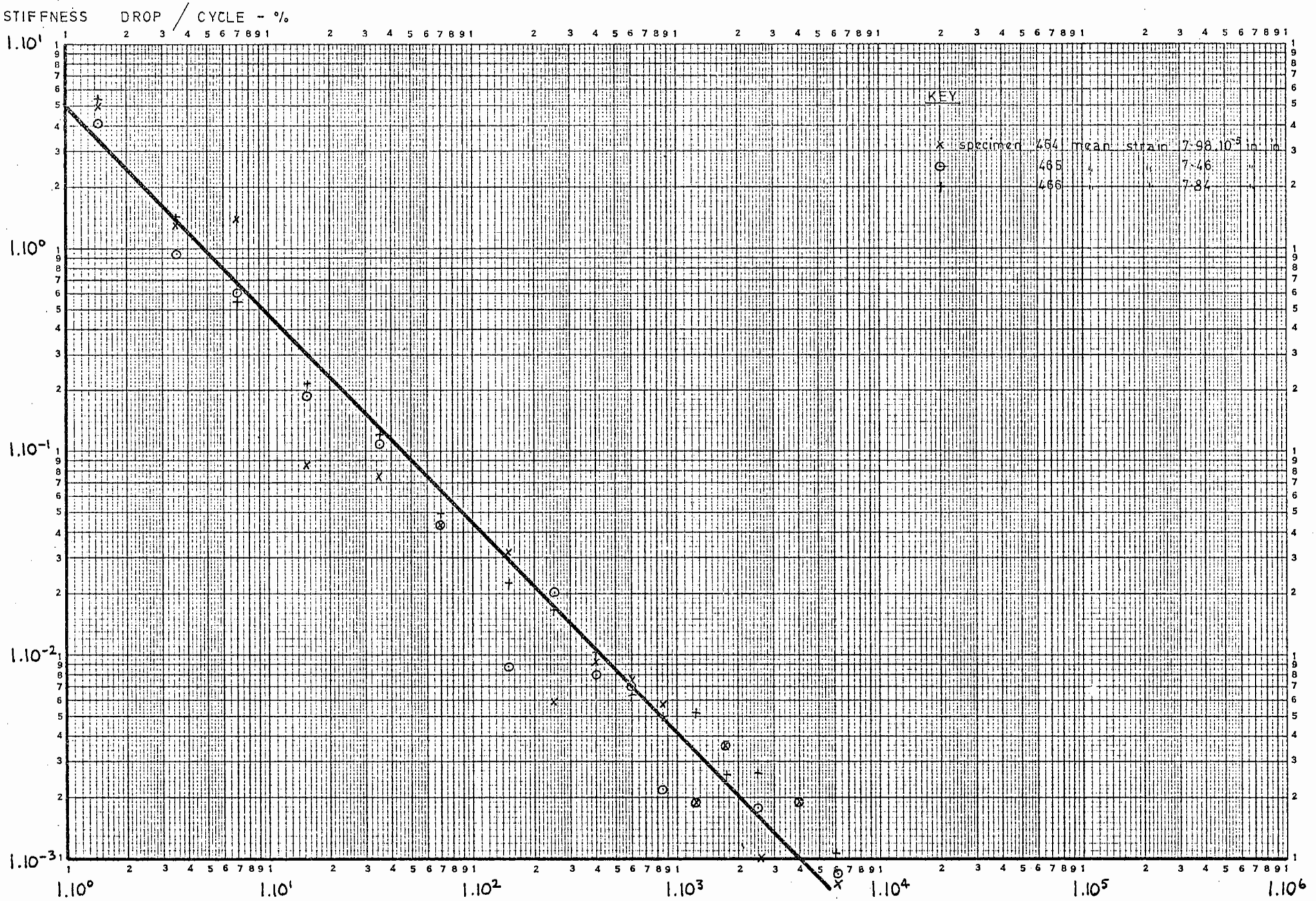

FIG. 117 CHANGE IN STIFFNESS CURVES OF D.T.M. AT LOW STRAIN LEVEL AT +30°C

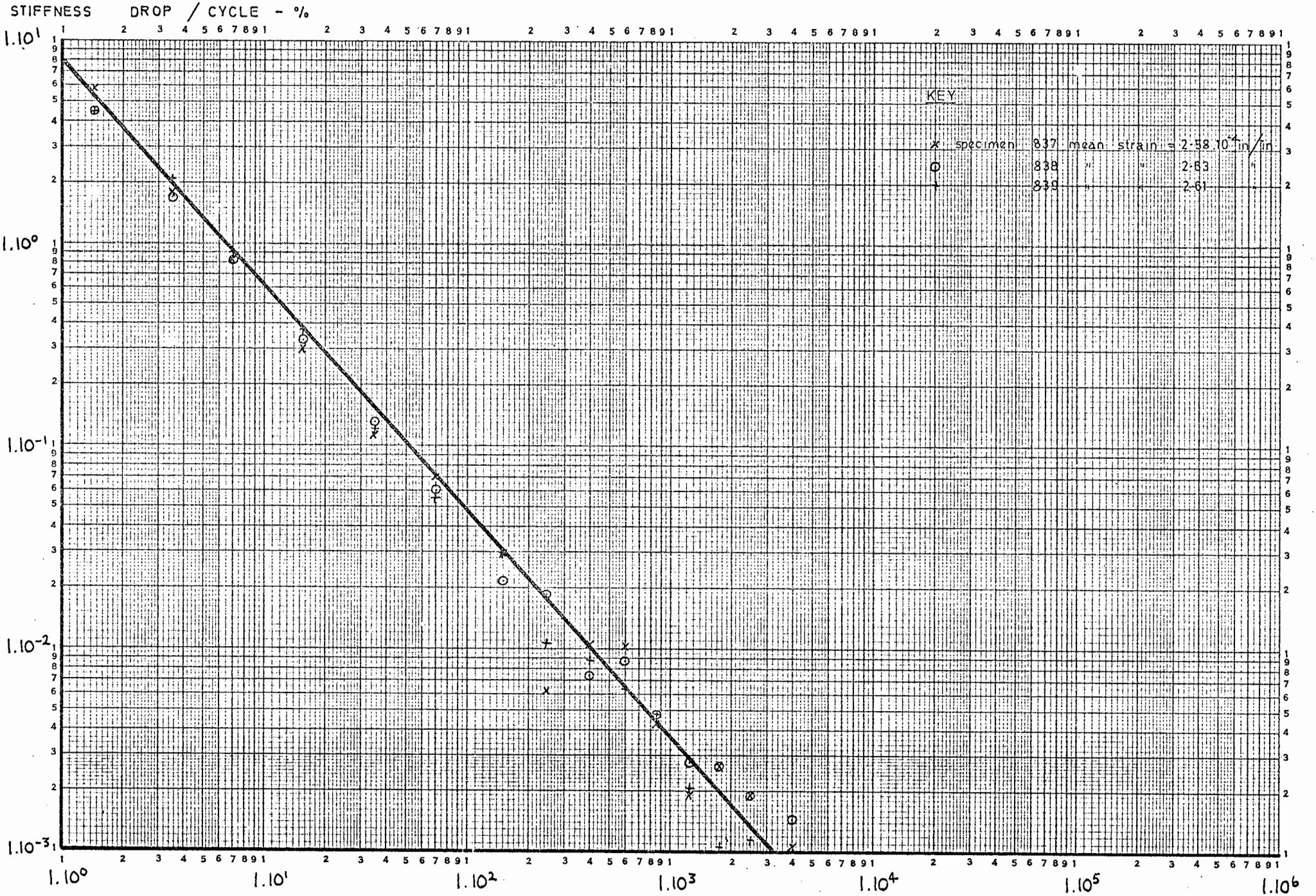

FIG. 118 CHANGE IN STIFFNESS CURVES OF D.T.M. AT MEDIUM STRAIN LEVEL AT +30°C

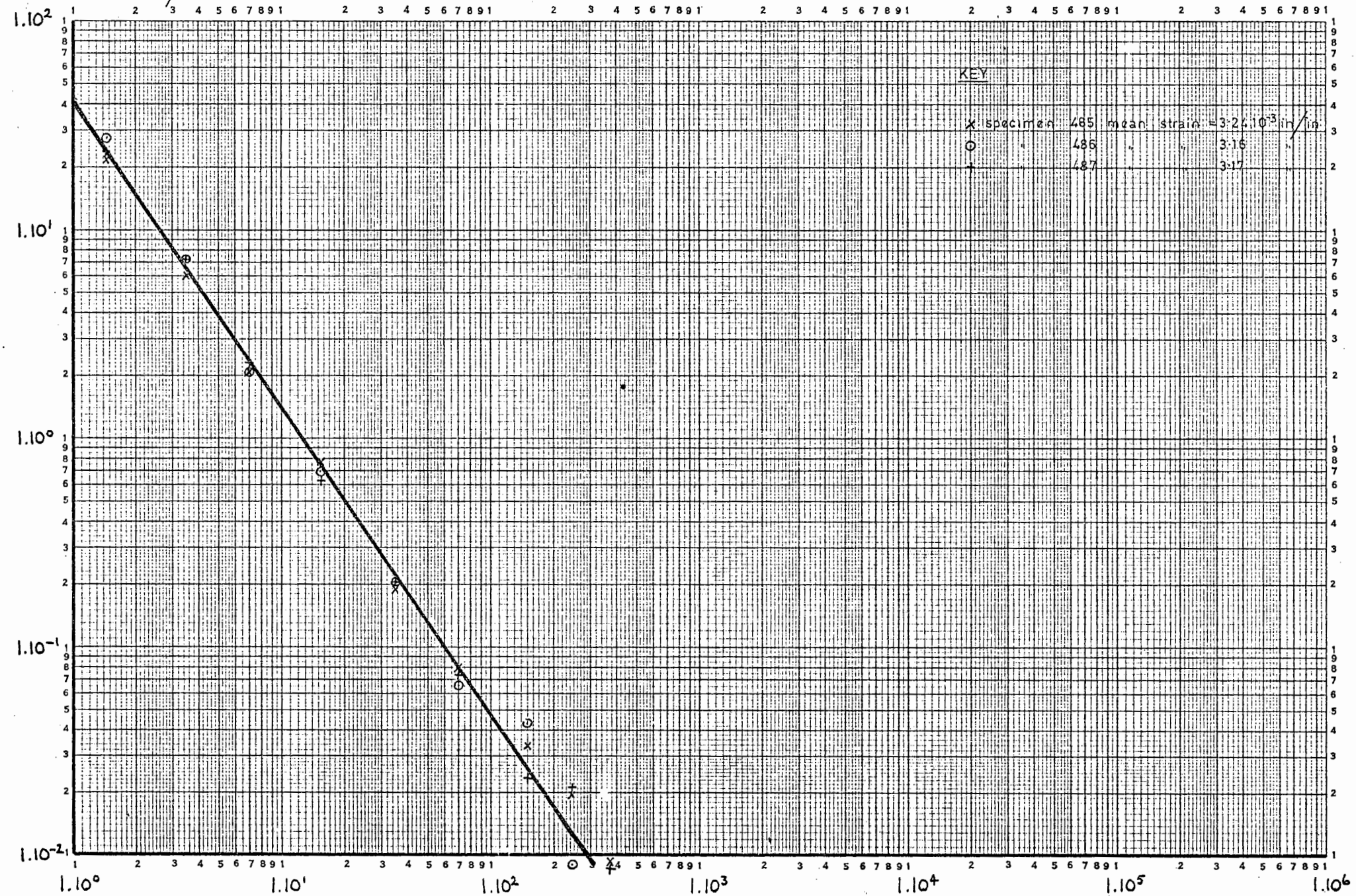

FIG. 119 CHANGE IN STIFFNESS CURVES OF H.R.A. AT HIGH STRAIN LEVEL AT +30°C

WELL Graph Data Ref. 5946 Log 4 Cycles x 6 Cycles

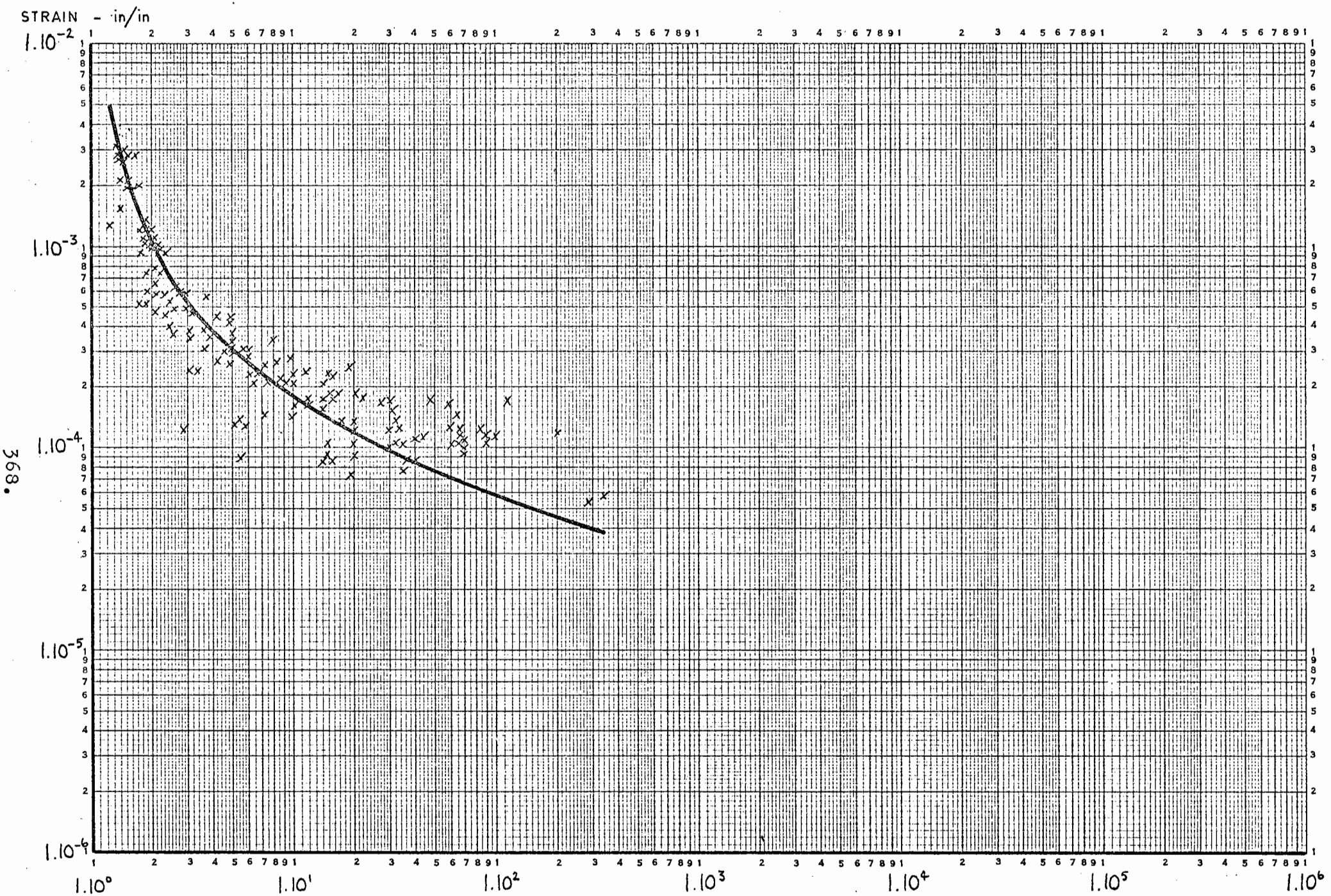

FIG. 120 CALCULATED CYCLES TO 90% OF INITIAL STIFFNESS OF 90/110 AND 190/210 D.B.M. at 0°C CYCLES TO 90%S

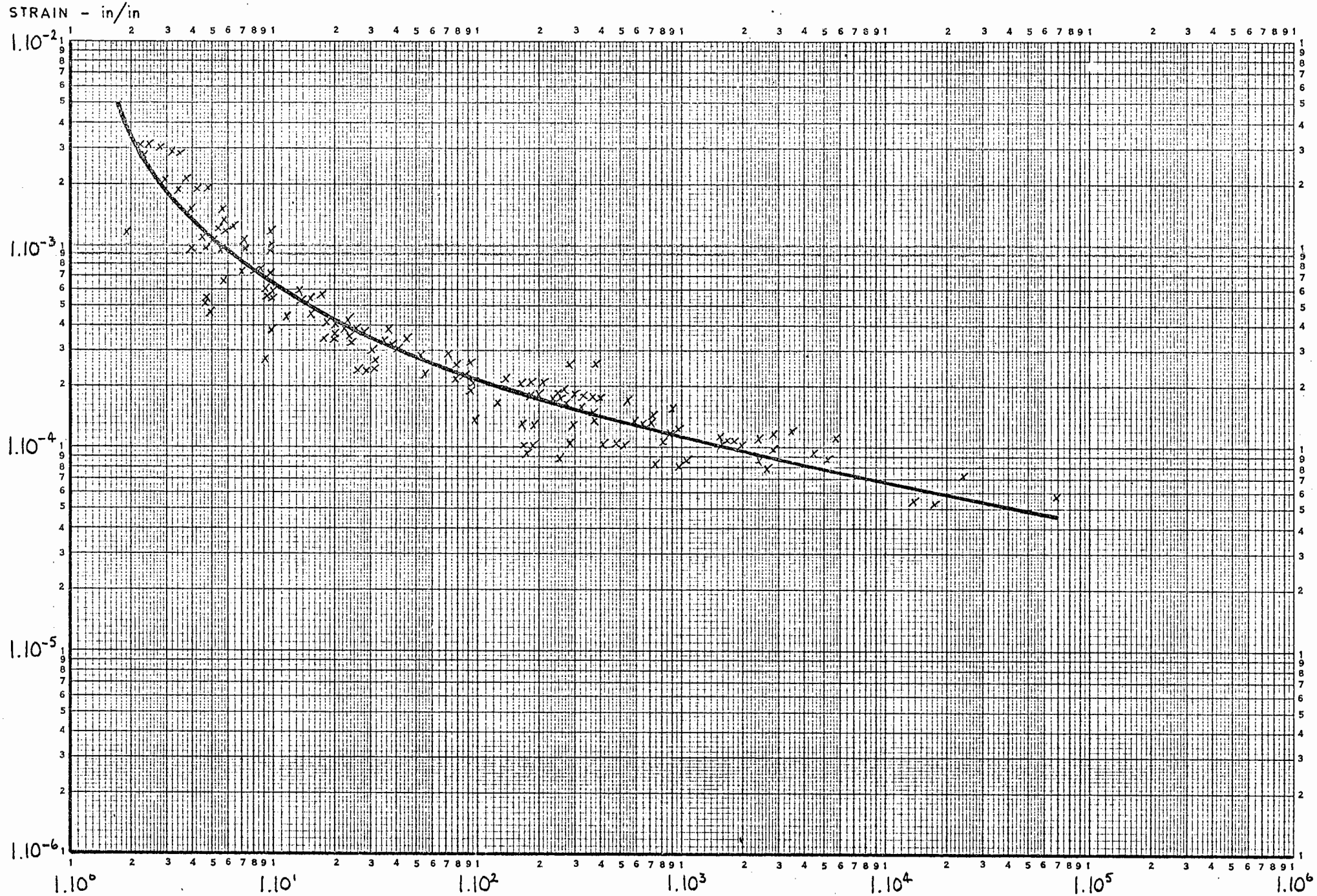

FIG. 121 CALCULATED CYCLES TO 75% OF INITIAL STIFFNESS OF 90/110 AND 190/210 D.B.M. AT $^{0°C}_{CYCLES}$ TO $^{+40°C}_{75\%S_i}$

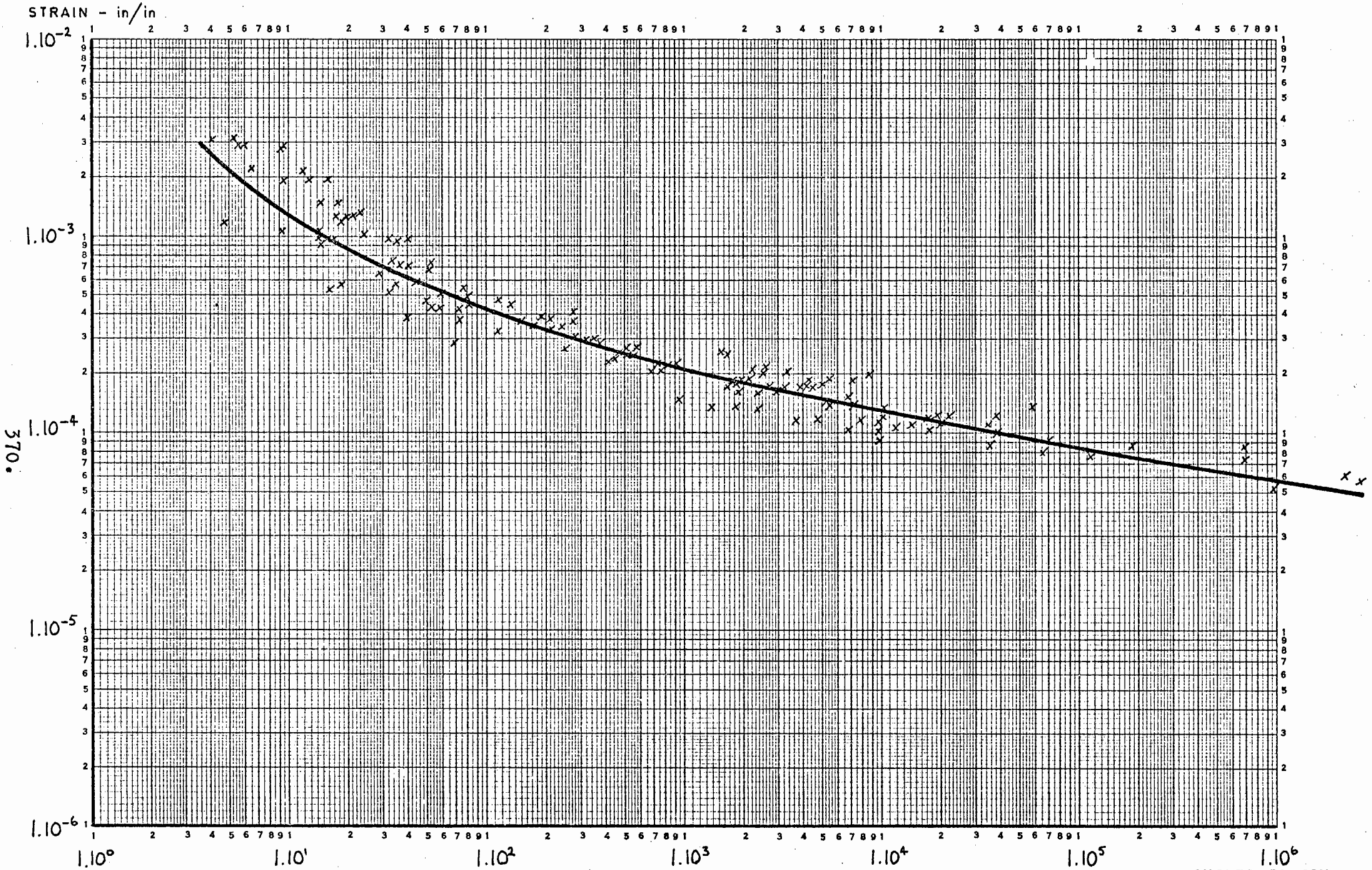

FIG. 122 CALCULATED CYCLES TO 60% OF INITIAL STIFFNESS OF 90/110 AND 190/210 D.B.M. AT 0°C to +40°C

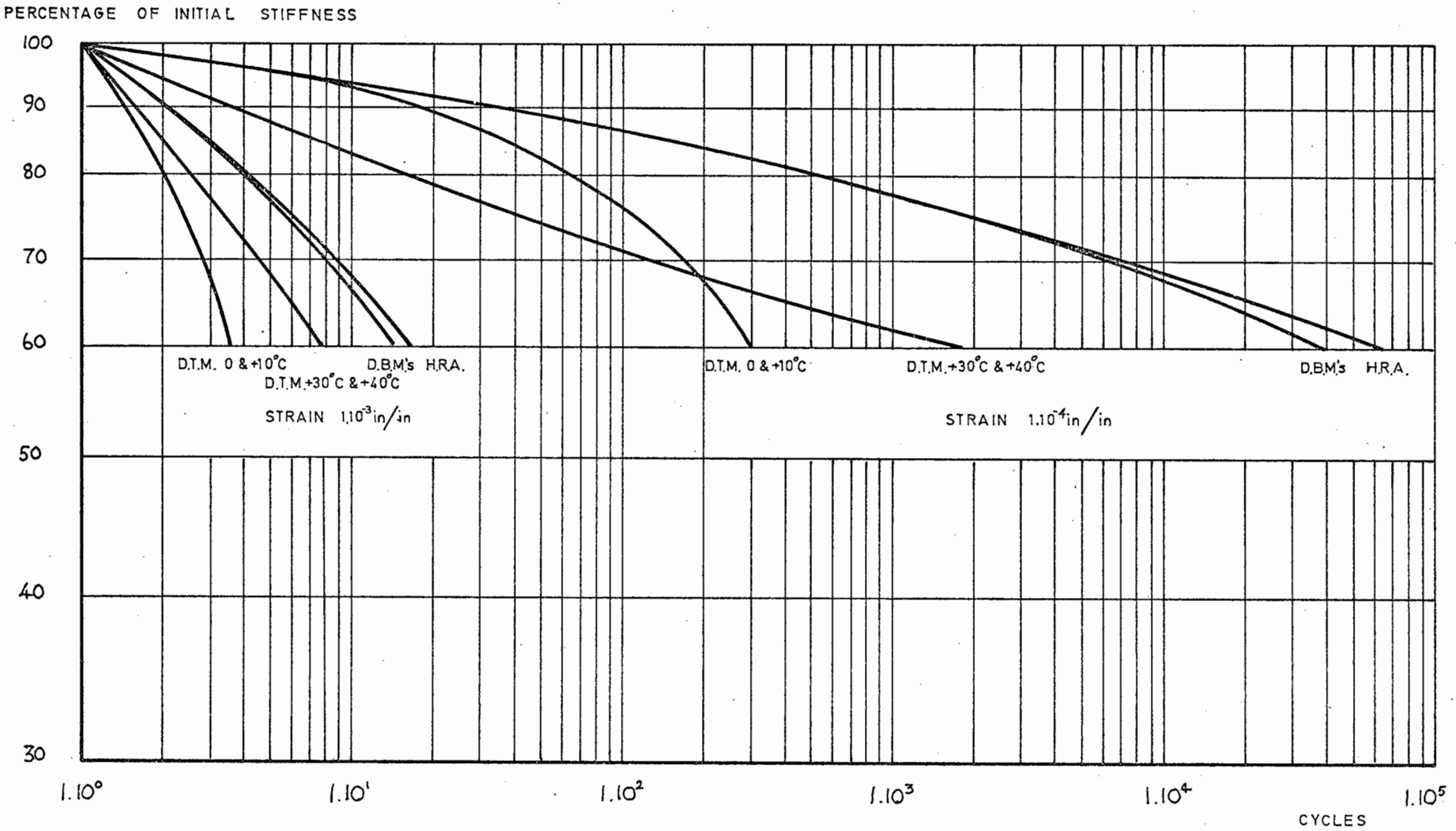

FIG. 123 CALCULATED STIFFNESS CURVES OF ALL BITUMINOUS MATERIALS STUDIED

LOAD CURVE SHAPES

TYPE A TENSILE AND COMPRESSIVE LOADS BOTH DECREASE ROUGHLY PROPORTIONALLY OVER DURATION OF TEST
B TENSILE LOAD DECREASES OVER DURATION OF TEST BUT COMPRESSIVE LOAD UNAFFECTED OVER FIRST FEW CYCLES
C COMPRESSIVE LOAD DECREASES OVER DURATION OF TEST BUT TENSILE LOAD SHOWS SLIGHT INCREASE OVER FIRST FEW CYCLES

DEFORMATION CURVE SHAPES

TYPE 1 TENSILE AND COMPRESSIVE DEFORMATIONS REMAIN CONSTANT OR DECREASE SLIGHTLY OVER DURATION OF TEST
2 TENSILE AND COMPRESSIVE DEFORMATIONS INCREASE OVER FIRST FEW CYCLES THEN DECREASE GRADUALLY FOR REMAINDER OF TEST
3 TENSILE AND COMPRESSIVE DEFORMATIONS INCREASE SIGNIFICANTLY FOR AT LEAST FIRST 50 CYCLES THEN DECREASE FOR REMAINDER OF TEST
4 TENSILE AND COMPRESSIVE DEFORMATIONS INCREASE OVER DURATION OF TEST

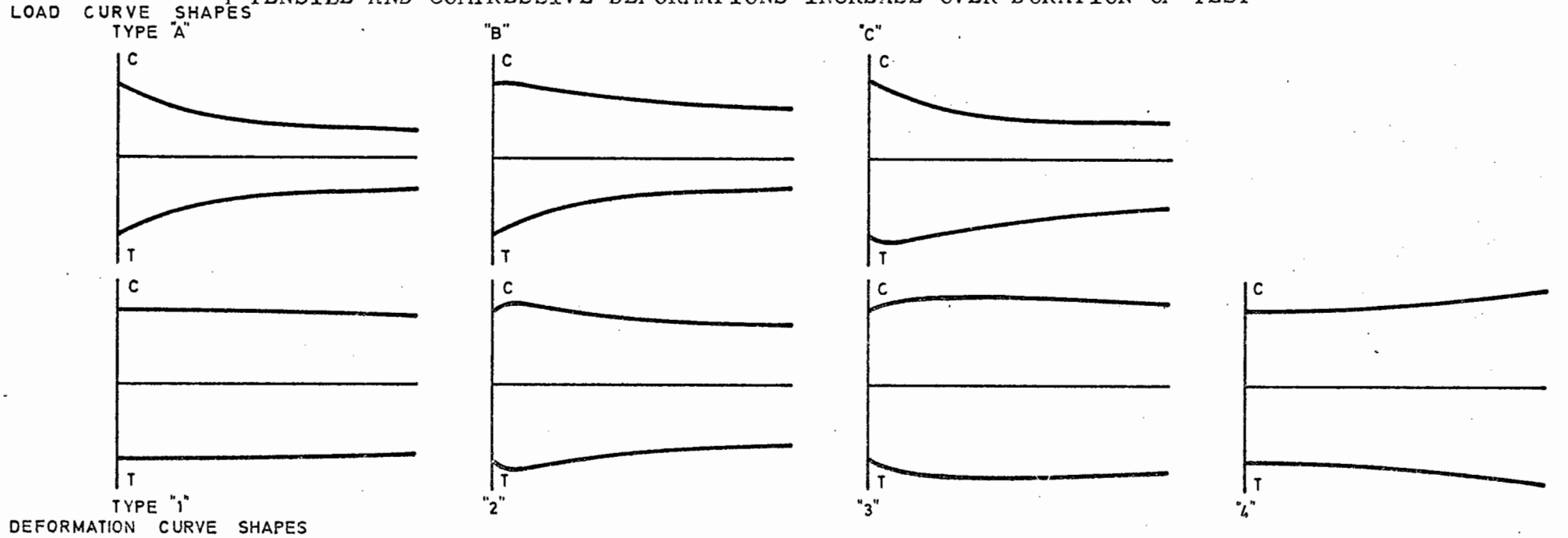

FIG. 124 SHAPES OF LOAD AND DEFLECTION CURVES OF BITUMINOUS MATERIALS DURING REPEATED LOADING TESTS

 Graph Data Ref. 5925 Log 2 Cycles x 5 Cycles

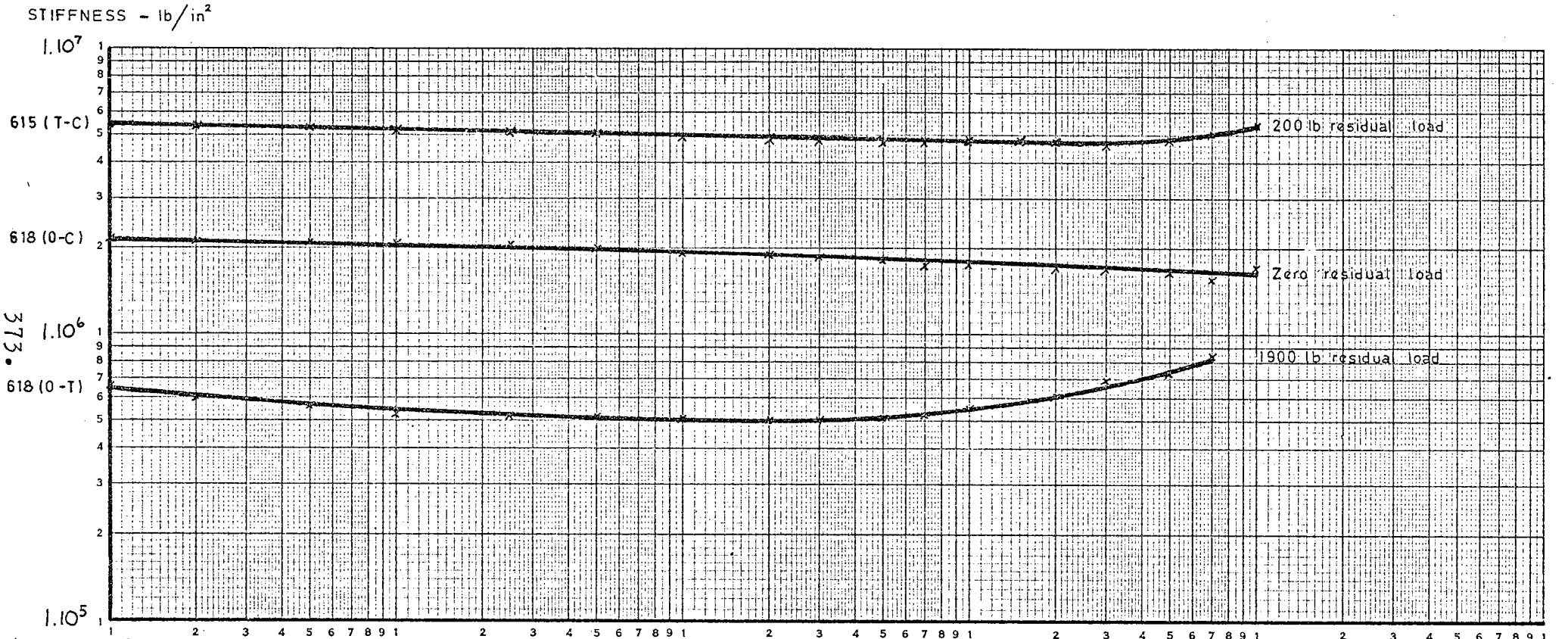

373.

specimen	strain				
615 (T-C)	$2{\cdot}88.10^{-5}$	$2{\cdot}74.10^{-5}$	$2{\cdot}76.10^{-5}$	$2{\cdot}70.10^{-5}$	$2{\cdot}90.10^{-5}$
618 (0-C)	$1{\cdot}94.10^{-4}$	$1{\cdot}94.10^{-4}$	$1{\cdot}94.10^{-4}$	$1{\cdot}92.10^{-4}$	$1{\cdot}92.10^{-4}$
618 (0-T)	$2{\cdot}02.10^{-4}$	$1{\cdot}96.10^{-4}$	$1{\cdot}94.10^{-4}$	$1{\cdot}94.10^{-4}$	—

FIG. 125 STIFFNESS CURVES OF DRY LEAN CONCRETE IN STRAIN-CONTROLLED REPEATED LOADING

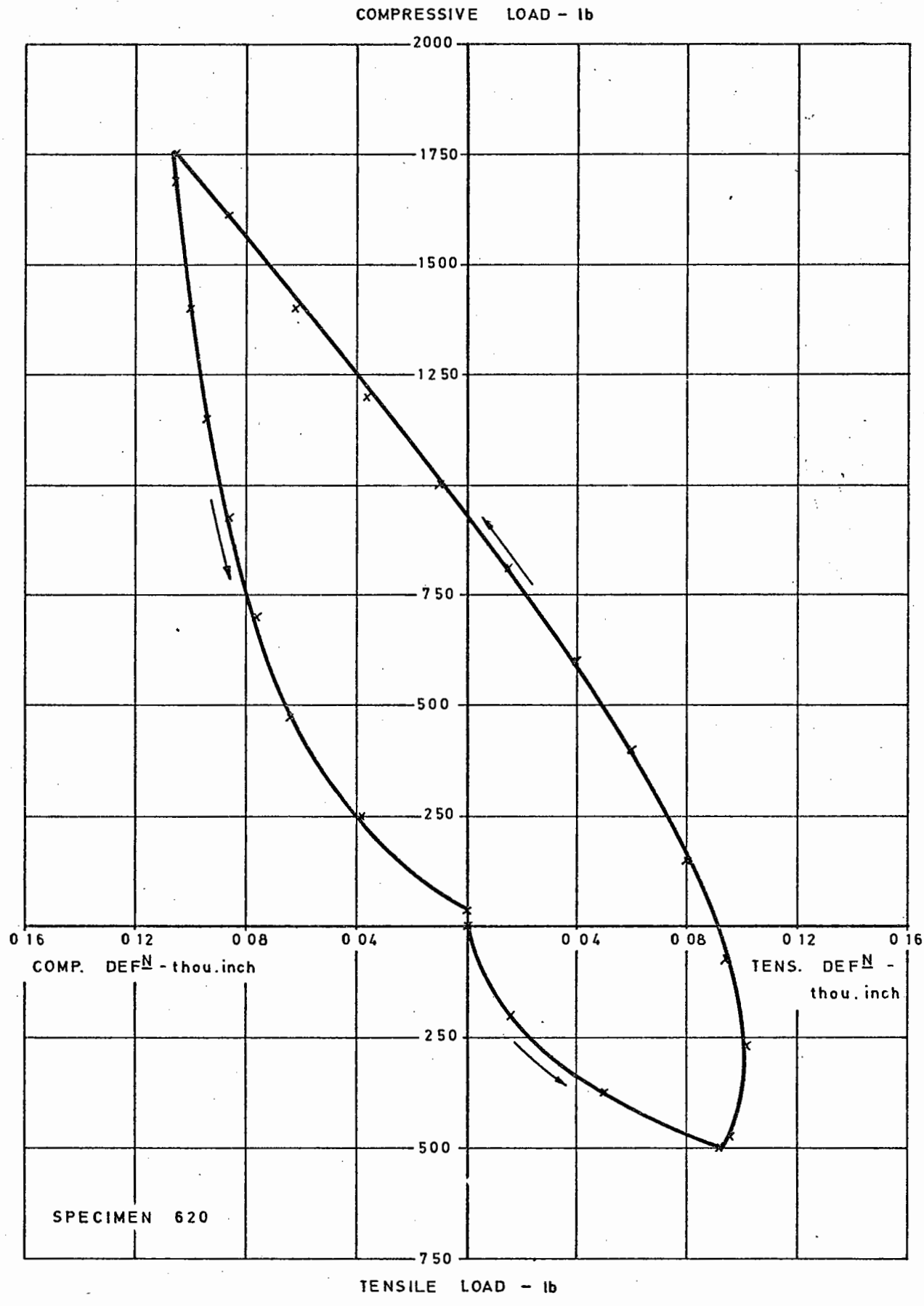

FIG. 126 HYSTERESIS LOOP OF SPECIMEN OF DRY LEAN CONCRETE IN FIRST CYCLE OF FLUCTUATING STRAIN-CONTROLLED REPEATED LOADING

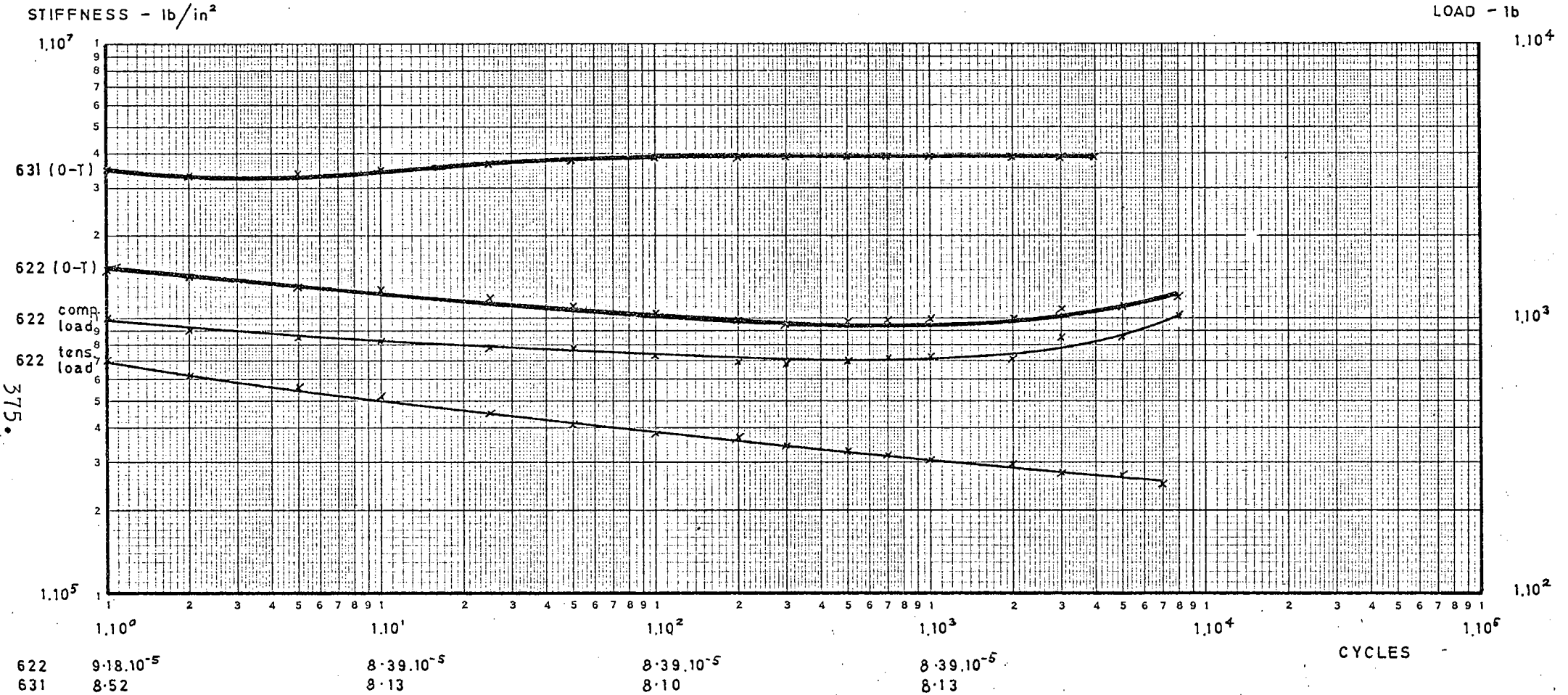

FIG. 127 STIFFNESS CURVES OF DRY LEAN CONCRETE IN TENSILE STRAIN-CONTROLLED REPEATED LOADING

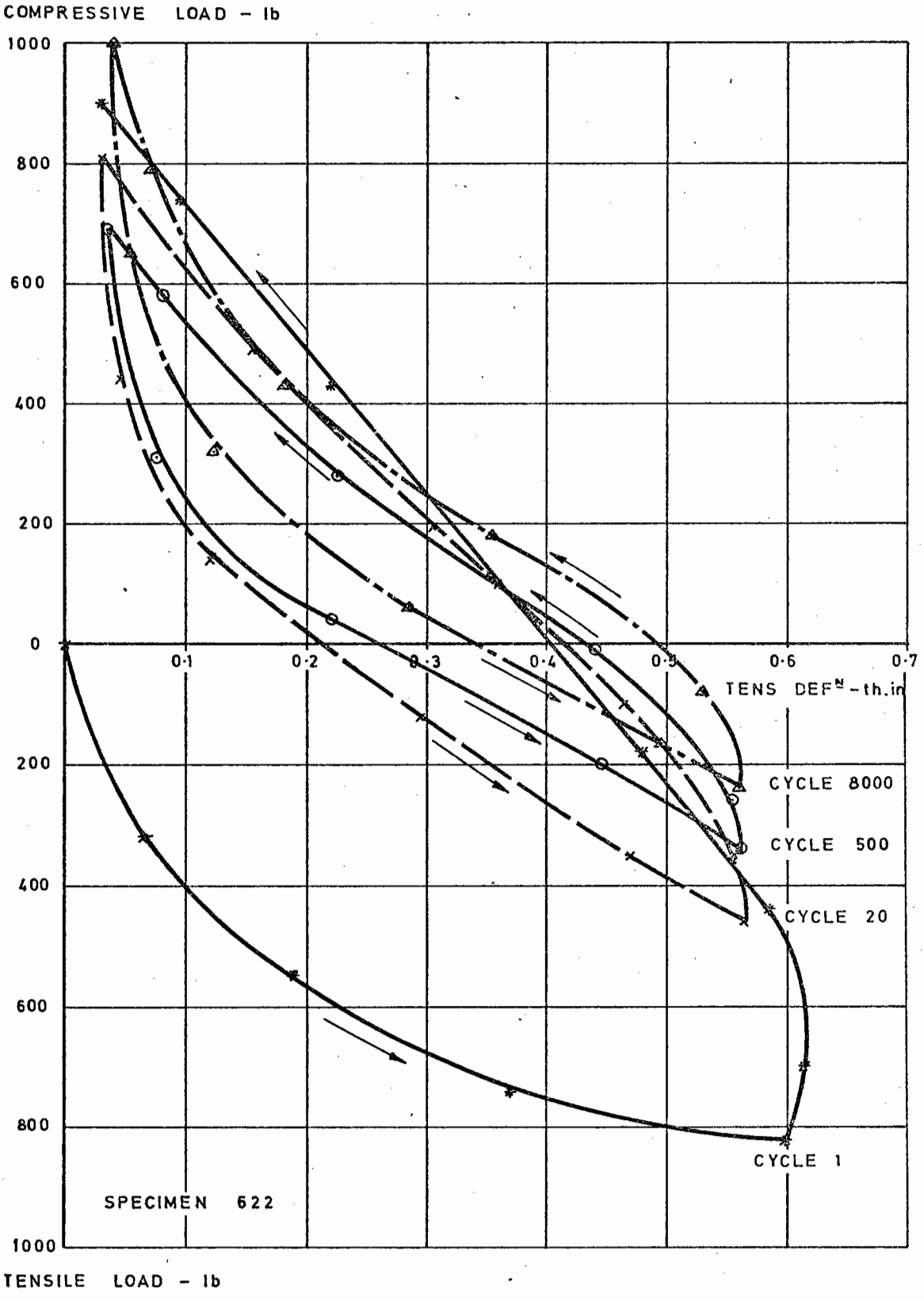

FIG. 128 HYSTERESIS LOOPS OF SPECIMEN OF DRY LEAN CONCRETE IN TENSILE STRAIN-CONTROLLED REPEATED LOADING

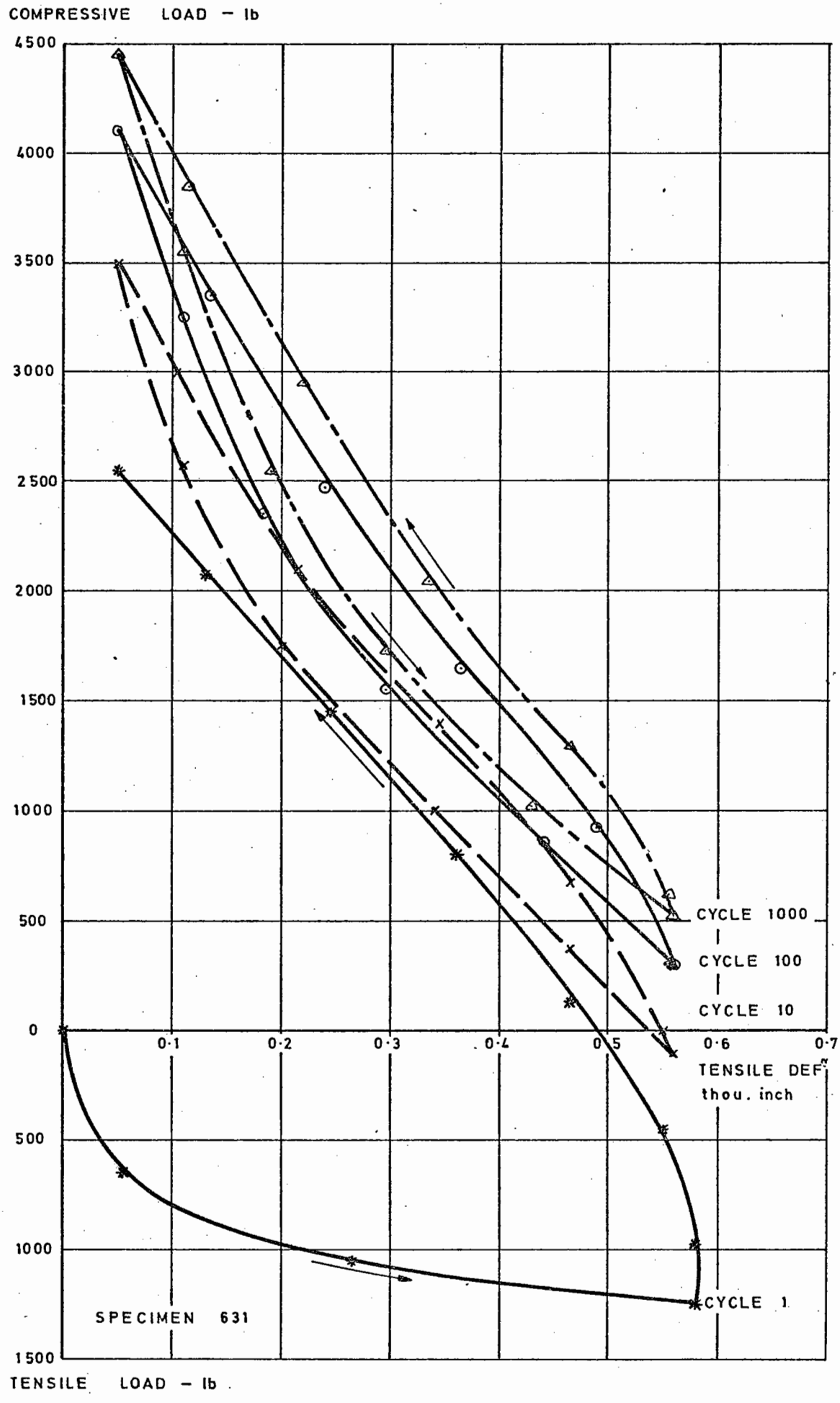

FIG. 129 HYSTERESIS LOOPS OF SPECIMEN OF DRY LEAN CONCRETE IN TENSILE STRAIN-CONTROLLED REPEATED LOADING

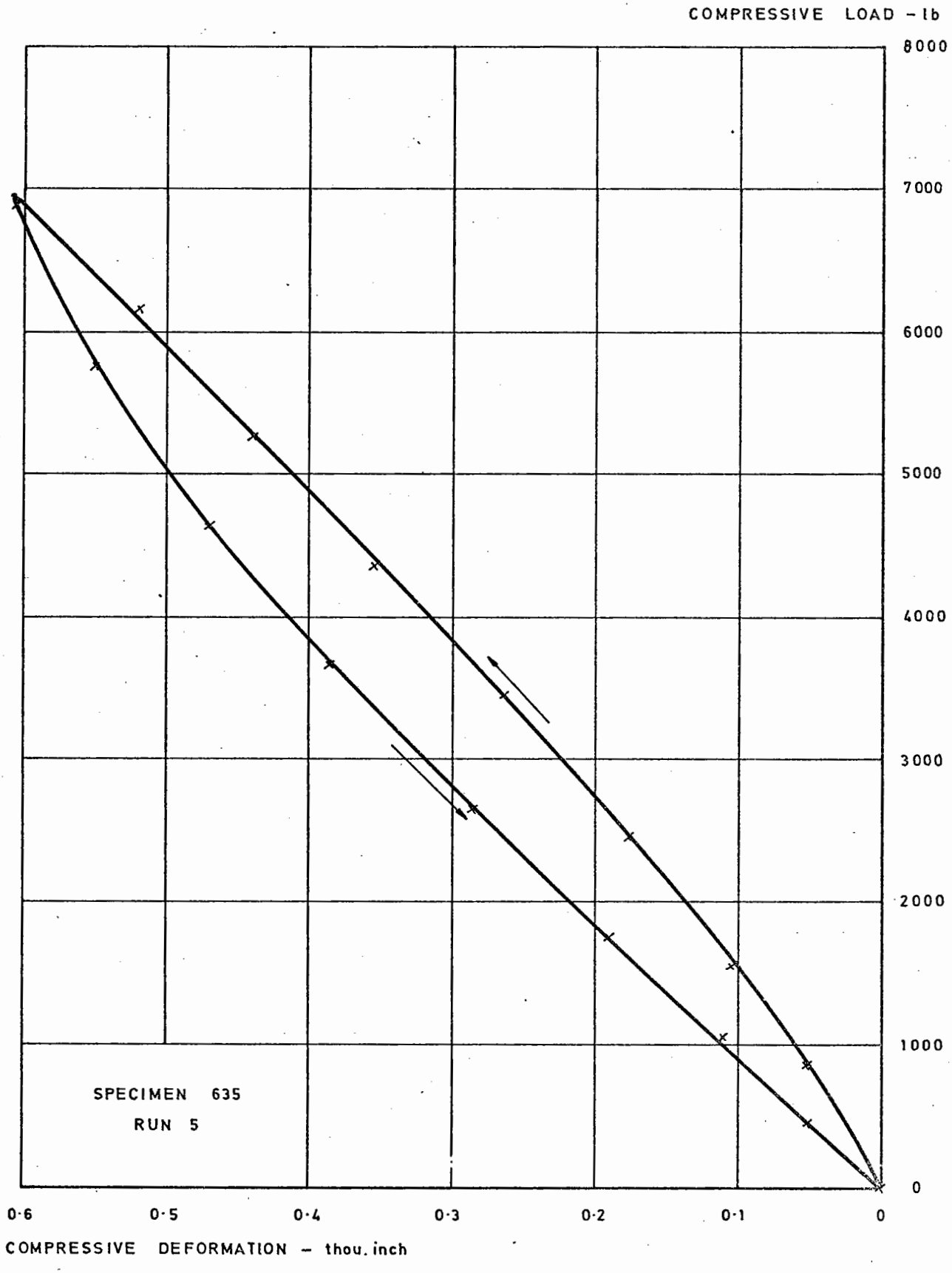

FIG. 130 HYSTERESIS LOOP OF SPECIMEN OF DRY LEAN CONCRETE IN FIRST CYCLE OF COMPRESSIVE STRAIN-CONTROLLED REPEATED LOADING

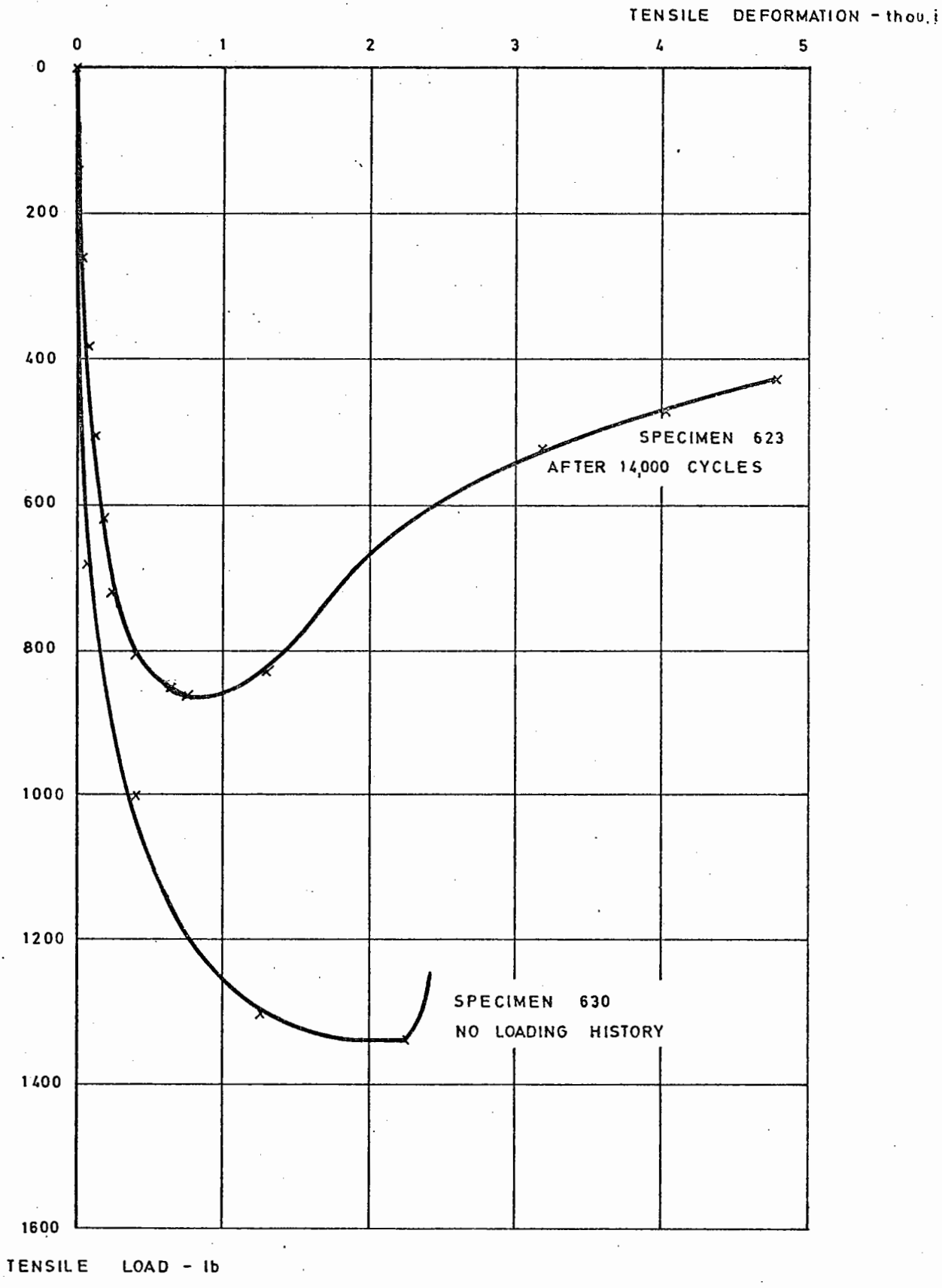

FIG. 131 DEFORMATION CHARACTERISTICS OF TYPICAL SPECIMENS OF DRY LEAN CONCRETE, WITH AND WITHOUT PREVIOUS LOADING HISTORY, LOADED TO FRACTURE

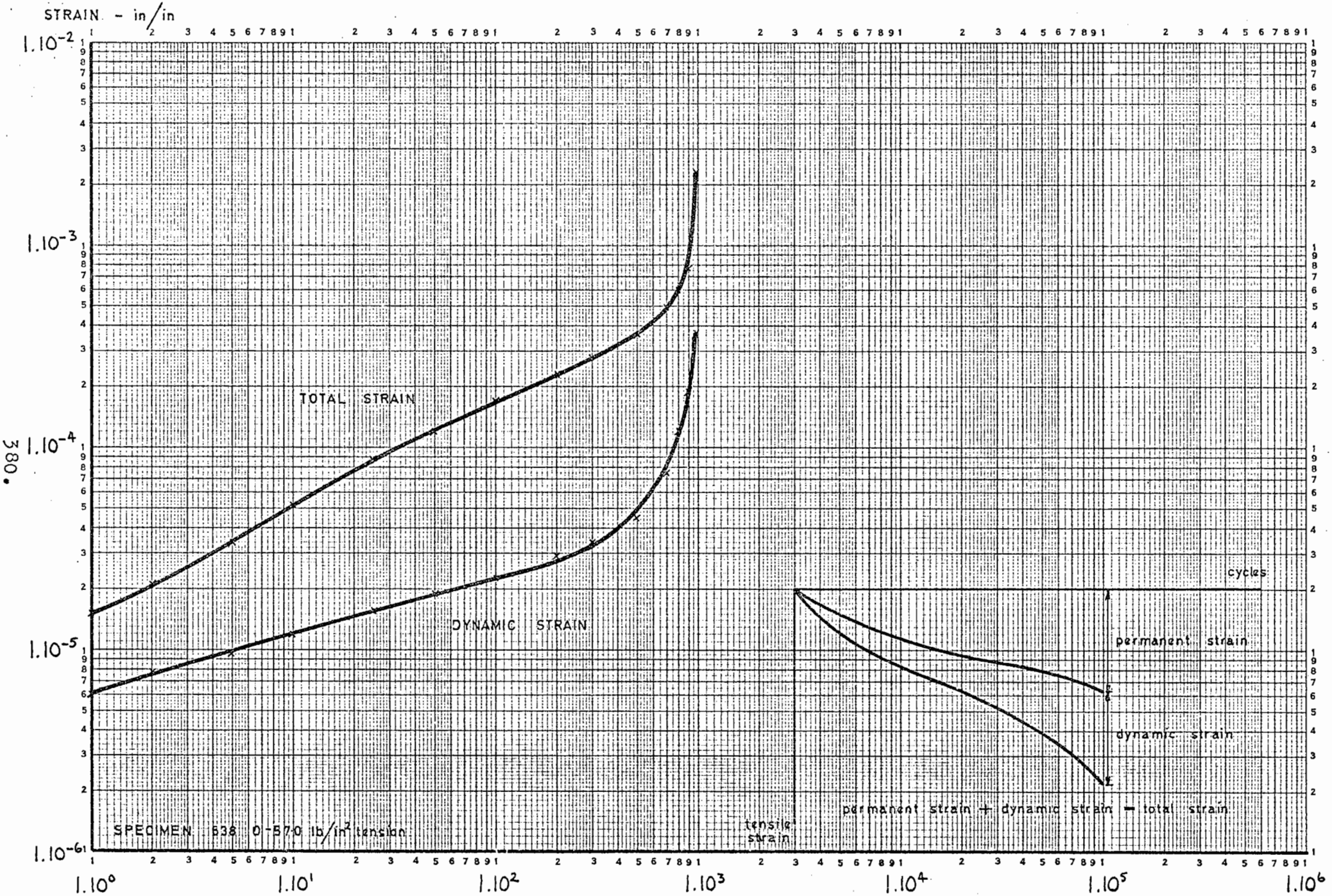

FIG. 132 STRAIN CURVES OF SPECIMEN OF DRY LEAN CONCRETE IN TENSILE STRESS-CONTROLLED REPEATED LOADING

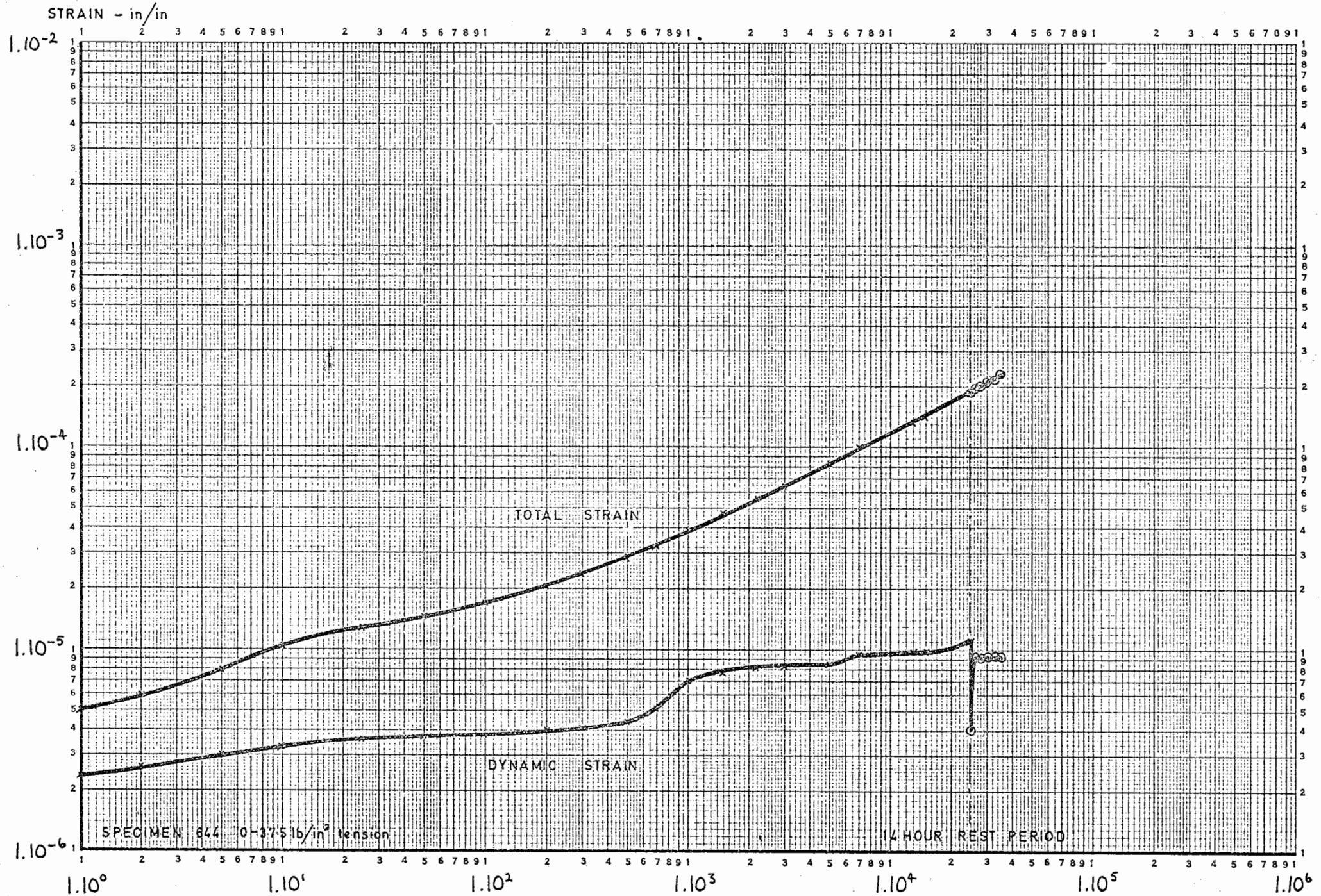

FIG. 133. STRAIN CURVES OF SPECIMEN OF DRY LEAN CONCRETE IN LOW TENSILE STRESS-CONTROLLED REPEATED LOADING

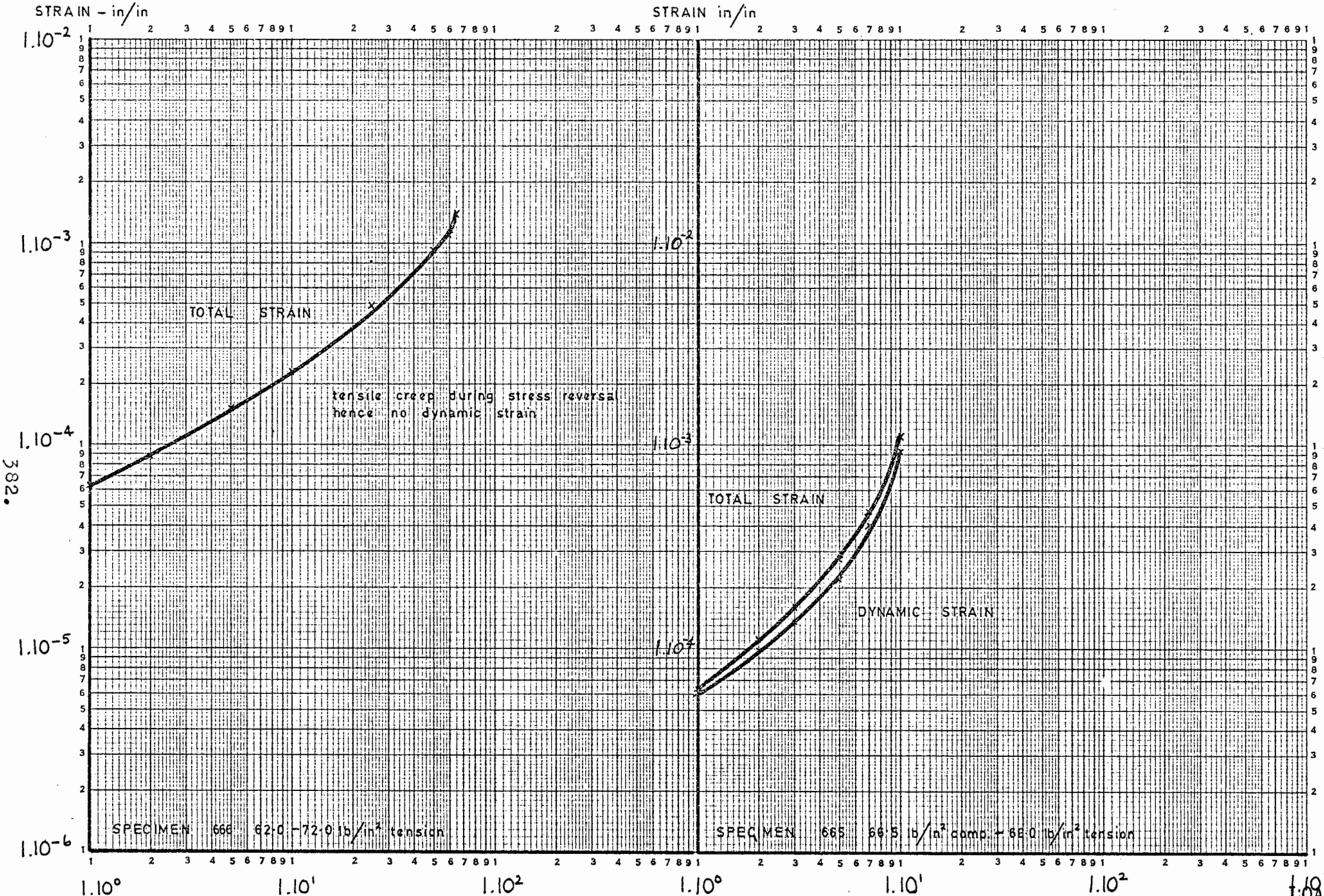

FIG. 134. STRAIN CURVES OF SPECIMEN OF DRY LEAN CONCRETE IN FLUCTUATING & ALTERNATING STRESS-CONTROLLED REPEATED

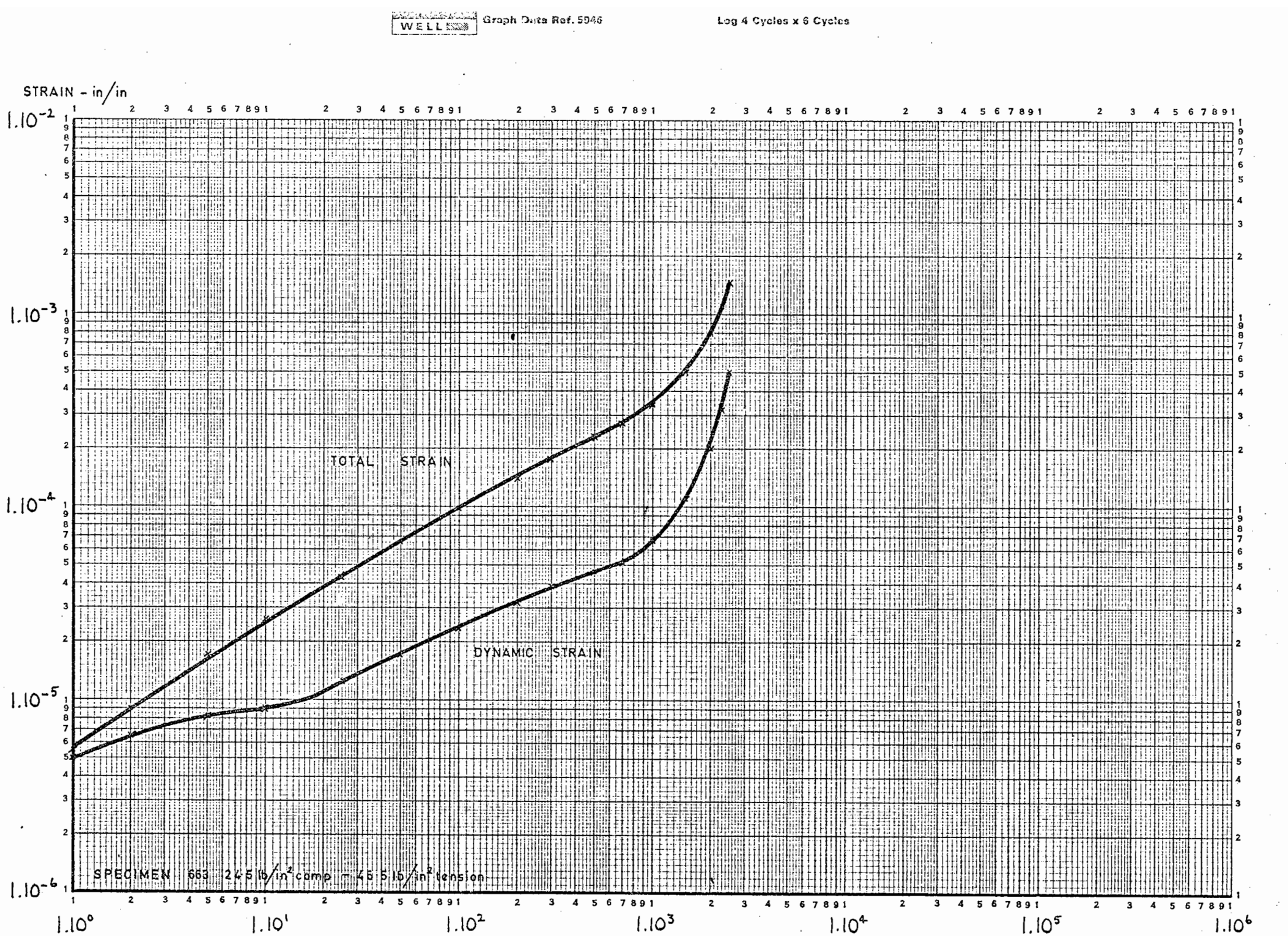

FIG. 135 STRAIN CURVES OF SPECIMEN OF DRY LEAN CONCRETE IN FLUCTUATING STRESS-CONTROLLED REPEATED LOADING

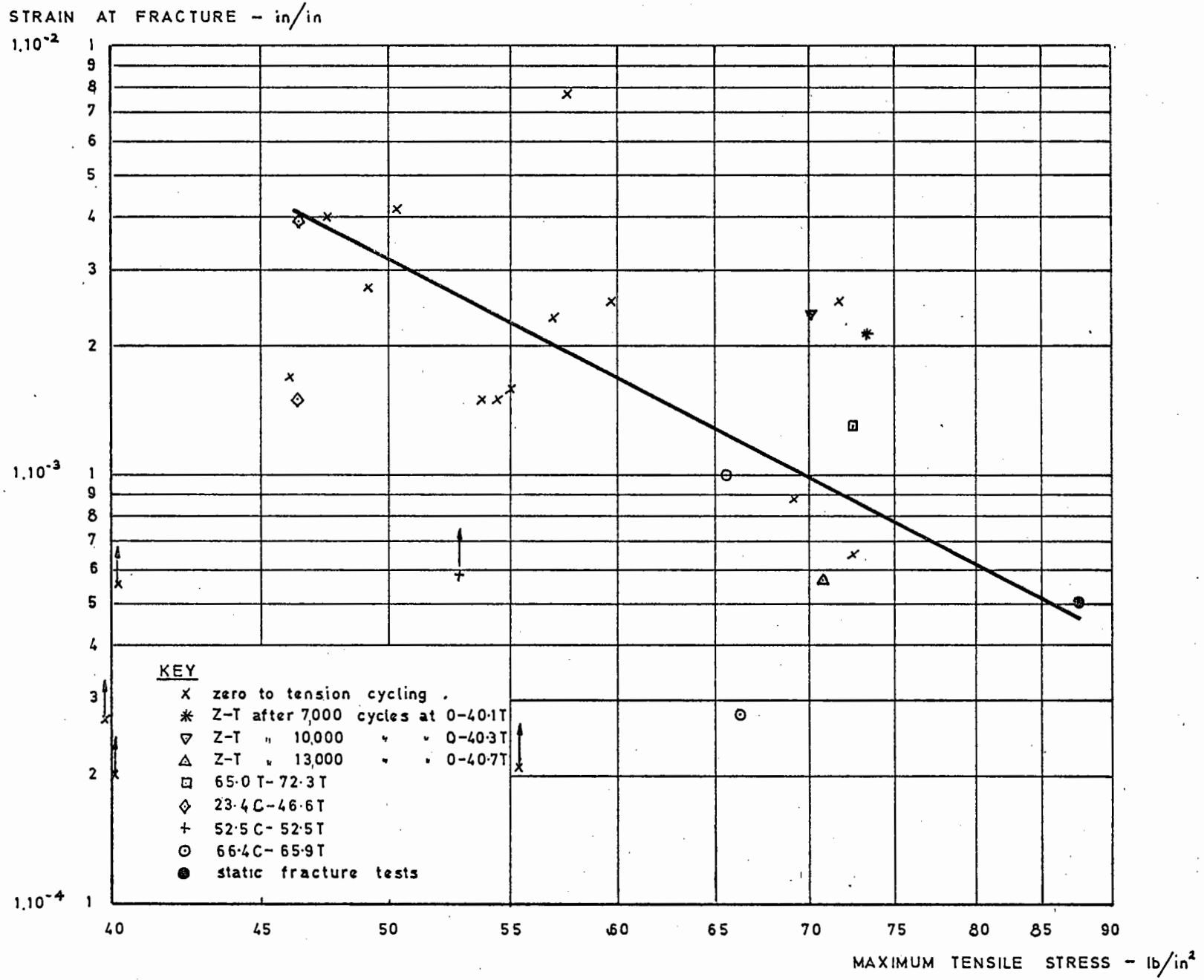

FIG. 136 FRACTURE STRAIN OF DRY LEAN CONCRETE AFTER ALL STRESS-CONTROLLED MODES OF REPEATED LOADING

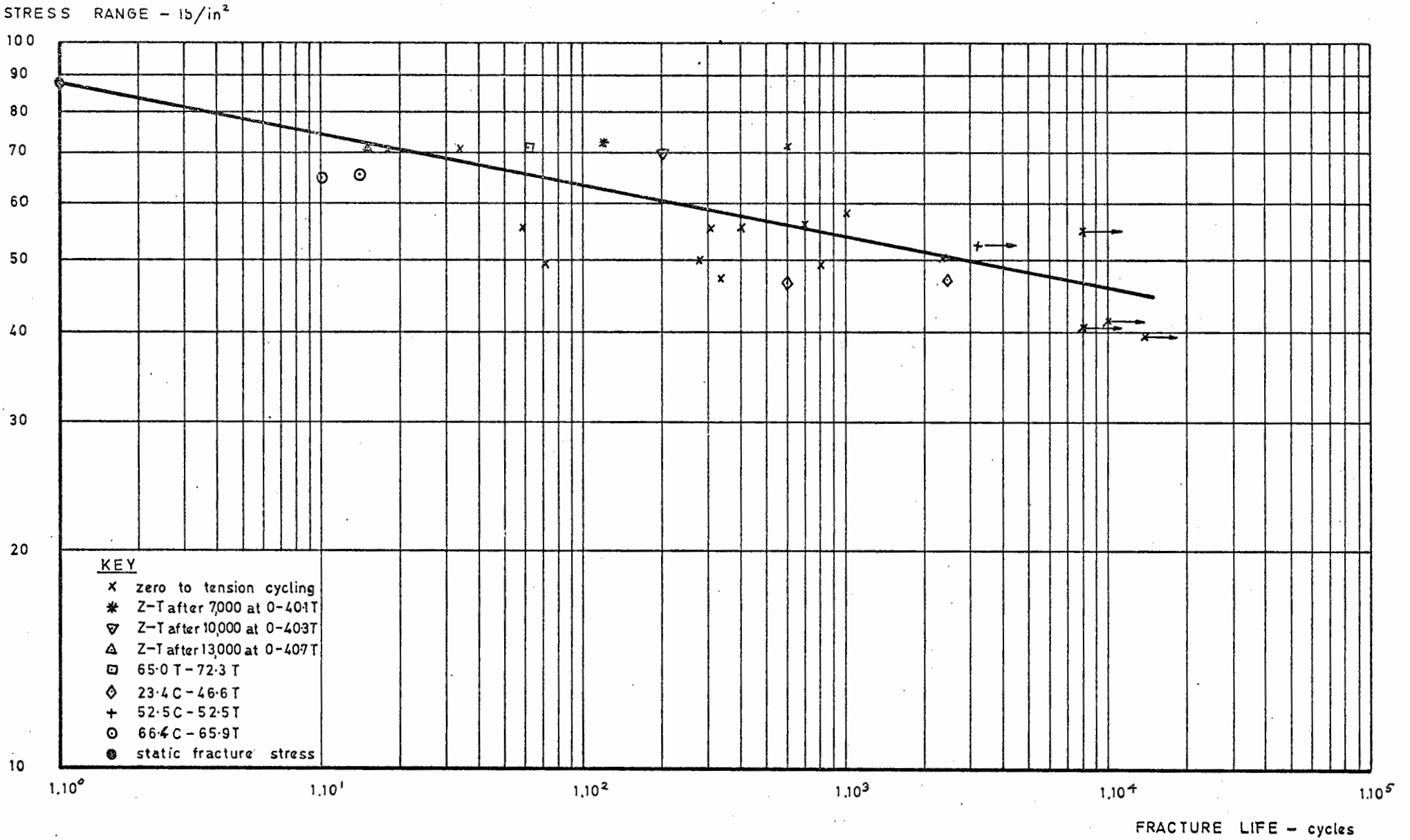

FIG. 137 FRACTURE LIFE OF DRY LEAN CONCRETE AFTER ALL STRESS-CONTROLLED MODES OF REPEATED LOADING

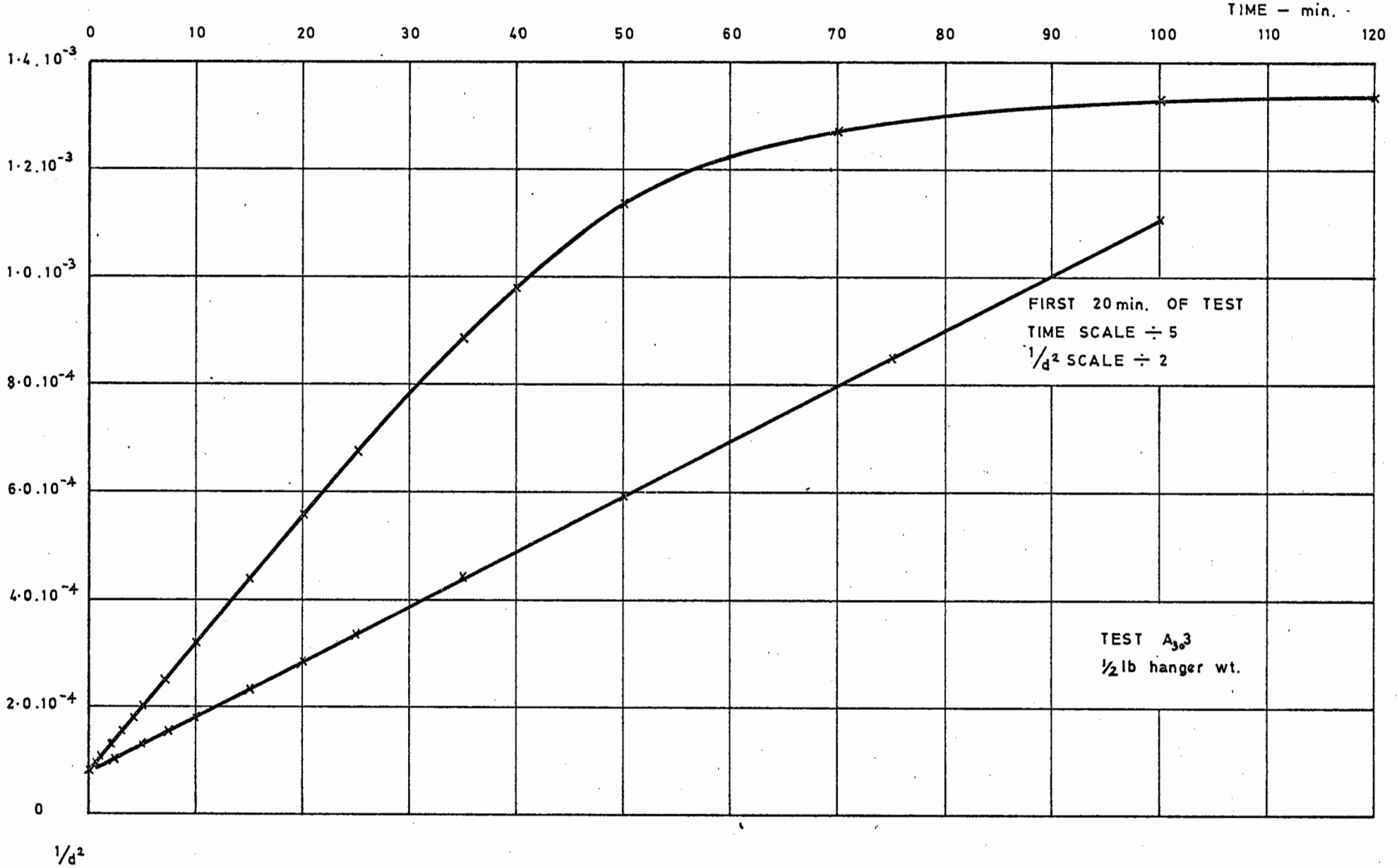

FIG. 138 PLATE SEPARATIONS OF PARALLEL PLATE VISCOMETER TEST ON 90/110 pen. BITUMEN AT +30° C

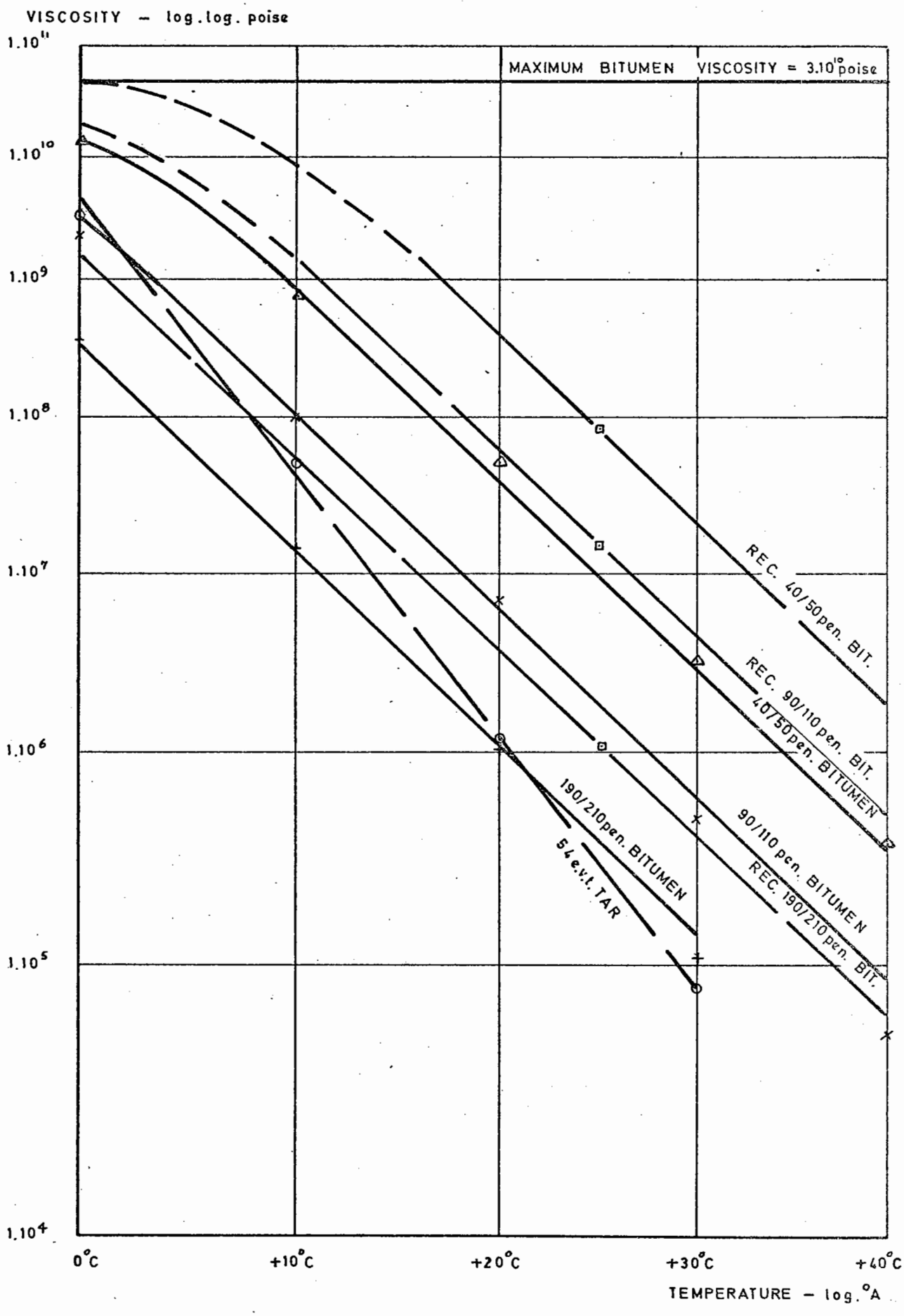

FIG. 139 MEASURED VISCOSITIES OF UNHEATED BINDERS AT 0°C to +40°C

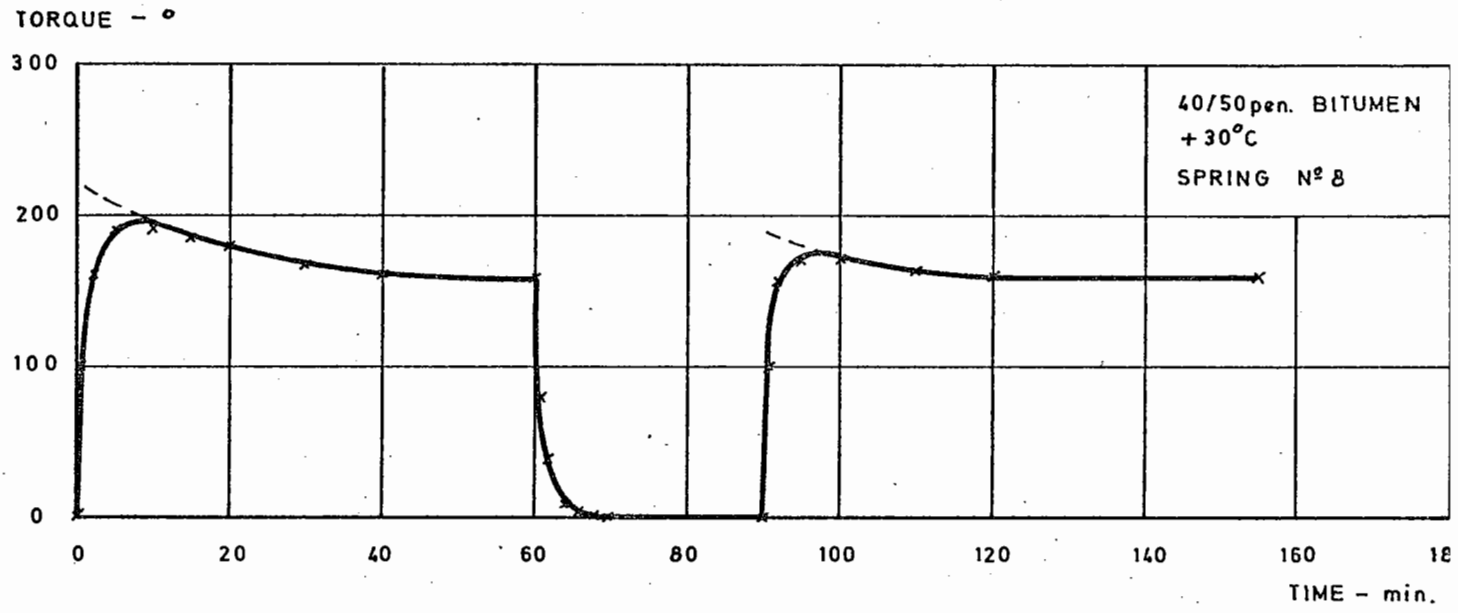

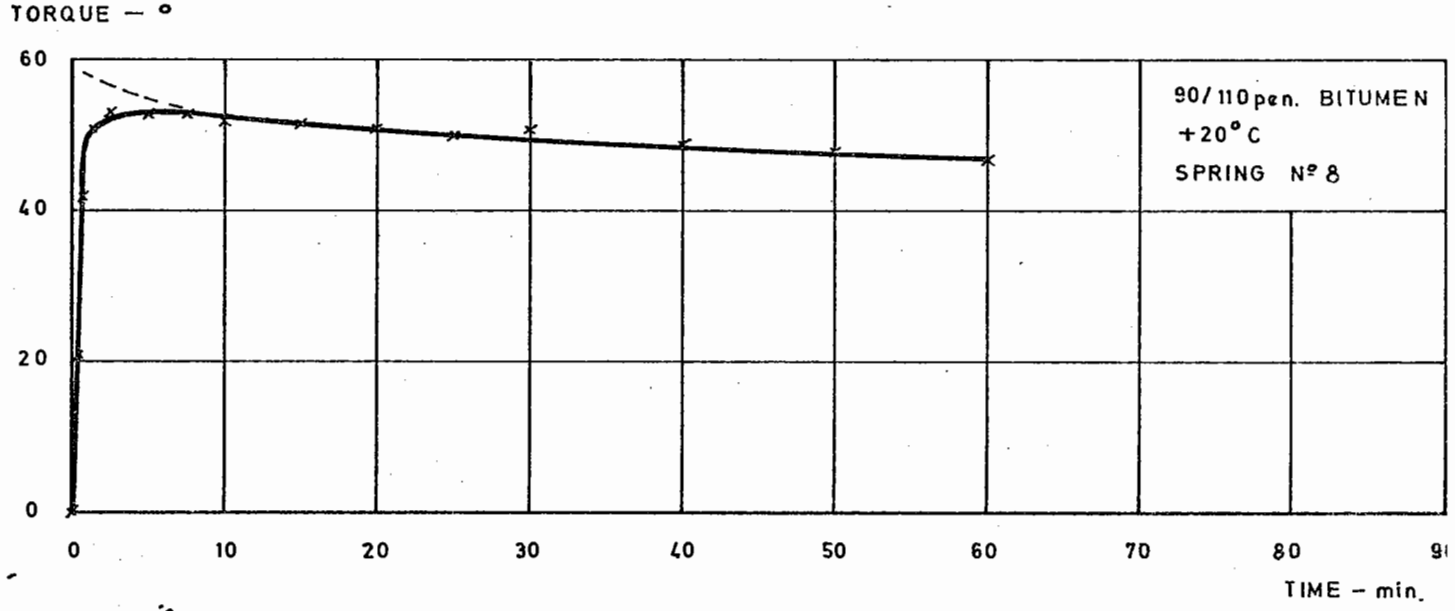

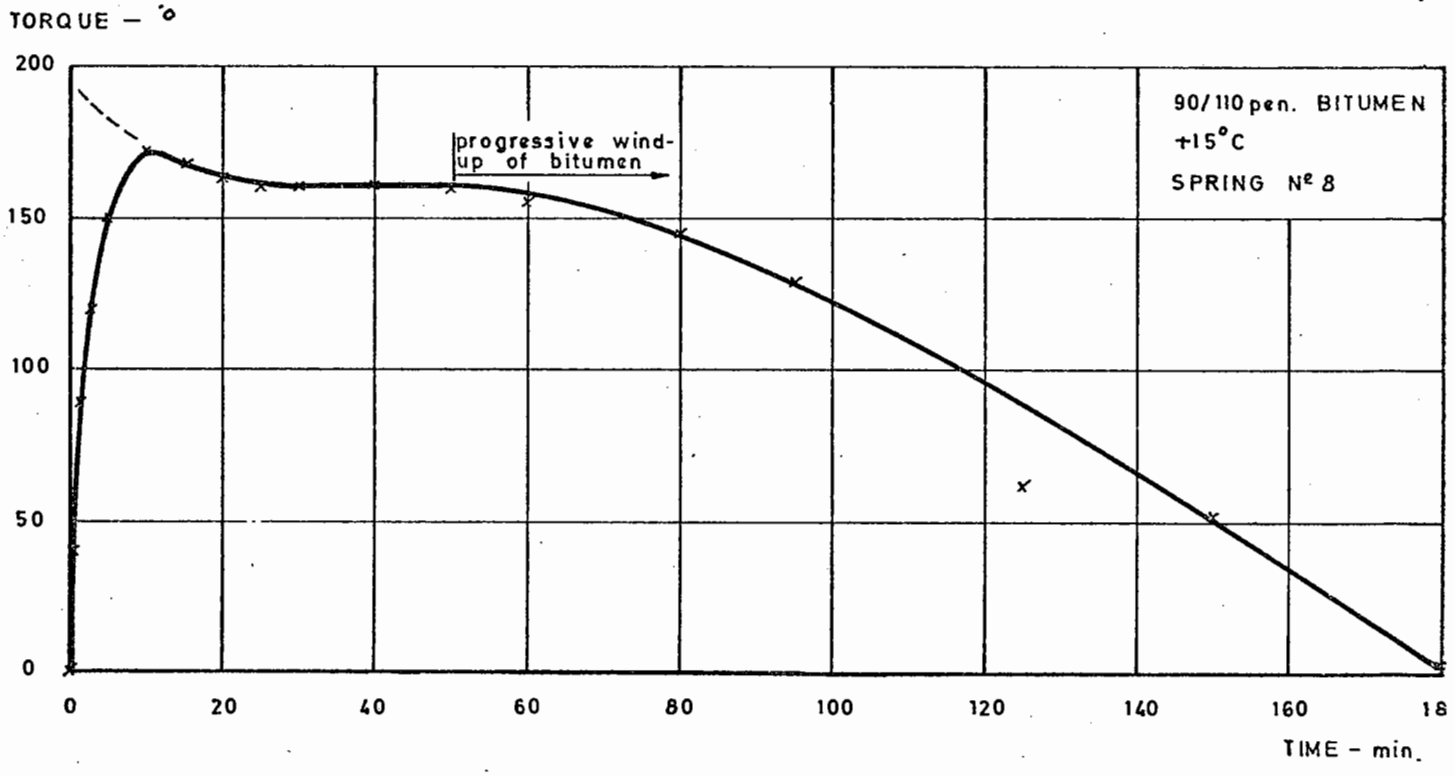

FIG. 140 TORQUE CURVES OF UNHEATED BITUMENS IN COAXIAL CYLINDER VISCOMETER

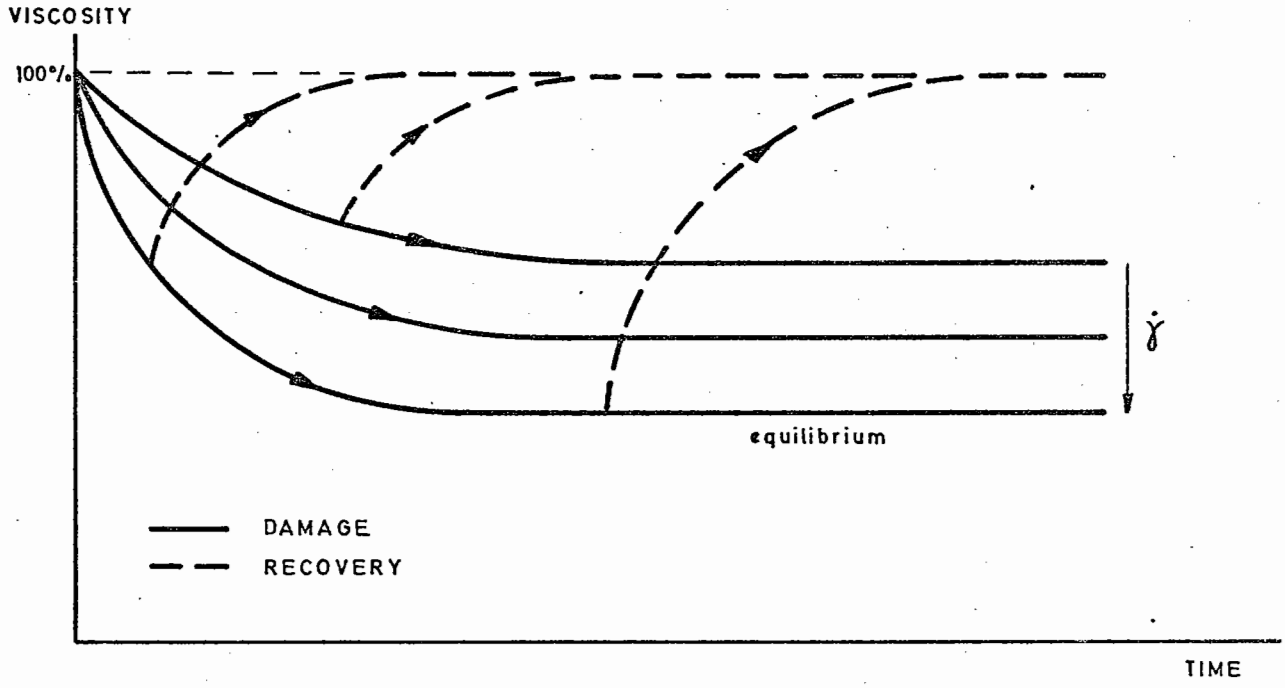

FIG. 141 ILLUSTRATION OF THIXOTROPY OF FLUID IN STEADY SHEAR after Wilkinson (98)

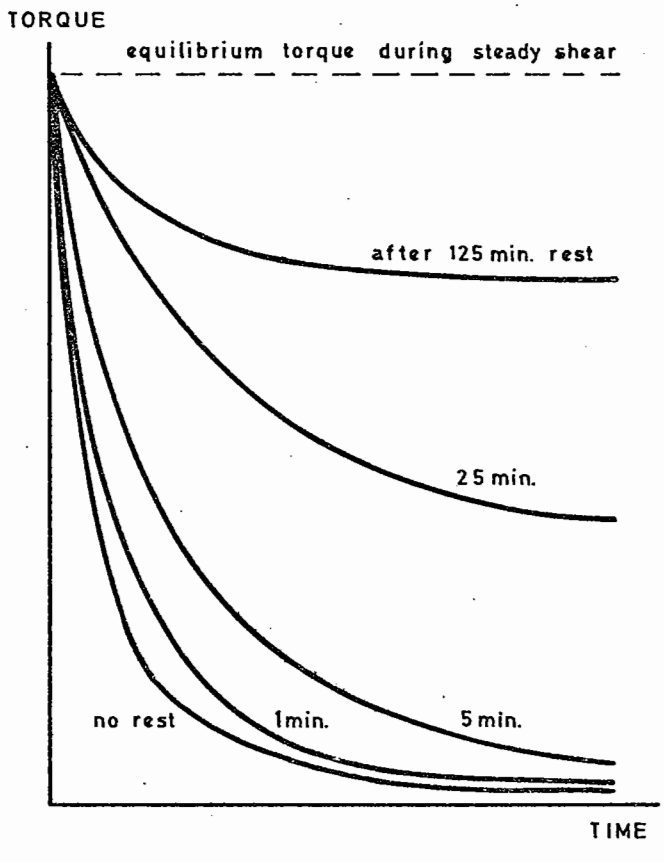

FIG. 142 THIXOTROPIC RECOVERY CURVES AFTER EQUILIBRIUM TORQUE IN STEADY SHEAR after Pryce Jones (221)

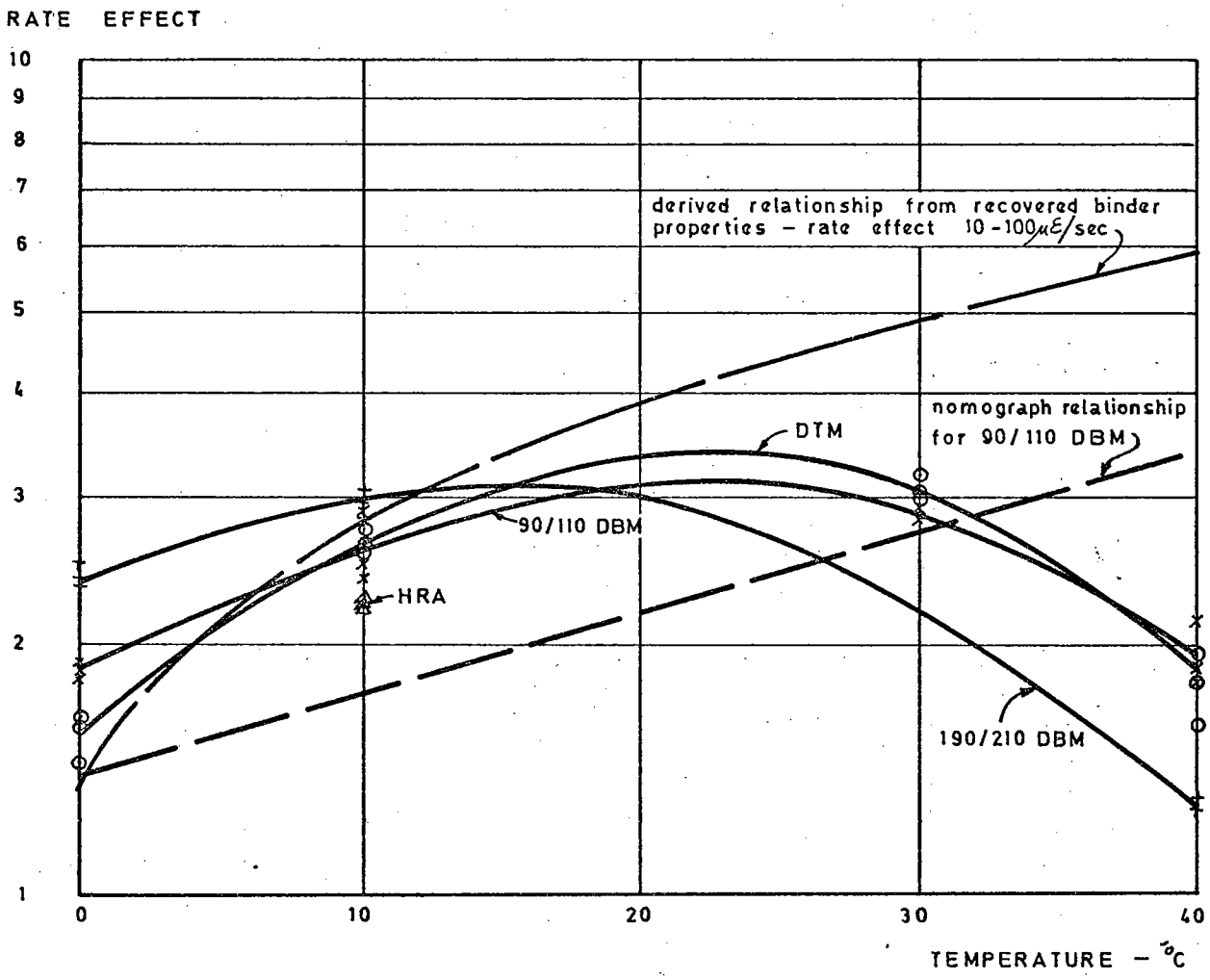

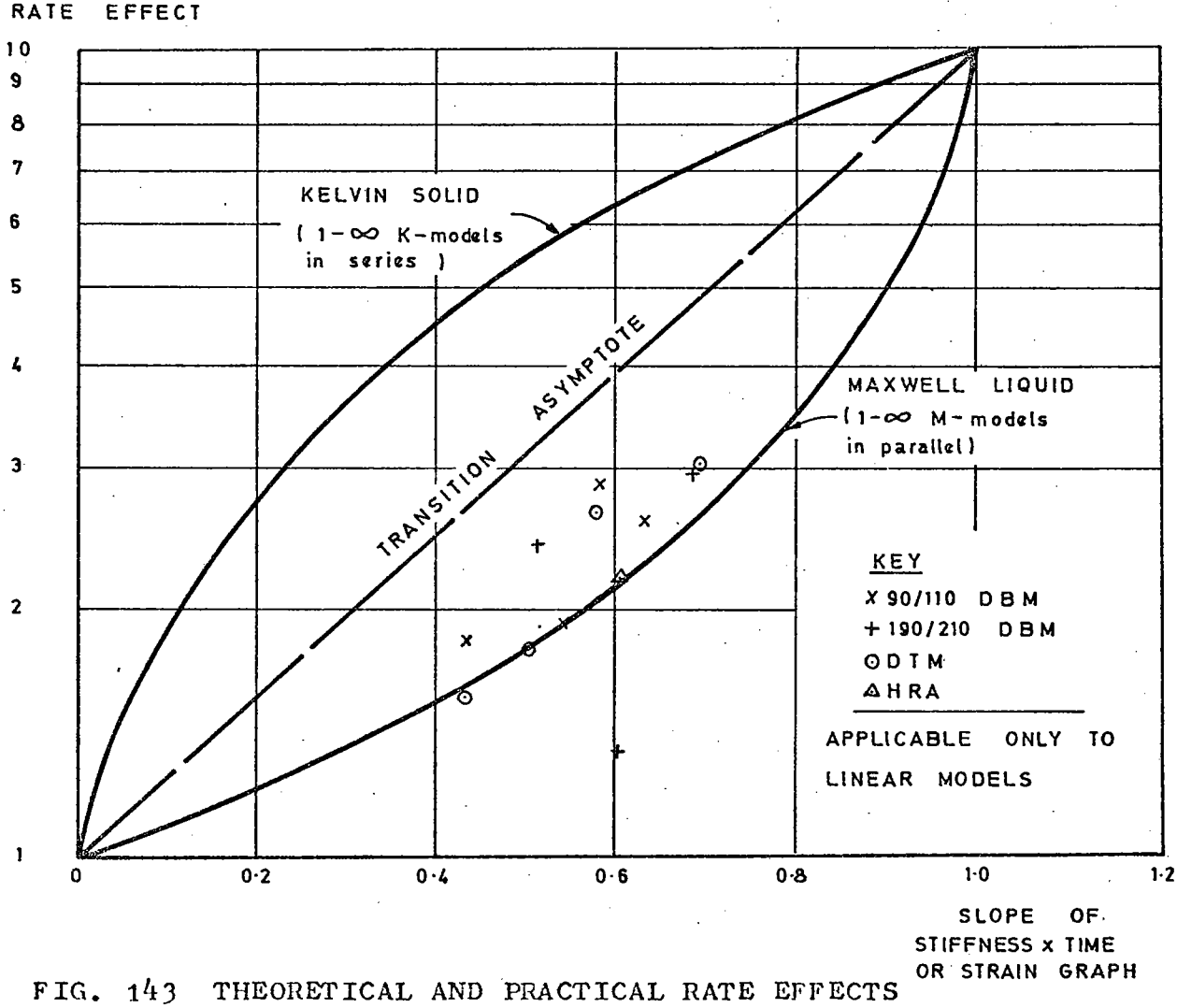

FIG. 143 THEORETICAL AND PRACTICAL RATE EFFECTS FOR BITUMINOUS MIXTURES

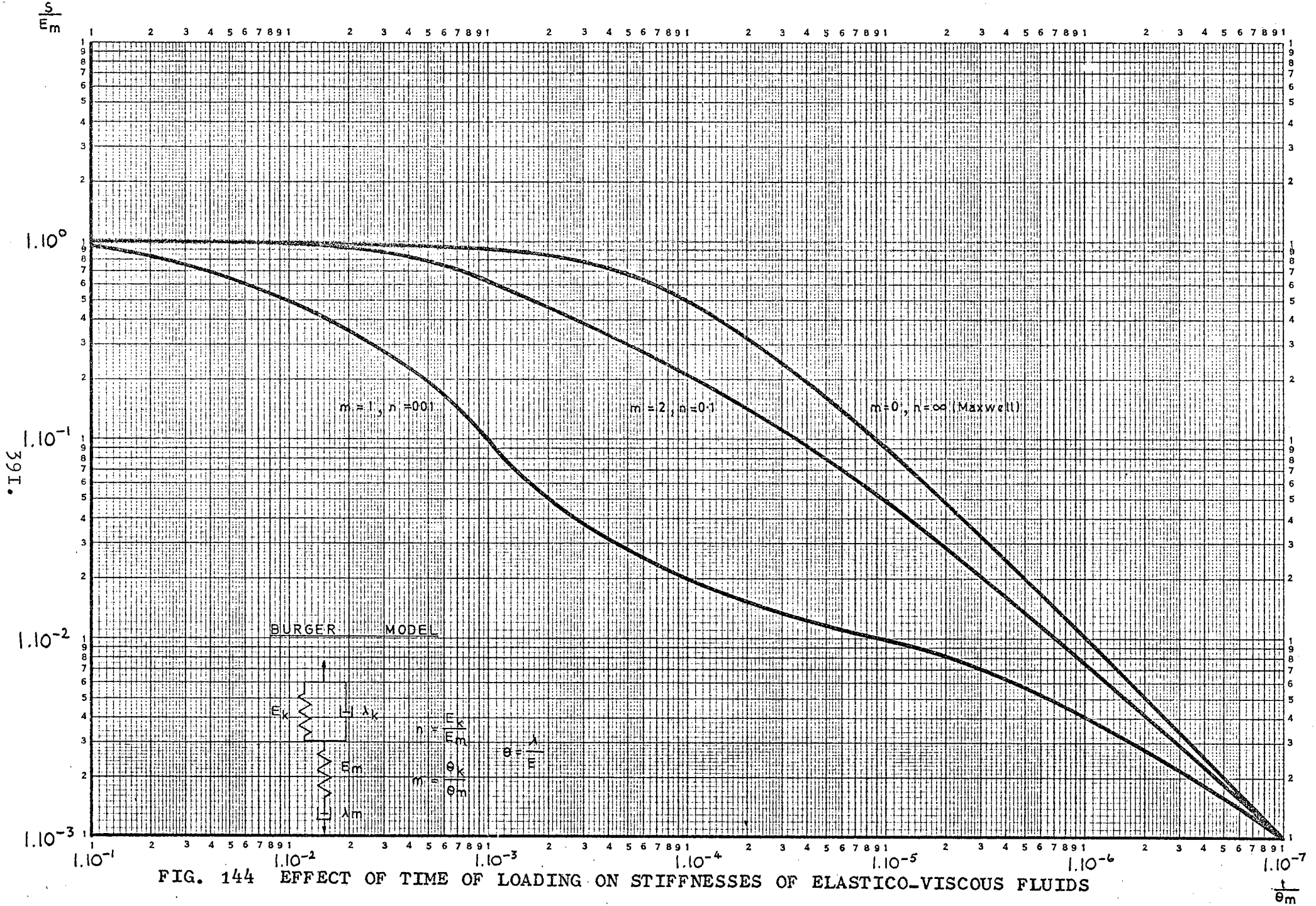

FIG. 144 EFFECT OF TIME OF LOADING ON STIFFNESSES OF ELASTICO-VISCOUS FLUIDS

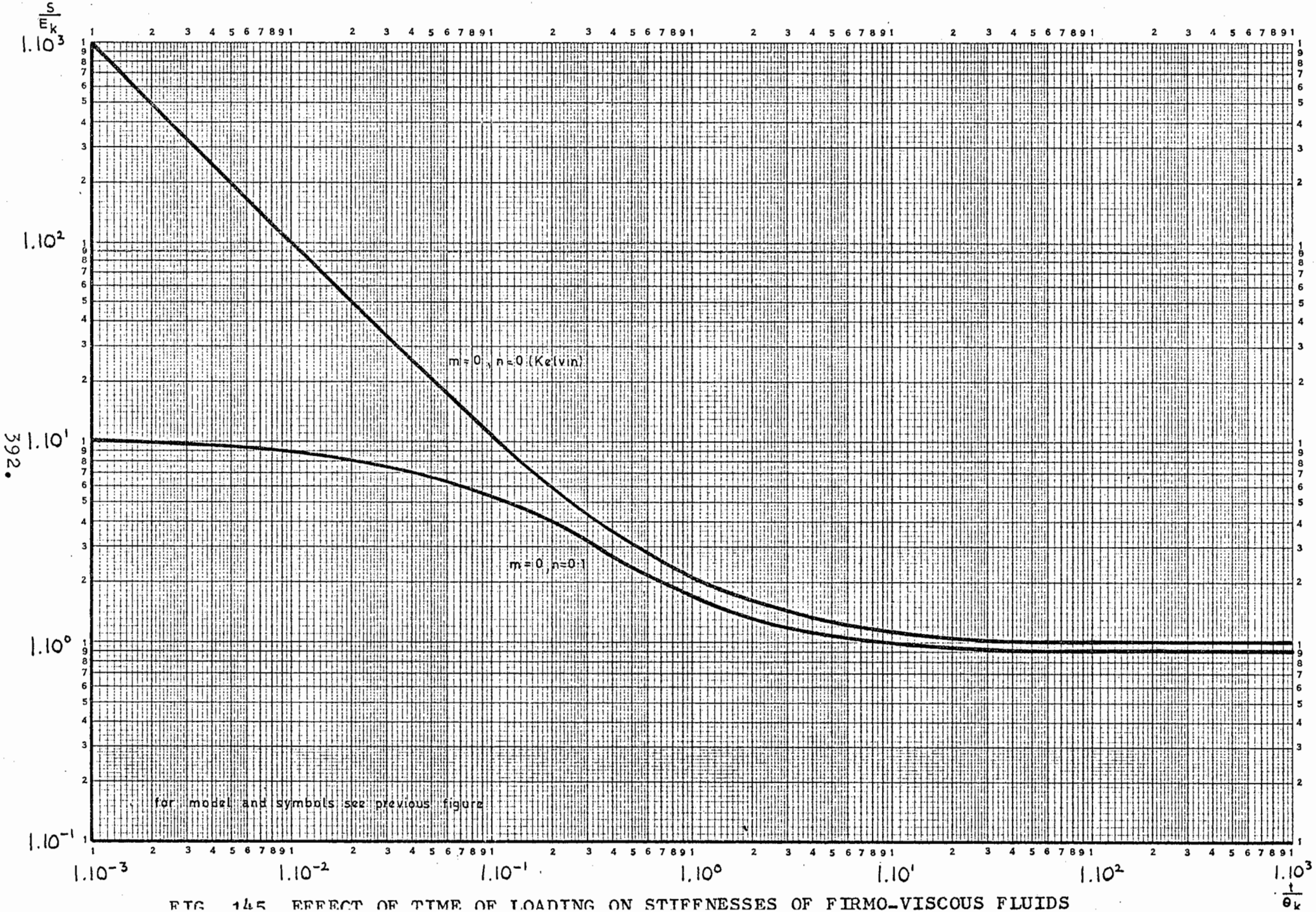

FIG. 145 EFFECT OF TIME OF LOADING ON STIFFNESSES OF FIRMO-VISCOUS FLUIDS

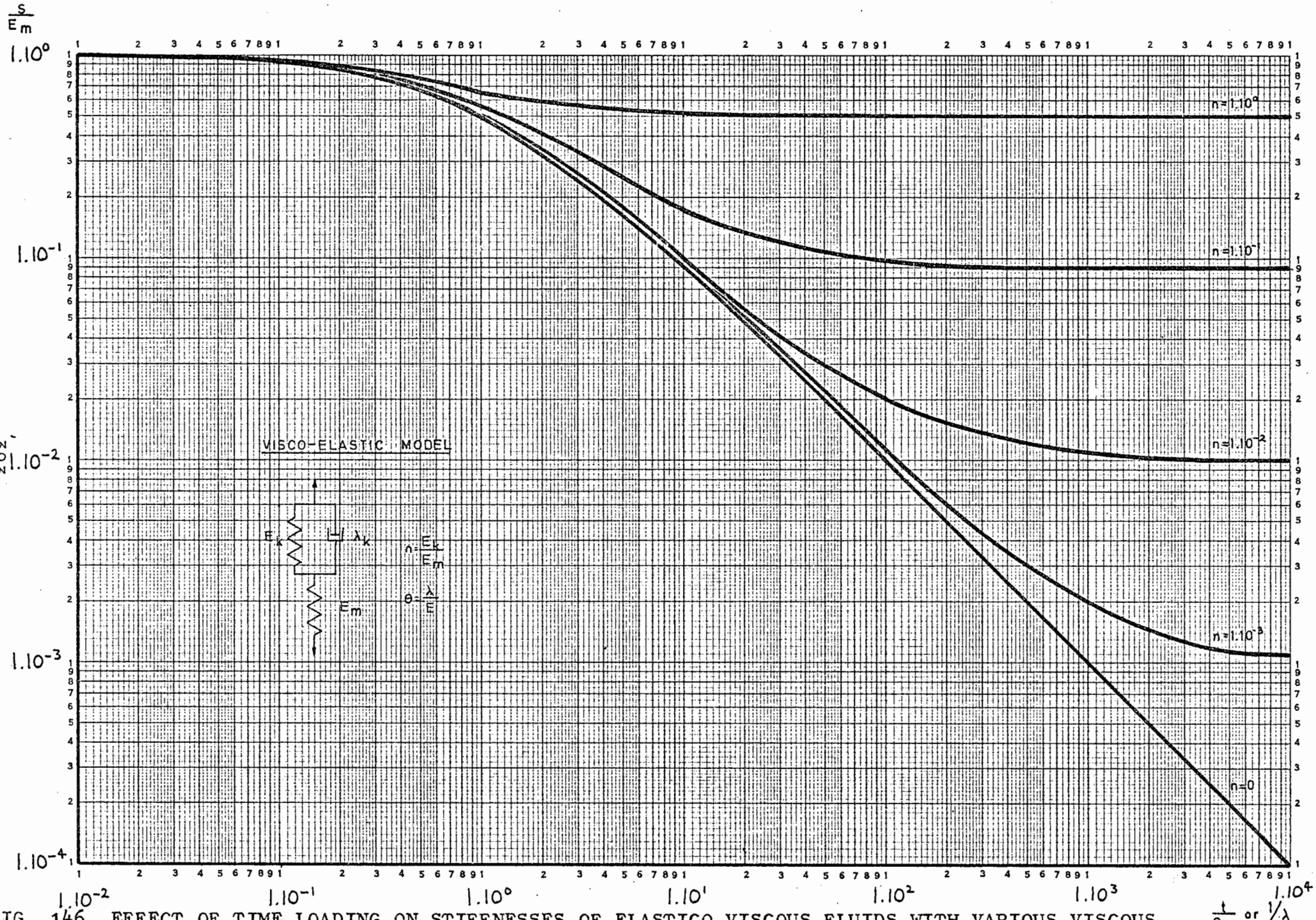

FIG. 146 EFFECT OF TIME LOADING ON STIFFNESSES OF ELASTICO-VISCOUS FLUIDS WITH VARIOUS VISCOUS COMPONENTS

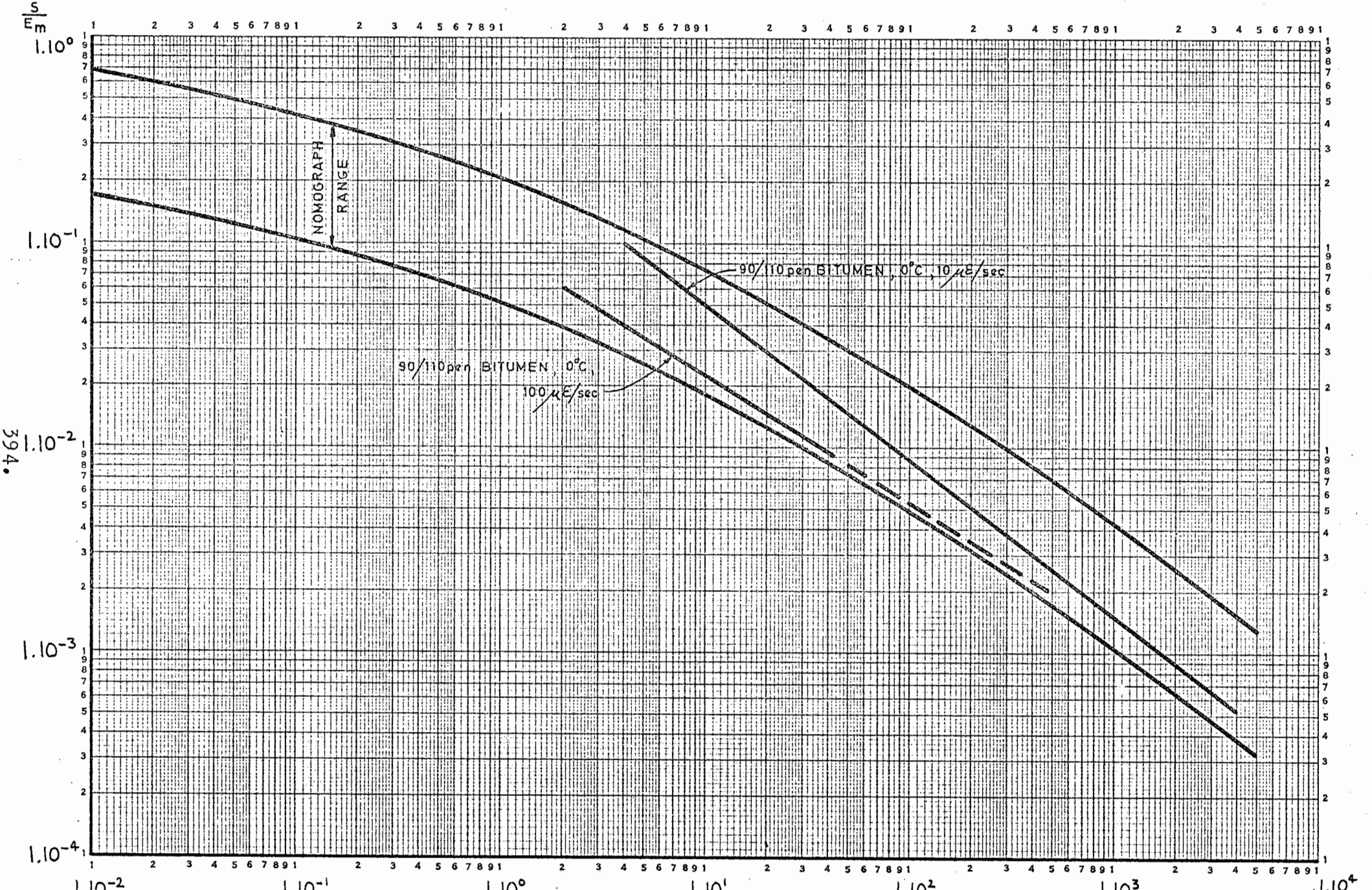

FIG. 147 NOMOGRAPH AND PRACTICAL EFFECT OF TIME OF LOADING ON STIFFNESS OF 90/110 pen. BITUMEN AT $\frac{t}{\theta_m}$ or $\frac{1}{\frac{\lambda}{\theta_m}}$

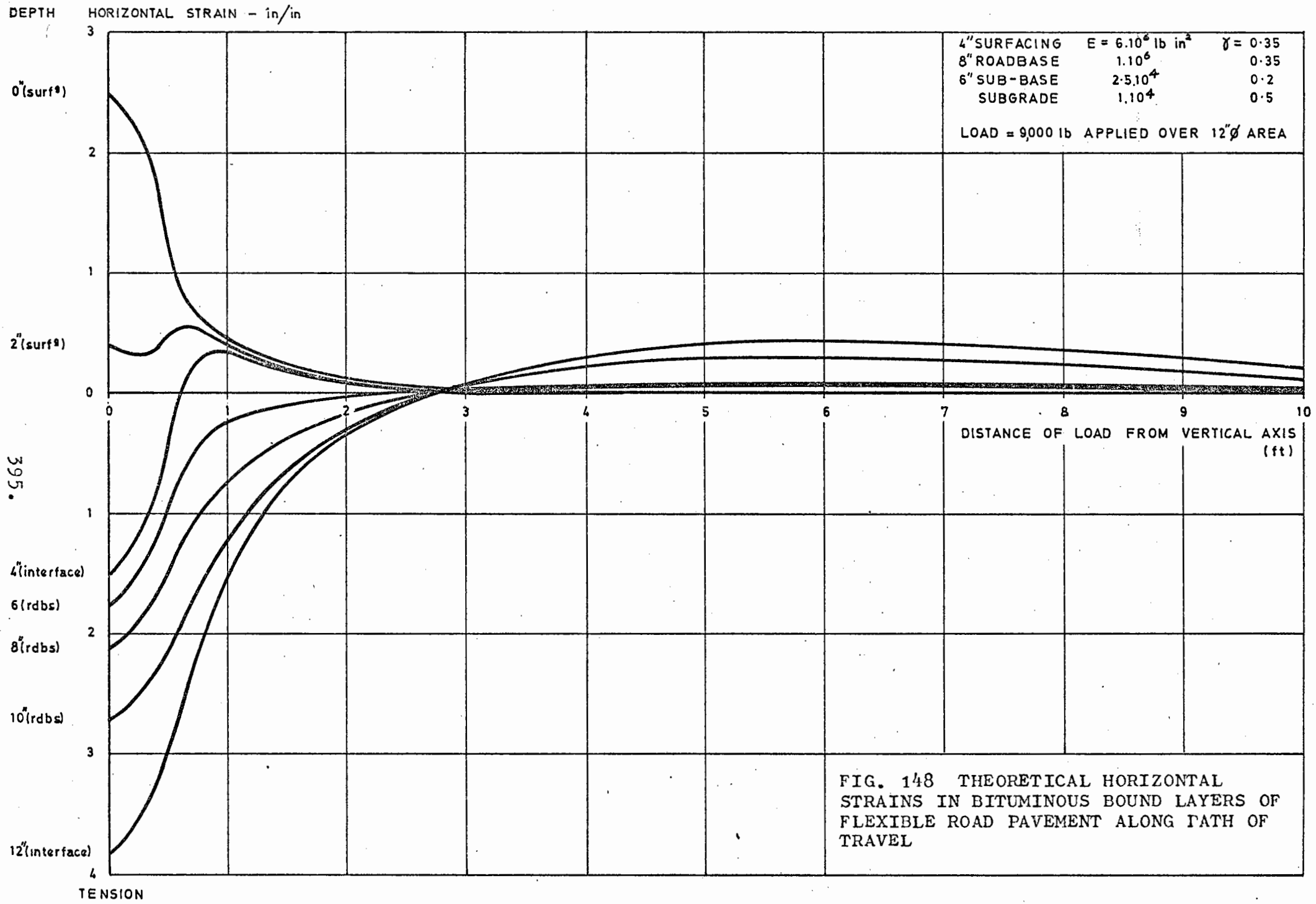

FIG. 148 THEORETICAL HORIZONTAL STRAINS IN BITUMINOUS BOUND LAYERS OF FLEXIBLE ROAD PAVEMENT ALONG PATH OF TRAVEL

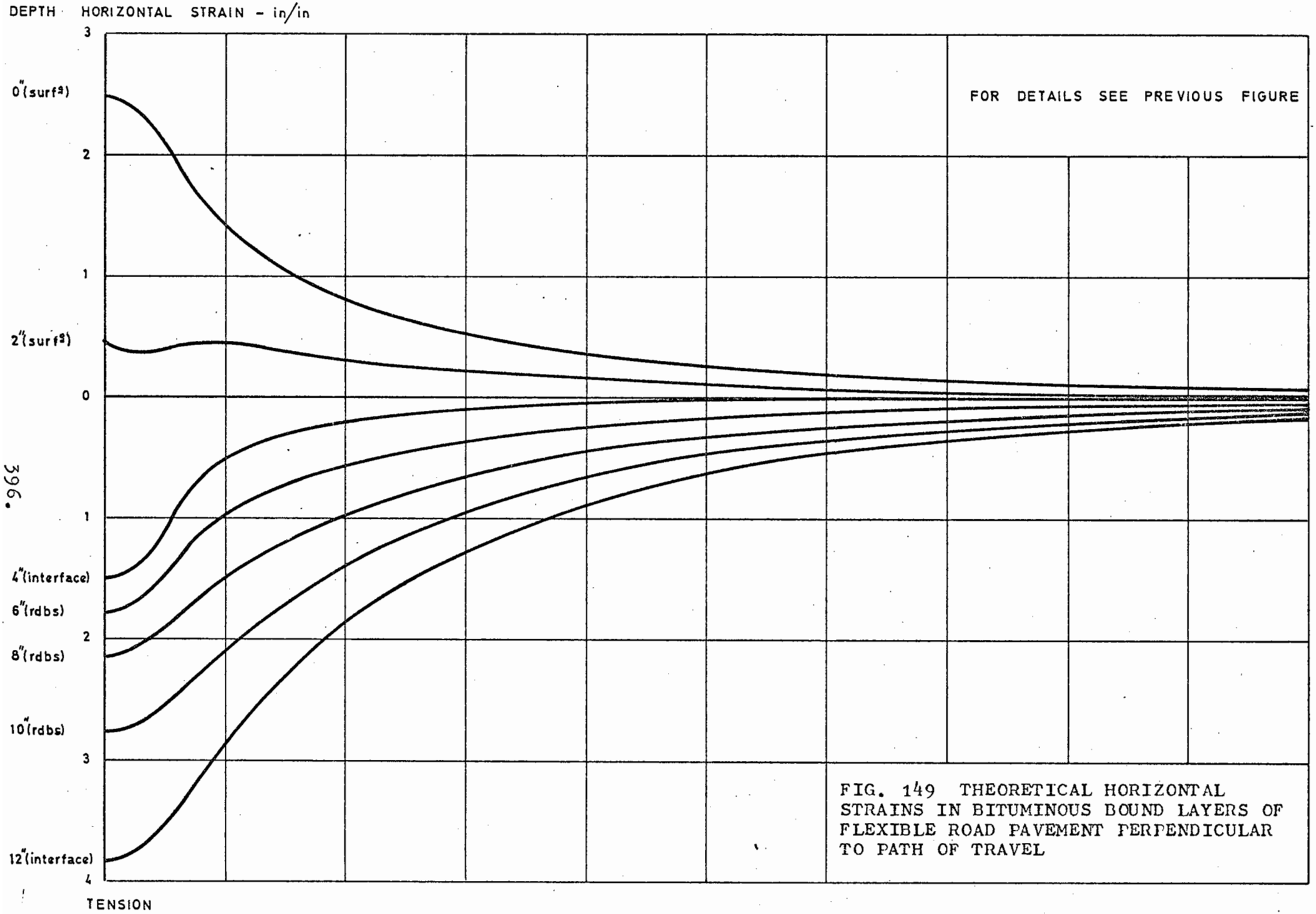

FIG. 149 THEORETICAL HORIZONTAL STRAINS IN BITUMINOUS BOUND LAYERS OF FLEXIBLE ROAD PAVEMENT PERPENDICULAR TO PATH OF TRAVEL

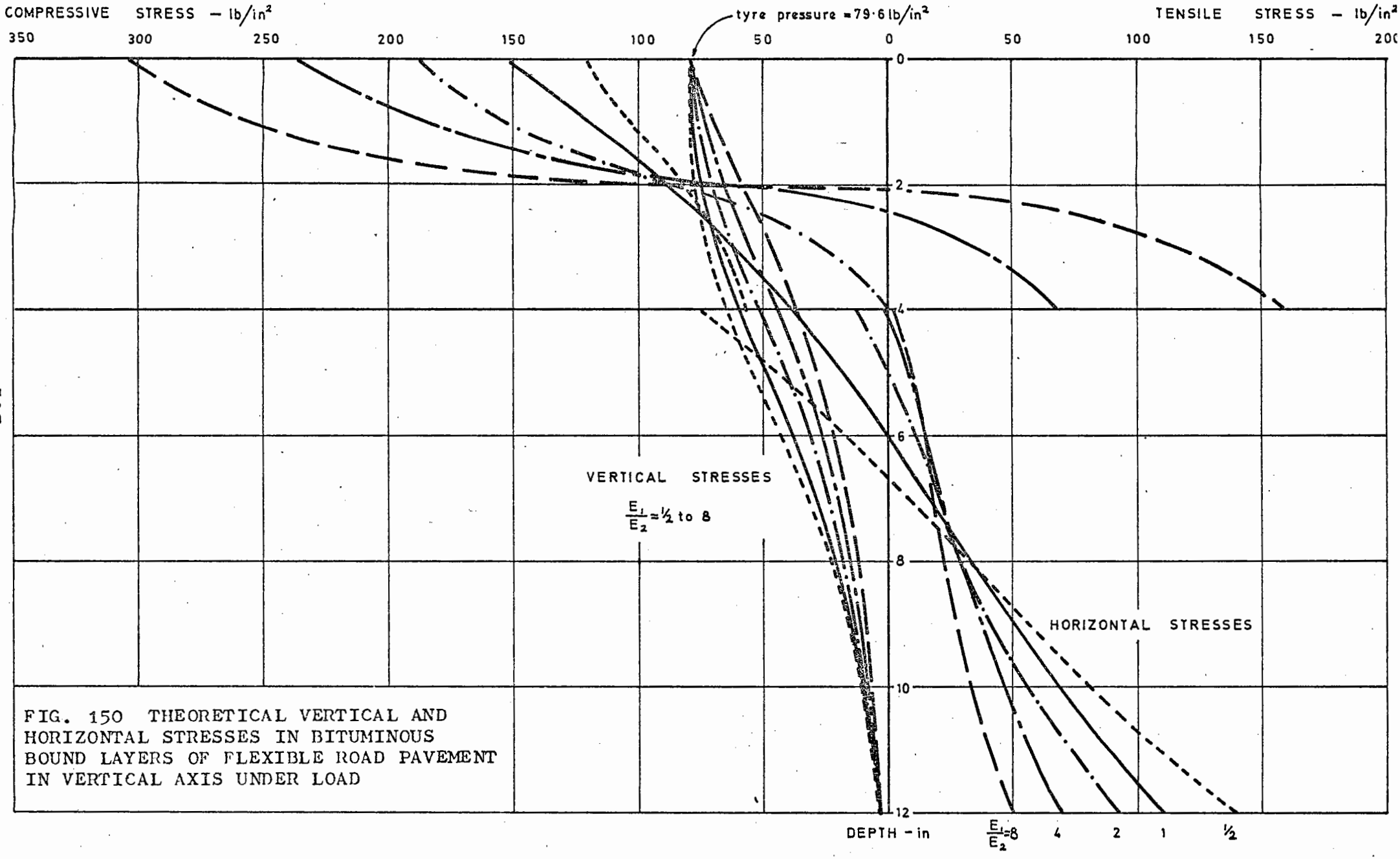

FIG. 150 THEORETICAL VERTICAL AND HORIZONTAL STRESSES IN BITUMINOUS BOUND LAYERS OF FLEXIBLE ROAD PAVEMENT IN VERTICAL AXIS UNDER LOAD

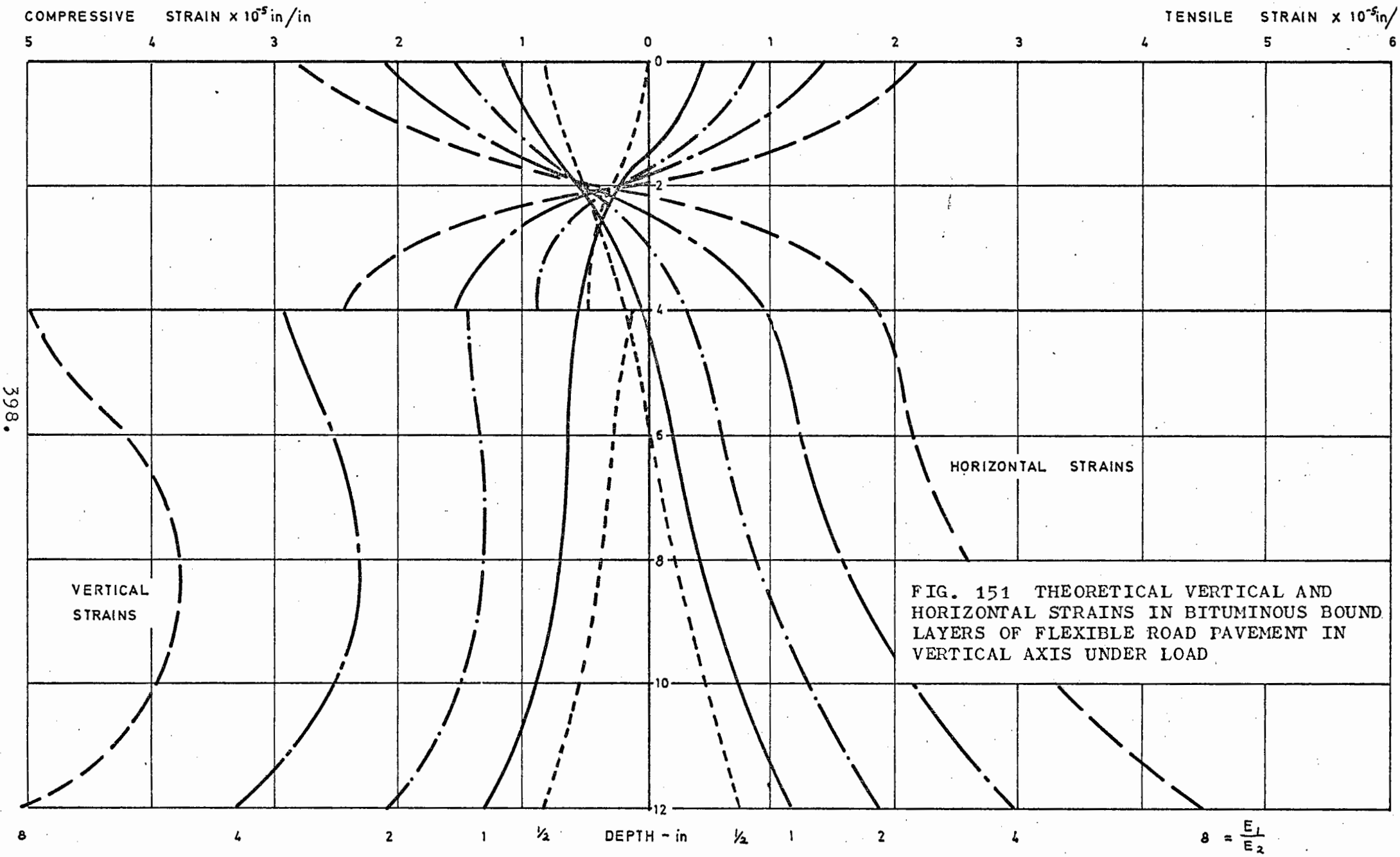

FIG. 151 THEORETICAL VERTICAL AND HORIZONTAL STRAINS IN BITUMINOUS BOUND LAYERS OF FLEXIBLE ROAD PAVEMENT IN VERTICAL AXIS UNDER LOAD

TABLES

TABLE 1 PARALLEL PLATE VISCOMETER DETAILS

a. Viscometer calibrations

b. Viscometer loadings

c. Recommended viscometer weights

TABLE 2 SPECIMEN MIXING DETAILS

TABLE 3 KEY TO SPECIMENS AND THEIR TESTING

TABLE 4 LOAD CELL CALIBRATION

a. Static tension with dead weights

b. Static compression with proving ring

c. Dynamic compression with proving ring

TABLE 5 SPECIFIC GRAVITIES OF AGGREGATES AND BINDERS

TABLE 6 DRY LEAN CONCRETE CUBE STRENGTHS

TABLE 7 DRYING OUT OF DRY LEAN CONCRETE SPECIMENS

TABLE 8 BALLOTINI WEIGHTS WHEN MEASURING SPECIMEN END VOIDS BY DIFFERENT METHODS

TABLE 9 SPECIMEN MOULD LENGTHS

TABLE 10 TYPICAL VOID DETERMINATIONS FOR BATCH OF BITUMINOUS SPECIMENS

TABLE 11 SPECIMEN VOIDS

a. 90/110 Dense bitumen macadam

b. 190/210 Dense bitumen macadam

c. Dense tar macadam

d. Hot rolled asphalt

e. Dry lean concrete

TABLE 12 SLOPES AND RATE EFFECTS FROM STIFFNESS MEASUREMENT TESTS ON BITUMINOUS SPECIMENS

TABLE 13 BEST FIT LINE VALUES FROM STIFFNESS AND REPEATED LOADING TESTS ON BITUMINOUS SPECIMENS

TABLE 14 TRENDS IN SHAPES OF LOAD AND DEFORMATION RECORDS DURING REPEATED LOADING TESTS ON BITUMINOUS SPECIMENS

TABLE 15 RESULTS FROM DRY LEAN CONCRETE SPECIMENS

a. Static ultimate strengths after strain-controlled repeated loading

b. Fracture lives and strains after stress-controlled repeated loading (specimens tested wet)

TABLE 16 VISCOSITY RESULTS FROM HIGH TEMPERATURE PARALLEL PLATE VISCOMETER TESTS ON 90/110 pen. BITUMEN

a. Unheated binder at +30°C

b. Unheated binder at +40°C

TABLE 17 PARALLEL PLATE VISCOMETER TEST RESULTS

a. 90/110 pen. bitumen

b. 190/210 pen. bitumen

c. 40/50 pen. bitumen

d. 54 e.v.t. tar

e. Recovered bitumens

TABLE 18 RESULTS OF STANDARD TESTS ON BINDERS

a. Bitumens

b. Tar

TABLE 19 RECOVERY OF STIFFNESS OF BITUMINOUS SPECIMENS DURING REST PERIOD AFTER STRAIN-CONTROLLED REPEATED LOADING

TABLE 20 DETAILS OF LAYERED SYSTEMS STUDIED IN THEORETICAL ANALYSIS

TABLE 21 REITERATIONS OF THEORETICAL STRAINS IN ROADBASE MATERIALS USING MULTI-LAYER THEORY

TABLE 22 SUMMARY OF RESULTS OF THEORETICAL ANALYSIS

TABLE 1

PARALLEL PLATE VISCOMETER DETAILS

a) Viscometer calibrations

Detail	Viscometer 1	Viscometer 2
Weight of disc and plunger less friction	121 gm	117 gm
Weight loading ball	67	67
Weight spacer	2	2
Force of dial gauge return spring	66	66
TOTAL STATIC WEIGHT	256 gm	252 gm
Plate separation $\frac{1}{8}$" nominal spacing	116 thou.in.	115 thou.in.
Plate separation $\frac{1}{16}$" nominal spacing	56 thou.in.	55 thou.in.

b) Viscometer loadings

Hanger Weight	Direct Wt. (nominal)	Extra Wt. on Disc	Total Loading Viscometer 1	Total Loading Viscometer 2
100 lb	-	500 kg	500 kg	500 kg
50	-	250	250	250
20	-	100	100.3	100.3
10	-	50	50.25	50.25
5	-	25	25.25	25.25
2	-	10	10.25	10.25
1	-	5	5.25	5.25
$\frac{1}{2}$	-	2.5	2.76	2.75
$\frac{1}{4}$	-	1.248	1.504	1.500
-	1 kg	0.987	1.243	1.239
-	$\frac{1}{2}$	0.505	0.761	0.757
-	$\frac{1}{4}$	0.252	0.508	0.504
-	none	none	0.256	0.252

TABLE 1 (contd.)

c) Recommended viscometer weights

Loading for 1 hour with $\frac{1}{8}$" initial plate separation

Predicted viscosity range (poise)	Additional loading
1.10^5 - 2.10^5	no additional load
2.10^5 - 3.10^5	$\frac{1}{4}$ kg direct weight
3.10^5 - 5.10^5	$\frac{1}{2}$ kg " "
5.10^5 - 1.10^6	1 kg " "
1.10^6 - 2.10^6	$\frac{1}{2}$ lb hanger weight
2.10^6 - 4.10^6	1 lb " "
4.10^6 - 1.10^7	2 lb " "
1.10^7 - 2.10^7	5 lb " "
2.10^7 - 4.10^7	10 lb " "
4.10^7 - 1.10^8	20 lb " "
1.10^8 - 2.10^8	50 lb " "
2.10^8 - 4.10^8	100 lb " "
4.10^8 and above	100 lb with extra time

TABLE 2

SPECIMEN MIXING DETAILS

Item	90/110 Dense Bitumen Macadam	190/210 Dense Bitumen Macadam	Dense Tar Macadam	Hot Rolled Asphalt	Dry Lean Concrete
%age passing					
1" sieve	100	100	100	100	100
¾"	83	83	83	98½	100
½"	68	68	68	52	76
⅜"	60	60	60	40	60
3/16"	45	45	45	32	40
No. 7	35	35	35	31	33
14	27	27	27	28½	26
25	21	21	21	26	19
52	15	15	15	8½	4
100	10	10	10	2	0

/contd.

TABLE 2 (contd.)

Item	90/110 Dense Bitumen Macadam	190/210 Dense Bitumen Macadam	Dense Tar Macadam	Hot Rolled Asphalt	Dry Lean Concrete
Stone type	Cr. Granite	Cr. Granite	Cr. Granite	Cr. Granite	Cr. Gravel
Sand type	Cr. Granite	Cr. Granite	Cr. Granite	Cr. Gravel	Cr. Gravel
Binder type	90/110 pen.	190/210 pen.	54 e.v.t. "B"	40/50 pen.	O.P.C.
Binder content by wt.	4%	4%	4.55%	5.7%	agg:cem=15:1 w/c=0.8:1
Agg. temp.	175°C	160°C	125°C	180°C (oven max.)	-
Binder temp.	150°C	135°C	100°C	165°C	-

TABLE 3

KEY TO SPECIMENS AND THEIR TESTING

Specimen	Material	Compaction	Special features	Test temp.	Test control	Frequency control	Purpose of test
1	HRA	Three layer	None	Room	X'hd	None	Exploratory studies
2-4	HRA	"	"	"	Load	"	- old machine
5-7	HRA	"	"	"	X'hd	"	" "
8-9	HRA	"	"	"	Load	"	" "
10-16	HRA	"	"	"	"	"	ditto - new machine 1 LVDT, x-y plotter
17,18	HRA	"	"	"	"	"	ditto - new machine 1 LVDT Dig. Volt.
19-22	HRA	"	"	+20°C	"	"	ditto
23-28	90/110 DBM	"	"	"	"	"	ditto
29-32	90/110 DBM	"	"	+10°C	"	"	ditto
33	"	"	"	"	X'hd	"	ditto
34	"	"	"	"	Extn	"	ditto
35-40	"	"	"	"	"	"	ditto - twin LVDT
41-46	"	"	Compn. method varies	"	"	Cones	Compaction study

/contd.

TABLE 3 (contd.)

Specimen	Material	Compaction	Special features	Test temp.	Test control	Frequency control	Purpose of test
47-52	90/110 DBM	Single layer	do thermo in 44	+10° C	Extn	Synch/Var	Modulator trials 3-pen. rec. Failure criterion (Loops)
53-58	SA	"	Thermocouples	"	"	"	Failure criterion Rest periods
59-124	90/110 DBM	"	None	"	"	"	Routine
125-148	"	"	"	+30° C	"	"	"
149-160	"	"	"	+40° C	"	"	"
161-178	"	"	"	0° C	"	"	"
179-182	"	"	"	+10° C	"	"	"
183,184	"	"	"	+30° C	"	"	"
185-187	"	"	"	+40° C	"	"	"
188-193	"	"	"	+10° C	"	"	"
401-412	DTM	"	Compn temp. varies	-	-	-	Compaction trials
413-418	"	"	None	0° C	Extn	Synch/Var	Routine
419-454	"	"	"	+10° C	"	"	"
455-490	"	"	"	+30° C	"	"	"

/contd.

TABLE 3 (contd.)

Specimen	Material	Compaction	Special features	Test temp.	Test control	Frequency control	Purpose of test
491-508	DTM	Single layer	None	+40° C	Extn	Synch/Var	Routine
509-526	"	"	"	0° C	"	"	"
601-612	DLC	"	Water content varies	-	-	-	Mixture trials
613-626	"	"	Tested wet	+20° C	Extn	Synch/Var	Exploratory studies
627-630	"	"	"	"	-	-	ditto - direct tension
631-636	"	"	Tested dry	"	Extn	Synch/Var	Exploratory studies
637-666	"	"	Tested wet	"	Load	None	Routine
701-730	190/210 DBM	"	None	+10° C	Extn	Synch/Var	"
731-742	"	"	"	0° C	"	"	"
743-754	"	"	"	+40° C	"	"	"
801-818	HRA	"	"	+10° C	"	"	"
819-849	"	"	"	+30° C	"	"	"
849-854	"	"	"	+10° C	"	"	"
855-860	"	"	"	+30° C	"	"	"
861-866	"	"	"	+40° C	"	"	"

TABLE 4

LOAD CELL CALIBRATION

a) Static tension with dead weights

Dead weight 0 lb	Load cell output 0 ± 1 lb
10	10
20	20
30	30
40	40
50	50
60	60
70	70
80	80
100	100
70	71½
50	51½
20	21½
10	11½
0	1½

b) Static compression with proving ring

Load cell output 0 ± 2.5 lb	Proving ring load 0 ± 0.5 lb
50	48
100	96
150	146
200	197
250	251
275	273
300	298
310	310
320	320
330	329
340	340
350	351
375	377
0	1

c) Dynamic compression with proving ring

Crosshead speed	Load cell output	Proving ring load
0.01 in/min	314 ± 2.5 lb	312 ± 0.5 lb
0.02	314	312
0.05	314	312
0.1	314	313
0.2	314	314
0.5	315	316
1.0	318	319
2.0	324	324

TABLE 5

SPECIFIC GRAVITIES OF AGGREGATES AND BINDERS

Material	mean S.G.
Graded crushed granite as used in dense macadams	2.825
Graded granite/gravel as used in hot rolled asphalt	2.775
Graded crushed gravel as used in dry lean concrete	2.626
Passing 100 mesh gravel sand excluded above	2.668
40/50, 90/110 and 190/210 pen. bitumens	1.019
54 e.v.t. tar	1.160
O.P.C. - not determined - assumed value	3.12

TABLE 6

DRY LEAN CONCRETE CUBE STRENGTHS

Cube details (all 4" cubes)	Agg/cem ratio (5% water)	Age	Strength (mean of 3)
Trial mix	17.5:1	7 days	825 lb/in^2
Trial mix	17.5:1	28	735
Standard mix - first specimen production	15.0:1	7	1293
Standard mix - first specimen production	15.0:1	28	1590
Standard mix - last specimen production	15.0:1	7	1185
Standard mix - last specimen production	15.0:1	28	1391

TABLE 7

DRYING OUT OF DRY LEAN CONCRETE SPECIMENS

Elapsed time	Moisture loss (601) (with rubber membrane)	Moisture loss (602) (without rubber membrane)
3 hours	0 gm	8 gm
6	0	16
9	0	24
12	0	29½
24	0	51
31	0	61½
4 days	1	91
5	1½	97½
7	1½	103½
13	3½	118
4 weeks	7½	125½

TABLE 8

BALLOTINI WEIGHTS WHEN MEASURING SPECIMEN END VOIDS BY DIFFERENT METHODS

(0.2 mm Ballotini, 4.000" ø recess x 0.496" deep)

End filling method	Wt. Ballotini	Repeatability
Ballotini poured in rotary manner from height of approximately ½"	183.1 gm 183.2 183.2 182.9 183.0 183.2	Very good " method adopted
Ballotini poured in rotary manner from height of approximately 3"	183.8 184.0 184.5	Fair
Ballotini poured into centre from height of 1"	181.4 182.0 180.1	Poor

TABLE 9

SPECIMEN MOULD LENGTHS

Mould Number	Length (mean of 4 determinations)
1	9.011 inch
2	9.009
3	9.007
4	9.010
5	9.011
6	9.011
Mean	9.010

TABLE 10

TYPICAL VOID DETERMINATIONS FOR BATCH OF BITUMINOUS SPECIMENS

Specimens: 143-148

Material: 90/110 DBM

Date: 28.2.69 Mix: 27.2.69

Specimen	143	144	145	146	147	148
Wt. Ballotini (gm): Upper End	285.6	284.3	282.0	290.1	287.7	290.6
	285.8	283.3	281.5	289.5	286.0	290.9
	286.8	284.6	281.3	288.0	285.9	290.9
Mean	286.1	284.1	281.6	289.2	286.5	290.8
Lower End	316.9	330.8	306.2	300.6	302.8	355.9
	316.1	331.6	306.9	299.6	302.8	355.6
	316.8	330.7	306.4	300.1	302.6	357.5
Mean	316.6	331.0	306.5	300.1	302.7	356.3
Total	602.7	615.1	588.1	589.3	589.2	647.1
Volume Ballotini (cc)	332.2	339.0	324.1	324.8	324.7	356.6
Volume specimen (cc)	1523.1	1516.3	1531.2	1530.5	1530.6	1498.7
Wt. specimen in air (gm)	3493	3478½	3526	3544½	3483	3429½
Wt. specimen in water (gm)	2065½	2061	2080½	2106	2055	2025½
Volume of material (cc)	1427½	1417½	1445½	1438½	1428	1404
S.G. specimen	2.293	2.294	2.303	2.316	2.276	2.288
Total (specimen) voids (%)	12.95	12.91	12.57	12.07	13.59	13.14
S.G. material	2.447	2.454	2.439	2.464	2.439	2.443
Internal (material) voids (%)	7.10	6.83	7.40	6.45	7.40	7.25
Volume surface voids (cc)	95.6	98.8	85.7	92.0	102.6	94.7
Surface voids (%)	6.28	6.52	5.60	6.01	6.70	6.32

TABLE 11

SPECIMEN VOIDS

a) 90/110 Dense Bitumen Macadam

Specimens	Internal voids			Surface voids			Total voids		
	mean (%)	S.D. (%)	%age S.D.	mean (%)	S.D. (%)	%age S.D.	mean (%)	S.D. (%)	%age S.D.
59-64	6.56	0.32	4.85	6.78	1.82	26.79	12.90	1.52	11.78
65-70	6.81	0.96	14.05	7.63	1.69	22.14	14.09	0.81	5.75
71-76	6.66	0.26	3.88	7.21	0.46	6.36	13.42	0.62	4.64
77-82	6.12	0.55	8.95	7.01	0.71	10.16	12.70	0.26	2.03
83-88	6.79	0.19	2.77	5.97	0.57	9.82	12.36	0.54	4.37
89-94	6.55	0.41	6.30	6.95	0.82	11.79	13.05	0.44	3.36
95-100	6.85	0.29	4.27	6.18	0.47	7.68	12.59	0.33	2.64
101-106	6.70	0.53	7.90	6.77	0.63	9.32	12.93	0.36	2.82
107-112	6.85	0.40	5.81	5.66	0.45	7.86	12.12	0.32	2.65
113-118	7.77	0.43	5.54	5.68	0.52	9.09	13.00	0.14	1.11
119-124	7.39	0.40	5.41	6.34	0.54	8.53	13.25	0.23	1.70
125-130	7.13	0.57	8.01	6.43	0.64	9.97	13.09	0.34	2.58
131-136	7.35	0.26	3.50	5.88	0.37	6.28	12.81	0.28	2.17
137-142	7.28	0.35	4.80	6.02	0.35	5.82	12.84	0.55	4.24
143-148	7.07	0.37	5.26	6.24	0.39	6.25	12.87	0.52	4.01
149-154	7.33	0.34	4.59	5.80	0.60	10.30	12.66	0.58	4.57
155-160	7.44	0.25	3.40	5.95	0.39	6.61	12.84	0.40	3.11
161-166	7.34	0.27	3.74	5.57	0.61	10.97	12.51	0.37	2.95
167-172	7.14	0.23	3.25	5.82	0.54	9.24	12.54	0.30	2.39
173-178	6.51	0.36	5.45	4.90	0.61	12.39	11.11	0.51	4.56
179-184	6.54	0.45	6.91	4.96	0.39	7.91	11.19	0.58	5.15
188-183	6.08	0.40	6.64	5.89	0.75	12.77	11.61	0.37	3.20
mean	6.92	0.31	5.70	6.17	0.65	10.36	12.66	0.47	3.70
59-193	6.92	0.58	8.37	6.16	0.96	15.57	12.66	0.83	6.59

N.B. One group of three specimens (185-187) was produced but is not included in the statistical analysis above. The average values of voids in this group were:-

Internal voids: 6.69% Surface voids: 5.65%

Total voids: 11.96%

TABLE 11 (contd.)

SPECIMEN VOIDS

b) 190/210 Dense Bitumen Macadam

Specimens	Internal voids			Surface voids			Total voids		
	mean (%)	S.D. (%)	%age S.D.	mean (%)	S.D. (%)	%age S.D.	mean (%)	S.D. (%)	%age S.D.
701-706	6.44	0.35	5.45	5.02	0.40	7.98	11.12	0.47	4.21
707-712	6.46	0.47	7.23	4.79	0.36	7.53	10.96	0.27	2.46
713-718	6.47	0.48	7.36	5.33	0.48	9.07	11.46	0.31	2.69
719-724	6.68	0.37	5.48	4.65	0.37	7.91	11.00	0.40	3.61
725-730	6.77	0.24	3.61	4.90	0.34	6.94	11.32	0.36	3.22
731-736	6.86	0.44	6.38	4.89	0.36	7.43	11.38	0.30	2.62
737-742	6.51	0.39	6.00	5.94	0.29	4.84	12.06	0.15	1.24
743-748	7.03	0.32	4.51	4.95	0.52	10.51	11.64	0.36	3.07
749-754	6.20	0.32	5.24	5.74	0.55	10.23	11.21	0.24	2.15
mean	6.60	0.38	5.70	5.09	0.40	8.05	11.35	0.32	2.81
701-754	6.60	0.43	6.46	5.09	0.53	10.50	11.35	0.45	3.93

TABLE 11 (contd.)

SPECIMEN VOIDS

c) Dense Tar Macadam

Specimens	Internal voids			Surface voids			Total voids		
	mean (%)	S.D. (%)	%age S.D.	mean (%)	S.D. (%)	%age S.D.	mean (%)	S.D. (%)	%age S.D.
413-418	6.77	0.41	6.09	4.30	0.43	10.03	10.78	0.29	2.73
419-424	6.59	0.34	5.15	5.65	0.74	13.12	11.84	0.41	3.49
425-430	6.18	0.24	3.86	5.69	0.38	6.65	11.51	0.35	3.07
431-436	7.52	0.25	3.33	4.32	0.47	10.99	11.45	0.44	3.80
437-442	6.82	0.44	6.51	4.80	0.74	15.49	11.33	0.32	2.84
443-448	7.36	0.30	4.10	4.65	0.42	9.12	11.68	0.26	2.26
449-454	7.53	0.43	5.71	4.71	0.40	8.52	11.88	0.41	3.49
455-460	6.93	0.43	6.16	5.13	0.32	6.33	11.66	0.38	3.27
461-466	6.53	0.30	4.64	5.44	0.21	3.80	11.61	0.36	3.08
467-472	6.74	0.51	7.55	5.17	0.60	11.56	11.56	0.30	2.57
473-478	6.91	0.27	3.92	5.62	0.30	5.29	12.15	0.45	3.73
479-484	6.98	0.41	5.89	5.59	0.42	7.60	12.17	0.74	3.51
485-490	6.77	0.54	7.99	5.77	0.52	8.93	12.16	0.85	7.01
491-496	7.03	0.35	5.01	5.23	0.43	8.13	11.87	0.38	3.22
497-502	6.86	0.93	13.60	5.29	0.77	14.64	11.77	0.61	5.17
503-508	7.27	0.21	2.92	5.08	0.50	9.91	11.98	0.62	5.15
509-514	7.67	0.23	2.94	4.64	0.09	2.04	11.90	0.31	2.62
515-520	7.67	0.30	3.97	4.66	0.61	13.21	11.68	0.33	2.85
521-526	7.29	0.44	6.06	5.59	0.55	9.77	12.46	0.28	2.23
527-532	7.12	0.67	9.40	5.01	0.68	13.61	11.79	0.36	3.08
mean	7.03	0.40	5.74	5.12	0.41	9.44	11.76	0.40	3.46
413-532	7.02	0.56	7.97	5.12	0.65	12.78	11.76	0.53	4.50

TABLE 11 (contd.)

SPECIMEN VOIDS

d) Hot Rolled Asphalt

Specimens	Internal voids			Surface voids			Total voids		
	mean (%)	S.D. (%)	%age S.D.	mean (%)	S.D. (%)	%age S.D.	mean (%)	S.D. (%)	%age S.D.
801-806	4.05	0.29	7.19	2.35	0.42	17.73	6.30	0.45	7.08
807-812	3.90	0.41	10.47	2.20	0.52	23.79	6.01	0.37	6.19
813-818	3.83	0.20	5.30	2.87	0.52	18.29	6.58	0.63	9.91
819-814	3.84	0.26	6.83	2.41	0.37	15.37	6.15	0.49	7.89
825-830	4.27	0.24	5.71	2.77	0.51	18.54	6.93	0.97	6.80
831-836	4.35	0.19	4.42	2.63	0.34	13.07	6.87	0.49	7.10
837-842	3.89	0.22	5.73	2.46	0.35	14.08	6.27	0.44	7.04
843-848	4.13	0.24	5.76	3.11	0.46	14.73	7.10	0.36	5.01
849-854	4.12	0.10	2.53	2.64	0.36	13.46	6.66	0.31	4.68
855-860	4.41	0.34	7.80	3.02	0.60	19.84	7.29	0.64	8.75
861-866	4.03	0.18	4.41	2.50	0.40	16.19	6.41	0.52	8.17
mean	4.07	0.24	6.01	2.63	0.44	16.83	6.60	0.47	7.12
801-866	4.07	0.31	7.49	2.63	0.50	18.84	6.60	0.59	8.97

e) Dry Lean Concrete

Specimens	mean (%)	S.D. (%)	%age S.D.
613-618	6.00	0.12	2.00
619-629	5.94	0.31	5.23
625-630	6.52	0.52	7.99
631-636	5.68	0.50	8.80
637-642	5.54	0.10	1.81
643-648	5.87	0.35	5.97
649-654	5.60	0.14	2.50
655-660	5.71	0.26	4.55
660-666	5.63	0.30	5.33
mean	5.83	0.29	4.91
613-666	5.83	0.42	7.21

TABLE 12

SLOPES AND RATE EFFECTS FROM STIFFNESS MEASUREMENT TESTS ON BITUMINOUS SPECIMENS

Material	Temp.	Slope stiff x strain (-ive)				Rate effect				m+logR
		m_1	m_2	m_3	mean	R_1	R_2	R_3	mean	
90/110 DBM	0°C	0.41	0.43	0.44	0.43	1.84	1.89	1.83	1.85	-0.16
	+10°C	0.58	0.62	0.68	0.63	2.40	2.50	2.90	2.60	-0.21
	+30°C	0.63	0.54	-	0.58	2.86	2.92	-	2.90	-0.12
	+40°C	0.55	0.42	0.64	0.54	1.88	2.16	1.80	1.95	-0.25
190/210 DBM	0°C	0.45	0.53	0.55	0.51	2.40	2.35	2.50	2.42	-0.13
	+10°C	0.65	0.82	0.58	0.68	2.82	3.07	2.95	2.95	-0.21
	+30°C	0.59	0.56	0.64	0.60	1.33	1.33	1.33	1.33	-0.48
DTM	0°C	0.41	0.44	0.44	0.43	1.60	1.45	1.65	1.57	-0.23
	+10°C	0.58	0.60	0.54	0.57	2.75	2.65	2.54	2.65	-0.16
	+30°C	0.72	0.64	0.72	0.69	3.20	3.00	3.00	3.07	-0.20
	+40°C	0.43	0.62	0.46	0.50	1.60	1.86	1.95	1.80	-0.24
HRA	+10°C	0.62	0.61	0.58	0.60	2.22	2.24	2.21	2.22	-0.25
	+30°C	varies				2.98	2.92	2.62	2.84	-

Rate effect for HRA at +30°C taken at $\epsilon = 5.10^{-4}$ in/in

TABLE 13

BEST FIT LINE VALUES FROM STIFFNESS AND REPEATED

LOADING TESTS ON BITUMINOUS SPECIMENS

Material	Temp.	No. of Specimens	Stiffness/Strain		Repeated loading: Cycles to -					
			Slope (-ive)	Intercept at $\varepsilon=1.$	90% Initial stiffness		75% Initial stiffness		60% Initial stiffness	
					Constant	Indicee	Constant	Indicee	Constant	Indicee
90/110 DBM	0°C	11	0.592	$2.12.10^6$	0.340	12.5	0.491	59.9	0.538	107
	+10°C	61	0.630	$7.10.10^5$	0.789	156	0.621	131	0.555	135
	+30°C	24	0.573	$1.53.10^5$	0.335	7.92	0.570	98.1	0.516	119
	+40°C	12	0.337	$6.92.10^4$	0.651	49.4	0.647	135	0.567	152
	0°C to +40°C	108	-	-	0.646	62.1	0.597	112	0.529	118
190/210 DBM	0°C	5	0.773	$1.02.10^5$	0.514	46.1	0.508	78.6	0.427	65.7
	+10°C	27	0.752	$3.80.10^5$	0.762	144	0.582	111	0.489	98.9
	+40°C	9	0.576	$1.18.10^4$	0.713	58.6	0.876	42.4	0.934	107
	0°C to +40°C	41	-	-	0.724	101	0.593	111	0.483	89.7
90/110 + 190/210	0°C to +40°C	149	-	-	0.665	69.7	0.596	112	0.519	111

/contd.

TABLE 13 (contd.)

Material	Temp.	No. of Specimens	Stiffness/Strain		Repeated loading: Cycles to -					
			Slope (-ive)	Intercept at $\varepsilon=1.10^{-4}$	90% Initial stiffness		75% Initial stiffness		60% Initial stiffness	
					Constant	Indicee	Constant	Indicee	Constant	Indicee
DTM	0°C	10	0.384	$4.08.10^{6}$	0.528	32.3	0.460	40.1	0.419	40.8
	+10°C	30	0.611	$2.01.10^{6}$	0.891	163	0.717	121	0.653	111
	+30°C	35	0.736	$7.57.10^{4}$	0.507	14.5	0.558	63.2	0.562	112
	+40°C	15	0.606	$1.86.10^{4}$	0.441	9.23	0.422	26.6	0.541	110
	0°C & +10°C	40	-	-	0.856	138	0.695	110	0.634	108
	+30°C & +40°C	50	-	-	0.492	13.1	0.517	47.9	0.562	116
HRA	+10°C	16	0.567	$1.07.10^{6}$	0.718	106	0.655	161	0.528	118
	+30°C	33	0.642	$8.28.10^{4}$	0.545	31.3	0.572	107	0.597	242
	+40°C	6	-	-	-	-	-	-	-	-
	+10°C to 40°C	55	-	-	0.649	63.6	0.558	95.9	0.489	110

$\log_e \text{cycles} = \frac{K}{\mu\varepsilon^x}$ where constant "K" defines position of curve being the cycles at $\mu\varepsilon = 1$, i.e. $\varepsilon = 1.10^{-6}$ in/in

and indicee "x" defines shape of curve

TABLE 14

TRENDS IN SHAPES OF LOAD AND DEFORMATION RECORDS

DURING REPEATED LOADING TESTS ON BITUMINOUS SPECIMENS

Material	Temp.	Load/Deflection record shape			Trend in ratio S_c/S_T		
		Low ϵ	Med. ϵ	High ϵ	Low ϵ	Med. ϵ	High ϵ
90/110 DBM	0°C	*B2	A3	-	INC	INC	-
	+10°C	*A3	A3	A1	INC	N/C	N/C
	+30°C	C1	A1	A1	DEC	DEC	DEC
	+40°C	C1	A1	A1	DEC	DEC	DEC
190/210 DBM	0°C	-	*C2	-	-	N/C	-
	+10°C	-	A2	A1	-	N/C	DEC
	+40°C	-	A1	-	-	DEC	-
DTM	0°C	*B1	A1	-	INC	N/C	-
	+10°C	*A1	*A2	A4	N/C	N/C	DEC
	+30°C	A1	A1	A1	DEC	DEC	DEC
	+40°C	A1	A1	-	DEC	DEC	-
HRA	+10°C	*C3	A1	-	N/C	DEC	-
	+30°C	-	A1	A1	-	DEC	DEC
	+40°C	-	-	A1	-	-	DEC

For key to definitions see Figure 125

Low strain taken as $< 1.10^{-4}$ in/in

Medium strain taken as 1.10^{-4} to 5.10^{-4} in/in

High strain taken as $> 5.10^{-4}$ in/in

INC - increase in ratio S_c/S_T during test

N/C - no change " " " " "

DEC - decrease " " " " "

TABLE 15

RESULTS FROM DRY LEAN CONCRETE SPECIMENS

a) Static ultimate strengths after strain-controlled repeated loading

Specimen	Condition	Type of cycling	Ult. tensile strength lb/in^2	Strain at ult. stress in/in
615	Wet	C-T	47.6	-
616	Wet	C-T	51.6	-
617	Wet	-	-	-
618	Wet	C-O/O-T	46.4	$4.70.10^{-4}$
619	Wet	-	-	-
620	Wet	Single cycle	92.7	$5.88.10^{-4}$
621	Wet	-	-	-
622	Wet	O-T	78.5	$2.00.10^{-4}$
623	Wet	O-C	68.2	$1.28.10^{-4}$
624	Wet	O-T	49.2	$4.28.10^{-4}$
625	Wet	O-T	48.8	$3.12.10^{-4}$
626	Wet	O-T	102.0	$1.36.10^{-4}$
627	Wet	None	104.7	$1.60.10^{-4}$
628	Wet	None	98.0	$1.28.10^{-3}$
629	Wet	None	48.0	$2.16.10^{-4}$
630	Wet	None	106.1	$3.60.10^{-4}$
631	Dry	O-T	102.8	$1.44.10^{-4}$
632	Dry	O-T	134.9	$4.88.10^{-4}$
633	Dry	O-T	121.0	$3.60.10^{-4}$
634	Dry	O-C	134.0	$2.24.10^{-4}$
635	Dry	Single cycle	138.9	$1.70.10^{-4}$

TABLE 15 (contd.)

b) Fracture lives and strains after stress-controlled repeated loading (specimens tested wet)

Specimen	Stress limits lb/in^2	Cycles to failure	Strain at failure in/in	Cycles to run out	Strain at run out in/in
636	various	-	-	-	-
637	0-55.5T	-	-	8,000	$2.10.10^{-4}$
638	0-56.8T	1003	$2.35.10^{-3}$	-	-
639	0-57.1T	702	$7.80.10^{-3}$	-	-
640	0-54.2T	58	$1.50.10^{-3}$	-	-
641	0-54.9T	265	$1.50.10^{-3}$	-	-
642	0-55.5T	462	$1.60.10^{-3}$	-	-
643	52.5c-52.5T	-	-	3,300	$5.78.10^{-4}$
644	0-56.1T	-	-	25,000	$1.85.10^{-4}$
645	m/c failure	-	-	-	-
646	0-50.4T	2400	-	-	-
647	0-46.0T	338	$1.70.10^{-3}$	-	-
648	0-47.4T	69	$4.05.10^{-3}$	-	-
649(1)	0-40.3T	-	-	10,000	$5.60.10^{-4}$
649(2)	0-69.8T	205	$8.90.10^{-4}$	-	-
650(1)	0-40.7T	-	-	13,000	$2.57.10^{-4}$
650(2)	0-71.4T	16	$2.55.10^{-3}$	-	-
651(1)	0-40.1T	-	-	7,000	$1.80.10^{-3}$
651(2)	0-73.0T	124	$6.60.10^{-4}$	-	-
652	0-73.4T	560	$2.15.10^{-3}$	-	-
653	0-70.1T	41	$2.37.10^{-3}$	-	-
654-656	0-abt 70T	1	-	-	-
657	0-70.6T	18	$5.65.10^{-4}$	-	-
658	0-59.3T	-	-	1,000	$3.05.10^{-4}$
659	0-50.0T	233	$4.20.10^{-4}$	-	-
660	0-49.2T	840	$2.75.10^{-4}$	-	-
661	0-abt 70T	1	-	-	-
662	23.5c-46.7T	590	$3.90.10^{-3}$	-	-
663	24.3c-46.6T	2500	$1.50.10^{-3}$	-	-
664	66.4c-65.9T	14	$2.81.10^{-4}$	-	-
665	66.5c-66.0T	10	$1.10.10^{-3}$	-	-
666	65.0T-72.3T	65	$1.33.10^{-3}$	-	-

TABLE 16

VISCOSITY RESULTS FROM HIGH TEMPERATURE PARALLEL PLATE VISCOMETER TESTS ON 90/110 pen. BITUMEN

a) Unheated binder at +30°C

Hanger wt.	Direct wt. (nominal)	Loading on viscometer	Initial plate separation	Binder viscosity
1 lb	-	5.25 kg	$\frac{1}{8}$"	$4.89.10^5$ poise
2	-	10.25	$\frac{1}{8}$	3.80
$\frac{1}{2}$	-	2.76	$\frac{1}{8}$	4.59
$\frac{1}{4}$	-	1.500	$\frac{1}{8}$	4.81
1	-	5.25	$\frac{1}{4}$	4.95
1	-	5.25	$\frac{1}{16}$	5.09
1	-	5.25	$\frac{1}{16}$	6.22
-	1 kg	1.243	$\frac{1}{8}$	4.34
-	1	1.239	$\frac{1}{8}$	5.44
-	1	1.243	$\frac{1}{8}$	4.22
-	1	1.239	$\frac{1}{8}$	5.75

b) Unheated binder at +40°C

Hanger wt.	Direct wt. (nominal)	Loading on viscometer	Initial plate separation	Binder viscosity
$\frac{1}{2}$ lb	-	2.76 kg	$\frac{1}{16}$"	$5.60.10^4$ poise
$\frac{1}{4}$	-	1.500	$\frac{1}{16}$	5.37
1	-	5.25	$\frac{1}{16}$	4.95
$\frac{1}{2}$	-	2.75	$\frac{1}{16}$	5.66
-	$\frac{1}{4}$ kg	0.508	$\frac{1}{8}$	4.88
-	$\frac{1}{4}$	0.504	$\frac{1}{8}$	6.24
-	none	0.256	$\frac{1}{8}$	6.30
-	none	0.252	$\frac{1}{8}$	4.46

TABLE 17

PARALLEL PLATE VISCOMETER TEST RESULTS

(all viscosities in poise)

a) 90/110 pen. Bitumen

Binder condition	0° C	+10° C	+20° C	+30° C	+40° C
Unheated	$2.39.10^9$	$1.23.10^8$	$6.42.10^6$	$4.89.10^5$	$5.60.10^4$
	2.78	$9.98.10^7$	7.63	3.80	5.37
	2.15	$1.23.10^8$	8.90	4.59	4.95
	-	-	7.46	4.81	5.66
	-	-	5.90	4.95	4.88
	-	-	-	5.09	6.24
	-	-	-	6.22	6.30
	-	-	-	4.34	4.46
	-	-	-	5.44	-
	-	-	-	4.22	-
	-	-	-	5.75	-
mean	$2.44.10^9$	$1.15.10^8$	$7.26.10^6$	$4.92.10^5$	$5.44.10^4$
Heated	-	$9.35.10^7$	-	-	$4.35.10^4$
	-	$1.06.10^8$	-	-	6.35
	-	$9.51.10^7$	-	-	5.35
	-	$1.14.10^8$	-	-	-
mean	-	$1.02.10^8$	-	-	$5.35.10^4$
Heated & Unheated	$2.44.10^9$	$1.08.10^8$	$7.26.10^6$	$4.92.10^5$	$5.41.10^4$

TABLE 17 (contd.)

b) 190/210 pen. Bitumen

Binder condition	0° C	+10° C	+20° C	+30° C	+40° C
Unheated	$3.44.10^{8}$	$1.36.10^{7}$	$9.65.10^{5}$	$1.33.10^{5}$	-
	3.71	1.50	$1.02.10^{6}$	1.03	-
	3.46	1.36	-	1.06	-
mean	$3.54.10^{8}$	$1.41.10^{7}$	$9.93.10^{5}$	$1.14.10^{5}$	-
Heated	$5.43.10^{8}$	$1.86.10^{7}$	$1.70.10^{6}$	$1.23.10^{5}$	-
	$6.83.10^{8}$	2.16	1.26	1.37	-
	-	1.94	-	1.39	-
	-	2.15	-	-	-
mean	$6.13.10^{8}$	$2.03.10^{7}$	$1.48.10^{6}$	$1.33.10^{5}$	-
Heated & Unheated	N/A	N/A	N/A	N/A	-

c) 40/50 pen. Bitumen

Binder condition	0° C	+10° C	+20° C	+30° C	+40° C
Unheated	$2.32.10^{10}$	$7.18.10^{8}$	$5.27.10^{7}$	$3.32.10^{6}$	$3.04.10^{5}$
	2.25	7.75	5.03	3.39	4.27
	-	-	-	-	3.24
mean	$2.29.10^{10}$	$7.47.10^{8}$	$5.14.10^{7}$	$3.36.10^{6}$	$3.52.10^{5}$
Heated	-	$7.18.10^{8}$	-	-	$3.45.10^{5}$
	-	7.40	-	-	3.84
	-	6.85	-	-	3.88
	-	-	-	-	3.70
	-	-	-	-	3.78
mean	-	$7.14.10^{8}$	-	-	$3.73.10^{5}$
Heated & Unheated	$2.29.10^{10}$	$7.27.10^{8}$	$5.14.10^{7}$	$3.36.10^{6}$	$3.65.10^{5}$

TABLE 17 (contd.)

d) 54 e.v.t. Tar

Binder condition	0° C	+10° C	+20° C	+30° C	+40° C
Unheated	$3.00.10^9$	$4.90.10^7$	$1.21.10^6$	$1.04.10^5$	-
	2.41	5.60	1.29	1.09	-
	4.50	4.34	1.25	$8.74.10^4$	-
	3.45	4.98	1.28	9.21	-
mean	$3.34.10^9$	$4.96.10^7$	$1.26.10^6$	$9.81.10^4$	-
Heated	$1.29.10^9$	$5.67.10^7$	$1.34.10^6$	$6.05.10^4$	-
	$8.60.10^8$	6.40	1.54	5.77	-
	-	5.87	-	-	-
	-	6.15	-	-	-
mean	$1.08.10^9$	$6.02.10^7$	$1.44.10^6$	$5.91.10^4$	-
Heated & Unheated	N/A	N/A	N/A	N/A	-

e) Recovered Bitumens

	90/110 pen.		190/210 pen.		40/50 pen.	
	Temp.	Viscosity	Temp.	Viscosity	Temp.	Viscosity
Test 1	25.6° C	$1.41.10^7$	25.2° C	$1.16.10^6$	24.8° C	$8.04.10^7$
Test 2	25.8° C	$1.39.10^7$	25.7° C	$1.18.10^6$	24.7° C	$9.40.10^7$
Mean	25.7° C	$1.40.10^7$	25.5° C	$1.17.10^6$	24.8° C	$8.72.10^7$

TABLE 18

RESULTS OF STANDARD TESTS ON BINDERS

a) Bitumens

Bitumen	Penetration (mean of 3)	Ring & Ball (mean of 4)	Penetration Index
Unheated 90/110	90	47.0°C	-1.1
Heated 90/110	85	48.0°C	-1.0
Recovered 90/110	40	55.5°C	-0.9
Unheated 190/210	179	38.5°C	-2.0
Heated 190/210	169	38.6°C	-2.2
Recovered 190/210	100	45.5°C	-1.2
Unheated 40/50	44	56.5°C	-0.4
Heated 40/50	42	57.3°C	-0.5
Recovered 40/50	27	64.0°C	0.0

b) Tar

Unheated e.v.t. (mean of 3) = 54.8°C

Heated e.v.t. (mean of 3) = 56.0°C

No tar recovered

TABLE 19

RECOVERY OF STIFFNESS OF BITUMINOUS SPECIMENS DURING REST PERIOD AFTER STRAIN-CONTROLLED REPEATED LOADING

Specimen	Material	Test temp.	Strain level in/in	Stiffness at end of test (% S_I)	Rest period in stress-free state	Stiffness at start 2nd run (% S_I)
128	90/110 DBM	+30° C	$3.68.10^{-4}$	43.8	1 hr	79.3
133	90/110 DBM	+30° C	$1.92.10^{-4}$	57.5	1 hr	83.8
742	190/210 DBM	0° C	$1.15.10^{-4}$	59.0	18 hrs	97.5
705	190/210 DBM	+10° C	$1.12.10^{-4}$	64.0	15 min	75.5
706	190/210 DBM	+10° C	$2.27.10^{-4}$	62.7	14 hrs	95.8
709	190/210 DBM	+10° C	$2.27.10^{-4}$	59.2	66 hrs	104.0
712	190/210 DBM	+10° C	$4.47.10^{-4}$	41.5	17 hrs	87.2
715	190/210 DBM	+10° C	$9.81.10^{-4}$	52.0	1 hr	90.6
718	190/210 DBM	+10° C	$2.15.10^{-3}$	26.3	1 hr	76.1
721	190/210 DBM	+10° C	$3.01.10^{-4}$	63.2	1 hr	92.0
724	190/210 DBM	+10° C	$3.05.10^{-4}$	62.3	16 hrs	95.5
727	190/210 DBM	+10° C	$1.94.10^{-3}$	55.9	18 hrs	102.0

/contd.

TABLE 19 (contd.)

Specimen	Material	Test temp.	Strain level in/in	Stiffness at end of test (% S_I)	Rest period in stress-free state	Stiffness at start 2nd run (% S_I)
745	190/210 DBM	+40° C	$5.27.10^{-4}$	40.4	17 hrs	72.5
440	DTM	+10° C	$2.44.10^{-4}$	18.3	16 hrs	54.3
450	DTM	+10° C	$9.15.10^{-5}$	62.8	15 hrs	84.0
454	DTM	+10° C	$4.91.10^{-5}$	69.9	16 hrs	93.7
460	DTM	+30° C	$1.54.10^{-4}$	44.0	17 hrs	86.5
466	DTM	+30° C	$7.84.10^{-5}$	53.7	16 hrs	84.4
472	DTM	+30° C	$1.97.10^{-4}$	54.0	65 hrs	82.0
478	DTM	+30° C	$4.13.10^{-4}$	48.0	15 hrs	80.6
496	DTM	+40° C	$2.61.10^{-4}$	56.1	14 hrs	94.5
502	DTM	+40° C	$4.80.10^{-4}$	48.1	15 hrs	85.3
865	HRA	+40° C	$2.62.10^{-5}$	77.0	15 min	91.6

TABLE 20

DETAILS OF LAYERED SYSTEMS STUDIED IN THEORETICAL ANALYSIS

System	Temp.	Frequency of loading (cy/sec)	Surfacing stiffness (lb/in^2)	Roadbase material	Roadbase stiffness (lb/in^2)	Roadbase thickness (in)	Load position	Purpose of analysis
1	+10° C	1	$6.0.10^6$	-	$1.0.10^6$	8	Varies	To assess change in frequency in bound layers
2a	+10° C	1	$6.0.10^6$	-	$7.5.10^5$	8	Axial	To study effect of roadbase stiffness on stresses and strains in bound layers.
2b	+10° C	1	$6.0.10^6$	-	$1.5.10^6$	8	Axial	
2c	+10° C	1	$6.0.10^6$	-	$3.0.10^6$	8	Axial	
2d	+10° C	1	$6.0.10^6$	-	$6.0.10^6$	8	Axial	
2e	+10° C	1	$6.0.10^6$	-	$1.2.10^7$	8	Axial	
3	+10° C	1	$6.0.10^6$	90/110 DBM	-	8	Axial	To find stresses and strains with 90/110 DBM roadbase
4	+10° C	1	$6.0.10^6$	90/110 DBM	-	4x2" layers	Axial	To compare results with System 3
5	+10° C	1	$6.0.10^6$	190/210 DBM	-	8	Axial	To find stresses and strains with 190/210 DBM roadbase
6	+10° C	1	$6.0.10^6$	DTM	-	8	Axial	ditto for DTM roadbase

/contd.

TABLE 20 (contd.)

System	Temp.	Frequency of loading (cy/sec)	Surfacing stiffness (lb/in^2)	Roadbase material	Roadbase stiffness (lb/in^2)	Roadbase thickness (in)	Load position	Purpose of analysis
7	+10° C	1	$6.0.10^6$	HRA	-	7	Axial	ditto for HRA roadbase
8	+10° C	1	$6.0.10^6$	HRA DLC	-	3 7	Axial	ditto for composite roadbase
9	+10° C	10	$6.0.10^6$	90/110 DBM	-	8	Axial	High frequency to compare with System 3
10	+30° C	1	$6.0.10^5$	90/110 DBM	-	8	Axial	High temperature to compare with System 3
11	0° C	1	$6.0.10^6$	90/110 DBM	-	8	Axial	Low temperature to compare with System 3
12	+10° C	1	$6.0.10^6$	90/110 DBM	60%	8	Axial	Damaged roadbase to compare with System 3
13	+10° C	1	$6.0.10^6$	HRA DLC	normal cracked	3 7	Axial	Cracked concrete to compare with System 8
14	0° C	10	$6.0.10^6$	DTM	-	8	Axial	Highest bituminous bound system stiffness
15	+30° C	1	$6.0.10^5$	DTM	-	8	Axial	Lowest bituminous bound system stiffness

TABLE 21

REITERATIONS OF THEORETICAL STRAINS IN ROADBASE MATERIALS USING MULTI-LAYER THEORY

System	Predicted strain (in/in)	Stiffness (lb/in^2)	Computed strains (in/in)	Modified stiffness (lb/in^2)	Computed strain (in/in)	Modified stiffness (lb/in^2)	Computed strain (in/in)	Modified stiffness (lb/in^2)	Computed strain (in/in)
1	-	$1.0.10^6$	N/A	N/A	-	-	-	-	-
2a-e	-	N/A	N/A	N/A	-	-	-	-	-
3	$1.0.10^{-5}$	$1.55.10^6$	$1.7.10^{-5}$	$1.4.10^6$	$1.85.10^{-5}$	$1.35.10^6$	$1.85.10^{-5}$	-	-
4 layer 1	$1.25.10^{-5}$	$1.45.10^6$	$1.25.10^{-5}$	-	-	-	-	-	-
2	$1.55.10^{-5}$	$1.4.10^6$	$1.55.10^{-5}$	-	-	-	-	-	-
3	$2.0.10^{-5}$	$1.35.10^6$	$2.05.10^{-5}$	-	-	-	-	-	-
4	$2.65.10^{-5}$	$1.25.10^6$	$2.75.10^{-5}$	-	-	-	-	-	-
5	$2.97.10^{-5}$	$7.35.10^5$	$2.8.10^{-5}$	$7.45.10^5$	$2.8.10^{-5}$	-	-	-	-
6	$6.75.10^{-5}$	$4.5.10^6$	$6.4.10^{-6}$	$4.55.10^6$	$6.4.10^{-6}$	-	-	-	-
7	$1.22.10^{-5}$	$2.25.10^6$	$1.45.10^{-5}$	$2.15.10^6$	$1.5.10^{-5}$	-	-	-	-
8 HRA	$5.0.10^{-6}$	$2.8.10^6$	$1.85.10^{-6}$	$3.5.10^6$	$0.9.10^{-6}$	$4.1.10^6$	$0.25.10^{-6}$	$*6.0.10^6$	$0.4.10^{-6}$
DLC	$1.0.10^{-5}$	$5.6.10^6$	$5.3.10^{-6}$	$9.0.10^6$	$3.6.10^{-6}$	$1.2.10^7$	$2.75.10^{-6}$	$1.45.10^7$	$2.2.10^{-6}$
9	$7.04.10^{-6}$	$4.4.10^6$	$6.6.10^{-6}$	$4.5.10^6$	$6.6.10^{-6}$	-	-	-	-

/contd.

TABLE 21 (contd.)

System	Predicted strain (in/in)	Stiffness (lb/in^2)	Computed strains (in/in)	Modified stiffness (lb/in^2)	Computed strain (in/in)	Modified stiffness (lb/in^2)	Computed strain (in/in)	Modified stiffness (lb/in^2)	Computed strain (in/in)
10	$5.0.10^{-5}$	$2.4.10^{5}$	$7.7.10^{-5}$	$2.25.10^{5}$	$8.1.10^{-5}$	$2.2.10^{5}$	$8.2.10^{-5}$	-	-
11	$5.56.10^{-6}$	$*6.45.10^{6}$	$4.8.10^{-6}$	-	-	-	-	-	-
12	$3.09.10^{-5}$	$7.35.10^{5}$	$2.8.10^{-5}$	$7.5.10^{5}$	$2.8.10^{-5}$	-	-	-	-
13 HRA	$2.0.10^{-4}$	$1.2.10^{6}$	$4.4.10^{-5}$	$1.65.10^{6}$	$3.75.10^{-5}$	$1.75.10^{6}$	$3.7.10^{-5}$	-	-
DLC	cracked	$2.5.10^{4}$	-	$2.5.10^{4}$	-	$2.5.10^{4}$	-	-	-
14	$3.55.10^{-6}$	$*7.05.10^{6}$	$4.3.10^{-6}$	-	-	-	-	-	-
15	$1.57.10^{-4}$	$9.7.10^{4}$	$1.37.10^{-4}$	$1.0.10^{5}$	$1.37.10^{-4}$	-	-	-	-

* theoretical maximum stiffness

TABLE 22

SUMMARY OF RESULTS OF THEORETICAL ANALYSIS

Sign convention - tension positive

System	Position	Vertical stress (lb/in^2)	Vertical strain (μ in/in)	Horizontal stress (lb/in^2)	Horizontal strain (μ in/in)	Surface deflection ($x10^{-3}$ in)	Cycles to 60% S_I
1	Load position	Varies	-	see Figures 148 and 149			
2a-e	Roadbase stiffness	Varies	-	see Figures 150 and 151			
3	Underside surfacing	-42.8	-16.3	+78.8	+11.0	6.87	10^{10}+
	Topside roadbase	-42.8	-31.7	-0.15	+11.0		
	Underside roadbase	-1.52	-35.2	+65.7	+32.0		$7.0.10^7$
	Topside subgrade	-1.00	-70.0	-0.30	+35.0		
4	Underside surfacing	-43.0	-16.0	+75.3	+10.7	6.90	10^{10}+
	Topside roadbase	-43.0	-30.0	+0.64	+10.7		
	Underside roadbase	-1.52	-35.9	+61.8	+32.6		$6.5.10^7$
	Topside subgrade	NOT COMPUTED					
5	Underside surfacing	-34.7	-24.3	+159	+19.2	7.92	10^{10}+
	Topside roadbase	-34.7	-49.7	+3.31	+19.2		
	Underside roadbase	-2.00	-50.6	+51.0	+45.4		$4.6.10^6$
	Topside subgrade	-1.23	-96.9	-0.26	+48.4		

/contd.

TABLE 22 (contd.)

System	Position	Vertical stress (lb/in^2)	Vertical strain (μ in/in)	Horizontal stress (lb/in^2)	Horizontal strain (μ in/in)	Surface deflection ($x10^{-3}$ in)	Cycles to 60% S_I
6	Underside surfacing	-56.8	-6.51	-25.3	+0.57	5.29	10^{1} ° +
	Topside roadbase	-56.8	-8.40	-26.6	+0.57		
	Underside roadbase	-0.86	-15.6	+100	+14.4		$7.0.10^{4}$
	Topside subgrade	-0.61	-34.9	-0.26	+17.5		
7	Underside surfacing	-46.6	-12.2	+38.1	+6.84	6.69	10^{1} ° +
	Topside roadbase	-46.6	-20.9	-2.47	+6.84		
	Underside roadbase	-1.43	-29.8	+89.4	+27.3		$2.1.10^{9}$
	Topside subgrade	-0.93	-62.1	-0.31	+31.1		
8	Underside surfacing	-67.3	-6.24	-42.7	-0.70	3.82	10^{1} ° +
	Topside HRA roadbase	-67.3	-6.24	-42.7	-0.70		
	Underside HRA "	-42.6	-3.80	-28.2	-0.57		10^{1} ° +
	Underside DLC "	-0.42	-2.80	+100	+5.55		> ult σ
	Topside subgrade	-0.33	-15.0	-0.18	+7.50		
9	Underside surfacing	-56.7	-6.56	-24.8	+0.63	5.30	10^{1} ° +
	Topside roadbase	-56.7	-8.53	-26.2	+0.63		
	Underside roadbase	-0.87	-15.7	+99.8	+14.5		10^{1} ° +
	Topside subgrade	-0.61	-35.1	-0.26	+17.6		
10	Underside surfacing	-51.2	-117	+27.5	+59.7	13.8	$2.3.10^{6}$
	Topside roadbase	-51.2	-209	-7.36	+59.7		
	Underside roadbase	-5.97	-159	+41.4	+132		$8.7.10^{3}$
	Topside subgrade	-2.98	-264	-0.34	+132		

/contd.

TABLE 22 (contd.)

System	Position	Vertical stress (lb/in^2)	Vertical strain (μ in/in)	Horizontal stress (lb/in^2)	Horizontal strain (μ in/in)	Surface deflection ($\times 10^{-3}$ in)	Cycles to 60% S_I
11	Underside surfacing	-59.9	-5.26	-40.5	-0.89	4.95	10^{10}+
	Topside roadbase	-59.9	-4.83	-41.1	-0.89		
	Underside roadbase	-0.74	-12.3	+112	+11.4		10^{10}+
	Topside subgrade	-0.54	-28.8	-0.25	+14.4		
12	Underside surfacing	-34.8	-24.2	+158	+19.1	7.90	10^{10}+
	Topside roadbase	-34.8	-49.5	+3.29	+19.1		
	Underside roadbase	-1.99	-50.4	+51.1	+45.2		-
	Topside subgrade	-1.23	-96.6	-0.26	+48.3		
13	Underside surfacing	-26.1	-26.3	+188	+21.9	9.85	10^{10}+
	Topside HRA roadbase	-26.1	-32.9	+45.0	+21.9		
	Underside HRA "	-3.94	-59.9	+144	+54.3		$4.4.10^6$
	Underside DLC "	-2.17	-101	+0.89	+45.9		-
	Topside subgrade	-1.54	-116	-0.38	+58.2		
14	Underside surfacing	-60.6	-5.04	-43.5	-1.17	4.87	10^{10}+
	Topside roadbase	-60.6	-4.10	-45.4	-1.17		
	Underside roadbase	-0.71	-11.6	+115	+10.7		$2.5.10^5$
	Topside subgrade	-0.53	-27.4	-0.25	+13.7		
15	Underside surfacing	-42.2	-183	+96.4	+129	16.5	$1.6.10^4$
	Topside roadbase	-42.2	-402	-2.87	+129		
	Underside roadbase	-7.92	-240	+22.9	+177		$1.7.10^2$
	Topside subgrade	-3.79	-354	-0.25	+177		

APPENDICES

APPENDIX 1	Equations of basic rheological models
APPENDIX 2	Theory of void determinations
APPENDIX 3	Stiffness corrections for changes in strain
APPENDIX 4	Computer programme for void analysis
APPENDIX 5	Computer programme for stiffness corrections and best fit lines for stiffness and lives under repeated loading
APPENDIX 6	Mathematical expressions for stiffness/cycles curves
APPENDIX 7	Proposed theory for cumulative damage due to thixotropic breakdown

APPENDIX 1

EQUATIONS OF BASIC RHEOLOGICAL MODELS

τ = shear stress
γ = shear strain
$\dot{\gamma}$ = rate of shear strain = where t = time
G = shear modulus = τ/γ
σ = axial stress
ε = axial strain
$\dot{\varepsilon}$ = rate of strain = ε/t
E = modulus of elasticity = σ/ε
η = coefficient of viscosity = $\tau/\dot{\gamma}$
λ = coefficient of viscous traction = $\sigma/\dot{\varepsilon}$
μ = Poisson's ratio
Θ = relaxation time = λ/E
S = stiffness

Considering a Kelvin model consisting of a spring and a dashpot in parallel, as shown in Figure 26, then, under static stress, the total stress on the model at time "t" is the sum of the stresses on the individual elements - i.e. for shear $\tau = G\gamma + \eta\dot{\gamma}$ -eq. 1

$\therefore$ model stiffness = $\frac{\tau}{\gamma} = G + \frac{\eta}{t}$ -eq. 2

similarly for axial load $\sigma = E\varepsilon + \lambda\dot{\varepsilon}$ -eq. 3

$\therefore$ model stiffness = $\frac{\sigma}{\varepsilon} = E + \frac{\lambda}{t}$ -eq. 4

For a Maxwell model consisting of a spring and a dashpot in series, also shown in Figure 26, the total strain on the model at time "t", under static stress, is the sum of the strains on the individual elements - i.e. for shear $\gamma = \frac{\tau}{G} + \frac{\tau t}{\eta}$ -eq. 5

$\therefore$ model stiffness = $\frac{\tau}{\gamma} = \frac{G\eta}{\eta + Gt}$ -eq. 6

similarly for axial loading $\varepsilon = \frac{\sigma}{E} + \frac{\sigma t}{\lambda}$ -eq. 7

$\therefore$ model stiffness = $\frac{\sigma}{\varepsilon} = \frac{\lambda E}{\lambda + Et} = \frac{E}{1 + t/\Theta}$ -eq. 8

In a Mohr's circle diagram for a viscous liquid the angle of friction is zero and therefore $\tau = \frac{\sigma_2 - \sigma_1}{2}$

For axial loading $\tau = \frac{\sigma}{2}$

$\therefore$ combining equations 1 and 3 $2(G\gamma + \eta\dot{\gamma}) = (E\varepsilon + \lambda\dot{\varepsilon})$ -eq. 9

Now from basic elastic theory $E = 2G(1+\mu)$. Taking bituminous binders as incompressible $\mu = \frac{1}{2}$ $\therefore E = 3G$.

Also $\tau = \frac{\sigma}{2}$ hence $\gamma = \frac{3}{2}\varepsilon$ $\therefore$ from eq. 9 $\lambda = 3\eta$

(This relationship may also be derived by combining equations 5 and 7).

Although the derived relationship $\lambda = 3\eta$ applies strictly to simple models, Trouton (239, 240) has shown that it is also applicable to Newtonian and near-Newtonian pitches and may therefore be considered as applicable to simple bitumens.

From equation 4 the stiffness of a Kelvin model is given by $S_K = E + \frac{\lambda}{t}$

as $t \rightarrow 0$, $S_K \rightarrow \infty$

as $t \rightarrow \infty$, $S_K \rightarrow E$.

Thus the bounding asymptotes are $S_K = \frac{\lambda}{t}$ and $S_K = E$ with a concave transition, and the intersection of the asymptotes $t = \theta$.

From equation 8 the stiffness of a Maxwell model is given by $S_M = \frac{E}{1+t/\theta}$

as $t \rightarrow 0$, $S_M \rightarrow E$

as $t \rightarrow \infty$, $S_M \rightarrow 0$

Thus the bounding asymptotes are $S_M = E$ and $S_M = \frac{\lambda}{t}$ with a convex transition, again, at the intersection of the asymptotes $t = \theta$.

The equations of the stiffness/time curves of these two models assume creep loading conditions, i.e. static stress. Constant strain rate and sinusoidal loading conditions will be bounded by the same asymptotes and the maximum variation in stiffness (at $t = \theta$) is less than a factor of 1.5.

The stiffness/time relationship for a viscous liquid, and hence the viscous asymptote for a visco-elastic liquid, is $S = \frac{\lambda}{t}$. In repeated loading, assuming a triangular waveform, the stress induced by a constant strain rate is reversed as the direction of application of strain is reversed.

Thus $S_d = \frac{2\lambda}{t} = 2\lambda\frac{\dot{\varepsilon}}{\varepsilon}$, where ε is the strain range.

APPENDIX 2

THEORY OF VOID DETERMINATIONS

If ω_c = fraction, by weight, of constituent material in mixture

and G_c = specific gravity of constituent material

and n = number of constituent materials in mixture

then vol/unit weight of voidless mixture = $\sum_{c=1}^{c=n} \frac{\omega_c}{G_c}$

$\therefore$ specific gravity of voidless mixture $G_S = \underline{\underline{\dfrac{1}{\sum_{c=1}^{c=n} \frac{\omega_c}{G_c}}}}$.

If G = specific gravity of compacted material

and V_v = volume of voids/unit weight of compacted material

then vol/unit weight of material = $\frac{1}{G_S} + V_v = \frac{1}{G}$

$\therefore$ vol. voids/unit volume of material = $V_v . G = \underline{\underline{\dfrac{G_S - G}{G_S}}}$.

If W_S = weight of specimen in air

and W_w = weight of specimen in water

and V_S = total volume of specimen (including surface voids)

then specific gravity of specimen $G_T = \frac{W_S}{V_S}$

$\therefore$ Total voids = $\underline{\underline{\dfrac{G_S - G_T}{G_S}}}$

also specific gravity of specimen material = $G_M = \frac{W_S}{W_S - W_w}$

$\therefore$ Internal (material) voids = $\underline{\underline{\dfrac{G_S - G_M}{G_S}}}$

and surface voids = $\underline{\underline{\dfrac{V_S - (W_S - W_w)}{V_S}}}$

APPENDIX 3

STIFFNESS CORRECTIONS FOR CHANGES IN STRAIN

From basic stiffness measurement work it has been found that, at constant strain rate, a linear relationship exists between the logarithms of stiffness and strain, with slope "m".

$$\therefore \quad m = \frac{\log\left(\frac{S_2}{S_1}\right)_\varepsilon}{\log\left(\frac{\varepsilon_2}{\varepsilon_1}\right)}$$

suffix ε denoting the effect of strain on stiffness at constant strain rate.

It has also been found that, at constant strain, a decade increase in strain rate increases stiffness by a constant amount, termed the rate effect "R".

$$\therefore \quad \left(\frac{S_2}{S_1}\right)_T = R^{\log_{10}\left(\frac{R_2}{R_1}\right)}$$

suffix r denoting the effect of strain rate on stiffness at constant strain.

Applying the principle of superposition by which the above two effects have been separated, then the effect of strain and strain rate on the resulting stiffness is:-

$$\log\left(\frac{S_2}{S_1}\right)_T = \log\left(\frac{S_2}{S_1}\right)_\varepsilon + \log\left(\frac{S_2}{S_1}\right)_r$$

suffix T denoting resulting stiffness

hence $\log\left(\frac{S_2}{S_1}\right)_T = m \log\left(\frac{\varepsilon_2}{\varepsilon_1}\right) + \log R \log_{10}\left(\frac{R_2}{R_1}\right)$

for constant frequency $\frac{\varepsilon_2}{\varepsilon_1} = \frac{R_2}{R_1}$ $\quad \therefore \quad \left(\frac{S_2}{S_1}\right)_T = \left(\frac{\varepsilon_2}{\varepsilon_1}\right)^{m+\log_{10}R}$

(For Newtonian fluids $\quad m = -1,\ R = 10,\ m + \log R = 0$

for linear elastic solids $m = 0,\ R = 1,\ \ m + \log R = 0$

$\therefore$ for linear visco-elastic liquids $-1 < (m + \log_{10} R) < 0$)

During repeated loading tests it was required to compensate stiffness for changes in strain level, and hence strain rate, resulting in changes in stiffness exceeding 1%.

The average value of $(m + \log R)$ was found from stiffness measurement tests to be in the order of -0.2 (see Table 12) $\quad \therefore \left(\frac{S_2}{S_1}\right)_T = \left(\frac{\varepsilon_2}{\varepsilon_1}\right)^{-0.2}$

for changes of stiffness less than 1% $\quad \left(\frac{S_2}{S_1}\right)_T < 1.01$

$$\therefore \quad 1.01 > \left(\frac{\varepsilon_2}{\varepsilon_1}\right)^{-0.2} \qquad \text{hence} \quad 1.05 > \left(\frac{\varepsilon_1}{\varepsilon_2}\right)$$

Therefore, changes of strain of less than 5% will alter stiffness by less than 1% and may be ignored. If the change in strain exceeds 5% then the corrected

stiffness is given by:-

$$S_c = \left(\frac{\varepsilon_A}{\varepsilon_n}\right)^{m+\log_{10} R} \cdot S_n$$

where Sc = corrected stiffness to strain ε_A
Sn = stiffness at strain ε_n
ε_A = average strain over test.

N.B. The above corrections are based upon the assumption that the values of "m" and "R" are not significantly affected by the action of repeated applications of load. If the cause of non-linearity in stiffness and reduction in stiffness under repeated loading are similar then the assumption is valid.

APPENDIX 4

COMPUTER PROGRAMME FOR VOID ANALYSIS

Symbols in programme

SPEC = specimen number
VI = internal voids
VS = surface voids
VT = total voids
N = number of blocks of 6 specimens
prefix SUM = sum
prefix T = total
prefix M = mean
prefix D = deviation from mean

Symbols in output

ST DEV = standard deviation about mean
PC ST DEV = percentage standard deviation (= st.dev. as %age of mean)
prefix OA = overall

The typical output shown is that for the 90/110 dense bitumen macadam specimens.

Input format

Job heading in parenthesis (automatic print out),
N, then N cards each with SPEC, VI, VS, VT.

```
HANSON          ORDINAL NUMBER  14     FROM TAPE Y TSN OUT013

PRINTING STARTED                                29/07/70    13.30

JOB VOIDSSD/EVPJRH/HANSON/CIVENG/10             29/07/70    13.16.15
                    *XEQ
                    *CARDLIST
                    *TABLES
                    *SUBFILECIVLIB//CIVENG
                    *SUBFILETRANSLIB//SYS

JOB C-GANISER VERSION 12/6/70 ENTERED  13.16.22     29/07/70          UNDER DIRECTOR
*CHAIN1
*ALGOL


NOTTINGHAM UNIVERSITY ALGOL 6C VERSION 18/12/69  TIME  13.16.27

    1       OPTION=2,3
    2       'BEGIN'
    3       'INTEGER' I,J,I;
    4       'REAL' SUMTVI,SUMTVS,SUMTVT,SUMTDVI,SUMTDVS,SUMTDVT,
    5       TVI,TVS,TVT,
    6       SDTVI,SDTVS,SDTVT,PSDTVI,PSDTVS,PSDTVT;
    7       N=11;
    8       'BEGIN'
    9       'REAL ARRAY' SUMVI,SUMVS,SUMVT,MVI,MVS,MVT,SUMDVI,SUMDVS,SUMDVT,
   10       SDVI,SDVS,SDVT,PSDVI,PSDVS,PSDVT(1','N);
   11       'REAL ARRAY' SPEC,VI,VS,VT(1','6:1','N);
   12       'REAL ARRAY' DVI,DVS,DVT,DTVI,DTVS,DTVT(1','6);
   13       SUMTVI=SUMTVS=SUMTVI=SUMTDVI=SUMTDVS=SUMTDVI=0;
   14       'FOR' J=1 'STEP' 1 'UNTIL' N 'DO'  'BEGIN'
   15       SUMVI(J)=SUMVS(J)=SUMVT(J)=0;
   16       SUMDVI(J)=SUMDVS(J)=SUMDVT(J)=0;
   17       'FOR' I=1 'STEP' 1 'UNTIL' 6 'DO'  'BEGIN'
   18       SPEC(I,J)=RIN; VI(I,J)=RIN; VS(I,J)=RIN; VT(I,J)=RIN;
   19       SUMVI(J)=SUMVI(J)+VI(I,J);
   20       SUMVS(J)=SUMVS(J)+VS(I,J);
   21       SUMVT(J)=SUMVT(J)+VT(I,J);
   22       'END';
   23       SUMTVI=SUMTVI+SUMVI(J);
   24       SUMTVS=SUMTVS+SUMVS(J);
   25       SUMTVT=SUMTVI+SUMVT(J);
   26       MVI(J)=SUMVI(J)/6;
   27       MVS(J)=SUMVS(J)/6;
   28       MVT(J)=SUMVT(J)/6;
   29       'FOR' I=1 'STEP' 1 'UNTIL' 6 'DO'  'BEGIN'
   30       DVI(I)=(VI(I,J)-MVI(J))**2;
   31       DVS(I)=(VS(I,J)-VS(J))**2;
   32       DVT(I)=(VT(I,J)-MVT(J))**2;
   33       SUMDVI(J)=SUMDVI(J)+DVI(I);
   34       SUMDVS(J)=SUMDVS(J)+DVS(I);
   35       SUMDVT(J)=SUMDVT(J)+DVI(I);
   36       'END';
   37       SDVI(J)=(SUMDVI(J)/5)**0.5;
   38       SDVS(J)=(SUMDVS(J)/5)**0.5;
```

```
39      SDVT(J)=(SUMDVT(J)/5)**0.5;
40      PSDVI(J)=(SDVI(J)/MVI(J))*100;
41      PSDVS(J)=(SDVS(J)/MVS(J))*100;
42      PSDVT(J)=(SDVT(J)/MVT(J))*100;
43      'END';
44      MTVI=SUMTVI/(6*N);
45      MTVS=SUMTVS/(6*N);
46      MTVT=SUMTVT/(6*N);
47      'FOR' J=1 'STEP' 1 'UNTIL' N 'DO'  'BEGIN'
48      'FOR' I=1 'STEP' 1 'UNTIL' 6 'DO'  'BEGIN'
49      DTVI(J)=(VI(I,J)-MTVI)**2;
50      DTVS(I)=(VS(I,J)-MTVS)**2;
51      DTVT(I)=(VT(I,J)-MTVT)**2;
52      SUMTDVI=SUMTDVI+DTVI(I);
53      SUMTDVS=SUMTDVS+DTVS(I);
54      SUMTDVT=SUMTDVT+DTVT(I);
55      'END'; 'END';
56      SDTVI=((SUMTDVI/(6*N-1))**0.5);
57      SDTVS=((SUMTDVS/(6*N-1))**0.5);
58      SDTVT=((SUMTDVT/(6*N-1))**0.5);
59      PSDTVI=(SDTVI/MTVI)*100;
60      PSDTVS=(SDTVS/MTVS)*100;
61      PSDTVT=(SDTVT/MTVT)*100;
62      LINES(2);
63      TEXT('('('9S')'SPECIMEN'('9S')'INT'*'VOIDS'('10S')'
64      SURF'*'VOIDS'('10S')'TOTE'*'VOIDS')'); LINES(2);
65      'FOR' J=1 'STEP' 1 'UNTIL' N 'DO'  'BEGIN'
66      'FOR' I=1 'STEP' 1 'UNTIL' 6 'DO'  'BEGIN'
67      SPACES(9); PRINT(SPEC(I,J),3,0);
68      SPACES(11); PRINT(VI(I,J),2,2); SPACES(11);
69      PRINT(VS(I,J),2,2); SPACES(11);
70      PRINT(VT(I,J),2,2); LINES(1);
71      'END';
72      SPACES(9); TEXT('('MEAN')'); SPACES(10); PRINT(MTVI,2,2);
73      SPACES(11); PRINT(MVS(J),2,2); SPACES(11); PRINT(MVT(J),2,2); LINES(1);
74      SPACES(5); TEXT('('ST'*'DEV')'); SPACES(11); PRINT(SDVI(J),2,2);
75      SPACES(11); PRINT(SDVS(J),2,2); SPACES(11); PRINT(SDVT(J),2,2);
76      LINES(1);
77      SPACES(9); TEXT('('PC'*'ST'*'DEV')'); SPACES(8); PRINT(PSDVI(J),2,2);
78      SPACES(11); PRINT(PSDVS(J),2,2); SPACES(11); PRINT(PSDVT(J),2,2);
79      LINES(2);
80      'END';
81      SPACES(9); TEXT('('DA'*'MEAN')'); SPACES(10); PRINT(MTVI,2,2);
82      SPACES(11); PRINT(MTVS,2,2); SPACES(11); PRINT(MTVT,2,2); LINES(1);
83      SPACES(9); TEXT('('DA'*'ST'*'DEV')'); SPACES(8); PRINT(SDTVI,2,2);
84      SPACES(11); PRINT(SDTVS,2,2); SPACES(11); PRINT(SDTVT,2,2); LINES(1);
85      SPACES(9); TEXT('('PC'*'DA'*'ST'*'DEV')'); SPACES(5);
86      PRINT(PSDTVI,2,2); SPACES(11); PRINT(PSDTVS,2,2); SPACES(11);
87      PRINT(PSDTVT,2,2);
88      'END'; STOP; 'END'
REFERENCE TABLE
 ADDRESS  NAME


569 WORDS OF CODING.

EXTERNAL NAMES USED:
        L5300   L5302     IIN     RIN    LINES    TEXT  SPACES   PRINT    STOP


*DATA
```

NOTTINGHAM TRANSPORT SCHEME VERSION 09/12/69

*** LABEL TRACE NOW COUNTS IN DECIMAL ***

DENSE BITUMEN MACADAM 90/110

SPECIMEN	INT VOIDS	SUR VOIDS	TOT VOIDS
59	6.19	10.35	15.90
60	6.23	6.00	11.88
61	6.95	6.00	12.53
62	6.76	5.69	12.07
63	6.80	5.64	12.07
64	6.45	7.00	12.98
MEAN	6.56	6.78	12.90
ST DEV	0.32	1.82	1.52
PC ST DEV	4.85	26.79	11.78
65	5.13	11.00	15.53
66	7.21	7.35	14.05
67	7.02	6.93	13.44
68	7.78	6.86	14.09
69	6.30	7.32	14.20
70	7.40	6.34	13.21
MEAN	6.81	7.63	14.09
ST DEV	0.96	1.69	0.81
PC ST DEV	14.05	22.14	5.75
71	6.30	6.92	12.76
72	6.53	7.23	13.29
73	6.57	6.53	12.64
74	7.06	7.14	13.71
75	6.76	7.71	13.97
76	6.76	7.71	14.12
MEAN	6.66	7.21	13.42
ST DEV	0.26	0.46	0.62
PC ST DEV	3.88	6.36	4.64
77	6.67	6.29	12.72
78	6.34	6.72	12.64
79	5.62	7.40	12.60
80	5.43	8.05	13.06
81	6.49	6.24	12.30
82	5.96	7.33	12.87
MEAN	6.12	7.01	12.70
ST DEV	0.55	0.71	0.26
PC ST DEV	8.95	10.16	2.03
83	6.68	6.93	13.14
84	6.53	5.41	11.62
85	6.85	6.22	12.49
86	6.67	5.53	12.03
87	6.95	5.61	12.15
88	7.02	6.14	12.72
MEAN	6.79	5.97	12.36
ST DEV	0.19	0.57	0.54

PC ST DEV	2.77	9.62	4.37
89	6.57	6.95	13.06
90	6.26	7.60	13.40
91	6.64	6.39	12.60
92	6.67	6.92	13.29
93	5.92	8.07	13.52
94	7.06	5.78	12.45
MEAN	6.55	6.95	13.05
ST DEV	0.41	0.82	0.44
PC ST DEV	6.30	11.79	3.36
95	6.68	5.98	12.22
96	6.42	6.93	12.91
97	6.83	5.75	12.19
98	6.99	6.05	12.60
99	7.29	5.77	12.64
100	6.87	6.57	12.98
MEAN	6.85	6.18	12.59
ST DEV	0.29	0.47	0.33
PC ST DEV	4.27	7.68	2.64
101	6.34	7.67	13.52
102	6.04	7.33	12.91
103	7.10	6.73	12.98
104	6.57	6.49	12.83
105	7.44	5.96	12.98
106	6.39	6.41	12.38
MEAN	6.70	6.77	12.93
ST DEV	0.53	0.63	0.36
PC ST DEV	7.90	9.32	2.82
107	7.14	5.04	11.81
108	6.50	6.15	12.07
109	6.67	5.71	12.19
110	6.53	6.12	12.26
111	7.40	5.67	12.64
112	6.57	5.27	11.77
MEAN	6.65	5.66	12.12
ST DEV	0.40	0.45	0.32
PC ST DEV	5.81	7.86	2.65
113	7.56	6.06	13.17
114	7.14	6.20	12.91
115	8.24	5.01	12.83
116	7.52	6.12	13.17
117	8.05	5.45	13.02
118	8.12	5.21	12.91
MEAN	7.77	5.68	13.00
ST DEV	0.43	0.52	0.14
PC ST DEV	5.54	9.09	1.11
119	7.48	5.93	12.98
120	8.09	5.59	13.21
121	7.25	6.50	13.29
122	6.67	7.06	13.44
123	7.37	6.22	13.02
124	7.29	6.76	13.55
MEAN	7.39	6.34	13.25
ST DEV	0.60	0.54	0.23
PC ST DEV	5.41	8.53	1.70

125	6.64	6.62	12.98
126	6.49	6.56	12.64
127	7.33	6.18	13.06
128	8.09	5.27	12.91
129	7.21	6.63	13.36
130	7.02	7.09	13.59
MEAN	7.13	6.43	13.09
ST DEV	0.57	0.64	0.34
PC ST DEV	8.01	9.97	2.58
131	7.10	6.06	12.72
132	7.40	5.67	12.64
133	6.99	6.50	13.02
134	7.63	5.92	13.25
135	7.59	5.57	12.72
136	7.37	5.53	12.49
MEAN	7.35	5.88	12.81
ST DEV	0.26	0.37	0.28
PC ST DEV	3.50	6.28	2.17
137	7.44	6.34	13.33
138	6.68	5.85	11.96
139	7.56	5.60	12.72
140	7.14	6.46	13.14
141	7.63	6.17	13.36
142	7.21	5.72	12.53
MEAN	7.28	6.02	12.84
ST DEV	0.35	0.35	0.55
PC ST DEV	4.80	5.82	4.24
143	7.10	6.28	12.95
144	6.83	6.52	12.91
145	7.40	5.60	12.57
146	6.45	6.01	12.07
147	7.40	6.70	13.59
148	7.25	6.32	13.14
MEAN	7.07	6.24	12.87
ST DEV	0.37	0.39	0.52
PC ST DEV	5.26	6.25	4.01
149	7.40	5.97	12.91
150	7.71	5.76	13.02
151	7.71	5.41	12.45
152	7.18	5.38	12.19
153	6.91	5.36	11.92
154	7.06	6.91	13.48
MEAN	7.33	5.80	12.66
ST DEV	0.34	0.60	0.58
PC ST DEV	4.59	10.30	4.57
155	7.48	5.73	12.76
156	7.48	6.32	12.72
157	7.59	5.30	12.49
158	7.10	6.06	12.76
159	7.19	5.92	12.68
160	7.78	6.34	13.63
MEAN	7.44	5.95	12.84
ST DEV	0.25	0.39	0.40
PC ST DEV	3.40	6.61	3.11

161	7.48	5.52	12.64
162	7.10	6.34	12.98
163	7.71	4.65	12.00
164	6.99	6.14	12.72
165	7.52	5.48	12.60
166	7.25	5.27	12.15
MEAN	7.34	5.57	12.51
ST DEV	0.27	0.61	0.37
PC ST DEV	3.74	10.97	2.95
167	6.80	6.47	12.83
168	7.48	5.09	12.19
169	7.29	5.52	12.41
170	7.10	5.55	12.57
171	7.02	6.40	12.95
172	7.14	5.57	12.30
MEAN	7.14	5.82	12.54
ST DEV	0.23	0.54	0.30
PC ST DEV	3.25	9.24	2.39
173	7.14	4.00	10.86
174	6.04	4.72	10.48
175	6.42	5.12	11.24
176	6.49	4.50	10.71
177	6.45	5.62	11.73
178	6.53	5.42	11.62
MEAN	6.51	4.90	11.11
ST DEV	0.36	0.61	0.51
PC ST DEV	5.45	12.39	4.56
179	7.10	5.39	12.11
180	6.64	4.33	10.71
181	5.81	5.07	10.59
182	6.83	5.13	11.58
183	6.57	4.66	10.93
184	6.26	5.20	11.24
MEAN	6.54	4.96	11.19
ST DEV	0.45	0.39	0.56
PC ST DEV	6.91	7.91	5.15
188	5.62	6.89	12.11
189	6.36	5.23	11.20
190	5.58	6.78	11.96
191	6.23	5.74	11.62
192	6.11	5.46	11.24
193	6.61	5.26	11.50
MEAN	6.08	5.89	11.61
ST DEV	0.40	0.75	0.37
PC ST DEV	6.64	12.77	3.20
OA MEAN	6.92	6.16	12.66
OA ST DEV	0.58	0.96	0.83
PC OA ST DEV	8.37	15.57	6.59

**** CPU TIME 000048 SECONDS. ELAPSED TIME 000077 SECONDS. INPUT 000134 CARDS.

TIME 13.17.36 RAN/EL/000M49S/001M20S

HANSON ORDINAL NUMBER 14 FROM TAPE Y TSN 0UT013

APPENDIX 5

COMPUTER PROGRAMME FOR STIFFNESS CORRECTIONS AND BEST FIT LINES FOR STIFFNESS AND LIVES UNDER REPEATED LOADING

Programme "BEST FIT LINE LOG." computes best fit line for stiffness and strain with no strain rate correction on logarithmic scales.

Programme "STIFF + BFLS" computes stiffnesses adjusted to strain rate of and the best fit line for adjusted stiffness and strain on logarithmic scales. Also the best fit lines for log.strain/log.log. cycles relationships.

Symbols in programmes

	SPEC	=	specimen number
	STR	=	strain
	RS	=	strain rate
	STI	=	stiffness
	NTY	=	cycles to 90% initial stiffnesses
	SYF	=	" " 75% " "
	SXY	=	" " 60% " "
	DSTR	=	strain in $\mu\varepsilon$
	M	=	number of sets of conditions (i.e. temperature)
	N	=	number of specimens
	R	=	rate effect
prefix	SUM	=	sum
	N	=	number of - -
	A	=	slope of best fit line
	B	=	value of best fit line at $1\mu\varepsilon$
	C	=	value of best fit line at strain level A to H ($A = 5.10^{-3}$, $B = 2.10^{-3}$, $C = 1.10^{-3}$ --- $H = 2.10^{-5}$)

Input format for "STIFF + BFLS"

Job heading in parenthesis (automatic print out),
M, then M sets of cards each with N, R, followed by N cards each with SPEC, STR, RS, STI, NTY, SYF, SXY.

```
HANSON          ORDINAL NUMBER  02      FROM TAPE Y TSN OUTC17

PRINTING STARTED                                21/07/70   29.51

JOB BESTFITLINELOG./EVAJMH/HANSON/CIVENG/5      21/07/70   29.31.30


****** WARNING - AT START OF THIS JOB YOU HAD ONLY 0000144 MINS ELAPSED TIME LEFT ***
                *XEQ
                *CARDLIST
                *TABLES
                *SUBFILECIVLIB//CIVENG
                *SUBFILETRANSLIB//SYS

JOB ORGANISER VERSION 17/06/70 ENTERED   29.31.40     21/07/70          UNDER DIRECTOR
*CHAIN;
*ALGOL


NOTTINGHAM UNIVERSITY ALGOL 60 VERSION 18/12/69  TIME  29.31.43

    1         OPTION2,3
    2     'BEGIN'
    3     'INTEGER' N,I;
    4     'REAL' STR,STI,SUM X,SUM Y,SUM XX, SUM XY,A,B,C;
    5     N=IIN;
    6     'BEGIN'
    7     'REAL ARRAY' STR,STI,DSTR,DSTI,X,Y,XX,XY(1:N);
    8     'FOR' I=1 'STEP' 1 'UNTIL' N 'DO'   'BEGIN'
    9     STR(I)=RIN;       STI(I)=RIN;
   10     DSTR(I)=STR(I)*(1'E'6);
   11     DSTI(I)=STI(I);
   12     X(I)=LN(DSTR(I));
   13     Y(I)=LN(DSTI(I));
   14     'END';
   15     SUM X=0;   SUM Y=0;   SUM XX=0;   SUM XY=0;
   16     'FOR' I=1 'STEP' 1 'UNTIL' N 'DO'   'BEGIN'
   17     XX(I)=X(I)**2;
   18     XY(I)=X(I)*Y(I);
   19     SUM X=SUM X + X(I);
   20     SUM Y=SUM Y+Y(I);
   21     SUM XX=SUM XX + XX(I);
   22     SUM XY = SUM XY + XY(I);
   23     'END';
   24     A=(SUM X*SUM Y - N*SUM XY)/(SUM X**2 - N*SUM XX);
   25     B=(SUM Y - A*SUM X) / N;
   26     C=B+A*LN(100);
   27     LINES(2);
   28     TEXT ( '(' BEST '*' FIT '*' LINE ')' ) ;
   29     LINES (2) ;
   30     TEXT('(' SLOPE '**' = '*''1' ) ; E PRINT (A,4);
   31     LINES (1) ;
   32     TEXT('('INTERCEPT'*'AT'*''1E-4'*'='*''')'); EPRINT(EXP(C),2);
   33     'END' ;
   34     STOP ;
   35     'END'
```

```
HANSON          ORDINAL NUMBER  09     FROM TAPE Y TSN 0UTO17

PRINTING STARTED                              06/07/70   19.27

JOB STIFF.LIFEBFLS/EVPJHH/HANSON/CIVENG/10     06/07/70   19.06.07

                *XEQ
                *CARDLIST
                *TABLES
                *SUBFILECIVLIB//CIVENG
                *SUBFILETRANSLIB//SYS

JOB ORGANISER VERSION 17/06/70 ENTERED   19.06.15     06/07/70          UNDER DIRECTOR
*CHAIN)
*ALGOL


NOTTINGHAM UNIVERSITY ALGOL 60 VERSION 18/12/69  TIME  19.06.18

    1          OPTION2,3
    2       'BEGIN'
    3       'INTEGER' N,NNTY,NSYF,NSXY,I,J,M;
    4       'REAL' R,SUMX,SUMY,SUMXX,SUMXY,SUMXNTY,SUMYNTY,SUMXXNTY,SUMXYNTY,
    5       SUMXSYF,SUMYSYF,SUMXXSYF,SUMXYSYF,SUMXSXY,SUMYSXY,SUMXXSXY,SUMXYSXY,
    6        A,B,C,ANTY,BNTY,CANTY,CBNTY,CCNTY,CDNTY,CENTY,CFNTY,CGNTY,CHNTY,
    7       ASYF,BSYF,CASYF,CBSYF,CCSYF,CDSYF,CESYF,CFSYF,CGSYF,CHSYF,
    8       ASXY,BSXY,CASXY,CBSXY,CCSXY,CDSXY,CESXY,CFSXY,CGSXY,CHSXY;
    9       M=IIN;
   10       'FOR' J=1 'STEP' 1 'UNTIL' M 'DO' 'BEGIN'
   11       N=IIN ;      R=RIN;
   12       'BEGIN'
   13       'REAL ARRAY' SPEC,STR,RS,STI,NTY,SYF,SXY,DSTR,X,Y,Z,XX,XY,
   14       XNTY,YNTY,XXNTY,XYNTY,XSYF,YSYF,XXSYF,XYSYF,
   15       XSXY,YSXY,XXSXY,XYSXY[1:'N];
   16       NNTY=NSYF=NSXY=0;
   17       'FOR' I=1 'STEP' 1 'UNTIL' N 'DO' 'BEGIN'
   18       SPEC[I]=RIN;STR[I]=RIN;RS[I]=RIN;STI[I]=RIN;NTY[I]=RIN;
   19       SYF[I]=RIN;SXY[I]=RIN;
   20       DSTR[I]=STR[I]*('E'6);
   21       X[I]=LN(DSTR[I]);
   22       Y[I]=LN(STI[I])*(LN(R)*(LN(100)-LN(RS[I]))/LN(10));
   23       'IF'NTY[I]'EQ'0'THEN''GOTO'NONTY;
   24       'IF'NTY[I]'NE'0'THEN''GOTO'YESNTY;
   25       NONTY',' XNTY[I]=0; YNTY[I]=0; 'GOTO'BOTHNTY;
   26       YESNTY',' NNTY=NNTY+1; XNTY[I]=X[I]; YNTY[I]=LN(LN(NTY[I]));
   27       'GOTO'BOTHNTY;
   28       BOTHNTY',' 'IF'SYF[I] 'EQ'0'THEN''GOTO'NOSYF;
   29       'IF'SYF[I]'NE'0'THEN''GOTO'YESSYF;
   30       NOSYF',' XSYF[I]=0; YSYF[I]=0; 'GOTO'BOTHSYF;
   31       YESSYF',' NSYF=NSYF+1; XSYF[I]=X[I]; YSYF[I]=LN(LN(SYF[I]));
   32       'GOTO'BOTHSYF;
   33       BOTHSYF',' 'IF'SXY[I]'EQ'0'THEN''GOTO'NOSXY;
   34       'IF'SXY[I]'NE'0'THEN''GOTO'YESSXY;
   35       NOSXY',' XSXY[I]=0; YSXY[I]=0; 'GOTO'BOTHSXY;
   36       YESSXY',' NSXY=NSXY+1; XSXY[I]=X[I]; YSXY[I]=LN(LN(SXY[I]));
   37       'GOTO'BOTHSXY;
   38       BOTHSXY',' 'END';
```

```
SUMX=SUMY=SUMXX=SUMXY=SUMXNTY=SUMYNTY=SUMXXNTY=SUMXYNTY=0;
SUMXSYF=SUMYSYF=SUMXXSYF=SUMXYSYF=SUMXSXY=SUMYSXY=SUMXXSXY=SUMXYSXY=0;
'FOR' I=1 'STEP' 1 'UNTIL' N 'DO'   'BEGIN'
XX(I)=X(I)**2;
XY(I)=X(I)*Y(I);
SUM X=SUM X + X(I);
SUM Y=SUM Y+Y(I);
SUM XX=SUM XX + XX(I);
SUM XY = SUM XY + XY(I);
XXNTY(I)=XNTY(I)**2;
XYNTY(I)=XNTY(I)*YNTY(I);
SUMXNTY=SUMXNTY+XNTY(I);
SUMYNTY=SUMYNTY+YNTY(I);
SUMXXNTY=SUMXXNTY+XXNTY(I);
SUMXYNTY=SUMXYNTY+XYNTY(I);
XXSYF(I)=XSYF(I)**2;
XYSYF(I)=XSYF(I)*YSYF(I);
SUMXSYF=SUMXSYF+XSYF(I);
SUMYSYF=SUMYSYF+YSYF(I);
SUMXXSYF=SUMXXSYF+XXSYF(I);
SUMXYSYF=SUMXYSYF+XYSYF(I);
XXSXY(I)=XSXY(I)**2;
XYSXY(I)=XSXY(I)*YSXY(I);
SUMXSXY=SUMXSXY+XSXY(I);
SUMYSXY=SUMYSXY+YSXY(I);
SUMXXSXY=SUMXXSXY+XXSXY(I);
SUMXYSXY=SUMXYSXY+XYSXY(I);
'END';
A=(SUM X*SUM Y - N*SUM XY)/(SUM X**2 - N*SUM XX);
B=(SUM Y - A*SUM X) / N;
C=B+A*LN(100);
ANTY=(SUMXNTY*SUMYNTY-NNTY*SUMXYNTY)/(SUMXNTY**2-NNTY*SUMXXNTY);
BNTY=(SUMYNTY-ANTY*SUMXNTY)/NNTY;
CANTY=BNTY+ANTY*LN(5000);
CBNTY=BNTY+ANTY*LN(2000);
CCNTY=BNTY+ANTY*LN(1000);
CDNTY=BNTY+ANTY*LN( 500);
CENTY=BNTY+ANTY*LN( 200);
CFNTY=BNTY+ANTY*LN( 100);
CGNTY=BNTY+ANTY*LN(  50);
CHNTY=BNTY+ANTY*LN(  20);
ASYF=(SUMXSYF*SUMYSYF-NSYF*SUMXYSYF)/(SUMXSYF**2-NSYF*SUMXXSYF);
BSYF=(SUMYSYF-ASYF*SUMXSYF)/NSYF;
CASYF=BSYF+ASYF*LN(5000);
CBSYF=BSYF+ASYF*LN(2000);
CCSYF=BSYF+ASYF*LN(1000);
CDSYF=BSYF+ASYF*LN( 500);
CESYF=BSYF+ASYF*LN( 200);
CFSYF=BSYF+ASYF*LN( 100);
CGSYF=BSYF+ASYF*LN(  50);
CHSYF=BSYF+ASYF*LN(  20);
ASXY=(SUMXSXY-SUMYSXY-NSXY+SUMXYSXY)/(SUMXSXY**2-NSXY+SUMXXSXY);
BSXY=(SUMYSXY-ASXY*SUMXSXY)/NSXY;
CASXY=BSXY+ASXY*LN(5000);
CBSXY=BSXY+ASXY*LN(2000);
CCSXY=BSXY+ASXY*LN(1000);
CDSXY=BSXY+ASXY*LN( 500);
CESXY=BSXY+ASXY*LN( 200);
CFSXY=BSXY+ASXY*LN( 100);
CGSXY=BSXY+ASXY*LN(  50);
CHSXY=BSXY+ASXY*LN(  20);
```

```
100       LINES(2);
101       TEXT('('BEST'*'FIT'*'LINE'*'STRAIN*STIFFNESS'('2SS')''');
102       TEXT('(' SLOPE '*' = '*''')' ) ; E PRINT (A,4); SPACES(10)
103       TEXT('('INTERCEPT'*'AT'*'1E-4'*'='*''')');
104       EPRINT(EXP(C),2); LINES(1);
105       TEXT('('BEST'*'FIT'*'LINE
106       '*'STRAIN*CYCLES'*'TO'*'90PC'*'STIFFNESS'('10S')''');
107       TEXT('(' SLOPE '*' = '*''')' ) ; E PRINT (ANTY,4);    SPACES(10);
108       TEXT('('LOG'*'BASE'*'E'*'OF'*'INTERCEPT'*'AT'*'1E-6'*'='*''')');
109       EPRINT(EXP(BNTY),2); LINES(1);
110       TEXT('('BEST'*'FIT'*'LINE
111       '*'STRAIN*CYCLES'*'TO'*'75PC'*'STIFFNESS'('10S')''');
112       TEXT('(' SLOPE '*' = '*''')' ) ; E PRINT (ASYF,4);    SPACES(10);
113       TEXT('('LOG'*'BASE'*'E'*'OF'*'INTERCEPT'*'AT'*'1E-6'*'='*''')');
114       EPRINT(EXP(BSYF),2); LINES(1);
115       TEXT('('BEST'*'FIT'*'LINE
116       '*'STRAIN*CYCLES'*'TO'*'60PC'*'STIFFNESS'('10S')''');
117       TEXT('(' SLOPE '*' = '*''')' ) ; E PRINT (ASXY,4);    SPACES(10);
118       TEXT('('LOG'*'BASE'*'E'*'OF'*'INTERCEPT'*'AT'*'1E-6'*'='*''')');
119       EPRINT(EXP(BSXY),2); LINES(4);
120       TEXT('(''('04S')'SPECIMEN'('10S')'STIFFNESS'('10S')'STRAIN'('11S')'
121       R'*'OF'*'S'('11S')'ADJ'*'STIFFNESS'('10S')'
122       CYCLES'*'*'TO'*'*'*'PERCENTAGE'*'*'*'STIFFNESS')');
123       LINES(1);
124       TEXT('('('099S')'
125       90PC'('9S')'75PC'('9S')'60PC')'); LINES(2);
126       'FOR'I=1'STEP'1'UNTIL'N'DO''BEGIN'
127       SPACES(03); PRINT(SPEC(I),3,0); SPACES(10); EPRINT(ST1(I),2);
128       SPACES(07); EPRINT(STR(I),2); SPACES(06); EPRINT(RS(I),2); SPACES(10);
129       EPRINT(EXP(Y(I)),2); SPACES(09); EPRINT(NTY(I),1); SPACES(3);
130       EPRINT(SYF(I),1); SPACES(3); EPRINT(SXY(I),1); LINES(1);
131       'END'; LINES(4);
132       TEXT('('BEST'*'FIT'*'LINES'*'STRAIN*CYCLES'*'TO'*'90PC'*'75PC'*'60PC
133       '*'STIFFNESS')');  LINES(2);
134       TEXT('('('05S')'STRAIN'('17S')'CYCLES'*'*'TO'('18S')'CYCLES'*'*'TO
135       '('18S')'CYCLES'*'*'TO')'); LINES(1);
136       TEXT('('('26S')'90PC'*'STIFFNESS'('14S')'75PC'*'STIFFNESS'('14S')'
137       60PC'*'STIFFNESS')');
138       LINES(2);
139       TEXT('('('6S')'5E-3'('16S')''')'); EPRINT(EXP(EXP(CANTY)),2);
140       SPACES(17); EPRINT(EXP(EXP(CASYF)),2); SPACES(17);
141       EPRINT(EXP(EXP(CASXY)),2); LINES(1);
142       TEXT('('('6S')'2E-3'('16S')''')'); EPRINT(EXP(EXP(CBNTY)),2);
143       SPACES(17); EPRINT(EXP(EXP(CBSYF)),2); SPACES(17);
144       EPRINT(EXP(EXP(CBSXY)),2); LINES(1);
145       TEXT('('('6S')'1E-3'('16S')''')'); EPRINT(EXP(EXP(CCNTY)),2);
146       SPACES(17); EPRINT(EXP(EXP(CCSYF)),2); SPACES(17);
147       EPRINT(EXP(EXP(CCSXY)),2); LINES(1);
148       TEXT('('('6S')'5E-4'('16S')''')'); EPRINT(EXP(EXP(CDNTY)),2);
149       SPACES(17); EPRINT(EXP(EXP(CDSYF)),2); SPACES(17);
150       EPRINT(EXP(EXP(CDSXY)),2); LINES(1);
151       TEXT('('('6S')'2E-4'('16S')''')'); EPRINT(EXP(EXP(CENTY)),2);
152       SPACES(17); EPRINT(EXP(EXP(CESYF)),2); SPACES(17);
153       EPRINT(EXP(EXP(CESXY)),2); LINES(1);
154       TEXT('('('6S')'1E-4'('16S')''')'); EPRINT(EXP(EXP(CFNTY)),2);
155       SPACES(17); EPRINT(EXP(EXP(CFSYF)),2); SPACES(17);
156       EPRINT(EXP(EXP(CFSXY)),2); LINES(1);
157       TEXT('('('6S')'5E-5'('16S')''')'); EPRINT(EXP(EXP(CGNTY)),2);
158       SPACES(17); EPRINT(EXP(EXP(CGSYF)),2); SPACES(17);
159       EPRINT(EXP(EXP(CGSXY)),2); LINES(1);
160       TEXT('('('6S')'2E-5'('16S')''')'); EPRINT(EXP(EXP(CHNTY)),2);
161       SPACES(17); EPRINT(EXP(EXP(CHSYF)),2); SPACES(17);
162       EPRINT(EXP(EXP(CHSXY)),2); PAGE;
163       'END';'END';STOP;'END'
REFERENCE TABLE
  ADDRESS  NAME
```

DENSE BITUMEN MACADAM 90/110 0 C

BEST FIT LINE STRAIN*STIFFNESS SLOPE = -5.9171E -1 INTERCEPT AT 1E-4 = 2.12E 6
BEST FIT LINE STRAIN*CYCLES TO 90PC STIFFNESS SLOPE = -3.3959E -1 LOG BASE E OF INTERCEPT AT 1E-6 = 1.25E 1
BEST FIT LINE STRAIN*CYCLES TO 75PC STIFFNESS SLOPE = -4.9118E -1 LOG BASE E OF INTERCEPT AT 1E-6 = 5.99E 1
BEST FIT LINE STRAIN*CYCLES TO 60PC STIFFNESS SLOPE = -5.3765E -1 LOG BASE E OF INTERCEPT AT 1E-6 = 1.07E 2

SPECIMEN	STIFFNESS	STRAIN	R OF S	ADJ STIFFNESS	CYCLES TO 90PC	PERCENTAGE 75PC	STIFFNESS 60PC
161	2.36E 6	1.33E -4	1.82E 2	2.01E 6	2.0E 1	3.5E 2	1.8E 3
162	2.38E 6	1.41E -4	1.96E 2	1.99E 6	1.0E 1	1.0E 2	1.0E 3
163	2.96E 6	1.29E -4	1.79E 2	2.54E 6	1.8E 1	3.0E 2	1.4E 3
164	3.10E 6	8.87E -5	2.98E 1	4.29E 6	5.3E 0	2.4E 2	3.5E 4
166	2.48E 6	8.40E -5	2.80E 1	3.42E 6	1.6E 1	7.0E 2	1.0E 4
167	1.41E 6	3.42E -4	5.15E 2	9.16E 5	8.0E 0	4.6E 1	1.2E 2
168	1.26E 6	3.92E -4	6.35E 2	7.74E 5	2.5E 0	9.7E 0	4.0E 1
169	8.81E 5	4.13E -4	7.27E 2	5.18E 5	6.0E 0	2.0E 1	7.5E 1
170	1.02E 6	2.06E -4	6.89E 1	1.13E 6	9.0E 0	1.6E 2	7.0E 2
171	1.01E 6	2.06E -4	6.88E 1	1.12E 6	9.0E 0	1.6E 2	8.0E 2
172	1.72E 6	2.05E -4	6.83E 1	1.91E 6	1.5E 1	1.5E 2	8.0E 2
173	3.30E 6	1.29E -5	1.69E 1	5.32E 6	0.0	0.0	0.0
174	4.19E 6	1.16E -5	1.30E 1	7.16E 6	0.0	0.0	0.0
176	2.92E 6	1.70E -5	2.08E 1	4.45E 6	0.0	0.0	0.0

BEST FIT LINES STRAIN*CYCLES TO 90PC 75PC 60PC STIFFNESS

STRAIN	CYCLES TO 90PC STIFFNESS	CYCLES TO 75PC STIFFNESS	CYCLES TO 60PC STIFFNESS
5E-3	2.01E 0	2.49E 0	2.99E 0
2E-3	2.59E 0	4.19E 0	6.03E 0
1E-3	3.34E 0	7.49E 0	1.35E 1
5E-4	4.60E 0	1.69E 1	4.41E 1
2E-4	8.03E 0	8.47E 1	4.92E 2
1E-4	1.39E 1	5.13E 2	8.10E 3
5E-5	2.81E 1	6.45E 3	4.71E 5
2E-5	9.51E 1	9.44E 5	1.93E 9

DENSE BITUMEN MACADAM 90/110 +10 C

BEST FIT LINE STRAIN*STIFFNESS SLOPE = -6.3026E -1 INTERCEPT AT 1E-6 = 7.10E 5
BEST FIT LINE STRAIN*CYCLES TO 90PC STIFFNESS SLOPE = -7.8895E -1 LOG BASE E OF INTERCEPT AT 1E-6 = 1.56E 2
BEST FIT LINE STRAIN*CYCLES TO 75PC STIFFNESS SLOPE = -6.2127E -1 LOG BASE E OF INTERCEPT AT 1E-6 = 1.31E 2
BEST FIT LINE STRAIN*CYCLES TO 60PC STIFFNESS SLOPE = -5.5546E -1 LOG BASE E OF INTERCEPT AT 1E-6 = 1.35E 2

SPECIMEN	STIFFNESS	STRAIN	R OF S	ADJ STIFFNESS	CYCLES TO 90PC	PERCENTAGE 75PC	STIFFNESS 60PC
59	4.11E 5	1.44E -4	2.02E 2	3.06E 5	6.5E 1	7.0E 2	6.1E 3
60	7.33E 5	1.16E -4	1.48E 2	6.23E 5	1.0E 2	3.0E 3	3.5E 4
61	5.59E 5	1.22E -4	1.63E 2	4.56E 5	8.5E 1	3.5E 3	4.0E 4
62	5.29E 5	1.18E -4	1.61E 2	4.34E 5	9.0E 1	1.5E 3	2.1E 4
63	8.10E 5	1.08E -4	1.44E 2	6.96E 5	7.0E 1	2.1E 3	1.6E 4
64	6.89E 5	9.50E -5	1.27E 2	6.22E 5	7.0E 1	2.8E 3	4.0E 4
65	7.19E 5	1.73E -4	2.36E 2	5.04E 5	1.2E 1	2.5E 2	2.0E 3
66	6.55E 5	1.57E -4	2.13E 2	4.78E 5	3.1E 1	3.6E 2	2.4E 3
67	6.11E 5	1.61E -4	2.15E 2	4.45E 5	6.0E 1	9.0E 2	4.3E 3
68	7.00E 5	1.68E -4	2.25E 2	4.99E 5	1.4E 1	3.0E 2	3.0E 3
69	7.29E 5	1.70E -4	2.31E 2	5.14E 5	2.8E 1	4.0E 2	4.3E 3
70	8.78E 5	1.74E -4	2.34E 2	6.15E 5	4.8E 1	5.3E 2	3.2E 3
71	5.30E 5	3.90E -4	5.60E 2	2.61E 5	5.1E 0	3.7E 1	2.0E 2
72	6.51E 5	3.65E -4	5.02E 2	3.33E 5	5.0E 0	2.8E 1	1.5E 2
73	8.59E 5	3.64E -4	5.04E 2	4.36E 5	2.5E 0	1.8E 1	7.1E 1
74	4.98E 5	2.34E -4	3.19E 2	3.07E 5	6.0E 0	5.3E 1	3.7E 2
75	3.83E 5	2.54E -4	3.43E 2	2.30E 5	2.0E 1	4.1E 2	8.5E 3
76	2.86E 5	2.13E -4	2.88E 2	1.85E 5	6.3E 0	1.0E 2	2.5E 3
77	1.00E 6	2.58E -4	3.50E 2	5.93E 5	7.0E 0	8.2E 1	5.5E 2
78	8.04E 5	2.75E -4	3.73E 2	5.00E 5	1.0E 1	2.8E 2	1.5E 3
79	9.13E 5	2.62E -4	3.52E 2	5.41E 5	8.3E 0	1.0E 2	4.6E 2
80	8.95E 5	1.34E -4	1.35E 2	7.88E 5	3.3E 1	3.5E 2	4.5E 3
81	8.28E 5	1.30E -4	1.33E 2	7.34E 5	3.0E 1	6.0E 2	1.0E 4
82	4.71E 5	1.25E -4	1.27E 2	4.26E 5	6.5E 1	1.0E 3	1.6E 4
83	9.51E 5	1.04E -4	6.94E 1	1.10E 6	3.2E 1	2.8E 2	3.5E 3
85	4.93E 5	1.06E -4	7.19E 1	5.66E 5	1.5E 1	4.0E 2	1.2E 4
86	1.06E 6	1.10E -4	7.40E 1	1.21E 6	4.5E 1	8.1E 2	1.0E 4
87	9.25E 5	1.04E -4	7.17E 1	1.06E 6	2.0E 1	4.8E 2	6.1E 3
88	8.58E 5	1.05E -4	7.19E 1	9.84E 5	3.6E 1	5.1E 2	7.5E 3
89	2.37E 5	1.59E -4	1.09E 2	2.29E 5	1.0E 1	1.2E 2	1.8E 3
90	7.40E 5	1.73E -4	1.18E 2	6.91E 5	1.5E 1	2.0E 2	1.4E 3
91	9.79E 5	1.70E -4	1.14E 2	9.24E 5	3.0E 1	3.1E 2	2.6E 3
92	9.25E 5	1.76E -4	1.16E 2	8.67E 5	2.3E 1	2.8E 2	1.5E 3
93	5.27E 5	1.75E -4	1.20E 2	4.89E 5	1.4E 1	2.1E 2	5.0E 3
94	3.46E 5	1.78E -4	1.20E 2	3.21E 5	1.6E 1	3.5E 2	5.6E 3

95	7.33E	5	2.67E	-4	1.92E	2	5.57E	5	4.1E	0	3.1E	1	2.4E	2
96	5.87E	5	2.90E	-4	1.99E	2	4.41E	5	6.0E	0	7.1E	1	5.0E	2
97	3.94E	5	2.63E	-4	2.04E	2	2.93E	5	4.0E	0	9.0E	0	7.0E	1
99	3.39E	5	7.77E	-4	1.00E	3	1.30E	5	2.0E	0	8.0E	0	3.6E	1
100	5.29E	5	6.83E	-4	7.43E	2	2.30E	5	2.1E	0	5.8E	0	2.0E	1
101	5.40E	5	5.67E	-4	3.69E	2	3.14E	5	2.1E	0	1.0E	1	6.0E	1
102	3.97E	5	6.12E	-4	4.69E	2	2.09E	5	2.6E	0	1.4E	1	4.5E	1
103	3.78E	5	5.83E	-4	4.41E	2	2.04E	5	2.3E	0	1.0E	1	3.3E	1
104	5.67E	5	6.05E	-4	4.16E	2	3.14E	5	2.0E	0	9.3E	0	5.1E	1
105	6.06E	5	5.91E	-4	3.56E	2	3.57E	5	2.8E	0	1.5E	1	8.0E	1
106	6.28E	5	5.83E	-4	3.79E	2	3.61E	5	3.0E	0	1.8E	1	8.0E	1
107	3.79E	5	1.26E	-3	9.54E	2	1.48E	5	1.8E	0	1.0E	1	1.8E	1
108	3.51E	5	1.19E	-3	8.44E	2	1.45E	5	2.0E	0	6.1E	0	1.8E	1
109	2.70E	5	1.22E	-3	9.69E	2	1.05E	5	2.0E	0	6.8E	0	2.1E	1
110	3.95E	5	1.22E	-3	8.39E	2	1.63E	5	1.9E	0	5.8E	0	1.8E	1
111	3.05E	5	1.09E	-3	4.69E	2	1.60E	5	1.8E	0	4.8E	0	9.0E	0
112	3.61E	5	1.18E	-3	4.20E	2	1.99E	5	1.2E	0	1.9E	0	4.5E	0
113	2.30E	5	1.09E	-3	4.59E	2	1.22E	5	1.9E	0	5.3E	0	1.5E	1
114	1.31E	5	1.04E	-3	4.64E	2	6.97E	4	2.1E	0	7.0E	0	2.4E	1
115	3.89E	5	1.05E	-3	3.50E	2	2.31E	5	1.8E	0	4.8E	0	1.5E	1
116	1.20E	5	3.04E	-3	6.59E	2	5.48E	4	1.4E	0	2.5E	0	5.3E	0
117	1.72E	5	2.95E	-3	6.02E	2	8.16E	4	1.4E	0	2.5E	0	5.6E	0
118	2.19E	5	3.05E	-3	5.80E	2	1.06E	5	1.4E	0	2.3E	0	4.1E	0
122	8.50E	5	5.67E	-5	7.63E	1	9.50E	5	3.5E	2	7.0E	4	2.5E	7
123	7.69E	5	5.29E	-5	7.13E	1	8.85E	5	3.0E	2	1.8E	4	1.0E	6
124	9.67E	5	5.33E	-5	7.17E	1	1.11E	6	1.5E	2	1.3E	4	3.0E	6
179	7.36E	5	4.73E	-5	6.58E	1	8.76E	5	0.0		0.0		0.0	
180	1.00E	6	3.96E	-5	5.35E	1	1.29E	6	0.0		0.0		0.0	
181	9.30E	5	4.16E	-5	5.50E	1	1.19E	6	0.0		0.0		0.0	

BEST FIT LINES STRAIN-CYCLES TO 90PC 75PC 60PC STIFFNESS

STRAIN	CYCLES TO 90PC STIFFNESS		CYCLES TO 75PC STIFFNESS		CYCLES TO 60PC STIFFNESS	
5E-3	1.20E	0	1.93E	0	3.29E	0
2E-3	1.47E	0	3.22E	0	7.26E	0
1E-3	1.95E	0	6.05E	0	1.84E	1
5E-4	3.19E	0	1.59E	1	7.24E	1
2E-4	1.09E	1	1.33E	2	1.24E	3
1E-4	6.22E	1	1.86E	3	3.52E	4
5E-5	1.25E	3	1.07E	5	4.82E	6
2E-5	2.43E	6	7.70E	8	1.31E	11

DENSE BITUMEN MACADAM 90/110 +30 C

BEST FIT LINE STRAIN*STIFFNESS SLOPE = -5.7265E -1 INTERCEPT AT 1E-4 = 1.53E 5
BEST FIT LINE STRAIN*CYCLES TO 90PC STIFFNESS SLOPE = -3.3504E -1 LOG BASE E OF INTERCEPT AT 1E-6 = 7.92E 0
BEST FIT LINE STRAIN*CYCLES TO 75PC STIFFNESS SLOPE = -5.7029E -1 LOG BASE E OF INTERCEPT AT 1E-6 = 9.82E 1
BEST FIT LINE STRAIN*CYCLES TO 60PC STIFFNESS SLOPE = -5.1617E -1 LOG BASE E OF INTERCEPT AT 1E-6 = 1.19E 2

SPECIMEN	STIFFNESS	STRAIN	R OF S	ADJ STIFFNESS	CYCLES TO 90PC	PERCENTAGE 75PC	STIFFNESS 60PC
125	1.22E 5	4.27E -4	6.64E 2	5.13E 4	3.0E 0	2.3E 1	2.8E 2
126	1.20E 5	3.77E -4	5.26E 2	5.90E 4	3.5E 0	2.0E 1	1.8E 2
127	1.63E 5	3.65E -4	5.00E 2	7.80E 4	3.6E 0	2.5E 1	2.1E 2
128	1.44E 5	3.67E -4	4.88E 2	6.98E 4	3.0E 0	2.3E 1	2.1E 2
129	1.47E 5	3.67E -4	5.04E 2	7.01E 4	4.0E 0	2.5E 1	2.8E 2
130	1.25E 5	3.75E -4	5.23E 2	5.82E 4	3.0E 0	2.0E 1	2.5E 2
131	1.26E 5	1.82E -4	2.31E 2	8.61E 4	7.5E 0	2.0E 2	4.6E 3
132	1.27E 5	1.92E -4	2.54E 2	8.32E 4	1.0E 1	2.5E 2	7.5E 3
133	1.28E 5	1.91E -4	2.51E 2	8.42E 4	9.0E 0	9.0E 1	2.2E 3
134	1.25E 5	7.80E -5	1.04E 2	1.22E 5	3.5E 0	2.6E 3	1.2E 5
135	2.43E 5	7.94E -5	1.02E 2	2.37E 5	1.4E 0	9.5E 2	6.5E 4
136	2.15E 5	7.84E -5	1.04E 2	2.10E 5	4.0E 0	2.5E 4	7.0E 5
137	7.73E 4	2.16E -4	7.29E 1	8.94E 4	7.6E 0	1.6E 2	9.5E 3
138	1.09E 5	2.22E -4	7.34E 1	1.25E 5	1.4E 1	2.2E 2	2.6E 3
139	1.41E 5	2.09E -4	7.00E 1	1.67E 5	9.0E 0	1.8E 2	3.5E 3
140	1.02E 5	1.34E -3	1.58E 3	2.87E 4	1.9E 0	6.0E 0	2.4E 1
141	8.77E 4	1.50E -3	1.85E 3	2.28E 4	1.4E 0	3.9E 0	1.8E 1
142	8.50E 4	1.57E -3	2.13E 3	2.07E 4	4.1E 0	5.6E 0	1.5E 1
143	7.96E 4	9.64E -4	1.66E 2	6.29E 4	1.8E 0	4.3E 0	1.5E 1
144	7.31E 4	9.77E -4	1.63E 2	5.82E 4	1.7E 0	3.9E 0	1.5E 1
145	7.94E 4	9.64E -4	1.66E 2	6.27E 4	2.0E 0	5.6E 0	1.8E 1
146	5.21E 4	2.90E -3	4.90E 2	2.50E 4	1.7E 0	3.5E 0	9.0E 0
147	4.34E 4	2.90E -3	4.90E 2	2.08E 4	1.6E 0	3.5E 0	9.0E 0
148	5.64E 4	2.96E -3	5.08E 2	2.67E 4	1.5E 0	2.8E 0	6.1E 0
183	1.10E 5	1.03E -5	9.17E 0	3.33E 5	0.0	0.0	0.0
184	1.38E 5	1.82E -5	2.31E 0	7.89E 5	0.0	0.0	0.0

BEST FIT LINES STRAIN*CYCLES TO 90PC 75PC 60PC STIFFNESS

STRAIN	CYCLES TO 90PC STIFFNESS	CYCLES TO 75PC STIFFNESS	CYCLES TO 60PC STIFFNESS
5E-3	1.57E 0	2.14E 0	4.37E 0
2E-3	1.86E 0	3.62E 0	1.06E 1
1E-3	2.18E 0	6.76E 0	2.96E 1
5E-4	2.68E 0	1.70E 1	1.27E 2
2E-4	3.82E 0	1.19E 2	2.39E 3
1E-4	5.43E 0	1.22E 3	6.78E 4
5E-5	8.46E 0	3.82E 4	8.13E 6
2E-5	1.82E 1	5.35E 7	1.22E 11

DENSE BITUMEN MACADAM 90/110 +40 C

BEST FIT LINE STRAIN*STIFFNESS SLOPE = -3.3734E -1 INTERCEPT AT 1E-4 = 6.92E 4
BEST FIT LINE STRAIN*CYCLES TO 90PC STIFFNESS SLOPE = -6.5148E -1 LOG BASE E OF INTERCEPT AT 1E-6 = 4.94E 1
BEST FIT LINE STRAIN*CYCLES TO 75PC STIFFNESS SLOPE = -6.4682E -1 LOG BASE E OF INTERCEPT AT 1E-6 = 1.35E 2
BEST FIT LINE STRAIN*CYCLES TO 60PC STIFFNESS SLOPE = -5.6686E -1 LOG BASE E OF INTERCEPT AT 1E-6 = 1.52E 2

SPECIMEN	STIFFNESS	STRAIN	R OF S	ADJ STIFFNESS	CYCLES TO 90PC	PERCENTAGE 75PC	STIFFNESS 60PC
149	5.89E 4	1.34E -4	1.83E 2	4.94E 4	5.0E 0	7.0E 2	6.0E 4
150	9.19E 4	1.36E -4	1.76E 2	7.80E 4	5.1E 0	1.6E 2	7.0E 3
151	9.89E 4	1.36E -4	1.85E 2	8.28E 4	7.0E 0	1.8E 2	5.1E 3
152	7.31E 4	8.91E -5	2.92E 1	1.04E 5	2.0E 1	5.0E 3	7.0E 5
153	6.60E 4	8.79E -5	2.91E 1	9.45E 4	1.5E 1	1.0E 3	7.0E 4
154	5.27E 4	8.47E -5	2.80E 1	7.63E 4	3.6E 1	2.5E 3	1.8E 5
155	7.00E 4	7.23E -4	9.76E 2	3.61E 4	1.9E 0	7.1E 0	4.1E 1
156	5.89E 4	7.32E -4	1.00E 3	3.01E 4	2.3E 0	9.6E 0	5.3E 1
157	7.38E 4	7.60E -4	1.02E 3	3.75E 4	2.0E 0	7.6E 0	3.5E 1
158	4.13E 4	4.77E -4	7.97E 1	4.40E 4	2.0E 0	4.8E 0	5.0E 1
159	3.23E 4	4.70E -4	7.84E 1	3.47E 4	2.6E 0	1.5E 1	1.2E 2
160	3.72E 4	4.62E -4	7.79E 1	4.00E 4	2.3E 0	1.4E 1	8.6E 1
185	3.97E 4	5.78E -5	1.06E 2	3.90E 4	0.0	0.0	0.0
186	5.44E 4	1.30E -5	6.60E 0	1.19E 5	0.0	0.0	0.0
187	8.24E 4	4.99E -6	3.61E 0	2.15E 5	0.0	0.0	0.0

BEST FIT LINES STRAIN*CYCLES TO 90PC 75PC 60PC STIFFNESS

STRAIN	CYCLES TO 90PC STIFFNESS	CYCLES TO 75PC STIFFNESS	CYCLES TO 60PC STIFFNESS
5E-3	1.21E 0	1.73E 0	3.38E 0
2E-3	1.41E 0	2.69E 0	7.74E 0
1E-3	1.73E 0	4.73E 0	2.07E 1
5E-4	2.37E 0	1.14E 1	8.94E 1
2E-4	4.79E 0	8.17E 1	1.90E 3
1E-4	1.17E 1	9.87E 2	7.23E 4
5E-5	4.78E 1	4.88E 4	1.57E 7
2E-5	1.12E 3	3.02E 8	1.26E 12

APPENDIX 6

MATHEMATICAL EXPRESSIONS FOR STIFFNESS/CYCLES CURVES

From typical stiffness/cycles test results it has been found that, over the range of cycles reducing initial stiffness by at least 40% of its initial value, a linear relationship exists between the logarithms of cycles and percentage drop in stiffness/cycle (see Figures 113-119).

Thus:- $\log P = -m \log N + \log K$

or $P = \frac{K}{N^m}$ where P = %age drop in stiffness/cycle

K = %age drop in stiffness in cycle 1

N = number of cycles

m = mod. slope of relationship.

If ND is the number of cycles required to reduce the initial stiffness by D%

then:- $D = \int_{N=1}^{N=N_D} P \, dN$ $\therefore$ $D = \frac{K}{1-m}\left(N_D^{(1-m)} - 1\right)$

(where $m \neq 1$, if $m = 1$ then $D = K \log N_D$)

From the results of repeated loading tests for each material and temperature, best fit lines have been established relating strain level to cycles for 90%, 75% and 60% of initial stiffness, i.e. D = 10, 25 and 40 respectively. Using these relationships and assuming that "K" is a function of strain for a specific material and temperature and that "m" is a material and temperature constant, then three simultaneous equations may be established for a specific strain level for each material and temperature

These are $\frac{40}{10} = \frac{(N_{40}^{(1-m)} - 1)}{(N_{10}^{(1-m)} - 1)}$, $\frac{25}{10} = \frac{(N_{25}^{(1-m)} - 1)}{(N_{10}^{(1-m)} - 1)}$

and $\frac{40}{25} = \frac{(N_{40}^{(1-m)} - 1)}{(N_{25}^{(1-m)} - 1)}$.

For each material and temperature (if relevant) the values of (1-m) may be determined for each of the following strain levels:- 2.10^{-5}, 5.10^{-5}, 1.10^{-4}, 2.10^{-4}, 5.10^{-4}, 1.10^{-3}, 2.10^{-3}, 5.10^{-3} in/in.

For each strain level for each material and temperature (if relevant) the determined values of (1-m) enable the constant (strain dependent) term "K" to be evaluated. For each material the three values of K corresponding to D = 10, 25 and 40 may be plotted against the corresponding strain level on log./log. paper and the resulting straight line used to define "K" in terms of strain level. Thus, for each material and test temperature the expression $D = \frac{K}{1-m}\left(N_D^{(1-m)} - 1\right)$ may be quantified.

For the materials studied in strain-controlled repeated loading, the constants (1-m) and functions "K" were found to be:-

Materials	Temperatures	(1-m)	Slope "m"	K
90/110 DBM - 190/210 DBM	All	0.0622	0.938	$0.102.\varepsilon^{0.71}$
DTM	0°C and +10°C	0.365	0.635	$0.015.\varepsilon^{1.07}$
DTM	+30°C and +40°C	-0.132	1.132	$1.17.\varepsilon^{0.428}$
HRA	+10°C and +30°C	0.0354	0.965	$0.138.\varepsilon^{0.662}$

where ε is in micro strains.

These result in expressions for reduction in stiffness with repeated applications of strain-controlled load of:-

90/110 and 190/210 DBM all temperatures	$D = 1{\cdot}64\ \varepsilon^{0{\cdot}71}\ (N_D^{0{\cdot}0622} - 1)$
D.T.M. at 0°C and +10°C	$D = 0{\cdot}0412\varepsilon^{1{\cdot}07}\ (N_D^{0{\cdot}365} - 1)$
DTM at +30°C and +40°C	$D = 8{\cdot}67\ \varepsilon^{0{\cdot}428}\ (1 - N_D^{-0{\cdot}132})$
HRA at +10°C and +30°C	$D = 3{\cdot}90\varepsilon^{0{\cdot}662}\ (N_D^{0{\cdot}0354} - 1)$

Using these relationships the cycles to 90%, 75% and 60% initial stiffness are as shown in the table overleaf.

Material and Temp.	Proportion In. Stiff.	Cycles required to reduce stiffness at strain level:-							
		2.10^{-5}	5.10^{-5}	1.10^{-4}	2.10^{-4}	5.10^{-4}	1.10^{-3}	2.10^{-3}	5.10^{-3}
90/110 and	90%	$6.56.10^{3}$	$1.71.10^{2}$	$2.87.10^{1}$	$8.42.10^{0}$	$3.15.10^{0}$	$2.03.10^{0}$	$1.54.10^{0}$	$1.26.10^{0}$
190/210 DBM	75%	$1.72.10^{7}$	$4.32.10^{4}$	$1.57.10^{3}$	$1.31.10^{2}$	$1.53.10^{1}$	$5.57.10^{0}$	$2.89.10^{0}$	$1.78.10^{0}$
all temps.	60%	$3.32.10^{9}$	$2.63.10^{6}$	$3.85.10^{4}$	$1.37.10^{3}$	$6.48.10^{1}$	$1.44.10^{0}$	$5.29.10^{0}$	$2.49.10^{0}$
DTM	90%	$6.94.10^{2}$	$6.33.10^{1}$	$1.62.10^{1}$	$4.90.10^{0}$	$2.12.10^{0}$	$1.47.10^{0}$	$1.21.10^{0}$	$1.08.10^{0}$
$0^{o}C$ - $+10^{o}C$	75%	$7.31.10^{3}$	$5.28.10^{2}$	$1.02.10^{2}$	$1.97.10^{1}$	$4.90.10^{0}$	$2.40.10^{0}$	$1.57.10^{0}$	$1.19.10^{0}$
	60%	$2.55.10^{4}$	$1.72.10^{3}$	$3.04.10^{2}$	$4.92.10^{1}$	$9.32.10^{0}$	$3.63.10^{0}$	$2.00.10^{0}$	$1.32.10^{0}$
DTM	90%	$1.67.10^{1}$	$5.99.10^{0}$	$3.63.10^{0}$	$2.56.10^{0}$	$1.86.10^{0}$	$1.58.10^{0}$	$1.40.10^{0}$	$1.26.10^{0}$
$+30^{o}C$ - $+40^{o}C$	75%	$8.50.10^{4}$	$2.87.10^{2}$	$4.31.10^{1}$	$1.37.10^{1}$	$5.24.10^{0}$	$3.33.10^{0}$	$2.40.10^{0}$	$1.79.10^{0}$
	60%	*	$1.18.10^{6}$	$1.73.10^{3}$	$1.82.10^{2}$	$1.74.10^{1}$	$7.58.10^{0}$	$4.29.10^{0}$	$2.60.10^{0}$
HRA	90%	$5.22.10^{3}$	$1.48.10^{2}$	$2.56.10^{1}$	$8.19.10^{0}$	$3.24.10^{0}$	$2.08.10^{0}$	$1.61.10^{0}$	$1.25.10^{0}$
$+10^{o}C$ - $+30^{o}C$	75%	$5.99.10^{7}$	$6.91.10^{4}$	$1.81.10^{3}$	$1.47.10^{2}$	$1.73.10^{1}$	$6.01.10^{0}$	$3.25.10^{0}$	$1.74.10^{0}$
	60%	$6.64.10^{10}$	$1.07.10^{7}$	$7.32.10^{4}$	$2.02.10^{3}$	$8.43.10^{1}$	$1.67.10^{1}$	$6.43.10^{0}$	$2.41.10^{0}$

* expression invalid for $\varepsilon < 33.9$ at $D = 40$.

APPENDIX 7

PROPOSED THEORY FOR CUMULATIVE DAMAGE DUE TO THIXOTROPIC BREAKDOWN

It was shown in Chapter 10 that the damage "D" sustained by a bituminous specimen after "N" applications of load at strain level "E" is given by:-

$$D = K E^n (N^m - 1) \quad - - - \quad \text{eq.1}$$

The values of K, n and m are material constants being independent of strain rate and, in some cases, temperature.

If N_1 applications of load at strain level E_1 are followed continuously with N_2 applications of load at strain level E_2, then the total damage sustained is equal to the sum of the damage due to N_1 applications of E_1, starting from rest, and N_2 applications of E_2, starting from the damaged state after N_1 applications of E_1.

Now the damage sustained by the specimen after N_1 applications of E_1 is $K E_1^n (N_1^m - 1)$. If "N_{21}" is the number of applications of load at strain level E_2 causing the same damage as N_1 applications of E_1 then:-

$$K E_1^n (N_1^m - 1) = K E_2^n (N_{21}^m - 1)$$

$$\text{hence } N_{21}^m = \left(\frac{E1}{E2}\right)^n (N_1^m - 1) + 1 \quad - - \quad \text{eq. 2}$$

Therefore, the damage caused by N_1 applications of E_1 followed by N_2 applications of E_2 is :-

$$D_2 = K E_2^n ((N_{21} + N_2)^m - 1) \quad - - \text{eq. 3}$$

Thus for any number "x" of continuously applied block loadings the final damage "Dx" may be calculated by determining the cumulative number of equivalent load applications "$N_{x(x-1)}$" prior to the final strain level and applying the final number of total equivalent load applications to the equation:-

$$D_x = K Ex^n ((Nx (x-1) + Nx)^m - 1) \quad - - \text{eq.4}$$

Example - assume K = 1, m = 0.1, n = $^2/_3$

loading sequence 1 - stage 1 1000 applications of 10 $\mu\varepsilon$

stage 2 10 " " 1000 $\mu\varepsilon$

stage 3 100 " " 100 $\mu\varepsilon$

At beginning of stage 2, number of applications of $1000\mu\varepsilon$ for damage equivalent to that of stage 1 is (from eq. 2):-

$$N_{21}^{0.1} = \left(\frac{10}{1000}\right)^{2}/_{3} \quad (1000^{0.1} - 1) + 1 = 1.046 , \quad N_{21} = 1.582$$

$\therefore$ at end of stage 2 the damage is equal to that sustained by :-
$1.582 + 10 = 11.582$ applications of $1000\mu\varepsilon$.
At beginning of stage 3, number of applications of $100\mu\varepsilon$ for damage equivalent to that at end of stage 2 is:-

$$N_{32}^{0.1} = \left(\frac{1000}{100}\right)^{2}/_{3} \; (11.582^{0.1} - 1) + 1 = 2.282 , \; N_{32} = 3834$$

$\therefore$ at end of stage 3 damage is equal to that sustained by :-
$3834 + 100 = 3934$ applications of $100\mu\varepsilon$.
At end of stage 3, total damage is (from eq.4) :-

$$D_3 = 1.100^{2}/_{3} \; (3934^{0.1} - 1) = \underline{\underline{27.75\%}}$$

loading sequence 2 - stage 1 100 applications of $100\mu\varepsilon$
stage 2 1000 " " $10\mu\varepsilon$
stage 3 10 " " $1000\mu\varepsilon$

$$N_{21}^{0.1} = \left(\frac{100}{10}\right)^{2}/_{3} \quad (100^{0.1} - 1) + 1 = 3.548 , \quad N_{21} = 3.158.10^{5}$$

$\therefore N_2 \equiv 3.158.10^{5} + 1.0.10^{3} = 3.168.10^{5}$

$$N_{31}^{0.1} = \left(\frac{10}{1000}\right)^{2}/_{3} \; ((3.168.10^{5})^{0.1} - 1) + 1 = 1.118 , \; N_{31} = 3.055$$

$\therefore N_3 = 3.055 + 10 = 13.055$

$\therefore D_3 = 1.\ 1000^{2}/_{3} \; (13.055^{0.1} - 1) = \underline{\underline{28.99\%}}$